

**Ongoing Face Recognition
Vendor Test (FRVT)**
Part 1: Verification

Patrick Grother
Mei Ngan
Kayee Hanaoka
Joyce C. Yang
Austin Hom

*Information Access Division
Information Technology Laboratory*

This publication is available free of charge from:
<https://www.nist.gov/programs-projects/face-recognition-vendor-test-frvt-ongoing>

2022/02/23

ACKNOWLEDGMENTS

The authors are grateful for the long-standing support and collaboration of the the Department of Homeland Security's Science & Technology Directorate (S&T) and the Office of Biometric Identity Management (OBIM).

Additionally, the authors are grateful to staff in the NIST Biometrics Research Laboratory for infrastructure supporting rapid evaluation of algorithms.

DISCLAIMER

Specific hardware and software products identified in this report were used in order to perform the evaluations described in this document. In no case does identification of any commercial product, trade name, or vendor, imply recommendation or endorsement by the National Institute of Standards and Technology, nor does it imply that the products and equipment identified are necessarily the best available for the purpose.

INSTITUTIONAL REVIEW BOARD

The National Institute of Standards and Technology's Research Protections Office reviewed the protocol for this project and determined it is not human subjects research as defined in Department of Commerce Regulations, 15 CFR 27, also known as the Common Rule for the Protection of Human Subjects (45 CFR 46, Subpart A).

FRVT STATUS

This report is a draft NIST Interagency Report, and is open for comment. It is the thirty sixth edition of the report since the first was published in June 2017. Prior editions of this report are maintained on the FRVT [website](#), and may contain useful information about older algorithms and datasets no longer used in FRVT.

FRVT remains open: All [four tracks](#) of the FRVT are open to new algorithm submissions.

2022-02-23 changes since 2022-01-24:

- ▷ We have added results for first algorithms from four developers: AFIS and Biometrics Consulting, Digi-data, Graymatics, Hangzhuo Allu Network Information Technology, KnowUTech LLC, Sukshi Technology Innovation, T4iSB, and TuringTech.vip
- ▷ We have added results for new algorithms from 18 returning developers: Cognitec Systems GmbH, GeoVision Inc, Glory, Herta Security, Intel Research Group, InsightFace AI, Kakao Enterprise, N-Tech Lab, Omnidarde Ltd, Papilon Savunma, Paravision, Reveal Networks Inc, Reveal Media Ltd, Shenzhen Inst Adv Integrated Tech CAS, Suprema AI Inc, Toshiba, Universidade de Coimbra, and Yuan High-Tech Development
- ▷ We have retired results for 14 algorithms per our policy to only list results for two algorithms per developer. Results for retired algorithms appear in prior versions of this report in the [archive](#).

2022-01-24 changes since 2022-01-20:

- ▷ We have added results for new algorithms from one returning developer: Vocord.

2022-01-20 changes since 2021-12-18:

- ▷ We have added results for first algorithms from four developers: Armatura, Beyne.AI, One More Security, and VinBigData
- ▷ We have added results for new algorithms from 19 returning developers: AuthenMetric, BOE Technology Group, Cybercore, Cyberlink, Dahua Technology, FaceTag Co, Innovatrics, Megvii, Mobbeel Solutions, Neurotechnology, Oz Forensics, Rank One Computing, Regula Forensics, Samsung S1, Securif AI, Sensetime Group, TigerIT Americas, Videmo Intelligente Videoanalyse, and YooniK.
- ▷ We have retired results for 14 algorithms per our policy to only list results for two algorithms per developer. Results for retired algorithms appear in prior versions of this report in the [archive](#).

: **2021-12-16** changes since 2021-11-22:

- ▷ We have added results for first algorithms from five developers: Alfabeta, Cloudmatrix, Euronovate SA, FaceOnLive Inc, and Mobicin Technology.
- ▷ We have added results for new algorithms from ten returning developers: ACI Software, ITMO University, NEO Systems, Guangzhou Pixel Solutions, Panasonic R+D Center Singapore, Qnap Security, Scanovate, Tevian, Unissey, and Vietnam Posts and Telecommunications Group.
- ▷ We have retired results for eight algorithms per our policy to only list results for two algorithms per developer. Results for retired algorithms appear in prior versions of this report in the [archive](#).

- ▷ We have revamped Figure 19 showing performance on 20 pairs of open-source images. It now color-codes false negatives and positives against a default threshold value.

2021-11-22 changes since 2021-10-28:

- ▷ We have added results to the [website](#) for kiosk-collected images where the design and geometry configuration mean that many images have considerable downward pitch angle. In some images, the face is partially cropped. Some images have other background faces.
- ▷ We have stopped using child exploitation images in FRVT, as we lost access to the imagery. All results for that set have been removed from the [website](#), and will be removed from future PDF reports.
- ▷ We have added results for first algorithms from seven new developers: CUDO Communication, Daon, KuKe3D Technology, Mantra Softtech India, Maxvision Technology, Multi-Modality Intelligence, and Samsung-SDS.
- ▷ We have added results for new algorithms from seven returning developers: Acer Incorporated, Cloudwalk-Moontime Smart Technology, Gorilla Technology, ID3 Technology, Incode Technologies, NSENSE Corp., and SQIssoft.
- ▷ We have retired results for six algorithms per our policy to only list results for two algorithms per developer. Results for retired algorithms appear in prior versions of this report in the [archive](#).

2021-10-28 changes since 2021-09-08:

- ▷ We have substantially revised the algorithm-specific report cards that are linked from the [FRVT results page](#). (Example: [HTML](#)).
- ▷ We have added results for first algorithms from eight new developers: Beijing Mendaxia Technology, Beijing Hisign Technology, Biocube Matrics, Clearview AI, Reveal Media, Toppan ID Gate, Verigram, and Viettel High Technology.
- ▷ We have added results for new algorithms from thirty returning developers: 20Face, 3divi, Canon Inc Chunghwa Telecom, Corsight, Decatur Industries, Deepglint, Dermalog, FaceTag, Fiberhome Telecommunication Technologies, GeoVision, ICM Airport Technics, Imagus Technology, InsightFace AI, Kakao Enterprise, Kookmin University, Line Corporation, N-Tech Lab, NotionTag Technologies, Realnetworks, Suprema ID, Taiwan-Certificate Authority, Toshiba, Tripleize, Trueface.ai, Veridas Digital Authentication, Visidon, VisionLabs, YooniK, and Yuan High-Tech Development.
- ▷ We have retired results for twenty algorithms per our policy to only list results for two algorithms per developer. Results for retired algorithms appear in prior versions of this report in the [archive](#).

2021-09-08 changes since 2021-08-02:

- ▷ We have added results for first algorithms from seven new developers: Griaule, SQIssoft, Qnap Security, Techsign, Smart Engines, Verihubs, and Wuhan Tianyu Information Industry.
- ▷ We have added results for new algorithms from sixteen returning developers: ADVANCE.AI, AuthenMetric, CloudSmart Consulting, Code Everest Pvt, Cognitec Systems, Thales Gemalto Cogent, Intel Research Group, Omnidarde, Oz Forensics, Rank One Computing, Samsung S1 Corp, Securif AI, Tevian, TigerIT Americas, Universidade de Coimbra, and Vigilant Solutions
- ▷ We have retired results for eleven algorithms per our policy to only list results for two algorithms per developer. Results for retired algorithms appear in prior versions of this report in the [archive](#).

2021-08-02 changes since 2021-06-25:

- ▷ We have added results for first algorithms from eight new developers: Bee the Data, Closeli Inc, Coretech Knowledge Inc, Deepsense (France), ioNetworks Inc, Kakao Pay Corp, Seventh Sense Artificial Intelligence, and SK Telecom.
- ▷ We have added results for new algorithms from fifteen returning developers: Alchera Inc, Adera Global PTE, Aware, Bresee Technology, Cyberlink Corp, Expasoft LLC, Fujitsu Research and Development Center, Gorilla Technology, Idemia, Neurotechnology, NEO Systems, NHN Corp, Paravision, Panasonic R+D Center Singapore, and Shenzhen University-Macau University of Science and Technology.
- ▷ We have retired results for twelve algorithms per our policy to only list results for two algorithms per developer. Results for retired algorithms appear in prior versions of this report in the [archive](#).

2021-06-25 changes since 2021-05-21:

- ▷ We have added results for first algorithms from six new developers: Alice Biometrics, BOE Technology Group, Fincore, Neosecu, Sodec App, and Yuntu Data and Technology.
- ▷ We have added results for new algorithms from seven returning developers: Incode Technologies, HyperVerge, Mobbeel Solutions, Guangzhou Pixel Solutions, Remark Holdings, Sensetime, and Vietnam Posts and Telecommunications Group.
- ▷ We have retired results for four algorithms per our policy to only list results for two algorithms per developer. Results for retired algorithms appear in prior versions of this report in the [archive](#).

2021-05-21 changes since 2021-04-26:

- ▷ We have added results for first algorithms from five new developers: Ekin Smart City Technologies, Suprema ID, Tripleize, Taiwan-Certificate Authority, and Vision Intelligence Center of Meituan.
- ▷ We have added results for new algorithms from eight returning developers: ID3 Technology, Imagus Technology, Momentum Digital, N-Tech Lab, NSENSE, Shanghai Jiao Tong University, Vision-Box, and Yuan High-Tech Development
- ▷ We have retired results for seven algorithms per our policy to only list results for two algorithms per developer. Results for retired algorithms appear in prior versions of this report in the [archive](#).

2021-04-26 changes since 2021-04-16:

- ▷ We have added results for first algorithms from three new developers: Quantasoft, Rendip, and NEO Systems.
- ▷ We have added results for new algorithms from four returning developers: 3Divi, Realnetworks, Veridas Digital Authentication Solutions, and Universidade de Coimbra.
- ▷ We have retired results for three algorithms per our policy to only list results for two algorithms per developer. Results for retired algorithms appear in prior versions of this report in the [archive](#).

2021-04-16 changes since 2021-03-19:

- ▷ We have added results for first algorithms from six new developers: 20Face, Beijing DeepSense Technologies, BitCenter UK, Enface, FaceTag, InsightFace AI, Line Corporation, Lema Labs, Nanjing Kiwi Network Technology, Omnidarde, Regula Forensics, and Suprema.
- ▷ We have added results for new algorithms from ten returning developers: CloudSmart Consulting, Dermalog, GeoVision, Neurotechnology, Panasonic R+D Center Singapore, Samsung S1, Securif AI, Trueface.ai, Vigilant Solutions, and Visidon.
- ▷ We have retired results for ten algorithms per our policy to only list results for two algorithms per developer. Results for retired algorithms appear in prior versions of this report in the [archive](#).

2021-03-19 changes since 2021-03-05:

- ▷ We have added results for first algorithms from six new developers: Ajou University, AuthenMetric, Code Everest, Corsight, Papilon Savunma, and NHN Corp
- ▷ We have added results for new algorithms from seven returning developers: Alchera, Deepglint, Fiber-home Telecommunication Technologies, Kakao Enterprise, Kookmin University, Megvii/Face++, and NotionTag Technologies.
- ▷ We have updated many of the hyperlinked HTML report-cards to include seven figures on demographic dependence. Figures of this kind first appeared, and are documented in, the December 2019 document, [NIST Interagency Report 8280](#) on demographic differentials in face recognition. The figures quantify false negative dependence on demographics using “visa-border” comparisons, and false positive dependence using comparisons of “application” photos that uniformly of quality and similar to visa photos.

2021-03-05 changes since 2021-01-19:

- ▷ We have added results for first algorithms from three new developers: IVA Cognitive, Mobbeel, and MoreDian Technology.
- ▷ We have added results for new algorithms from returning developers: Ability Enterprise - Andro Video, ACI Software, Adera Global, AnyVision, BioID Technologies, China Electronics Import-Export, Cognitec Systems, Fujitsu Research and Development Center, Glory, Guangzhou Pixel Solutions, Hengrui AI Technology, Incode Technologies, Intel Research, iQIYI, Mobai, Oz Forensics, Paravision, VisionLabs, and Xforward AI Technology.
- ▷ We have added a new “resources” tab to the main [webpage](#). It includes sortable columns for data related to speed, model size, storage, and memory consumption.
- ▷ We have retired results for 13 algorithms per our policy to only list results for two algorithms per developer. Results for retired algorithms appear in prior versions of this report in the [archive](#).

2021-01-19 changes since 2020-12-18:

- ▷ This report adds results for first algorithms from four developers: Herta Security, Irex AI, Shenzhen University-Macau University of Science and Technology, and Vietnam Posts and Telecommunications Group. See Table 6 for more information.
- ▷ The report also includes results for thirteen developers who have previously submitted algorithms: Bresee Technology, Canon (previously Canon Information Technology (Beijing)), Cyberlink, CSA IntelliCloud Technology, Dahua Technology, ID3 Technology, Imagus Technology (Vixvizion), Moontime Smart Technology, N-Tech Lab, Thales Cogent, Veridas Digital Authentication Solutions, Vocord, and Yuan High-Tech Development.

- ▷ We have retired results for ten algorithms per our policy to only list results for two algorithms per developer. Results for retired algorithms appear in prior versions of this report in the [archive](#).

2020-12-18 changes since 2020-10-09:

- ▷ This report adds results for first algorithms from ten developers: BitCenter UK, CloudSmart Consulting, Cubox, Institute of Computing Technology, Naver Corp, Minivision, NSENSE Corp, Viettel Group, Visage Technologies, and Xiamen University. See Table 6 for more information.
- ▷ The report also includes results for eighteen developers who have previously submitted algorithms: ADVANCE.AI, Awudit Systems, Chosun University, Dermalog, GeoVision, ICM Airport Technics, Idemia, Institute of Information Technologies, Kakao Enterprise, Neurotechnology, Panasonic R+D Center Singapore, Rank One Computing, SenseTime Group, Shanghai Jiao Tong University, TigerIT Americas LLC, Vigilant Solutions, Winsense, and YooniK
- ▷ We have retired results for twelve algorithms per our policy to only list results for two algorithms per developer. Results for retired algorithms appear in prior versions of this report in the [archive](#).

Changes since September 18, 2020:

- ▷ This report adds results for first algorithms from five developers: Aigen, Cortica, Kookmin University, Securif AI and Vinai.
- ▷ The report also includes results for three developers who have previously submitted algorithms: Fujitsu Laboratories, Hengrui AI, and X-Forward AI.
- ▷ In the per-algorithm report-cards linked from tables and the main webpage, we have added a chart to showing reduction in error rates over the course of FRVT i.e. from 2017 onwards for all algorithms supplied by that developer. Similarly we have added a chart showing error rate reductions for our test of protective face mask verification.
- ▷ We plan to continue evaluating algorithms on various mask datasets. We hold that algorithms should be capable of detecting masks and verifying identity of all combinations of masked and unmasked faces. We have accordingly increased the amount of time allowed to extract those features from 1.0 to 1.5 seconds.

Changes since August 25, 2020:

- ▷ This report adds results for first algorithms from eight new developers. Akurat Satu Indonesia, Cybercore, Decatur Industries, Innef Labs, Satellite Innovation/Eocortex, Expasoft, and Mobai.
- ▷ The report includes results for seven developers who have previously submitted algorithms: 3Divi, BioID Technologies, Incode Technologies, Innovatrics, iSAP Solution, Synology, and Tevian.
- ▷ We have retired results for five algorithms per our policy to only list results for two algorithms per developer. Results for retired algorithms appear in prior versions of this report in the [archive](#).

Changes since July 27, 2020:

- ▷ We have introduced per-algorithm report sheets. These are HTML documents linked from the accuracy tables in this report (i.e. Table 25) and on the FRVT 1:1 [homepage](#). The sheets contain interactive graphics allowing, for example, mouseover exploration of FNMR(T) and FMR(T). Some of their content had previously appeared in this document.
- ▷ This report adds results for algorithms from six new developers. ACI Software, Bresee Technology, Fiberhome Telecommunication Technologies, Imageware Systems, Oz Forensics, and Pensees.
- ▷ The report includes results for thirteen developers who have previously submitted algorithms: Canon Information Technology (Beijing), Cyberlink, Dahua Technology, Gorilla Technology, ID3 Technology, Intel Research Group, iQIYI Inc, Momentum Digital, Netbridge Technology, Tech5 SA, Shenzhen AiMall Tech, Vigilant Solutions, and VisionLabs.
- ▷ We have retired results for nine algorithms per our policy to only list results for two algorithms per developer. Results for retired algorithms appear in prior versions of this report in the [archive](#).

Changes since May 18, 2020:

- ▷ The report is the first FRVT update since the pandemic closed it from March to June 2020.
- ▷ This report includes results for algorithms from nine new developers: GeoVision Inc, Su Zhou NaZhi-TianDi Intelligent Technology, YooniK, AYF Technology, PXL Vision AG, Yuan High-Tech Development, Beihang University-ERCACAT, ICM Airport Technics, and Staqu Technologies
- ▷ This report includes results for algorithms from 15 returning developers Acer Incorporated, Antheus Technologia, Chosun University, Chunghwa Telecom, Idemia, Moontime Smart Technology, Neurotechnology, Guangzhou Pixel Solutions, Panasonic R+D Center Singapore, Rank One Computing, Scanovate, Shanghai Universiy - Shanghai Film Academy, Synesis, Trueface.ai, and Veridas Digital Authentication Solutions
- ▷ We have retired results for ten algorithms per our policy to only list results for two algorithms per developer. Results for retired algorithms appear in prior versions of this report in the [archive](#).
- ▷ We separated timing and other resource consumption from the main participation table. The new Table 15 includes template generation durations for four kinds of images, not just mugshots.
- ▷ We have published a separate report, [NIST Interagency Report 8311](#) on accuracy of pre-pandemic algorithms on subjects wearing face masks. We plan to track improvements in accuracy on masked images going forward. In particular, we invite submission of algorithms that can detect whether a person is wearing a mask, extract features from the full face or the exposed periocular region, and do appropriate comparison. We do not intend to evaluate algorithms that assume 100% of images will be of masked individuals.

Changes since March 25, 2020:

- ▷ The report is a maintenance release - it does not add any new algorithms, and FRVT has been closed to new algorithms since mid March 2020.
- ▷ We modified the primary accuracy summary, Table 25, as follows:
 - ▷▷ For visa images, the column for FNMR at FMR = 0.0001 has been removed. The visa images are so highly controlled that the error rates for the most accurate algorithms are dominated by false rejection of very young children and by the presence of a few noisy greyscale images. For now, two visa columns remain: FNMR at FMR= 10^{-6} and, for matched covariates, FNMR at FMR= 10^{-4} .

- ▷▷ We have inserted a new column labelled “BORDER” giving accuracy for comparison of moderately poor webcam border-crossing photos that exhibit pose variations, poor compression, and low contrast due to strong background illumination. The accuracies are the worst from all cooperative image datasets used in FRVT.
- ▷ Accordingly, we updated the failure-to-template rates in Table 32.
- ▷ We withdrew a figure showing how false matches are concentrated in certain visa images used in cross-comparison, because it didn’t attempt to include demographic information.

Changes since February 27, 2020:

- ▷ The report adds results algorithms from two new developers: Beijing Alleyes Technology, and the Chinese University of Hong Kong. Results for newly submitted algorithms from two other developers will appear in the next report.
- ▷ The report adds results for algorithms from thirteen returning developers: ASUSTek Computer, Aware, Cyberlink Corp, Gorilla Technology, Innovative Technology, Kakao Enterprise, Lomonosov Moscow State University, Panasonic R+D Center Singapore, Shenzhen AiMall Technology, Shenzhen Intellifusion Technologies, Synology, Tech5 SA, and Via Technologies.
- ▷ Per policy to only list results for two algorithms per developer, we have dropped results for algorithms from Aware, Cyberlink, Gorilla Technology, Kakao Enterprise, Lomonosov Moscow State University, Panasonic R+D Center Singapore, and Tech5 SA.

Changes since January 20, 2020:

- ▷ The report adds results for five new developers: Ability Enterprise (Andro Video), Chosun University, Fujitsu Research and Development Center, University of Coimbra, and Xforward AI Technology.
- ▷ The report adds results for algorithms from six returning developers: AlphaSSTG, Incode Technologies, Kneron, Shanghai Jiao Tong University, Vocord, and X-Laboratory.
- ▷ We have corrected template comparison timing numbers for algorithms submitted September 2019 to January 2020. The values reported previously were slower due to a software bug.
- ▷ We have dropped results for algorithms from Vocord and Incode per policy to only list results for two algorithms per developer.
- ▷ The [FRVT 1:1 homepage](#) has been updated with latest accuracy results.
- ▷ The [FRVT 1:N homepage](#) now includes an update to the September 2019 NIST Interagency Report 8271. The new report adds results for one-to-many search algorithms submitted to NIST from June 2019 to January 2020.

Changes since January 6, 2020:

- ▷ Section 2 has been updated to better describe the Visa and Border images. The caption for Table 25 has been updated to better relate the accuracy values to particular image comparisons.
- ▷ The report adds results for five new developers: Acer, Advance.AI, Expasoft, Netbridge Technology, and Videmo Intelligent Videoanalyse.
- ▷ The report adds results for algorithms from 7 returning developers: China Electronics Import-Export Corp, Intel Research Group, ITMO University, Neurotechnology, N-Tech Lab, Rokid, and VisionLabs.

- ▷ We have dropped results from this edition of the report per policy to only list results for two algorithms per developer: N-Tech Lab, Neurotechnology, ITMO, Visionlabs, and CEIEC.
- ▷ The [FRVT homepage](#) has been updated with latest accuracy results.

Changes since November 11, 2019:

- ▷ Table 15 has been updated to include runtime memory usage. This is the first time such a quantity has been reported. The value is the peak size of the resident set size logged during enrollment of single images.
- ▷ We have migrated summary results table to a new platform that supports sortable tables:
<https://pages.nist.gov/frvt/html/frvt11.html>
- ▷ The report adds results for four new developers: Antheus Technologia, BioID Technologies SA, Canon Information Tech. (Beijing), Samsung S1 (listed in the tables as S1), and Taiwan AI Labs.
- ▷ The report adds results for algorithms from 13 returning developers: Anke Investments, Chunghwa Telecom, Deepglint, Institute of Information Technologies, iQIYI, Kneron, Ping An Technology, Paravision, KanKan Ai, Rokid Corporation, Shanghai Universiy - Shanghai Film Academy, Veridas Digital Authentication Solutions, and Videonetics Technology.
- ▷ We have dropped results from this edition of the report per policy to only list results for two algorithms per developer: remarkai-000, veridas-001, senesetime-001, iit-000, anke-003, and everai-002. Results for these are available in prior editions of this report linked from the FRVT page.
- ▷ We issued [NIST Interagency Report 8280: FRVT Part 3: Demographics](#) on 2019-12-19. It includes results for many of the algorithms covered by this report.

Changes since October 16, 2019:

- ▷ The report adds results for ten new developers: Ai-Union Technology, ASUSTek Computer, DiDi ChuXing Technology, Innovative Technology, Luxand, MVision, Pyramid Cyber Security + Forensic, Scanovate, Shenzhen AiMall Tech, and TUPU Technology.
- ▷ The report adds results for 12 returning developers: CTBC Bank Glory Gorilla Technology Guangzhou Pixel Solutions Imagus Technology Incode Technologies Lomonosov Moscow State University Rank One Computing Samtech InfoNet Shanghai Ulucu Electronics Technology Synesis, and Winsense.
- ▷ We have dropped results from this edition of the report per policy to only list results for two algorithms per developer: glory-000, gorilla-002, incode-003, rankone-006, and synesis-004.
- ▷ Results for five recently submitted algorithms will appear in the next report.

Changes since September 11, 2019:

- ▷ The report adds results for five new participants: Awidit Systems (Awiros), Momentum Digital (Sertis), Trueface AI, Shanghai Jiao Tong University, and X-Laboratory.
- ▷ The report adds results for five new algorithms from returning developers: Cyberlink, Hengrui AI Technology, Idemia, Panasonic R+D Singapore, and Tevian. This causes three algorithms to be de-listed from the report per policy to list results for two algorithms per developer.

Changes since July 31 2019:

- ▷ The HTML table on the [FRVT 1:1 homepage](#) has been updated to include a column for cross-domain Visa-Border verification. Results for this new dataset appeared in the July 29 report under the name "CrossEV" - these are now renamed "Visa-Border".
- ▷ The [FRVT 1:1 homepage](#) lists algorithms according to lowest mean rank accuracy:

$$\begin{aligned} &\text{Rank(FNMR}_{\text{VISA}} \text{ at FMR = 0.000001}) + \\ &\text{Rank(FNMR}_{\text{VISA-BORDER}} \text{ at FMR = 0.000001}) + \\ &\text{Rank(FNMR}_{\text{MUGSHOT}} \text{ at FMR = 0.00001 after 14 years}) + \\ &\text{Rank(FNMR}_{\text{WILD}} \text{ at FMR = 0.00001}) \end{aligned}$$

This ordering rewards high accuracy across all datasets.
- ▷ The main results in Table 25 is now in landscape format to accomodate extra columns for the Visa-Border set, and mugshot comparisons after at least 12 years.
- ▷ The report adds results for nine new participants: Alpha SSTG, Intel Research, ULSee, Chungwa Telecon, iSAP Solution, Rokid, Shenzhen EI Networks, CSA Intellicloud, Shenzhen Intellifusion Technologies.
- ▷ The reports adds results for six new algorithms from returning developers: Innovatrics, Dahua Technology, Tech5 SA, Intellivision, Nodeflux and Imperial College, London. One algorithm, from Imperial has been retired, per policy to list results for two algorithms per developer.
- ▷ The cross-country false match rate heatmaps have been replotted to reveal more structure by listing countries by region instead of alphabetically.
- ▷ The next version of this report will be posted around October 18, 2019.

Changes since July 3 2019:

- ▷ The HTML table on the [FRVT 1:1 homepage](#) has been updated to list the 20 most accurate developers rather than algorithms, choosing the most accurate algorithm from each developer based on visa and mugshot results. Also, the algorithms are ordered in terms of lowest mean rank across mugshot, visa and wild datasets, rewarding broad accuracy over a good result on one particular dataset.
- ▷ This report includes results for a new dataset - see the column labelled "visa-border" in Table 5. It compares a new set of high quality visa-like portraits with a set webcam border-crossing photos that exhibit moderately poor pose variations and background illumination. The two new sets are described in sections 2.2 and 2.3. The comparisons are "cross-domain" in that the algorithm must compare "visa" and "wild" images. Results for other algorithms will be added in future reports as they become available.
- ▷ This report adds results for algorithms from 9 developers submitted in early July 2019. These are from 3DiVi, Camvi, EverAI-Paravision, Facesoft, Farbar (F8), Institute of Information Technologies, Shanghai U. Film Academy, Via Technologies, and Ulucu Electronics Tech. Six of these are new participants.
- ▷ Several other algorithms have been submitted and are being evaluated. Results will be released in the next report, scheduled for September 5. That report will include results for new datasets.
- ▷ Older algorithms from Everai, Camvi and 3DiVi, have been retired, per the policy to list only two algorithms per developer.

Changes since June 20 2019:

- ▷ This report adds results for algorithms from 18 developers submitted in early June 2019. These are from CTBC Bank, Deep Glint, Thales Cogent, Ever AI Paravision, Gorilla Technology, Imagus, Incode, Kneron, N-Tech Lab, Neurotechnology, Notiontag Technologies, Star Hybrid, Videonetics, Vigilant Solutions, Winsense, Anke Investments, CEIEC, and DSK. Nine of these are new participants.
- ▷ Several other algorithms have been submitted and are being evaluated. Results will be released in the next report, scheduled for August 1.
- ▷ Older algorithms from Everai, Thales Cogent, Gorilla Technology, Incode, Neurotechnology, N-Tech Lab and Vigilant Solutions have been retired, per the policy to list only two algorithms per developer.

Changes since April 2019:

- ▷ This report adds results for nine algorithms from nine developers submitted in early June 2019. These are from Tencent Deepsea, Hengrui, Kedacom, Moontime, Guangzhou Pixel, Rank One Computing, Synesis, Sensetime and Vocord.
- ▷ Another 23 algorithms have been submitted and are being evaluated. Results will be released in the next report, scheduled for July 3.
- ▷ Older algorithms for Rank One, Synesis, and Vocord have been retired, per the policy to list only two algorithms per developer.

Changes since February 2019:

- ▷ This report adds results for 49 algorithms from 42 developers submitted in early March 2019.
- ▷ This report omits results for algorithms that we retired. We retired for three reasons: 1. The developer submitted a new algorithm, and we only list two. 2. The algorithm needs a GPU, and we no longer allow GPU-based algorithms. 3. Inoperable algorithms.
- ▷ Previous results for retired algorithms are available in older editions of this report linked [here](#).
- ▷ The mugshot database used from February 2017 to January 2019 has been replaced with an extract of the mugshot database documented in NIST Interagency Report 8238, November 2018. The new mugshot set is described in section [2.4](#) and is adopted because:
 - ▷▷ It has much better identity label integrity, so that false non-match rates are substantially lower than those reported in FRVT 1:1 reports to date - see Figure [79](#).
 - ▷▷ It includes images collected over a 17 year period such that ageing can be much better characterized - - see Figure [286](#).
- ▷ Using the new mugshot database, Figure [286](#) shows accuracy for four demographic groups identified in the biographic metadata that accompanies the data: black females, black males, white females and white males.
- ▷ The report adds Figure [19](#) with results for the twenty human-difficult pairs used in the May 2018 paper *Face recognition accuracy of forensic examiners, superrecognizers, and face recognition algorithms* by Phillips et al. [[1](#)].
- ▷ The report uses an update to the wild image database that corrects some ground truth labels.
- ▷ Some results for the child exploitation database are not complete. They are typically updated less frequently than for other image sets.

Contents

ACKNOWLEDGMENTS	1
DISCLAIMER	1
INSTITUTIONAL REVIEW BOARD	1
1 METRICS	47
1.1 CORE ACCURACY	47
2 DATASETS	48
2.1 VISA IMAGES	48
2.2 APPLICATION IMAGES	48
2.3 BORDER CROSSING IMAGES	48
2.4 MUGSHOT IMAGES	49
2.5 WILD IMAGES	49
3 RESULTS	49
3.1 TEST GOALS	49
3.2 TEST DESIGN	50
3.3 FAILURE TO ENROLL	53
3.4 RECOGNITION ACCURACY	61
3.5 GENUINE DISTRIBUTION STABILITY	288
3.5.1 EFFECT OF BIRTH PLACE ON THE GENUINE DISTRIBUTION	288
3.5.2 EFFECT OF AGEING	322
3.5.3 EFFECT OF AGE ON GENUINE SUBJECTS	347
3.6 IMPOSTOR DISTRIBUTION STABILITY	382
3.6.1 EFFECT OF BIRTH PLACE ON THE IMPOSTOR DISTRIBUTION	382
3.6.2 EFFECT OF AGE ON IMPOSTORS	386

List of Tables

1 PARTICIPANT INFORMATION	20
2 PARTICIPANT INFORMATION	21
3 PARTICIPANT INFORMATION	22
4 PARTICIPANT INFORMATION	23
5 PARTICIPANT INFORMATION	24
6 PARTICIPANT INFORMATION	25
7 ALGORITHM SUMMARY	26
8 ALGORITHM SUMMARY	27
9 ALGORITHM SUMMARY	28
10 ALGORITHM SUMMARY	29
11 ALGORITHM SUMMARY	30
12 ALGORITHM SUMMARY	31
13 ALGORITHM SUMMARY	32
14 ALGORITHM SUMMARY	33
15 ALGORITHM SUMMARY	34
16 FALSE NON-MATCH RATE	35
17 FALSE NON-MATCH RATE	36
18 FALSE NON-MATCH RATE	37
19 FALSE NON-MATCH RATE	38
20 FALSE NON-MATCH RATE	39
21 FALSE NON-MATCH RATE	40

22	FALSE NON-MATCH RATE	41
23	FALSE NON-MATCH RATE	42
24	FALSE NON-MATCH RATE	43
25	FALSE NON-MATCH RATE	44
26	FAILURE TO ENROL RATES	54
27	FAILURE TO ENROL RATES	55
28	FAILURE TO ENROL RATES	56
29	FAILURE TO ENROL RATES	57
30	FAILURE TO ENROL RATES	58
31	FAILURE TO ENROL RATES	59
32	FAILURE TO ENROL RATES	60

List of Figures

1	PERFORMANCE SUMMARY: FNMR VS. TEMPLATE SIZE TRADEOFF	45
2	PERFORMANCE SUMMARY: FNMR VS. TEMPLATE TIME TRADEOFF	46
3	EXAMPLE IMAGES	50
(A)	VISA	50
(B)	MUGSHOT	50
(C)	WILD	50
(D)	BORDER	50
4	PERFORMANCE ON 20 HUMAN-DIFFICULT PAIRS	62
5	PERFORMANCE ON 20 HUMAN-DIFFICULT PAIRS	63
6	PERFORMANCE ON 20 HUMAN-DIFFICULT PAIRS	64
7	PERFORMANCE ON 20 HUMAN-DIFFICULT PAIRS	65
8	PERFORMANCE ON 20 HUMAN-DIFFICULT PAIRS	66
9	PERFORMANCE ON 20 HUMAN-DIFFICULT PAIRS	67
10	PERFORMANCE ON 20 HUMAN-DIFFICULT PAIRS	68
11	PERFORMANCE ON 20 HUMAN-DIFFICULT PAIRS	69
12	PERFORMANCE ON 20 HUMAN-DIFFICULT PAIRS	70
13	PERFORMANCE ON 20 HUMAN-DIFFICULT PAIRS	71
14	PERFORMANCE ON 20 HUMAN-DIFFICULT PAIRS	72
15	PERFORMANCE ON 20 HUMAN-DIFFICULT PAIRS	73
16	PERFORMANCE ON 20 HUMAN-DIFFICULT PAIRS	74
17	PERFORMANCE ON 20 HUMAN-DIFFICULT PAIRS	75
18	PERFORMANCE ON 20 HUMAN-DIFFICULT PAIRS	76
19	PERFORMANCE ON 20 HUMAN-DIFFICULT PAIRS	77
20	ERROR TRADEOFF CHARACTERISTIC: VISA IMAGES	78
21	ERROR TRADEOFF CHARACTERISTIC: VISA IMAGES	79
22	ERROR TRADEOFF CHARACTERISTIC: VISA IMAGES	80
23	ERROR TRADEOFF CHARACTERISTIC: VISA IMAGES	81
24	ERROR TRADEOFF CHARACTERISTIC: VISA IMAGES	82
25	ERROR TRADEOFF CHARACTERISTIC: VISA IMAGES	83
26	ERROR TRADEOFF CHARACTERISTIC: VISA IMAGES	84
27	ERROR TRADEOFF CHARACTERISTIC: VISA IMAGES	85
28	ERROR TRADEOFF CHARACTERISTIC: VISA IMAGES	86
29	ERROR TRADEOFF CHARACTERISTIC: VISA IMAGES	87
30	ERROR TRADEOFF CHARACTERISTIC: VISA IMAGES	88
31	ERROR TRADEOFF CHARACTERISTIC: VISA IMAGES	89
32	ERROR TRADEOFF CHARACTERISTIC: VISA IMAGES	90
33	ERROR TRADEOFF CHARACTERISTIC: VISA IMAGES	91
34	ERROR TRADEOFF CHARACTERISTIC: VISA IMAGES	92
35	ERROR TRADEOFF CHARACTERISTIC: VISA IMAGES	93
36	ERROR TRADEOFF CHARACTERISTIC: VISA IMAGES	94
37	ERROR TRADEOFF CHARACTERISTIC: VISA IMAGES	95

38	ERROR TRADEOFF CHARACTERISTIC: VISA IMAGES	96
39	ERROR TRADEOFF CHARACTERISTIC: VISA IMAGES	97
40	ERROR TRADEOFF CHARACTERISTIC: VISA IMAGES	98
41	ERROR TRADEOFF CHARACTERISTIC: VISA IMAGES	99
42	ERROR TRADEOFF CHARACTERISTIC: VISA IMAGES	100
43	ERROR TRADEOFF CHARACTERISTIC: VISA IMAGES	101
44	ERROR TRADEOFF CHARACTERISTIC: VISA IMAGES	102
45	ERROR TRADEOFF CHARACTERISTIC: VISA IMAGES	103
46	ERROR TRADEOFF CHARACTERISTIC: VISA IMAGES	104
47	ERROR TRADEOFF CHARACTERISTIC: VISA IMAGES	105
48	ERROR TRADEOFF CHARACTERISTIC: VISA IMAGES	106
49	ERROR TRADEOFF CHARACTERISTIC: VISA IMAGES	107
50	ERROR TRADEOFF CHARACTERISTIC: VISA IMAGES	108
51	ERROR TRADEOFF CHARACTERISTIC: VISA IMAGES	109
52	ERROR TRADEOFF CHARACTERISTIC: VISA IMAGES	110
53	ERROR TRADEOFF CHARACTERISTIC: VISA IMAGES	111
54	ERROR TRADEOFF CHARACTERISTIC: VISA IMAGES	112
55	ERROR TRADEOFF CHARACTERISTIC: VISA IMAGES	113
56	ERROR TRADEOFF CHARACTERISTIC: VISA IMAGES	114
57	ERROR TRADEOFF CHARACTERISTIC: VISA IMAGES	115
58	ERROR TRADEOFF CHARACTERISTIC: VISA IMAGES	116
59	ERROR TRADEOFF CHARACTERISTIC: VISA IMAGES	117
60	ERROR TRADEOFF CHARACTERISTIC: MUGSHOT IMAGES	118
61	ERROR TRADEOFF CHARACTERISTIC: MUGSHOT IMAGES	119
62	ERROR TRADEOFF CHARACTERISTIC: MUGSHOT IMAGES	120
63	ERROR TRADEOFF CHARACTERISTIC: MUGSHOT IMAGES	121
64	ERROR TRADEOFF CHARACTERISTIC: MUGSHOT IMAGES	122
65	ERROR TRADEOFF CHARACTERISTIC: MUGSHOT IMAGES	123
66	ERROR TRADEOFF CHARACTERISTIC: MUGSHOT IMAGES	124
67	ERROR TRADEOFF CHARACTERISTIC: MUGSHOT IMAGES	125
68	ERROR TRADEOFF CHARACTERISTIC: MUGSHOT IMAGES	126
69	ERROR TRADEOFF CHARACTERISTIC: MUGSHOT IMAGES	127
70	ERROR TRADEOFF CHARACTERISTIC: MUGSHOT IMAGES	128
71	ERROR TRADEOFF CHARACTERISTIC: MUGSHOT IMAGES	129
72	ERROR TRADEOFF CHARACTERISTIC: MUGSHOT IMAGES	130
73	ERROR TRADEOFF CHARACTERISTIC: MUGSHOT IMAGES	131
74	ERROR TRADEOFF CHARACTERISTIC: MUGSHOT IMAGES	132
75	ERROR TRADEOFF CHARACTERISTIC: MUGSHOT IMAGES	133
76	ERROR TRADEOFF CHARACTERISTIC: MUGSHOT IMAGES	134
77	ERROR TRADEOFF CHARACTERISTIC: MUGSHOT IMAGES	135
78	ERROR TRADEOFF CHARACTERISTIC: MUGSHOT IMAGES	136
79	ERROR TRADEOFF CHARACTERISTIC: MUGSHOT IMAGES	137
80	ERROR TRADEOFF CHARACTERISTIC: WILD IMAGES	138
81	ERROR TRADEOFF CHARACTERISTIC: WILD IMAGES	139
82	ERROR TRADEOFF CHARACTERISTIC: WILD IMAGES	140
83	ERROR TRADEOFF CHARACTERISTIC: WILD IMAGES	141
84	ERROR TRADEOFF CHARACTERISTIC: WILD IMAGES	142
85	ERROR TRADEOFF CHARACTERISTIC: WILD IMAGES	143
86	ERROR TRADEOFF CHARACTERISTIC: WILD IMAGES	144
87	ERROR TRADEOFF CHARACTERISTIC: WILD IMAGES	145
88	ERROR TRADEOFF CHARACTERISTIC: WILD IMAGES	146
89	ERROR TRADEOFF CHARACTERISTIC: WILD IMAGES	147
90	ERROR TRADEOFF CHARACTERISTIC: WILD IMAGES	148
91	ERROR TRADEOFF CHARACTERISTIC: WILD IMAGES	149
92	ERROR TRADEOFF CHARACTERISTIC: WILD IMAGES	150
93	ERROR TRADEOFF CHARACTERISTIC: WILD IMAGES	151

94	ERROR TRADEOFF CHARACTERISTIC: WILD IMAGES	152
95	ERROR TRADEOFF CHARACTERISTIC: WILD IMAGES	153
96	ERROR TRADEOFF CHARACTERISTIC: WILD IMAGES	154
97	FALSE MATCH RATES WITHIN AND ACROSS DEMOGRAPHIC GROUPS	155
98	FALSE MATCH RATES WITHIN AND ACROSS DEMOGRAPHIC GROUPS	156
99	FALSE MATCH RATES WITHIN AND ACROSS DEMOGRAPHIC GROUPS	157
100	FALSE MATCH RATES WITHIN AND ACROSS DEMOGRAPHIC GROUPS	158
101	FALSE MATCH RATES WITHIN AND ACROSS DEMOGRAPHIC GROUPS	159
102	FALSE MATCH RATES WITHIN AND ACROSS DEMOGRAPHIC GROUPS	160
103	FALSE MATCH RATES WITHIN AND ACROSS DEMOGRAPHIC GROUPS	161
104	FALSE MATCH RATES WITHIN AND ACROSS DEMOGRAPHIC GROUPS	162
105	FALSE MATCH RATES WITHIN AND ACROSS DEMOGRAPHIC GROUPS	163
106	FALSE MATCH RATES WITHIN AND ACROSS DEMOGRAPHIC GROUPS	164
107	FALSE MATCH RATES WITHIN AND ACROSS DEMOGRAPHIC GROUPS	165
108	FALSE MATCH RATES WITHIN AND ACROSS DEMOGRAPHIC GROUPS	166
109	FALSE MATCH RATES WITHIN AND ACROSS DEMOGRAPHIC GROUPS	167
110	FALSE MATCH RATES WITHIN AND ACROSS DEMOGRAPHIC GROUPS	168
111	FALSE MATCH RATES WITHIN AND ACROSS DEMOGRAPHIC GROUPS	169
112	FALSE MATCH RATES WITHIN AND ACROSS DEMOGRAPHIC GROUPS	170
113	FALSE MATCH RATES WITHIN AND ACROSS DEMOGRAPHIC GROUPS	171
114	FALSE MATCH RATES WITHIN AND ACROSS DEMOGRAPHIC GROUPS	172
115	FALSE MATCH RATES WITHIN AND ACROSS DEMOGRAPHIC GROUPS	173
116	FALSE MATCH RATES WITHIN AND ACROSS DEMOGRAPHIC GROUPS	174
117	SEX AND RACE EFFECTS: MUGSHOT IMAGES	175
118	SEX AND RACE EFFECTS: MUGSHOT IMAGES	176
119	SEX AND RACE EFFECTS: MUGSHOT IMAGES	177
120	SEX AND RACE EFFECTS: MUGSHOT IMAGES	178
121	SEX AND RACE EFFECTS: MUGSHOT IMAGES	179
122	SEX AND RACE EFFECTS: MUGSHOT IMAGES	180
123	SEX AND RACE EFFECTS: MUGSHOT IMAGES	181
124	SEX AND RACE EFFECTS: MUGSHOT IMAGES	182
125	SEX AND RACE EFFECTS: MUGSHOT IMAGES	183
126	SEX AND RACE EFFECTS: MUGSHOT IMAGES	184
127	SEX AND RACE EFFECTS: MUGSHOT IMAGES	185
128	SEX AND RACE EFFECTS: MUGSHOT IMAGES	186
129	SEX AND RACE EFFECTS: MUGSHOT IMAGES	187
130	SEX AND RACE EFFECTS: MUGSHOT IMAGES	188
131	SEX AND RACE EFFECTS: MUGSHOT IMAGES	189
132	SEX AND RACE EFFECTS: MUGSHOT IMAGES	190
133	SEX AND RACE EFFECTS: MUGSHOT IMAGES	191
134	SEX AND RACE EFFECTS: MUGSHOT IMAGES	192
135	SEX AND RACE EFFECTS: MUGSHOT IMAGES	193
136	SEX AND RACE EFFECTS: MUGSHOT IMAGES	194
137	SEX EFFECTS: VISA IMAGES	195
138	SEX EFFECTS: VISA IMAGES	196
139	SEX EFFECTS: VISA IMAGES	197
140	SEX EFFECTS: VISA IMAGES	198
141	SEX EFFECTS: VISA IMAGES	199
142	SEX EFFECTS: VISA IMAGES	200
143	SEX EFFECTS: VISA IMAGES	201
144	SEX EFFECTS: VISA IMAGES	202
145	SEX EFFECTS: VISA IMAGES	203
146	SEX EFFECTS: VISA IMAGES	204
147	SEX EFFECTS: VISA IMAGES	205
148	SEX EFFECTS: VISA IMAGES	206
149	SEX EFFECTS: VISA IMAGES	207
150	SEX EFFECTS: VISA IMAGES	208

151	SEX EFFECTS: VISA IMAGES	209
152	SEX EFFECTS: VISA IMAGES	210
153	SEX EFFECTS: VISA IMAGES	211
154	SEX EFFECTS: VISA IMAGES	212
155	SEX EFFECTS: VISA IMAGES	213
156	SEX EFFECTS: VISA IMAGES	214
157	SEX EFFECTS: VISA IMAGES	215
158	SEX EFFECTS: VISA IMAGES	216
159	SEX EFFECTS: VISA IMAGES	217
160	SEX EFFECTS: VISA IMAGES	218
161	SEX EFFECTS: VISA IMAGES	219
162	SEX EFFECTS: VISA IMAGES	220
163	SEX EFFECTS: VISA IMAGES	221
164	SEX EFFECTS: VISA IMAGES	222
165	SEX EFFECTS: VISA IMAGES	223
166	SEX EFFECTS: VISA IMAGES	224
167	SEX EFFECTS: VISA IMAGES	225
168	SEX EFFECTS: VISA IMAGES	226
169	SEX EFFECTS: VISA IMAGES	227
170	FALSE MATCH RATE CALIBRATION: MUGSHOT IMAGES	228
171	FALSE MATCH RATE CALIBRATION: MUGSHOT IMAGES	229
172	FALSE MATCH RATE CALIBRATION: MUGSHOT IMAGES	230
173	FALSE MATCH RATE CALIBRATION: MUGSHOT IMAGES	231
174	FALSE MATCH RATE CALIBRATION: MUGSHOT IMAGES	232
175	FALSE MATCH RATE CALIBRATION: MUGSHOT IMAGES	233
176	FALSE MATCH RATE CALIBRATION: MUGSHOT IMAGES	234
177	FALSE MATCH RATE CALIBRATION: MUGSHOT IMAGES	235
178	FALSE MATCH RATE CALIBRATION: MUGSHOT IMAGES	236
179	FALSE MATCH RATE CALIBRATION: MUGSHOT IMAGES	237
180	FALSE MATCH RATE CALIBRATION: MUGSHOT IMAGES	238
181	FALSE MATCH RATE CALIBRATION: MUGSHOT IMAGES	239
182	FALSE MATCH RATE CALIBRATION: MUGSHOT IMAGES	240
183	FALSE MATCH RATE CALIBRATION: MUGSHOT IMAGES	241
184	FALSE MATCH RATE CALIBRATION: MUGSHOT IMAGES	242
185	FALSE MATCH RATE CALIBRATION: MUGSHOT IMAGES	243
186	FALSE MATCH RATE CALIBRATION: MUGSHOT IMAGES	244
187	FALSE MATCH RATE CALIBRATION: MUGSHOT IMAGES	245
188	FALSE MATCH RATE CALIBRATION: MUGSHOT IMAGES	246
189	FALSE MATCH RATE CALIBRATION: MUGSHOT IMAGES	247
190	FALSE MATCH RATE CALIBRATION: VISA IMAGES	248
191	FALSE MATCH RATE CALIBRATION: VISA IMAGES	249
192	FALSE MATCH RATE CALIBRATION: VISA IMAGES	250
193	FALSE MATCH RATE CALIBRATION: VISA IMAGES	251
194	FALSE MATCH RATE CALIBRATION: VISA IMAGES	252
195	FALSE MATCH RATE CALIBRATION: VISA IMAGES	253
196	FALSE MATCH RATE CALIBRATION: VISA IMAGES	254
197	FALSE MATCH RATE CALIBRATION: VISA IMAGES	255
198	FALSE MATCH RATE CALIBRATION: VISA IMAGES	256
199	FALSE MATCH RATE CALIBRATION: VISA IMAGES	257
200	FALSE MATCH RATE CALIBRATION: VISA IMAGES	258
201	FALSE MATCH RATE CALIBRATION: VISA IMAGES	259
202	FALSE MATCH RATE CALIBRATION: VISA IMAGES	260
203	FALSE MATCH RATE CALIBRATION: VISA IMAGES	261
204	FALSE MATCH RATE CALIBRATION: VISA IMAGES	262
205	FALSE MATCH RATE CALIBRATION: VISA IMAGES	263
206	FALSE MATCH RATE CALIBRATION: VISA IMAGES	264
207	FALSE MATCH RATE CALIBRATION: VISA IMAGES	265

208	FALSE MATCH RATE CALIBRATION: VISA IMAGES	266
209	FALSE MATCH RATE CALIBRATION: VISA IMAGES	267
210	FALSE MATCH RATE CALIBRATION: VISA IMAGES	268
211	FALSE MATCH RATE CALIBRATION: VISA IMAGES	269
212	FALSE MATCH RATE CALIBRATION: VISA IMAGES	270
213	FALSE MATCH RATE CALIBRATION: VISA IMAGES	271
214	FALSE MATCH RATE CALIBRATION: VISA IMAGES	272
215	FALSE MATCH RATE CALIBRATION: VISA IMAGES	273
216	FALSE MATCH RATE CALIBRATION: VISA IMAGES	274
217	FALSE MATCH RATE CALIBRATION: VISA IMAGES	275
218	FALSE MATCH RATE CALIBRATION: VISA IMAGES	276
219	FALSE MATCH RATE CALIBRATION: VISA IMAGES	277
220	FALSE MATCH RATE CALIBRATION: VISA IMAGES	278
221	FALSE MATCH RATE CALIBRATION: VISA IMAGES	279
222	FALSE MATCH RATE CALIBRATION: VISA IMAGES	280
223	FALSE MATCH RATE CALIBRATION: VISA IMAGES	281
224	FALSE MATCH RATE CALIBRATION: VISA IMAGES	282
225	FALSE MATCH RATE CALIBRATION: VISA IMAGES	283
226	FALSE MATCH RATE CALIBRATION: VISA IMAGES	284
227	FALSE MATCH RATE CALIBRATION: VISA IMAGES	285
228	FALSE MATCH RATE CALIBRATION: VISA IMAGES	286
229	FALSE MATCH RATE CALIBRATION: VISA IMAGES	287
230	EFFECT OF COUNTRY OF BIRTH ON FNMR	289
231	EFFECT OF COUNTRY OF BIRTH ON FNMR	290
232	EFFECT OF COUNTRY OF BIRTH ON FNMR	291
233	EFFECT OF COUNTRY OF BIRTH ON FNMR	292
234	EFFECT OF COUNTRY OF BIRTH ON FNMR	293
235	EFFECT OF COUNTRY OF BIRTH ON FNMR	294
236	EFFECT OF COUNTRY OF BIRTH ON FNMR	295
237	EFFECT OF COUNTRY OF BIRTH ON FNMR	296
238	EFFECT OF COUNTRY OF BIRTH ON FNMR	297
239	EFFECT OF COUNTRY OF BIRTH ON FNMR	298
240	EFFECT OF COUNTRY OF BIRTH ON FNMR	299
241	EFFECT OF COUNTRY OF BIRTH ON FNMR	300
242	EFFECT OF COUNTRY OF BIRTH ON FNMR	301
243	EFFECT OF COUNTRY OF BIRTH ON FNMR	302
244	EFFECT OF COUNTRY OF BIRTH ON FNMR	303
245	EFFECT OF COUNTRY OF BIRTH ON FNMR	304
246	EFFECT OF COUNTRY OF BIRTH ON FNMR	305
247	EFFECT OF COUNTRY OF BIRTH ON FNMR	306
248	EFFECT OF COUNTRY OF BIRTH ON FNMR	307
249	EFFECT OF COUNTRY OF BIRTH ON FNMR	308
250	EFFECT OF COUNTRY OF BIRTH ON FNMR	309
251	EFFECT OF COUNTRY OF BIRTH ON FNMR	310
252	EFFECT OF COUNTRY OF BIRTH ON FNMR	311
253	EFFECT OF COUNTRY OF BIRTH ON FNMR	312
254	EFFECT OF COUNTRY OF BIRTH ON FNMR	313
255	EFFECT OF COUNTRY OF BIRTH ON FNMR	314
256	EFFECT OF COUNTRY OF BIRTH ON FNMR	315
257	EFFECT OF COUNTRY OF BIRTH ON FNMR	316
258	EFFECT OF COUNTRY OF BIRTH ON FNMR	317
259	EFFECT OF COUNTRY OF BIRTH ON FNMR	318
260	EFFECT OF COUNTRY OF BIRTH ON FNMR	319
261	EFFECT OF COUNTRY OF BIRTH ON FNMR	320
262	EFFECT OF COUNTRY OF BIRTH ON FNMR	321
263	ERROR TRADEOFF CHARACTERISTIC: MUGSHOT IMAGES	323
264	ERROR TRADEOFF CHARACTERISTIC: MUGSHOT IMAGES	324

265	ERROR TRADEOFF CHARACTERISTIC: MUGSHOT IMAGES	325
266	ERROR TRADEOFF CHARACTERISTIC: MUGSHOT IMAGES	326
267	ERROR TRADEOFF CHARACTERISTIC: MUGSHOT IMAGES	327
268	ERROR TRADEOFF CHARACTERISTIC: MUGSHOT IMAGES	328
269	ERROR TRADEOFF CHARACTERISTIC: MUGSHOT IMAGES	329
270	ERROR TRADEOFF CHARACTERISTIC: MUGSHOT IMAGES	330
271	ERROR TRADEOFF CHARACTERISTIC: MUGSHOT IMAGES	331
272	ERROR TRADEOFF CHARACTERISTIC: MUGSHOT IMAGES	332
273	ERROR TRADEOFF CHARACTERISTIC: MUGSHOT IMAGES	333
274	ERROR TRADEOFF CHARACTERISTIC: MUGSHOT IMAGES	334
275	ERROR TRADEOFF CHARACTERISTIC: MUGSHOT IMAGES	335
276	ERROR TRADEOFF CHARACTERISTIC: MUGSHOT IMAGES	336
277	ERROR TRADEOFF CHARACTERISTIC: MUGSHOT IMAGES	337
278	ERROR TRADEOFF CHARACTERISTIC: MUGSHOT IMAGES	338
279	ERROR TRADEOFF CHARACTERISTIC: MUGSHOT IMAGES	339
280	ERROR TRADEOFF CHARACTERISTIC: MUGSHOT IMAGES	340
281	ERROR TRADEOFF CHARACTERISTIC: MUGSHOT IMAGES	341
282	ERROR TRADEOFF CHARACTERISTIC: MUGSHOT IMAGES	342
283	ERROR TRADEOFF CHARACTERISTIC: MUGSHOT IMAGES	343
284	ERROR TRADEOFF CHARACTERISTIC: MUGSHOT IMAGES	344
285	ERROR TRADEOFF CHARACTERISTIC: MUGSHOT IMAGES	345
286	ERROR TRADEOFF CHARACTERISTIC: MUGSHOT IMAGES	346
287	EFFECT OF SUBJECT AGE ON FNMR	348
288	EFFECT OF SUBJECT AGE ON FNMR	349
289	EFFECT OF SUBJECT AGE ON FNMR	350
290	EFFECT OF SUBJECT AGE ON FNMR	351
291	EFFECT OF SUBJECT AGE ON FNMR	352
292	EFFECT OF SUBJECT AGE ON FNMR	353
293	EFFECT OF SUBJECT AGE ON FNMR	354
294	EFFECT OF SUBJECT AGE ON FNMR	355
295	EFFECT OF SUBJECT AGE ON FNMR	356
296	EFFECT OF SUBJECT AGE ON FNMR	357
297	EFFECT OF SUBJECT AGE ON FNMR	358
298	EFFECT OF SUBJECT AGE ON FNMR	359
299	EFFECT OF SUBJECT AGE ON FNMR	360
300	EFFECT OF SUBJECT AGE ON FNMR	361
301	EFFECT OF SUBJECT AGE ON FNMR	362
302	EFFECT OF SUBJECT AGE ON FNMR	363
303	EFFECT OF SUBJECT AGE ON FNMR	364
304	EFFECT OF SUBJECT AGE ON FNMR	365
305	EFFECT OF SUBJECT AGE ON FNMR	366
306	EFFECT OF SUBJECT AGE ON FNMR	367
307	EFFECT OF SUBJECT AGE ON FNMR	368
308	EFFECT OF SUBJECT AGE ON FNMR	369
309	EFFECT OF SUBJECT AGE ON FNMR	370
310	EFFECT OF SUBJECT AGE ON FNMR	371
311	EFFECT OF SUBJECT AGE ON FNMR	372
312	EFFECT OF SUBJECT AGE ON FNMR	373
313	EFFECT OF SUBJECT AGE ON FNMR	374
314	EFFECT OF SUBJECT AGE ON FNMR	375
315	EFFECT OF SUBJECT AGE ON FNMR	376
316	EFFECT OF SUBJECT AGE ON FNMR	377
317	EFFECT OF SUBJECT AGE ON FNMR	378

318	EFFECT OF SUBJECT AGE ON FNMR	379
319	EFFECT OF SUBJECT AGE ON FNMR	380
320	WORST CASE REGIONAL EFFECT FNMR	383
321	IMPOSTOR DISTRIBUTION SHIFTS FOR SELECT COUNTRY PAIRS	385

	Location	Developer Name	Short Name	Seq. Num.	Validation Date
1	NL	20Face	20face-000	000	2021-04-12
2	NL	20Face	20face-001	001	2021-09-29
3	US	3Divi	3divi-006	006	2021-04-14
4	US	3Divi	3divi-007	007	2021-09-27
5	TH	ACI Software	acisw-003	003	2020-08-03
6	TH	ACI Software	acisw-007	007	2021-11-15
7	SG	ADVANCE.AI	advance-002	002	2019-12-19
8	SG	ADVANCE.AI	advance-003	003	2021-08-05
9	US	AFIS and Biometrics Consulting	afisbiometrics-000	000	2022-01-27
10	TW	ASUSTek Computer Inc	asusaics-000	000	2019-10-24
11	TW	ASUSTek Computer Inc	asusaics-001	001	2020-02-25
12	CN	AYF Technology	ayftech-001	001	2020-07-06
13	TW	Ability Enterprise - Andro Video	androvideo-000	000	2021-01-25
14	TW	Acer Incorporated	acer-001	001	2020-06-30
15	TW	Acer Incorporated	acer-002	002	2021-11-10
16	SG	Adera Global PTE	adera-002	002	2021-02-16
17	SG	Adera Global PTE	adera-003	003	2021-07-12
18	TH	Ai First	aifirst-001	001	2019-11-21
19	TW	AiUnion Technology	aiunionface-000	000	2019-10-22
20	TH	Aigen	aigen-001	001	2020-10-06
21	TH	Aigen	aigen-002	002	2021-03-15
22	KR	Ajou University	ajou-001	001	2021-03-08
23	ID	Akurat Satu Indonesia	ptakuratsatu-000	000	2020-09-11
24	KR	Alchera Inc	alchera-002	002	2021-03-05
25	KR	Alchera Inc	alchera-003	003	2021-07-13
26	ID	Alfabeta	alfabeta-001	001	2021-12-02
27	ES	Alice Biometrics	alice-000	000	2021-06-15
28	RU	Alivia / Innovation Sys	isystems-001	001	2018-06-12
29	RU	Alivia / Innovation Sys	isystems-002	002	2018-10-18
30	IN	AllGoVision	allgovision-000	000	2019-03-01
31	CN	AlphaSSTG	alphaface-001	001	2019-09-03
32	CN	AlphaSSTG	alphaface-002	002	2020-02-20
33	GB	Amplified Group	amplifiedgroup-001	001	2019-03-01
34	CN	Anke Investments	anke-004	004	2019-06-27
35	CN	Anke Investments	anke-005	005	2019-11-21
36	BR	Antheus Technologia	antheus-000	000	2019-12-05
37	BR	Antheus Technologia	antheus-001	001	2020-06-25
38	GB	AnyVision	anyvision-004	004	2018-06-15
39	GB	AnyVision	anyvision-005	005	2021-02-03
40	US	Armatura LLC	armatura-001	001	2022-01-04
41	CN	AuthenMetric	authenmetric-003	003	2021-08-09
42	CN	AuthenMetric	authenmetric-004	004	2022-01-03
43	US	Aware	aware-005	005	2020-02-27
44	US	Aware	aware-006	006	2021-07-03
45	IN	Awidit Systems	awiros-001	001	2019-09-23
46	IN	Awidit Systems	awiros-002	002	2020-10-28
47	JP	Ayonix	ayonix-000	000	2017-06-22
48	CN	BOE Technology Group	boetech-001	001	2021-06-22
49	CN	BOE Technology Group	boetech-002	002	2021-12-21
50	ES	Bee the Data	beethedata-000	000	2021-07-26
51	CN	Beihang University-ERCACAT	ercacat-001	001	2020-07-06
52	CN	Beijing Alleyes Technology	alleyes-000	000	2020-03-09
53	CN	Beijing DeepSense Technologies	deepsense-000	000	2021-03-19
54	CN	Beijing Hisign Technology	hisign-001	001	2021-09-24
55	CN	Beijing Mendaxia Technology	mendaxiatech-000	000	2021-09-15
56	CN	Beijing Vion Technology Inc	vion-000	000	2018-10-19
57	KZ	Beyne.AI	beyneai-000	000	2022-01-03
58	CH	BioID Technologies SA	bioidechswiss-001	001	2020-08-28
59	CH	BioID Technologies SA	bioidechswiss-002	002	2021-02-17
60	IN	Biocube Matrixs	biocube-001	001	2021-09-08
61	UK	BitCenter UK	farfaces-001	001	2021-04-09
62	CN	Bitmain	bm-001	001	2018-10-17
63	CN	Bresee Technology	bresee-001	001	2020-12-30
64	CN	Bresee Technology	bresee-002	002	2021-06-30
65	CN	CSA IntelliCloud Technology	intellicloudai-001	001	2019-08-13
66	CN	CSA IntelliCloud Technology	intellicloudai-002	002	2020-12-17
67	TW	CTBC Bank	ctbcbank-000	000	2019-06-28
68	TW	CTBC Bank	ctbcbank-001	001	2019-10-28
69	KR	CUDO Communication	cudocommunication-001	001	2021-10-20
70	US	Camvi Technologies	camvi-002	002	2018-10-19

Table 1: Summary of participant information included in this report.

	Location	Developer Name	Short Name	Seq. Num.	Validation Date
71	US	Camvi Technologies	camvi-004	004	2019-07-12
72	CN	Canon Inc	canon-002	002	2020-12-29
73	JP	Canon Inc	canon-003	003	2021-09-15
74	CN	China Electronics Import-Export Corp	ceiec-003	003	2020-01-06
75	CN	China Electronics Import-Export Corp	ceiec-004	004	2021-01-18
76	CN	China University of Petroleum	upc-001	001	2019-06-05
77	CN	Chinese University of Hong Kong	cuhkee-001	001	2020-03-18
78	KR	Chosun University	chosun-001	001	2020-07-01
79	KR	Chosun University	chosun-002	002	2020-11-25
80	TW	Chunghwa Telecom	chtface-003	003	2020-06-24
81	TW	Chunghwa Telecom	chtface-004	004	2021-10-08
82	US	Clearview AI Inc	clearviewai-000	000	2021-09-22
83	CN	Closeli Inc	closeli-001	001	2021-07-15
84	US	CloudSmart Consulting LLC	csc-002	002	2021-03-24
85	US	CloudSmart Consulting LLC	csc-003	003	2021-08-26
86	TW	Cloudmatrix	cloudmatrix-000	000	2021-10-22
87	CN	Cloudwalk - Hengrui AI Technology	cloudwalk-hr-003	003	2020-09-25
88	CN	Cloudwalk - Hengrui AI Technology	cloudwalk-hr-004	004	2021-02-10
89	CN	Cloudwalk - Moontime Smart Technology	cloudwalk-mt-003	003	2020-12-22
90	CN	Cloudwalk - Moontime Smart Technology	cloudwalk-mt-004	004	2021-11-09
91	IN	Code Everest Pvt	facex-001	001	2021-03-08
92	IN	Code Everest Pvt	facex-002	002	2021-08-24
93	DE	Cognitec Systems GmbH	cognitec-003	003	2021-07-30
94	DE	Cognitec Systems GmbH	cognitec-004	004	2022-02-10
95	TW	Coretech Knowledge Inc	coretech-000	000	2021-07-12
96	IL	Corsight	corsight-001	001	2021-03-11
97	IL	Corsight	corsight-002	002	2021-09-01
98	IL	Cortica	cor-001	001	2020-09-24
99	KR	Cubox	cubox-001	001	2020-12-07
100	KR	Cubox	cubox-002	002	2021-08-24
101	JP	Cybercore	cybercore-000	000	2020-08-26
102	JP	Cybercore	cybercore-001	001	2021-12-15
103	US	Cyberextruder	cyberextruder-001	001	2017-08-02
104	US	Cyberextruder	cyberextruder-002	002	2018-01-30
105	TW	Cyberlink Corp	cyberlink-007	007	2021-07-16
106	TW	Cyberlink Corp	cyberlink-008	008	2022-01-07
107	CN	DSK	dsk-000	000	2019-06-28
108	CN	Dahua Technology	dahua-006	006	2020-12-30
109	CN	Dahua Technology	dahua-007	007	2021-12-20
110	IE	Daon	daon-000	000	2021-11-03
111	US	Decatur Industries Inc	decatur-000	000	2020-08-18
112	US	Decatur Industries Inc	decatur-001	001	2021-09-27
113	CN	Deepglint	deepglint-003	003	2021-03-03
114	CN	Deepglint	deepglint-004	004	2021-09-17
115	FR	Depsense	dps-000	000	2021-07-16
116	DE	Dermalog	dermalog-008	008	2021-03-25
117	DE	Dermalog	dermalog-009	009	2021-10-06
118	CN	DiDi ChuXing Technology	didiglobalface-001	001	2019-10-23
119	IN	Digidata	digidata-000	000	2022-01-27
120	GB	Digital Barriers	digitalbarriers-002	002	2019-03-01
121	TR	Ekin Smart City Technologies	ekin-002	002	2021-05-04
122	RU	Enface	enface-000	000	2021-04-09
123	RU	Enface	enface-001	001	2021-12-17
124	CH	Euronovate SA	euronovate-001	001	2021-11-15
125	RU	Expasoft LLC	expasoft-001	001	2020-09-03
126	RU	Expasoft LLC	expasoft-002	002	2021-07-26
127	DE	FaceOnLive Inc	faceonlive-001	001	2021-11-23
128	GB	FaceSoft	facesoft-000	000	2019-07-10
129	KR	FaceTag Co	facetag-000	000	2021-03-22
130	KR	FaceTag Co	facetag-002	002	2022-01-06
131	TW	FarBar Inc	f8-001	001	2019-07-11
132	CN	Fiberhome Telecommunication Technologies	fiberhome-nanjing-003	003	2021-03-12
133	CN	Fiberhome Telecommunication Technologies	fiberhome-nanjing-004	004	2021-09-14
134	UK	Fincore Ltd	fincore-000	000	2021-06-07
135	CN	Fujitsu Research and Development Center	fujitsulab-002	002	2021-02-24
136	CN	Fujitsu Research and Development Center	fujitsulab-003	003	2021-07-12
137	US	Gemalto Cogent	cogent-005	005	2020-12-29
138	US	Gemalto Cogent	cogent-006	006	2021-07-28
139	TW	GeoVision Inc	geo-002	002	2021-04-01
140	TW	GeoVision Inc	geo-004	004	2022-02-10

Table 2: Summary of participant information included in this report.

	Location	Developer Name	Short Name	Seq. Num.	Validation Date
141	JP	Glory	glory-003	003	2021-01-15
142	JP	Glory	glory-004	004	2022-02-08
143	TW	Gorilla Technology	gorilla-007	007	2021-06-28
144	TW	Gorilla Technology	gorilla-008	008	2021-11-08
145	US	Graymatics	graymatics-001	001	2022-01-13
146	US	Griaule	griaule-000	000	2021-08-20
147	CN	Guangzhou Pixel Solutions	pixelall-006	006	2021-06-17
148	CN	Guangzhou Pixel Solutions	pixelall-007	007	2021-12-01
149	CN	Hangzhuo Allu Network Information Technology	hzailu-001	001	2022-01-27
150	ES	Herta Security	hertasecurity-000	000	2021-01-05
151	ES	Herta Security	hertasecurity-001	001	2022-01-18
152	CN	Hikvision Research Institute	hik-001	001	2019-03-01
153	IN	HyperVerge Inc	hyperverge-001	001	2020-12-13
154	IN	HyperVerge Inc	hyperverge-002	002	2021-05-27
155	AU	ICM Airport Technics	icm-002	002	2020-11-13
156	AU	ICM Airport Technics	icm-003	003	2021-09-06
157	FR	ID3 Technology	id3-006	006	2020-12-17
158	FR	ID3 Technology	id3-008	008	2021-11-10
159	RU	ITMO University	itmo-007	007	2020-01-06
160	RU	ITMO University	itmo-008	008	2021-11-19
161	RU	IVA Cognitive	ivacognitive-001	001	2021-01-29
162	FR	Idemia	idemia-007	007	2020-12-04
163	FR	Idemia	idemia-008	008	2021-07-07
164	US	Imageware Systems	iws-000	000	2020-08-12
165	AU	Imagus Technology Pty	imagus-002	002	2020-12-31
166	AU	Imagus Technology Pty	imagus-004	004	2021-09-20
167	GB	Imperial College London	imperial-000	000	2019-03-01
168	GB	Imperial College London	imperial-002	002	2019-08-28
169	US	Incode Technologies Inc	incode-009	009	2021-06-22
170	US	Incode Technologies Inc	incode-010	010	2021-10-22
171	IN	Innef Labs	innefulabs-000	000	2020-09-04
172	GB	Innovative Technology	innovativetechnologyltd-001	001	2019-10-22
173	GB	Innovative Technology	innovativetechnologyltd-002	002	2020-02-26
174	SK	Innovatrics	innovatrics-007	007	2020-08-19
175	SK	Innovatrics	innovatrics-008	008	2021-12-15
176	CN	InsightFace AI	insightface-001	001	2021-09-27
177	CN	InsightFace AI	insighiface-002	002	2022-01-31
178	CN	Institute of Computing Technology	icthtc-000	000	2020-11-29
179	RU	Institute of Information Technologies	iit-002	002	2019-12-04
180	RU	Institute of Information Technologies	iit-003	003	2020-12-01
181	IS	Intel Research Group	intelresearch-004	004	2021-08-24
182	IS	Intel Research Group	intelresearch-005	005	2022-02-13
183	US	Intellivision	intellivision-001	001	2017-10-10
184	US	Intellivision	intellivision-002	002	2019-08-23
185	US	IrexAI	irex-000	000	2020-12-17
186	IL	Is It You	isityou-000	000	2017-06-26
187	KR	Kakao Enterprise	kakao-005	005	2021-03-09
188	KR	Kakao Enterprise	kakao-007	007	2022-01-12
189	KR	Kakao Pay Corp	kakaopay-001	001	2021-07-06
190	SG	Kedacom International Pte	kedacom-000	000	2019-06-03
191	US	Kneron Inc	kneron-003	003	2019-07-01
192	US	Kneron Inc	kneron-005	005	2020-02-21
193	US	KnowUTech LLC	knowutech-000	000	2022-02-13
194	KR	Kookmin University	kookmin-002	002	2021-03-05
195	CN	KuKe3D Technology	kuke3d-001	001	2021-10-28
196	IN	Lema Labs	lemalabs-001	001	2021-04-13
197	JP	Line Corporation	line-000	000	2021-03-31
198	JP	Line Corporation	line-001	001	2021-09-26
199	RU	Lomonosov Moscow State University	intsyssmu-001	001	2019-10-22
200	RU	Lomonosov Moscow State University	intsyssmu-002	002	2020-03-12
201	IN	Lookman Electroplast Industries	lookman-002	002	2018-06-13
202	IN	Lookman Electroplast Industries	lookman-004	004	2019-06-03
203	US	Luxand Inc	luxand-000	000	2019-11-07
204	RU	MVision	mvision-001	001	2019-11-12
205	IN	Mantra Softech India	mantra-000	000	2021-10-28
206	CN	Maxvision Technology	maxvision-000	000	2021-10-27
207	CN	Megvii/Face++	megvii-003	003	2021-03-08
208	CN	Megvii/Face++	megvii-004	004	2021-11-19
209	GB	MicroFocus	microfocus-001	001	2018-06-13
210	GB	MicroFocus	microfocus-002	002	2018-10-17

Table 3: Summary of participant information included in this report.

	Location	Developer Name	Short Name	Seq. Num.	Validation Date
211	CN	Minivision	minivision-000	000	2020-10-28
212	NO	Mobai	mobai-000	000	2020-08-26
213	NO	Mobai	mobai-001	001	2021-02-17
214	ES	Mobbeel Solutions	mobbl-001	001	2021-06-16
215	ES	Mobbeel Solutions	mobbl-002	002	2021-12-16
216	KR	Mobipin Technology	mobilpintech-000	000	2021-11-23
217	TH	Momentum Digital	sertis-000	000	2019-10-07
218	TH	Momentum Digital	sertis-002	002	2021-05-13
219	CN	MoreDian Technology	moreidian-000	000	2021-02-24
220	CN	Multi-Modality Intelligence	multimodality-000	000	2021-10-19
221	RU	N-Tech Lab	ntechlab-011	011	2021-09-13
222	RU	N-Tech Lab	ntechlab-012	012	2022-01-20
223	CA	NEO Systems	neosystems-002	002	2021-07-03
224	CA	NEO Systems	neosystems-003	003	2021-11-11
225	KR	NHN Corp	nhn-001	001	2021-03-15
226	KR	NHN Corp	nhn-002	002	2021-07-15
227	KR	NSENSE Corp	nsensecorp-002	002	2021-05-06
228	KR	NSENSE Corp	nsensecorp-003	003	2021-10-29
229	CN	Nanjing Kiwi Network Technology	kiwitech-000	000	2021-03-19
230	KR	Naver Corp	clova-000	000	2020-10-21
231	KR	Neosecu Co	openface-001	001	2021-06-15
232	TW	Netbridge Technology Incoporation	netbridgetech-001	001	2020-01-08
233	TW	Netbridge Technology Incoporation	netbridgetech-002	002	2020-08-11
234	LT	Neurotechnology	neurotechnology-012	012	2021-07-26
235	LT	Neurotechnology	neurotechnology-013	013	2022-01-07
236	ID	Nodeflux	nodeflux-002	002	2019-08-13
237	IN	NotionTag Technologies Private Limited	notiontag-001	001	2021-03-04
238	IN	NotionTag Technologies Private Limited	notiontag-002	002	2021-09-17
239	US	Omnigarde Ltd	omnigarde-001	001	2021-08-23
240	US	Omnigarde Ltd	omnigarde-002	002	2022-01-19
241	KR	One More Security	omsecurity-000	000	2021-12-15
242	RU	Oz Forensics LLC	oz-003	003	2021-08-09
243	RU	Oz Forensics LLC	oz-004	004	2021-12-13
244	CH	PXL Vision AG	pxl-001	001	2020-06-30
245	SG	Panasonic R+D Center Singapore	psl-008	008	2021-07-21
246	SG	Panasonic R+D Center Singapore	psl-009	009	2021-12-08
247	TR	Papilon Savunma	papsav1923-001	001	2021-03-10
248	TR	Papilon Savunma	papsav1923-002	002	2022-01-20
249	US	Paravision	paravision-008	008	2021-06-30
250	US	Paravision (EverAI)	paravision-010	010	2022-02-02
251	SG	Pensees Pte	pensees-001	001	2020-08-17
252	IN	Pyramid Cyber Security + Forensic (P)	pyramid-000	000	2019-11-04
253	TW	Qnap Security	qnap-000	000	2021-08-09
254	TW	Qnap Security	qnap-001	001	2021-12-09
255	CZ	Quantasoft	quantasoft-003	003	2021-04-19
256	US	Rank One Computing	rankone-011	011	2021-08-27
257	US	Rank One Computing	rankone-012	012	2021-12-27
258	US	Realnetworks Inc	realnetworks-005	005	2021-09-27
259	US	Realnetworks Inc	realnetworks-006	006	2022-02-09
260	US	Regula Forensics	regula-000	000	2021-04-13
261	US	Regula Forensics	regula-001	001	2021-12-14
262	CN	Remark Holdings	remarkai-001	001	2019-03-01
263	CN	Remark Holdings	remarkai-003	003	2021-06-22
264	SG	Rendip	rendip-000	000	2021-04-19
265	UK	Reveal Media Ltd	revealmedia-005	005	2021-09-24
266	UK	Reveal Media Ltd	revealmedia-006	006	2022-01-26
267	CN	Rokid Corporation	rokid-000	000	2019-08-01
268	CN	Rokid Corporation	rokid-001	001	2019-12-13
269	KR	SK Telecom	sktelecom-000	000	2021-07-09
270	KR	SQIsoft	sqiisoft-001	001	2021-07-27
271	KR	SQIsoft	sqiisoft-002	002	2021-11-03
272	DE	Saffe	saffe-001	001	2018-10-19
273	DE	Saffe	saffe-002	002	2019-03-01
274	KR	Samsung S1 Corp	s1-003	003	2021-08-24
275	KR	Samsung S1 Corp	s1-004	004	2022-01-04
276	KR	Samsung-SDS	samsungsds-000	000	2021-10-28
277	IN	Samtech InfoNet Limited	samtech-001	001	2019-10-15
278	RU	Satellite Innovation/Eocortex	eocortex-000	000	2020-08-26
279	IL	Scanovate	scanovate-002	002	2020-06-26
280	IL	Scanovate	scanovate-003	003	2021-11-15

Table 4: Summary of participant information included in this report.

	Location	Developer Name	Short Name	Seq. Num.	Validation Date
281	RO	Securif AI	securifai-003	003	2021-08-03
282	RO	Securif AI	securifai-004	004	2021-12-21
283	CN	Sensetime Group	sensetime-005	005	2021-05-24
284	CN	Sensetime Group	sensetime-006	006	2021-12-28
285	SG	Seventh Sense Artificial Intelligence	sevensense-000	000	2021-06-29
286	US	Shaman Software	shaman-000	000	2017-12-05
287	US	Shaman Software	shaman-001	001	2018-01-13
288	CN	Shanghai Jiao Tong University	sjtu-003	003	2020-11-02
289	CN	Shanghai Jiao Tong University	sjtu-004	004	2021-05-13
290	CN	Shanghai Ulucus Electronics Technology	uluface-002	002	2019-07-10
291	CN	Shanghai Ulucus Electronics Technology	uluface-003	003	2019-11-12
292	CN	Shanghai University - Shanghai Film Academy	shu-002	002	2019-12-10
293	CN	Shanghai University - Shanghai Film Academy	shu-003	003	2020-06-24
294	CN	Shanghai Yitu Technology	yitu-003	003	2019-03-01
295	CN	Shenzhen AiMall Tech	aimall-002	002	2020-03-12
296	CN	Shenzhen AiMall Tech	aimall-003	003	2020-08-12
297	CN	Shenzhen EI Networks	einetworks-000	000	2019-08-13
298	CN	Shenzhen Inst Adv Integrated Tech CAS	siat-002	002	2018-06-13
299	CN	Shenzhen Inst Adv Integrated Tech CAS	siat-005	005	2022-02-08
300	CN	Shenzhen Intellifusion Technologies	intellifusion-001	001	2019-08-22
301	CN	Shenzhen Intellifusion Technologies	intellifusion-002	002	2020-03-18
302	CN	Shenzhen University-Macau University of Science and Technology	sztu-000	000	2020-12-17
303	CN	Shenzhen University-Macau University of Science and Technology	sztu-001	001	2021-07-13
304	RU	Smart Engines	smartengines-000	000	2021-08-25
305	DE	Smilart	smilart-002	002	2018-02-06
306	DE	Smilart	smilart-003	003	2018-06-18
307	TR	Sodec App Inc	sodec-000	000	2021-06-02
308	IN	Staqua Technologies	staqua-000	000	2020-07-15
309	CN	Star Hybrid Limited	starhybrid-001	001	2019-06-19
310	CN	Su Zhou NaZhiTianDi intelligent technology	nazhiai-000	000	2020-06-25
311	IN	Sukshi Technology Innovation	sukshi-000	000	2022-02-13
312	KR	Suprema AI Inc	suprema-001	001	2021-09-23
313	KR	Suprema AI Inc	suprema-002	002	2022-02-11
314	KR	Suprema ID Inc	supremaid-001	001	2021-05-04
315	RU	Synesis	synesis-006	006	2019-10-10
316	RU	Synesis	synesis-007	007	2020-06-24
317	TW	Synology Inc	synology-000	000	2019-10-23
318	TW	Synology Inc	synology-002	002	2020-08-20
319	BR	T4iSB	t4isb-000	000	2022-01-28
320	CN	TUPU Technology	tuputech-000	000	2019-10-11
321	TW	Taiwan AI Labs	ailabs-001	001	2019-12-18
322	TW	Taiwan-Certificate Authority Incorporation	twface-000	000	2021-05-14
323	TW	Taiwan-Certificate Authority Incorporation	twface-001	001	2021-09-14
324	CH	Tech5 SA	tech5-004	004	2020-03-09
325	CH	Tech5 SA	tech5-005	005	2020-07-24
326	TR	Techsign	techsign-000	000	2021-08-25
327	CN	Tencent Deepsea Lab	deepsea-001	001	2019-06-03
328	RU	Tevian	tevian-007	007	2021-08-06
329	RU	Tevian	tevian-008	008	2021-12-06
330	US	TigerIT Americas LLC	tiger-005	005	2021-07-29
331	US	TigerIT Americas LLC	tiger-006	006	2021-12-13
332	RU	Tinkoff Bank	tinkoff-001	001	2021-05-13
333	CN	TongYi Transportation Technology	tongyi-005	005	2019-06-12
334	TW	Toppan ID Gate	toppanidgate-000	000	2021-09-28
335	JP	Toshiba	toshiba-004	004	2021-09-27
336	JP	Toshiba	toshiba-005	005	2022-02-09
337	JP	Tripleize	aize-001	001	2021-04-23
338	JP	Tripleize	aize-002	002	2021-10-08
339	US	Trueface.ai	trueface-002	002	2021-03-29
340	US	Trueface.ai	trueface-003	003	2021-09-30
341	CN	TuringTech.vip	turingtechvip-001	001	2022-02-03
342	CN	ULSee Inc	ulsee-001	001	2019-07-31
343	FR	Unissey	unissey-001	001	2021-11-29
344	PT	Universidade de Coimbra	visteam-002	002	2021-08-20
345	PT	Universidade de Coimbra	visteam-003	003	2022-01-31
346	US	VCognition	vcog-002	002	2017-06-12
347	ES	Veridas Digital Authentication Solutions S.L.	veridas-006	006	2021-04-15
348	ES	Veridas Digital Authentication Solutions S.L.	veridas-007	007	2021-09-02
349	KZ	Verigram	verigram-000	000	2021-09-06
350	ID	Verihubs	verihubs-inteligensia-000	000	2021-07-27

Table 5: Summary of participant information included in this report.

	Location	Developer Name	Short Name	Seq. Num.	Validation Date
351	TW	Via Technologies Inc	via-000	000	2019-07-08
352	TW	Via Technologies Inc	via-001	001	2020-01-08
353	DE	Videmo Intelligente Videoanalyse	videmo-000	000	2019-12-19
354	DE	Videmo Intelligente Videoanalyse	videmo-001	001	2021-12-22
355	IN	Videonetics Technology Pvt	videonetics-001	001	2019-06-19
356	IN	Videonetics Technology Pvt	videonetics-002	002	2019-11-21
357	VN	Vietnam Posts and Telecommunications Group	vnpt-002	002	2021-06-08
358	VN	Vietnam Posts and Telecommunications Group	vnpt-003	003	2021-12-01
359	VN	Viettel Group	vts-000	000	2020-11-04
360	VN	Viettel High Technology	viettelhightech-000	000	2021-08-04
361	US	Vigilant Solutions	vigilantsolutions-010	010	2021-04-07
362	US	Vigilant Solutions	vigilantsolutions-011	011	2021-08-07
363	VN	VinAI Research VietNam	vinai-000	000	2020-09-24
364	VN	VinBigData	vinbigdata-001	001	2022-01-06
365	SE	Visage Technologies	visage-000	000	2020-12-09
366	FI	Visidon	vd-002	002	2021-04-12
367	FI	Visidon	vd-003	003	2021-10-12
368	CN	Vision Intelligence Center of Meituan	meituan-000	000	2021-05-14
369	PT	Vision-Box	visionbox-001	001	2019-03-01
370	PT	Vision-Box	visionbox-002	002	2021-04-29
371	RU	VisionLabs	visionlabs-010	010	2021-01-25
372	RU	VisionLabs	visionlabs-011	011	2021-10-13
373	RU	Vocord	vocord-009	009	2020-12-28
374	RU	Vocord	vocord-010	010	2021-12-20
375	CN	Winsense	winsense-001	001	2019-10-16
376	CN	Winsense	winsense-002	002	2020-11-20
377	CN	Wuhan Tianyu Information Industry	wuhantianyu-001	001	2021-08-05
378	CN	X-Laboratory	x-laboratory-000	000	2019-09-03
379	CN	X-Laboratory	x-laboratory-001	001	2020-01-21
380	CN	Xforward AI Technology	xforwardai-001	001	2020-09-25
381	CN	Xforward AI Technology	xforwardai-002	002	2021-02-10
382	CN	Xiamen Meiya Pico Information	meiya-001	001	2019-03-01
383	CN	Xiamen University	xm-000	000	2020-10-19
384	PT	YooniK	yooniK-002	002	2021-09-06
385	PT	YooniK	yooniK-003	003	2022-01-06
386	TW	Yuan High-Tech Development	yuan-003	003	2021-09-17
387	TW	Yuan High-Tech Development	yuan-004	004	2022-01-14
388	CN	Yuntu Data and Technology	ytu-000	000	2021-06-16
389	CN	Zhuhai Yisheng Electronics Technology	yisheng-004	004	2018-06-12
390	CN	iQIYI Inc	iqface-000	000	2019-06-04
391	CN	iQIYI Inc	iqface-003	003	2021-02-23
392	TW	iSAP Solution Corporation	isap-001	001	2019-08-07
393	TW	iSAP Solution Corporation	isap-002	002	2020-09-01
394	TW	ioNetworks Inc	ionetworks-000	000	2021-07-20

Table 6: Summary of participant information included in this report.

	ALGORITHM	CONFIG	LIBRARY	TEMPLATE								COMPARISON ⁴								
				NAME	DATA	DATA	MEMORY	SIZE	GENERATION TIME (ms) ⁴				TIME (ns) ⁵							
									(KB) ¹	(KB) ²	(MB) ³	(B)	MUGSHOT	480x720	960x1440	1600x2400	3000x4500	GENUINE	IMPOSTOR	
1	20face-000	117155	324083	190	905	193	2048 ± 0	32	232 ± 1	21	223 ± 1	16	226 ± 4	14	222 ± 1	10	224 ± 1	367	44880 ± 134	366 44462 ± 163
2	20face-001	226824	324119	316	1940	353	4096 ± 0	42	279 ± 2	25	266 ± 1	18	266 ± 1	17	267 ± 1	13	267 ± 0	292	5553 ± 54	290 5541 ± 65
3	3divi-006	273866	52656	77	472	105	2048 ± 0	185	654 ± 1	150	651 ± 0	132	660 ± 1	115	678 ± 2	117	759 ± 13	96	775 ± 19	95 770 ± 22
4	3divi-007	483115	24723	251	1285	252	2048 ± 0	168	615 ± 1	140	616 ± 1	118	623 ± 1	104	644 ± 1	107	727 ± 5	82	707 ± 31	85 712 ± 25
5	acer-001	36650	66086	63	417	24	512 ± 0	29	199 ± 0	22	237 ± 28	17	229 ± 26	16	242 ± 37	12	259 ± 21	220	2453 ± 44	222 2461 ± 62
6	acer-002	43922	624858	30	187	194	2048 ± 0	25	184 ± 0	16	184 ± 0	10	185 ± 0	8	185 ± 0	8	186 ± 0	257	3370 ± 47	257 3350 ± 54
7	acisw-003	282029	35664	43	282	391	18467 ± 8	33	232 ± 1	26	267 ± 22	71	488 ± 28	210	990 ± 24	321	2977 ± 129	393	847908 ± 16757	393 851850 ± 17018
8	acisw-007	267619	36111	44	286	240	2048 ± 0	47	283 ± 0	35	293 ± 3	43	414 ± 0	32	404 ± 0	39	484 ± 1	149	1316 ± 22	149 1297 ± 23
9	ader-a-002	0	749797	198	921	382	5120 ± 0	380	1394 ± 11	336	1381 ± 1	334	1393 ± 1	309	1403 ± 1	265	1464 ± 2	212	2163 ± 32	213 2158 ± 28
10	ader-a-003	0	749778	193	917	381	5120 ± 0	375	1381 ± 12	338	1385 ± 1	335	1394 ± 1	306	1401 ± 1	266	1469 ± 1	211	2148 ± 34	210 2130 ± 32
11	advance-002	257173	20434	48	295	109	2048 ± 0	240	811 ± 2	196	803 ± 2	148	696 ± 2	122	699 ± 4	103	718 ± 1	113	987 ± 10	112 988 ± 45
12	advance-003	258867	78699	95	518	90	2048 ± 0	152	586 ± 0	125	584 ± 0	103	583 ± 0	85	588 ± 0	66	591 ± 1	192	1813 ± 17	188 1788 ± 26
13	afisbiometrics-000	545886	32882	225	1088	27	512 ± 0	346	1219 ± 1	290	1135 ± 1	275	1137 ± 2	244	1137 ± 1	201	1147 ± 1	155	1400 ± 29	152 1357 ± 32
14	aifirst-001	224157	808777	80	485	251	2048 ± 0	153	587 ± 2	119	568 ± 2	104	584 ± 3	90	601 ± 6	115	755 ± 5	130	1099 ± 14	132 1087 ± 45
15	aigen-001	256958	595227	232	1136	129	2048 ± 0	389	1448 ± 9	349	1451 ± 8	353	1759 ± 6	351	2594 ± 4	337	5691 ± 44	272	3772 ± 57	271 3736 ± 56
16	aigen-002	205300	1316138	185	874	249	2048 ± 0	151	586 ± 24	124	582 ± 4	212	920 ± 4	333	1758 ± 5	354	5427 ± 17	268	3678 ± 44	266 3646 ± 48
17	ailabs-001	1054663	338989	245	1252	149	2048 ± 0	192	664 ± 4	191	774 ± 50	278	1145 ± 12	339	1972 ± 74	321	5205 ± 272	384	104034 ± 661	384 103415 ± 7722
18	aimall-002	370156	25210	285	1576	260	2048 ± 0	228	776 ± 4	243	927 ± 27	221	940 ± 21	201	955 ± 34	172	1003 ± 75	381	72811 ± 7399	380 71216 ± 6286
19	aimall-003	504324	171935	312	1913	66	1024 ± 0	189	662 ± 1	179	740 ± 51	165	752 ± 62	139	741 ± 46	128	807 ± 47	361	34565 ± 93	362 34598 ± 118
20	aiunionface-000	241642	840295	59	402	133	2048 ± 0	177	637 ± 13	184	754 ± 41	247	1025 ± 28	255	1179 ± 29	282	1639 ± 47	124	1072 ± 19	130 1080 ± 47
21	aize-001	268456	168970	274	1436	153	2048 ± 0	93	437 ± 10	71	440 ± 8	90	542 ± 17	143	756 ± 27	278	1583 ± 53	200	1937 ± 22	197 1919 ± 23
22	aize-002	257106	182517	114	586	114	2048 ± 0	104	467 ± 1	84	479 ± 1	167	756 ± 1	321	1477 ± 1	331	4617 ± 41	50	597 ± 16	55 598 ± 14
23	ajou-001	363257	31734	69	442	255	2048 ± 0	125	530 ± 0	105	536 ± 0	87	535 ± 0	76	549 ± 0	63	577 ± 0	49	597 ± 19	53 596 ± 13
24	alchera-002	405409	22275	243	1233	125	2048 ± 0	299	968 ± 1	233	976 ± 2	234	979 ± 1	209	988 ± 1	177	1025 ± 2	263	3488 ± 63	261 3430 ± 63
25	alchera-003	487718	24613	263	1376	190	2048 ± 0	260	854 ± 3	216	862 ± 2	192	870 ± 1	175	882 ± 2	152	918 ± 1	260	3426 ± 57	258 3383 ± 53
26	alfabeta-001	128232	21780	6	73	33	512 ± 0	39	271 ± 0	30	276 ± 0	58	459 ± 2	177	886 ± 2	312	2547 ± 9	35	470 ± 25	37 458 ± 20
27	alice-000	1741293	19355	300	1732	340	4096 ± 0	293	950 ± 2	245	933 ± 1	226	949 ± 1	217	1011 ± 3	225	1264 ± 8	335	14975 ± 201	334 14890 ± 229
28	alleyes-000	507636	997090	182	857	205	2048 ± 0	231	784 ± 1	252	970 ± 61	232	974 ± 62	197	943 ± 69	185	1057 ± 23	148	1298 ± 34	150 1303 ± 51
29	allgovision-000	172509	155862	107	561	159	2048 ± 0	75	384 ± 8	55	395 ± 17	42	413 ± 14	53	471 ± 14	100	710 ± 21	359	29903 ± 406	360 29735 ± 194
30	alphaface-001	259849	81636	97	527	220	2048 ± 0	162	612 ± 1	135	613 ± 3	115	612 ± 1	95	619 ± 1	82	640 ± 2	117	1008 ± 10	117 1002 ± 19
31	alphaface-002	768995	70692	273	1434	224	2048 ± 0	173	628 ± 2	181	746 ± 19	164	751 ± 18	148	779 ± 22	133	828 ± 40	108	945 ± 25	109 935 ± 17
32	amplifiedgroup-001	0	47053	10	81	54	866 ± 2	8	93 ± 0	-	-	-	-	-	-	-	370	57803 ± 4210	373 56365 ± 1196	
33	androvideo-000	174847	585063	60	403	256	2048 ± 0	41	277 ± 0	33	285 ± 0	23	314 ± 0	28	372 ± 1	73	620 ± 0	238	2860 ± 28	238 2847 ± 22
34	anke-004	349388	410776	143	706	304	2056 ± 0	171	625 ± 1	141	627 ± 2	126	635 ± 3	109	653 ± 2	168	982 ± 8	66	633 ± 22	69 632 ± 34
35	anke-005	328553	429160	230	1134	299	2056 ± 0	154	590 ± 2	131	594 ± 5	111	601 ± 3	103	638 ± 4	132	821 ± 24	78	685 ± 19	81 687 ± 26
36	antheus-000	119453	41994	16	116	43	520 ± 0	12	109 ± 1	17	187 ± 1	13	189 ± 1	10	195 ± 1	11	236 ± 2	309	6901 ± 268	309 6936 ± 103
37	antheus-001	119453	41962	17	118	44	520 ± 0	14	120 ± 1	24	265 ± 13	63	468 ± 22	266	1223 ± 27	313	2660 ± 87	305	6218 ± 47	304 6216 ± 45
38	anyvision-004	401001	630797	227	1102	65	1024 ± 0	62	355 ± 1	-	-	-	-	-	-	-	198	1891 ± 51	192 1829 ± 85	
39	anyvision-005	190979	116595	203	963	63	1024 ± 0	302	985 ± 1	257	997 ± 1	244	1004 ± 1	211	995 ± 1	170	995 ± 1	88	733 ± 14	89 733 ± 16
40	armatura-001	0	374608	233	1151	142	2048 ± 0	202	688 ± 1	161	689 ± 1	146	693 ± 1	128	708 ± 3	116	756 ± 13	15	270 ± 17	18 268 ± 11
41	asusaics-000	257418	245320	122	605	112	2048 ± 0	112	484 ± 13	99	506 ± 21	188	850 ± 26	334	1789 ± 61	339	6305 ± 188	290	5455 ± 78	289 5422 ± 112
42	asusaics-001	257418	245330	119	595	358	4096 ± 0	257	842 ± 17	261	1008 ± 20	329	1377 ± 28	350	2423 ± 90	345	7284 ± 277	319	8618 ± 42	319 8638 ± 136
43	authenmetric-003	293599	39492	207	982	99	2048 ± 0	305	992 ± 1	260	1006 ± 1	243	1003 ± 2	215	1002 ± 1	179	1036 ± 1	181	1757 ± 19	181 1755 ± 19
44	authenmetric-004	381165	39492	238	1214	106	2048 ± 0	278	910 ± 1	236	909 ± 1	208	915 ± 1	188	921 ± 2	160	950 ± 1	176	1724 ± 14	173 1691 ± 29

Notes

- The configuration size does not capture static data included in libraries.
- The library size is the combined total of all files provided in the submission lib folder. These libraries e.g. OpenCV may or may not be installed on any end user's platform natively and would not need to be installed with the algorithm. Some developers put neural network models in their libraries.
- The memory usage is the peak resident set size reported by the ps system call during template generation.
- The median template creation times are measured on Intel®Xeon®CPU E5-2630 v4 @ 2.20GHz processors.
- The comparison durations, in nanoseconds, are estimated using std::chrono::high_resolution_clock which on the machine in (2) counts 1ns clock ticks. Precision is somewhat worse than that however. The ± value is the median absolute deviation times 1.48 for Normal consistency.

Table 7: Summary of algorithms and properties included in this report. The red superscripts give ranking for the quantity in that column.

	ALGORITHM	CONFIG	LIBRARY	TEMPLATE								COMPARISON ⁴									
				NAME	DATA	DATA	MEMORY	SIZE	GENERATION TIME (ms) ⁴				TIME (ns) ⁵								
									(KB) ¹	(KB) ²	(MB) ³	(B)	MUGSHOT	480x720	960x1440	1600x2400	3000x4500	GENUINE	IMPOSTOR		
45	aware-005	300017	26320	247	1265	86	1572 ± 0	274	886 ± 23	272	1038 ± 21	270	1121 ± 22	287	1337 ± 58	297	2195 ± 144	162	1475 ± 63	158	1427 ± 115
46	aware-006	298543	14124	201	943	14	352 ± 0	335	1148 ± 3	295	1146 ± 2	289	1190 ± 2	279	1306 ± 20	290	1754 ± 84	229	2598 ± 42	229	2559 ± 60
47	awiros-001	15499	87480	12	88	26	512 ± 0	9	97 ± 6	5	98 ± 4	6	138 ± 6	15	225 ± 7	59	556 ± 8	126	1079 ± 44	125	1050 ± 45
48	awiros-002	289016	203723	108	562	216	2048 ± 0	109	479 ± 0	97	500 ± 0	86	534 ± 0	94	618 ± 0	158	946 ± 1	201	1966 ± 31	201	1957 ± 25
49	ayftech-001	195423	43580	154	731	23	512 ± 0	82	408 ± 23	83	476 ± 52	177	814 ± 108	335	1827 ± 384	334	5412 ± 1029	59	615 ± 16	106	885 ± 44
50	ayonix-000	58505	5252	69	71	1036 ± 0	2	18 ± 2	-	-	-	-	-	-	-	62	621 ± 23	64	620 ± 26		
51	beethedata-000	227849	1087592	106	555	178	2048 ± 0	102	465 ± 0	82	467 ± 0	62	468 ± 0	51	467 ± 0	34	467 ± 0	209	2121 ± 34	209	2110 ± 38
52	beynai-000	256958	591433	228	1124	108	2048 ± 0	96	451 ± 8	74	449 ± 1	169	767 ± 7	329	1603 ± 25	332	4669 ± 124	270	3730 ± 57	268	3668 ± 54
53	biocube-001	25030	6192987	73	458	333	4096 ± 0	40	282 ± 22	34	292 ± 24	84	521 ± 57	116	684 ± 59	228	1282 ± 68	348	21787 ± 96	348	21812 ± 109
54	bioidechswiss-001	1178769	120811	276	1455	29	512 ± 0	298	966 ± 4	317	1270 ± 270	309	1294 ± 96	310	1409 ± 157	292	1793 ± 79	230	2610 ± 25	230	2624 ± 32
55	bioidechswiss-002	744786	114842	210	993	35	512 ± 0	281	917 ± 2	244	930 ± 2	229	952 ± 2	199	947 ± 3	186	1058 ± 11	213	2177 ± 29	214	2170 ± 31
56	bm-001	287734	38076	23	148	1	64 ± 0	94	444 ± 88	-	-	-	-	-	-	197	1887 ± 31	196	1877 ± 26		
57	boetech-001	261376	88710	266	1384	188	2048 ± 0	38	271 ± 1	27	268 ± 1	19	273 ± 0	18	286 ± 1	15	318 ± 1	378	68519 ± 1921	378	67648 ± 822
58	boetech-002	294347	88710	279	1489	113	2048 ± 0	53	305 ± 4	37	296 ± 1	21	302 ± 1	19	313 ± 1	18	348 ± 2	379	68921 ± 2137	379	69473 ± 2104
59	bresee-001	287880	23227	239	1214	172	2048 ± 0	348	1223 ± 3	305	1216 ± 1	320	1331 ± 1	268	1227 ± 1	240	1360 ± 1	362	37240 ± 655	363	37167 ± 584
60	bresee-002	313627	30902	318	1956	179	2048 ± 0	218	743 ± 4	293	1143 ± 2	279	1146 ± 2	248	1148 ± 2	212	1176 ± 2	184	1778 ± 22	183	1775 ± 23
61	camvi-002	236278	225285	155	737	59	1024 ± 0	195	677 ± 7	175	726 ± 36	191	869 ± 28	240	1129 ± 43	318	2785 ± 113	58	612 ± 26	58	603 ± 20
62	camvi-004	280733	615819	194	919	119	2048 ± 0	222	759 ± 10	215	861 ± 17	238	986 ± 34	276	1279 ± 51	320	2891 ± 158	109	948 ± 40	110	963 ± 31
63	canon-002	446491	130232	188	891	342	4096 ± 0	365	1308 ± 2	325	1315 ± 1	318	1326 ± 2	290	1345 ± 1	262	1452 ± 1	304	6211 ± 25	303	6194 ± 25
64	canon-003	2550850	101378	381	5472	385	6180 ± 0	355	1263 ± 3	315	1263 ± 1	303	1283 ± 1	289	1320 ± 1	270	1482 ± 2	282	4783 ± 17	279	4780 ± 19
65	ceiec-003	260371	88707	67	430	248	2048 ± 0	244	817 ± 4	227	883 ± 57	200	897 ± 60	181	899 ± 72	157	944 ± 72	217	2256 ± 38	217	2241 ± 54
66	ceiec-004	2634746	67011	61	408	180	2048 ± 0	311	1024 ± 1	264	1027 ± 1	249	1027 ± 1	219	1030 ± 1	183	1055 ± 1	194	1844 ± 26	193	1836 ± 20
67	chosun-001	765615	707	85	491	165	2048 ± 0	230	783 ± 2	203	826 ± 4	352	1662 ± 13	356	3679 ± 67	353	11694 ± 243	114	998 ± 25	123	1035 ± 11
68	chosun-002	234001	31875	70	450	117	2048 ± 0	34	248 ± 3	28	273 ± 3	349	1495 ± 14	357	7920 ± 90	354	80302 ± 1349	63	623 ± 17	71	634 ± 13
69	chtface-003	363153	369529	235	1178	222	2048 ± 0	158	594 ± 16	173	720 ± 33	258	1050 ± 41	338	1884 ± 90	336	5606 ± 334	208	2110 ± 37	216	2219 ± 65
70	chtface-004	409656	311027	278	1487	148	2048 ± 0	56	332 ± 0	39	323 ± 1	26	329 ± 1	21	335 ± 1	21	377 ± 1	177	1727 ± 17	176	1720 ± 16
71	clearviewai-000	342491	211852	347	2750	215	2048 ± 0	384	1402 ± 1	344	1403 ± 1	338	1412 ± 1	314	1420 ± 1	255	1418 ± 1	167	1592 ± 37	165	1561 ± 37
72	closeli-001	420342	9851	161	773	351	4096 ± 0	256	839 ± 1	210	843 ± 1	186	841 ± 1	165	845 ± 1	143	865 ± 1	289	5404 ± 17	288	5400 ± 25
73	cloudmatrix-000	309939	542141	151	727	151	2048 ± 0	221	754 ± 10	182	750 ± 2	166	754 ± 4	147	764 ± 1	125	793 ± 2	371	49192 ± 206	371	49275 ± 176
74	cloudwalk-hr-003	383733	144263	209	984	310	2057 ± 0	161	606 ± 0	127	588 ± 0	107	594 ± 0	93	612 ± 1	-	-	312	6982 ± 80	311	6972 ± 84
75	cloudwalk-hr-004	502916	520169	268	1394	268	2049 ± 0	268	873 ± 1	196	876 ± 1	174	879 ± 1	149	902 ± 3	327	11652 ± 127	326	11608 ± 123		
76	cloudwalk-mt-003	490365	494959	258	1342	267	2049 ± 0	284	923 ± 1	238	918 ± 1	217	926 ± 1	189	925 ± 1	155	936 ± 1	326	11620 ± 179	328	11661 ± 128
77	cloudwalk-mt-004	1384602	512628	379	5426	182	2048 ± 0	285	923 ± 2	239	919 ± 1	210	918 ± 0	187	919 ± 0	153	927 ± 1	328	11744 ± 170	327	11631 ± 126
78	clova-000	198420	6824	75	464	140	2048 ± 0	92	437 ± 0	67	431 ± 0	50	435 ± 0	45	452 ± 2	43	508 ± 7	186	1794 ± 16	189	1795 ± 19
79	cogent-005	1876796	75276	349	2806	321	2523 ± 0	347	1221 ± 2	310	1236 ± 1	304	1289 ± 2	313	1420 ± 4	279	1602 ± 5	354	24854 ± 69	354	24858 ± 71
80	cogent-006	1078167	58108	283	1547	74	1062 ± 0	226	768 ± 0	193	789 ± 1	182	831 ± 2	191	930 ± 1	166	971 ± 1	188	1802 ± 17	190	1797 ± 23
81	cognitec-003	471458	62502	172	817	273	2052 ± 0	70	366 ± 9	58	403 ± 9	40	408 ± 9	38	424 ± 9	44	509 ± 13	259	3417 ± 51	262	3433 ± 53
82	cognitec-004	705645	62678	113	585	272	2052 ± 0	100	463 ± 9	94	497 ± 9	77	504 ± 10	67	521 ± 10	74	631 ± 12	245	3028 ± 197	246	3059 ± 238
83	cor-001	1194948	11240	244	1249	312	2060 ± 0	208	699 ± 3	217	863 ± 76	189	865 ± 80	171	872 ± 89	161	952 ± 39	389	270145 ± 2259	389	282686 ± 11788
84	coretech-000	186423	43964	58	393	22	512 ± 0	160	602 ± 15	151	659 ± 12	276	1139 ± 24	249	1149 ± 25	208	1165 ± 23	23	333 ± 14	23	321 ± 13
85	corsight-001	1437763	31525	324	2040	314	2064 ± 0	361	1291 ± 3	319	1285 ± 1	307	1293 ± 1	278	1303 ± 2	242	1379 ± 3	388	249340 ± 1713	388	248929 ± 1909
86	corsight-002	1474921	32093	325	2061	316	2080 ± 0	360	1290 ± 1	320	1287 ± 1	305	1290 ± 1	280	1307 ± 2	248	1388 ± 4	355	24953 ± 637	353	24263 ± 578
87	csc-002	0	519768	264	1376	49	544 ± 0	106	473 ± 0	92	494 ± 0	66	481 ± 1	58	490 ± 1	47	514 ± 5	29	367 ± 11	29	371 ± 10
88	csc-003	0	400435	292	1609	48	544 ± 0	117	499 ± 0	96	500 ± 1	75	502 ± 0	63	508 ± 1	52	535 ± 4	31	393 ± 8	32	397 ± 7

Notes

- 1 The configuration size does not capture static data included in libraries.
- 2 The library size is the combined total of all files provided in the submission lib folder. These libraries e.g. OpenCV may or may not be installed on any end user's platform natively and would not need to be installed with the algorithm. Some developers put neural network models in their libraries.
- 3 The memory usage is the peak resident set size reported by the ps system call during template generation.
- 4 The median template creation times are measured on Intel®Xeon®CPU E5-2630 v4 @ 2.20GHz processors.
- 5 The comparison durations, in nanoseconds, are estimated using std::chrono::high_resolution_clock which on the machine in (2) counts 1ns clock ticks. Precision is somewhat worse than that however. The ± value is the median absolute deviation times 1.48 for Normal consistency.

Table 8: Summary of algorithms and properties included in this report. The red superscripts give ranking for the quantity in that column.

	ALGORITHM	CONFIG	LIBRARY	TEMPLATE								COMPARISON ⁴									
				NAME		DATA		MEMORY		SIZE		GENERATION TIME (ms) ⁴				TIME (ns) ⁵					
				(KB) ¹	(KB) ²	(MB) ³	(B)	MUGSHOT	480x720	960x1440	1600x2400	3000x4500	GENUINE	IMPOSTOR							
89	ctbcbank-000	257208	599238	111	570	230	2048 ± 0	143	568 ± 43	133	606 ± 38	145	690 ± 53	129	711 ± 50	135	831 ± 51	264	3551 ± 87	281	4805 ± 209
90	ctbcbank-001	275511	599238	120	603	244	2048 ± 0	182	652 ± 35	192	781 ± 30	195	875 ± 43	180	898 ± 51	178	1030 ± 47	273	3926 ± 45	272	3924 ± 56
91	cubox-001	369627	75427	127	649	155	2048 ± 0	277	907 ± 1	234	902 ± 1	203	903 ± 0	186	917 ± 0	154	931 ± 0	151	1379 ± 37	157	1417 ± 38
92	cubox-002	542254	90975	319	1964	229	2048 ± 0	282	921 ± 1	240	921 ± 1	213	922 ± 1	193	933 ± 1	173	1003 ± 1	203	2008 ± 72	203	1969 ± 57
93	cudocommunication-001	385258	341277	221	1077	241	2048 ± 0	286	925 ± 1	241	923 ± 1	219	928 ± 1	192	932 ± 0	163	964 ± 1	224	2534 ± 20	226	2537 ± 20
94	cuhkee-001	787853	74917	338	2515	270	2052 ± 0	300	977 ± 31	-	-	-	-	-	-	232	2719 ± 60	236	2783 ± 56		
95	cybercore-000	86008	55441	35	200	34	512 ± 0	186	655 ± 3	162	689 ± 71	131	649 ± 6	105	648 ± 8	91	680 ± 6	334	14800 ± 75	336	15757 ± 782
96	cybercore-001	166096	7791	340	2574	209	2048 ± 0	114	487 ± 0	88	486 ± 0	70	488 ± 0	57	487 ± 0	42	502 ± 0	372	52119 ± 111	372	52127 ± 111
97	cyberextruder-001	121211	13629	29	178	4	256 ± 0	276	893 ± 25	-	-	-	-	-	-	127	1083 ± 16	129	1079 ± 19		
98	cyberextruder-002	168909	13924	34	194	161	2048 ± 0	128	532 ± 6	-	-	-	-	-	-	190	1803 ± 14	186	1779 ± 22		
99	cyberlink-007	380046	102446	301	1743	387	6212 ± 0	211	725 ± 1	178	732 ± 1	160	734 ± 1	137	736 ± 1	122	767 ± 1	20	304 ± 19	21	304 ± 16
100	cyberlink-008	380047	102470	302	1748	386	6212 ± 0	213	729 ± 1	174	725 ± 0	157	727 ± 0	135	732 ± 0	118	760 ± 0	14	263 ± 17	17	255 ± 13
101	dahua-006	831641	119261	377	5068	101	2048 ± 0	382	1398 ± 2	343	1397 ± 1	337	1404 ± 1	308	1402 ± 1	251	1402 ± 1	12	249 ± 13	10	250 ± 11
102	dahua-007	1578737	119418	387	7237	348	4096 ± 0	379	1393 ± 2	335	1373 ± 1	330	1378 ± 1	299	1378 ± 1	243	1379 ± 2	28	367 ± 102	33	434 ± 108
103	daon-000	280726	2307	323	2013	315	2065 ± 0	138	562 ± 3	122	581 ± 5	172	791 ± 9	162	838 ± 15	184	1055 ± 32	337	16052 ± 88	337	16041 ± 85
104	decatur-000	350495	171271	191	907	366	4100 ± 0	310	1024 ± 2	-	-	-	-	-	-	324	11439 ± 80	324	11418 ± 112		
105	decatur-001	342866	253734	280	1507	284	2052 ± 0	324	1103 ± 2	276	1064 ± 2	261	1063 ± 2	230	1067 ± 2	190	1084 ± 2	57	610 ± 19	57	602 ± 8
106	deepglint-003	838065	262081	334	2374	384	6144 ± 0	336	1159 ± 1	294	1145 ± 1	280	1148 ± 1	247	1148 ± 1	207	1163 ± 1	339	17227 ± 41	339	17210 ± 51
107	deepglint-004	1073382	261571	357	3084	253	2048 ± 0	392	1470 ± 1	354	1474 ± 1	348	1485 ± 1	320	1474 ± 1	271	1492 ± 2	298	5961 ± 34	299	5955 ± 29
108	deepsea-001	147497	336250	55	358	55	1024 ± 0	174	630 ± 7	183	752 ± 37	163	746 ± 30	133	727 ± 32	131	820 ± 32	156	1401 ± 37	159	1467 ± 50
109	deeepsense-000	357113	936618	388	7618	186	2048 ± 0	191	664 ± 3	149	645 ± 1	133	660 ± 2	118	687 ± 2	129	808 ± 3	36	480 ± 22	38	459 ± 34
110	dermalog-008	0	937895	376	4989	20	512 ± 0	78	404 ± 2	59	410 ± 3	47	424 ± 5	40	430 ± 5	37	477 ± 5	33	468 ± 31	25	328 ± 13
111	dermalog-009	0	319363	131	664	21	512 ± 0	61	349 ± 0	45	351 ± 0	29	352 ± 0	25	357 ± 0	24	389 ± 0	38	487 ± 34	31	385 ± 29
112	didiglobalface-001	259849	70680	96	527	145	2048 ± 0	164	612 ± 1	145	633 ± 3	125	634 ± 3	107	650 ± 15	88	666 ± 4	111	973 ± 20	111	988 ± 20
113	digidata-000	133370	30249	39	257	217	2048 ± 0	68	361 ± 0	49	360 ± 0	32	361 ± 0	26	363 ± 0	22	380 ± 0	207	2084 ± 37	205	2039 ± 42
114	digitalbarriers-002	83002	598577	314	1930	302	2056 ± 0	30	209 ± 11	23	250 ± 19	41	411 ± 37	153	808 ± 72	299	2236 ± 123	331	13409 ± 228	332	13267 ± 206
115	dps-000	0	2211812	216	1058	361	4096 ± 0	262	868 ± 2	231	893 ± 6	342	1445 ± 9	353	2910 ± 38	348	9345 ± 17	161	1473 ± 37	161	1479 ± 37
116	dsk-000	11967	782905	38	252	18	512 ± 0	51	304 ± 47	38	317 ± 33	242	1001 ± 96	352	2660 ± 170	351	10451 ± 832	315	7152 ± 115	313	7134 ± 111
117	einetworks-000	372608	219883	186	880	309	2056 ± 0	180	645 ± 3	-	-	-	-	-	-	284	4876 ± 66	285	5156 ± 77		
118	ekin-002	51434	278	20	139	325	3072 ± 0	342	1186 ± 13	301	1180 ± 12	286	1181 ± 11	262	1191 ± 11	217	1207 ± 8	276	4294 ± 80	292	5569 ± 112
119	enface-000	369598	153781	130	662	61	1024 ± 0	137	555 ± 4	117	558 ± 4	137	669 ± 6	208	987 ± 15	304	2349 ± 54	313	7059 ± 62	312	6980 ± 65
120	enface-001	370710	173609	134	670	62	1024 ± 0	135	550 ± 4	115	555 ± 3	136	668 ± 7	205	981 ± 15	307	2416 ± 59	307	6734 ± 68	307	6766 ± 69
121	eocortex-000	255937	59432	37	224	257	2048 ± 0	52	305 ± 22	43	341 ± 25	54	440 ± 47	48	464 ± 45	45	513 ± 44	107	923 ± 11	108	918 ± 11
122	ercacat-001	811623	58012	350	2816	277	2052 ± 0	319	1052 ± 3	-	-	-	-	-	-	226	2551 ± 62	223	2501 ± 81		
123	euronovate-001	0	1774966	256	1308	77	1177 ± 0	315	1034 ± 2	296	1165 ± 3	282	1160 ± 3	254	1177 ± 3	211	1172 ± 2	383	81294 ± 591	383	81631 ± 931
124	expasoft-001	39057	983064	21	142	264	2048 ± 0	6	70 ± 0	374 ± 0	377 ± 0	373 ± 0	374 ± 0	171	1660 ± 35	171	1676 ± 48				
125	expasoft-002	38760	59825	26	168	157	2048 ± 0	4	34 ± 0	234 ± 0	234 ± 0	1	34 ± 0	1	34 ± 0	320	8870 ± 78	320	8838 ± 77		
126	f8-001	272977	19668	248	1276	156	2048 ± 0	250	822 ± 39	-	-	-	-	-	-	336	15262 ± 139	335	15277 ± 212		
127	faceonlive-001	0	71529	50	302	293	2056 ± 0	22	179 ± 0	12	179 ± 0	14	190 ± 0	13	217 ± 0	17	343 ± 1	123	1064 ± 37	122	1033 ± 35
128	facesoft-000	370120	10612	165	796	214	2048 ± 0	194	675 ± 18	155	669 ± 3	143	686 ± 3	113	675 ± 5	94	687 ± 2	216	2239 ± 28	218	2277 ± 96
129	facetag-000	1232331	4022	205	965	53	684 ± 0	63	355 ± 17	51	369 ± 8	240	989 ± 33	349	2408 ± 91	346	7930 ± 316	380	72003 ± 625	381	71912 ± 612
130	facetag-002	819806	4021	150	726	173	2048 ± 0	131	544 ± 1	109	544 ± 0	89	542 ± 0	74	545 ± 0	58	554 ± 0	178	1730 ± 25	178	1733 ± 25
131	facex-001	305074	930372	356	2931	93	2048 ± 0	86	422 ± 4	69	434 ± 4	83	520 ± 7	138	737 ± 13	284	1670 ± 27	195	1871 ± 23	194	1846 ± 29
132	facex-002	305074	928334	358	3095	262	2048 ± 0	87	426 ± 5	66	429 ± 4	81	516 ± 8	134	730 ± 12	289	1738 ± 36	65	631 ± 25	62	614 ± 19

Notes

- 1 The configuration size does not capture static data included in libraries.
- 2 The library size is the combined total of all files provided in the submission lib folder. These libraries e.g. OpenCV may or may not be installed on any end user's platform natively and would not need to be installed with the algorithm. Some developers put neural network models in their libraries.
- 3 The memory usage is the peak resident set size reported by the ps system call during template generation.
- 4 The median template creation times are measured on Intel®Xeon®CPU E5-2630 v4 @ 2.20GHz processors.
- 5 The comparison durations, in nanoseconds, are estimated using std::chrono::high_resolution_clock which on the machine in (2) counts 1ns clock ticks. Precision is somewhat worse than that however. The ± value is the median absolute deviation times 1.48 for Normal consistency.

	ALGORITHM	CONFIG	LIBRARY	TEMPLATE								COMPARISON ⁴					
				NAME		DATA		MEMORY		SIZE		GENERATION TIME (ms) ⁴				TIME (ns) ⁵	
				(KB) ¹	(KB) ²	(MB) ³	(B)	MUGSHOT	480x720	960x1440	1600x2400	3000x4500	GENUINE	IMPOSTOR			
133	farfaces-001	346494	44581	40 ²⁶¹	38 ^{512 ± 0}	338 ^{1179 ± 1}	300 ^{1180 ± 1}	285 ^{1180 ± 0}	257 ^{1185 ± 1}	218 ^{1209 ± 2}	104 ^{855 ± 25}	103 ^{860 ± 31}					
134	fiberhome-nanjing-003	352895	1482309	179 ⁸⁴⁵	245 ^{2048 ± 0}	330 ^{1136 ± 7}	289 ^{1134 ± 4}	274 ^{1132 ± 3}	245 ^{1139 ± 3}	202 ^{1154 ± 5}	129 ^{1097 ± 38}	131 ^{1083 ± 42}					
135	fiberhome-nanjing-004	443779	1482313	213 ¹⁰⁴⁸	346 ^{4096 ± 0}	369 ^{1321 ± 5}	323 ^{1304 ± 3}	312 ^{1307 ± 2}	281 ^{1308 ± 3}	237 ^{1326 ± 5}	147 ^{1276 ± 40}	147 ^{1265 ± 38}					
136	fincore-000	256615	19409	100 ⁵³⁵	189 ^{2048 ± 0}	121 ^{508 ± 3}	98 ^{505 ± 0}	78 ^{508 ± 1}	65 ^{513 ± 2}	51 ^{535 ± 1}	182 ^{1765 ± 31}	182 ^{1763 ± 22}					
137	fujitsulab-002	0	1088887	293 ¹⁶¹³	371 ^{4104 ± 0}	350 ^{1237 ± 2}	307 ^{1222 ± 2}	295 ^{1236 ± 1}	269 ^{1251 ± 2}	238 ^{1327 ± 2}	236 ^{2836 ± 25}	237 ^{2809 ± 44}					
138	fujitsulab-003	662263	318209	386 ⁶⁹⁰⁷	374 ^{4104 ± 0}	294 ^{951 ± 20}	247 ^{941 ± 19}	228 ^{952 ± 19}	204 ^{971 ± 20}	181 ^{1045 ± 21}	237 ^{2855 ± 16}	239 ^{2849 ± 19}					
139	geo-002	369903	98667	211 ¹⁰¹⁸	97 ^{2048 ± 0}	235 ^{791 ± 1}	194 ^{793 ± 0}	173 ^{794 ± 0}	150 ^{795 ± 1}	126 ^{803 ± 1}	258 ^{3407 ± 45}	260 ^{3422 ± 65}					
140	geo-004	168980	107714	250 ¹²⁸⁰	139 ^{2048 ± 0}	336 ^{1268 ± 1}	318 ^{1279 ± 1}	302 ^{1274 ± 0}	272 ^{1259 ± 1}	231 ^{1296 ± 1}	120 ^{1023 ± 20}	121 ^{1028 ± 22}					
141	glory-003	0	536910	269 ¹⁴⁰⁰	377 ^{4234 ± 0}	115 ^{489 ± 0}	118 ^{565 ± 0}	158 ^{732 ± 0}	337 ^{1876 ± 2}	347 ^{8941 ± 20}	300 ^{6020 ± 90}	302 ^{6003 ± 72}					
142	glory-004	0	999639	330 ²¹⁸¹	376 ^{4182 ± 0}	201 ^{588 ± 0}	186 ^{759 ± 1}	224 ^{941 ± 1}	342 ^{2134 ± 4}	349 ^{9360 ± 47}	286 ^{4982 ± 66}	284 ^{4990 ± 63}					
143	gorilla-007	441058	708166	294 ¹⁶⁹¹	388 ^{6288 ± 0}	156 ^{592 ± 1}	129 ^{592 ± 1}	112 ^{603 ± 1}	99 ^{625 ± 2}	106 ^{722 ± 9}	269 ^{3686 ± 37}	270 ^{3709 ± 36}					
144	gorilla-008	450175	707000	305 ¹⁷⁸⁹	390 ^{8338 ± 0}	159 ^{595 ± 1}	128 ^{590 ± 0}	110 ^{600 ± 1}	97 ^{621 ± 2}	104 ^{720 ± 9}	279 ^{4530 ± 44}	277 ^{4524 ± 38}					
145	graymatics-001	13095	70406	18 ¹²⁷	338 ^{4096 ± 0}	27 ^{191 ± 1}	18 ^{203 ± 1}	106 ^{592 ± 5}	331 ^{1698 ± 9}	343 ^{7150 ± 34}	364 ^{39874 ± 309}	364 ^{39762 ± 295}					
146	griaule-000	0	598214	215 ¹⁰⁵⁴	274 ^{2052 ± 0}	85 ^{416 ± 6}	64 ^{425 ± 7}	170 ^{770 ± 14}	332 ^{1749 ± 43}	341 ^{6406 ± 189}	274 ^{3987 ± 42}	273 ^{3938 ± 38}					
147	hertasecurity-000	0	780014	94 ⁵¹⁶	6 ^{256 ± 0}	10 ^{99 ± 0}	6 ^{98 ± 0}	5 ^{100 ± 0}	5 ^{107 ± 0}	5 ^{139 ± 0}	84 ^{710 ± 31}	77 ^{667 ± 28}					
148	hertasecurity-001	0	944427	236 ¹¹⁸³	19 ^{512 ± 0}	60 ^{346 ± 0}	44 ^{345 ± 0}	28 ^{349 ± 0}	23 ^{354 ± 0}	23 ^{388 ± 0}	183 ^{1770 ± 45}	177 ^{1726 ± 48}					
149	hik-001	667866	9290	384 ⁶⁵⁹⁷	81 ^{1408 ± 0}	181 ^{651 ± 0}	154 ^{667 ± 8}	140 ^{677 ± 16}	117 ^{686 ± 13}	110 ^{737 ± 12}	39 ^{488 ± 19}	39 ^{477 ± 22}					
150	hisign-001	732412	167488	284 ¹⁵⁵³	317 ^{2080 ± 0}	364 ^{1306 ± 1}	327 ^{1320 ± 1}	314 ^{1315 ± 1}	284 ^{1312 ± 1}	236 ^{1325 ± 1}	7 ^{201 ± 10}	6 ^{185 ± 13}					
151	hyperverge-001	260819	88624	89 ⁵⁰⁷	197 ^{2048 ± 0}	197 ^{682 ± 20}	164 ^{695 ± 17}	292 ^{1196 ± 37}	348 ^{2400 ± 68}	344 ^{7178 ± 204}	302 ^{6026 ± 40}	301 ^{5984 ± 38}					
152	hyperverge-002	2951900	198832	320 ¹⁹⁷⁵	58 ^{1024 ± 0}	288 ^{938 ± 1}	246 ^{939 ± 1}	222 ^{941 ± 1}	198 ^{945 ± 1}	167 ^{975 ± 1}	301 ^{6023 ± 37}	300 ^{5966 ± 40}					
153	hzailiu-001	0	372018	109 ⁵⁶³	301 ^{2056 ± 0}	328 ^{1126 ± 1}	288 ^{1128 ± 1}	273 ^{1130 ± 1}	241 ^{1132 ± 1}	204 ^{1159 ± 1}	106 ^{894 ± 19}	107 ^{899 ± 22}					
154	icm-002	621586	903	79 ⁴⁸⁴	225 ^{2048 ± 0}	314 ^{1031 ± 7}	-	-	-	-	352 ^{24052 ± 118}	351 ^{24049 ± 124}					
155	icm-003	1513988	940	87 ⁵⁰⁰	124 ^{2048 ± 0}	196 ^{681 ± 6}	156 ^{672 ± 4}	154 ^{714 ± 11}	160 ^{837 ± 41}	244 ^{1381 ± 131}	353 ^{24351 ± 161}	352 ^{24227 ± 146}					
156	ichttc-000	172459	1471004	307 ¹⁸⁰⁵	94 ^{2048 ± 0}	59 ^{338 ± 11}	42 ^{338 ± 9}	51 ^{437 ± 16}	125 ^{705 ± 24}	288 ^{1719 ± 44}	288 ^{5284 ± 63}	287 ^{5290 ± 54}					
157	id3-006	210116	7706	208 ⁹⁸²	45 ^{520 ± 0}	198 ^{583 ± 0}	279 ^{1088 ± 1}	290 ^{1192 ± 1}	265 ^{1209 ± 1}	226 ^{1270 ± 1}	291 ^{5547 ± 34}	291 ^{5563 ± 34}					
158	id3-008	242416	8151	219 ¹⁰⁶⁸	9 ^{264 ± 0}	246 ^{819 ± 0}	304 ^{1209 ± 2}	310 ^{1297 ± 2}	286 ^{1329 ± 1}	260 ^{1433 ± 1}	294 ^{5658 ± 44}	294 ^{5624 ± 40}					
159	idemida-007	353242	67485	214 ¹⁰⁵¹	15 ^{468 ± 0}	73 ^{384 ± 0}	54 ^{389 ± 0}	37 ^{393 ± 1}	33 ^{405 ± 2}	29 ^{441 ± 8}	253 ^{3243 ± 63}	253 ^{3202 ± 63}					
160	idemida-008	374017	69922	237 ¹¹⁹⁴	13 ^{348 ± 0}	98 ^{457 ± 1}	80 ^{461 ± 0}	60 ^{466 ± 1}	54 ^{476 ± 2}	46 ^{513 ± 10}	248 ^{3080 ± 41}	244 ^{3046 ± 56}					
161	iit-002	259579	52070	153 ⁷³¹	107 ^{2048 ± 0}	122 ^{514 ± 1}	101 ^{531 ± 2}	94 ^{547 ± 1}	80 ^{583 ± 1}	108 ^{733 ± 2}	119 ^{1023 ± 7}	118 ^{1011 ± 66}					
162	iit-003	261288	53791	174 ⁸¹⁷	128 ^{2048 ± 0}	111 ^{482 ± 0}	91 ^{493 ± 0}	79 ^{509 ± 0}	72 ^{541 ± 0}	86 ^{661 ± 0}	22 ^{324 ± 17}	24 ^{326 ± 8}					
163	imagus-002	227766	318409	62 ⁴¹¹	168 ^{2048 ± 0}	232 ^{786 ± 1}	187 ^{766 ± 2}	198 ^{885 ± 3}	315 ^{1430 ± 3}	329 ^{4080 ± 10}	74 ^{676 ± 16}	66 ^{630 ± 20}					
164	imagus-004	254405	380049	142 ⁶⁹⁷	158 ^{2048 ± 0}	170 ^{624 ± 1}	126 ^{587 ± 10}	119 ^{626 ± 3}	88 ^{592 ± 3}	102 ^{717 ± 6}	92 ^{760 ± 22}	84 ^{703 ± 28}					
165	imperial-000	370120	10623	166 ⁷⁹⁶	170 ^{2048 ± 0}	193 ^{669 ± 1}	157 ^{675 ± 3}	142 ^{683 ± 17}	114 ^{676 ± 2}	95 ^{689 ± 2}	210 ^{2130 ± 32}	207 ^{2052 ± 100}					
166	imperial-002	472327	16134	308 ¹⁸²⁶	258 ^{2048 ± 0}	144 ^{569 ± 1}	123 ^{581 ± 15}	101 ^{575 ± 5}	78 ^{576 ± 2}	65 ^{588 ± 3}	218 ^{2278 ± 90}	211 ^{2131 ± 44}					
167	incode-009	266103	21014	199 ⁹³⁹	218 ^{2048 ± 0}	118 ^{503 ± 0}	90 ^{490 ± 1}	74 ^{498 ± 0}	62 ^{505 ± 0}	53 ^{537 ± 0}	131 ^{1102 ± 28}	134 ^{1113 ± 29}					
168	incode-010	627808	21014	342 ²⁶²⁸	227 ^{2048 ± 0}	339 ^{1180 ± 2}	298 ^{1178 ± 1}	287 ^{1182 ± 1}	256 ^{1184 ± 1}	219 ^{1221 ± 1}	137 ^{1164 ± 32}	138 ^{1144 ± 32}					
169	innefulabs-000	370588	162172	68 ⁴³⁹	242 ^{2048 ± 0}	308 ^{1006 ± 3}	263 ^{1025 ± 3}	251 ^{1030 ± 4}	223 ^{1041 ± 2}	199 ^{1135 ± 3}	295 ^{5782 ± 41}	297 ^{5741 ± 45}					
170	innovativetechnologyltd-001	177232	335757	52 ³⁴¹	162 ^{2048 ± 0}	90 ^{433 ± 7}	73 ^{446 ± 8}	52 ^{439 ± 4}	44 ^{452 ± 4}	40 ^{485 ± 7}	196 ^{1877 ± 42}	198 ^{1924 ± 97}					
171	innovativetechnologyltd-002	173939	372324	192 ⁹¹²	213 ^{2048 ± 0}	187 ^{661 ± 2}	176 ^{726 ± 4}	235 ^{981 ± 27}	212 ^{997 ± 40}	121 ^{766 ± 3}	193 ^{1841 ± 50}	195 ^{1857 ± 59}					
172	innovatrics-007	0	493269	315 ¹⁹³⁷	75 ^{1064 ± 0}	394 ^{1485 ± 7}	356 ^{1785 ± 184}	355 ^{2078 ± 24}	341 ^{2123 ± 15}	298 ^{2210 ± 42}	299 ^{5978 ± 88}	296 ^{5690 ± 102}					
173	innovatrics-008	307323	59842	271 ¹⁴²⁴	47 ^{538 ± 0}	229 ^{778 ± 6}	188 ^{767 ± 3}	171 ^{770 ± 3}	151 ^{803 ± 3}	140 ^{853 ± 10}	243 ^{3021 ± 66}	232 ^{2673 ± 88}					
174	insightface-001	776777	16606	367 ³⁸⁵²	201 ^{2048 ± 0}	373 ^{1366 ± 2}	332 ^{1368 ± 3}	326 ^{1372 ± 3}	298 ^{1375 ± 5}	246 ^{1386 ± 4}	133 ^{1119 ± 29}	133 ^{1108 ± 34}					
175	insightface-002	800572	16606	366 ³⁸¹⁹	171 ^{2048 ± 0}	381 ^{1396 ± 2}	340 ^{1389 ± 4}	336 ^{1403 ± 3}	307 ^{1402 ± 2}	254 ^{1413 ± 3}	138 ^{1169 ± 40}	135 ^{1118 ± 38}					
176	intelllicloudai-001	220831	868246	128 ⁶⁵⁵	233 ^{2048 ± 0}	105 ^{468 ± 2}	76 ^{456 ± 1}	61 ^{466 ± 3}	61 ^{492 ± 1}	75 ^{632 ± 2}	121 ^{1056 ± 4}	126 ^{1051 ± 72}					

	ALGORITHM	CONFIG	LIBRARY	TEMPLATE								COMPARISON ⁴						
				NAME	DATA	DATA	MEMORY	SIZE	GENERATION TIME (ms) ⁴				TIME (ns) ⁵					
									(KB) ¹	(KB) ²	(MB) ³	(B)	MUGSHOT	480x720	960x1440	1600x2400	3000x4500	Genuine
177	intellicloudai-002	259047	58559	³⁶² 3584	³⁶⁸ 4100 ± 0	²⁵⁸ 847 ± 1	²¹¹ 847 ± 2	¹⁸⁷ 849 ± 1	¹⁶⁷ 853 ± 1	¹⁴⁵ 878 ± 4	¹⁰¹ 822 ± 28	¹⁰¹ 818 ± 23						
178	intellifusion-001	271872	289387	¹⁵⁹ 762	¹⁷⁴ 2048 ± 0	²²³ 764 ± 38	¹⁹⁰ 774 ± 39	¹⁷⁴ 797 ± 42	¹⁵² 803 ± 34	¹²⁷ 805 ± 33	¹³² 1112 ± 28	¹³⁶ 1128 ± 41						
179	intellifusion-002	762731	385841	²⁰⁰ 941	³⁴⁹ 4096 ± 0	²⁹² 950 ± 2	²⁸³ 1096 ± 42	²⁶⁵ 1088 ± 33	²⁵² 1168 ± 31	²⁰⁹ 1171 ± 10	¹⁷⁴ 1713 ± 57	¹⁷⁰ 1665 ± 87						
180	intellivision-001	43692	11649	⁸ 74	²⁹² 2056 ± 0	⁵ 62 ± 2	-	-	-	-	-	²²⁸ 2573 ± 91	²²⁷ 2544 ± 38					
181	intellivision-002	43692	14505	¹¹ 81	²⁹⁰ 2056 ± 0	⁵³ 322 ± 1	⁴⁷ 355 ± 2	³⁴ 372 ± 1	³⁷ 422 ± 2	⁶⁸ 600 ± 1	³³² 13525 ± 134	³³¹ 12782 ± 278						
182	intelresearch-004	646918	85290	³¹¹ 1856	¹⁷⁷ 2048 ± 0	³⁶⁸ 1319 ± 2	³²⁸ 1322 ± 3	³¹⁹ 1330 ± 3	²⁸⁹ 1345 ± 3	²⁵³ 1411 ± 5	²⁸⁰ 4696 ± 63	²⁷⁸ 4692 ± 66						
183	intelresearch-005	398137	85290	²³⁴ 1158	²⁶⁵ 2048 ± 0	³⁷⁰ 1328 ± 1	³³⁰ 1334 ± 2	³²² 1344 ± 2	²⁹² 1356 ± 2	²⁵⁷ 1423 ± 4	²⁷⁸ 4524 ± 87	²⁷⁶ 4461 ± 74						
184	intsysmsu-001	384409	172480	¹⁶⁴ 789	¹⁸³ 2048 ± 0	¹⁶³ 614 ± 2	¹³⁹ 615 ± 2	¹²⁹ 642 ± 2	¹⁴¹ 750 ± 3	²⁰⁵ 1159 ± 4	⁶¹ 621 ± 8	⁶⁰ 611 ± 31						
185	intsysmsu-002	765921	172298	¹⁶³ 786	⁶⁴ 1024 ± 0	¹⁵⁷ 593 ± 1	¹⁹⁹ 793 ± 2	¹⁸⁰ 827 ± 1	¹⁷² 875 ± 104	²³⁰ 1293 ± 3	⁴³ 549 ± 25	⁴⁵ 548 ± 29						
186	ionetworks-000	287609	51236	⁵⁴ 351	²¹⁹ 2048 ± 0	⁸⁹ 430 ± 0	⁷⁰ 435 ± 0	⁴⁹ 433 ± 0	⁴¹ 432 ± 0	³¹ 444 ± 0	³¹⁰ 6913 ± 102	³¹⁴ 7150 ± 160						
187	iqface-000	268819	596337	¹⁴⁴ 704	³⁷⁹ 4750 ± 32	¹³⁰ 538 ± 26	⁹³ 494 ± 2	⁹² 543 ± 3	¹³⁶ 734 ± 4	²⁵⁰ 1393 ± 4	³⁹² 636433 ± 38446	³⁹² 632654 ± 85615						
188	iqface-003	370803	963398	¹⁷¹ 817	³⁸⁰ 4763 ± 37	¹²⁴ 529 ± 1	¹⁰² 532 ± 2	¹⁰⁹ 599 ± 8	¹⁶⁶ 850 ± 2	²⁸⁵ 1694 ± 2	³⁹¹ 575924 ± 2601	³⁹¹ 576653 ± 2051						
189	irex-000	741899	47419	³²⁶ 2086	³²⁶ 3080 ± 0	²⁵⁹ 852 ± 2	²¹³ 850 ± 1	¹⁹⁴ 874 ± 2	¹⁹⁸ 939 ± 1	²²² 1249 ± 5	⁸ 201 ± 11	⁹ 208 ± 8						
190	isap-001	99049	204201	¹ 18	³⁴³ 4096 ± 0	¹ 0 ± 0	-	-	-	-	³² 459 ± 17	³⁶ 456 ± 11						
191	isap-002	256765	49931	⁴⁶ 288	²¹⁰ 2048 ± 0	²²⁷ 769 ± 3	²⁶⁵ 1027 ± 2	¹⁹⁷ 877 ± 2	¹⁴⁶ 761 ± 1	¹⁵⁰ 912 ± 2	²⁴⁶ 3045 ± 94	²⁴¹ 2973 ± 66						
192	isityou-000	48010	36621	¹⁴ 110	³⁹² 1920 ± 0	¹³ 113 ± 5	-	-	-	-	³⁸⁷ 237517 ± 1318	³⁸⁷ 237374 ± 1279						
193	isystems-001	274621	639268	²²⁶ 1091	²⁵⁹ 2048 ± 0	⁴⁸ 291 ± 9	-	-	-	-	⁴⁵ 557 ± 16	⁴⁷ 564 ± 22						
194	isystems-002	358984	803389	²⁹⁰ 1595	²³⁶ 2048 ± 0	²⁴⁹ 822 ± 8	-	-	-	-	⁸⁹ 749 ± 31	⁶⁸ 632 ± 28						
195	itmo-007	415979	245376	³³² 2199	¹²¹ 2048 ± 0	²¹⁷ 741 ± 2	-	-	-	-	²²⁵ 2551 ± 50	²²⁵ 2529 ± 80						
196	itmo-008	726866	318238	²⁶⁵ 1377	³⁶² 4096 ± 0	³²⁰ 1060 ± 1	²⁷⁵ 1058 ± 1	²⁶⁰ 1059 ± 1	²³¹ 1072 ± 4	¹⁹⁴ 1104 ± 1	²⁶⁵ 3578 ± 25	²⁶⁵ 3580 ± 28						
197	ivacognitive-001	256958	62791	²⁰² 947	²⁰⁶ 2048 ± 0	³⁶² 1292 ± 3	³²¹ 1289 ± 4	³⁰⁶ 1292 ± 4	²⁷⁷ 1292 ± 3	²³⁵ 1321 ± 4	²⁷⁵ 4228 ± 41	²⁷⁴ 4226 ± 41						
198	iws-000	30875	3063	⁹ 77	³² 512 ± 0	⁴⁰ 277 ± 5	³² 283 ± 1	⁷² 494 ± 3	²⁰⁷ 984 ± 3	³²² 2987 ± 39	¹¹⁵ 999 ± 40	¹¹⁴ 992 ± 22						
199	kakao-005	414316	152216	²⁸⁶ 1581	²⁸⁷ 2052 ± 0	³²¹ 1068 ± 1	²⁷⁸ 1073 ± 1	²⁶³ 1079 ± 0	²³² 1077 ± 1	¹⁹² 1089 ± 1	²⁰⁶ 2067 ± 26	²⁰⁶ 2043 ± 34						
200	kakao-007	526993	129545	³⁷¹ 3953	¹²³ 2048 ± 0	²⁹⁹ 952 ± 1	²⁵⁰ 961 ± 1	²³⁰ 958 ± 1	²⁰³ 962 ± 1	¹⁶³ 968 ± 1	¹²² 1056 ± 16	¹²⁴ 1047 ± 28						
201	kakaopay-001	397864	179869	¹³⁶ 684	³³⁰ 4096 ± 0	⁹³ 448 ± 0	¹⁰⁷ 542 ± 0	⁹¹ 542 ± 0	⁷³ 542 ± 0	⁵⁷ 553 ± 0	⁶⁷ 633 ± 22	⁶⁷ 630 ± 22						
202	kedacom-000	245292	37401	³⁹³ 23574	¹¹ 292 ± 0	¹¹⁹ 506 ± 3	¹¹² 547 ± 10	¹¹⁷ 614 ± 9	⁸⁴ 588 ± 10	⁸⁷ 665 ± 24	⁷⁵ 684 ± 14	⁷⁹ 682 ± 16						
203	kiwitech-000	369711	21375	¹⁶⁹ 808	¹⁰⁴ 2048 ± 0	¹⁵⁵ 591 ± 0	¹³⁰ 594 ± 0	¹⁰⁸ 595 ± 1	⁸⁹ 596 ± 0	⁷⁰ 609 ± 0	¹⁸⁰ 1755 ± 20	¹⁸⁰ 1734 ± 16						
204	kneron-003	58366	1747	³¹ 188	¹¹⁸ 2048 ± 0	⁴³ 281 ± 3	³¹ 280 ± 1	²⁴ 315 ± 13	²⁷ 365 ± 7	²²¹ 1224 ± 30	²⁸⁷ 5237 ± 63	²⁸⁶ 5274 ± 99						
205	kneron-005	375374	13633	⁷² 457	¹⁹³ 2048 ± 0	¹²³ 518 ± 2	¹⁰⁰ 522 ± 4	⁹⁷ 556 ± 5	¹⁴⁴ 757 ± 19	²⁹¹ 1760 ± 25	¹⁹⁹ 1922 ± 11	¹⁹⁹ 1926 ± 20						
206	knowutech-000	808045	32886	²⁵⁵ 1303	⁸³ 1536 ± 0	³⁸⁷ 1419 ± 2	³³⁴ 1372 ± 1	³²⁸ 1377 ± 1	³⁰⁰ 1382 ± 2	²⁴⁷ 1386 ± 2	²⁷¹ 3743 ± 31	²⁶⁹ 3693 ± 38						
207	kookmin-002	371771	30734	¹⁷⁶ 827	¹⁴⁷ 2048 ± 0	³¹⁷ 1038 ± 2	²⁷³ 1047 ± 1	²⁵⁶ 1045 ± 1	²²⁸ 1061 ± 1	¹⁹⁵ 1116 ± 1	⁷⁰ 638 ± 19	⁷² 636 ± 20						
208	kuke3d-001	403462	68786	⁹⁸ 530	³⁴⁷ 4096 ± 0	²⁴² 814 ± 2	¹⁹⁸ 811 ± 2	¹⁷⁸ 814 ± 2	¹⁵⁴ 814 ± 1	¹³⁸ 834 ± 1	³⁰⁶ 6412 ± 57	³⁰⁶ 6413 ± 51						
209	lemalabs-001	748400	198794	³⁴⁶ 2738	²⁰⁴ 2048 ± 0	²³⁹ 810 ± 0	¹⁹⁹ 812 ± 0	¹⁷⁶ 813 ± 0	¹⁵⁶ 819 ± 0	¹³⁹ 844 ± 1	³³⁰ 11930 ± 35	³³⁰ 11913 ± 37						
210	line-000	264443	407003	¹¹⁶ 590	²⁰⁷ 2048 ± 0	¹⁴⁹ 586 ± 0	¹³⁴ 612 ± 0	¹¹⁴ 609 ± 1	⁹² 611 ± 0	⁷² 618 ± 1	²³⁵ 2753 ± 19	²³⁵ 2745 ± 23						
211	line-001	944355	407058	³³³ 2373	²²³ 2048 ± 0	²⁵⁴ 833 ± 10	²⁰⁶ 830 ± 3	¹⁸¹ 828 ± 4	¹⁶¹ 838 ± 8	¹³⁶ 833 ± 4	²³¹ 2696 ± 23	²³³ 2677 ± 35						
212	lookman-002	138200	25410	³⁹¹ 16518	⁵¹ 548 ± 0	²⁰ 173 ± 1	-	-	-	-	⁵⁶ 610 ± 19	⁶¹ 612 ± 22						
213	lookman-004	244775	37401	³⁹² 23548	⁵⁰ 548 ± 0	¹²⁰ 507 ± 5	¹¹⁰ 545 ± 12	¹¹⁶ 613 ± 12	⁸⁷ 590 ± 11	⁸³ 656 ± 16	¹⁰⁵ 871 ± 29	¹⁰⁵ 878 ± 29						
214	luxand-000	0	57908	²⁶² 1366	⁷² 1040 ± 0	⁷⁹ 407 ± 23	⁶⁸ 433 ± 11	⁵⁵ 444 ± 14	⁵⁰ 464 ± 14	⁶¹ 562 ± 25	¹⁰² 828 ± 28	¹⁰² 828 ± 32						
215	mantra-000	471458	62566	¹⁵⁷ 749	²⁷⁹ 2052 ± 0	⁸³ 413 ± 18	⁸⁹ 487 ± 19	⁷³ 494 ± 18	⁶⁴ 511 ± 18	⁶⁷ 598 ± 19	²⁵⁰ 3151 ± 51	²⁴⁹ 3127 ± 63						
216	maxvision-000	133114	56426	³⁰⁶ 1791	³¹ 512 ± 0	⁶⁶ 359 ± 0	⁴⁸ 356 ± 0	³¹ 359 ± 0	²⁴ 356 ± 0	²⁰ 370 ± 1	²²¹ 2461 ± 20	²²⁰ 2452 ± 17						
217	megvii-003	4430290	42790	³⁷⁵ 4878	³⁵⁰ 4096 ± 0	³⁴⁴ 1210 ± 1	³⁰⁸ 1223 ± 0	³²⁴ 1356 ± 4	³²⁷ 1582 ± 7	³¹⁵ 2727 ± 23	³⁸⁶ 225342 ± 3574	³⁸⁶ 225413 ± 6344						
218	megvii-004	3962505	44019	³⁷⁴ 4436	³⁶⁴ 4097 ± 0	³⁵⁹ 1287 ± 1	³³³ 1369 ± 2	³¹³ 1310 ± 2	³⁰² 1384 ± 3	²⁶¹ 1436 ± 5	³⁶⁹ 46801 ± 204	³⁶⁹ 46832 ± 207						
219	meituan-000	259514	333178	¹⁰⁴ 554	¹²⁷ 2048 ± 0	⁹¹ 436 ± 4	⁷² 441 ± 1	¹²⁰ 626 ± 5	²³⁵ 1098 ± 15	³²⁴ 3126 ± 53	⁶⁹ 638 ± 17	⁷⁰ 633 ± 16						
220	meiya-001	280055	264913	⁹⁰ 507	²⁶⁹ 2049 ± 0	¹⁶⁹ 622 ± 12	-	-	-	-	³¹⁸ 8356 ± 615	³¹⁸ 8134 ± 97						

	ALGORITHM	CONFIG	LIBRARY	TEMPLATE								COMPARISON ⁴						
				NAME	DATA	DATA	MEMORY	SIZE	GENERATION TIME (ms) ⁴				TIME (ns) ⁵					
									(KB) ¹	(KB) ²	(MB) ³	(B)	MUGSHOT	480x720	960x1440	1600x2400	3000x4500	GENUINE
221	mendaxiatech-000	1941475	45484	³⁶⁰ 3195	³⁶⁵ 4097 ± 0	³⁵¹ 1243 ± 2	³¹³ 1255 ± 1	³²⁷ 1373 ± 2	³²⁸ 1598 ± 3	³¹⁴ 2689 ± 8	³⁷⁰ 46906 ± 275	³⁷⁰ 46872 ± 217						
222	microfocus-001	104524	27242	³² 190	² 256 ± 0	³⁷ 264 ± 18	-	-	-	-	¹¹ 215 ± 8	¹¹ 217 ± 10						
223	microfocus-002	96288	27362	²⁸ 176	³ 256 ± 0	³⁵ 259 ± 18	-	-	-	-	²⁴ 337 ± 34	¹³ 230 ± 25						
224	minivision-000	836697	16597	³⁷² 4013	³⁵⁷ 4096 ± 0	³¹⁶ 1035 ± 1	²⁶⁹ 1033 ± 2	²⁵⁴ 1035 ± 1	²²¹ 1037 ± 1	¹⁸⁷ 1059 ± 2	²²² 2466 ± 26	²²¹ 2460 ± 25						
225	mobai-000	365451	80573	¹⁶² 786	³⁸³ 6144 ± 0	²²⁴ 766 ± 8	²²⁰ 869 ± 6	²⁹³ 1205 ± 31	³³⁶ 1867 ± 45	³²⁸ 3549 ± 190	³³⁸ 16458 ± 333	³³⁸ 16423 ± 1473						
226	mobai-001	265297	60164	⁹⁹ 534	²⁴³ 2048 ± 0	¹⁶³ 612 ± 3	¹³⁷ 614 ± 3	¹⁴⁴ 687 ± 9	¹⁷⁶ 886 ± 31	²⁸⁶ 1707 ± 103	¹⁵² 1386 ± 25	¹⁵³ 1377 ± 26						
227	mobbl-001	231160	58706	³⁶ 223	²³² 2048 ± 0	²⁴ 183 ± 32	¹⁵ 184 ± 25	³⁰ 354 ± 76	¹⁵⁹ 823 ± 396	³¹⁷ 2781 ± 1166	³²⁹ 11832 ± 109	³²⁹ 11851 ± 88						
228	mobbl-002	242920	60119	⁴⁷ 288	¹⁹⁶ 2048 ± 0	¹⁹⁰ 663 ± 6	¹⁵² 660 ± 5	¹³⁵ 662 ± 5	¹¹¹ 663 ± 5	⁹⁰ 676 ± 5	³²⁵ 11616 ± 78	³²⁵ 11588 ± 97						
229	mobilpintech-000	370514	303291	²²⁹ 1130	¹⁶⁴ 2048 ± 0	³⁵² 1245 ± 1	³⁰⁹ 1234 ± 1	²⁹⁹ 1264 ± 1	²⁹³ 1360 ± 1	²⁸⁷ 1707 ± 1	³³³ 14506 ± 214	³³³ 14433 ± 197						
230	moreedian-000	525259	21374	¹⁹⁷ 932	¹⁶⁷ 2048 ± 0	²⁰⁵ 694 ± 0	¹⁶⁵ 698 ± 0	¹⁵⁰ 699 ± 0	¹²³ 700 ± 0	¹⁰¹ 713 ± 1	¹⁸⁹ 1803 ± 11	¹⁸⁵ 1779 ± 23						
231	multimodality-000	0	503924	²⁷⁰ 1417	²²¹ 2048 ± 0	⁸⁴ 416 ± 0	⁶³ 420 ± 0	⁴⁵ 423 ± 0	³⁹ 427 ± 0	³³ 463 ± 0	¹⁰³ 848 ± 25	⁹⁹ 800 ± 28						
232	mvision-001	227502	149531	¹⁴⁹ 723	³⁶ 512 ± 0	²⁰³ 691 ± 21	¹⁶⁷ 702 ± 19	¹⁴⁹ 697 ± 24	¹²⁷ 708 ± 29	⁹⁹ 710 ± 27	¹³⁴ 1123 ± 40	¹³⁹ 1154 ± 38						
233	nazhiai-000	547484	16141	³⁴³ 2716	²³⁹ 2048 ± 0	¹⁹⁹ 683 ± 3	¹⁶⁰ 687 ± 2	¹⁸³ 835 ± 27	¹⁶⁴ 840 ± 31	¹³⁷ 834 ± 34	²¹⁵ 2230 ± 34	²¹² 2133 ± 81						
234	neosystems-002	599441	349942	²⁴² 1222	¹²² 2048 ± 0	³²⁹ 1135 ± 2	³⁵⁸ 1855 ± 3	³⁵⁶ 2258 ± 5	³⁴² 2228 ± 3	³⁰⁰ 2247 ± 3	³⁴¹ 18752 ± 167	³⁴² 18610 ± 213						
235	neosystems-003	599442	349942	²⁴⁰ 1215	¹⁹⁸ 2048 ± 0	³³² 1143 ± 2	³⁵⁷ 1836 ± 7	³⁵⁷ 2260 ± 3	³⁴⁷ 2273 ± 6	³⁰¹ 2273 ± 3	³⁴⁴ 19130 ± 223	³⁴⁴ 19167 ± 186						
236	netbridge-tech-001	133108	205875	⁹¹ 508	³⁵⁴ 4096 ± 0	⁷⁸⁵ 85 ± 1	⁴⁸³ 80 ± 0	⁴⁸⁴ 80 ± 0	⁴⁹² 80 ± 0	⁴¹¹³ 84 ± 4	³²¹ 9280 ± 74	³²¹ 9446 ± 512						
237	netbridge-tech-002	257687	49931	⁴⁹ 299	²²⁸ 2048 ± 0	²⁵⁵ 838 ± 6	²⁰⁹ 838 ± 2	¹⁸⁵ 839 ± 1	¹⁶³ 839 ± 3	¹⁴¹ 859 ± 5	²³⁹ 2893 ± 65	²⁴⁵ 3050 ± 123						
238	neurotechnology-012	147830	51395	¹⁷⁰ 814	⁵ 256 ± 0	⁷⁴ 384 ± 0	⁵³ 387 ± 0	³⁹ 404 ± 1	⁴³ 435 ± 1	⁶⁴ 583 ± 7	³¹¹⁹ 87 ± 7	³¹¹⁶ 87 ± 7						
239	neurotechnology-013	474749	85552	³⁵⁵ 2894	⁴¹ 514 ± 0	³⁰⁶ 1000 ± 1	²⁵⁹ 1006 ± 2	²⁴⁶ 1022 ± 2	²²⁷ 1053 ± 2	²¹³ 1195 ± 8	² 109 ± 4	¹ 110 ± 4						
240	nhn-001	336391	817674	¹²⁹ 662	³⁶³ 4096 ± 0	³¹³ 1027 ± 3	²⁶⁷ 1029 ± 1	²⁵⁰ 1029 ± 1	²²⁴ 1044 ± 1	¹⁹³ 1090 ± 1	³⁷⁴ 56650 ± 260	³⁷⁵ 56639 ± 210						
241	nhn-002	363471	817674	¹³³ 667	³⁴⁴ 4096 ± 0	³³¹ 1141 ± 3	²⁹¹ 1138 ± 2	²⁷⁷ 1141 ± 2	²⁵⁰ 1151 ± 6	²¹⁵ 1203 ± 2	³⁷³ 56608 ± 579	³⁷⁴ 56549 ± 606						
242	nodeflux-002	774668	690213	⁷⁶ 466	²⁰⁸ 2048 ± 0	²¹⁰ 708 ± 4	¹⁶⁹ 709 ± 4	¹⁵⁵ 716 ± 5	¹³² 716 ± 7	¹⁰⁹ 736 ± 3	²⁶² 3475 ± 62	²⁵⁹ 3408 ± 143						
243	notiontag-001	92753	427967	¹¹⁰ 566	⁵² 584 ± 0	²⁸⁷ 929 ± 35	²⁸⁰ 1092 ± 39	³⁵⁸ 3709 ± 81	³⁵⁸ 10233 ± 180	-	³⁶⁵ 43636 ± 286	³⁶⁵ 43724 ± 330						
244	notiontag-002	271987	967207	³⁵¹ 2840	³²⁰ 2120 ± 0	⁹⁷ 453 ± 2	⁷⁵ 453 ± 3	⁵⁶ 453 ± 3	⁴⁶ 458 ± 2	³⁵ 471 ± 3	³⁴⁷ 20278 ± 194	³⁴⁷ 20195 ± 186						
245	nsensecorp-002	187421	122407	¹⁰⁵ 554	¹⁸⁴ 2048 ± 0	⁵⁷ 333 ± 0	⁴¹ 333 ± 0	²⁷ 337 ± 0	²² 338 ± 0	¹⁹ 351 ± 0	³⁶⁸ 45965 ± 213	³⁶⁸ 45988 ± 158						
246	nsensecorp-003	199895	117041	¹⁴⁷ 710	²⁶³ 2048 ± 0	¹⁸⁸ 661 ± 0	¹⁵³ 664 ± 0	¹³⁴ 662 ± 1	¹¹⁰ 659 ± 1	⁸⁴ 659 ± 0	³⁶⁶ 44658 ± 51	³⁶⁷ 44654 ± 72						
247	ntechlab-011	786933	209458	³⁸⁵ 867	⁸⁰ 1280 ± 0	³³⁴ 1148 ± 2	²⁹² 1142 ± 1	²⁸¹ 1159 ± 1	²⁵⁸ 1185 ± 1	²²⁹ 1290 ± 3	⁴ 179 ± 11	⁵ 173 ± 11						
248	ntechlab-012	570796	212350	³⁸⁰ 5451	³²² 2560 ± 0	³⁶⁶ 1309 ± 1	³²⁹ 1323 ± 1	³²¹ 1331 ± 1	²⁹⁷ 1360 ± 1	²⁶⁴ 1460 ± 3	¹⁰ 211 ± 8	¹⁰ 211 ± 7						
249	omnigarde-001	200523	328882	⁷⁴ 464	¹⁶ 512 ± 0	²⁸⁹ 941 ± 0	²²⁶ 883 ± 1	¹⁹⁹ 886 ± 1	¹⁷⁹ 891 ± 1	¹⁴⁷ 898 ± 0	¹⁵⁷ 1405 ± 31	¹⁵⁴ 1379 ± 26						
250	omnigarde-002	368860	328882	¹⁵⁸ 757	⁵⁶ 1024 ± 0	³⁶³ 1303 ± 1	³¹¹ 1246 ± 1	²⁹⁶ 1249 ± 1	²⁷⁰ 1253 ± 1	²²⁴ 1261 ± 1	²³⁴ 2727 ± 34	²³⁴ 2686 ± 32						
251	omsecurity-000	45945	844976	²⁴ 150	⁶⁰ 1024 ± 0	²⁶ 185 ± 1	²⁰ 206 ± 2	¹⁵ 203 ± 1	⁹ 195 ± 1	⁹ 193 ± 1	³⁷ 481 ± 42	³⁵ 456 ± 20						
252	openface-001	0	40111	¹³ 100	¹⁸⁷ 2048 ± 0	¹⁷ 148 ± 1	¹⁰ 154 ± 0	³³ 365 ± 3	³⁵ 409 ± 9	⁷¹ 616 ± 31	⁵⁵ 608 ± 14	⁵⁹ 604 ± 13						
253	oz-003	484147	519652	³⁹⁰ 11949	²⁹⁰ 2053 ± 0	³⁷⁴ 1375 ± 12	³³⁹ 1388 ± 3	³⁵⁴ 1773 ± 16	³⁴⁰ 2039 ± 6	³²⁶ 3209 ± 5	³⁸² 73905 ± 456	³⁸² 73892 ± 444						
254	oz-004	373982	1075452	³⁸⁹ 8071	²⁸⁹ 2053 ± 0	²⁵³ 832 ± 7	²²¹ 871 ± 6	²⁰² 899 ± 10	²³³ 1078 ± 12	²⁸⁰ 1608 ± 10	³⁷⁷ 61654 ± 418	³⁷⁶ 61749 ± 450						
255	papsav1923-001	279210	52652	⁷⁸ 473	¹⁴³ 2048 ± 0	¹⁷² 626 ± 1	¹⁴² 628 ± 1	¹²² 630 ± 1	¹⁰⁶ 648 ± 2	¹¹³ 744 ± 3	⁸⁷ 725 ± 25	⁸⁸ 731 ± 28						
256	papsav1923-002	491185	24727	²³¹ 1136	²⁷⁸ 2052 ± 0	²³⁶ 792 ± 1	²⁵⁴ 978 ± 1	²⁵⁵ 1042 ± 1	²⁵¹ 1158 ± 1	²⁸³ 1641 ± 19	¹⁴⁰ 1209 ± 29	¹⁴³ 1206 ± 38						
257	paravision-008	542190	204400	²⁷⁵ 1448	³⁵⁵ 4096 ± 0	²⁰⁷ 699 ± 0	¹⁶⁶ 700 ± 0	¹⁵¹ 701 ± 0	¹²⁴ 702 ± 1	⁹⁸ 702 ± 0	²⁵ 337 ± 17	²⁶ 330 ± 13						
258	paravision-010	688291	205854	³²⁸ 2150	³⁶⁹ 4100 ± 0	¹⁷⁶ 634 ± 0	¹⁴⁷ 635 ± 0	¹²⁷ 635 ± 0	¹⁰¹ 635 ± 0	⁷⁹ 635 ± 1	¹⁶⁶ 1577 ± 35	¹⁶⁶ 1571 ± 32						
259	pensees-001	1619431	408932	³¹³ 1922	³⁸⁹ 8200 ± 0	³²⁶ 1108 ± 3	³⁴⁸ 1448 ± 17	³⁴⁰ 1439 ± 10	³¹⁹ 1464 ± 5	²⁷⁶ 1546 ± 9	²⁵¹ 3151 ± 34	²⁵⁰ 3143 ± 25						
260	pixelall-006	0	746305	¹⁹⁸ 934	³²³ 2560 ± 0	³⁰⁹ 1024 ± 3	²⁶⁶ 1028 ± 2	²⁵² 1033 ± 1	²²⁰ 1032 ± 1	¹⁸² 1054 ± 2	⁹⁰ 754 ± 14	⁸⁷ 722 ± 10						
261	pixelall-007	0	444912	²⁶⁰ 1349	¹³⁰ 2048 ± 0	³¹² 1026 ± 4	²⁷⁰ 1038 ± 2	²⁶⁶ 1089 ± 2	²³⁴ 1087 ± 2	¹⁹⁶ 1124 ± 2	⁸³ 708 ± 14	⁸³ 701 ± 19						
262	psl-008	954351	524525	³⁶⁵ 3807	³²⁸ 3144 ± 0	³⁸⁰ 1412 ± 4	³⁴⁷ 1415 ± 3	³³⁹ 1416 ± 2	³¹² 1418 ± 2	²⁵⁶ 1418 ± 2	¹³ 259 ± 22	¹⁶ 252 ± 22						
263	psl-009	411027	411504	³⁷⁸ 5369	³⁷⁵ 4168 ± 0	³⁷⁶ 1382 ± 2	³³⁷ 1381 ± 1	³³¹ 1383 ± 1										

	ALGORITHM	CONFIG	LIBRARY	TEMPLATE								COMPARISON ⁴		
				NAME				GENERATION TIME (ms) ⁴				TIME (ns) ⁵		
				(KB) ¹	(KB) ²	(MB) ³	(B)	MUGSHOT	480x720	960x1440	1600x2400	3000x4500	GENUINE	IMPOSTOR
265	pxl-001	110116	78231	²⁵ 168	²⁵ 512 ± 0	¹¹ 101 ± 5	⁷ 104 ± 5	¹² 189 ± 12	³⁴ 408 ± 27	²⁶⁷ 1470 ± 144	²⁹³ 5598 ± 45	²⁹³ 5590 ± 68		
266	pyramid-000	372608	219883	¹⁶⁷ 804	³⁰⁵ 2056 ± 0	¹⁴⁶ 583 ± 2	-	-	-	-	³¹⁴ 7147 ± 59	³¹⁶ 7586 ± 425		
267	qnap-000	186731	15598	⁴² 272	²³⁸ 2048 ± 0	²¹² 726 ± 9	⁷⁷ 457 ± 1	⁵⁷ 458 ± 0	⁴⁹ 464 ± 1	³⁸ 482 ± 2	⁷³ 660 ± 25	⁷⁵ 654 ± 29		
268	qnap-001	196210	13399	⁴⁵ 286	¹¹¹ 2048 ± 0	¹⁶⁶ 614 ± 1	¹³⁸ 615 ± 1	¹²¹ 627 ± 1	⁹⁸ 623 ± 1	⁷⁷ 634 ± 2	⁷¹ 649 ± 11	⁷³ 648 ± 14		
269	quantasoft-003	370518	211354	²¹⁷ 1058	¹⁷⁵ 2048 ± 0	¹⁷⁵ 632 ± 2	¹⁴⁶ 634 ± 0	¹²³ 632 ± 0	¹⁰⁰ 631 ± 1	⁷⁶ 634 ± 0	⁹ 201 ± 7	⁵ 203 ± 8		
270	rankone-011	0	179209	²² 146	⁸ 261 ± 0	¹⁴⁰ 567 ± 1	¹¹⁶ 557 ± 1	⁹⁹ 567 ± 1	⁸¹ 586 ± 1	⁹² 682 ± 3	¹⁷ 283 ± 14	¹² 220 ± 19		
271	rankone-012	0	264182	¹⁹ 134	⁷ 261 ± 0	¹³⁹ 564 ± 3	¹¹⁴ 554 ± 1	⁹⁸ 564 ± 1	⁸² 586 ± 1	⁹⁶ 695 ± 1	¹⁶ 273 ± 17	¹⁴ 231 ± 14		
272	realnetworks-005	172253	56755	¹⁴¹ 697	²⁹⁸ 2056 ± 0	³¹ 211 ± 4	¹⁹ 205 ± 3	²⁰ 290 ± 6	⁶⁶ 515 ± 17	²³² 1312 ± 78	¹⁴¹ 1213 ± 17	¹⁴⁴ 1207 ± 16		
273	realnetworks-006	466225	56771	²⁸⁸ 1588	²⁹⁵ 2056 ± 0	¹⁷⁸ 638 ± 4	¹⁴³ 630 ± 3	¹³⁸ 672 ± 5	¹²⁶ 706 ± 5	¹²³ 774 ± 5	³⁴ 469 ± 19	⁴⁰ 478 ± 25		
274	regula-000	262444	29384	¹²³ 610	¹³⁶ 2048 ± 0	³⁴³ 1187 ± 1	²⁸⁷ 1126 ± 1	²⁷² 1129 ± 0	²⁴² 1132 ± 1	²⁰⁶ 1159 ± 1	⁴¹ 491 ± 16	⁴² 500 ± 22		
275	regula-001	256075	25980	²⁰⁶ 976	¹⁹¹ 2048 ± 0	³⁵⁸ 1284 ± 1	³⁰⁶ 1220 ± 1	²⁹⁴ 1222 ± 1	²⁶⁷ 1226 ± 1	²²³ 1255 ± 1	²⁷ 361 ± 10	²⁷ 342 ± 25		
276	remarkai-001	241857	868314	¹⁵² 730	²⁸⁸ 2052 ± 0	²⁵² 831 ± 6	²¹² 849 ± 18	²⁵⁹ 1055 ± 25	²⁶³ 1198 ± 34	²⁷³ 1519 ± 38	¹⁴⁵ 1229 ± 20	¹⁰⁰ 805 ± 56		
277	remarkai-003	280516	58559	³⁶⁹ 3896	³⁷⁰ 4100 ± 0	³⁰³ 986 ± 1	²⁵⁶ 993 ± 1	²⁴¹ 992 ± 1	²¹³ 999 ± 3	¹⁷⁵ 1019 ± 2	⁹⁸ 787 ± 20	⁹⁷ 793 ± 22		
278	rendip-000	0	437653	¹³⁵ 682	⁹¹ 2048 ± 0	¹⁰¹ 464 ± 2	⁷⁸ 458 ± 0	⁶⁵ 473 ± 0	⁵⁵ 483 ± 1	⁶⁰ 556 ± 4	⁴⁶ 576 ± 13	⁴⁸ 573 ± 11		
279	revealmedia-005	293933	202465	¹⁶⁰ 763	³⁶⁷ 4100 ± 0	⁸⁸ 428 ± 0	⁶⁵ 428 ± 0	⁴⁸ 430 ± 0	⁴² 433 ± 0	³⁰ 442 ± 0	²⁰⁴ 2023 ± 38	²⁰⁴ 2009 ± 26		
280	revealmedia-006	293933	200912	¹⁵⁶ 741	²⁸³ 2052 ± 0	⁷² 381 ± 0	⁵² 381 ± 0	³⁶ 382 ± 0	²⁹ 384 ± 0	²⁶ 394 ± 0	⁶⁴ 626 ± 35	⁵⁶ 600 ± 2		
281	rokid-000	258612	396624	²⁴¹ 1218	³⁰⁸ 2056 ± 0	¹³² 546 ± 3	¹⁰⁸ 542 ± 2	⁹³ 545 ± 1	⁶⁸ 522 ± 3	⁶² 563 ± 4	²⁶¹ 3457 ± 62	²⁶³ 3463 ± 77		
282	rokid-001	641223	413733	²²⁰ 1071	³¹³ 2060 ± 0	²⁷⁹ 911 ± 2	²³³ 901 ± 5	²⁰¹ 899 ± 2	¹⁸² 900 ± 3	¹⁴⁸ 901 ± 3	²⁵⁰ 3345 ± 50	²⁵⁶ 3346 ± 149		
283	s1-003	145509	95446	¹⁷³ 817	³³⁹ 4096 ± 0	²⁹¹ 947 ± 0	²⁴⁹ 959 ± 0	²²⁷ 952 ± 0	²⁰⁰ 952 ± 1	¹⁶² 955 ± 1	²⁶⁷ 3657 ± 19	²⁶⁷ 3652 ± 16		
284	s1-004	246514	202623	¹⁴³ 700	²⁰⁰ 2048 ± 0	²⁴³ 815 ± 0	²⁰⁰ 818 ± 1	¹⁷⁹ 818 ± 1	¹⁵⁷ 820 ± 1	¹³⁴ 828 ± 1	²⁵⁴ 3245 ± 100	²⁵¹ 3161 ± 88		
285	saffe-001	85973	62488	²⁷ 168	⁷⁸ 1280 ± 0	⁴⁴ 281 ± 1	-	-	-	-	¹⁴⁶ 1274 ± 19	¹⁴⁸ 1277 ± 26		
286	saffe-002	260622	28285	¹⁸¹ 855	¹¹⁶ 2048 ± 0	²⁴⁵ 817 ± 11	¹⁹⁷ 805 ± 15	¹⁷⁵ 809 ± 19	¹⁵⁵ 815 ± 29	¹³⁰ 813 ± 23	⁸⁵ 717 ± 7	⁸⁶ 714 ± 29		
287	samsungsds-000	0	307431	²²³ 1083	¹²⁶ 2048 ± 0	⁵⁴ 316 ± 0	⁴⁰ 326 ± 5	²⁵ 328 ± 4	²⁰ 327 ± 1	¹⁶ 343 ± 0	³⁵⁰ 23722 ± 295	³⁵⁰ 23874 ± 305		
288	samtech-001	288082	219883	¹²¹ 605	²⁹⁷ 2056 ± 0	⁵⁰ 294 ± 3	-	-	-	-	³¹⁷ 7694 ± 59	³¹⁷ 7678 ± 91		
289	scanovate-002	256986	457227	¹⁸⁰ 850	¹⁵² 2048 ± 0	²⁰⁶ 696 ± 32	¹⁷⁰ 713 ± 33	¹⁶¹ 738 ± 28	¹⁴⁹ 779 ± 32	²¹⁰ 1172 ± 53	²⁴⁴ 3021 ± 38	²⁴⁸ 3120 ± 163		
290	scanovate-003	135585	89469	¹⁶⁸ 808	¹⁹⁹ 2048 ± 0	¹⁴⁸ 585 ± 1	¹³⁶ 613 ± 12	¹⁰⁵ 591 ± 1	⁹¹ 610 ± 2	⁹³ 684 ± 1	²⁴⁰ 2926 ± 22	²⁴⁰ 2925 ± 20		
291	securifai-003	303794	13512	³⁵³ 2868	³⁷³ 4104 ± 0	¹³³ 549 ± 7	¹¹³ 550 ± 7	⁹⁵ 549 ± 7	⁷⁵ 546 ± 6	⁵⁴ 546 ± 6	¹⁷⁵ 1714 ± 26	¹⁷⁵ 1713 ± 37		
292	securifai-004	282177	12027	¹²⁶ 636	¹³⁸ 2048 ± 0	²⁶³ 869 ± 1	²¹⁹ 867 ± 1	¹⁹⁰ 867 ± 1	¹⁷⁰ 867 ± 1	¹⁴⁴ 865 ± 1	¹⁷³ 1711 ± 19	¹⁷⁴ 1705 ± 29		
293	sensetime-005	765353	37673	³⁸³ 6133	⁶⁷ 1028 ± 0	³⁷² 1361 ± 27	³²² 1304 ± 1	³¹⁶ 1319 ± 1	²⁹⁰ 1360 ± 1	²⁷² 1514 ± 1	¹⁴⁴ 1223 ± 28	¹⁴² 1184 ± 29		
294	sensetime-006	765353	37673	³⁸² 5994	⁶⁸ 1028 ± 0	³⁷¹ 1352 ± 17	³²⁴ 1311 ± 1	³¹⁷ 1323 ± 1	²⁹³ 1357 ± 1	²⁷⁴ 1523 ± 2	¹³⁹ 1179 ± 28	¹⁴¹ 1157 ± 29		
295	sertis-000	265572	68770	⁶⁵ 427	¹⁰³ 2048 ± 0	²²⁰ 754 ± 0	¹⁸⁵ 759 ± 0	¹⁶⁸ 764 ± 0	¹⁴⁵ 760 ± 0	¹²⁰ 763 ± 0	¹⁶³ 1497 ± 29	¹⁶⁷ 1582 ± 38		
296	sertis-002	460790	68929	²⁶⁷ 1391	¹⁰⁰ 2048 ± 0	³⁴¹ 1181 ± 1	²⁹⁷ 1178 ± 0	²⁸⁸ 1183 ± 0	²⁶¹ 1187 ± 0	²²⁰ 1221 ± 0	¹²⁸ 1086 ± 32	¹²⁷ 1076 ± 31		
297	seventhsense-000	369850	1561668	¹⁷⁵ 824	²⁷¹ 2052 ± 0	³⁵⁴ 1250 ± 3	³¹⁴ 1257 ± 1	²⁹⁸ 1261 ± 1	²⁷³ 1259 ± 1	²²⁷ 1272 ± 2	¹⁸⁷ 1800 ± 35	¹⁸⁷ 1787 ± 32		
298	shaman-000	0	120033	⁸⁸ 507	³⁶⁰ 4096 ± 0	¹⁸³ 653 ± 16	-	-	-	-	³⁰ 380 ± 25	³⁰ 379 ± 31		
299	shaman-001	0	174446	⁹³ 511	³³² 4096 ± 0	⁴⁹ 294 ± 2	-	-	-	-	⁶⁸ 635 ± 19	³⁴ 441 ± 25		
300	shu-002	731250	148309	¹⁸⁷ 890	³⁵² 4096 ± 0	²¹⁹ 751 ± 2	¹⁸⁹ 769 ± 4	²¹⁴ 922 ± 4	³¹⁶ 1431 ± 9	³²⁷ 3489 ± 47	³⁹⁴ 2930763 ± 47355	³⁹⁴ 2929759 ± 39149		
301	shu-003	428774	146940	⁹² 511	¹³² 2048 ± 0	²⁴⁷ 820 ± 6	²⁰⁵ 828 ± 3	²²³ 941 ± 9	²⁸² 1308 ± 15	³²³ 3045 ± 44	²²³ 2506 ± 26	²²⁴ 2512 ± 38		
302	siat-002	486842	7738	³³⁵ 2434	²⁸² 2052 ± 0	¹⁴⁵ 579 ± 0	-	-	-	-	⁹⁵ 769 ± 13	⁹² 750 ± 13		
303	siat-005	380936	16935	²⁵⁴ 1298	¹⁶³ 2048 ± 0	⁷⁷ 403 ± 0	⁵⁷ 400 ± 0	³⁸ 401 ± 0	³¹ 403 ± 1	²⁸ 422 ± 7	⁴⁷ 577 ± 13	⁴⁹ 580 ± 17		
304	sjtu-003	480795	148243	¹⁰¹ 538	²⁴⁷ 2048 ± 0	²⁴⁸ 821 ± 2	²⁰¹ 820 ± 2	²¹⁵ 923 ± 3	²⁶⁴ 1201 ± 3	³⁰⁵ 2373 ± 9	¹⁶⁵ 1560 ± 20	¹⁶⁴ 1560 ± 14		
305	sjtu-004	1953267	241108	³⁴⁴ 2727	³⁷⁸ 4608 ± 0	³⁴⁹ 1236 ± 2	³⁰³ 1209 ± 2	³⁰⁸ 1294 ± 4	³²⁵ 1554 ± 5	³¹⁶ 2738 ± 8	²⁴⁷ 3057 ± 14	²⁴⁷ 3070 ± 20		
306	sktelecom-000	527132	298496	²⁵⁷ 1311	⁸² 1536 ± 0	³²⁷ 1110 ± 1	²⁸⁴ 1113 ± 1	²⁶⁹ 1114 ± 1	²³⁷ 1120 ± 1	²⁰³ 1155 ± 1	³⁵⁸ 26583 ± 128	³⁵⁷ 26508 ± 126		
307	smartengines-000	1711	3025	³ 50	¹⁰ 288 ± 0	¹⁹ 168 ± 7	¹³ 180 ± 1	¹¹ 188 ± 3	¹² 217 ± 3	¹⁴ 275 ± 1	⁶ 197 ± 5	⁴ 167 ± 11		
308	smilart-002	111826	87805	⁴¹ 263	⁵⁷ 1024 ± 0	²¹ 176 ± 16	-	-	-	-	³⁴² 18784 ± 136	³⁴³ 18795 ± 151		

Notes

- 1 The configuration size does not capture static data included in libraries.
- 2 The library size is the combined total of all files provided in the submission lib folder. These libraries e.g. OpenCV may or may not be installed on any end user's platform natively and would not need to be installed with the algorithm. Some developers put neural network models in their libraries.
- 3 The memory usage is the peak resident set size reported by the ps system call during template generation.
- 4 The median template creation times are measured on Intel®Xeon®CPU E5-2630 v4 @ 2.20GHz processors.
- 5 The comparison durations, in nanoseconds, are estimated using std::chrono::high_resolution_clock which on the machine in (2) counts 1ns clock ticks. Precision is somewhat worse than that however. The ± value is the median absolute deviation times 1.48 for Normal consistency.

Table 13: Summary of algorithms and properties included in this report. The red superscripts give ranking for the quantity in that column.

	ALGORITHM	CONFIG	LIBRARY	TEMPLATE								COMPARISON ⁴		
				NAME	DATA	DATA	MEMORY	SIZE	GENERATION TIME (ms) ⁴				TIME (ns) ⁵	
									(KB) ¹	(KB) ²	(MB) ³	(B)	MUGSHOT	480x720
309	smilart-003	67339	91670	33192	30512 ± 0	23180 ± 12	14181 ± 10	22313 ± 22	112665 ± 49	3022299 ± 196	1531395 ± 74	1201027 ± 66		
310	sodec-000	836592	13142	3593186	3354096 ± 0	3181041 ± 2	2681032 ± 1	2531035 ± 1	2221037 ± 2	1881061 ± 2	1851794 ± 37	1841775 ± 23		
311	sqisoft-001	278968	386291	138688	3062056 ± 0	107477 ± 5	3311348 ± 18	3231353 ± 26	2881340 ± 14	2491393 ± 28	99797 ± 22	96788 ± 22		
312	sqisoft-002	278039	386291	132666	2912056 ± 0	103466 ± 8	81466 ± 2	64468 ± 11	47461 ± 6	36472 ± 4	91758 ± 11	93760 ± 23		
313	stachu-000	879661	624676	2181064	3564096 ± 0	241813 ± 25	-	-	-	-	2412979 ± 31	2433007 ± 75		
314	starhybrid-001	100509	289356	178845	1762048 ± 0	65358 ± 82	46355 ± 49	35379 ± 58	30401 ± 79	25393 ± 67	1251075 ± 51	1281078 ± 53		
315	sukshi-000	94035	688738	56372	39332768 ± 0	81407 ± 11	60413 ± 8	76504 ± 8	119689 ± 11	2771574 ± 28	3239817 ± 50	3229787 ± 62		
316	suprema-001	373423	41460	2991731	2112048 ± 0	234788 ± 1	204826 ± 2	207914 ± 2	2461146 ± 7	3092443 ± 4	2523212 ± 16	2543220 ± 22		
317	suprema-002	373808	41473	2981731	1442048 ± 0	233787 ± 3	208833 ± 3	216924 ± 4	2591185 ± 6	3112479 ± 3	2553255 ± 17	2553253 ± 14		
318	supremaid-001	258193	23479	102541	2032048 ± 0	108479 ± 1	85481 ± 0	67481 ± 0	59490 ± 0	50522 ± 0	81704 ± 19	74652 ± 19		
319	synesis-006	7319411	21817	2771472	3724104 ± 0	134549 ± 1	111546 ± 1	96552 ± 1	77558 ± 2	81639 ± 28	80697 ± 32	82688 ± 31		
320	synesis-007	1442961	24145	3362443	3273080 ± 0	3451215 ± 5	3161268 ± 30	3111306 ± 67	2831311 ± 58	2581423 ± 52	77684 ± 32	80686 ± 25		
321	synology-000	221021	25809	71453	1342048 ± 0	80407 ± 14	61415 ± 14	147694 ± 31	3051396 ± 58	3304568 ± 211	34619720 ± 203	34519767 ± 379		
322	synology-002	256713	25943	82488	1542048 ± 0	275886 ± 4	230892 ± 3	211920 ± 2	2141000 ± 5	2331317 ± 12	1601466 ± 32	1621496 ± 45		
323	sztu-000	338637	15871	2521298	1352048 ± 0	127531 ± 0	103532 ± 0	88533 ± 0	69537 ± 0	55548 ± 0	48585 ± 11	52592 ± 13		
324	sztu-001	338650	15871	2531298	1202048 ± 0	129535 ± 0	106537 ± 0	88538 ± 0	71540 ± 0	56553 ± 0	52599 ± 10	54598 ± 10		
325	t4isb-000	234227	115237	53343	2312048 ± 0	3071006 ± 5	2581001 ± 1	2451006 ± 1	2161009 ± 1	1761022 ± 2	2663586 ± 34	2643534 ± 34		
326	tech5-004	2410272	118858	3452733	12321 ± 0	266872 ± 2	2851117 ± 164	2681114 ± 182	2431134 ± 179	171999 ± 44	51597 ± 13	51592 ± 16		
327	tech5-005	1178769	120517	2721426	37512 ± 0	3571272 ± 109	2711038 ± 63	2571046 ± 39	2381124 ± 38	2391351 ± 44	2272573 ± 37	2282545 ± 32		
328	techsign-000	0	1101622	3171955	982048 ± 0	69366 ± 1	56398 ± 1	2831172 ± 3	3553065 ± 18	35210460 ± 65	2814758 ± 112	2804789 ± 93		
329	tevian-007	779934	19523	2971714	701032 ± 0	147583 ± 1	121579 ± 0	102580 ± 0	83588 ± 1	80636 ± 0	2854894 ± 65	2834841 ± 83		
330	tevian-008	847177	19519	3613490	691032 ± 0	273884 ± 2	235903 ± 1	204903 ± 1	184911 ± 1	159946 ± 1	2834828 ± 40	2824811 ± 41		
331	tiger-005	342866	253734	2821531	2862052 ± 0	3221097 ± 2	2771065 ± 2	2621066 ± 2	2291067 ± 3	1911088 ± 3	60620 ± 19	63615 ± 16		
332	tiger-006	421186	394688	146707	2752052 ± 0	3781392 ± 16	3451411 ± 10	3411444 ± 10	3231531 ± 11	2931848 ± 10	1911810 ± 20	1911801 ± 13		
333	tinkoff-001	274660	389272	118592	962048 ± 0	3311176 ± 3	2991179 ± 3	2841178 ± 3	2531169 ± 2	2161203 ± 3	2774361 ± 74	2754364 ± 75		
334	tongyi-005	1140701	138919	3272121	3192089 ± 0	18165 ± 1	-	-	-	-	34318924 ± 65	34620158 ± 103		
335	toppanidgate-000	671181	711850	3041786	3414096 ± 0	280915 ± 1	237916 ± 1	209916 ± 1	185917 ± 1	151917 ± 1	35625262 ± 84	35525264 ± 97		
336	toshiba-004	599297	27880	2911595	3032056 ± 0	3881447 ± 3	3501453 ± 2	3451457 ± 9	3181457 ± 3	2691479 ± 4	1181020 ± 25	115998 ± 32		
337	toshiba-005	599298	61113	2891593	3002056 ± 0	3901456 ± 4	3511454 ± 2	3461461 ± 2	3171455 ± 2	2631459 ± 2	1681613 ± 34	1681607 ± 28		
338	trueface-002	253947	123116	81486	882000 ± 0	67360 ± 0	50361 ± 0	46423 ± 0	86590 ± 1	-	5192 ± 14	7186 ± 19		
339	trueface-003	346530	24308	3703915	2122048 ± 0	3251107 ± 22	158677 ± 3	159732 ± 7	183905 ± 5	-	1103 ± 11	2112 ± 29		
340	tuputech-000	11476	17185	23233	1502048 ± 0	15122 ± 4	8120 ± 1	7142 ± 2	11196 ± 5	27411 ± 14	35123893 ± 406	35625279 ± 406		
341	turingtechvip-001	399874	54535	125617	1372048 ± 0	3771384 ± 4	3411391 ± 1	3331393 ± 1	3111411 ± 1	2681476 ± 2	1791733 ± 19	1791734 ± 20		
342	twface-000	661735	11782	3412610	1412048 ± 0	264871 ± 1	222873 ± 1	193873 ± 2	173876 ± 2	146898 ± 1	1641504 ± 29	1631510 ± 34		
343	twface-001	671511	11782	3522855	2542048 ± 0	283923 ± 1	242925 ± 2	218926 ± 1	190929 ± 2	156940 ± 2	1541400 ± 32	1551402 ± 37		
344	ulsee-001	370519	57261	-	2022048 ± 0	184654 ± 2	-	-	-	-	3036065 ± 94	3056228 ± 77		
345	uluface-002	0	480761	2241088	2502048 ± 0	267873 ± 42	214855 ± 9	233978 ± 24	2741271 ± 40	3032333 ± 68	34519207 ± 1114	34118501 ± 274		
346	uluface-003	97357	529422	2461264	3243072 ± 0	297965 ± 11	251968 ± 10	2641087 ± 20	3031387 ± 36	3102469 ± 86	35726057 ± 195	35926865 ± 566		
347	unissey-001	0	1956593	2871584	3434096 ± 0	272880 ± 3	229892 ± 3	3441452 ± 8	3543048 ± 12	35010017 ± 387	1591463 ± 35	1601471 ± 34		
348	upc-001	0	89914	2221077	731052 ± 0	136551 ± 15	168703 ± 56	156724 ± 51	142751 ± 49	142863 ± 33	2493114 ± 44	2523165 ± 97		
349	vcog-002	3229434	118946	3633666	39461504 ± 5	64357 ± 25	-	-	-	-	390296154 ± 3077	390296436 ± 4183		
350	vd-002	254498	34389	139688	42516 ± 0	200684 ± 5	159679 ± 4	139676 ± 5	121693 ± 5	114754 ± 5	193300 ± 14	22319 ± 32		
351	vd-003	254505	44051	140696	2762052 ± 0	204691 ± 5	163690 ± 5	141683 ± 4	120691 ± 5	105722 ± 5	1161003 ± 11	1161001 ± 7		
352	veridas-006	355669	896424	3221990	892048 ± 0	271880 ± 8	228885 ± 8	3011271 ± 18	3462242 ± 38	3426414 ± 156	37556940 ± 149	37766077 ± 194		

Notes

- 1 The configuration size does not capture static data included in libraries.
- 2 The library size is the combined total of all files provided in the submission lib folder. These libraries e.g. OpenCV may or may not be installed on any end user's platform natively and would not need to be installed with the algorithm. Some developers put neural network models in their libraries.
- 3 The memory usage is the peak resident set size reported by the ps system call during template generation.
- 4 The median template creation times are measured on Intel®Xeon®CPU E5-2630 v4 @ 2.20GHz processors.
- 5 The comparison durations, in nanoseconds, are estimated using std::chrono::high_resolution_clock which on the machine in (2) counts 1ns clock ticks. Precision is somewhat worse than that however. The ± value is the median absolute deviation times 1.48 for Normal consistency.

Table 14: Summary of algorithms and properties included in this report. The red superscripts give ranking for the quantity in that column.

	ALGORITHM	CONFIG	LIBRARY	TEMPLATE									COMPARISON ⁴			
				NAME		DATA		MEMORY		SIZE		GENERATION TIME (ms) ⁴			TIME (ns) ⁵	
				(KB) ¹	(KB) ²	(MB) ³	(B)	MUGSHOT	480x720	960x1440	1600x2400	3000x4500	GENUINE	IMPOSTOR		
353	veridas-007	355105	891492	³³⁹ 2527	¹¹⁰ 2048 ± 0	²⁶⁵ 872 ± 9	²²³ 875 ± 8	²⁹⁷ 1261 ± 18	³⁴⁵ 2238 ± 38	³⁴⁰ 6374 ± 147	⁷² 655 ± 16	⁷⁸ 660 ± 19				
354	verigram-000	256209	7798	³⁰⁹ 1842	²³⁷ 2048 ± 0	²³⁷ 807 ± 1	²⁰² 821 ± 1	²³¹ 972 ± 2	²⁹⁴ 1358 ± 3	³¹⁹ 2848 ± 13	¹⁴³ 1222 ± 17	¹⁴⁵ 1219 ± 17				
355	verihubs-inteligensia-000	209562	51877	⁶⁶ 427	⁹² 2048 ± 0	¹⁴² 567 ± 0	³⁵⁵ 1558 ± 8	³⁵¹ 1560 ± 8	³²⁶ 1568 ± 8	²⁸¹ 1621 ± 8	³⁴⁹ 22351 ± 91	³⁴⁹ 22371 ± 81				
356	via-000	124422	11151	²⁰⁴ 964	²²⁶ 2048 ± 0	²⁰⁹ 707 ± 8	¹⁸⁰ 740 ± 5	²⁰⁵ 906 ± 41	¹⁹⁶ 941 ± 40	¹⁸⁰ 1040 ± 5	¹¹⁰ 966 ± 28	¹¹⁹ 1021 ± 44				
357	via-001	370255	11151	²⁹⁵ 1697	²³⁵ 2048 ± 0	²⁹⁶ 964 ± 3	²⁶² 1011 ± 3	²⁴⁸ 1026 ± 4	²²⁵ 1045 ± 3	²⁰⁰ 1137 ± 28	¹¹² 983 ± 31	¹¹³ 989 ± 40				
358	videmo-000	139643	39470	⁵⁷ 390	²⁴⁶ 2048 ± 0	¹⁶ 142 ± 5	⁹ 150 ± 4	⁸ 150 ± 6	⁶ 151 ± 4	⁶ 155 ± 8	⁴² 513 ± 16	⁴² 523 ± 38				
359	videmo-001	212051	95063	⁵¹ 304	¹³¹ 2048 ± 0	²⁸ 199 ± 0	¹¹ 164 ± 0	⁹ 164 ± 0	⁷ 164 ± 0	¹⁸ 165 ± 0	¹⁸ 296 ± 17	¹⁹ 288 ± 16				
360	videonetics-001	30875	5963	⁴ 61	²⁸ 512 ± 0	³⁶ 262 ± 3	²⁹ 273 ± 1	⁵³ 439 ± 3	¹⁵⁸ 820 ± 3	³⁰⁶ 2393 ± 43	¹³⁵ 1153 ± 38	¹³⁷ 1142 ± 65				
361	videonetics-002	121981	6289	¹⁵ 115	²⁸⁵ 2052 ± 0	⁴⁵ 282 ± 5	³⁶ 295 ± 1	⁸⁰ 513 ± 4	²¹⁸ 1029 ± 3	³²⁵ 3151 ± 46	¹⁴² 1219 ± 57	¹⁴⁶ 1262 ± 56				
362	viettelnighttech-000	259471	215557	⁶⁴ 419	¹⁶⁰ 2048 ± 0	⁹⁹ 461 ± 1	⁷⁹ 461 ± 2	⁵⁹ 461 ± 1	⁵² 467 ± 2	⁴¹ 494 ± 0	⁵³ 599 ± 11	⁵⁰ 591 ± 13				
363	vigilantsolutions-010	348798	49973	¹⁷⁷ 840	⁸⁴ 1548 ± 0	¹⁶⁷ 615 ± 0	¹⁴⁴ 631 ± 0	¹²⁴ 632 ± 0	¹⁰² 636 ± 0	⁸⁵ 659 ± 0	⁴⁰ 490 ± 13	⁴¹ 488 ± 11				
364	vigilantsolutions-011	255661	49973	¹¹⁷ 591	⁸⁵ 1548 ± 0	⁷⁶ 402 ± 0	⁶² 418 ± 0	⁴⁴ 418 ± 0	³⁶ 422 ± 0	³² 445 ± 0	²⁶ 339 ± 20	²⁸ 366 ± 37				
365	vinai-000	402391	866522	²¹² 1032	⁹⁵ 2048 ± 0	³²³ 1099 ± 1	²⁸² 1095 ± 1	²⁶⁷ 1093 ± 1	²³⁶ 1099 ± 1	¹⁹⁸ 1126 ± 1	²⁴² 2996 ± 20	²⁴² 2993 ± 26				
366	vinbigdata-001	271405	44746	¹¹⁵ 589	¹⁴⁶ 2048 ± 0	³⁸³ 1400 ± 5	³⁴² 1393 ± 2	³³² 1391 ± 2	³⁰⁴ 1393 ± 1	²⁵² 1404 ± 1	¹⁵⁰ 1351 ± 50	¹⁵¹ 1310 ± 38				
367	vion-000	228219	7533	⁸⁶ 498	²⁸¹ 2052 ± 0	⁵⁸ 333 ± 1	-	-	-	-	-	³⁶³ 39839 ± 3561	³⁵⁸ 26830 ± 2241			
368	visage-000	49218	70150	⁷ 73	¹⁷ 512 ± 0	³ 27 ± 0	¹ 27 ± 0	¹ 31 ± 0	² 38 ± 0	² 63 ± 0	²¹⁴ 2220 ± 14	²¹⁵ 2218 ± 14				
369	visionbox-001	256869	190645	¹¹² 579	²³⁴ 2048 ± 0	³⁰¹ 983 ± 7	²⁸¹ 1093 ± 46	³²⁵ 1360 ± 68	³⁴³ 2181 ± 105	³³⁸ 5955 ± 281	¹³⁶ 1161 ± 22	¹⁴⁰ 1154 ± 20				
370	visionbox-002	259063	135281	¹²⁴ 612	³¹¹ 2059 ± 0	¹¹⁰ 482 ± 1	⁸⁷ 482 ± 0	⁶⁸ 484 ± 1	⁶⁰ 492 ± 1	⁴⁸ 517 ± 3	²⁰² 1969 ± 44	²⁰⁰ 1931 ± 42				
371	visionlabs-010	1067280	19357	¹⁸⁹ 902	⁴⁰ 513 ± 0	²¹⁴ 730 ± 0	¹⁷¹ 717 ± 1	¹⁵² 709 ± 0	¹³⁰ 713 ± 1	¹¹¹ 739 ± 0	⁵⁴ 600 ± 41	⁶⁵ 626 ± 35				
372	visionlabs-011	1067280	19353	¹⁸³ 862	³⁹ 513 ± 0	²¹⁵ 731 ± 1	¹⁷² 717 ± 1	¹⁵³ 710 ± 1	¹³¹ 714 ± 1	¹¹² 741 ± 1	⁴⁴ 556 ± 26	⁴⁶ 559 ± 25				
373	visteam-002	186440	30888	¹⁰³ 547	³³⁶ 4096 ± 0	²⁵¹ 829 ± 5	²⁰⁷ 832 ± 6	¹⁸⁴ 839 ± 7	¹⁶⁸ 853 ± 6	¹⁷⁴ 1013 ± 14	³¹¹ 6952 ± 118	³¹⁰ 6970 ± 120				
374	visteam-003	215359	33730	⁸⁴ 489	³³⁷ 4096 ± 0	³⁵³ 1249 ± 4	³¹² 1251 ± 4	³⁰⁰ 1266 ± 5	²⁷⁵ 1272 ± 5	²⁴¹ 1370 ± 9	³⁰⁸ 6816 ± 111	³⁰⁸ 6816 ± 105				
375	vnpt-002	271649	3203296	⁸³ 489	¹⁹² 2048 ± 0	²¹⁶ 739 ± 2	¹⁷⁷ 731 ± 2	¹⁶² 740 ± 1	¹⁴⁰ 742 ± 2	¹¹⁹ 763 ± 2	⁹⁴ 766 ± 13	⁹⁴ 762 ± 13				
376	vnpt-003	369956	297799	¹⁴⁸ 714	³³⁴ 4096 ± 0	³⁶⁷ 1315 ± 4	³²⁶ 1315 ± 4	³¹⁵ 1318 ± 2	²⁹¹ 1350 ± 3	²⁵⁹ 1428 ± 3	³¹⁶ 7397 ± 31	³¹⁵ 7384 ± 29				
377	vocord-009	1380132	201560	³⁷³ 4162	⁸⁷ 1920 ± 0	³⁹³ 1472 ± 2	³⁵³ 1472 ± 1	³⁵⁰ 1549 ± 1	³³⁰ 1667 ± 2	²⁹⁶ 2064 ± 2	²⁰⁵ 2052 ± 50	²⁰⁸ 2056 ± 39				
378	vocord-010	902552	206873	³⁶⁸ 3858	⁷⁶ 1088 ± 0	³⁹¹ 1459 ± 2	³⁵² 1459 ± 1	³⁴⁷ 1463 ± 2	³²² 1484 ± 1	²⁷⁵ 1535 ± 3	²³³ 2724 ± 31	²³¹ 2653 ± 45				
379	vts-000	256589	169760	²⁹⁶ 1704	¹⁸³ 2048 ± 0	¹¹³ 486 ± 1	⁸⁶ 481 ± 0	⁶⁹ 484 ± 0	⁵⁶ 485 ± 1	⁴⁹ 517 ± 0	³⁸⁵ 124209 ± 352	³⁸⁵ 123652 ± 358				
380	winsense-001	264428	32035	¹⁹⁶ 922	⁷⁹ 1280 ± 0	²²⁵ 766 ± 7	²⁷⁴ 1058 ± 47	²³⁶ 983 ± 97	²²⁶ 1053 ± 119	²³⁴ 1320 ± 84	¹⁶⁹ 1631 ± 28	²⁰² 1964 ± 171				
381	winsense-002	281379	25780	³⁰³ 1781	¹⁰² 2048 ± 0	¹¹⁶ 494 ± 2	⁹⁵ 498 ± 1	⁸² 519 ± 1	⁷⁰ 537 ± 1	⁷⁸ 634 ± 1	¹⁷² 1683 ± 8	¹⁷² 1685 ± 7				
382	wuhantianyu-001	465118	66457	¹⁸⁴ 866	¹⁶⁶ 2048 ± 0	¹⁷⁹ 642 ± 1	¹⁴⁸ 642 ± 1	¹³⁰ 644 ± 0	¹⁰⁸ 652 ± 0	⁹⁷ 697 ± 0	³²² 9502 ± 151	³²³ 9920 ± 253				
383	x-laboratory-000	520020	197310	²⁸¹ 1524	²⁹⁴ 2056 ± 0	²³⁸ 808 ± 7	²³² 897 ± 113	²⁰⁶ 907 ± 103	¹⁷⁸ 886 ± 103	⁸⁹ 673 ± 39	⁸⁸ 725 ± 19	⁹⁷ 749 ± 34				
384	x-laboratory-001	625140	398792	³¹⁰ 1844	³⁰⁷ 2056 ± 0	¹⁶⁰ 586 ± 2	¹³² 596 ± 5	¹¹³ 603 ± 6	⁹⁶ 620 ± 7	¹²⁴ 793 ± 14	¹⁰⁰ 813 ± 28	¹⁰⁴ 872 ± 32				
385	xforwardai-001	340100	51163	³²⁹ 2173	¹⁸¹ 2048 ± 0	³⁴⁰ 1180 ± 2	³⁰² 1182 ± 1	²⁹¹ 1194 ± 1	²⁶⁰ 1186 ± 2	²¹⁴ 1203 ± 1	⁹⁷ 779 ± 17	⁹⁸ 797 ± 13				
386	xforwardai-002	707715	51163	³²¹ 1989	³³¹ 4096 ± 0	²⁹⁰ 944 ± 1	²⁴⁸ 942 ± 1	²²⁵ 943 ± 4	¹⁹⁴ 935 ± 1	¹⁶⁴ 967 ± 1	¹⁵⁸ 1406 ± 8	¹⁵⁶ 1405 ± 13				
387	xm-000	578041	148920	¹³⁷ 688	²⁸⁰ 2052 ± 0	²⁷⁰ 878 ± 2	²²⁵ 882 ± 1	²³⁹ 988 ± 2	²⁷¹ 1258 ± 3	³⁰⁸ 2434 ± 7	¹⁷⁰ 1634 ± 17	¹⁶⁹ 1632 ± 20				
388	yisheng-004	486351	38653	²⁴⁹ 1279	³²⁹ 3704 ± 0	⁷¹ 378 ± 12	-	-	-	-	⁷⁹ 693 ± 137	⁴⁴ 526 ± 34				
389	yitu-003	1525719	138919	³⁶⁴ 3737	³¹⁸ 2082 ± 0	²⁶¹ 860 ± 0	-	-	-	-	³⁴⁰ 18305 ± 71	³⁴⁰ 18286 ± 62				
390	yooniik-002	453720	265415	³⁴⁸ 2755	¹⁶⁹ 2048 ± 0	³³³ 1145 ± 4	²⁸⁰ 1123 ± 2	²⁷¹ 1124 ± 2	²³⁹ 1125 ± 2	¹⁹⁷ 1126 ± 3	⁹³ 761 ± 32	⁹⁰ 736 ± 32				
391	yooniik-003	346691	265415	³³¹ 2196	²⁶⁶ 2048 ± 0	³⁰⁴ 991 ± 3	²⁵⁵ 980 ± 1	²³⁷ 984 ± 4	²⁰⁶ 982 ± 1	¹⁶⁹ 983 ± 1	⁷⁶ 684 ± 45	⁷⁸ 678 ± 41				
392	ytu-000	1477360	44032	³³⁷ 2484	¹¹⁵ 2048 ± 0	¹²⁶ 530 ± 0	¹⁰⁴ 533 ± 0	¹²⁸ 640 ± 0	¹⁶⁹ 861 ± 2	²⁹⁵ 1949 ± 8	³⁶⁰ 31797 ± 131	³⁶¹ 31794 ± 133				
393	yuan-003	370419	147783	³⁵⁴ 2885	²⁶¹ 2048 ± 0	³⁸⁵ 1405 ± 2	³⁴⁶ 1413 ± 3	³⁴³ 1446 ± 3	³²⁴ 1547 ± 5	²⁹⁴ 1878 ± 5	²¹⁹ 2320 ± 32	²¹⁹ 2287 ± 34				
394	yuan-004	428665	50011	²⁶¹ 1353	³⁵⁹ 4096 ± 0	¹⁴¹ 567 ± 0	¹²⁰ 569 ± 0	¹⁰⁰ 573 ± 0	⁷⁰ 579 ± 0	⁶⁹ 607 ± 0	²⁹⁶ 5816 ± 35	²⁹⁸ 5800 ± 31				

Notes
 1 The configuration size does not capture static data included in libraries.
 2 The library size is the combined total of all files provided in the submission lib folder. These libraries e.g. OpenCV may or may not be installed on any end user's platform natively and would not need to be installed with the algorithm. Some developers put neural network models in their libraries.
 3 The memory usage is the peak resident set size reported by the ps system call during template generation.
 4 The median template creation times are measured on Intel®Xeon®CPU E5-2630 v4 @ 2.20GHz processors.
 5 The comparison durations, in nanoseconds, are estimated using std::chrono::high_resolution_clock which on the machine in (2) counts 1ns clock ticks. Precision is somewhat worse than that however. The \pm value is the median absolute deviation times 1.48 for Normal consistency.

Table 15: Summary of algorithms and properties included in this report. The red superscripts give ranking for the quantity in that column.

	Algorithm	FALSE NON-MATCH RATE (FNMR)										LESS CONSTRAINED, NON-COOP.					
		CONSTRAINED, COOPERATIVE								WILD							
		Name	VISAMC	VISA	MUGSHOT	MUGSHOT12+YRS	VISABORDER	BORDER	BORDER	1E-05							
	FMR	0.0001	1E-06	1E-05	1E-05	1E-06	1E-06	1E-06	1E-05	0.0001							
1	20face-000	0.1268	337	0.1828	333	0.1748	342	0.2768	342	0.1765	331	0.1864	278	0.0927	305	0.0405	239
2	20face-001	0.0521	317	0.0732	317	0.1414	337	0.2549	340	0.0769	312	0.1354	274	0.0419	271	0.0295	143
3	3divi-006	0.0064	147	0.0094	144	0.0047	124	0.0066	129	0.0091	132	0.0191	149	0.0113	133	0.0289	123
4	3divi-007	0.0024	34	0.0038	39	0.0028	35	0.0034	32	0.0046	47	0.0101	67	0.0082	77	0.0300	156
5	acer-001	0.0294	298	0.0504	304	0.0240	297	0.0463	299	0.0436	293	0.0622	244	0.0360	264	0.0307	166
6	acer-002	0.0169	270	0.0262	271	0.0103	228	0.0167	239	0.0182	231	0.0281	192	0.0159	189	0.0297	149
7	acisw-003	0.9682	392	0.9971	392	0.7892	380	0.8738	380	0.8752	374	0.8275	338	0.6698	360	0.4470	365
8	acisw-007	0.4276	368	0.5493	369	0.8425	381	0.9185	381	0.8424	369	0.9976	363	0.9930	377	0.4963	369
9	ader-a-002	0.0052	112	0.0071	107	0.0047	122	0.0064	124	0.0087	125	0.0159	122	0.0136	161	0.0990	304
10	ader-a-003	0.0043	91	0.0059	88	0.0036	81	0.0043	66	0.0076	104	0.0151	109	0.0128	153	0.0989	303
11	advance-002	0.0089	192	0.0137	194	0.0073	187	0.0115	189	0.0400	286	0.0722	251	0.0593	288	0.0498	263
12	advance-003	0.0060	142	0.0087	135	0.0052	138	0.0067	130	0.0389	285	0.4914	308	0.1291	313	0.0508	265
13	afisbiometrics-000	0.0051	110	0.0073	111	0.0030	48	0.0050	87	0.0044	40	0.0077	31	0.0057	21	0.0282	78
14	aifirst-001	0.0119	232	0.0170	226	0.0084	207	0.0127	201	0.0131	191	0.0212	160	0.0138	164	0.0432	248
15	aigen-001	0.0124	237	0.0219	247	0.0143	267	0.0217	262	0.0236	256	0.8960	342	0.3255	337	0.0681	285
16	aigen-002	0.0192	281	0.0343	286	0.0256	298	0.0402	294	0.0389	284	0.9196	345	0.3876	343	0.1096	311
17	ailabs-001	0.0158	264	0.0276	277	0.0192	285	0.0317	287	0.0352	278	0.0608	241	0.0434	275	0.0338	204
18	aimall-002	0.0119	231	0.0167	224	0.0224	293	0.0411	295	0.0233	253	0.0373	219	0.0235	240	0.0327	193
19	aimall-003	0.0033	57	0.0041	44	0.0033	70	0.0035	38	0.0056	73	0.0109	74	0.0087	90	0.0312	176
20	aiunionface-000	0.0104	216	0.0154	214	0.0082	204	0.0122	192	0.0141	199	0.0243	175	0.0169	198	0.0306	164
21	aize-001	0.0223	289	0.0344	287	0.0199	286	0.0313	285	0.0367	280	0.0522	234	0.0359	263	0.0446	253
22	aize-002	0.0210	287	0.0327	282	0.0280	301	0.0489	302	0.0504	298	0.0692	248	0.0434	274	0.0854	298
23	ajou-001	0.0093	201	0.0147	206	0.0071	184	0.0126	196	0.0173	229	0.0274	187	0.0186	213	0.0348	211
24	alchera-002	0.0107	219	0.0157	215	0.0104	232	0.0229	265	0.0144	204	0.0246	176	0.0198	224	0.0328	195
25	alchera-003	0.0044	92	0.0055	79	0.0031	52	0.0039	54	0.0042	35	0.0077	33	0.0065	34	0.0339	206
26	alfabeta-001	0.4867	376	0.5831	373	0.6855	369	0.8156	373	0.8253	368	0.7765	334	0.6416	359	0.3427	356
27	alice-000	0.0119	233	0.0192	237	0.0106	236	0.0170	240	0.0167	221	0.0265	183	0.0150	181	0.0288	114
28	alleyes-000	0.0058	134	0.0090	140	0.0055	149	0.0087	168	0.0068	97	0.0105	72	0.0076	64	0.0282	76
29	allgovision-000	0.0346	306	0.0527	307	0.0232	294	0.0339	288	0.0372	283	0.0620	243	0.0443	278	0.0607	279
30	alphaface-001	0.0065	150	0.0097	153	0.0039	96	0.0063	123	0.0083	118	-	-	-	0.0280	62	
31	alphaface-002	0.0052	114	0.0075	118	0.0030	43	0.0044	69	1.0000	385	0.0115	84	0.0084	83	0.0279	51
32	amplifiedgroup-001	0.5034	378	0.5848	374	0.6973	373	0.8316	374	0.7807	363	0.7724	332	0.6354	356	0.4250	362
33	androvideo-000	0.0243	291	0.0438	300	0.0239	296	0.0365	292	0.0483	297	0.1870	279	0.0635	291	0.1163	313
34	anke-004	0.0080	182	0.0154	213	0.0073	186	0.0112	187	0.0102	159	0.0178	140	0.0118	140	0.0288	116
35	anke-005	0.0070	159	0.0109	173	0.0059	161	0.0094	174	0.0105	162	0.0142	99	0.0102	113	0.0289	121
36	antheus-000	0.2564	351	0.3776	355	0.7240	375	0.8699	377	0.8899	375	0.9872	354	0.9483	372	0.7668	375
37	antheus-001	0.1311	338	0.2306	340	0.5113	361	0.6797	362	0.8748	373	0.9908	358	0.9649	375	0.7586	374
38	anyvision-004	0.0267	296	0.0385	294	0.0258	299	0.0487	301	0.0234	255	0.0301	197	0.0191	217	0.0470	257
39	anyvision-005	0.0023	31	0.0037	36	0.0027	33	0.0035	37	0.0049	54	0.0084	43	0.0069	48	0.0285	95
40	armatura-001	0.0033	58	0.0042	51	0.0031	51	0.0037	45	0.0056	72	0.0110	75	0.0092	99	0.0815	297
41	asusaics-000	0.0125	240	0.0209	243	0.0085	208	0.0134	209	0.0143	202	0.7189	326	0.0285	252	0.0295	142
42	asusaics-001	0.0125	239	0.0210	244	0.0085	210	0.0134	210	0.0143	203	0.7437	329	0.0289	253	0.0295	141
43	authenmetric-003	0.0036	69	0.0053	76	0.0039	100	0.0051	90	0.0095	147	0.9930	359	0.5932	354	0.0290	127
44	authenmetric-004	0.0027	43	0.0042	52	0.0033	67	0.0036	42	0.0083	121	0.9879	356	0.4058	345	0.0290	130

Table 16: FNMR is the proportion of mated comparisons below a threshold set to achieve the FMR given in the header on the fourth row. FMR is the proportion of impostor comparisons at or above that threshold. The light grey values give rank over all algorithms in that column. The pink columns use only same-sex impostors; others are selected regardless of demographics. The exception, in the green column, uses "matched-covariates" i.e. impostors of the same sex, age group, and country of birth. The second pink column includes effects of extended ageing. Missing entries for border, visa, mugshot and wild images generally mean the algorithm did not run to completion. The VISA columns compare images described in section 2.1. The MUGSHOT columns compare images described in section 2.4. The VISA-BORDER column compare images described in section 2.2 with those of section 2.3. The BORDER column compares images described in section 2.3. The WILD columns compare images described in section 2.5.

	Algorithm	FALSE NON-MATCH RATE (FNMR)									
		CONSTRAINED, COOPERATIVE								LESS CONSTRAINED, NON-COOP.	
		Name	VISAMC	VISA	MUGSHOT	MUGSHOT12+YRS	VISABORDER	BORDER	BORDER	WILD	
	FMR	0.0001	1E-06	1E-05	1E-05	1E-05	1E-06	1E-06	1E-05	0.0001	
45	aware-005	0.0457	314	0.0643	312	0.0603	322	0.1094	324	0.0613	304
46	aware-006	0.0487	315	0.0819	321	0.0529	318	0.1090	323	0.1011	323
47	awiros-001	0.4044	365	0.4622	362	0.5530	362	0.6518	360	0.2008	335
48	awiros-002	0.1990	345	0.2561	343	0.3319	351	0.4411	351	0.3821	348
49	ayftech-001	0.0946	331	0.1941	334	0.2438	347	0.3625	347	0.1558	328
50	ayonix-000	0.4351	371	0.4872	363	0.6150	367	0.7510	367	0.6557	357
51	beethedata-000	0.0127	242	0.0195	238	0.0092	219	0.0157	230	0.0171	226
52	beyneai-000	0.0071	165	0.0107	171	0.0104	233	0.0131	207	0.0170	225
53	biocube-001	0.5596	382	0.6834	380	0.7700	379	0.8712	378	0.8446	370
54	bioidtechswiss-001	0.0054	120	0.0072	109	0.0069	179	0.0124	195	0.0060	81
55	bioidtechswiss-002	0.0049	100	0.0067	102	0.0064	168	0.0116	190	0.0067	95
56	bm-001	0.7431	387	0.9494	388	0.9586	385	0.9843	383	0.9049	376
57	boetech-001	0.0662	324	0.0802	320	0.0493	315	0.0791	315	0.0682	308
58	boetech-002	0.0535	319	0.0565	310	0.0114	251	0.0136	212	0.0403	287
59	bresee-001	0.0085	190	0.0143	201	0.0086	213	0.0153	228	0.0108	167
60	bresee-002	0.0079	181	0.0101	161	0.0065	173	0.0079	152	0.0129	187
61	camvi-002	0.0125	241	0.0221	249	0.0089	217	0.0145	221	0.0142	200
62	camvi-004	0.0171	274	0.0316	281	0.0042	111	0.0049	85	0.0097	152
63	canon-002	0.0034	65	0.0050	68	0.0026	24	0.0033	31	0.0043	38
64	canon-003	0.0041	88	0.0059	89	0.0030	42	0.0040	57	0.0040	28
65	ceiec-003	0.0071	166	0.0107	168	0.0061	164	0.0079	154	0.0160	213
66	ceiec-004	0.0038	76	0.0051	69	0.0045	121	0.0053	94	0.0062	88
67	chosun-001	0.0525	318	0.0936	323	0.0742	327	0.1263	328	0.0978	322
68	chosun-002	0.0390	309	0.0646	313	0.0339	308	0.0576	309	0.0455	295
69	chtface-003	0.0091	196	0.0146	203	0.0083	206	0.0128	203	0.0132	192
70	chtface-004	0.0046	97	0.0062	93	0.0052	137	0.0080	156	0.0088	129
71	clearviewai-000	0.0010	4	0.0019	8	0.0024	8	0.0028	17	0.0030	9
72	closeli-001	0.0136	245	0.0163	218	0.0039	97	0.0054	96	0.0072	100
73	cloudmatrix-000	0.0192	282	0.0340	285	0.0133	261	0.0220	263	0.9837	379
74	cloudwalk-hr-003	0.0026	40	0.0041	46	0.0040	104	0.0058	108	0.0060	86
75	cloudwalk-hr-004	0.0009	2	0.0018	5	0.0034	72	0.0028	21	0.0052	61
76	cloudwalk-mt-003	0.0013	11	0.0022	10	0.0026	19	0.0027	14	0.0039	24
77	cloudwalk-mt-004	0.0009	3	0.0013	1	0.0024	10	0.0021	2	0.0028	7
78	clova-000	0.0099	210	0.0150	208	0.0094	223	0.0147	224	0.0136	194
79	cogent-005	0.0060	138	0.0112	177	0.0064	171	0.0070	134	0.0095	146
80	cogent-006	0.0046	96	0.0059	91	0.0036	77	0.0047	75	0.0058	78
81	cognitec-003	0.0038	75	0.0052	71	0.0054	148	0.0057	106	0.0225	250
82	cognitec-004	0.0036	67	0.0053	75	0.0053	139	0.0056	101	0.0098	153
83	cor-001	0.0075	174	0.0113	180	0.0055	152	0.0084	162	0.0091	134
84	coretech-000	0.7699	389	1.0000	396	1.0000	391	-	1.0000	393	1.0000
85	corsight-001	0.0040	82	0.0057	85	0.0033	69	0.0047	74	0.0045	43
86	corsight-002	0.0053	116	0.0068	104	0.0030	46	0.0041	59	0.0039	26
87	csc-002	0.0099	211	0.0132	192	0.0077	192	0.0142	218	0.0126	185
88	csc-003	0.0053	117	0.0065	98	0.0037	85	0.0047	77	0.0074	102

FRVT - FACE RECOGNITION VENDOR TEST - VERIFICATION

Table 17: FNMR is the proportion of mated comparisons below a threshold set to achieve the FMR given in the header on the fourth row. FMR is the proportion of impostor comparisons at or above that threshold. The light grey values give rank over all algorithms in that column. The pink columns use only same-sex impostors; others are selected regardless of demographics. The exception, in the green column, uses “matched-covariates” i.e. impostors of the same sex, age group, and country of birth. The second pink column includes effects of extended ageing. Missing entries for border, visa, mugshot and wild images generally mean the algorithm did not run to completion. The VISA columns compare images described in section 2.1. The MUGSHOT columns compare images described in section 2.4. The VISA-BORDER column compare images described in section 2.2 with those of section 2.3. The BORDER column compares images described in section 2.3. The WILD columns compare images described in section 2.5.

Algorithm	FALSE NON-MATCH RATE (FNMR)																
	CONSTRAINED, COOPERATIVE								LESS CONSTRAINED, NON-COOP.								
	Name	VISAMC	VISA	MUGSHOT	MUGSHOT12+YRS	VISABORDER	BORDER	BORDER	WILD								
	FMR	0.0001	1E-06	1E-05	1E-05	1E-06	1E-06	1E-05	0.0001								
89	ctcbcbank-000	0.0168	269	0.0250	265	0.0146	270	0.0224	264	0.0211	247	0.8964	343	0.3779	342	1.0000	390
90	ctcbcbank-001	0.0155	262	0.0235	258	0.0148	275	0.0243	270	0.0207	244	0.9279	346	0.3469	339	1.0000	396
91	cubox-001	0.0064	149	0.0080	126	0.0037	84	0.0055	98	0.0060	82	0.0111	77	0.0077	65	0.0300	154
92	cubox-002	0.0034	64	0.0041	47	0.0025	15	0.0025	9	0.0033	13	0.0064	14	0.0058	23	0.0480	260
93	cudocommunication-001	0.4777	374	1.0000	394	0.4373	356	0.5360	354	1.0000	391	1.0000	387	1.0000	387	1.0000	387
94	cuhksee-001	0.0036	71	0.0045	59	0.0031	57	0.0046	72	0.0051	60	0.0095	60	0.0079	68	0.1492	320
95	cybercore-000	0.0728	326	0.1110	325	0.1521	339	0.2375	337	0.1874	334	0.1907	280	0.1178	312	0.1191	315
96	cybercore-001	0.3759	363	0.5677	371	0.6928	372	0.7926	369	0.8118	366	0.9291	349	0.7080	363	0.3811	358
97	cyberextruder-001	0.1972	343	0.2547	342	0.4686	360	0.6387	359	0.3807	347	0.3806	301	0.2582	327	0.1747	327
98	cyberextruder-002	0.0811	329	0.1336	327	0.1465	338	0.2266	336	0.2086	338	1.0000	383	1.0000	390	0.1000	306
99	cyberlink-007	0.0032	55	0.0053	73	0.0041	107	0.0043	64	0.0052	64	0.0243	174	0.0084	84	0.0280	58
100	cyberlink-008	0.0042	89	0.0056	83	0.0038	93	0.0048	79	0.0053	65	0.0099	64	0.0074	59	0.0274	16
101	dahua-006	0.0027	42	0.0039	40	0.0031	55	0.0039	55	0.0039	25	0.0067	19	0.0058	22	0.0280	54
102	dahua-007	0.0017	19	0.0023	12	0.0026	22	0.0032	30	0.0033	11	0.0060	10	0.0054	17	0.0278	38
103	daon-000	0.0095	204	0.0117	181	0.0068	176	0.0077	149	0.0092	138	0.0174	136	0.0137	163	0.0331	198
104	decatur-000	0.0714	325	0.1115	326	0.0608	323	0.1106	325	0.0866	316	1.0000	378	0.0714	297	0.0658	282
105	decatur-001	0.0424	311	0.0711	315	0.0237	295	0.0458	298	0.0447	294	1.0000	372	0.9969	379	0.0280	61
106	deepglint-003	0.0027	44	0.0038	37	0.0030	45	0.0032	29	0.0043	37	0.0082	40	0.0076	63	0.0279	44
107	deepglint-004	0.0025	39	0.0034	32	0.0039	98	0.0061	120	0.0050	58	0.0091	51	0.0082	76	0.0285	101
108	deepsea-001	0.0136	247	0.0215	245	0.0142	266	0.0214	261	0.0163	217	0.0250	178	0.0192	218	0.0347	210
109	deepsense-000	0.0145	253	0.0265	273	0.0113	249	0.0196	254	0.0151	207	0.0215	164	0.0129	154	0.0290	125
110	dermalog-008	0.0096	207	0.0166	223	0.0086	211	0.0133	208	0.0165	219	0.0586	238	0.0226	237	0.0277	33
111	dermalog-009	0.0067	154	0.0094	145	0.0051	135	0.0069	132	0.0116	176	0.0312	200	0.0177	205	0.0270	3
112	didiglobalface-001	0.0055	125	0.0092	142	0.0030	44	0.0045	70	0.0088	128	0.0119	89	0.0085	86	0.0282	74
113	digitdata-000	0.0967	332	0.1410	329	0.2596	348	0.3462	346	0.0293	271	0.0363	215	0.0212	230	0.0310	173
114	digitalbarriers-002	0.3360	360	0.3690	353	0.0877	329	0.1557	329	0.0971	321	0.0951	259	0.0497	281	0.0436	250
115	dps-000	0.0115	225	0.0176	229	0.0149	277	0.0185	249	0.0173	228	0.0275	189	0.0180	208	0.1067	309
116	dsk-000	0.1526	340	0.2169	338	0.3787	353	0.5426	356	0.3115	341	0.3089	297	0.1994	324	0.2201	337
117	einetworks-000	0.0099	212	0.0180	232	0.0088	216	0.0140	216	0.0130	189	0.0225	170	0.0147	177	0.0293	136
118	ekin-002	0.1168	335	0.2042	335	0.1530	340	0.2524	339	0.1777	333	0.2773	295	0.1347	315	0.4801	368
119	enface-000	0.0028	47	0.0049	64	0.0043	113	0.0072	136	0.0058	79	0.0150	107	0.0090	95	0.0290	132
120	enface-001	0.0072	168	0.0107	169	0.0071	181	0.0138	213	0.0068	98	0.0515	232	0.0094	104	0.0284	92
121	eocortex-000	0.3485	361	0.6943	381	0.1122	331	0.1574	330	0.2155	340	0.2257	290	0.1606	322	0.2546	348
122	ercacat-001	0.0036	68	0.0044	56	0.0033	66	0.0047	78	0.0106	164	0.0202	156	0.0184	211	0.0258	1
123	euronovate-001	0.2786	354	0.3608	352	0.4489	358	0.6105	358	0.5010	353	0.5392	313	0.3769	341	0.4333	363
124	expasoft-001	0.0328	304	0.0488	302	0.0211	290	0.0342	290	0.0629	307	0.6483	320	0.2816	334	0.0552	273
125	expasoft-002	0.0170	271	0.0274	275	0.0787	328	0.0768	314	0.1629	329	0.9996	368	0.9631	374	0.0337	202
126	f8-001	0.0249	292	0.0336	283	0.0178	283	0.0232	266	0.0303	274	0.0615	242	0.0408	270	0.0475	259
127	faceonlive-001	0.0269	297	0.0359	290	0.0387	311	0.0721	313	0.0246	265	0.0349	212	0.0220	233	0.0548	271
128	facesoft-000	0.0085	189	0.0112	178	0.0064	170	0.0107	184	0.0091	133	0.0171	133	0.0107	124	0.0275	21
129	facetag-000	0.2836	355	0.4081	359	0.2933	350	0.4303	350	0.3448	343	0.6312	318	0.3530	340	0.2087	336
130	facetag-002	0.0098	209	0.0147	205	0.0064	172	0.0110	185	0.0116	175	0.0190	148	0.0119	144	0.0675	284
131	facex-001	1.0000	395	1.0000	395	1.0000	389	-	1.0000	389	1.0000	386	1.0000	385	1.0000	386	
132	facex-002	0.0803	327	0.1404	328	0.1283	333	0.1979	334	0.1440	327	0.1952	282	0.1299	314	0.2377	340

Table 18: FNMR is the proportion of mated comparisons below a threshold set to achieve the FMR given in the header on the fourth row. FMR is the proportion of impostor comparisons at or above that threshold. The light grey values give rank over all algorithms in that column. The pink columns use only same-sex impostors; others are selected regardless of demographics. The exception, in the green column, uses "matched-covariates" i.e. impostors of the same sex, age group, and country of birth. The second pink column includes effects of extended ageing. Missing entries for border, visa, mugshot and wild images generally mean the algorithm did not run to completion. The VISA columns compare images described in section 2.1. The MUGSHOT columns compare images described in section 2.4. The VISA-BORDER column compare images described in section 2.2 with those of section 2.3. The BORDER column compares images described in section 2.3. The WILD columns compare images described in section 2.5.

Algorithm	FALSE NON-MATCH RATE (FNMR)										LESS CONSTRAINED, NON-COOP.					
	CONSTRAINED, COOPERATIVE								WILD							
	Name	VISAMC	VISA	MUGSHOT	MUGSHOT12+YRS	VISABORDER	BORDER	BORDER	1E-06	1E-05						
FMR	0.0001	1E-06	1E-05	1E-05	1E-06	1E-06	1E-06	1E-05	0.0001							
133 <i>farfaces-001</i>	0.4890	377	0.5860	375	0.5650	363	0.7268	365	0.8015	365	0.7511	330	0.5892	353	0.1976	334
134 <i>fiberhome-nanjing-003</i>	0.0090	193	0.0139	198	0.0082	203	0.0144	219	0.0110	169	0.0174	134	0.0107	125	0.0272	10
135 <i>fiberhome-nanjing-004</i>	0.0037	74	0.0056	84	0.0031	53	0.0043	65	0.0043	39	0.0083	41	0.0061	30	0.0272	8
136 <i>fincore-000</i>	0.0309	302	0.0502	303	0.0281	302	0.0510	304	0.0521	300	0.0815	253	0.0522	283	0.0681	286
137 <i>fujitsulab-002</i>	0.0091	197	0.0124	186	0.0105	234	0.0156	229	0.0169	224	0.0345	211	0.0146	176	0.0282	71
138 <i>fujitsulab-003</i>	0.0045	94	0.0065	99	0.0057	157	0.0083	160	0.0080	111	0.0154	115	0.0101	110	0.0280	53
139 <i>geo-002</i>	0.0171	273	0.0187	235	0.0035	76	0.0051	92	0.0064	90	0.0117	86	0.0083	81	0.0302	160
140 <i>geo-004</i>	0.0030	48	0.0041	45	0.0025	18	0.0030	25	0.0035	18	0.0065	16	0.0053	15	0.0286	103
141 <i>glory-003</i>	0.0076	176	0.0125	188	0.0077	194	0.0103	181	0.0130	188	0.0205	158	0.0143	172	0.0763	291
142 <i>glory-004</i>	0.0077	177	0.0123	183	0.0074	190	0.0098	178	0.0122	182	0.0193	150	0.0134	158	0.0743	290
143 <i>gorilla-007</i>	0.0074	172	0.0111	176	0.0065	174	0.0126	197	0.0100	157	0.0151	108	0.0102	112	0.0278	35
144 <i>gorilla-008</i>	0.0058	132	0.0091	141	0.0049	128	0.0079	153	0.0079	110	0.0126	94	0.0091	97	0.0278	42
145 <i>graymatics-001</i>	0.1039	334	0.1620	331	0.1344	335	0.1917	333	0.1648	330	0.5160	311	0.2689	332	0.3057	354
146 <i>griaule-000</i>	0.0071	164	0.0099	158	0.0050	131	0.0072	135	0.0160	211	0.0304	198	0.0267	249	0.0338	203
147 <i>hertasecurity-000</i>	0.0630	323	0.0780	319	0.0503	317	0.0898	317	0.0738	309	0.0693	250	0.0420	272	0.0575	276
148 <i>hertasecurity-001</i>	0.0249	293	0.0309	280	0.0105	235	0.0161	232	0.0245	263	0.0447	226	0.0359	262	0.0486	262
149 <i>hik-001</i>	0.0096	206	0.0125	189	0.0093	222	0.0164	237	0.0108	168	0.0937	257	0.0127	151	0.0271	5
150 <i>hisign-001</i>	0.0036	72	0.0050	67	0.0034	71	0.0046	71	0.0079	109	0.0153	114	0.0133	156	0.0286	106
151 <i>hyperverge-001</i>	1.0000	397	1.0000	393	1.0000	397	-	-	1.0000	392	1.0000	389	1.0000	386	1.0000	388
152 <i>hyperverge-002</i>	0.0050	103	0.0066	100	0.0035	75	0.0051	89	0.0062	87	0.0107	73	0.0074	60	0.0276	29
153 <i>hzailu-001</i>	0.0122	234	0.0164	220	0.0095	225	0.0196	253	0.0079	107	0.0118	87	0.0090	94	0.0392	234
154 <i>icm-002</i>	0.0143	251	0.0249	264	0.0144	268	0.0256	271	0.0236	258	0.0386	221	0.0263	248	0.0339	205
155 <i>icm-003</i>	0.0138	248	0.0222	250	0.0149	276	0.0282	280	0.0227	251	0.0384	220	0.0257	245	0.0333	200
156 <i>icthtc-000</i>	0.0260	295	0.0396	295	0.0207	289	0.0339	289	0.0291	270	0.0474	229	0.0346	259	0.0459	256
157 <i>id3-006</i>	0.0072	169	0.0103	163	0.0049	129	0.0074	142	0.0095	145	0.0165	130	0.0119	143	0.9938	385
158 <i>id3-008</i>	0.0039	78	0.0055	81	0.0032	62	0.0042	61	0.0081	115	0.0155	116	0.0134	157	0.8856	379
159 <i>idemia-007</i>	0.0024	35	0.0039	41	0.0032	64	0.0038	51	0.0046	46	0.0092	53	0.0070	52	0.0288	119
160 <i>idemia-008</i>	0.0023	32	0.0032	26	0.0023	5	0.0028	16	0.0034	16	0.0067	18	0.0056	20	0.0290	129
161 <i>iit-002</i>	0.0111	223	0.0177	231	0.0085	209	0.0140	215	0.0193	240	0.0332	207	0.0260	246	0.1373	317
162 <i>iit-003</i>	0.0082	187	0.0151	211	0.0053	141	0.0084	163	0.0122	181	0.0199	154	0.0137	162	0.0407	240
163 <i>imagus-002</i>	0.0062	144	0.0086	133	0.0053	143	0.0075	143	0.0121	179	0.0207	159	0.0161	191	0.0735	289
164 <i>imagus-004</i>	0.0063	145	0.0094	148	0.0055	151	0.0081	158	0.0098	154	0.0157	120	0.0111	129	0.0283	84
165 <i>imperial-000</i>	0.0067	155	0.0108	172	0.0080	200	0.0134	211	0.0087	126	0.0581	236	0.0102	114	0.0281	66
166 <i>imperial-002</i>	0.0058	130	0.0081	130	0.0055	150	0.0085	165	0.0083	119	0.0157	118	0.0103	115	0.0273	14
167 <i>incode-009</i>	0.0044	93	0.0067	103	0.0034	74	0.0051	88	0.0049	55	0.0091	50	0.0067	43	0.0296	147
168 <i>incode-010</i>	0.0041	86	0.0063	95	0.0028	38	0.0043	63	0.0047	51	0.0077	32	0.0061	29	0.0296	148
169 <i>innefulabs-000</i>	0.0122	235	0.0199	239	0.0112	248	0.0197	255	0.0222	249	0.0372	218	0.0271	250	0.0348	213
170 <i>innovativetechnologyltd-001</i>	0.0578	321	0.0938	324	0.0501	316	0.0981	318	0.0592	303	0.0779	252	0.0422	273	0.0449	255
171 <i>innovativetechnologyltd-002</i>	0.0451	313	0.0716	316	0.0541	319	0.1009	321	0.0506	299	0.0682	246	0.0371	265	0.0804	296
172 <i>innovatrics-007</i>	0.0040	83	0.0054	78	0.0057	156	0.0078	150	0.0079	108	0.0123	90	0.0088	91	0.0282	77
173 <i>innovatrics-008</i>	0.0047	98	0.0064	97	0.0038	92	0.0052	93	0.0053	66	0.0088	48	0.0069	49	0.0287	107
174 <i>insightface-001</i>	0.0009	1	0.0014	2	0.0027	28	0.0024	5	0.0035	17	0.0070	22	0.0065	36	0.0279	47
175 <i>insightface-002</i>	0.0011	6	0.0019	7	0.0027	30	0.0026	10	0.0036	21	0.0069	21	0.0065	35	0.0280	52
176 <i>intellicloudai-001</i>	0.0142	250	0.0234	256	0.0092	221	0.0145	220	0.0162	215	0.0371	217	0.0171	200	0.0409	241

Table 19: FNMR is the proportion of mated comparisons below a threshold set to achieve the FMR given in the header on the fourth row. FMR is the proportion of impostor comparisons at or above that threshold. The light grey values give rank over all algorithms in that column. The pink columns use only same-sex impostors; others are selected regardless of demographics. The exception, in the green column, uses “matched-covariates” i.e. impostors of the same sex, age group, and country of birth. The second pink column includes effects of extended ageing. Missing entries for border, visa, mugshot and wild images generally mean the algorithm did not run to completion. The VISA columns compare images described in section 2.1. The MUGSHOT columns compare images described in section 2.4. The VISA-BORDER column compare images described in section 2.2 with those of section 2.3. The BORDER column compares images described in section 2.3. The WILD columns compare images described in section 2.5.

Algorithm	FALSE NON-MATCH RATE (FNMR)												
	CONSTRAINED, COOPERATIVE											LESS CONSTRAINED, NON-COOP.	
	Name	VISAMC	VISA	MUGSHOT	MUGSHOT12+YRS	VISA BORDER	BORDER	BORDER	WILD				
FMR	0.0001	1E-06	1E-05	1E-05	1E-06	1E-06	1E-06	1E-05	0.0001				
177 <i>intellicloudai-002</i>	0.0059	137	0.0085	132	0.0060	163	0.0069	133	0.0108	166	0.2477	293	
178 <i>intellifusion-001</i>	0.0072	167	0.0094	149	0.0056	155	0.0085	166	0.0111	171	0.0212	161	
179 <i>intellifusion-002</i>	0.0059	135	0.0077	121	0.0040	103	0.0074	141	0.0085	124	0.5352	312	
180 <i>intellivision-001</i>	0.1335	339	0.2205	339	0.1090	330	0.1670	331	0.1385	324	0.1676	276	
181 <i>intellivision-002</i>	0.1000	333	0.1775	332	0.0610	324	0.1009	320	0.0805	314	0.1074	265	
182 <i>intelresearch-004</i>	0.0025	38	0.0035	33	0.0032	60	0.0038	49	0.0049	56	0.0094	55	
183 <i>intelresearch-005</i>	0.0016	16	0.0023	14	0.0028	34	0.0034	34	0.0042	36	0.0084	42	
184 <i>intsysmsu-001</i>	0.9543	391	0.9888	390	0.9923	386	-	0.9977	380	0.9955	361	0.9892	376
185 <i>intsysmsu-002</i>	0.0130	243	0.0254	267	0.0137	264	0.0267	278	0.0160	212	0.0267	185	
186 <i>ionetworks-000</i>	0.0060	141	0.0087	137	0.0044	114	0.0058	110	0.0080	114	0.0144	103	
187 <i>iqface-000</i>	0.0091	199	0.0143	200	0.0075	191	0.0110	186	0.0171	227	0.2234	288	
188 <i>iqface-003</i>	0.0058	133	0.0079	125	0.0051	136	0.0058	111	0.0104	161	0.0200	155	
189 <i>irex-000</i>	0.0052	111	0.0099	157	0.0056	154	0.0083	161	0.0137	197	0.0163	128	
190 <i>isap-001</i>	0.5092	379	0.6588	377	0.6899	371	0.7978	370	0.7200	359	0.7253	327	
191 <i>isap-002</i>	0.0114	224	0.0186	234	0.0087	214	0.0151	227	0.0156	210	0.5134	310	
192 <i>isityou-000</i>	0.5682	383	0.7033	382	1.0000	395	-	1.0000	386	1.0000	382	1.0000	391
193 <i>isystems-001</i>	0.0149	259	0.0245	262	0.0138	265	0.0210	259	0.0209	246	0.0332	206	
194 <i>isystems-002</i>	0.0118	228	0.0182	233	0.0111	245	0.0162	235	0.0166	220	0.0284	193	
195 <i>itmo-007</i>	0.0080	183	0.0125	187	0.0107	237	0.0185	247	0.0167	222	0.0222	169	
196 <i>itmo-008</i>	0.0090	195	0.0150	209	0.0058	159	0.0059	115	0.0187	236	0.0355	213	
197 <i>ivacognitive-001</i>	0.0189	279	0.0351	288	0.0123	256	0.0235	267	0.0198	242	0.0274	188	
198 <i>iws-000</i>	0.4824	375	0.5801	372	0.6859	370	0.8155	372	0.8251	367	0.7756	333	
199 <i>kakao-005</i>	0.0040	80	0.0059	87	0.0036	83	0.0057	105	0.0085	123	0.0239	173	
200 <i>kakao-007</i>	0.0019	24	0.0028	22	0.0024	7	0.0026	11	0.0033	12	0.0061	11	
201 <i>kakaopay-001</i>	0.0152	261	0.0252	266	0.0145	269	0.0270	279	0.0232	252	0.0344	210	
202 <i>kedacom-000</i>	0.0055	123	0.0081	129	0.0111	247	0.0120	191	0.0415	289	0.0966	261	
203 <i>kiwitech-000</i>	0.0076	175	0.0105	165	0.0081	202	0.0128	204	0.0096	148	0.0163	127	
204 <i>kneron-003</i>	0.0542	320	0.0902	322	0.0346	309	0.0562	307	0.0919	318	0.1251	271	
205 <i>kneron-005</i>	0.0157	263	0.0259	269	0.0126	259	0.0212	260	0.0406	288	0.0693	249	
206 <i>knowutech-000</i>	0.0039	79	0.0055	80	0.0028	39	0.0042	60	0.0042	33	0.0077	30	
207 <i>kookmin-002</i>	0.0054	121	0.0077	120	0.0043	112	0.0065	126	0.0123	183	0.7591	331	
208 <i>kuke3d-001</i>	0.0058	127	0.0104	164	0.0083	205	0.0093	173	0.0270	268	0.9901	357	
209 <i>lemalabs-001</i>	0.0111	222	0.0175	228	0.0088	215	0.0142	217	0.0143	201	0.0228	171	
210 <i>line-000</i>	0.0172	275	0.0236	259	0.0109	241	0.0194	252	0.0183	232	0.0291	194	
211 <i>line-001</i>	0.0025	37	0.0040	42	0.0026	27	0.0034	36	0.0045	44	0.4127	305	
212 <i>lookman-002</i>	0.0297	300	0.0547	309	0.0339	307	0.0562	306	0.0614	305	0.0960	260	
213 <i>lookman-004</i>	0.0074	173	0.0099	156	0.0124	258	0.0149	225	0.0430	292	0.0866	255	
214 <i>luxand-000</i>	0.2056	346	0.2814	346	0.4053	355	0.5365	355	0.3497	344	0.3743	300	
215 <i>mantra-000</i>	0.0037	73	0.0052	72	0.0054	146	0.0056	103	0.0097	151	0.0181	142	
216 <i>maxvision-000</i>	0.0078	179	0.0106	167	0.0110	243	0.0147	223	0.0368	282	1.0000	393	
217 <i>megvii-003</i>	0.0064	148	0.0094	146	0.0136	263	0.0260	273	0.0050	57	0.0080	36	
218 <i>megvii-004</i>	0.0020	25	0.0033	29	0.0028	37	0.0035	39	0.0037	23	0.0074	25	
219 <i>megvii-004-82</i>	-	-	-	-	0.0028	36	0.0036	41	-	-	-	-	
220 <i>meitan-000</i>	0.0197	283	0.0424	298	0.0078	195	0.0074	140	0.0103	160	0.0193	151	
											0.0164	194	
											0.1063	308	

Table 20: FNMR is the proportion of mated comparisons below a threshold set to achieve the FMR given in the header on the fourth row. FMR is the proportion of impostor comparisons at or above that threshold. The light grey values give rank over all algorithms in that column. The pink columns use only same-sex impostors; others are selected regardless of demographics. The exception, in the green column, uses “matched-covariates” i.e. impostors of the same sex, age group, and country of birth. The second pink column includes effects of extended ageing. Missing entries for border, visa, mugshot and wild images generally mean the algorithm did not run to completion. The VISA columns compare images described in section 2.1. The MUGSHOT columns compare images described in section 2.4. The VISA-BORDER column compare images described in section 2.2 with those of section 2.3. The BORDER column compares images described in section 2.3. The WILD columns compare images described in section 2.5.

	Algorithm	FALSE NON-MATCH RATE (FNMR)										LESS CONSTRAINED, NON-COOP.					
		CONSTRAINED, COOPERATIVE								WILD							
		Name	VISAMC	VISA	MUGSHOT	MUGSHOT12+YRS	VISABORDER	BORDER	BORDER								
	FMR	0.0001	1E-06	1E-05	1E-05	1E-05	1E-06	1E-06	1E-05		0.0001						
221	meiya-001	0.0171	272	0.0275	276	0.0159	280	0.0261	276	0.0311	275	0.2250	289	0.0245	243	0.0363	227
222	mendaxiatech-000	0.0027	45	0.0036	34	0.0029	40	0.0036	43	0.0031	10	0.0057	8	0.0051	11	0.0275	22
223	microfocus-001	0.4482	372	0.5524	370	0.7256	376	0.8416	375	0.7301	360	0.6926	324	0.5180	349	0.2567	349
224	microfocus-002	0.3605	362	0.5057	365	0.5783	365	0.7223	364	0.5909	354	0.5963	317	0.4160	346	0.1582	323
225	minivision-000	0.0033	56	0.0048	63	0.0038	90	0.0049	82	0.0055	70	0.0094	58	0.0079	70	0.0273	11
226	mobai-000	0.0360	308	0.0439	301	0.0372	310	0.0700	311	0.0367	281	0.0939	258	0.0795	302	0.2640	351
227	mobai-001	0.0199	286	0.0219	248	0.0047	123	0.0061	117	0.0093	143	0.0174	135	0.0138	165	0.1045	307
228	mobbl-001	0.3208	357	0.4375	360	0.5680	364	0.7193	363	0.6282	356	0.5783	316	0.3984	344	0.1866	331
229	mobbl-002	0.9914	393	0.9970	391	0.9355	383	-		1.0000	384	1.0000	375	0.9999	382	0.9921	383
230	mobipintech-000	0.0090	194	0.0149	207	0.0039	102	0.0057	104	0.0115	174	0.0465	228	0.0182	210	0.0315	181
231	moreedian-000	0.3874	364	0.4912	364	0.9988	387	-		0.9990	381	0.9999	370	0.9998	381	0.4788	367
232	multimodality-000	0.0034	62	0.0047	62	0.0036	82	0.0044	68	0.0077	105	0.9976	364	0.4456	347	0.0287	108
233	mvision-001	0.0191	280	0.0233	254	0.0204	288	0.0356	291	0.0198	243	0.0337	209	0.0242	242	0.0431	247
234	nazhiai-000	0.0040	84	0.0059	90	0.0036	78	0.0048	81	0.0057	75	0.0125	93	0.0083	80	0.0275	23
235	neosystems-002	0.2905	356	0.4077	358	0.2028	345	0.3252	344	0.4088	350	0.5519	314	0.3331	338	0.4500	366
236	neosystems-003	0.2429	348	0.3349	349	0.1844	343	0.2999	343	0.5942	355	0.3936	302	0.2292	325	0.1404	318
237	netbridgetech-001	0.4749	373	0.6599	378	0.4438	357	0.5676	357	0.4491	351	1.0000	373	0.9541	373	0.1098	312
238	netbridgetech-002	0.0101	214	0.0166	222	0.0077	193	0.0127	200	0.0133	193	0.8215	336	0.0523	284	0.0351	219
239	neurotechnology-012	0.0051	109	0.0070	106	0.0038	87	0.0056	102	0.0066	94	0.0112	80	0.0075	61	0.0279	49
240	neurotechnology-013	0.0032	53	0.0045	58	0.0026	26	0.0036	40	0.0037	22	0.0068	20	0.0052	13	0.0278	39
241	rhn-001	0.0066	153	0.0098	154	0.0053	142	0.0079	155	0.0093	139	0.0156	117	0.0109	127	0.0308	172
242	rhn-002	0.0068	157	0.0096	150	0.0057	158	0.0087	169	0.0136	196	0.0253	180	0.0186	215	0.0302	159
243	nodeflux-002	0.0186	278	0.0340	284	0.0261	300	0.0451	297	0.0548	301	1.0000	379	1.0000	384	0.0299	152
244	notiontag-001	0.6846	385	0.8006	385	0.3955	354	0.5247	353	0.8669	372	0.8313	339	0.6362	357	0.2221	338
245	notiontag-002	0.0066	151	0.0089	138	0.0045	120	0.0061	118	0.0077	106	0.0137	97	0.0104	118	0.0299	151
246	nsensecorp-002	0.4277	369	0.5375	368	0.6734	368	0.7924	368	0.7194	358	0.6937	325	0.5617	351	0.5530	370
247	nsensecorp-003	0.0251	294	0.0295	279	0.0212	291	0.0305	283	0.0131	190	0.2139	287	0.0141	169	0.0872	300
248	ntechlab-011	0.0012	10	0.0019	6	0.0024	13	0.0028	23	0.0029	8	0.0055	6	0.0047	6	0.0288	115
249	ntechlab-012	0.0011	5	0.0016	3	0.0023	6	0.0030	26	0.0026	4	0.0050	3	0.0043	4	0.0280	59
250	omnigarde-001	0.0168	268	0.0260	270	0.0203	287	0.0402	293	0.0243	261	0.0327	204	0.0177	203	0.0288	113
251	omnigarde-002	0.0033	59	0.0046	60	0.0027	32	0.0039	52	0.0041	30	0.0076	28	0.0059	28	0.0278	41
252	omsecurity-000	0.2573	352	0.3835	356	0.3590	352	0.4903	352	0.3956	349	0.5003	309	0.2595	328	0.2400	342
253	openface-001	0.1804	342	0.2921	347	0.2878	349	0.3906	349	0.2054	337	0.2338	292	0.1549	320	0.2445	344
254	oz-003	0.0095	205	0.0143	199	0.0054	147	0.0077	148	0.0096	149	0.0175	138	0.0118	141	0.0288	117
255	oz-004	0.0033	61	0.0049	65	0.0038	94	0.0055	97	0.0081	116	0.0163	129	0.0142	170	0.0329	196
256	papsav1923-001	0.0078	180	0.0130	191	0.0068	177	0.0105	183	0.0119	177	0.0221	168	0.0136	160	0.0293	135
257	papsav1923-002	0.0021	29	0.0034	30	0.0026	20	0.0030	28	0.0048	52	0.0093	54	0.0086	87	0.0312	177
258	paravision-008	0.0018	21	0.0025	18	0.0024	9	0.0025	8	0.0036	19	0.0070	23	0.0063	33	0.0279	45
259	paravision-010	0.0012	9	0.0021	9	0.0022	3	0.0021	4	0.0027	5	0.0055	7	0.0050	10	0.0288	118
260	pensees-001	0.0087	191	0.0133	193	0.0071	183	0.0122	194	0.0145	205	0.0252	179	0.0195	222	0.0283	81
261	pixelall-006	0.0032	54	0.0042	50	0.0032	59	0.0039	53	0.0063	89	0.9960	362	0.0723	298	0.0283	80
262	pixelall-007	0.0036	70	0.0049	66	0.0039	95	0.0044	67	0.0068	96	0.9873	355	0.0217	232	0.0285	102
263	psl-008	0.0026	41	0.0040	43	0.0024	12	0.0028	22	0.0041	31	0.0077	29	0.0055	19	0.0280	56
264	psl-009	0.0161	266	0.0294	278	0.0023	4	0.0025	6	0.0036	20	0.0065	17	0.0048	7	0.0482	261

Table 21: FNMR is the proportion of mated comparisons below a threshold set to achieve the FMR given in the header on the fourth row. FMR is the proportion of impostor comparisons at or above that threshold. The light grey values give rank over all algorithms in that column. The pink columns use only same-sex impostors; others are selected regardless of demographics. The exception, in the green column, uses "matched-covariates" i.e. impostors of the same sex, age group, and country of birth. The second pink column includes effects of extended ageing. Missing entries for border, visa, mugshot and wild images generally mean the algorithm did not run to completion. The VISA columns compare images described in section 2.1. The MUGSHOT columns compare images described in section 2.4. The VISA-BORDER column compare images described in section 2.2 with those of section 2.3. The BORDER column compares images described in section 2.3. The WILD columns compare images described in section 2.5.

Algorithm	FALSE NON-MATCH RATE (FNMR)															
	CONSTRAINED, COOPERATIVE															
	Name	VISAMC	VISA	MUGSHOT	MUGSHOT+12-YRS	VISABORDER	BORDER	BORDER	LESS CONSTRAINED, NON-COOP.							
	FMR	0.0001	1E-06	1E-05	1E-05	1E-06	1E-06	1E-05	WILD							
265 <i>ptakuratsatu-000</i>	0.0060	140	0.0089	139	0.0070	180	0.0104	182	0.0096	150	0.0152	112	0.0100	108	0.0284	89
266 <i>pxl-001</i>	0.0488	316	0.0752	318	0.0586	321	0.1087	322	0.0946	319	0.1065	264	0.0625	290	0.1088	310
267 <i>pyramid-000</i>	0.0136	246	0.0233	255	0.0117	254	0.0192	251	0.0185	235	0.0322	203	0.0206	228	0.0304	162
268 <i>qnap-000</i>	0.0149	258	0.0228	252	0.0155	278	0.0267	277	0.0238	260	0.8329	340	0.0396	269	0.0324	188
269 <i>qnap-001</i>	0.0148	255	0.0215	246	0.0103	229	0.0162	234	0.0183	234	0.0301	196	0.0186	214	0.0360	226
270 <i>quantasoft-003</i>	0.0081	186	0.0113	179	0.0056	153	0.0076	146	0.0091	135	0.0161	124	0.0107	126	0.0414	243
271 <i>rankone-011</i>	0.0049	101	0.0075	117	0.0038	86	0.0048	80	0.0060	85	0.0143	102	0.0080	73	0.0359	225
272 <i>rankone-012</i>	0.0043	90	0.0058	86	0.0031	58	0.0038	48	0.0047	49	0.0081	38	0.0065	37	0.0358	224
273 <i>realnetworks-005</i>	0.0070	158	0.0093	143	0.0063	167	0.0089	171	0.0092	137	0.0161	125	0.0104	119	0.0289	124
274 <i>realnetworks-006</i>	0.0040	85	0.0056	82	0.8657	382	-	0.0059	80	0.0112	78	0.0085	85	0.1790	330	
275 <i>regula-000</i>	0.0184	277	0.0376	293	0.0103	230	0.0185	246	0.0120	178	0.9983	365	0.0231	238	0.0273	13
276 <i>regula-001</i>	0.0072	170	0.0107	170	0.0102	227	0.0179	244	0.0123	184	0.0333	208	0.0174	201	0.0295	139
277 <i>remarkai-001</i>	0.0144	252	0.0256	268	0.0102	226	0.0159	231	0.0162	216	0.0582	237	0.0185	212	0.0308	170
278 <i>remarkai-003</i>	0.0047	99	0.0063	96	0.0033	68	0.0049	83	0.0054	67	0.0100	66	0.0072	54	0.0275	25
279 <i>rendip-000</i>	0.0055	124	0.0077	119	0.0048	126	0.0060	116	0.0080	112	0.0142	101	0.0110	128	0.0433	249
280 <i>revealmedia-005</i>	0.0050	105	0.0074	116	0.0050	132	0.0068	131	0.0075	103	0.0124	91	0.0104	122	0.3960	360
281 <i>revealmedia-006</i>	0.0040	81	0.0067	101	0.0041	109	0.0056	100	0.0056	71	0.0085	45	0.0068	45	0.0278	40
282 <i>rokid-000</i>	0.0093	202	0.0145	202	0.0073	188	0.0102	180	0.0164	218	0.0280	191	0.0214	231	0.0857	299
283 <i>rokid-001</i>	0.0105	218	0.0162	217	0.0094	224	0.0163	236	0.0181	230	0.0276	190	0.0165	196	0.0325	191
284 <i>s1-003</i>	0.0051	108	0.0073	112	0.0044	116	0.0063	122	0.0052	63	0.0096	62	0.0070	50	0.1321	316
285 <i>s1-004</i>	0.0053	115	0.0080	127	0.0038	88	0.0059	114	0.0057	74	0.0103	68	0.0073	57	0.0281	65
286 <i>saffe-001</i>	0.4339	370	0.5261	366	0.7539	378	0.8736	379	0.7977	364	0.9810	352	0.7435	365	0.3887	359
287 <i>saffe-002</i>	0.0119	230	0.0206	240	0.0107	240	0.0177	242	0.0244	262	0.9998	369	0.2785	333	0.0308	169
288 <i>samsungsds-000</i>	0.0046	95	0.0069	105	0.0132	260	0.0081	157	0.0099	155	0.0179	141	0.0162	192	0.1874	332
289 <i>samtech-001</i>	0.0197	284	0.0365	291	0.0146	273	0.0241	269	0.0238	259	0.0394	222	0.0251	244	0.0337	201
290 <i>scanovate-002</i>	0.0175	276	0.0355	289	0.0146	271	0.0286	281	0.0269	267	0.0301	195	0.0178	206	0.0301	158
291 <i>scanovate-003</i>	0.0054	119	0.0080	128	0.0054	144	0.0072	138	0.0312	276	0.0599	239	0.0568	286	0.0283	79
292 <i>securifai-003</i>	0.4086	366	0.7577	384	0.7233	374	0.8070	371	0.7787	362	1.0000	380	0.9988	380	0.8326	378
293 <i>securifai-004</i>	0.0136	244	0.0192	236	0.0064	169	0.0099	179	0.0115	173	0.0272	186	0.0127	152	0.0347	209
294 <i>sensetime-005</i>	0.0019	22	0.0029	23	0.0022	2	0.0021	3	0.0023	2	0.0044	2	0.0039	2	0.0273	12
295 <i>sensetime-006</i>	0.0014	12	0.0024	15	0.0021	1	0.0020	1	0.0021	1	0.0040	1	0.0036	1	0.0272	9
296 <i>sertis-000</i>	0.0118	229	0.0208	242	0.0080	198	0.0127	199	0.0110	170	0.0176	139	0.0114	135	0.0285	100
297 <i>sertis-002</i>	0.0049	102	0.0061	92	0.0039	101	0.0061	121	0.0055	69	0.0099	65	0.0070	51	0.0281	64
298 <i>seventhsense-000</i>	0.0067	156	0.0099	159	0.0045	118	0.0065	127	0.0093	140	0.0169	132	0.0124	148	0.0275	24
299 <i>shaman-000</i>	0.9297	390	0.9774	389	0.9990	388	-	0.9999	382	1.0000	376	0.9999	383	0.9575	381	
300 <i>shaman-001</i>	0.3346	359	0.4616	361	0.2368	346	0.3723	348	0.3574	345	0.3527	299	0.2304	326	0.1498	322
301 <i>shu-002</i>	-	0.0079	124	0.0146	272	0.0308	284	1.0000	383	0.0183	144	0.0115	136	0.0284	90	
302 <i>shu-003</i>	0.0028	46	0.0041	49	0.0050	130	0.0088	170	0.0081	117	0.0133	96	0.0094	102	0.0283	86
303 <i>siat-002</i>	0.0091	198	0.0126	190	0.0109	242	0.0190	250	0.0276	269	0.0516	233	0.0464	279	0.0520	268
304 <i>siat-005</i>	0.0021	28	0.0038	38	0.0059	160	0.0049	84	0.0742	310	0.9623	350	0.6801	361	0.0279	46
305 <i>sjtu-003</i>	0.0017	18	0.0033	28	0.0030	47	0.0037	46	0.0058	76	0.0104	69	0.0081	75	0.0284	94
306 <i>sjtu-004</i>	0.0014	13	0.0025	17	0.0027	29	0.0028	24	0.0046	45	0.0086	47	0.0073	56	0.0272	7
307 <i>sktelecom-000</i>	0.0038	77	0.0054	77	0.0031	49	0.0051	91	0.0042	32	0.3418	298	0.0061	31	0.0293	137
308 <i>smartengines-000</i>	0.6240	384	0.7562	383	0.9552	384	0.9784	382	0.9515	378	0.9288	348	0.8200	367	0.8037	377

Table 22: FNMR is the proportion of mated comparisons below a threshold set to achieve the FMR given in the header on the fourth row. FMR is the proportion of impostor comparisons at or above that threshold. The light grey values give rank over all algorithms in that column. The pink columns use only same-sex impostors; others are selected regardless of demographics. The exception, in the green column, uses “matched-covariates” i.e. impostors of the same sex, age group, and country of birth. The second pink column includes effects of extended ageing. Missing entries for border, visa, mugshot and wild images generally mean the algorithm did not run to completion. The VISA columns compare images described in section 2.1. The MUGSHOT columns compare images described in section 2.4. The VISA-BORDER column compare images described in section 2.2 with those of section 2.3. The BORDER column compares images described in section 2.3. The WILD columns compare images described in section 2.5.

Algorithm	FALSE NON-MATCH RATE (FNMR)																
	CONSTRAINED, COOPERATIVE																
	Name	VISAMC	VISA	MUGSHOT	MUGSHOT12+YRS	VISABORDER	BORDER	BORDER	WILD	LESS CONSTRAINED, NON-COOP.							
FMR	0.0001	1E-06	1E-05	1E-05	1E-06	1E-06	1E-06	1E-05	0.0001								
309	smilart-002	0.2440	349	0.3532	351	-	-	0.3785	346	0.4145	306	0.2611	330	-			
310	smilart-003	0.6944	386	0.8836	386	0.0695	326	0.1193	326	0.0894	317	0.1221	270	0.0737	299	0.1190	314
311	sodec-000	0.0033	60	0.0044	57	0.0040	105	0.0053	95	0.0054	68	0.0096	61	0.0080	71	0.0274	17
312	sqisoft-001	0.1220	336	0.2088	336	0.1978	344	0.3386	345	0.2111	339	0.2798	296	0.1474	318	0.0519	267
313	sqisoft-002	0.0082	188	0.0124	185	0.0051	134	0.0086	167	0.0102	158	0.0183	145	0.0122	146	0.0287	109
314	stachu-000	0.0139	249	0.0208	241	0.0104	231	0.0145	222	0.0156	209	0.8063	335	0.1408	317	0.0332	199
315	starhybrid-001	0.0108	220	0.0138	195	0.0081	201	0.0113	188	0.0152	208	0.0265	184	0.0189	216	0.0350	218
316	sukshi-000	0.5409	380	0.6612	379	0.4556	359	0.6567	361	0.9296	377	0.8898	341	0.7384	364	0.6892	372
317	suprema-001	0.0041	87	0.0053	74	0.0038	91	0.0047	76	0.0060	84	0.0111	76	0.0095	105	0.0382	231
318	suprema-002	0.0030	50	0.0041	48	0.0034	73	0.0040	56	0.0045	41	0.0085	44	0.0072	55	0.0295	140
319	supremaid-001	0.0053	118	0.0073	113	0.0045	119	0.0066	128	0.0099	156	0.0186	147	0.0148	178	0.0352	220
320	synesis-006	0.0070	161	0.0096	151	0.0107	238	0.0166	238	-	-	0.0128	95	0.0089	92	0.0292	134
321	synesis-007	0.0050	106	0.0073	114	0.0062	166	0.0076	145	-	-	0.0105	70	0.0080	74	0.0288	111
322	synology-000	0.0149	256	0.0238	260	0.0148	274	0.0261	274	0.0221	248	0.0331	205	0.0209	229	0.0330	197
323	synology-002	0.0104	217	0.0153	212	0.0107	239	0.0184	245	0.0189	238	0.2032	284	0.0180	207	0.0312	175
324	sztu-000	0.0092	200	0.0139	197	0.0091	218	0.0201	257	0.0136	195	0.0685	247	0.0118	142	0.0270	2
325	sztu-001	0.0031	51	0.0043	55	0.0025	16	0.0028	20	0.0051	59	0.0113	82	0.0089	93	0.0275	20
326	t4isb-000	0.0058	129	0.0087	136	0.0041	110	0.0064	125	0.0083	120	0.0157	119	0.0103	116	0.0282	72
327	tech5-004	0.0123	236	0.0234	257	0.0086	212	0.0162	233	0.0065	93	0.0112	79	0.0082	78	0.0281	69
328	tech5-005	0.0054	122	0.0072	108	0.0069	178	0.0122	193	0.0060	83	0.0094	57	0.0066	40	0.0349	215
329	techsign-000	0.0325	303	0.0511	305	0.0435	313	0.0710	312	0.0746	311	0.1104	268	0.0841	303	0.0639	281
330	tevian-007	0.0019	23	0.0027	21	0.0032	63	0.0041	58	0.0045	42	0.0086	46	0.0078	67	0.0310	174
331	tevian-008	0.0012	8	0.0017	4	0.0033	65	0.0042	62	0.0042	34	0.0081	37	0.0068	46	0.0290	126
332	tiger-005	0.0624	322	0.2450	341	0.0292	305	0.0556	305	0.0430	291	1.0000	371	0.9964	378	0.0278	37
333	tiger-006	0.0066	152	0.0101	162	0.0050	133	0.0075	144	0.0089	131	0.0158	121	0.0117	139	0.0290	133
334	tinkoff-001	0.0145	254	0.0244	261	0.0318	306	0.0636	310	0.0236	257	1.0000	388	0.0339	257	0.0563	275
335	tongyi-005	0.0073	171	0.0146	204	0.0187	284	0.0421	296	0.0161	214	0.0215	163	0.0149	180	0.0399	235
336	toppanidgate-000	0.0021	26	0.0033	27	0.0026	21	0.0028	18	0.0039	27	0.0075	26	0.0068	44	0.0376	229
337	toshiba-004	0.0030	49	0.0042	53	0.0025	17	0.0027	15	0.0034	15	0.0063	13	0.0053	16	0.0278	36
338	toshiba-005	0.0023	33	0.0037	35	0.0024	11	0.0026	12	0.0072	101	0.0141	98	0.0130	155	0.0281	67
339	trueface-002	0.0060	139	0.0096	152	0.0048	125	0.0061	119	0.0112	172	0.0198	153	0.0155	187	0.0793	295
340	trueface-003	0.0070	162	0.0094	147	0.0053	140	0.0081	159	0.0122	180	0.0217	166	0.0159	190	0.0785	294
341	tuputech-000	0.3218	358	0.3696	354	-	-	-	0.3237	342	0.4304	307	0.2973	336	0.9415	380	
342	turingtechchip-001	0.0330	305	0.0540	308	0.0458	314	0.1007	319	0.4715	352	0.9286	347	0.8448	370	0.4035	361
343	twface-000	0.0051	107	0.0072	110	0.0041	108	0.0058	107	0.0071	99	0.0153	113	0.0100	107	0.0276	28
344	twface-001	0.0036	66	0.0051	70	0.0031	56	0.0038	47	0.0049	53	0.0091	52	0.0075	62	0.0277	31
345	ulsee-001	0.0151	260	0.0246	263	0.0113	250	0.0185	248	0.0187	237	0.6766	322	0.0181	209	0.0316	182
346	ultinous-000	0.2343	347	0.3484	350	-	-	-	-	-	-	-	-	-	-	-	
347	ultinous-001	0.2485	350	0.4003	357	-	-	-	-	-	-	-	-	-	-	-	
348	uluface-002	0.0081	184	0.0123	182	0.0071	182	0.0095	177	0.0107	165	1.0000	390	0.0140	167	0.0444	251
349	uluface-003	0.0100	213	0.0150	210	0.0079	196	0.0128	202	-	-	-	-	-	-	0.0635	280
350	unissey-001	0.0095	203	0.0160	216	0.0134	262	0.0150	226	0.0147	206	0.0253	181	0.0163	193	0.0946	302
351	upc-001	0.0234	290	0.0519	306	0.0291	304	0.0490	303	0.0294	272	0.2316	291	0.0389	268	0.0314	179
352	vcog-002	0.7522	388	0.9033	387	-	-	-	-	-	-	-	-	-	-	-	

Table 23: FNMR is the proportion of mated comparisons below a threshold set to achieve the FMR given in the header on the fourth row. FMR is the proportion of impostor comparisons at or above that threshold. The light grey values give rank over all algorithms in that column. The pink columns use only same-sex impostors; others are selected regardless of demographics. The exception, in the green column, uses “matched-covariates” i.e. impostors of the same sex, age group, and country of birth. The second pink column includes effects of extended ageing. Missing entries for border, visa, mugshot and wild images generally mean the algorithm did not run to completion. The VISA columns compare images described in section 2.1. The MUGSHOT columns compare images described in section 2.4. The VISA-BORDER column compare images described in section 2.2 with those of section 2.3. The BORDER column compares images described in section 2.3. The WILD columns compare images described in section 2.5.

Algorithm	Name	FALSE NON-MATCH RATE (FNMR)										LESS CONSTRAINED, NON-COOP.					
		CONSTRAINED, COOPERATIVE								WILD							
		VISAMC	VISA	MUGSHOT	MUGSHOT12+YRS	VISABORDER	BORDER	BORDER	1E-05	0.0001							
FMR		0.0001	1E-06	1E-05	1E-05	1E-06	1E-06	1E-06		0.0001							
353	vd-002	0.0429	312	0.0704	314	0.0569	320	0.0844	316	0.0801	313	0.0937	256	0.0577	287	0.0556	274
354	vd-003	0.0199	285	0.0222	251	0.0115	253	0.0130	206	0.0138	198	0.0239	172	0.0177	204	0.0389	232
355	veridas-006	0.0098	208	0.0167	225	0.0079	197	0.0127	198	0.0127	186	0.0217	165	0.0151	183	0.0286	105
356	veridas-007	0.0063	146	0.0083	131	0.0044	115	0.0058	109	0.0080	113	0.0152	111	0.0120	145	0.0284	91
357	verigram-000	0.0032	52	0.0043	54	0.0031	50	0.0034	33	0.0093	142	0.0175	137	0.0164	195	0.0276	27
358	verihubs-inteligensia-000	0.0070	160	0.0098	155	0.0048	127	0.0076	147	0.0092	136	0.0160	123	0.0117	138	0.0283	82
359	via-000	0.0216	288	0.0365	292	0.0177	282	0.0287	282	0.0296	273	0.0572	235	0.0290	254	0.0349	214
360	via-001	0.0149	257	0.0229	253	0.0114	252	0.0177	243	0.0183	233	0.04056	304	0.0176	202	0.0373	228
361	videmo-000	0.0298	301	0.0423	297	0.0155	279	0.0260	272	0.0246	264	0.0397	223	0.0239	241	0.0541	270
362	videmo-001	0.0295	299	0.0417	296	0.0164	281	0.0261	275	0.0355	279	0.0603	240	0.0442	277	0.1473	319
363	videonetics-001	0.5483	381	0.6446	376	0.7517	377	0.8607	376	0.8664	371	0.8255	337	0.6956	362	0.2986	352
364	videonetics-002	0.4274	367	0.5329	367	0.6081	366	0.7438	366	0.7775	361	0.7297	328	0.5756	352	0.1976	335
365	viettelhightech-000	0.0117	227	0.0166	221	0.0110	244	0.0198	256	0.0167	223	0.0249	177	0.0158	188	0.0409	242
366	vigilantsolutions-010	0.0109	221	0.0164	219	0.0074	189	0.0095	176	0.0209	245	0.0365	216	0.0233	239	0.0277	32
367	vigilantsolutions-011	0.0124	238	0.0176	230	0.0073	185	0.0095	175	0.0196	241	0.0360	214	0.0221	234	0.0274	15
368	vinai-000	0.0081	185	0.0124	184	0.0045	117	0.0072	137	0.0089	130	0.1814	277	0.0112	131	0.0274	18
369	vinbigdata-001	0.2576	353	0.2763	344	0.1404	336	0.1988	335	0.1407	326	0.1150	269	0.0703	296	0.9767	382
370	vion-000	0.0419	310	0.0590	311	0.0422	312	0.0478	300	0.0581	302	0.0968	262	0.0847	304	0.2479	345
371	visage-000	0.0933	330	0.1441	330	0.1316	334	0.2416	338	0.1395	325	0.1920	281	0.1001	308	0.0500	264
372	visionbox-001	0.0159	265	0.0270	274	0.0111	246	0.0173	241	0.0190	239	0.0315	201	0.0205	227	0.0389	233
373	visionbox-002	0.0058	128	0.0079	123	0.0060	162	0.0074	139	0.0084	122	0.0149	106	0.0113	134	0.0447	254
374	visionlabs-010	0.0017	20	0.0024	16	0.0026	23	0.0030	27	0.0033	14	0.0061	12	0.0052	12	0.0282	75
375	visionlabs-011	0.0012	7	0.0022	11	0.0024	14	0.0026	13	0.0028	6	0.0053	4	0.0046	5	0.0280	57
376	visteam-002	0.1564	341	0.2789	345	0.1581	341	0.2567	341	0.1776	332	0.2090	286	0.1021	309	0.0349	216
377	visteam-003	0.0804	328	0.2166	337	0.0613	325	0.1204	327	0.0963	320	0.1269	272	0.0441	276	0.0296	146
378	vnpt-002	0.0351	307	0.0424	299	0.0220	292	0.0316	286	0.0471	296	0.0817	254	0.0698	295	0.0400	236
379	vnpt-003	0.0117	226	0.0138	196	0.0040	106	0.0058	112	0.0087	127	0.0161	126	0.0126	150	0.0284	88
380	vocord-009	0.0022	30	0.0029	24	0.0036	79	0.0046	73	0.0052	62	0.0098	63	0.0086	89	0.0284	93
381	vocord-010	0.0024	36	0.0031	25	0.0036	80	0.0049	86	0.0025	3	0.0065	15	0.0040	3	0.0280	55
382	vts-000	0.0103	215	0.0174	227	0.0080	199	0.0129	205	0.0250	266	0.0450	227	0.0372	266	0.0596	277
383	winsense-001	0.0062	143	0.0099	160	0.0092	220	0.0210	258	0.0093	141	0.0144	104	0.0098	106	0.0320	186
384	winsense-002	0.0050	104	0.0073	115	0.0038	89	0.0059	113	0.0064	91	0.0118	88	0.0084	82	0.0307	168
385	wuhantianyu-001	0.0163	267	0.0262	272	0.0281	303	0.0569	308	0.0316	277	0.0486	230	0.0344	258	0.0324	189
386	x-laboratory-000	0.0071	163	0.0106	166	0.0123	257	0.0138	214	0.0419	290	0.5629	315	0.2852	335	0.0295	144
387	x-laboratory-001	0.0059	136	0.0110	174	0.0054	145	0.0078	151	0.0094	144	0.0142	100	0.0100	109	0.0294	138
388	xforwardai-001	0.0021	27	0.0034	31	0.0027	31	0.0028	19	0.0046	48	0.0088	49	0.0079	69	0.0281	68
389	xforwardai-002	0.0016	17	0.0023	13	0.0026	25	0.0025	7	0.0040	29	0.0081	39	0.0074	58	0.0282	70
390	xm-000	0.0015	14	0.0026	20	0.0031	54	0.0038	50	0.0058	77	0.0105	71	0.0082	79	0.0282	73
391	yisheng-004	0.1988	344	0.3329	348	0.1147	332	0.1849	332	0.2044	336	-	-	-	0.0908	301	
392	ytu-003	0.0015	15	0.0026	19	0.0066	175	0.0085	164	0.0064	92	0.0114	83	0.0103	117	0.0325	192
393	yoonik-002	0.0052	113	0.0062	94	0.0029	41	0.0034	35	0.0615	306	0.1279	273	0.1166	310	0.0549	272
394	yoonik-003	0.0034	63	0.0047	61	0.0032	61	0.0037	44	0.0816	315	0.2033	285	0.1601	321	0.0699	288
395	ytu-000	0.0057	126	0.0087	134	0.0121	255	0.0238	268	0.0047	50	0.0078	34	0.0059	26	0.0286	104
396	yuan-003	0.0078	178	0.0111	175	0.0062	165	0.0091	172	0.0106	163	0.0511	231	0.0123	147	0.0320	187

Table 24: FNMR is the proportion of mated comparisons below a threshold set to achieve the FMR given in the header on the fourth row. FMR is the proportion of impostor comparisons at or above that threshold. The light grey values give rank over all algorithms in that column. The pink columns use only same-sex impostors; others are selected regardless of demographics. The exception, in the green column, uses “matched-covariates” i.e. impostors of the same sex, age group, and country of birth. The second pink column includes effects of extended ageing. Missing entries for border, visa, mugshot and wild images generally mean the algorithm did not run to completion. The VISA columns compare images described in section 2.1. The MUGSHOT columns compare images described in section 2.4. The VISA-BORDER column compare images described in section 2.2 with those of section 2.3. The BORDER column compares images described in section 2.3. The WILD columns compare images described in section 2.5.

		FALSE NON-MATCH RATE (FNMR)															
		CONSTRAINED, COOPERATIVE						LESS CONSTRAINED, NON-COOP.									
	Algorithm	VISAMC	VISA	MUGSHOT	MUGSHOT12+YRS	VISABORDER	BORDER	BORDER	WILD								
	FMR	0.0001	1E-06	1E-05	1E-05	1E-06	1E-06	1E-05	0.0001								
397	yuan-004	0.0058	131	0.0078	122	0.0039	99	0.0055	99	0.0234	254	0.0442	225	0.0353	260	0.0299	153

Table 25: FNMR is the proportion of mated comparisons below a threshold set to achieve the FMR given in the header on the fourth row. FMR is the proportion of impostor comparisons at or above that threshold. The light grey values give rank over all algorithms in that column. The pink columns use only same-sex impostors; others are selected regardless of demographics. The exception, in the green column, uses “matched-covariates” i.e. impostors of the same sex, age group, and country of birth. The second pink column includes effects of extended ageing. Missing entries for border, visa, mugshot and wild images generally mean the algorithm did not run to completion. The VISA columns compare images described in section 2.1. The MUGSHOT columns compare images described in section 2.4. The VISA-BORDER column compare images described in section 2.2 with those of section 2.3. The BORDER column compares images described in section 2.3. The WILD columns compare images described in section 2.5.

$\text{FNMR}(T)$
 $\text{FMR}(T)$
 “False non-match rate”
 “False match rate”

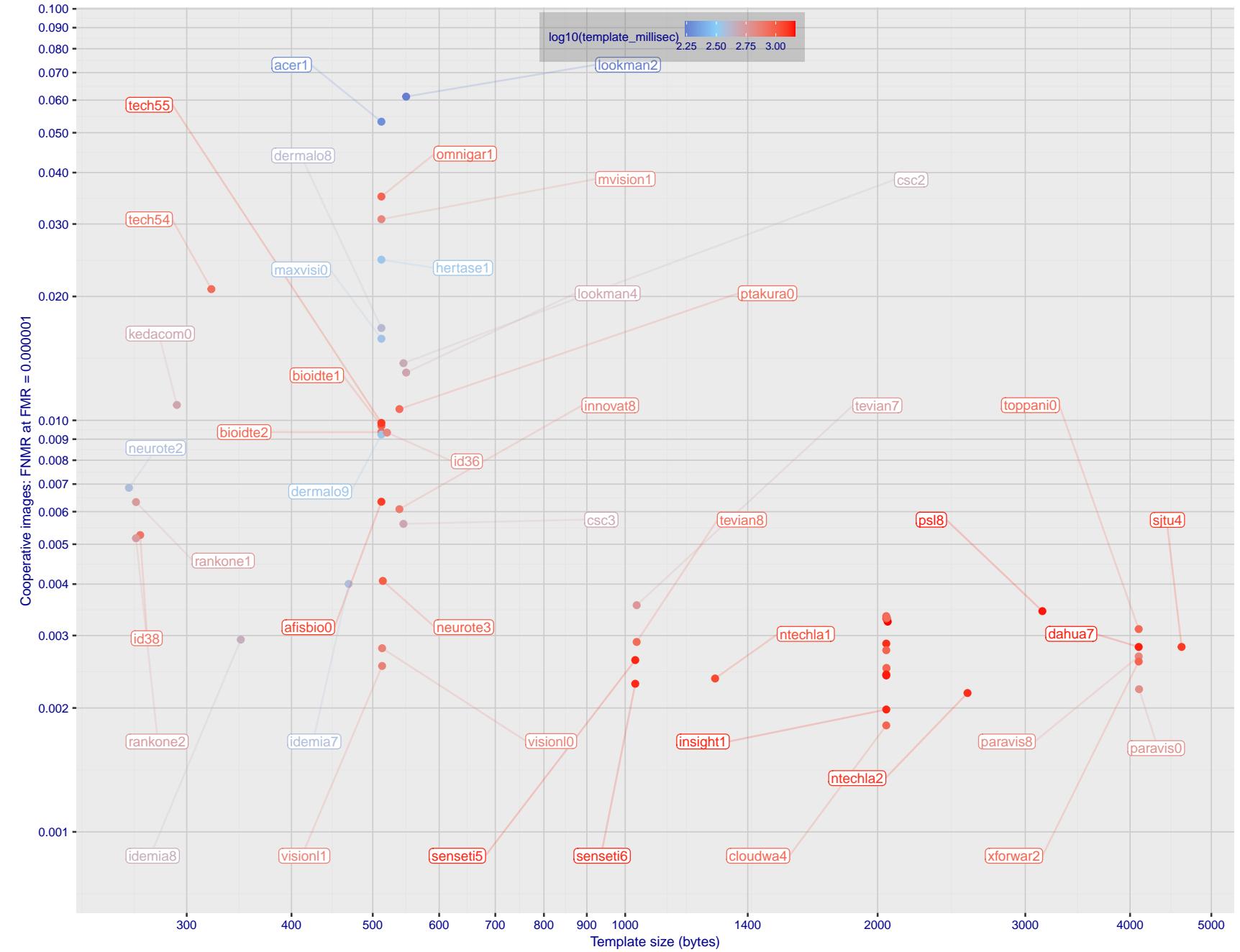


Figure 1: The points show false non-match rates (FNMR) versus the size of the encoded template. FNMR is the geometric mean of FNMR values for visa and mugshot images (from Figs. 59 and 79) at the false match rate (FMR) given in the y-axis label. The color of the points encodes template generation time - which spans at least one order of magnitude. Durations are measured on a single core of a c. 2016 Intel Xeon CPU E5-2630 v4 running at 2.20GHz. Algorithms with poor FNMR are omitted.

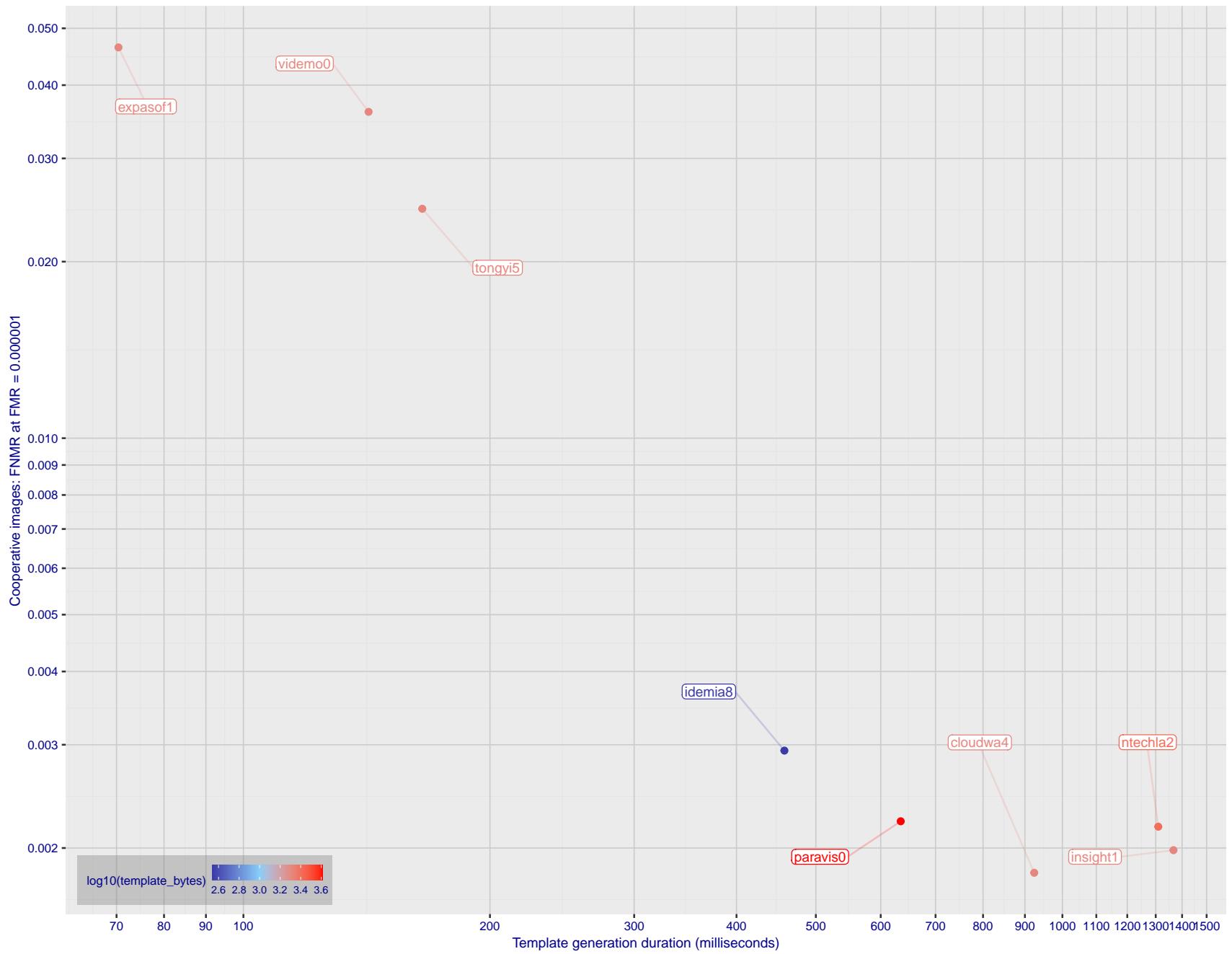


Figure 2: The points show false non-match rates (FNMR) versus the duration of the template generation operation. FNMR is the geometric mean of FNMR values for visa and mugshot images (from Figs. 59 and 79) at a false match rate (FMR) given in the y-axis label. Template generation time is a median estimated over 640 x 480 pixel portraits. It is measured on a single core of a c. 2016 Intel Xeon CPU E5-2630 v4 running at 2.20GHz. The color of the points encodes template size - which span two orders of magnitude. Algorithms with poor FNMR are omitted.

1 Metrics

1.1 Core accuracy

Given a vector of N genuine scores, u , the false non-match rate (FNMR) is computed as the proportion below some threshold, T:

$$\text{FNMR}(T) = 1 - \frac{1}{N} \sum_{i=1}^N H(u_i - T) \quad (1)$$

where $H(x)$ is the unit step function, and $H(0)$ taken to be 1.

Similarly, given a vector of N impostor scores, v , the false match rate (FMR) is computed as the proportion above T:

$$\text{FMR}(T) = \frac{1}{N} \sum_{i=1}^N H(v_i - T) \quad (2)$$

The threshold, T, can take on any value. We typically generate a set of thresholds from quantiles of the observed impostor scores, v , as follows. Given some interesting false match rate range, $[\text{FMR}_L, \text{FMR}_U]$, we form a vector of K thresholds corresponding to FMR measurements evenly spaced on a logarithmic scale

$$T_k = Q_v(1 - \text{FMR}_k) \quad (3)$$

where Q is the quantile function, and FMR_k comes from

$$\log_{10} \text{FMR}_k = \log_{10} \text{FMR}_L + \frac{k}{K} [\log_{10} \text{FMR}_U - \log_{10} \text{FMR}_L] \quad (4)$$

Error tradeoff characteristics are plots of FNMR(T) vs. FMR(T). These are plotted with $\text{FMR}_U \rightarrow 1$ and FMR_L as low as is sustained by the number of impostor comparisons, N. This is somewhat higher than the “rule of three” limit $3/N$ because samples are not independent, due to re-use of images.

2 Datasets

2.1 Visa images

- ▷ The number of images is on the order of 10^5 .
- ▷ The number of subjects is on the order of 10^5 .
- ▷ The number of subjects with two images is on the order of 10^4 .
- ▷ The images have geometry in reasonable conformance with the ISO/IEC 19794-5 Full Frontal image type. Pose is generally excellent.
- ▷ The images are of size 252x300 pixels. The mean interocular distance (IOD) is 69 pixels.
- ▷ The images are of subjects from greater than 100 countries, with significant imbalance due to visa issuance patterns.
- ▷ The images are of subjects of all ages, including children, again with imbalance due to visa issuance demand.
- ▷ Many of the images are live capture. A substantial number of the images are photographs of paper photographs.
- ▷ When these images are input to the algorithm, they are labelled as being of type "ISO" - see Table 4 of the FRVT API.

2.2 Application images

- ▷ The number of images is on the order of 10^6 .
- ▷ The number of subjects is on the order of 10^6 .
- ▷ The number of subjects with two images is on the order of 10^6 .
- ▷ The images have geometry in good conformance with the ISO/IEC 19794-5 Full Frontal image type. Pose is generally excellent.
- ▷ The images are of size 300x300 pixels. The mean interocular distance (IOD) is 61 pixels.
- ▷ The images are of subjects from greater than 100 countries, with significant imbalance due to population and immigration patterns.
- ▷ The images are of subjects of adults with imbalance due to population and immigration patterns and demand.
- ▷ All of the images are live capture.
- ▷ When these images are input to the algorithm, they are labelled as being of type "ISO" - see Table 4 of the FRVT API.

2.3 Border crossing images

- ▷ The number of images is on the order of 10^6 .
- ▷ The number of subjects is on the order of 10^6 .
- ▷ The number of subjects with two images is on the order of 10^6 .
- ▷ The images are taken with a camera oriented by an attendant toward a cooperating subject. This is done under time constraints so there are roll, pitch and yaw angle variations. Also background illumination is sometimes strong, so the face is under-exposed. There is some perspective distortion due to close range images. Some faces are partially cropped.
- ▷ The images are of subjects from greater than 100 countries, with significant imbalance due to population and immigration patterns.
- ▷ The images are of subjects of adults with imbalance due to population and immigration patterns and demand.

- ▷ The images have mean IOD of 38 pixels.
- ▷ The images are all live capture.
- ▷ When these images are input to the algorithm, they are labelled as being of type "WILD" - see Table 4 of the FRVT API.

2.4 Mugshot images

- ▷ The number of images is on the order of 10^6 .
- ▷ The number of subjects is on the order of 10^6 .
- ▷ The number of subjects with two images is on the order of 10^6 .
- ▷ The images have geometry in reasonable conformance with the ISO/IEC 19794-5 Full Frontal image type.
- ▷ The images are of variable sizes. The median IOD is 105 pixels. The mean IOD is 113 pixels. The 1-st, 5-th, 10-th, 25-th, 75-th, 90-th and 99-th percentiles are 34, 58, 70, 87, 121, 161 and 297 pixels.
- ▷ The images are of subjects from the United States.
- ▷ The images are of adults.
- ▷ The images are all live capture.
- ▷ When these images are input to the algorithm, they are labelled as being of type "mugshot" - see Table 4 of the FRVT API.

2.5 Wild images

- ▷ The number of images is on the order of 10^5 .
- ▷ The number of subjects is on the order of 10^3 .
- ▷ The number of subjects with two images on the order of 10^3 .
- ▷ The images include many photojournalism-style images. Images are given to the algorithm using a variable but generally tight crop of the head. Resolution varies very widely. The images are very unconstrained, with wide yaw and pitch pose variation. Faces can be occluded, including hair and hands.
- ▷ The images are of adults.
- ▷ All of the images are live capture, none are scanned.
- ▷ When these images are input to the algorithm, they are labelled as being of type "WILD" - see Table 4 of the FRVT API.

3 Results

3.1 Test goals

- ▷ To state absolute accuracy for different kinds of images, including those with and without subject cooperation.
- ▷ To state comparative accuracy, across algorithms.

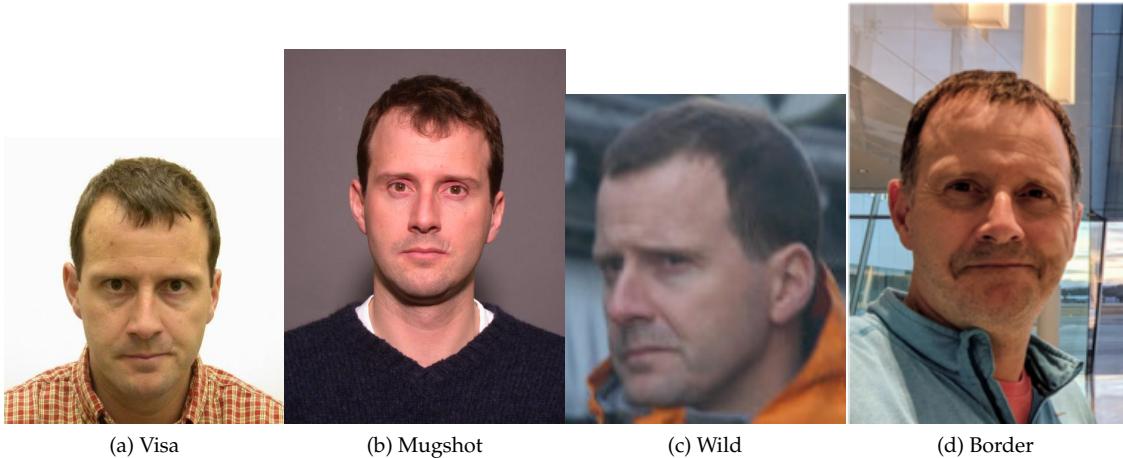


Figure 3: The figure gives simulated samples of image types used in this report.

3.2 Test design

Method: For visa images:

- ▷ The comparisons are of visa photos against visa photos.
 - ▷ The number of genuine comparisons is on the order of 10^4 .
 - ▷ The number of impostor comparisons is on the order of 10^{10} .
 - ▷ The comparisons are fully zero-effort, meaning impostors are paired without attention to sex, age or other covariates. However, later analysis is conducted on subsets.
 - ▷ The number of persons is on the order of 10^5 .
 - ▷ The number of images used to make 1 template is 1.
 - ▷ The number of templates used to make each comparison score is two corresponding to simple one-to-one verification.

Method: For mugshot images:

- ▷ The comparisons are of mugshot photos against mugshot photos.
 - ▷ The number of genuine comparisons is on the order of 10^6 .
 - ▷ The number of impostor comparisons is on the order of 10^8 .
 - ▷ The impostors are paired by sex, but not by age or other covariates.
 - ▷ The number of persons is on the order of 10^6 .
 - ▷ The number of images used to make 1 template is 1.
 - ▷ The number of templates used to make each comparison score is two corresponding to simple one-to-one verification.

Method: For visa-border comparisons:

- ▷ The comparisons are of visa-like frontals against border crossing webcam photos.
 - ▷ The number of genuine comparisons is on the order of 10^6 .
 - ▷ The number of impostor comparisons is on the order of 10^8 .

- ▷ The impostors are paired by sex, but not by age or other covariates.
- ▷ The number of persons is on the order of 10^6 .
- ▷ The number of images used to make 1 template is 1.
- ▷ The number of templates used to make each comparison score is two corresponding to simple one-to-one verification.

Method: For border-border comparisons:

- ▷ The comparisons are of border crossing webcam photos.
- ▷ The number of genuine comparisons is on the order of 10^6 .
- ▷ The number of impostor comparisons is on the order of 10^8 .
- ▷ The impostors are paired by sex, but not by age or other covariates.
- ▷ The number of persons is on the order of 10^6 .
- ▷ The number of images used to make 1 template is 1.
- ▷ The number of templates used to make each comparison score is two corresponding to simple one-to-one verification.

Method: For wild images:

- ▷ The comparisons are of wild photos against wild photos.
- ▷ The number of genuine comparisons is on the order of 10^6 .
- ▷ The number of impostor comparisons is on the order of 10^7 .
- ▷ The comparisons are fully zero-effort, meaning impostors are paired without attention to sex, age or other covariates.
- ▷ The number of persons is on the order of 10^4 .
- ▷ The number of images used to make 1 template is 1.
- ▷ The number of templates used to make each comparison score is two corresponding to simple one-to-one verification.

Method: For child exploitation images:

- ▷ The comparisons are of unconstrained child exploitation photos against others of the same type.
- ▷ The number of genuine comparisons is on the order of 10^4 .
- ▷ The number of impostor comparisons is on the order of 10^7 .
- ▷ The comparisons are fully zero-effort, meaning impostors are paired without attention to sex, age or other covariates.
- ▷ The number of persons is on the order of 10^3 .
- ▷ The number of images used to make 1 template is 1.
- ▷ The number of templates used to make each comparison score is two corresponding to simple one-to-one verification.
- ▷ We produce two performance statements. First, is a DET as used for visa and mugshot images. The second is a cumulative match characteristic (CMC) summarizing a simulated one-to-many search process. This is done as follows.
 - We regard M enrollment templates as items in a gallery.

- These M templates come from $M > N$ individuals, because multiple images of a subject are present in the gallery under separate identifiers.
- We regard the verification templates as search templates.
- For each search we compute the rank of the highest scoring mate.
- This process should properly be conducted with a 1:N algorithm, such as those tested in NIST IR 8009. We use the 1:1 algorithms in a simulated 1:N mode here to a) better reflect what a child exploitation analyst does, and b) to show algorithm efficacy is better than that revealed in the verification DETs.

3.3 Failure to enroll

Name	Algorithm	Failure to Enrol Rate ¹							
		APPLICATION		BORDER		CHILD-EXPLOIT		MUGSHOT	
		SEC. 2.2	SEC. 2.3	SEC. ??	SEC. 2.4	SEC. 2.1	SEC. 2.5		
1	20face-000	0.0000	253	0.0008	205	-	361	0.0000	122
2	20face-001	0.0000	200	0.0008	206	-	192	0.0000	120
3	3divi-006	0.0000	242	0.0007	180	-	388	0.0001	214
4	3divi-007	0.0000	221	0.0007	181	-	281	0.0001	215
5	acer-001	0.0000	233	0.0011	251	-	228	0.0001	190
6	acer-002	0.0000	326	0.0008	200	-	162	0.0003	280
7	acisw-003	0.0000	44	0.0000	84	-	75	0.0000	30
8	acisw-007	0.0000	89	0.0000	45	-	290	0.0000	101
9	adera-002	0.0000	308	0.0034	323	-	70	0.0003	287
10	adera-003	0.0000	307	0.0034	322	-	81	0.0003	288
11	advance-002	0.0000	189	0.0013	271	-	52	0.0000	173
12	advance-003	0.0000	296	0.0012	260	-	190	0.0001	229
13	afisbiometrics-000	0.0000	173	0.0008	194	-	126	0.0000	121
14	aifirst-001	0.0000	107	0.0000	55	0.0000	11	0.0000	94
15	aigen-001	0.0000	48	0.0000	72	-	204	0.0000	17
16	aigen-002	0.0000	98	0.0000	41	-	310	0.0000	107
17	ailabs-001	0.0000	238	0.0090	360	-	383	0.0007	337
18	aimall-002	0.0000	314	0.0043	336	-	273	0.0012	352
19	aimall-003	0.0000	286	0.0012	265	-	73	0.0004	302
20	aiunionface-000	0.0000	167	0.0000	12	-	331	0.0000	57
21	aize-001	0.0001	352	0.0040	331	-	104	0.0026	371
22	aize-002	0.0000	75	0.0014	274	-	186	0.0005	323
23	ajou-001	0.0000	204	0.0020	294	-	168	0.0001	217
24	alchera-002	0.0000	202	0.0008	211	-	200	0.0001	237
25	alchera-003	0.0001	363	0.0013	269	-	307	0.0002	266
26	alfabeto-001	0.0005	371	0.0650	390	-	372	0.0024	366
27	alice-000	0.0000	114	0.0006	157	-	284	0.0000	136
28	alleyes-000	0.0000	188	0.0010	234	-	86	0.0002	245
29	allgovision-000	0.0007	375	0.0062	353	-	111	0.0026	370
30	alphaface-001	0.0000	249	0.0012	256	-	351	0.0000	177
31	alphaface-002	0.0000	231	0.0012	257	-	260	0.0000	179
32	amplifiedgroup-001	0.0114	389	0.1023	392	-	119	0.0189	390
33	androvideo-000	0.0000	15	0.0000	95	-	141	0.0000	51
34	anke-004	0.0000	184	0.0011	248	0.0944	28	0.0001	222
35	anke-005	0.0000	194	0.0012	258	0.1228	30	0.0001	233
36	antheus-000	0.0000	31	0.0000	78	0.0000	5	0.0000	37
37	antheus-001	0.0000	64	0.0000	75	-	196	0.0000	11
38	anyvision-004	0.0000	298	0.0017	284	0.1660	33	0.0001	234
39	anyvision-005	0.0000	192	0.0013	266	-	54	0.0000	150
40	armatura-001	0.0000	315	0.0021	299	-	134	0.0005	318
41	asusaics-000	0.0000	50	0.0000	71	-	207	0.0000	16
42	asusaics-001	0.0000	118	0.0000	28	-	250	0.0000	81
43	authenmetric-003	0.0000	169	0.0000	10	-	338	0.0000	59
44	authenmetric-004	0.0000	110	0.0000	51	-	278	0.0000	96
45	aware-005	0.0000	281	0.0020	293	-	370	0.0001	244
46	aware-006	0.0000	175	0.0009	219	-	129	0.0000	153
47	awiros-001	0.0039	380	0.0369	384	-	255	0.0386	391
48	awiros-002	0.0000	327	0.0038	329	-	97	0.0007	336
49	ayftech-001	0.0002	365	0.0046	341	-	180	0.0043	381
50	ayonix-000	0.0053	383	0.0341	381	0.0000	1	0.0113	388
51	beethedata-000	0.0005	370	0.0042	335	-	385	0.0002	254
52	beyneai-000	0.0000	18	0.0000	102	-	113	0.0000	40
53	biocube-001	0.0006	373	0.0391	385	-	339	0.0015	357
54	bioditechswiss-001	0.0000	246	0.0007	175	-	364	0.0000	142
55	bioditechswiss-002	0.0000	226	0.0007	178	-	248	0.0000	146
56	bm-001	0.0000	51	0.0000	70	0.0000	8	0.0000	110
57	boetech-001	0.0087	387	0.0272	373	-	83	0.0032	377
58	boetech-002	0.0087	386	0.0272	374	-	144	0.0032	378

Table 26: FTE is the proportion of failed template generation attempts. Failures can occur because the software throws an exception, or because the software electively refuses to process the input image. This would typically occur if a face is not detected. FTE is measured as the number of function calls that give EITHER a non-zero error code OR that give a "small" template. This is defined as one whose size is less than 0.3 times the median template size for that algorithm. This second rule is needed because some algorithms incorrectly fail to return a non-zero error code when template generation fails.

A hyphen "-" indicates the dataset was not produced.¹ The effects of FTE are included in the accuracy results of this report by regarding any template comparison involving a failed template to produce a low similarity score. Thus higher FTE results in higher FNMR and lower FMR.

	Algorithm	Failure to Enrol Rate ¹											
		APPLICATION	BORDER	CHILD-EXPLOIT	MUGSHOT	VISA	WILD	SEC. 2.2	SEC. 2.3	SEC. ??	SEC. 2.4	SEC. 2.1	SEC. 2.5
59	bressee-001	0.0000	252	0.0010	240	-	356	0.0002	252	0.0003	157	0.0003	128
60	bressee-002	0.0000	306	0.0020	297	-	358	0.0008	338	0.0004	210	0.0031	291
61	camvi-002	0.0000	139	0.0000	16	0.0000	21	0.0000	71	0.0000	73	0.0000	43
62	camvi-004	0.0000	171	0.0000	109	0.0000	15	0.0000	60	0.0000	55	0.0000	50
63	canon-002	0.0000	112	0.0000	50	-	282	0.0000	99	0.0000	94	0.0000	63
64	canon-003	0.0000	225	0.0008	193	-	245	0.0000	172	0.0004	242	0.0003	159
65	ceiec-003	0.0000	81	0.0013	272	-	158	0.0001	194	0.0004	248	0.0004	168
66	ceiec-004	0.0000	46	0.0008	204	-	209	0.0000	147	0.0004	193	0.0004	201
67	chosun-001	0.0000	134	0.0000	33	-	239	0.0000	80	0.0000	76	0.0000	76
68	chosun-002	0.0000	22	0.0000	101	-	117	0.0000	42	0.0000	42	0.0000	21
69	chiface-003	0.0000	303	0.0018	287	-	67	0.0001	201	0.0006	330	0.0010	257
70	chiface-004	0.0000	77	0.0017	282	-	181	0.0000	160	0.0004	255	0.0020	283
71	clearviewai-000	0.0000	235	0.0003	133	-	240	0.0000	163	0.0003	143	0.0003	129
72	closeli-001	0.0000	115	0.0000	48	-	286	0.0000	98	0.0000	93	0.0001	115
73	cloudmatrix-000	0.0000	274	0.0012	261	-	317	0.0001	193	0.0004	184	0.0004	192
74	cloudwalk-hr-003	0.0000	180	0.0008	207	-	143	0.0001	200	0.0004	187	0.0113	324
75	cloudwalk-hr-004	0.0000	211	0.0011	254	-	164	0.0004	304	0.0003	166	0.0129	327
76	cloudwalk-mt-003	0.0000	255	0.0007	170	-	359	0.0002	262	0.0004	264	0.0004	175
77	cloudwalk-mt-004	0.0000	187	0.0009	212	-	82	0.0002	267	0.0004	276	0.0004	186
78	clova-000	0.0000	318	0.0022	300	-	103	0.0006	330	0.0005	294	0.0019	280
79	cogent-005	0.0000	145	0.0000	20	-	368	0.0000	67	0.0000	70	0.0000	41
80	cogent-006	0.0000	84	0.0000	62	-	156	0.0000	2	0.0000	3	0.0000	15
81	cognitec-003	0.0001	346	0.0194	369	-	305	0.0003	294	0.0005	305	0.0039	295
82	cognitec-004	0.0001	347	0.0037	328	-	313	0.0003	295	0.0005	304	0.0035	292
83	cor-001	0.0000	178	0.0006	161	-	135	0.0002	274	0.0004	225	0.0004	212
84	coretech-000	0.0000	29	0.0000	82	-	89	0.0000	35	0.0000	37	0.0000	39
85	corsight-001	0.0000	257	0.0006	166	-	326	0.0001	241	0.0004	209	0.0004	191
86	corsight-002	0.0000	217	0.0005	155	-	309	0.0001	224	0.0004	214	0.0003	158
87	csc-002	0.0015	377	0.0033	319	-	99	0.0006	331	0.0006	337	0.0968	376
88	csc-003	0.0015	378	0.0033	318	-	266	0.0006	332	0.0006	338	0.0968	377
89	ctbcbank-000	0.0001	349	0.0051	346	0.3285	40	0.0011	350	0.0019	371	0.0868	371
90	ctbcbank-001	0.0000	328	0.0036	327	-	106	0.0005	320	0.0010	345	0.0844	368
91	cubox-001	0.0000	141	0.0000	17	-	390	0.0000	72	0.0000	72	0.0000	44
92	cubox-002	0.0000	280	0.0006	164	-	371	0.0002	275	0.0005	321	0.0016	276
93	cudocommunication-001	0.0000	120	0.0000	31	-	244	0.0000	85	0.0000	89	0.0000	94
94	cuhkee-001	0.0000	212	0.0011	253	-	289	0.0000	125	0.0004	215	0.1278	384
95	cybercore-000	0.0000	245	0.0073	357	-	396	0.0001	211	0.0005	300	0.0383	357
96	cybercore-001	0.0000	313	0.0001	120	-	170	0.0002	248	0.0002	121	0.0018	279
97	cyberextruder-001	0.0029	379	0.0293	375	0.5338	46	0.0024	364	0.0029	384	0.0597	364
98	cyberextruder-002	0.0013	376	0.0840	391	0.2672	39	0.0027	372	0.0028	381	0.0335	354
99	cyberlink-007	0.0000	41	0.0003	127	-	72	0.0000	116	0.0003	156	0.0001	102
100	cyberlink-008	0.0000	143	0.0004	144	-	362	0.0000	117	0.0003	158	0.0002	126
101	dahua-006	0.0000	79	0.0000	108	-	153	0.0000	165	0.0003	167	0.0000	16
102	dahua-007	0.0000	149	0.0000	105	-	344	0.0000	167	0.0003	169	0.0000	60
103	daon-000	0.0000	332	0.0028	310	-	115	0.0014	356	0.0015	366	0.0030	290
104	decatur-000	0.0000	268	0.0020	292	-	208	0.0004	310	0.0005	291	0.0236	342
105	decatur-001	0.0000	237	0.0009	226	-	380	0.0001	204	0.0004	207	0.0004	206
106	deepglint-003	0.0000	234	0.0004	145	-	237	0.0002	268	0.0004	201	0.0003	145
107	deepglint-004	0.0000	214	0.0005	149	-	301	0.0002	272	0.0004	195	0.0003	147
108	deepsea-001	0.0000	38	0.0000	88	0.0000	2	0.0000	26	0.0000	31	0.0000	33
109	deepsense-000	0.0000	34	0.0006	167	-	51	0.0000	132	0.0004	170	0.0003	150
110	dermalog-008	0.0000	322	0.0031	316	-	56	0.0006	325	0.0003	131	0.0002	116
111	dermalog-009	0.0000	321	0.0031	315	-	96	0.0006	326	0.0003	132	0.0002	117
112	didiglobalface-001	0.0000	254	0.0012	255	0.2175	35	0.0000	178	0.0004	257	0.0004	174
113	digidata-000	0.0000	208	0.0023	301	-	149	0.0004	312	0.0006	333	0.0006	231
114	digitalbarriers-002	0.0001	355	0.0045	338	-	299	0.0028	374	0.0027	378	0.0071	311
115	dps-000	0.0000	130	0.0000	37	-	229	0.0000	75	0.0000	80	0.0000	80
116	dsk-000	0.0000	159	0.0000	2	0.0000	19	0.0000	66	0.0000	63	0.0000	56

Table 27: FTE is the proportion of failed template generation attempts. Failures can occur because the software throws an exception, or because the software electively refuses to process the input image. This would typically occur if a face is not detected. FTE is measured as the number of function calls that give EITHER a non-zero error code OR that give a “small” template. This is defined as one whose size is less than 0.3 times the median template size for that algorithm. This second rule is needed because some algorithms incorrectly fail to return a non-zero error code when template generation fails.

A hyphen “-” indicates the dataset was not produced.¹ The effects of FTE are included in the accuracy results of this report by regarding any template comparison involving a failed template to produce a low similarity score. Thus higher FTE results in higher FNMR and lower FMR.

	Algorithm	Failure to Enrol Rate ¹											
		APPLICATION	BORDER	CHILD-EXPLOIT	MUGSHOT	VISA	WILD	SEC. 2.2	SEC. 2.3	SEC. ??	SEC. 2.4	SEC. 2.1	SEC. 2.5
117	einetworks-000	0.0000	329	0.0017	283	-	212	0.0002	263	0.0005	314	0.0008	252
118	ekin-002	0.0000	56	0.0000	110	-	220	0.0000	115	0.0000	112	0.0019	281
119	enface-000	0.0000	165	0.0012	264	-	328	0.0000	157	0.0004	218	0.0004	193
120	enface-001	0.0000	53	0.0012	263	-	216	0.0000	140	0.0004	212	0.0004	179
121	eocortex-000	0.0095	388	0.0602	388	-	345	0.0094	387	0.0059	388	0.1405	388
122	ercacat-001	0.0000	16	0.0005	150	-	100	0.0000	156	0.0003	159	0.0002	120
123	euronovate-001	0.0255	393	0.0102	362	-	201	0.0021	361	0.0004	285	0.2451	390
124	expasoft-001	0.0000	122	0.0000	26	-	254	0.0000	87	0.0000	87	0.0000	87
125	expasoft-002	0.0000	11	0.0000	94	-	145	0.0000	50	0.0000	49	0.0000	26
126	f8-001	0.0003	366	0.0059	352	0.2026	34	0.0035	379	0.0030	385	0.0087	318
127	faceonlive-001	0.0000	338	0.0029	313	-	332	0.0013	354	0.0011	353	0.0160	333
128	facesoft-000	0.0000	153	0.0000	6	0.0000	17	0.0000	61	0.0000	66	0.0000	58
129	facetag-000	0.0000	95	0.0000	43	-	293	0.0000	106	0.0000	106	0.0000	74
130	facetag-002	0.0000	133	0.0000	34	-	236	0.0000	79	0.0000	77	0.0000	77
131	facex-001	0.0001	361	0.0360	383	-	62	0.0047	383	0.0027	379	0.1109	380
132	facex-002	0.0001	362	0.0360	382	-	352	0.0047	384	0.0027	380	0.1109	379
133	farfaces-001	0.0000	325	0.0007	177	-	223	0.0003	290	0.0003	148	0.0006	240
134	fiberhome-nanjing-003	0.0000	164	0.0004	141	-	319	0.0000	55	0.0003	138	0.0001	104
135	fiberhome-nanjing-004	0.0000	1	0.0004	142	-	120	0.0000	45	0.0003	136	0.0001	101
136	fincore-000	0.0000	247	0.0008	208	-	373	0.0001	185	0.0004	253	0.0006	233
137	fujitsulab-002	0.0000	166	0.0009	217	-	335	0.0001	230	0.0003	137	0.0003	135
138	fujitsulab-003	0.0000	91	0.0008	198	-	296	0.0001	221	0.0001	118	0.0003	132
139	geo-002	0.0000	199	0.0015	275	-	224	0.0001	181	0.0004	271	0.0017	278
140	geo-004	0.0000	174	0.0005	154	-	125	0.0001	212	0.0004	199	0.0009	256
141	glory-003	0.0000	293	0.0027	307	-	337	0.0004	303	0.0005	297	0.0244	345
142	glory-004	0.0000	279	0.0020	296	-	381	0.0001	227	0.0004	269	0.0167	334
143	gorilla-007	0.0000	207	0.0009	230	-	184	0.0001	202	0.0004	244	0.0004	184
144	gorilla-008	0.0000	250	0.0009	229	-	353	0.0001	203	0.0004	251	0.0004	183
145	graymatics-001	0.0000	49	0.0010	231	-	205	0.0001	240	0.0004	205	0.0006	234
146	griaule-000	0.0000	334	0.0026	305	-	138	0.0004	313	0.0010	346	0.0023	284
147	hertasecurity-000	0.0133	390	0.0077	359	-	336	0.0025	369	0.0243	394	0.0171	336
148	hertasecurity-001	0.0000	83	0.0000	112	-	155	0.0000	126	0.0001	114	0.0002	125
149	hik-001	0.0000	86	0.0000	114	-	165	0.0000	3	0.0000	2	0.0000	13
150	hisign-001	0.0000	94	0.0000	44	-	291	0.0000	105	0.0000	105	0.0000	73
151	hyperverge-001	0.0000	343	0.0072	355	-	321	0.0015	359	0.0014	365	0.0042	296
152	hyperverge-002	0.0000	74	0.0008	197	-	185	0.0002	276	0.0004	204	0.0004	203
153	hzailu-001	0.0000	316	0.0016	278	-	242	0.0003	297	0.0005	317	0.0075	313
154	icm-002	0.0000	131	0.0001	117	-	233	0.0000	77	0.0000	110	0.0000	97
155	icm-003	0.0000	92	0.0001	118	-	298	0.0000	104	0.0000	111	0.0000	96
156	icthtc-000	0.0001	360	0.0047	344	-	182	0.0028	375	0.0029	382	0.0086	317
157	id3-006	0.0000	285	0.0009	228	-	53	0.0004	306	0.0005	313	0.0008	251
158	id3-008	0.0000	7	0.0006	165	-	140	0.0001	239	0.0004	178	0.0003	130
159	idemria-007	0.0000	14	0.0004	147	-	148	0.0000	129	0.0003	161	0.0003	141
160	idemria-008	0.0000	36	0.0004	146	-	57	0.0000	128	0.0003	160	0.0003	142
161	iit-002	0.0000	333	0.0021	298	-	157	0.0009	346	0.0005	323	0.0443	359
162	iit-003	0.0000	223	0.0008	209	-	288	0.0000	149	0.0004	183	0.0069	310
163	imagus-002	0.0000	289	0.0018	285	-	238	0.0000	158	0.0004	238	0.0296	349
164	imagus-004	0.0000	161	0.0000	14	-	325	0.0000	52	0.0000	60	0.0000	52
165	imperial-000	0.0000	93	0.0000	42	-	303	0.0000	103	0.0000	107	0.0000	72
166	imperial-002	0.0000	121	0.0000	27	0.0000	10	0.0000	86	0.0000	86	0.0000	86
167	incode-009	0.0000	282	0.0009	220	-	323	0.0002	257	0.0004	200	0.0007	246
168	incode-010	0.0000	272	0.0009	221	-	302	0.0002	258	0.0004	203	0.0007	247
169	innefublars-000	0.0000	183	0.0024	302	-	114	0.0003	291	0.0005	310	0.0004	190
170	innovativetechnologyltd-001	0.0001	359	0.0050	345	-	163	0.0024	367	0.0025	377	0.0055	303
171	innovativetechnologyltd-002	0.0000	291	0.0046	339	-	395	0.0057	386	0.0005	311	0.0247	347
172	innovatrics-007	0.0000	195	0.0007	187	-	69	0.0001	182	0.0003	150	0.0003	143
173	innovatrics-008	0.0000	244	0.0009	223	-	393	0.0000	155	0.0004	174	0.0003	164
174	insightface-001	0.0000	128	0.0000	36	-	231	0.0000	74	0.0000	81	0.0000	79

Table 28: FTE is the proportion of failed template generation attempts. Failures can occur because the software throws an exception, or because the software electively refuses to process the input image. This would typically occur if a face is not detected. FTE is measured as the number of function calls that give EITHER a non-zero error code OR that give a “small” template. This is defined as one whose size is less than 0.3 times the median template size for that algorithm. This second rule is needed because some algorithms incorrectly fail to return a non-zero error code when template generation fails.

A hyphen “-” indicates the dataset was not produced.¹ The effects of FTE are included in the accuracy results of this report by regarding any template comparison involving a failed template to produce a low similarity score. Thus higher FTE results in higher FNMR and lower FMR.

	Algorithm	Failure to Enrol Rate ¹											
		APPLICATION	BORDER	CHILD-EXPLOIT	MUGSHOT	VISA	WILD	SEC. 2.2	SEC. 2.3	SEC. ??	SEC. 2.4	SEC. 2.1	SEC. 2.5
175	insightface-002	0.0000	66	0.0000	73	-	203	0.0000	13	0.0000	11	0.0000	1
176	intellicloudai-001	0.0000	8	0.0000	96	-	136	0.0000	48	0.0000	51	0.0001	108
177	intellicloudai-002	0.0000	27	0.0008	201	-	85	0.0000	148	0.0004	177	0.0012	268
178	intellifusion-001	0.0000	177	0.0005	151	0.0949	29	0.0001	198	0.0003	164	0.0005	222
179	intellifusion-002	0.0000	21	0.0000	111	-	116	0.0000	111	0.0000	41	0.0001	107
180	intellivision-001	0.0042	381	0.0296	376	0.5495	47	0.0048	385	0.0042	386	0.1358	385
181	intellivision-002	0.0000	344	0.0046	340	-	139	0.0012	351	0.0005	328	0.0146	330
182	intelresearch-004	0.0000	205	0.0006	160	-	176	0.0000	133	0.0004	191	0.0003	149
183	intelresearch-005	0.0000	230	0.0006	159	-	256	0.0000	135	0.0004	194	0.0003	151
184	intsysmsu-001	0.0000	154	0.0010	237	-	343	0.0001	219	0.0004	229	0.0004	200
185	intsysmsu-002	0.0000	78	0.0010	238	-	152	0.0001	216	0.0004	220	0.0004	199
186	ionetworks-000	0.0000	5	0.0016	280	-	133	0.0004	300	0.0005	298	0.0004	204
187	iqface-000	0.0000	152	0.0000	5	0.0000	16	0.0000	62	0.0000	67	0.0000	59
188	iqface-003	0.0000	330	0.0076	358	-	376	0.0006	327	0.0005	327	0.0069	309
189	irex-000	0.0000	297	0.0009	227	-	279	0.0000	164	0.0005	293	0.0003	157
190	isap-001	0.0000	37	0.0000	91	-	60	0.0000	24	0.0000	32	0.0000	36
191	isap-002	0.0000	62	0.0000	77	-	189	0.0000	10	0.0000	14	0.0000	4
192	isityou-000	0.0068	385	0.0316	379	0.4714	43	0.0023	363	0.0010	349	0.0663	365
193	isystems-001	0.0000	337	0.0035	324	0.1421	32	0.0010	348	0.0007	340	0.0128	326
194	isystems-002	0.0000	336	0.0035	325	0.1421	31	0.0010	347	0.0007	339	0.0128	325
195	itmo-007	0.0000	13	0.0009	215	-	146	0.0003	298	0.0000	47	0.0004	181
196	itmo-008	0.0000	32	0.0135	366	-	95	0.0024	368	0.0000	34	0.0836	367
197	ivacognitive-001	0.0000	264	0.0011	250	-	118	0.0001	191	0.0004	273	0.0011	260
198	iws-000	0.0005	372	0.0650	389	-	357	0.0024	365	0.0012	358	0.0936	373
199	kakao-005	0.0000	140	0.0000	106	-	389	0.0000	73	0.0000	113	0.0000	45
200	kakao-007	0.0000	61	0.0007	169	-	187	0.0001	209	0.0004	192	0.0097	322
201	kakaopay-001	0.0000	270	0.0013	270	-	188	0.0001	195	0.0004	274	0.0078	315
202	kedacom-000	0.0000	45	0.0000	87	0.0000	3	0.0000	32	0.0000	25	0.0000	32
203	kiwitech-000	0.0000	193	0.0009	213	-	55	0.0004	307	0.0005	295	0.0004	210
204	kneron-003	0.0239	391	0.0306	377	0.4883	45	0.0044	382	0.0016	369	0.1823	389
205	kneron-005	0.0000	339	0.0226	370	-	193	0.0006	324	0.0005	306	0.0097	321
206	knowutech-000	0.0000	229	0.0008	195	-	251	0.0000	151	0.0004	240	0.0003	166
207	kookmin-002	0.0000	19	0.0000	103	-	109	0.0000	41	0.0000	43	0.0000	23
208	kuke3d-001	0.0000	58	0.0000	65	-	222	0.0000	23	0.0000	17	0.0000	7
209	lemalabs-001	0.0000	163	0.0005	153	-	320	0.0002	261	0.0004	181	0.0004	173
210	line-000	0.0000	88	0.0000	60	-	161	0.0000	4	0.0000	1	0.0000	98
211	line-001	0.0000	55	0.0000	63	-	227	0.0000	20	0.0000	18	0.0001	109
212	lookman-002	0.0000	111	0.0000	47	-	287	0.0000	97	0.0000	96	0.0000	62
213	lookman-004	0.0000	106	0.0000	54	0.0000	12	0.0000	93	0.0000	101	0.0000	67
214	luxand-000	0.0000	116	0.0000	30	-	246	0.0000	82	0.0000	91	0.0000	89
215	mantra-000	0.0001	348	0.0041	334	-	167	0.0003	289	0.0004	284	0.0037	294
216	maxvision-000	0.0000	68	0.0000	107	-	169	0.0000	6	0.0000	9	0.0000	20
217	megvii-003	0.0000	258	0.0010	245	-	330	0.0002	270	0.0004	263	0.0011	266
218	megvii-004	0.0000	198	0.0010	236	-	211	0.0002	255	0.0004	233	0.0011	262
219	meituan-000	0.0000	85	0.0001	119	-	160	0.0000	127	0.0002	123	0.0001	110
220	meiya-001	0.0000	335	0.0028	311	-	217	0.0004	311	0.0010	350	0.0025	286
221	mendaxiatech-000	0.0000	215	0.0010	232	-	292	0.0002	273	0.0004	260	0.0011	263
222	microfocus-001	0.0001	357	0.0053	348	0.0791	27	0.0008	341	0.0016	368	0.0220	341
223	microfocus-002	0.0001	356	0.0053	349	0.0791	26	0.0008	340	0.0016	367	0.0220	340
224	minivision-000	0.0000	76	0.0000	57	-	179	0.0000	9	0.0000	5	0.0000	17
225	mobai-000	0.0000	301	0.0114	364	-	94	0.0003	293	0.0012	360	0.1242	383
226	mobai-001	0.0000	262	0.0040	330	-	130	0.0001	223	0.0012	359	0.0523	362
227	mobb1-001	0.0000	331	0.0052	347	-	300	0.0002	250	0.0005	316	0.0181	338
228	mobb1-002	0.0000	340	0.0029	314	-	272	0.0002	265	0.0009	344	0.0026	288
229	mobilpintech-000	0.0000	162	0.0000	13	-	327	0.0000	53	0.0000	61	0.0000	53
230	moreidian-000	0.0000	179	0.0009	214	-	142	0.0004	308	0.0005	296	0.0004	209
231	multimodality-000	0.0000	135	0.0000	19	-	382	0.0000	69	0.0000	75	0.0000	47
232	mvision-001	0.0000	3	0.0000	99	-	122	0.0000	43	0.0000	52	0.0000	28

Table 29: FTE is the proportion of failed template generation attempts. Failures can occur because the software throws an exception, or because the software electively refuses to process the input image. This would typically occur if a face is not detected. FTE is measured as the number of function calls that give EITHER a non-zero error code OR that give a “small” template. This is defined as one whose size is less than 0.3 times the median template size for that algorithm. This second rule is needed because some algorithms incorrectly fail to return a non-zero error code when template generation fails.

A hyphen “-” indicates the dataset was not produced.¹ The effects of FTE are included in the accuracy results of this report by regarding any template comparison involving a failed template to produce a low similarity score. Thus higher FTE results in higher FNMR and lower FMR.

	Algorithm Name	Failure to Enrol Rate ¹											
		APPLICATION	BORDER	CHILD-EXPLOIT	MUGSHOT	VISA	WILD	SEC. 2.2	SEC. 2.3	SEC. ??	SEC. 2.4	SEC. 2.1	SEC. 2.5
233	nazhiai-000	0.0000	123	0.0000	25	-	257	0.0000	88	0.0000	85	0.0000	85
234	neosystems-002	0.0000	40	0.0000	89	-	66	0.0000	27	0.0000	29	0.0000	34
235	neosystems-003	0.0000	43	0.0000	85	-	76	0.0000	31	0.0000	28	0.0000	31
236	netbridgetech-001	0.0000	105	0.0000	56	-	267	0.0000	92	0.0000	102	0.0000	68
237	netbridgetech-002	0.0000	127	0.0000	23	-	264	0.0000	90	0.0000	83	0.0000	82
238	neurotechnology-012	0.0000	323	0.0010	247	-	71	0.0001	232	0.0004	222	0.0005	223
239	neurotechnology-013	0.0000	71	0.0008	210	-	174	0.0000	119	0.0001	115	0.0004	188
240	nhn-001	0.0000	222	0.0019	289	-	274	0.0001	206	0.0004	283	0.0020	282
241	nhn-002	0.0000	136	0.0004	148	-	384	0.0000	145	0.0003	142	0.0003	133
242	nodeflux-002	0.0000	236	0.0261	372	-	241	0.0008	339	0.0005	312	0.0008	253
243	notiontag-001	0.0000	108	0.0000	53	-	275	0.0027	373	0.0000	99	0.0132	329
244	notiontag-002	0.0000	138	0.0000	18	-	386	0.0000	70	0.0000	74	0.0000	46
245	nsensecorp-002	0.0000	182	0.0009	216	-	112	0.0003	281	0.0011	351	0.0178	337
246	nsensecorp-003	0.0000	96	0.0000	115	-	306	0.0000	137	0.0007	342	0.0150	331
247	ntechlab-011	0.0000	156	0.0003	129	-	354	0.0000	168	0.0004	173	0.0003	155
248	ntechlab-012	0.0000	158	0.0003	128	-	360	0.0000	169	0.0004	172	0.0003	154
249	null-020	-	395	-	395	-	206	-	392	-	397	-	393
250	omnigarde-001	0.0000	251	0.0008	191	-	355	0.0000	141	0.0004	228	0.0003	165
251	omnigarde-002	0.0000	206	0.0008	192	-	178	0.0000	138	0.0004	221	0.0003	160
252	omsecurity-000	0.0000	4	0.0000	98	-	123	0.0000	44	0.0000	53	0.1160	381
253	openface-001	0.0000	312	0.0104	363	-	93	0.0004	305	0.0006	336	0.0856	370
254	oz-003	0.0000	104	0.0002	122	-	269	0.0000	118	0.0003	130	0.0002	119
255	oz-004	0.0000	319	0.0003	131	-	276	0.0000	123	0.0002	120	0.0006	230
256	papsav1923-001	0.0000	259	0.0007	179	-	334	0.0001	213	0.0002	125	0.0005	215
257	papsav1923-002	0.0000	213	0.0018	288	-	295	0.0000	159	0.0004	243	0.0004	189
258	paravision-008	0.0000	33	0.0010	235	-	50	0.0001	207	0.0004	176	0.0003	162
259	paravision-010	0.0000	142	0.0010	233	-	394	0.0001	208	0.0004	179	0.0003	163
260	pensees-001	0.0000	203	0.0000	59	-	171	0.0000	5	0.0000	8	0.0000	19
261	pixelall-006	0.0000	126	0.0000	22	-	265	0.0000	89	0.0000	82	0.0000	83
262	pixelall-007	0.0000	160	0.0000	15	-	322	0.0000	54	0.0000	62	0.0000	54
263	psl-008	0.0000	224	0.0003	130	-	285	0.0000	124	0.0003	155	0.0002	127
264	psl-009	0.0000	176	0.0004	140	-	131	0.0000	112	0.0004	171	0.0003	146
265	ptakuratsatu-000	0.0000	196	0.0007	188	-	65	0.0001	183	0.0003	149	0.0003	144
266	pxl-001	0.0000	345	0.0044	337	-	294	0.0005	317	0.0022	375	0.0323	351
267	pyramid-000	0.0001	354	0.0041	333	-	270	0.0005	316	0.0007	341	0.0015	275
268	qnap-000	0.0000	103	0.0007	189	-	315	0.0002	259	0.0002	119	0.0003	131
269	qnap-001	0.0000	181	0.0000	113	-	101	0.0000	161	0.0001	116	0.0001	112
270	quantasoft-003	0.0000	304	0.0015	276	-	197	0.0005	315	0.0006	334	0.0088	319
271	rankone-011	0.0000	129	0.0000	38	-	230	0.0000	76	0.0000	79	0.0000	81
272	rankone-012	0.0000	170	0.0000	9	-	341	0.0000	58	0.0000	56	0.0000	48
273	realnetworks-005	0.0000	216	0.0002	125	-	311	0.0000	114	0.0002	129	0.0003	140
274	realnetworks-006	0.0000	248	0.0002	126	-	348	0.0000	113	0.0002	128	0.0003	139
275	regula-000	0.0000	117	0.0000	29	-	247	0.0000	83	0.0000	92	0.0000	90
276	regula-001	0.0000	113	0.0000	49	-	283	0.0000	100	0.0000	95	0.0000	64
277	remarkai-001	0.0000	150	0.0000	7	-	346	0.0000	63	0.0000	68	0.0000	99
278	remarkai-003	0.0000	228	0.0007	176	-	253	0.0000	162	0.0004	189	0.0004	194
279	rendip-000	0.0000	283	0.0016	279	-	102	0.0002	256	0.0004	287	0.0013	273
280	revealmedia-005	0.0000	295	0.0007	183	-	213	0.0009	345	0.0004	288	0.0076	314
281	revealmedia-006	0.0000	148	0.0009	224	-	374	0.0001	220	0.0004	252	0.0004	211
282	rokid-000	0.0000	10	0.0072	356	-	137	0.0001	210	0.0005	307	0.0354	355
283	rokid-001	0.0000	73	0.0013	268	-	183	0.0000	8	0.0000	6	0.0007	244
284	s1-003	0.0000	87	0.0002	124	-	166	0.0007	333	0.0003	139	0.0415	358
285	s1-004	0.0000	80	0.0000	116	-	151	0.0000	176	0.0001	117	0.0001	100
286	saffe-001	0.0000	9	0.0000	97	0.0000	7	0.0000	47	0.0000	50	0.0000	27
287	saffe-002	0.0000	42	0.0000	86	-	74	0.0000	29	0.0000	26	0.0000	30
288	samsungsds-000	0.0000	292	0.0055	351	-	363	0.0038	380	0.0005	308	0.0925	372
289	samtech-001	0.0001	353	0.0032	317	-	297	0.0004	309	0.0008	343	0.0013	271
290	scanovate-002	0.0000	271	0.0018	286	-	154	0.0000	175	0.0004	278	0.0008	250

Table 30: FTE is the proportion of failed template generation attempts. Failures can occur because the software throws an exception, or because the software electively refuses to process the input image. This would typically occur if a face is not detected. FTE is measured as the number of function calls that give EITHER a non-zero error code OR that give a “small” template. This is defined as one whose size is less than 0.3 times the median template size for that algorithm. This second rule is needed because some algorithms incorrectly fail to return a non-zero error code when template generation fails.

A hyphen “-” indicates the dataset was not produced.¹ The effects of FTE are included in the accuracy results of this report by regarding any template comparison involving a failed template to produce a low similarity score. Thus higher FTE results in higher FNMR and lower FMR.

	Algorithm	Failure to Enrol Rate ¹							
		APPLICATION	BORDER	CHILD-EXPLOIT	MUGSHOT	VISA	WILD	SEC. 2.1	SEC. 2.5
Name	SEC. 2.2	SEC. 2.3	SEC. ??	SEC. 2.4	SEC. 2.1	SEC. 2.1	SEC. 2.5	SEC. 2.1	SEC. 2.5
291	scanovate-003	0.0000	275	0.0233	371	-	280	0.0006	328
292	securifai-003	0.0000	25	0.0000	80	-	90	0.0000	33
293	securifai-004	0.0000	39	0.0000	90	-	63	0.0000	28
294	sensetime-005	0.0000	147	0.0004	138	-	369	0.0000	144
295	sensetime-006	0.0000	23	0.0004	139	-	84	0.0000	143
296	sertis-000	0.0000	72	0.0007	182	-	177	0.0000	180
297	sertis-002	0.0000	124	0.0007	173	-	259	0.0000	174
298	seventhsense-000	0.0000	256	0.0006	168	-	324	0.0001	186
299	shaman-000	0.0000	2	0.0000	100	0.0000	6	0.0000	46
300	shaman-001	0.0000	157	0.0000	1	0.0000	20	0.0000	65
301	shu-002	0.0000	276	0.0010	241	-	249	0.0005	314
302	shu-003	0.0000	69	0.0007	171	-	172	0.0001	188
303	siat-002	0.0000	210	0.0012	262	0.0616	25	0.0000	154
304	siat-005	0.0000	12	0.0000	93	-	147	0.0000	49
305	sjtu-003	0.0000	6	0.0005	156	-	128	0.0000	166
306	sjtu-004	0.0000	99	0.0000	39	-	318	0.0000	108
307	sktelecom-000	0.0000	227	0.0008	203	-	252	0.0000	171
308	smartengines-000	0.0066	384	0.0150	367	-	235	0.0022	362
309	smilart-002	0.0000	341	0.0036	326	0.2422	38	-	396
310	smilart-003	0.0003	367	0.0100	361	-	329	0.0014	355
311	sodec-000	0.0000	67	0.0000	74	-	202	0.0000	14
312	sqisoft-001	0.0000	97	0.0003	135	-	308	0.0000	130
313	sqisoft-002	0.0000	63	0.0003	134	-	198	0.0000	131
314	staqu-000	0.0000	132	0.0000	35	-	232	0.0000	78
315	starhybrid-001	0.0001	358	0.0033	321	0.2340	37	0.0009	344
316	sukshi-000	0.0000	52	0.0000	67	-	219	0.0000	18
317	suprema-001	0.0000	288	0.0027	306	-	234	0.0003	283
318	suprema-002	0.0000	266	0.0010	243	-	61	0.0002	251
319	supremaid-001	0.0000	191	0.0020	295	-	58	0.0001	218
320	synesis-006	0.0000	137	0.0003	136	-	377	0.0000	170
321	synesis-007	0.0000	190	0.0013	267	-	49	0.0002	269
322	synology-000	0.0000	168	0.0000	11	-	333	0.0000	56
323	synology-002	0.0000	70	0.0000	58	-	173	0.0000	7
324	sztu-000	0.0000	125	0.0000	24	-	262	0.0000	91
325	sztu-001	0.0000	109	0.0000	52	-	277	0.0000	95
326	t4isb-000	0.0000	47	0.0000	69	-	210	0.0000	15
327	tech5-004	0.0000	172	0.0008	196	-	124	0.0003	284
328	tech5-005	0.0000	197	0.0007	190	-	215	0.0000	139
329	techsign-000	0.0007	374	0.0334	380	-	195	0.0020	360
330	tevian-007	0.0000	185	0.0015	277	-	78	0.0002	264
331	tevian-008	0.0000	243	0.0006	158	-	391	0.0000	134
332	tiger-005	0.0000	241	0.0009	225	-	387	0.0001	205
333	tiger-006	0.0000	277	0.0011	252	-	258	0.0001	238
334	tinkoff-001	0.0000	273	0.0008	202	-	304	0.0001	231
335	tongyi-005	0.0000	59	0.0000	64	0.0000	9	0.0000	21
336	toppanidgate-000	0.0000	220	0.0008	199	-	271	0.0004	301
337	toshiba-004	0.0000	28	0.0000	83	-	88	0.0000	36
338	toshiba-005	0.0000	201	0.0004	143	-	199	0.0001	235
339	trueface-002	0.0000	267	0.0046	343	-	64	0.0003	278
340	trueface-003	0.0000	278	0.0046	342	-	261	0.0003	279
341	tuputech-000	0.0003	368	0.0116	365	-	349	-	394
342	turingtechvip-001	0.0001	350	0.0007	185	-	175	0.0007	334
343	twface-000	0.0000	144	0.0000	21	-	366	0.0000	68
344	twface-001	0.0000	17	0.0000	104	-	105	0.0000	39
345	ulsee-001	0.0000	35	0.0000	92	-	59	0.0000	25
346	ultinous-000	-	394	-	397	0.0007	22	-	393
347	ultinous-001	-	396	-	394	0.0007	23	-	397
348	uluface-002	0.0000	30	0.0000	79	0.0000	4	0.0000	38
								0.0000	36
								0.0000	37

Table 31: FTE is the proportion of failed template generation attempts. Failures can occur because the software throws an exception, or because the software electively refuses to process the input image. This would typically occur if a face is not detected. FTE is measured as the number of function calls that give EITHER a non-zero error code OR that give a “small” template. This is defined as one whose size is less than 0.3 times the median template size for that algorithm. This second rule is needed because some algorithms incorrectly fail to return a non-zero error code when template generation fails.

A hyphen “-” indicates the dataset was not produced.¹ The effects of FTE are included in the accuracy results of this report by regarding any template comparison involving a failed template to produce a low similarity score. Thus higher FTE results in higher FNMR and lower FMR.

	Algorithm	Failure to Enrol Rate ¹						
		APPLICATION	BORDER	CHILD-EXPLOIT	MUGSHOT	VISA	WILD	
Name	SEC. 2.2	SEC. 2.3	SEC. ??	SEC. 2.4	SEC. 2.1	SEC. 2.5		
349 uluface-003	0.0000	101	0.0001	121	-	314	0.0002	247
350 unissey-001	0.0000	24	0.0000	81	-	91	0.0000	34
351 upc-001	0.0000	317	0.0003	132	0.0450	24	0.0003	282
352 vcog-002	-	397	-	393	0.2209	36	-	395
353 vd-002	0.0000	65	0.0000	76	-	194	0.0000	12
354 vd-003	0.0001	351	0.0041	332	-	392	0.0030	376
355 veridas-006	0.0000	310	0.0026	304	-	107	0.0001	226
356 veridas-007	0.0000	311	0.0026	303	-	77	0.0001	225
357 verigram-000	0.0000	290	0.0068	354	-	397	0.0003	299
358 verihubs-inteligensia-000	0.0000	260	0.0029	312	-	340	0.0001	192
359 via-000	0.0000	90	0.0000	46	0.0000	13	0.0000	102
360 via-001	0.0000	54	0.0000	68	-	218	0.0000	19
361 videmo-000	0.0000	263	0.0019	290	-	132	0.0003	292
362 videmo-001	0.0000	302	0.0170	368	-	68	0.0010	349
363 videonetics-001	0.0004	369	0.0309	378	0.4799	44	0.0015	358
364 videonetics-002	0.0000	284	0.0459	387	0.4598	42	0.0006	329
365 viettelhightech-000	0.0000	320	0.0019	291	-	127	0.0007	335
366 vigilantsolutions-010	0.0000	305	0.0028	308	-	375	0.0001	197
367 vigilantsolutions-011	0.0000	300	0.0028	309	-	108	0.0001	196
368 vinai-000	0.0000	82	0.0000	61	-	159	0.0000	1
369 vinbigdata-001	0.0000	155	0.0000	4	-	350	0.0000	64
370 vion-000	0.0050	382	0.0392	386	0.6388	48	0.0130	389
371 visage-000	0.0000	324	0.0054	350	-	226	0.0009	342
372 visionbox-001	0.0000	342	0.0033	320	-	342	0.0005	322
373 visionbox-002	0.0000	60	0.0017	281	-	191	0.0000	152
374 visionlabs-010	0.0000	294	0.0009	218	-	92	0.0001	236
375 visionlabs-011	0.0000	146	0.0006	163	-	365	0.0001	199
376 visteam-002	0.0000	299	0.0014	273	-	367	0.0002	253
377 visteam-003	0.0000	209	0.0010	242	-	150	0.0001	187
378 vnpt-002	0.0000	240	0.0002	123	-	379	0.0003	296
379 vnpt-003	0.0000	100	0.0004	137	-	312	0.0002	246
380 vocord-009	0.0000	219	0.0006	162	-	268	0.0001	242
381 vocord-010	0.0000	265	0.0005	152	-	80	0.0002	260
382 vts-000	0.0000	287	0.0011	249	-	214	0.0001	243
383 winsense-001	0.0000	102	0.0000	40	0.0000	14	0.0000	109
384 winsense-002	0.0000	119	0.0000	32	-	243	0.0000	84
385 wuhantianyu-001	0.0000	26	0.0007	174	-	87	0.0001	184
386 x-laboratory-000	0.0247	392	0.0000	3	0.0000	18	0.0005	321
387 x-laboratory-001	0.0000	239	0.0012	259	-	378	0.0001	228
388 xforwardai-001	0.0000	218	0.0007	184	-	316	0.0003	286
389 xforwardai-002	0.0000	186	0.0007	186	-	79	0.0003	285
390 xm-000	0.0000	20	0.0007	172	-	110	0.0001	189
391 yisheng-004	0.0002	364	-	396	0.4279	41	0.0013	353
392 yitu-003	0.0000	151	0.0000	8	-	347	0.0009	343
393 yoonik-002	0.0000	269	0.0010	239	-	225	0.0003	277
394 yoonik-003	0.0000	261	0.0009	222	-	121	0.0002	249
395 ytuo-000	0.0000	232	0.0010	246	-	263	0.0002	271
396 yuan-003	0.0000	309	0.0010	244	-	98	0.0005	319
397 yuan-004	0.0000	57	0.0000	66	-	221	0.0000	22

Table 32: FTE is the proportion of failed template generation attempts. Failures can occur because the software throws an exception, or because the software electively refuses to process the input image. This would typically occur if a face is not detected. FTE is measured as the number of function calls that give EITHER a non-zero error code OR that give a “small” template. This is defined as one whose size is less than 0.3 times the median template size for that algorithm. This second rule is needed because some algorithms incorrectly fail to return a non-zero error code when template generation fails.

A hyphen “-” indicates the dataset was not produced. ¹The effects of FTE are included in the accuracy results of this report by regarding any template comparison involving a failed template to produce a low similarity score. Thus higher FTE results in higher FNMR and lower FMR.

3.4 Recognition accuracy

Core algorithm accuracy is stated via:

▷ **Cooperative subjects**

- The summary table of Figure 25;
- The visa image DETs of Figure 59;
- The mugshot DETs of Figure 79;
- The mugshot ageing profiles of Figure 286;
- The human-difficult pairs of Figure 19

▷ **Non-cooperative subjects**

- The photojournalism DET of Figure 96

Figure 229 shows dependence of false match rate on algorithm score threshold. This allows a deployer to set a threshold to target a particular false match rate appropriate to the security objectives of the application.

Figure 189 likewise shows FMR(T) but for mugshots, and specially four subsets of the population.

Note that in both the mugshot and visa sets false match rates vary with the ethnicity, age, and sex, of the enrollee and impostor. For example figure 116 summarizes FMR for impostors paired from four groups black females, black males, white females, white males.

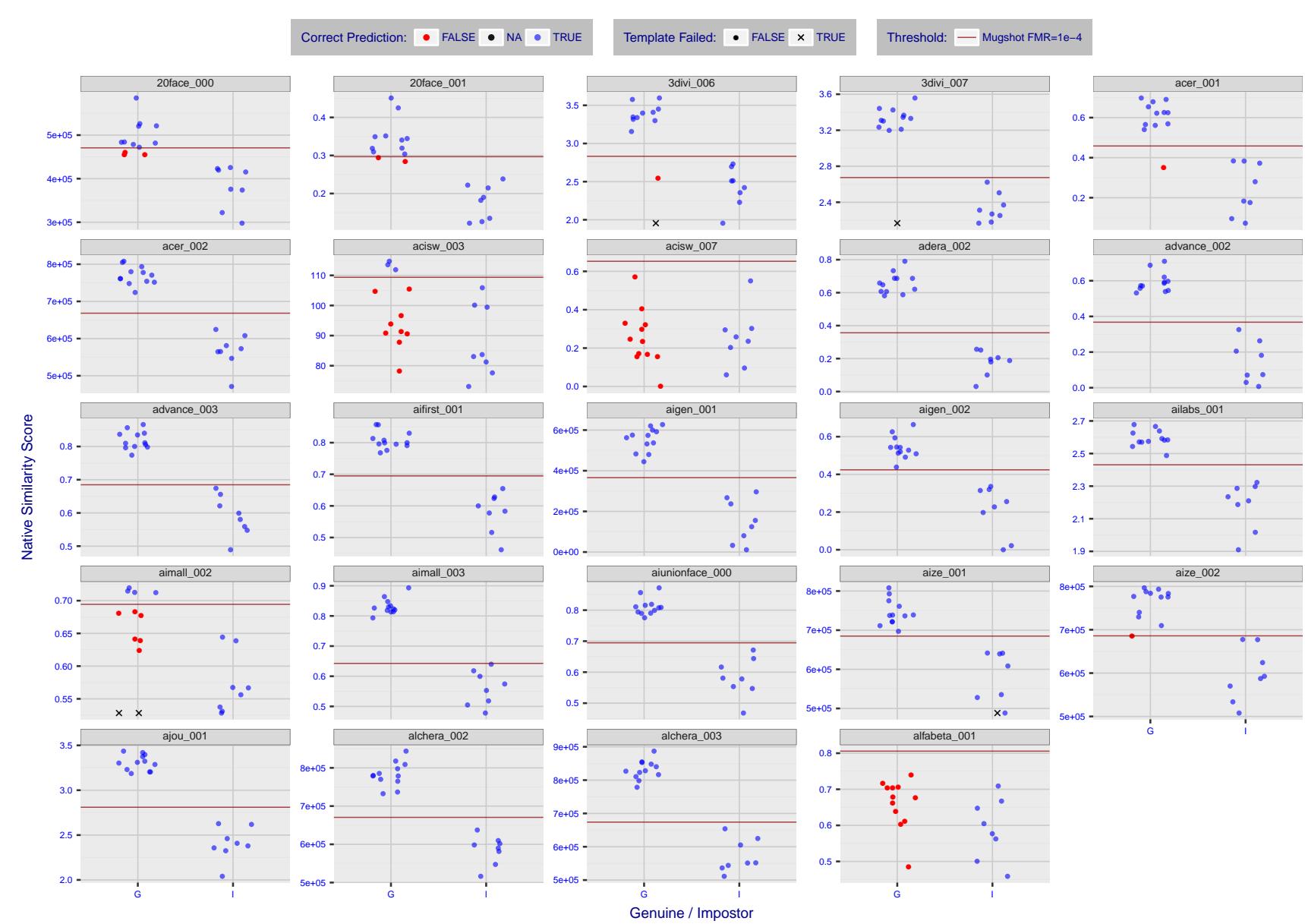


Figure 4: The figure shows algorithms' similarity scores for 12 genuine and 8 impostor image pairs used in the May 2018 paper Face recognition accuracy of forensic examiners, superrecognizers, and face recognition algorithms (Phillips et al. [1]). The threshold (red horizontal line) is a value calibrated to give $FMR = 0.0001$ on mugshot images. Points above the threshold correspond to pairs predicted to be genuine, and points below the threshold correspond to pairs predicted to be impostors. The figure shows whether the predicted class (genuine or impostor) matches the real class. Blue denotes a correct prediction, and red denotes incorrect. An "X" represents face detection failure in either of the images in the pair. Note that the sample size ($n=20$) is small, and the figure may change substantially if larger or different sets are used. The images can be downloaded from the [Supplemental Information](#) page provided with that publication.

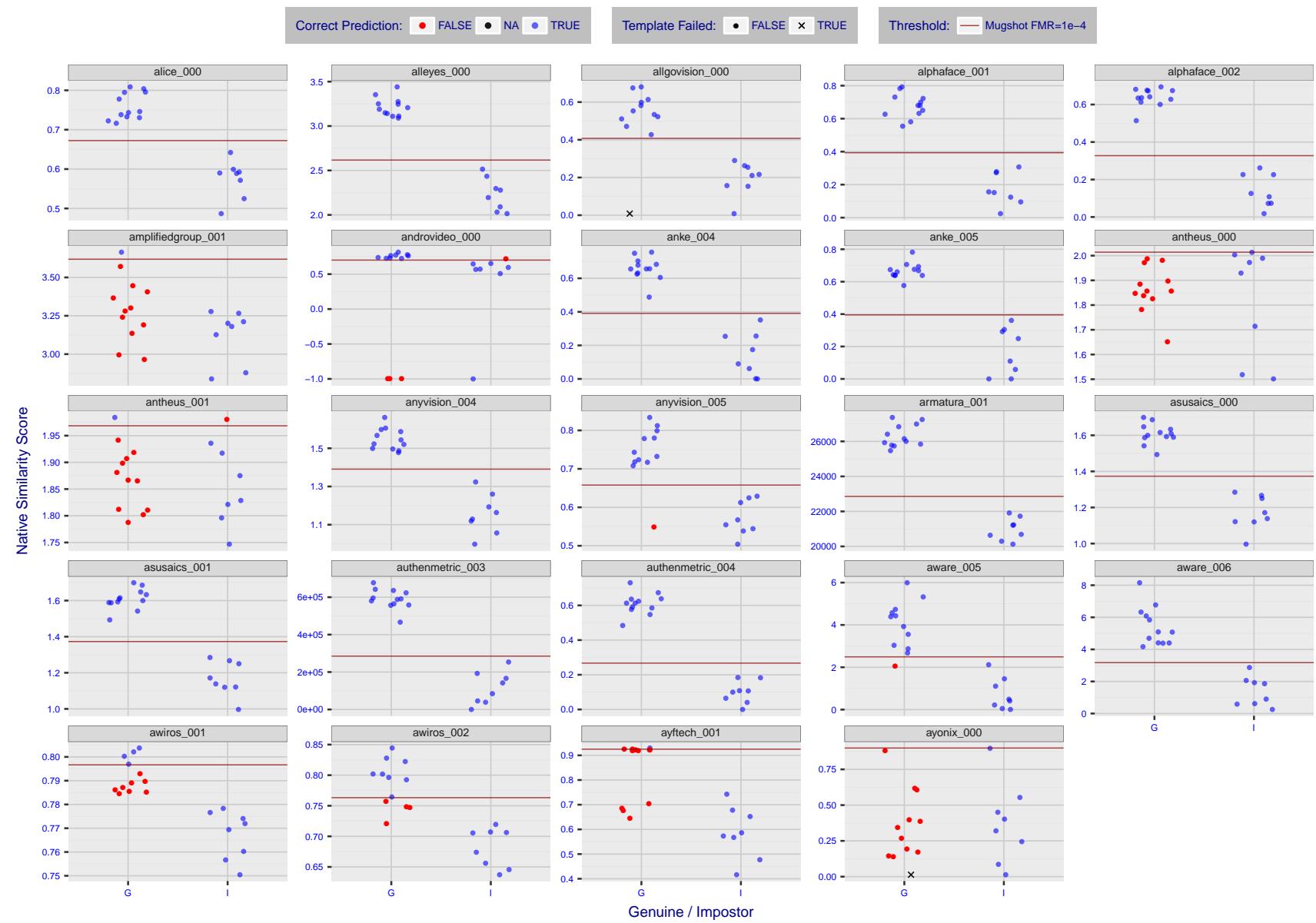


Figure 5: The figure shows algorithms' similarity scores for 12 genuine and 8 impostor image pairs used in the May 2018 paper Face recognition accuracy of forensic examiners, superrecognizers, and face recognition algorithms (Phillips et al. [1]). The threshold (red horizontal line) is a value calibrated to give $FMR = 0.0001$ on mugshot images. Points above the threshold correspond to pairs predicted to be genuine, and points below the threshold correspond to pairs predicted to be impostors. The figure shows whether the predicted class (genuine or impostor) matches the real class. Blue denotes a correct prediction, and red denotes incorrect. An "X" represents face detection failure in either of the images in the pair. Note that the sample size ($n=20$) is small, and the figure may change substantially if larger or different sets are used. The images can be downloaded from the [Supplemental Information](#) page provided with that publication.

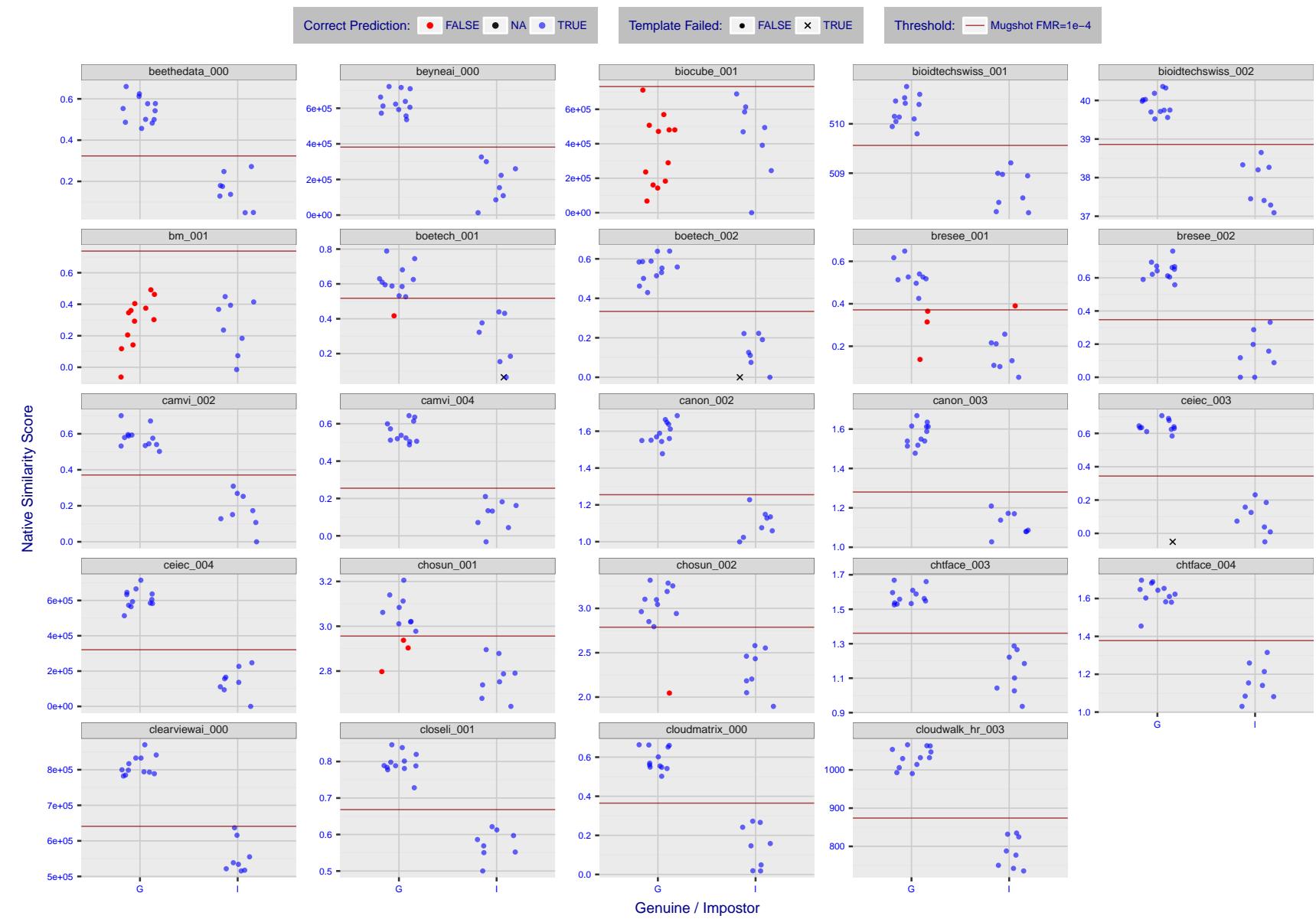


Figure 6: The figure shows algorithms' similarity scores for 12 genuine and 8 impostor image pairs used in the May 2018 paper Face recognition accuracy of forensic examiners, superrecognizers, and face recognition algorithms (Phillips et al. [1]). The threshold (red horizontal line) is a value calibrated to give $FMR = 0.0001$ on mugshot images. Points above the threshold correspond to pairs predicted to be genuine, and points below the threshold correspond to pairs predicted to be impostors. The figure shows whether the predicted class (genuine or impostor) matches the real class. Blue denotes a correct prediction, and red denotes incorrect. An "X" represents face detection failure in either of the images in the pair. Note that the sample size ($n=20$) is small, and the figure may change substantially if larger or different sets are used. The images can be downloaded from the [Supplemental Information](#) page provided with that publication.

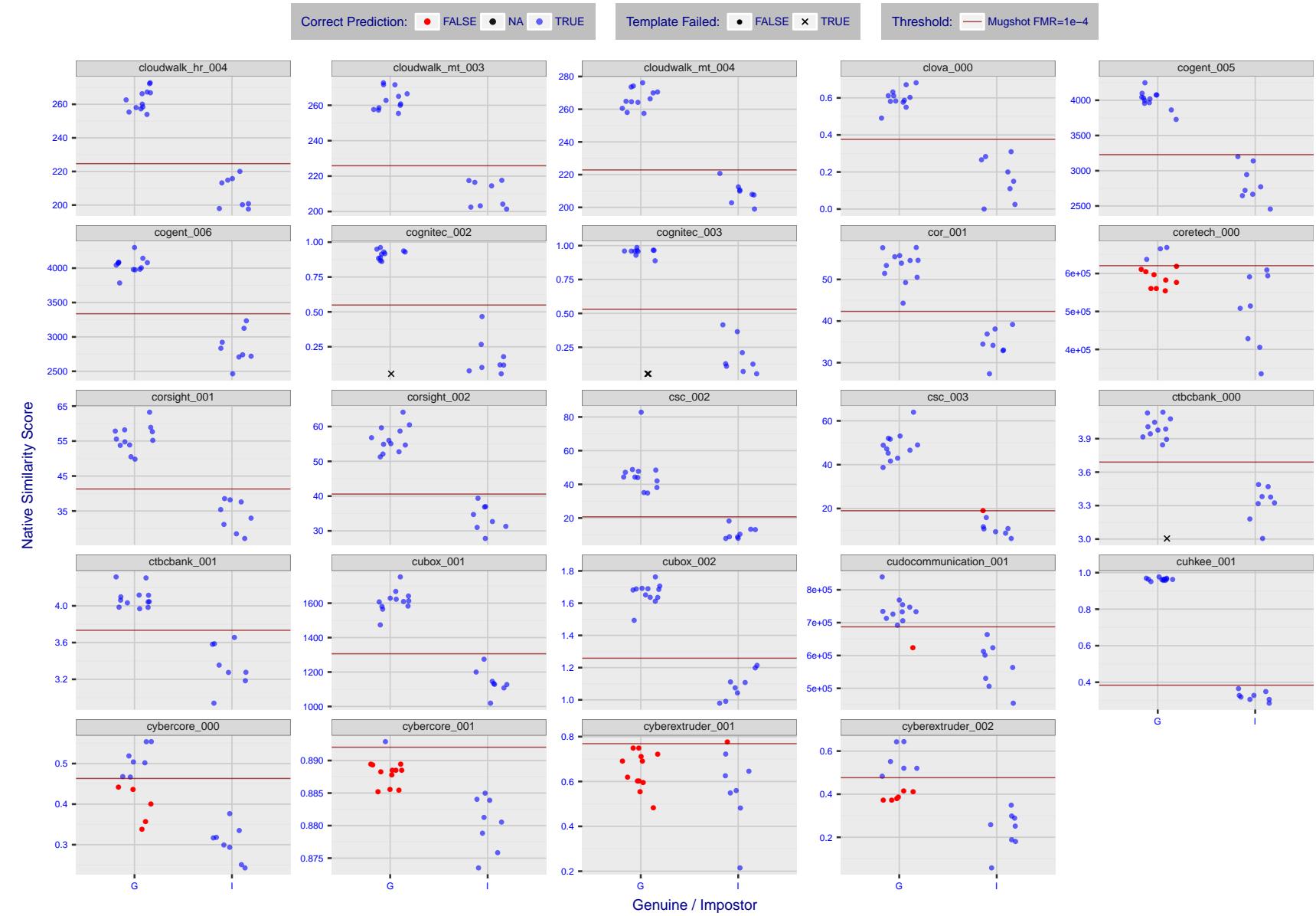


Figure 7: The figure shows algorithms' similarity scores for 12 genuine and 8 impostor image pairs used in the May 2018 paper Face recognition accuracy of forensic examiners, superrecognizers, and face recognition algorithms (Phillips et al. [1]). The threshold (red horizontal line) is a value calibrated to give $FMR = 0.0001$ on mugshot images. Points above the threshold correspond to pairs predicted to be genuine, and points below the threshold correspond to pairs predicted to be impostors. The figure shows whether the predicted class (genuine or impostor) matches the real class. Blue denotes a correct prediction, and red denotes incorrect. An "X" represents face detection failure in either of the images in the pair. Note that the sample size ($n=20$) is small, and the figure may change substantially if larger or different sets are used. The images can be downloaded from the [Supplemental Information](#) page provided with that publication.

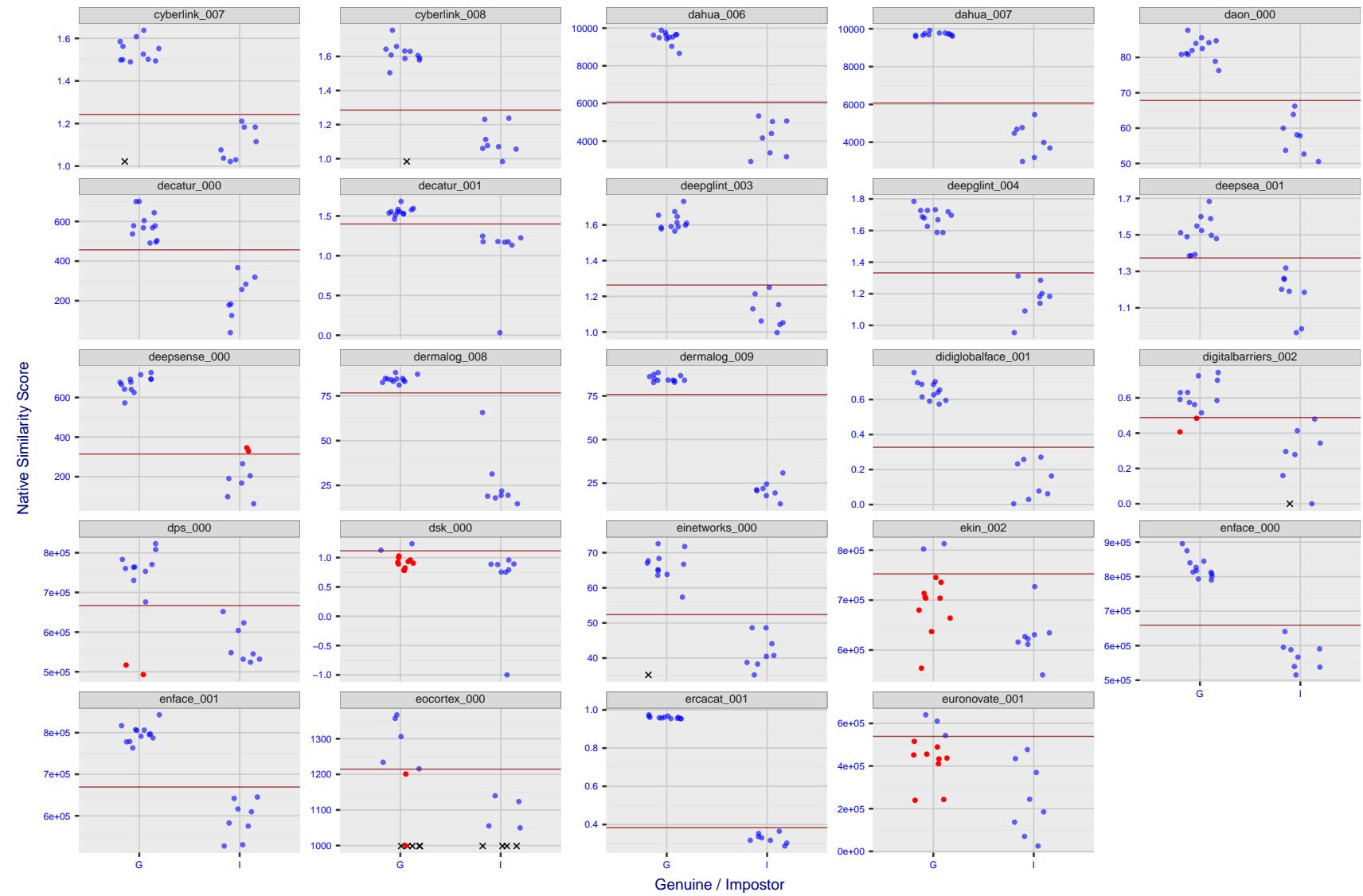


Figure 8: The figure shows algorithms' similarity scores for 12 genuine and 8 impostor image pairs used in the May 2018 paper Face recognition accuracy of forensic examiners, superrecognizers, and face recognition algorithms (Phillips et al. [1]). The threshold (red horizontal line) is a value calibrated to give $FMR = 0.0001$ on mugshot images. Points above the threshold correspond to pairs predicted to be genuine, and points below the threshold correspond to pairs predicted to be impostors. The figure shows whether the predicted class (genuine or impostor) matches the real class. Blue denotes a correct prediction, and red denotes incorrect. An "X" represents face detection failure in either of the images in the pair. Note that the sample size ($n=20$) is small, and the figure may change substantially if larger or different sets are used. The images can be downloaded from the [Supplemental Information](#) page provided with that publication.

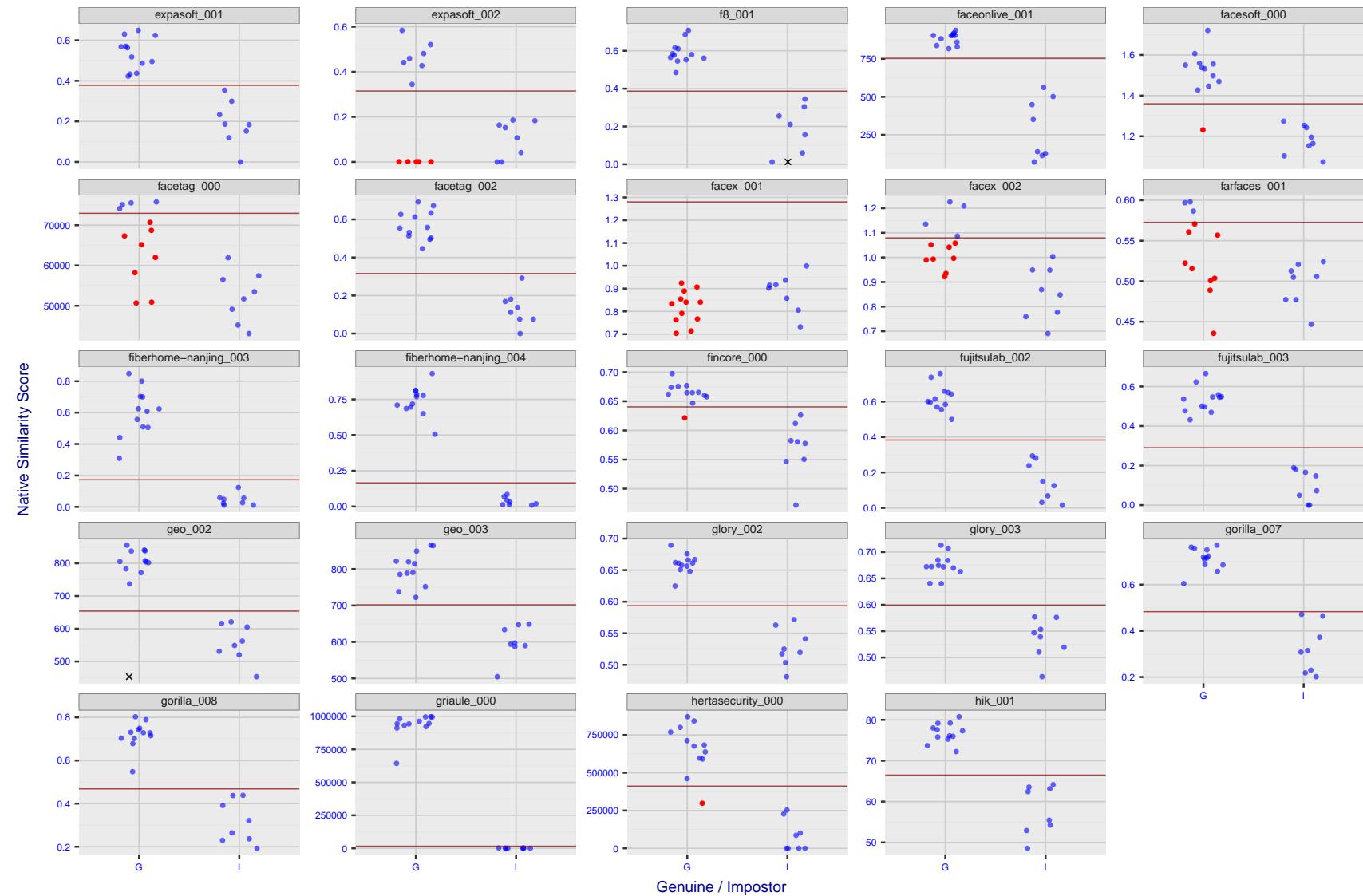


Figure 9: The figure shows algorithms' similarity scores for 12 genuine and 8 impostor image pairs used in the May 2018 paper Face recognition accuracy of forensic examiners, superrecognizers, and face recognition algorithms (Phillips et al. [1]). The threshold (red horizontal line) is a value calibrated to give $FMR = 0.0001$ on mugshot images. Points above the threshold correspond to pairs predicted to be genuine, and points below the threshold correspond to pairs predicted to be impostors. The figure shows whether the predicted class (genuine or impostor) matches the real class. Blue denotes a correct prediction, and red denotes incorrect. An "X" represents face detection failure in either of the images in the pair. Note that the sample size ($n=20$) is small, and the figure may change substantially if larger or different sets are used. The images can be downloaded from the [Supplemental Information](#) page provided with that publication.

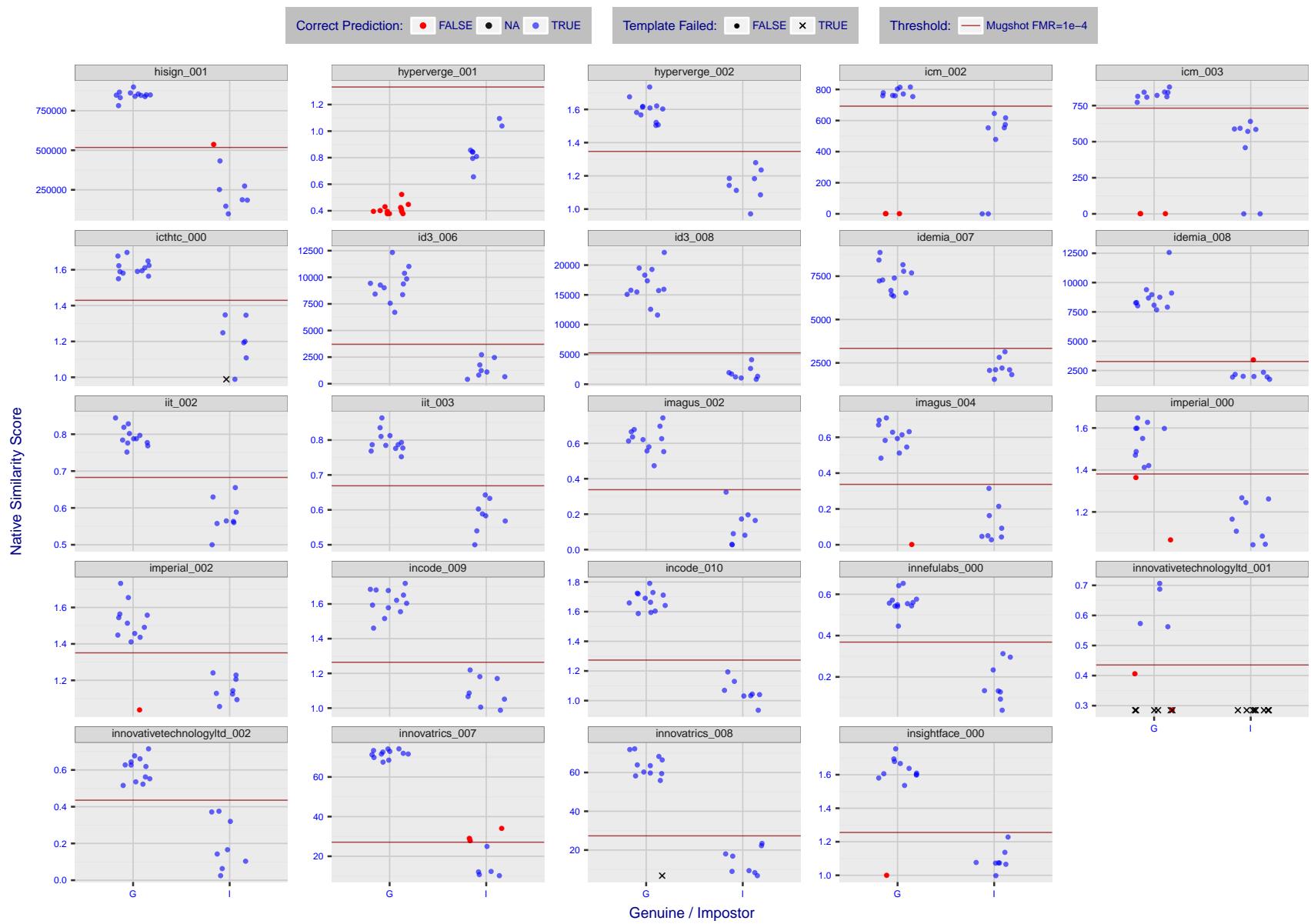


Figure 10: The figure shows algorithms' similarity scores for 12 genuine and 8 impostor image pairs used in the May 2018 paper Face recognition accuracy of forensic examiners, superrecognizers, and face recognition algorithms (Phillips et al. [1]). The threshold (red horizontal line) is a value calibrated to give $FMR = 0.0001$ on mugshot images. Points above the threshold correspond to pairs predicted to be genuine, and points below the threshold correspond to pairs predicted to be impostors. The figure shows whether the predicted class (genuine or impostor) matches the real class. Blue denotes a correct prediction, and red denotes incorrect. An "X" represents face detection failure in either of the images in the pair. Note that the sample size ($n=20$) is small, and the figure may change substantially if larger or different sets are used. The images can be downloaded from the [Supplemental Information](#) page provided with that publication.

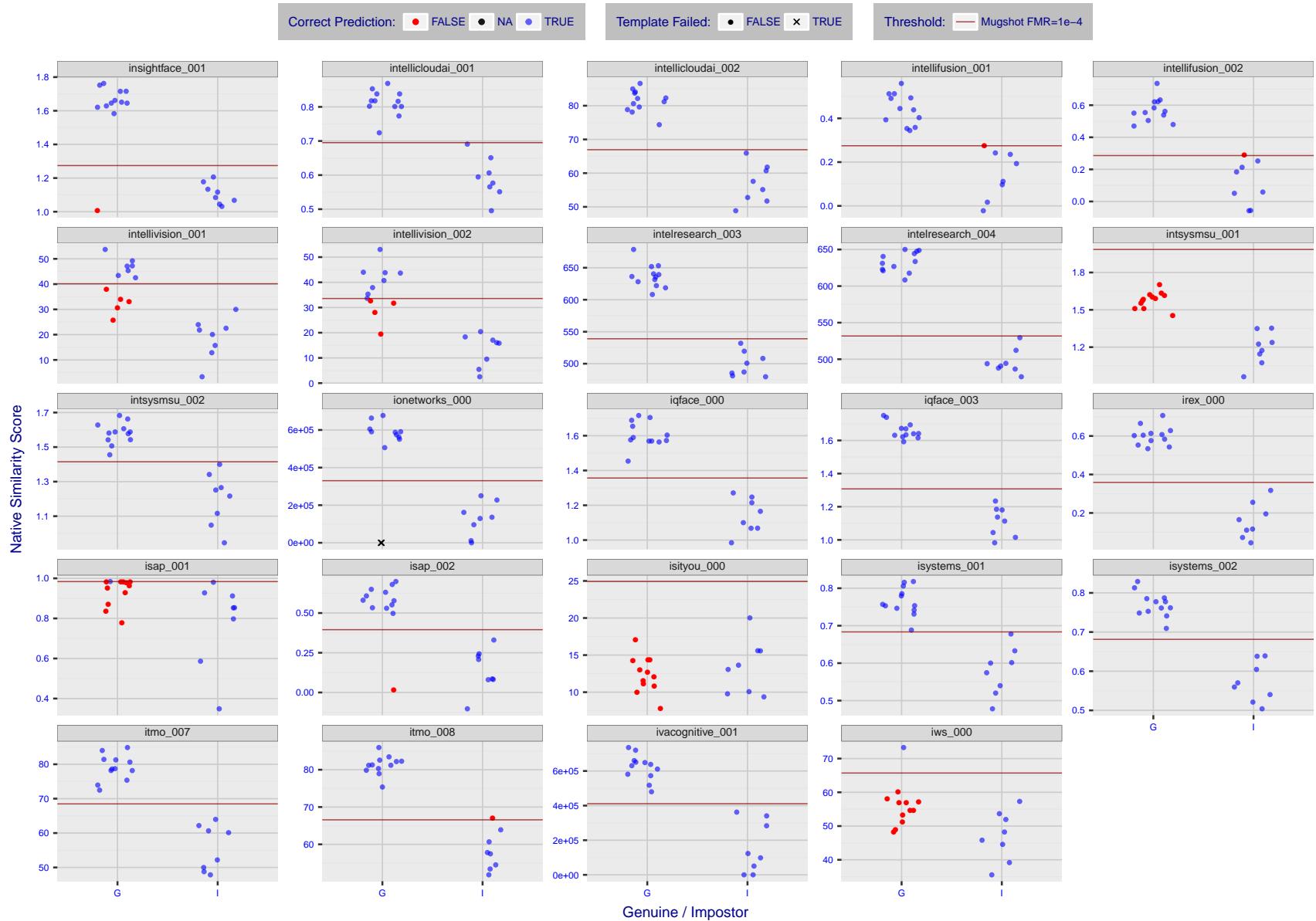


Figure 11: The figure shows algorithms' similarity scores for 12 genuine and 8 impostor image pairs used in the May 2018 paper Face recognition accuracy of forensic examiners, superrecognizers, and face recognition algorithms (Phillips et al. [1]). The threshold (red horizontal line) is a value calibrated to give FMR = 0.0001 on mugshot images. Points above the threshold correspond to pairs predicted to be genuine, and points below the threshold correspond to pairs predicted to be impostors. The figure shows whether the predicted class (genuine or impostor) matches the real class. Blue denotes a correct prediction, and red denotes incorrect. An "X" represents face detection failure in either of the images in the pair. Note that the sample size ($n=20$) is small, and the figure may change substantially if larger or different sets are used. The images can be downloaded from the [Supplemental Information](#) page provided with that publication.

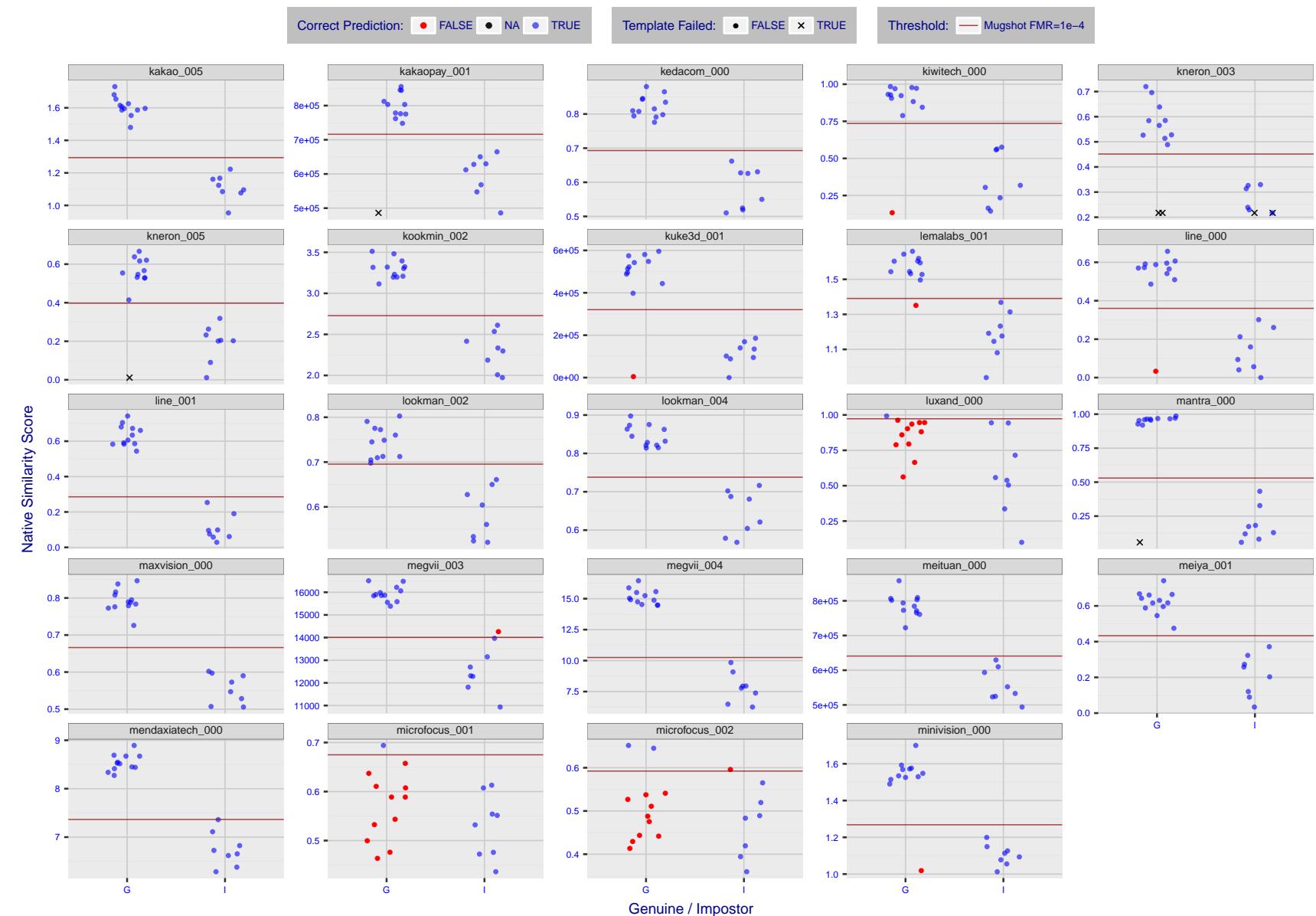


Figure 12: The figure shows algorithms' similarity scores for 12 genuine and 8 impostor image pairs used in the May 2018 paper Face recognition accuracy of forensic examiners, superrecognizers, and face recognition algorithms (Phillips et al. [1]). The threshold (red horizontal line) is a value calibrated to give $FMR = 0.0001$ on mugshot images. Points above the threshold correspond to pairs predicted to be genuine, and points below the threshold correspond to pairs predicted to be impostors. The figure shows whether the predicted class (genuine or impostor) matches the real class. Blue denotes a correct prediction, and red denotes incorrect. An "X" represents face detection failure in either of the images in the pair. Note that the sample size ($n=20$) is small, and the figure may change substantially if larger or different sets are used. The images can be downloaded from the [Supplemental Information](#) page provided with that publication.

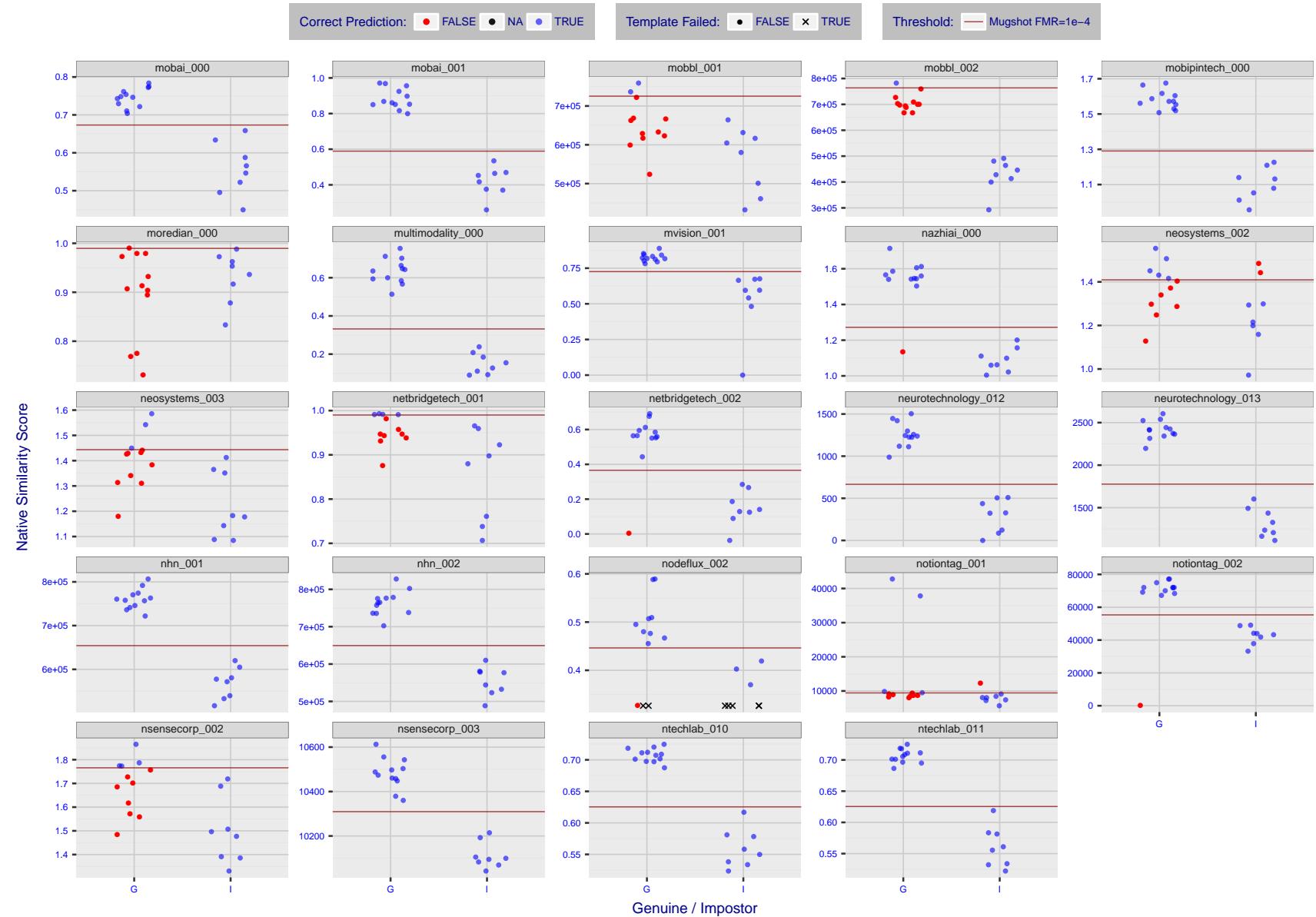


Figure 13: The figure shows algorithms' similarity scores for 12 genuine and 8 impostor image pairs used in the May 2018 paper Face recognition accuracy of forensic examiners, superrecognizers, and face recognition algorithms (Phillips et al. [1]). The threshold (red horizontal line) is a value calibrated to give $FMR = 0.0001$ on mugshot images. Points above the threshold correspond to pairs predicted to be genuine, and points below the threshold correspond to pairs predicted to be impostors. The figure shows whether the predicted class (genuine or impostor) matches the real class. Blue denotes a correct prediction, and red denotes incorrect. An "X" represents face detection failure in either of the images in the pair. Note that the sample size ($n=20$) is small, and the figure may change substantially if larger or different sets are used. The images can be downloaded from the [Supplemental Information](#) page provided with that publication.

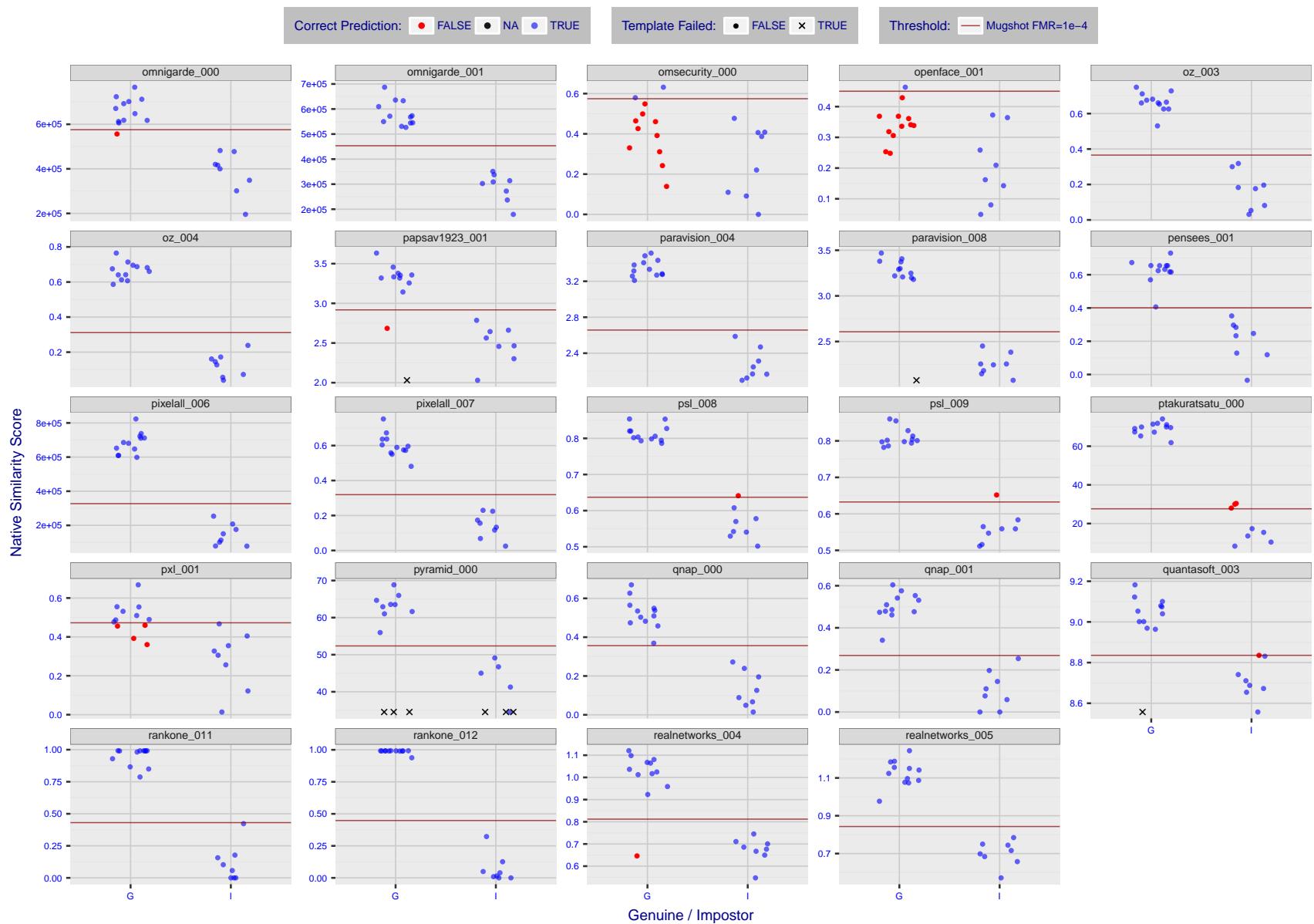


Figure 14: The figure shows algorithms' similarity scores for 12 genuine and 8 impostor image pairs used in the May 2018 paper Face recognition accuracy of forensic examiners, superrecognizers, and face recognition algorithms (Phillips et al. [1]). The threshold (red horizontal line) is a value calibrated to give $FMR = 0.0001$ on mugshot images. Points above the threshold correspond to pairs predicted to be genuine, and points below the threshold correspond to pairs predicted to be impostors. The figure shows whether the predicted class (genuine or impostor) matches the real class. Blue denotes a correct prediction, and red denotes incorrect. An "X" represents face detection failure in either of the images in the pair. Note that the sample size ($n=20$) is small, and the figure may change substantially if larger or different sets are used. The images can be downloaded from the [Supplemental Information](#) page provided with that publication.

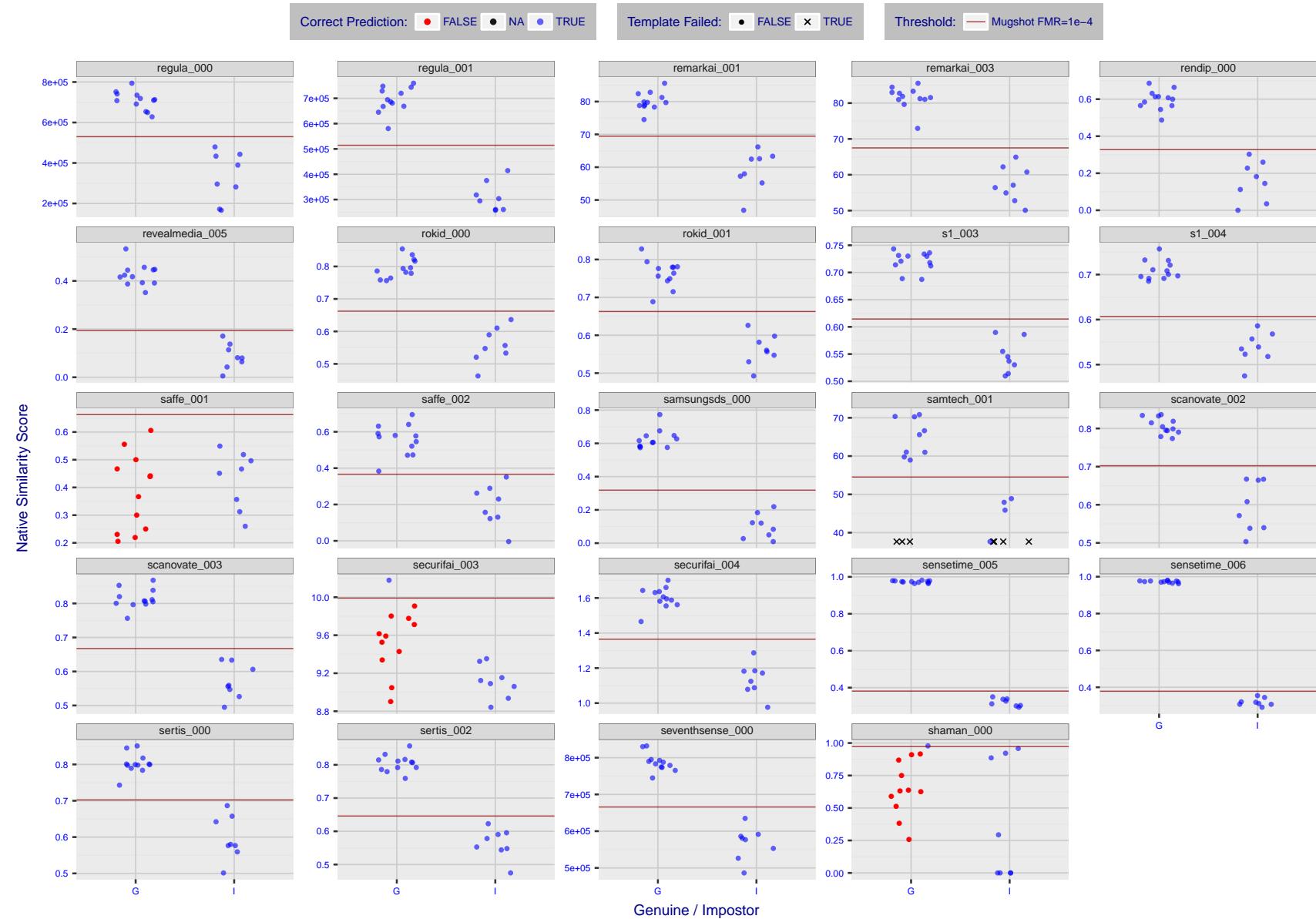


Figure 15: The figure shows algorithms' similarity scores for 12 genuine and 8 impostor image pairs used in the May 2018 paper Face recognition accuracy of forensic examiners, superrecognizers, and face recognition algorithms (Phillips et al. [1]). The threshold (red horizontal line) is a value calibrated to give $FMR = 0.0001$ on mugshot images. Points above the threshold correspond to pairs predicted to be genuine, and points below the threshold correspond to pairs predicted to be impostors. The figure shows whether the predicted class (genuine or impostor) matches the real class. Blue denotes a correct prediction, and red denotes incorrect. An "X" represents face detection failure in either of the images in the pair. Note that the sample size ($n=20$) is small, and the figure may change substantially if larger or different sets are used. The images can be downloaded from the [Supplemental Information](#) page provided with that publication.

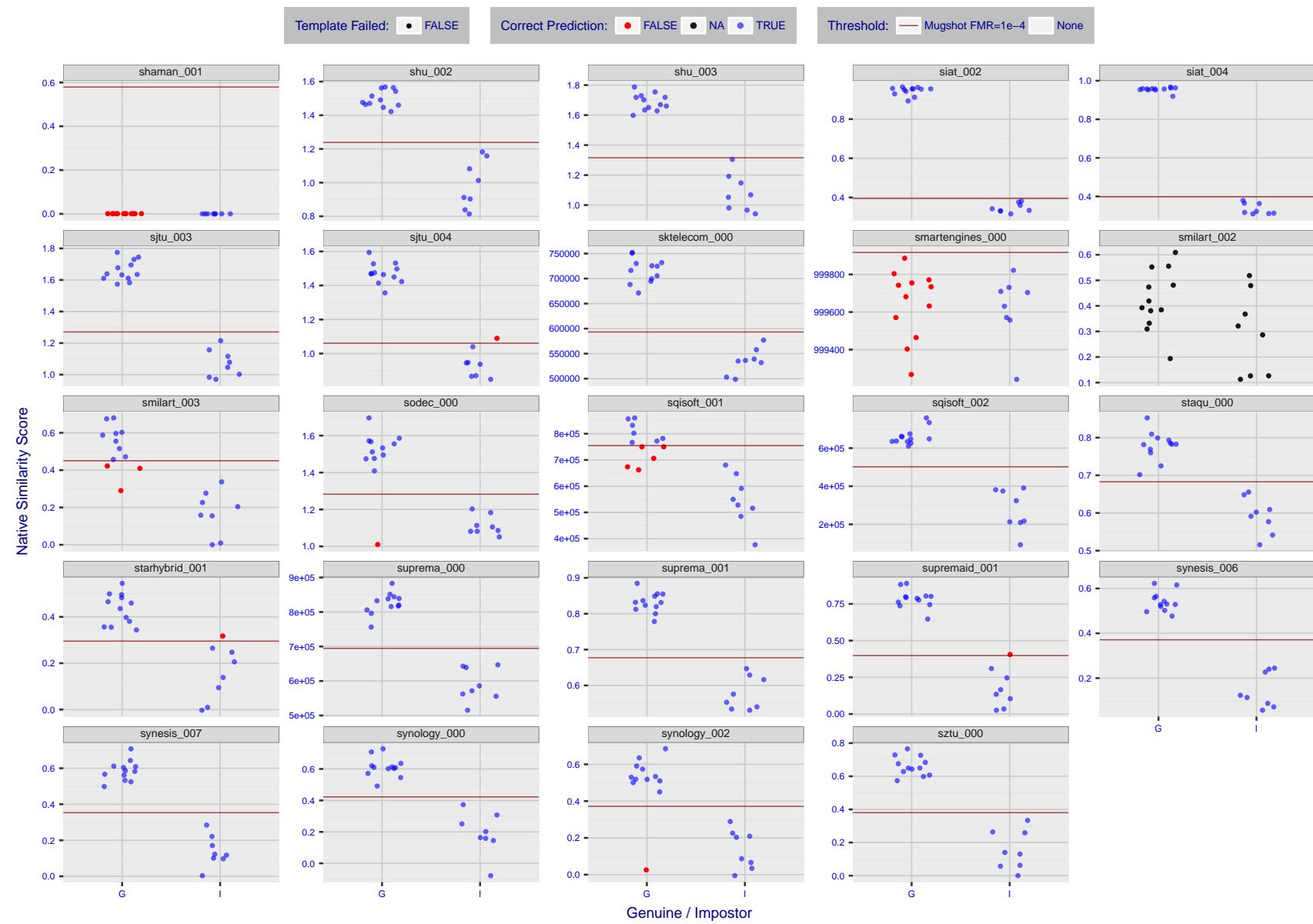


Figure 16: The figure shows algorithms' similarity scores for 12 genuine and 8 impostor image pairs used in the May 2018 paper Face recognition accuracy of forensic examiners, superrecognizers, and face recognition algorithms (Phillips et al. [1]). The threshold (red horizontal line) is a value calibrated to give $FMR = 0.0001$ on mugshot images. Points above the threshold correspond to pairs predicted to be genuine, and points below the threshold correspond to pairs predicted to be impostors. The figure shows whether the predicted class (genuine or impostor) matches the real class. Blue denotes a correct prediction, and red denotes incorrect. An "X" represents face detection failure in either of the images in the pair. Note that the sample size ($n=20$) is small, and the figure may change substantially if larger or different sets are used. The images can be downloaded from the [Supplemental Information](#) page provided with that publication.

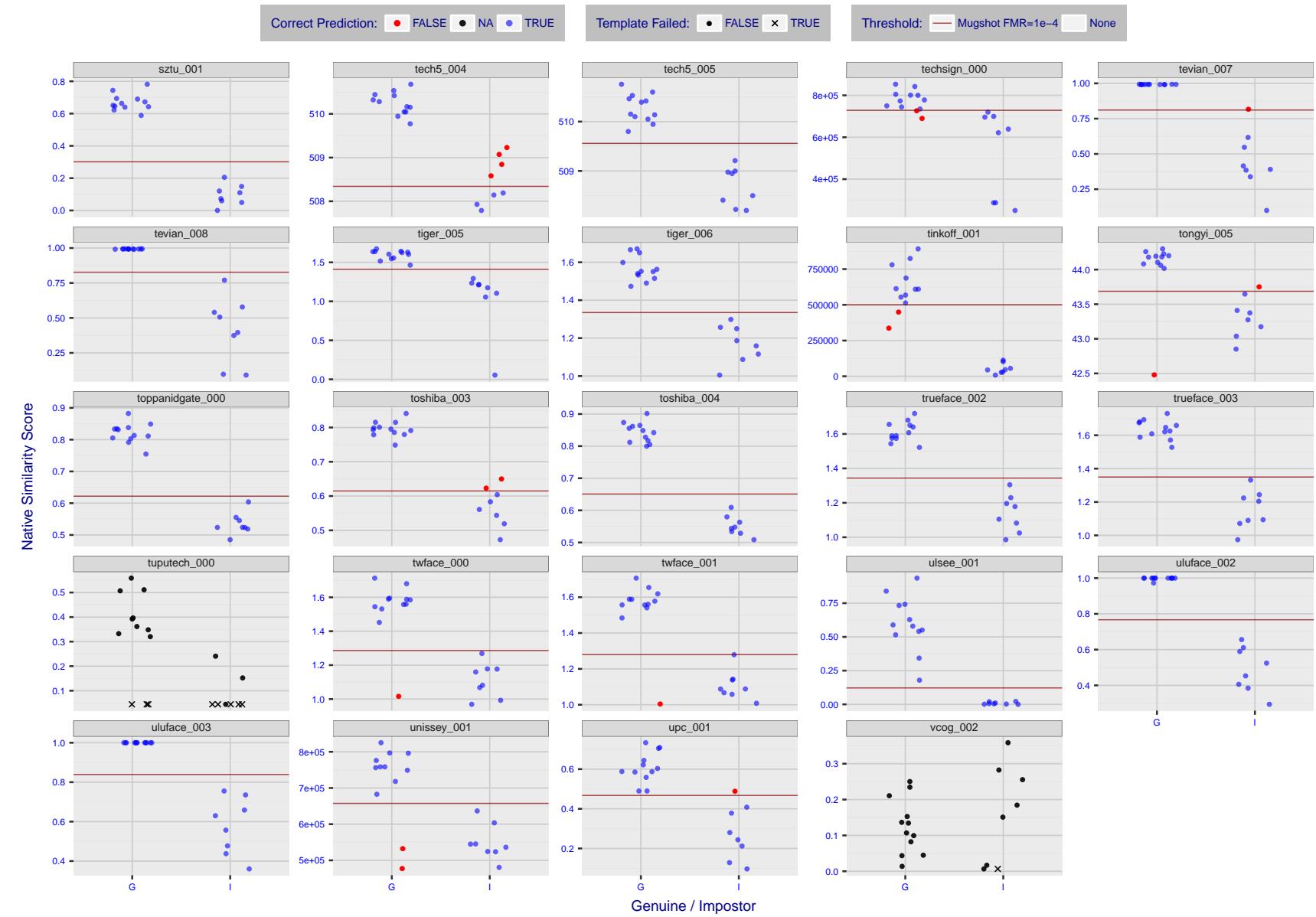


Figure 17: The figure shows algorithms' similarity scores for 12 genuine and 8 impostor image pairs used in the May 2018 paper Face recognition accuracy of forensic examiners, superrecognizers, and face recognition algorithms (Phillips et al. [1]). The threshold (red horizontal line) is a value calibrated to give $FMR = 0.0001$ on mugshot images. Points above the threshold correspond to pairs predicted to be genuine, and points below the threshold correspond to pairs predicted to be impostors. The figure shows whether the predicted class (genuine or impostor) matches the real class. Blue denotes a correct prediction, and red denotes incorrect. An "X" represents face detection failure in either of the images in the pair. Note that the sample size ($n=20$) is small, and the figure may change substantially if larger or different sets are used. The images can be downloaded from the [Supplemental Information](#) page provided with that publication.



Figure 18: The figure shows algorithms' similarity scores for 12 genuine and 8 impostor image pairs used in the May 2018 paper Face recognition accuracy of forensic examiners, superrecognizers, and face recognition algorithms (Phillips et al. [1]). The threshold (red horizontal line) is a value calibrated to give $FMR = 0.0001$ on mugshot images. Points above the threshold correspond to pairs predicted to be genuine, and points below the threshold correspond to pairs predicted to be impostors. The figure shows whether the predicted class (genuine or impostor) matches the real class. Blue denotes a correct prediction, and red denotes incorrect. An "X" represents face detection failure in either of the images in the pair. Note that the sample size ($n=20$) is small, and the figure may change substantially if larger or different sets are used. The images can be downloaded from the [Supplemental Information](#) page provided with that publication.

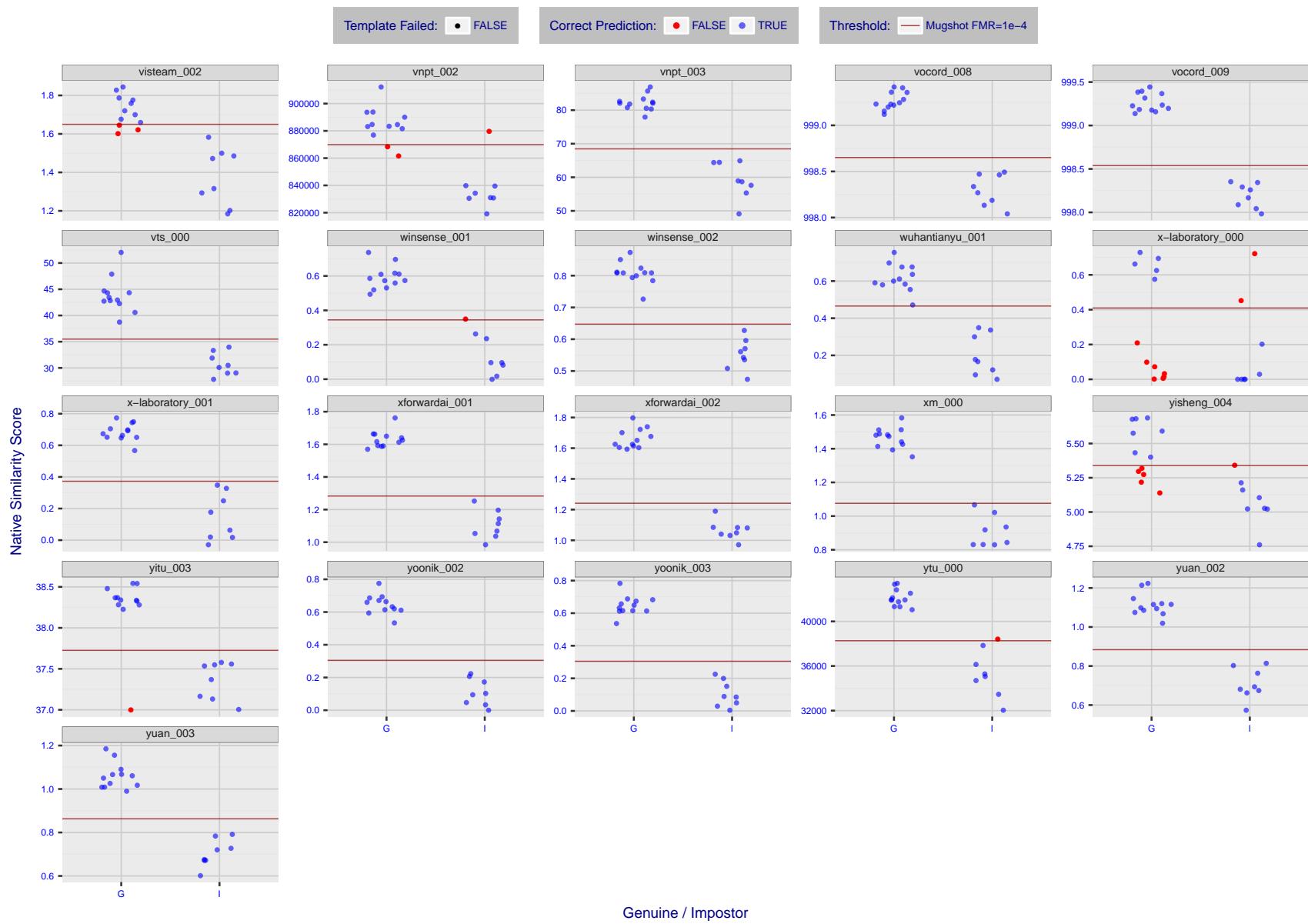


Figure 19: The figure shows algorithms' similarity scores for 12 genuine and 8 impostor image pairs used in the May 2018 paper Face recognition accuracy of forensic examiners, superrecognizers, and face recognition algorithms (Phillips et al. [1]). The threshold (red horizontal line) is a value calibrated to give $FMR = 0.0001$ on mugshot images. Points above the threshold correspond to pairs predicted to be genuine, and points below the threshold correspond to pairs predicted to be impostors. The figure shows whether the predicted class (genuine or impostor) matches the real class. Blue denotes a correct prediction, and red denotes incorrect. An "X" represents face detection failure in either of the images in the pair. Note that the sample size ($n=20$) is small, and the figure may change substantially if larger or different sets are used. The images can be downloaded from the [Supplemental Information](#) page provided with that publication.

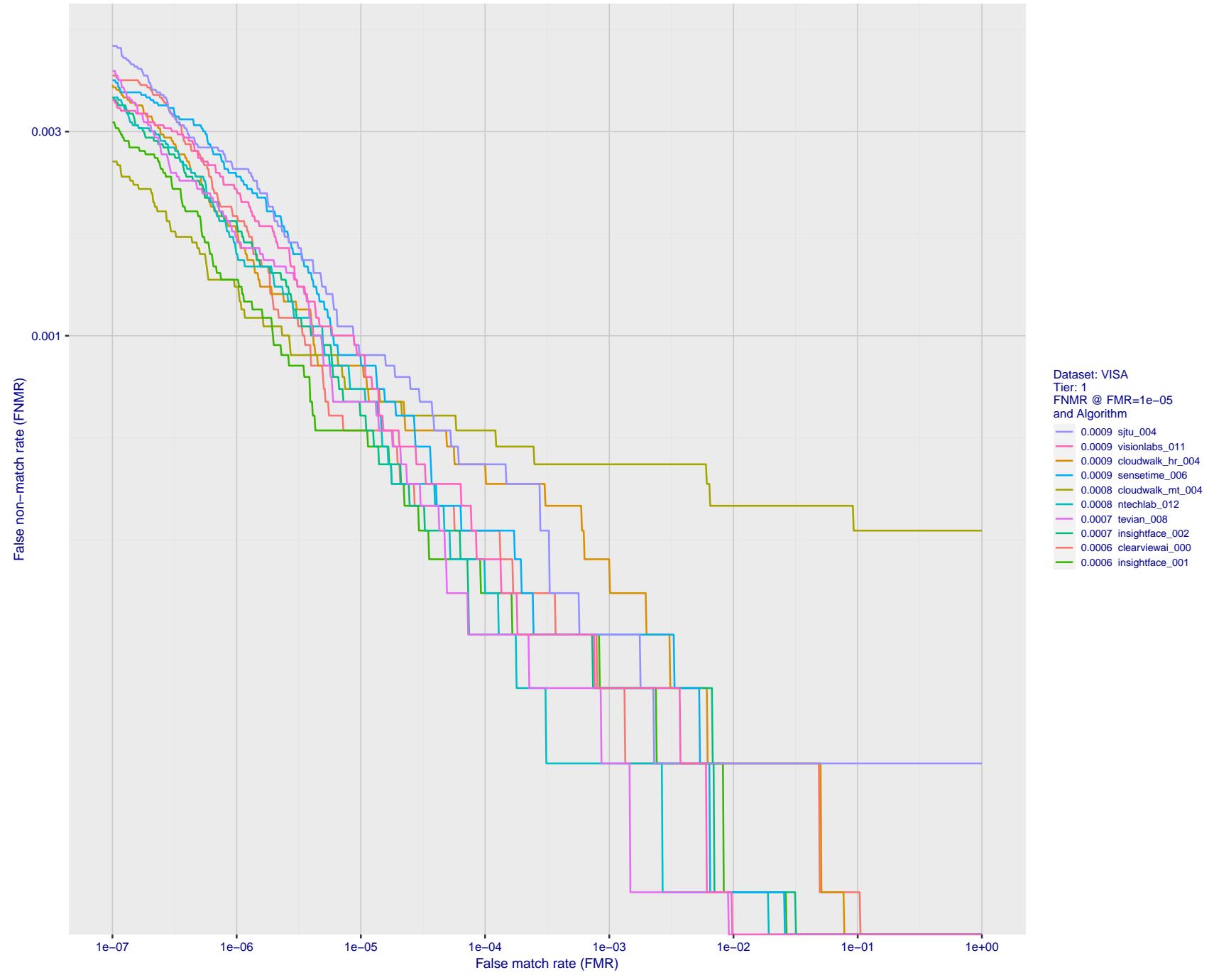


Figure 20: For the visa images, detection error tradeoff (DET) characteristics showing false non-match rate vs. false match rate plotted parametrically on threshold, T . The scales are logarithmic in order to show many decades of FMR.

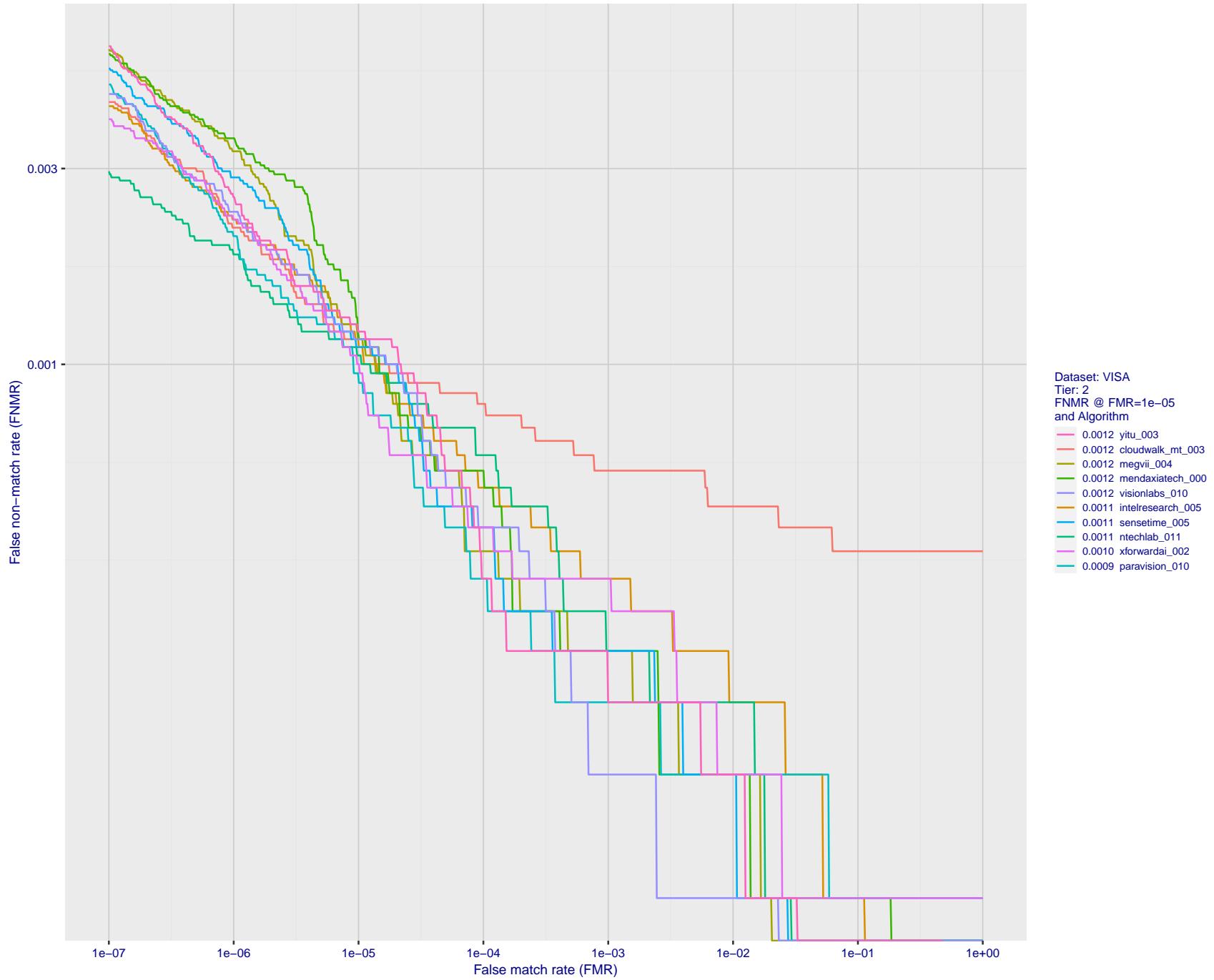


Figure 21: For the visa images, detection error tradeoff (DET) characteristics showing false non-match rate vs. false match rate plotted parametrically on threshold, T . The scales are logarithmic in order to show many decades of FMR.

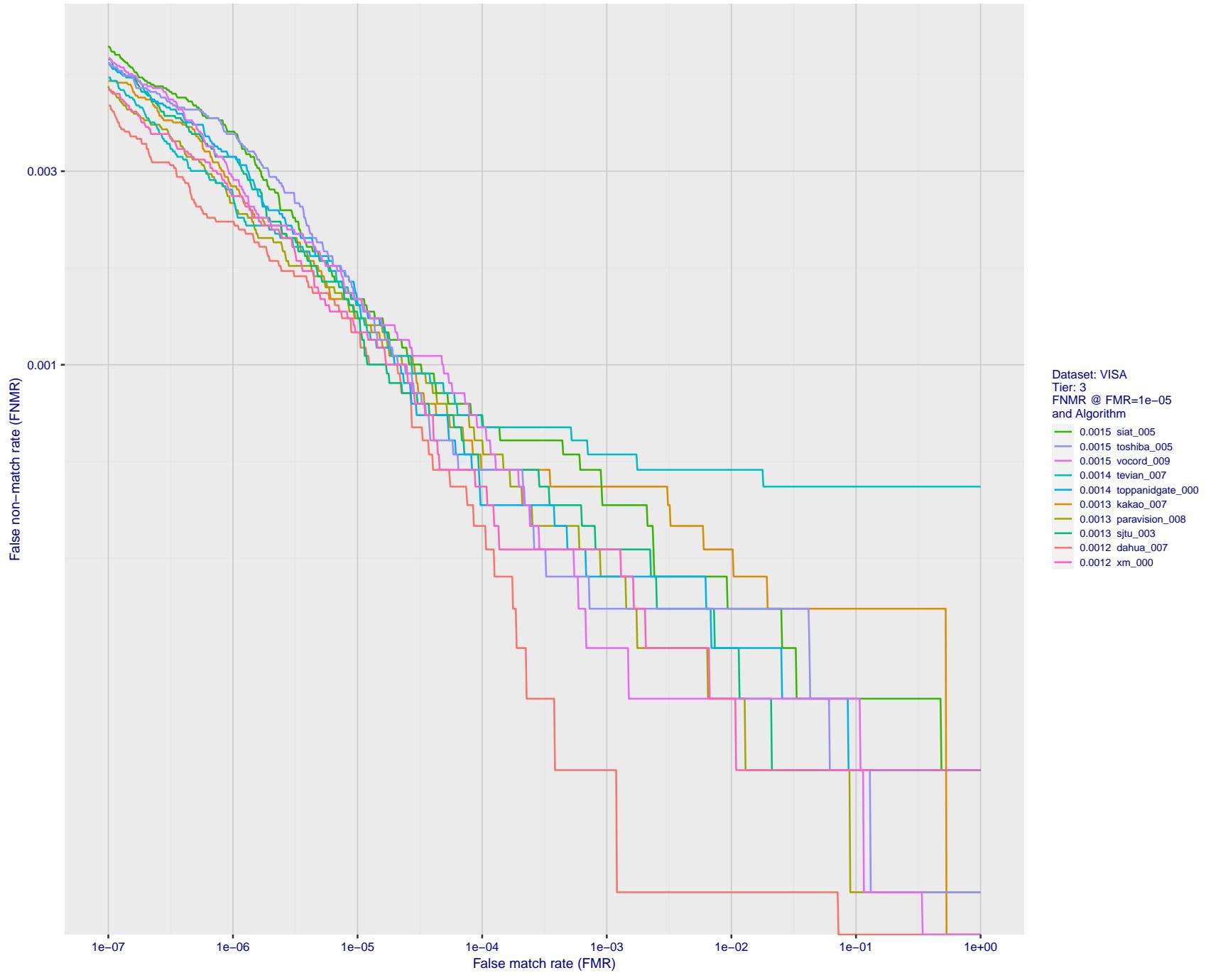


Figure 22: For the visa images, detection error tradeoff (DET) characteristics showing false non-match rate vs. false match rate plotted parametrically on threshold, T . The scales are logarithmic in order to show many decades of FMR.

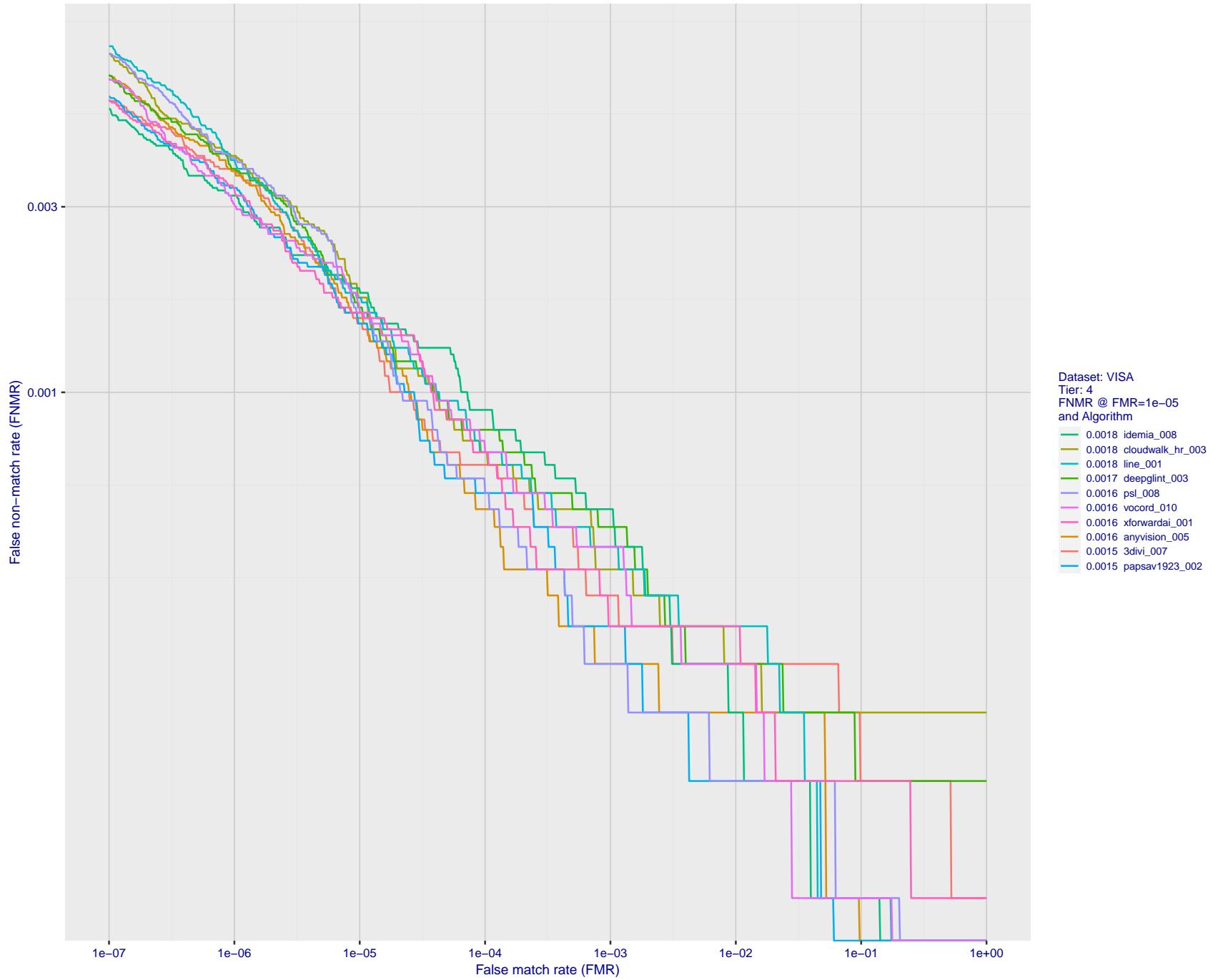


Figure 23: For the visa images, detection error tradeoff (DET) characteristics showing false non-match rate vs. false match rate plotted parametrically on threshold, T . The scales are logarithmic in order to show many decades of FMR.

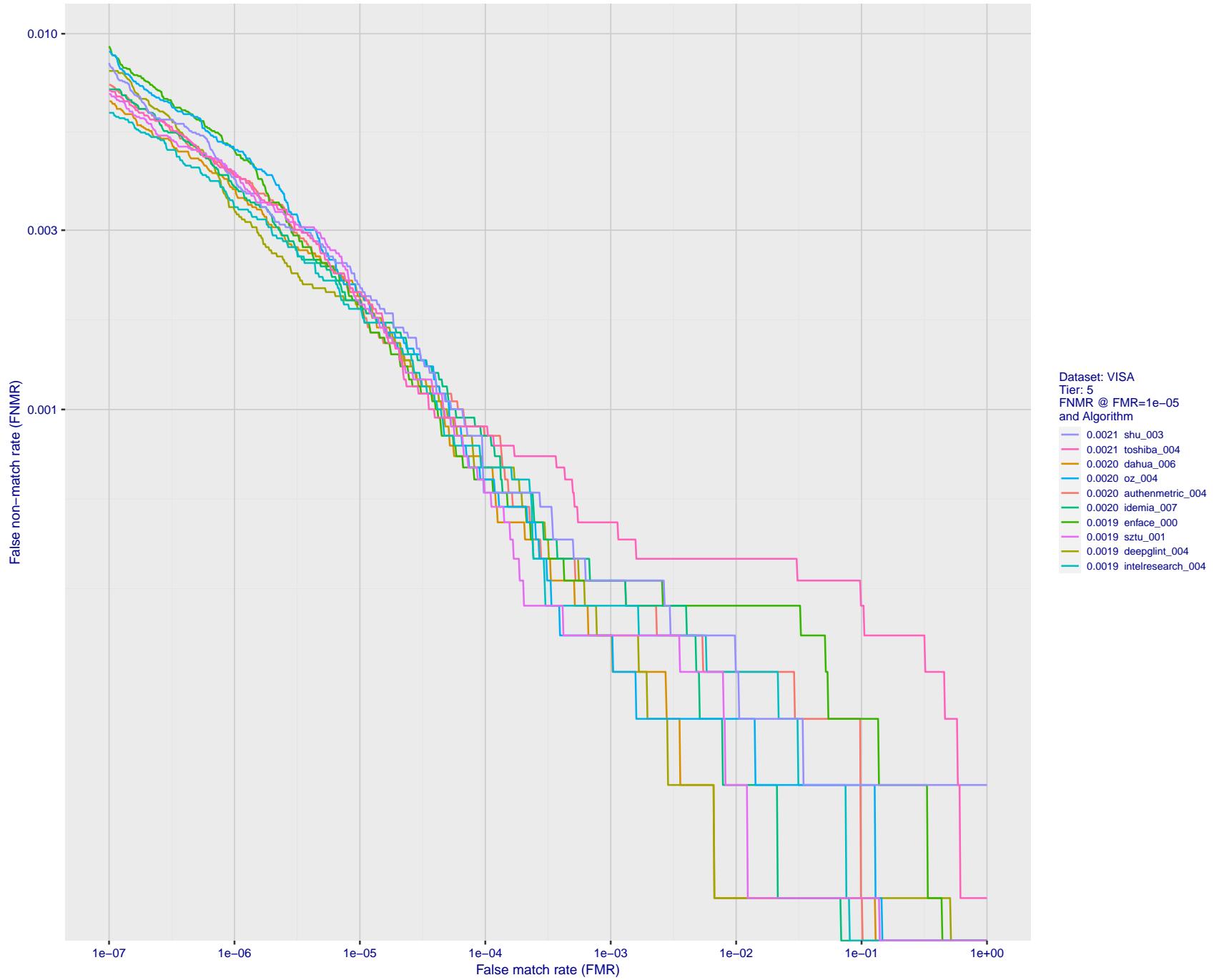


Figure 24: For the visa images, detection error tradeoff (DET) characteristics showing false non-match rate vs. false match rate plotted parametrically on threshold, T . The scales are logarithmic in order to show many decades of FMR.

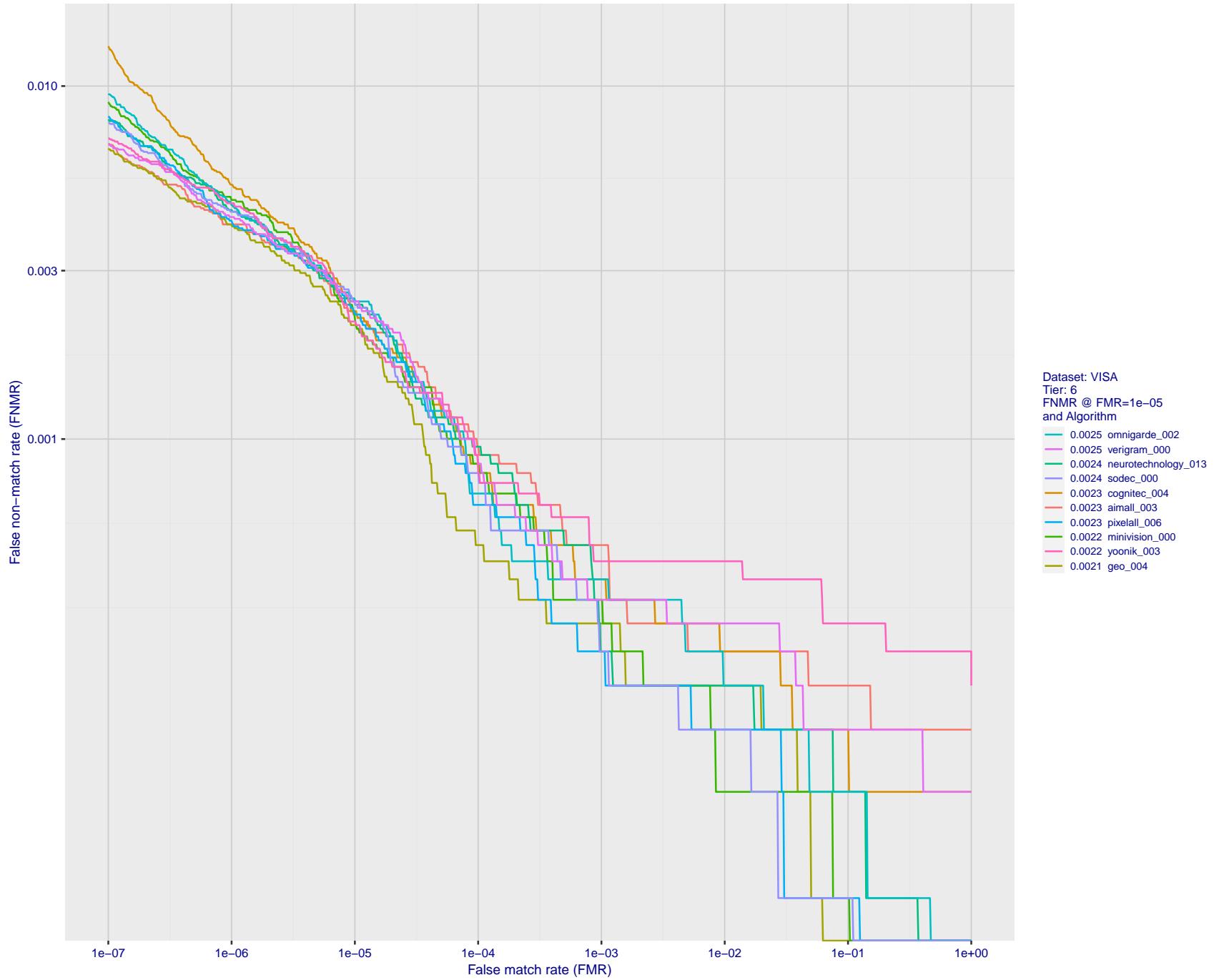


Figure 25: For the visa images, detection error tradeoff (DET) characteristics showing false non-match rate vs. false match rate plotted parametrically on threshold, T . The scales are logarithmic in order to show many decades of FMR.

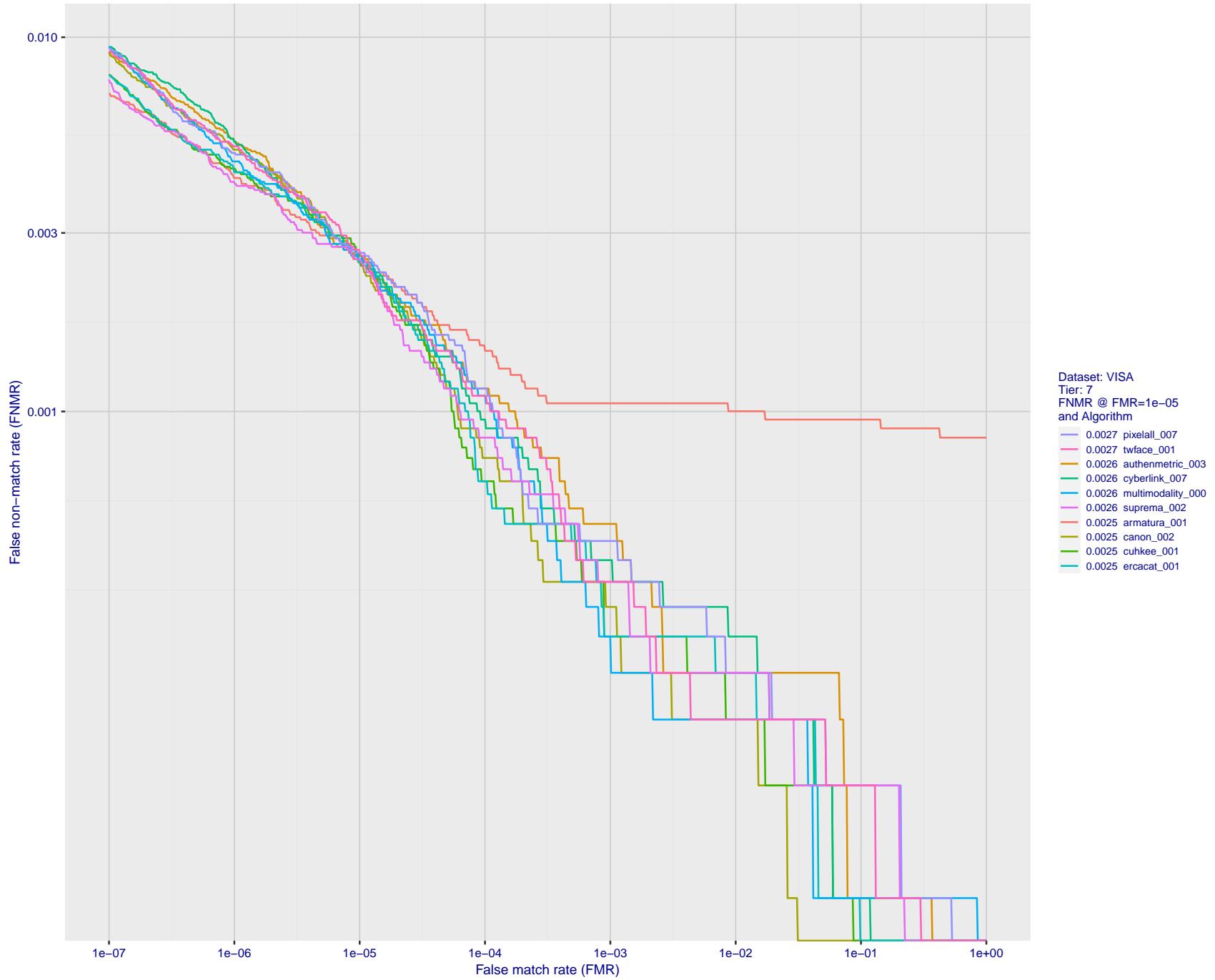


Figure 26: For the visa images, detection error tradeoff (DET) characteristics showing false non-match rate vs. false match rate plotted parametrically on threshold, T . The scales are logarithmic in order to show many decades of FMR.

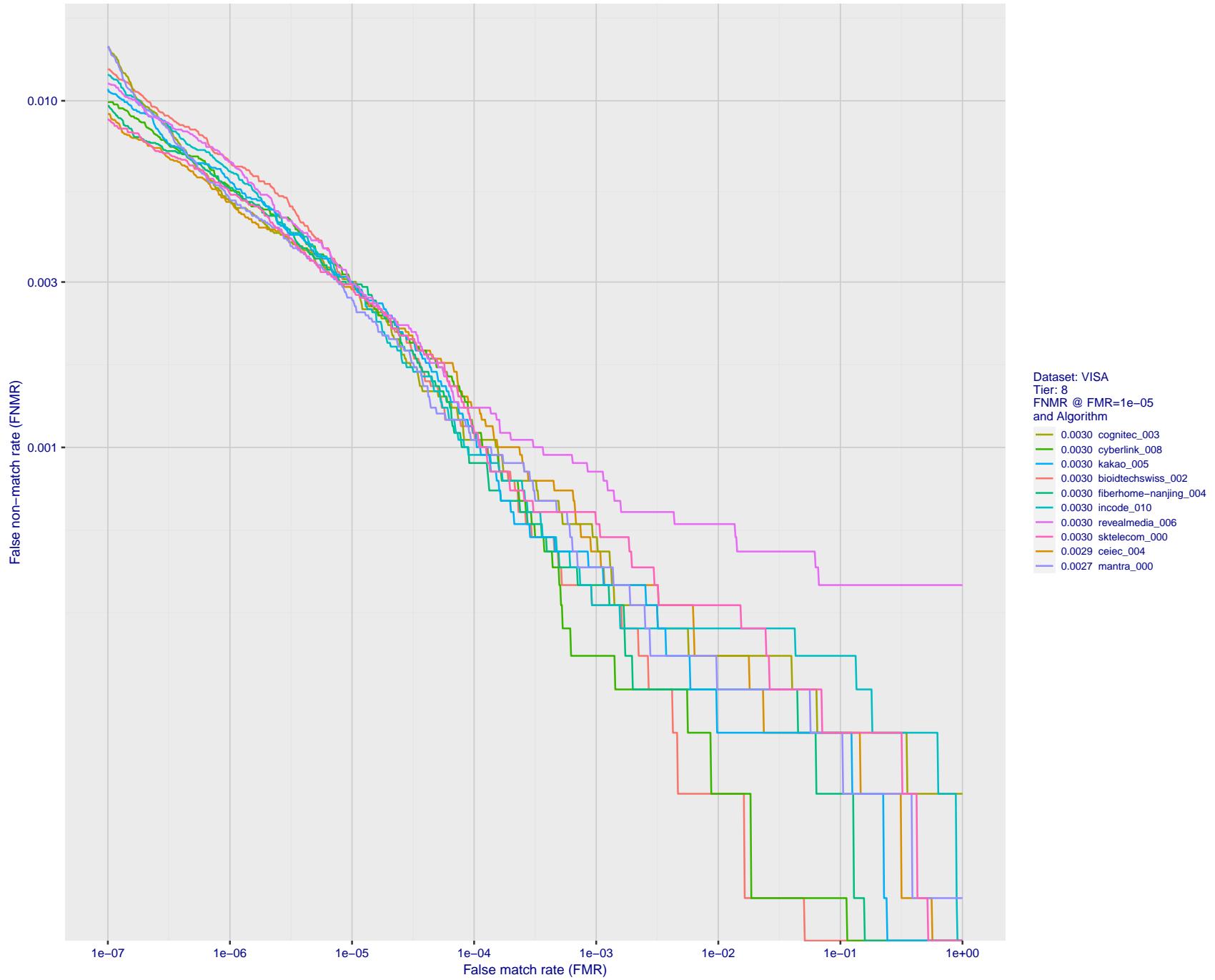


Figure 27: For the visa images, detection error tradeoff (DET) characteristics showing false non-match rate vs. false match rate plotted parametrically on threshold, T . The scales are logarithmic in order to show many decades of FMR.

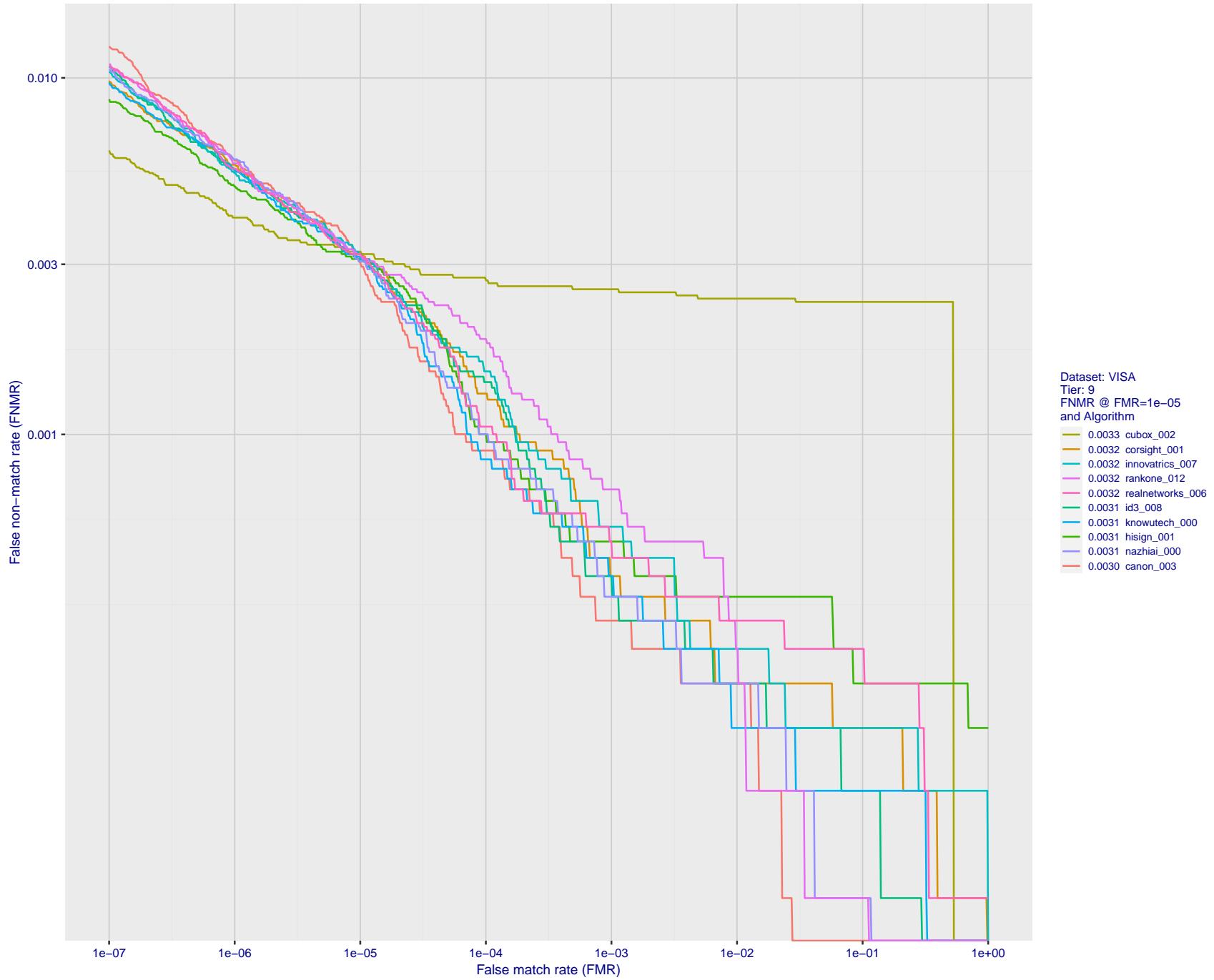


Figure 28: For the visa images, detection error tradeoff (DET) characteristics showing false non-match rate vs. false match rate plotted parametrically on threshold, T . The scales are logarithmic in order to show many decades of FMR.

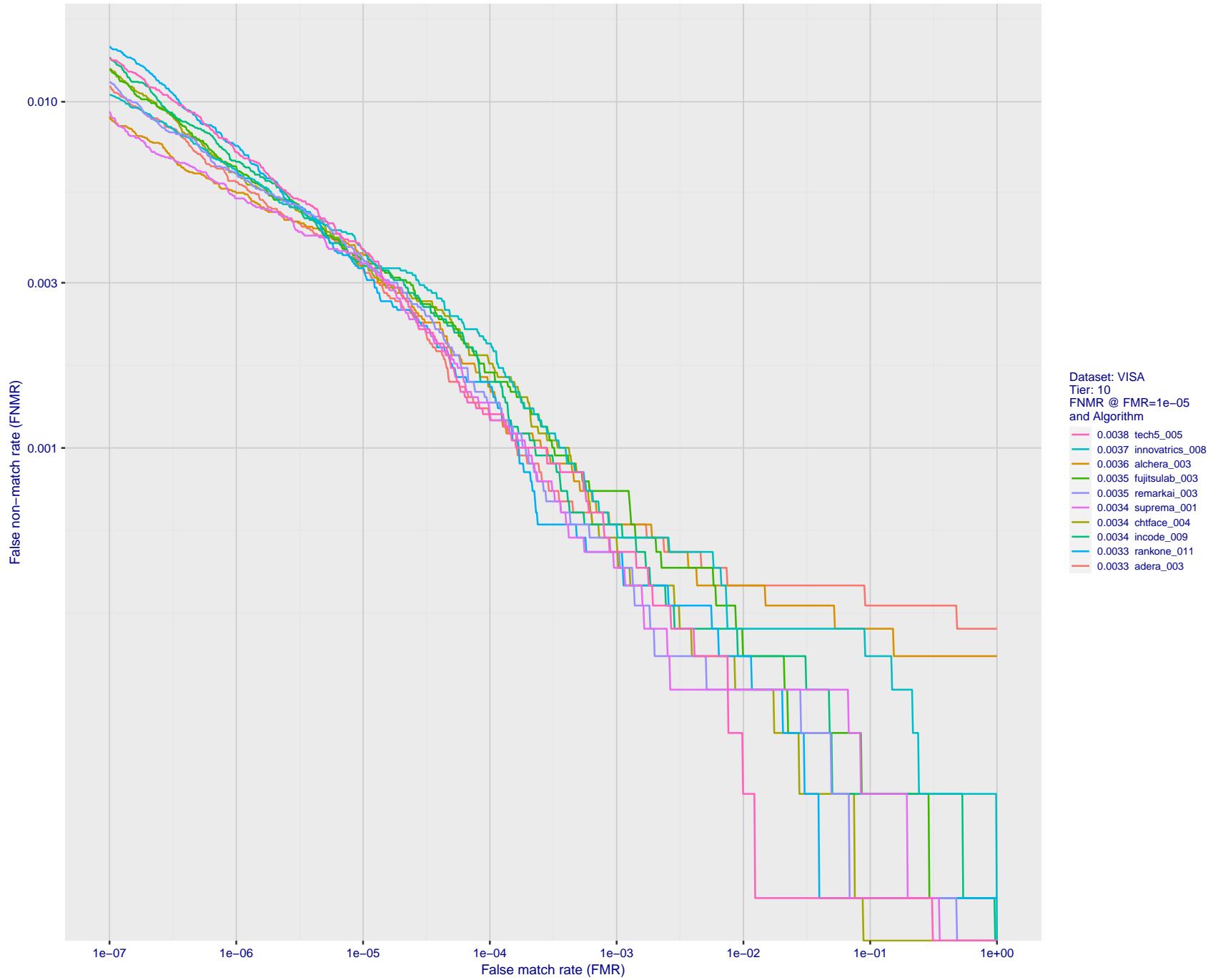


Figure 29: For the visa images, detection error tradeoff (DET) characteristics showing false non-match rate vs. false match rate plotted parametrically on threshold, T . The scales are logarithmic in order to show many decades of FMR.

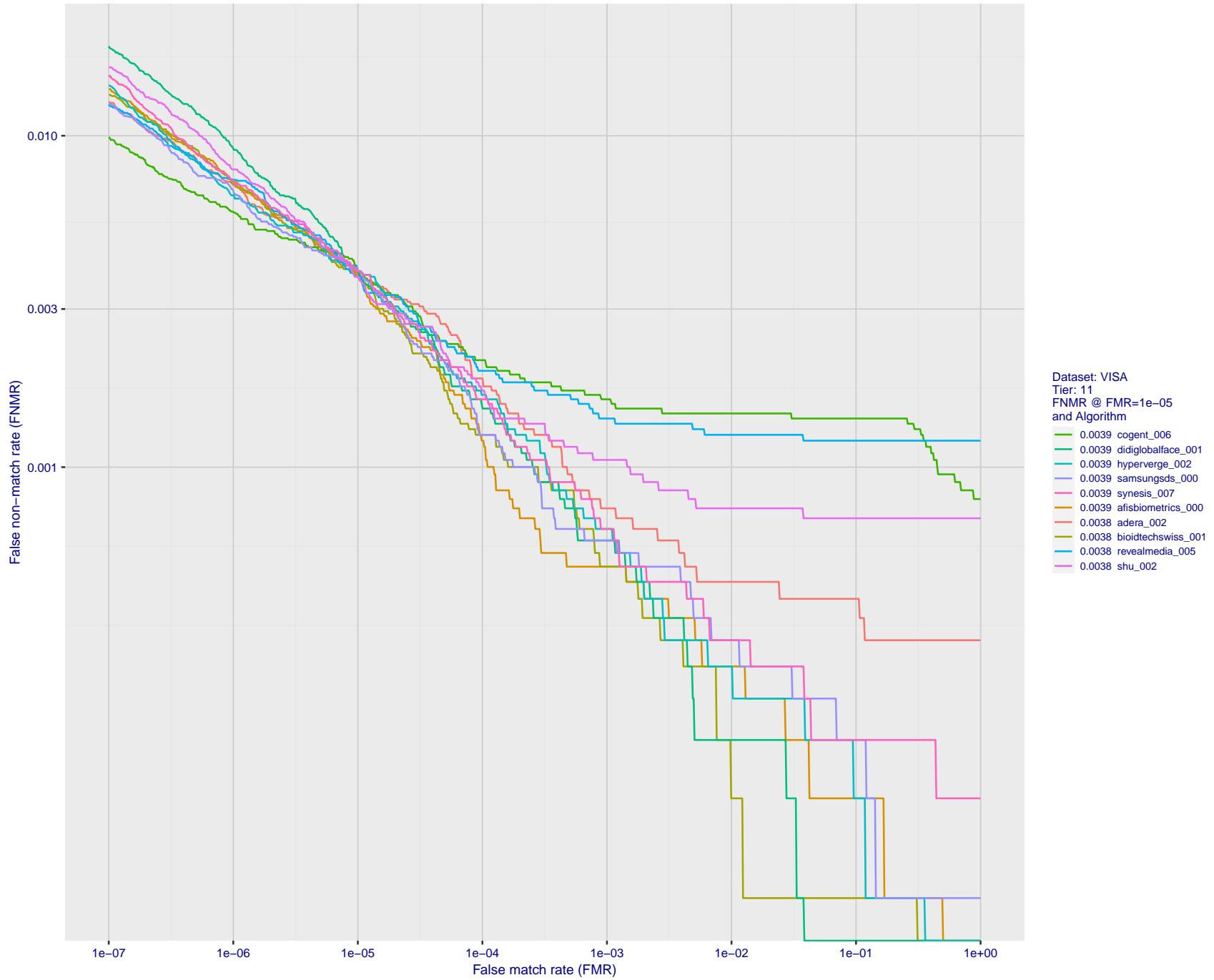


Figure 30: For the visa images, detection error tradeoff (DET) characteristics showing false non-match rate vs. false match rate plotted parametrically on threshold, T . The scales are logarithmic in order to show many decades of FMR.

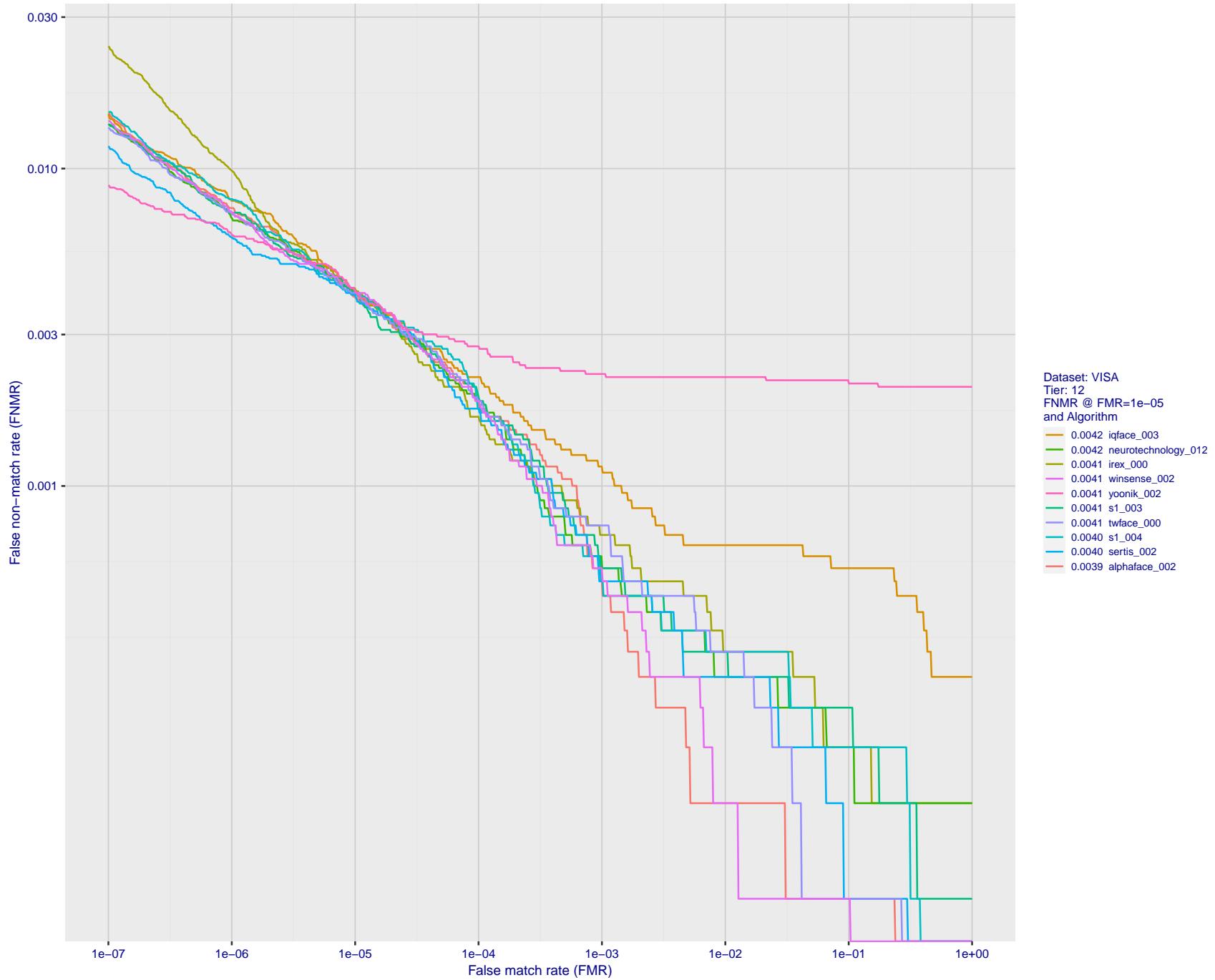


Figure 31: For the visa images, detection error tradeoff (DET) characteristics showing false non-match rate vs. false match rate plotted parametrically on threshold, T . The scales are logarithmic in order to show many decades of FMR.

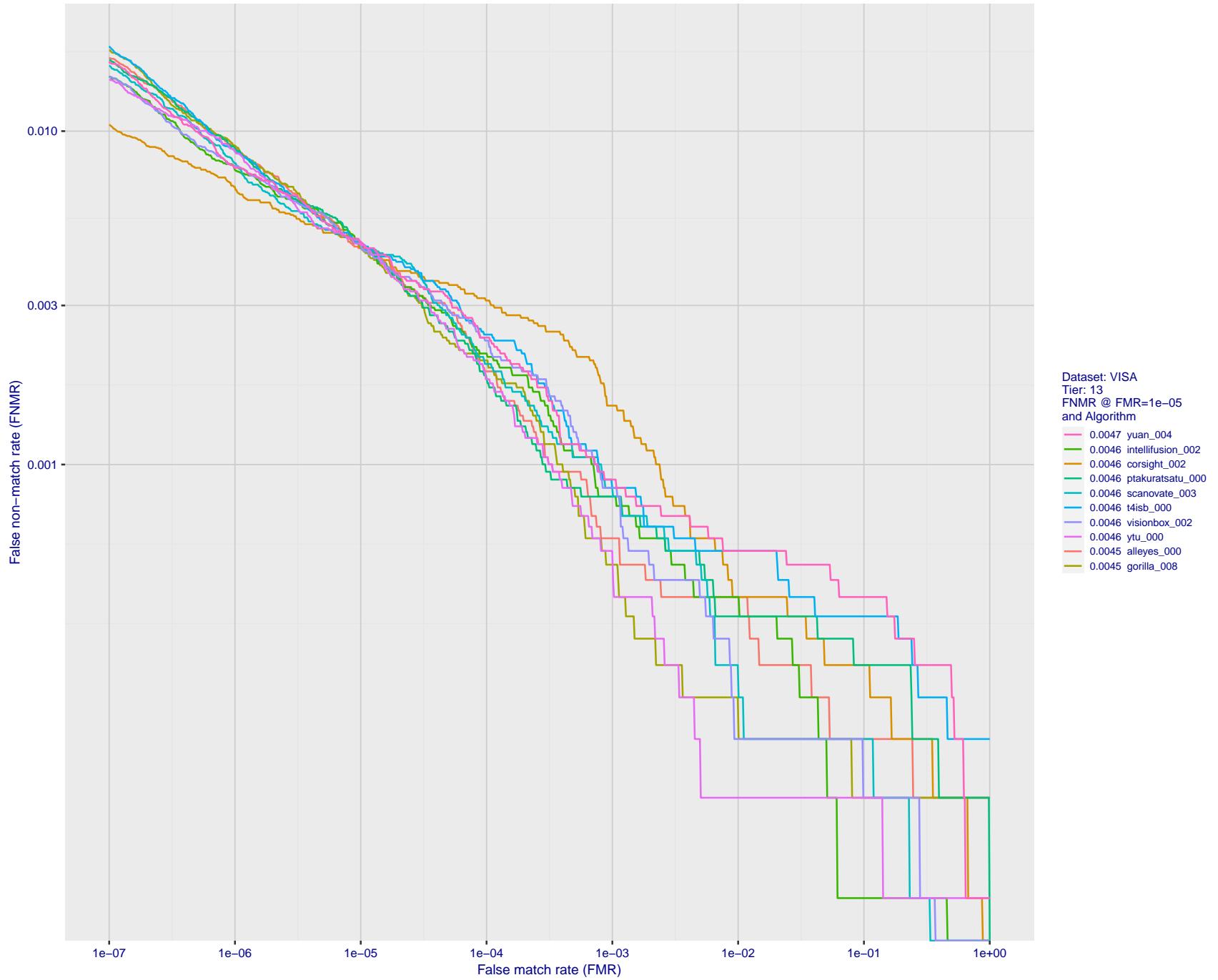


Figure 32: For the visa images, detection error tradeoff (DET) characteristics showing false non-match rate vs. false match rate plotted parametrically on threshold, T . The scales are logarithmic in order to show many decades of FMR.

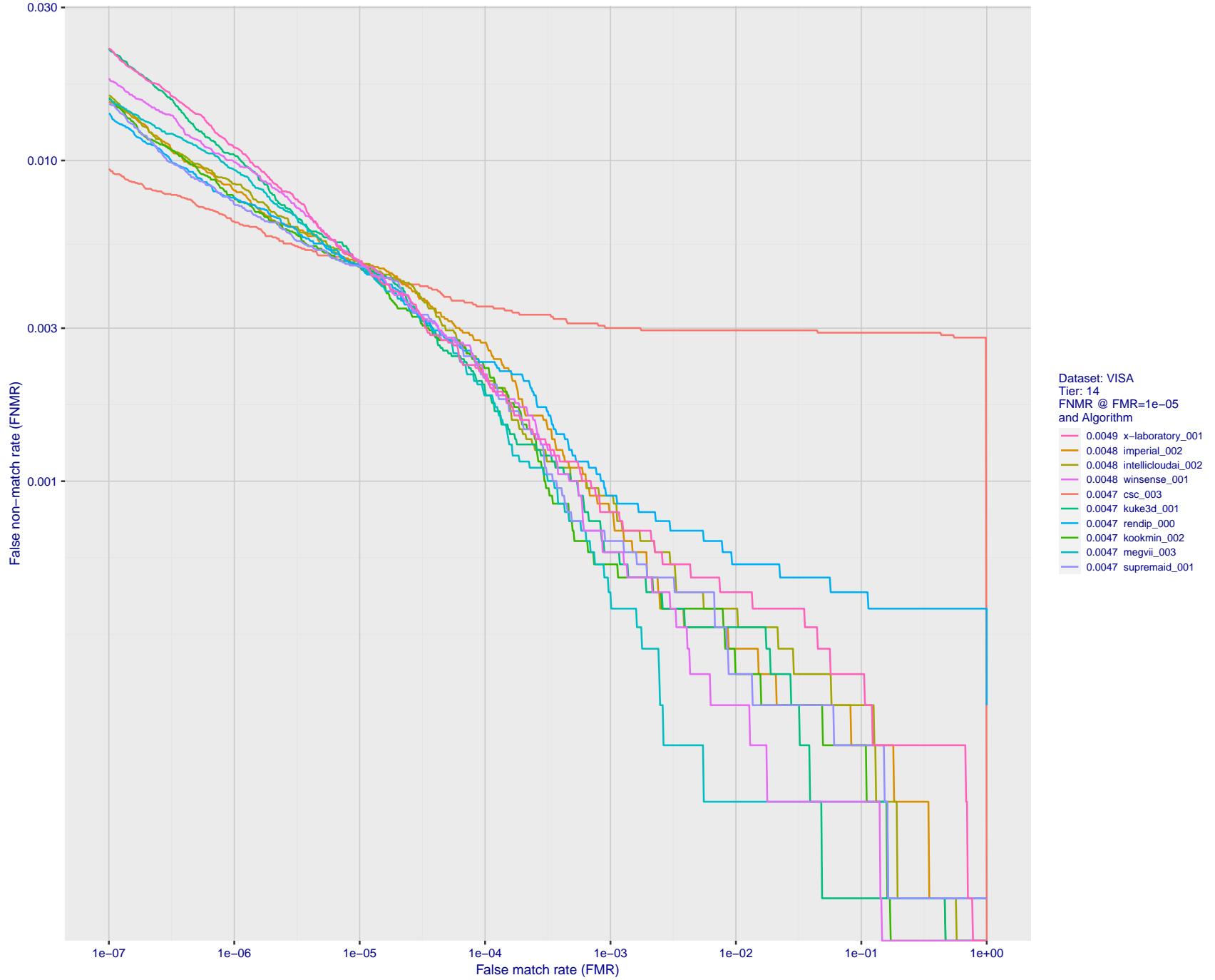


Figure 33: For the visa images, detection error tradeoff (DET) characteristics showing false non-match rate vs. false match rate plotted parametrically on threshold, T . The scales are logarithmic in order to show many decades of FMR.

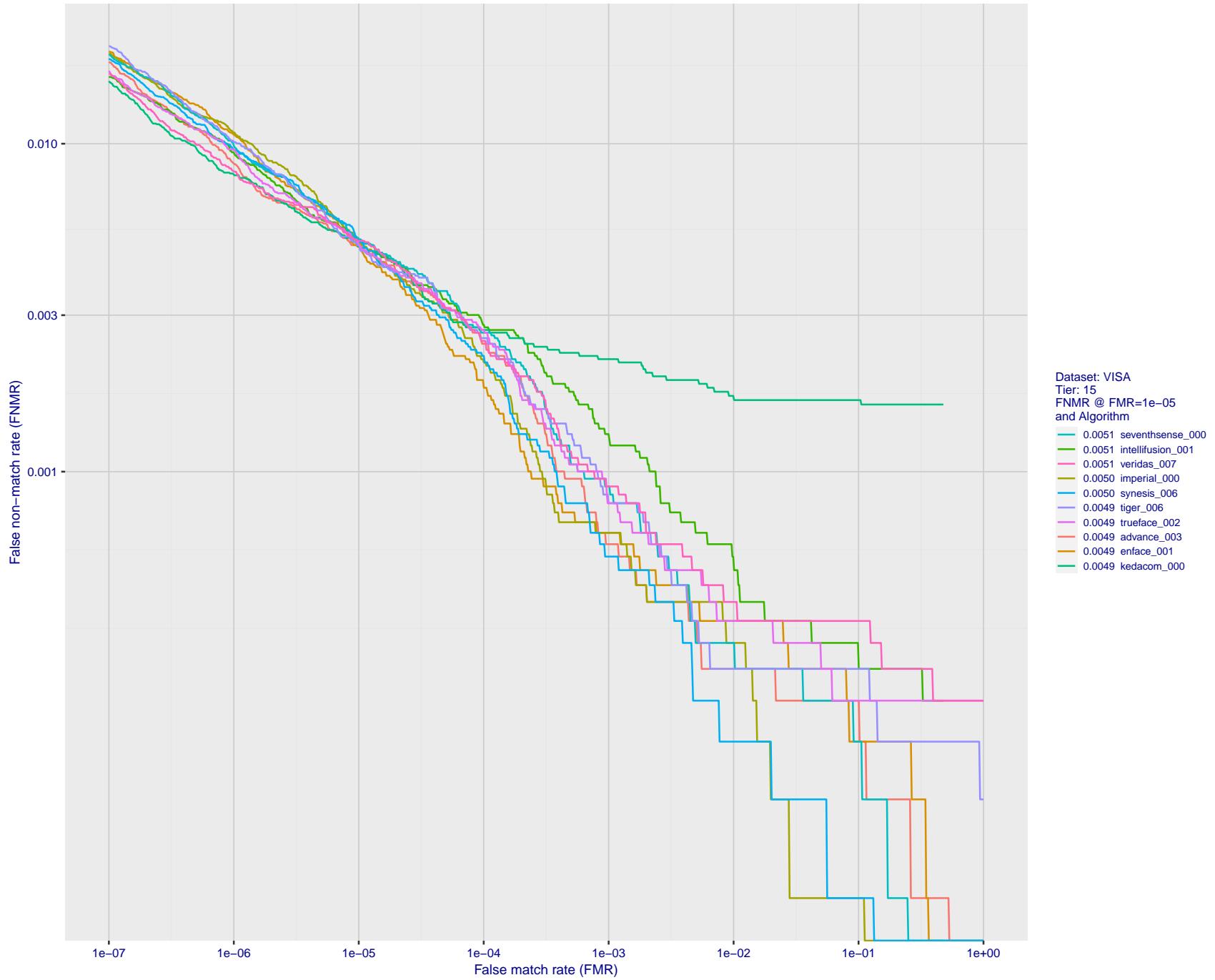


Figure 34: For the visa images, detection error tradeoff (DET) characteristics showing false non-match rate vs. false match rate plotted parametrically on threshold, T . The scales are logarithmic in order to show many decades of FMR.

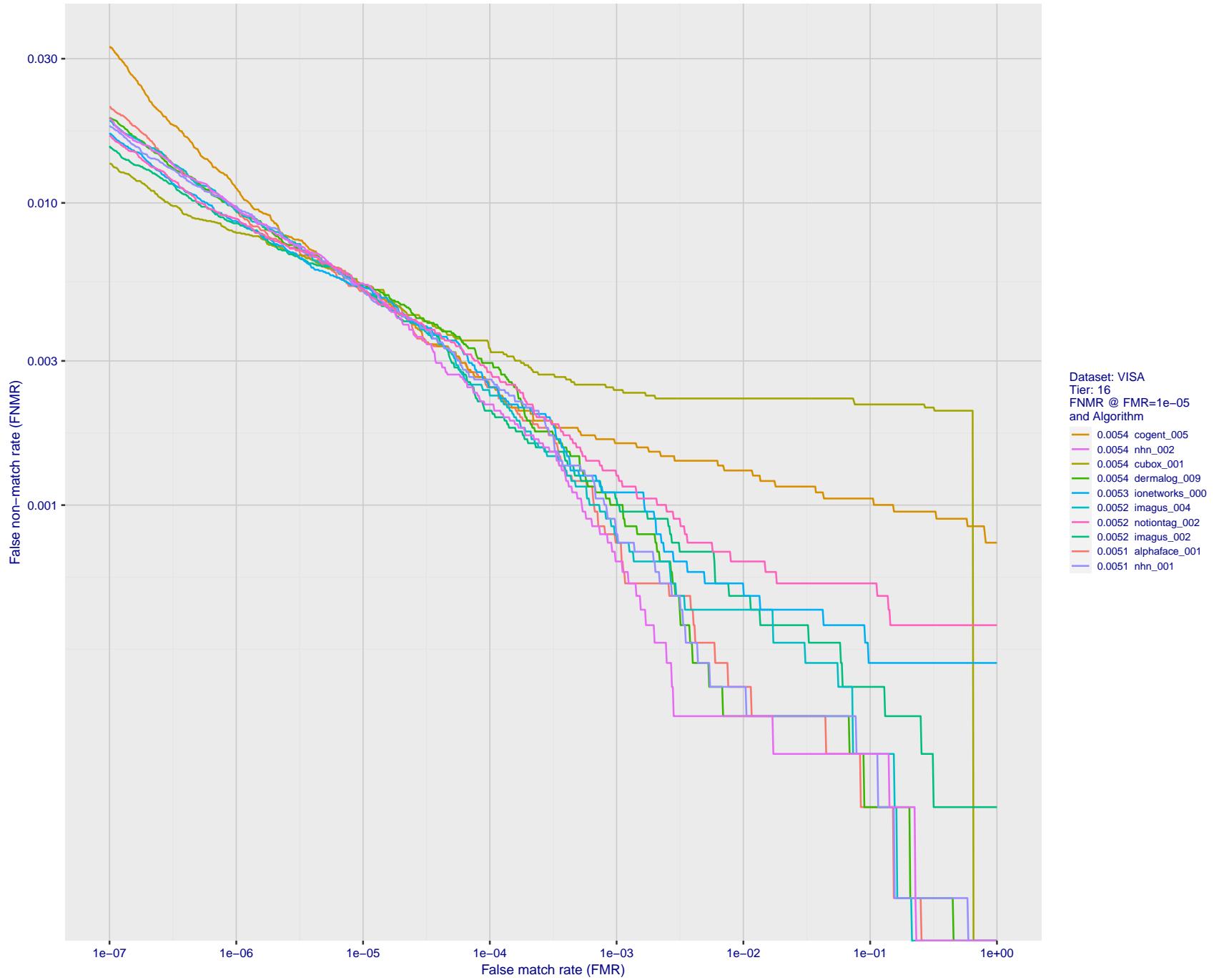


Figure 35: For the visa images, detection error tradeoff (DET) characteristics showing false non-match rate vs. false match rate plotted parametrically on threshold, T . The scales are logarithmic in order to show many decades of FMR.

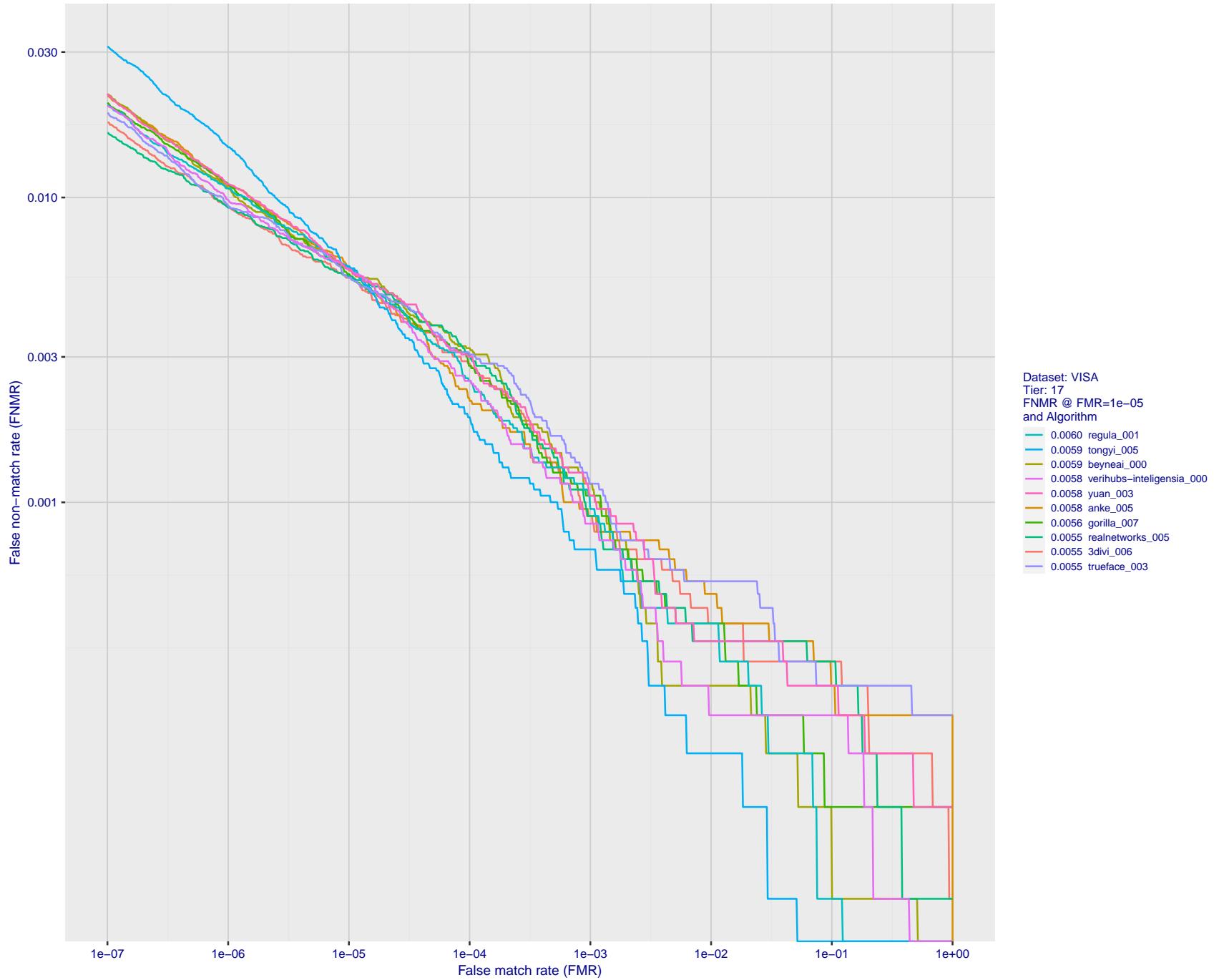


Figure 36: For the visa images, detection error tradeoff (DET) characteristics showing false non-match rate vs. false match rate plotted parametrically on threshold, T . The scales are logarithmic in order to show many decades of FMR.

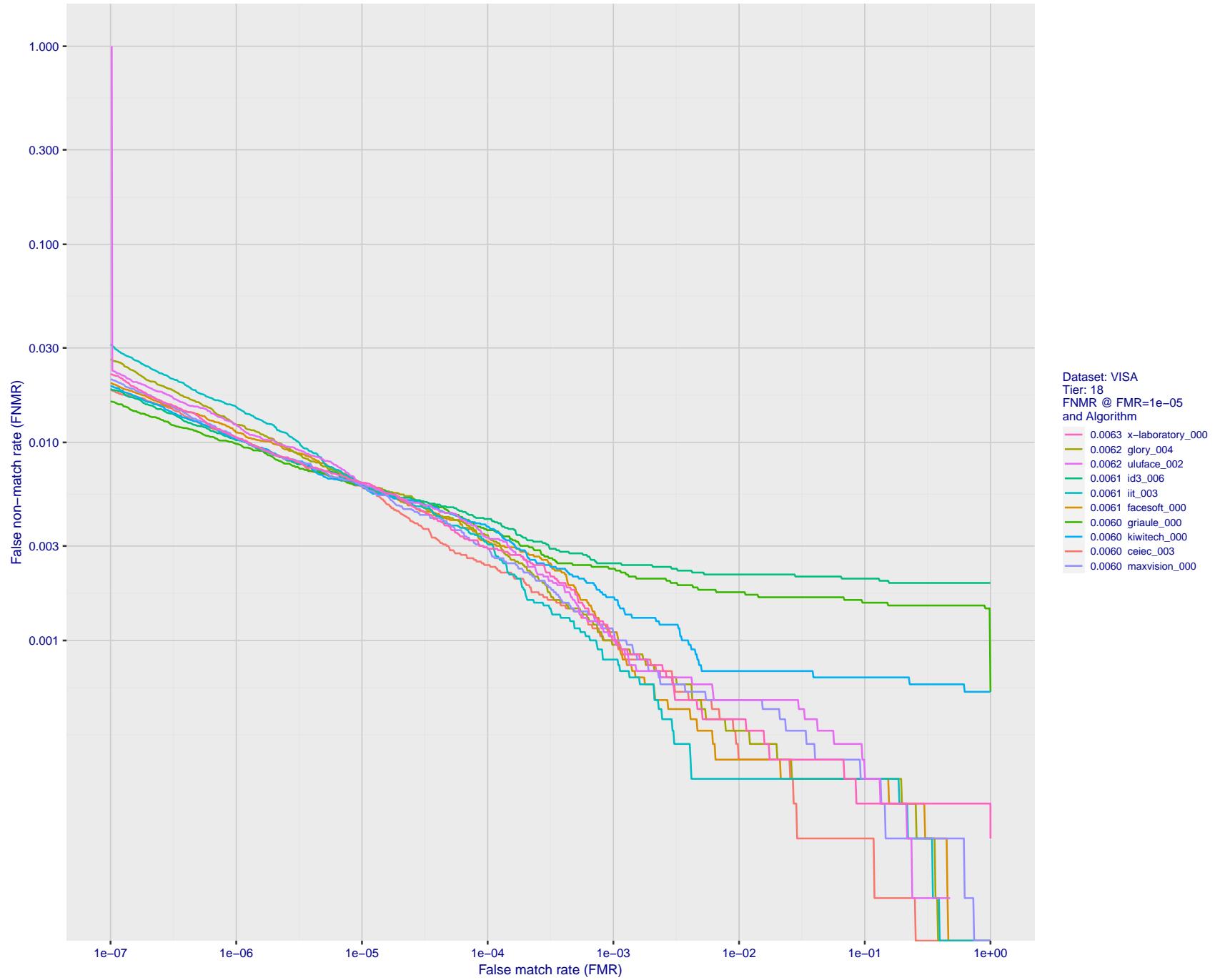


Figure 37: For the visa images, detection error tradeoff (DET) characteristics showing false non-match rate vs. false match rate plotted parametrically on threshold, T . The scales are logarithmic in order to show many decades of FMR.

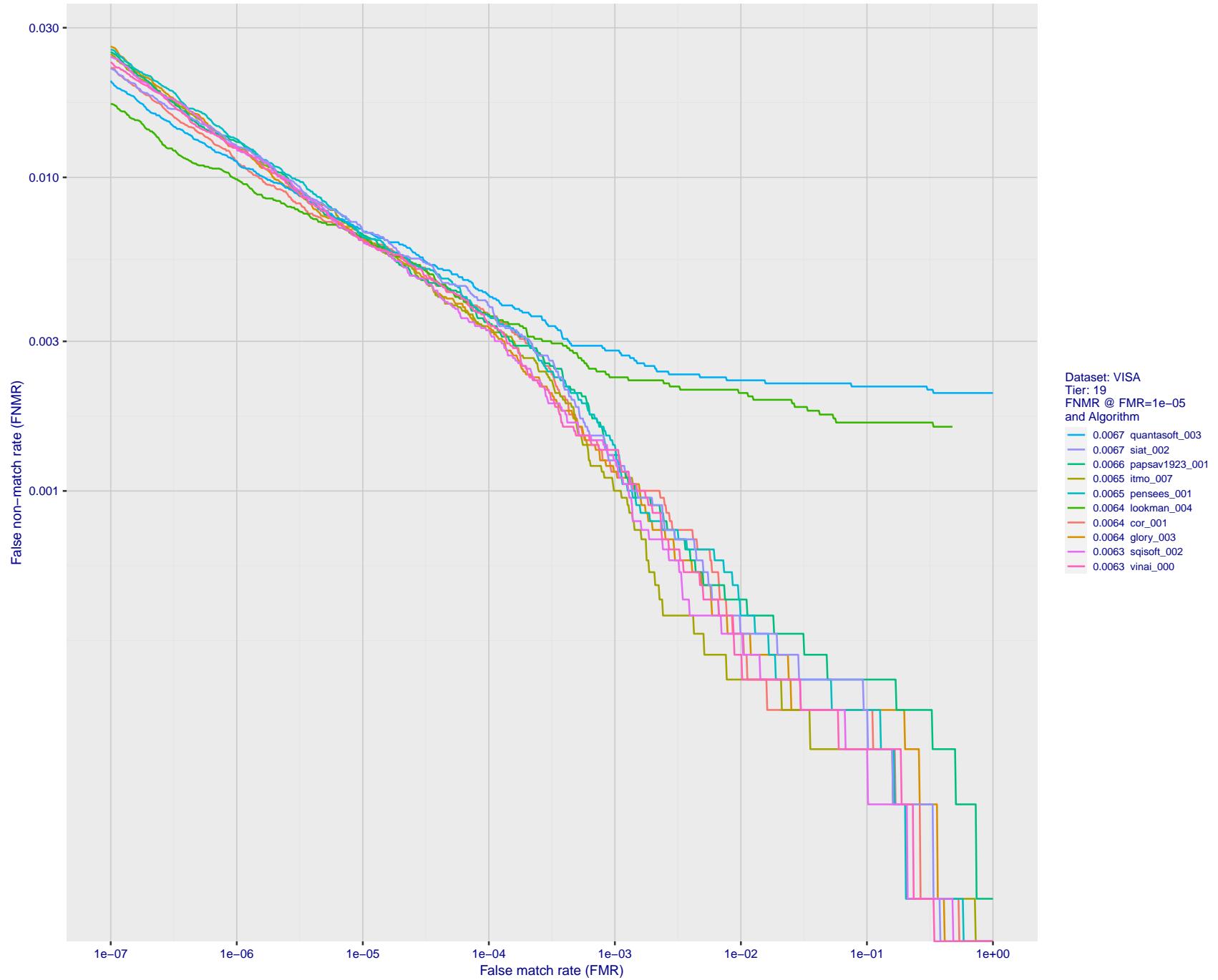


Figure 38: For the visa images, detection error tradeoff (DET) characteristics showing false non-match rate vs. false match rate plotted parametrically on threshold, T . The scales are logarithmic in order to show many decades of FMR.

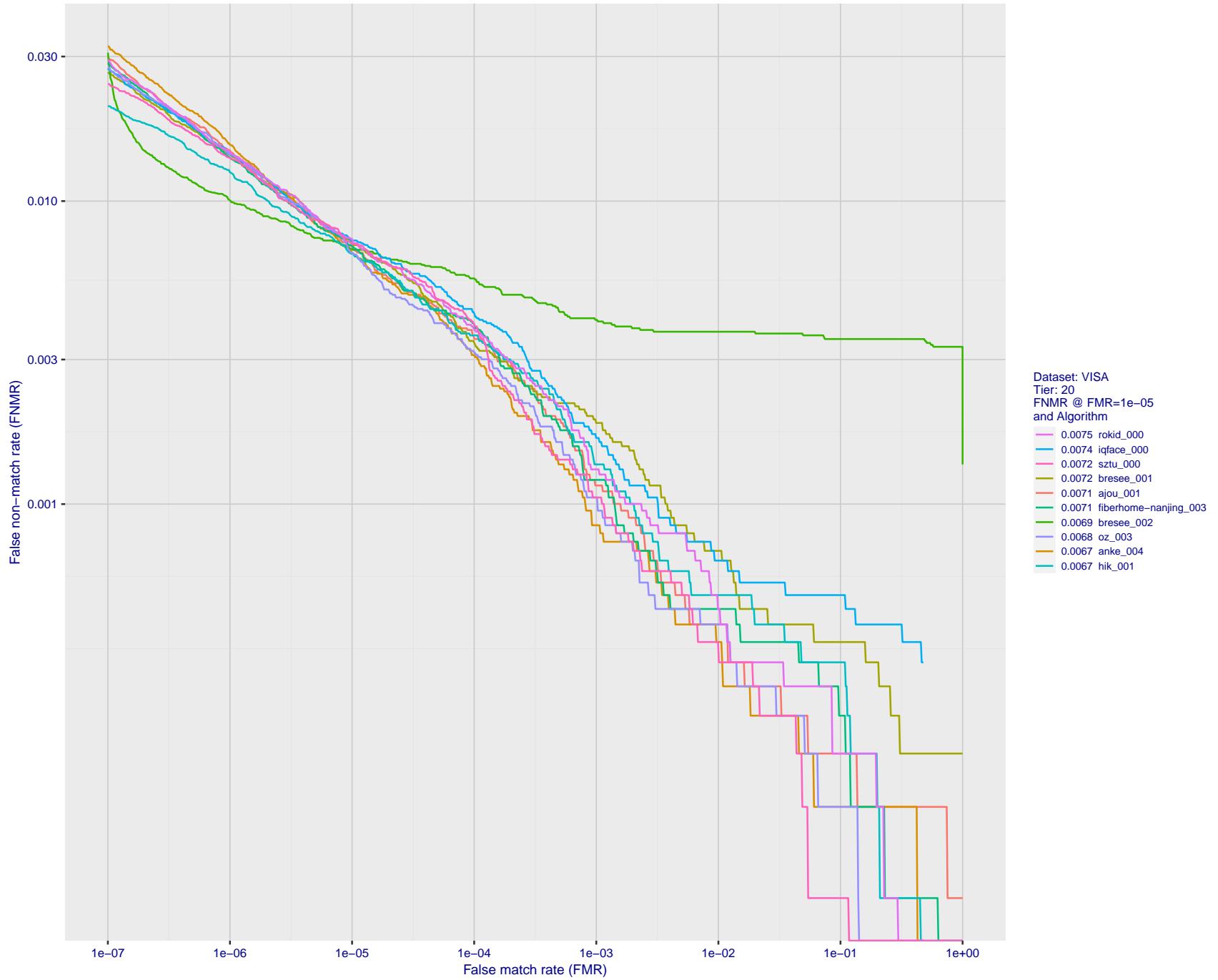


Figure 39: For the visa images, detection error tradeoff (DET) characteristics showing false non-match rate vs. false match rate plotted parametrically on threshold, T . The scales are logarithmic in order to show many decades of FMR.

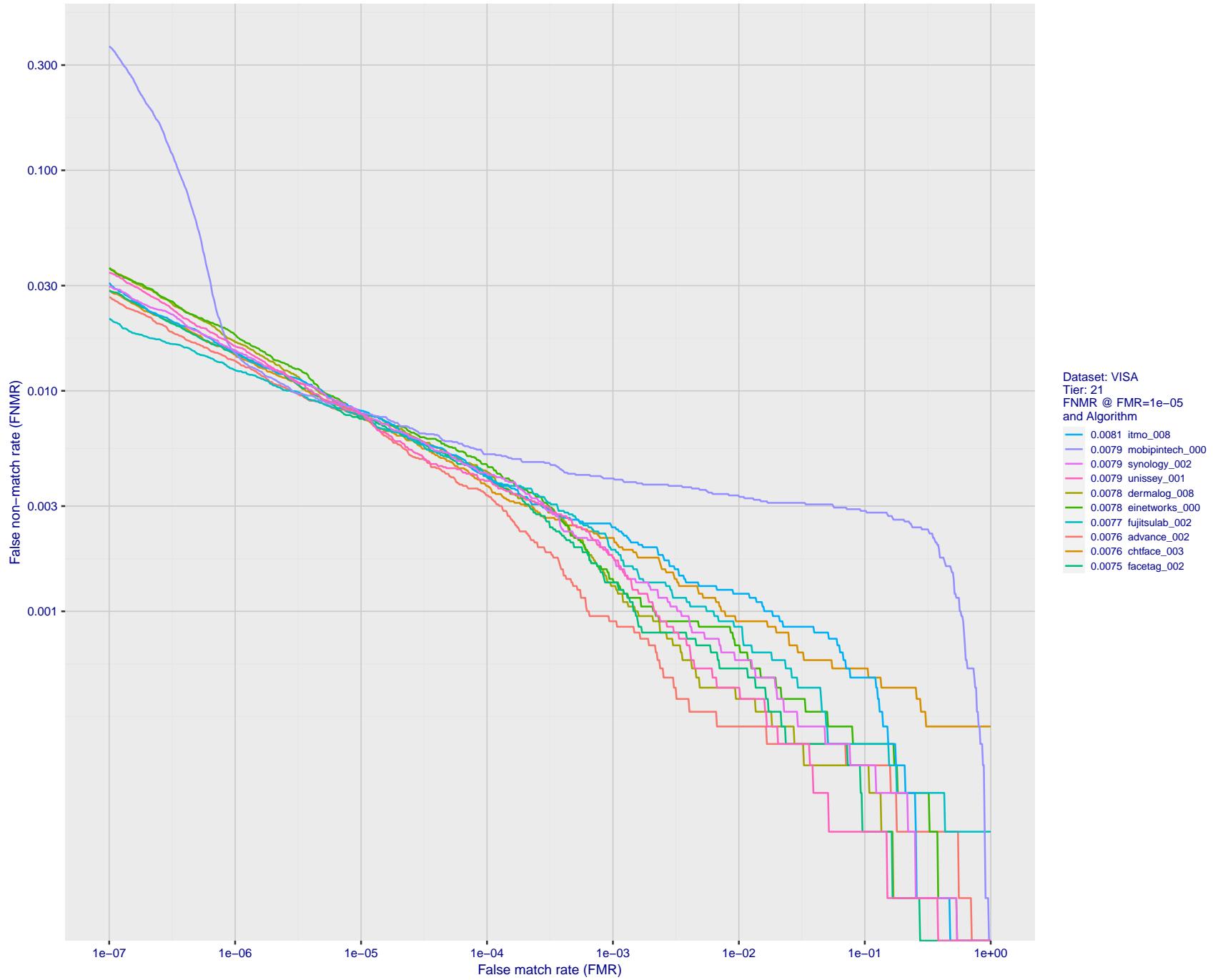


Figure 40: For the visa images, detection error tradeoff (DET) characteristics showing false non-match rate vs. false match rate plotted parametrically on threshold, T . The scales are logarithmic in order to show many decades of FMR.

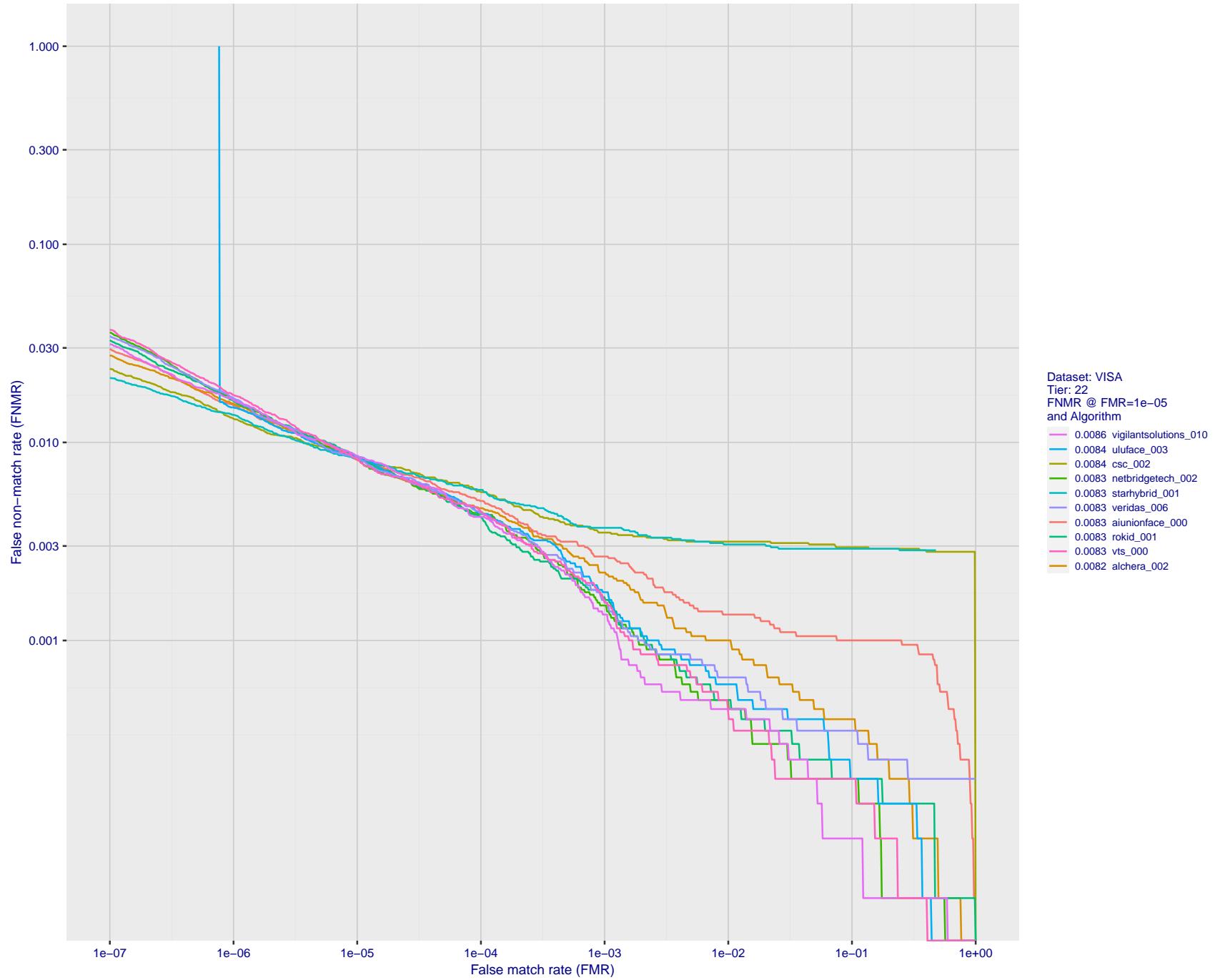


Figure 41: For the visa images, detection error tradeoff (DET) characteristics showing false non-match rate vs. false match rate plotted parametrically on threshold, T . The scales are logarithmic in order to show many decades of FMR.

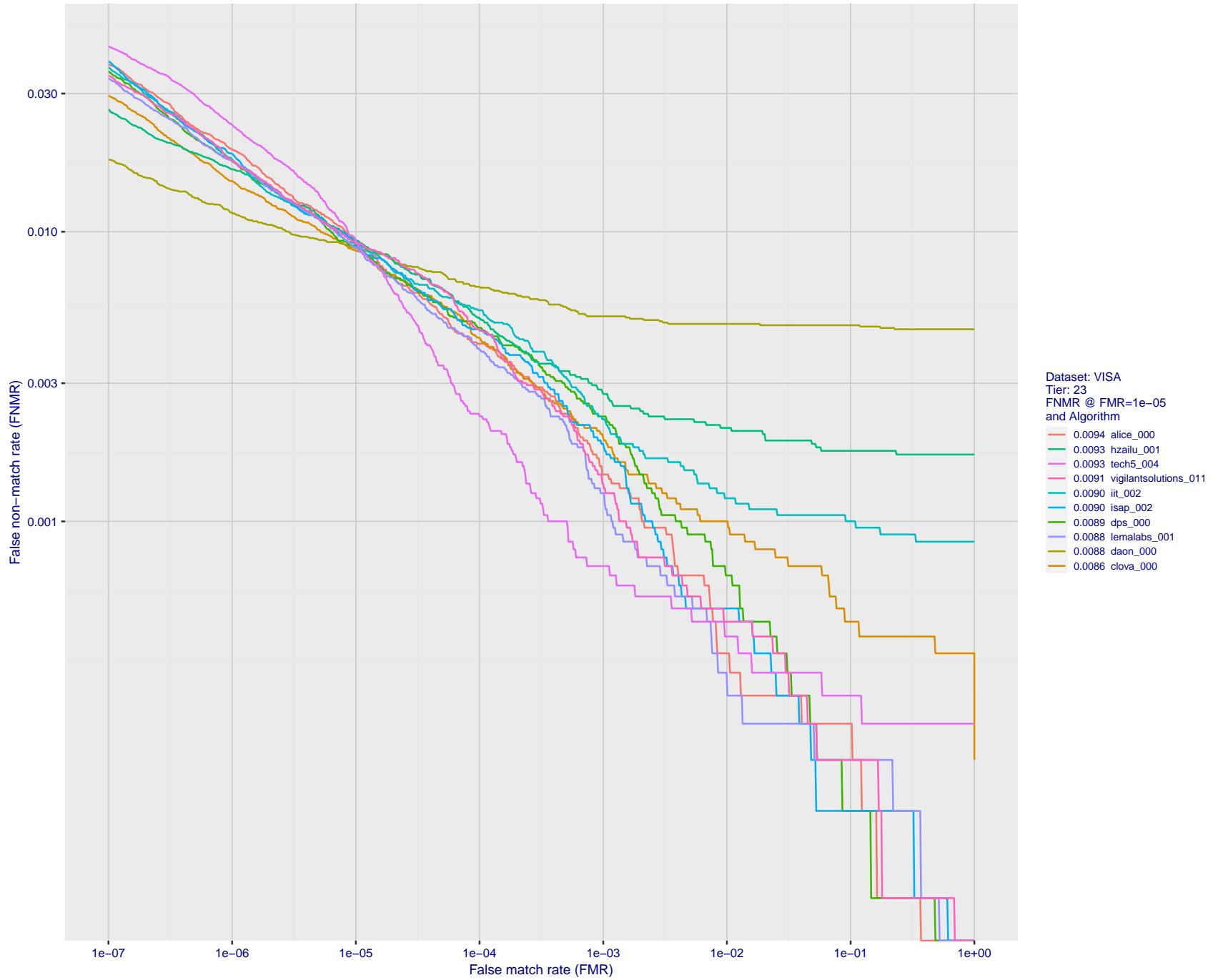


Figure 42: For the visa images, detection error tradeoff (DET) characteristics showing false non-match rate vs. false match rate plotted parametrically on threshold, T . The scales are logarithmic in order to show many decades of FMR.

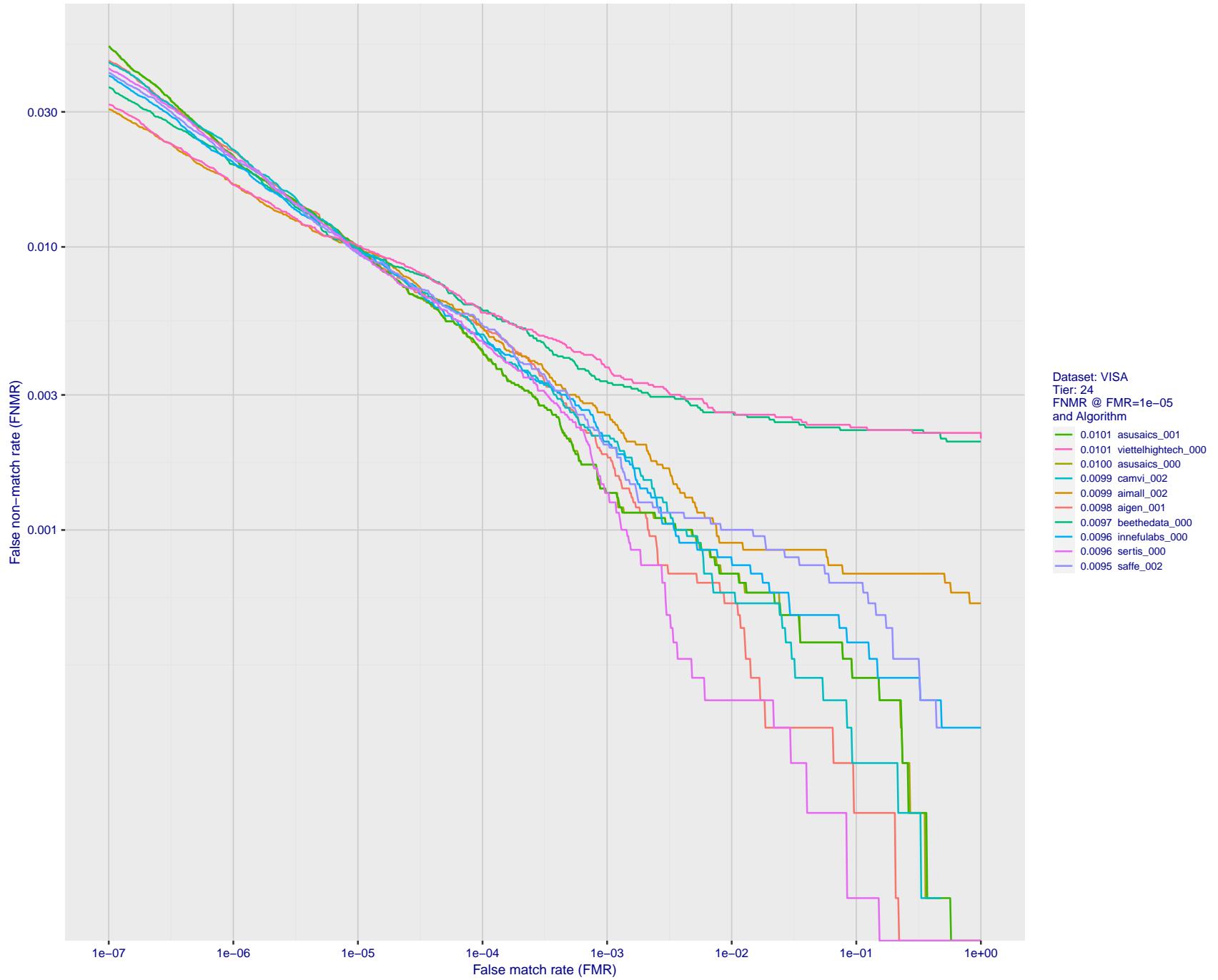


Figure 43: For the visa images, detection error tradeoff (DET) characteristics showing false non-match rate vs. false match rate plotted parametrically on threshold, T . The scales are logarithmic in order to show many decades of FMR.

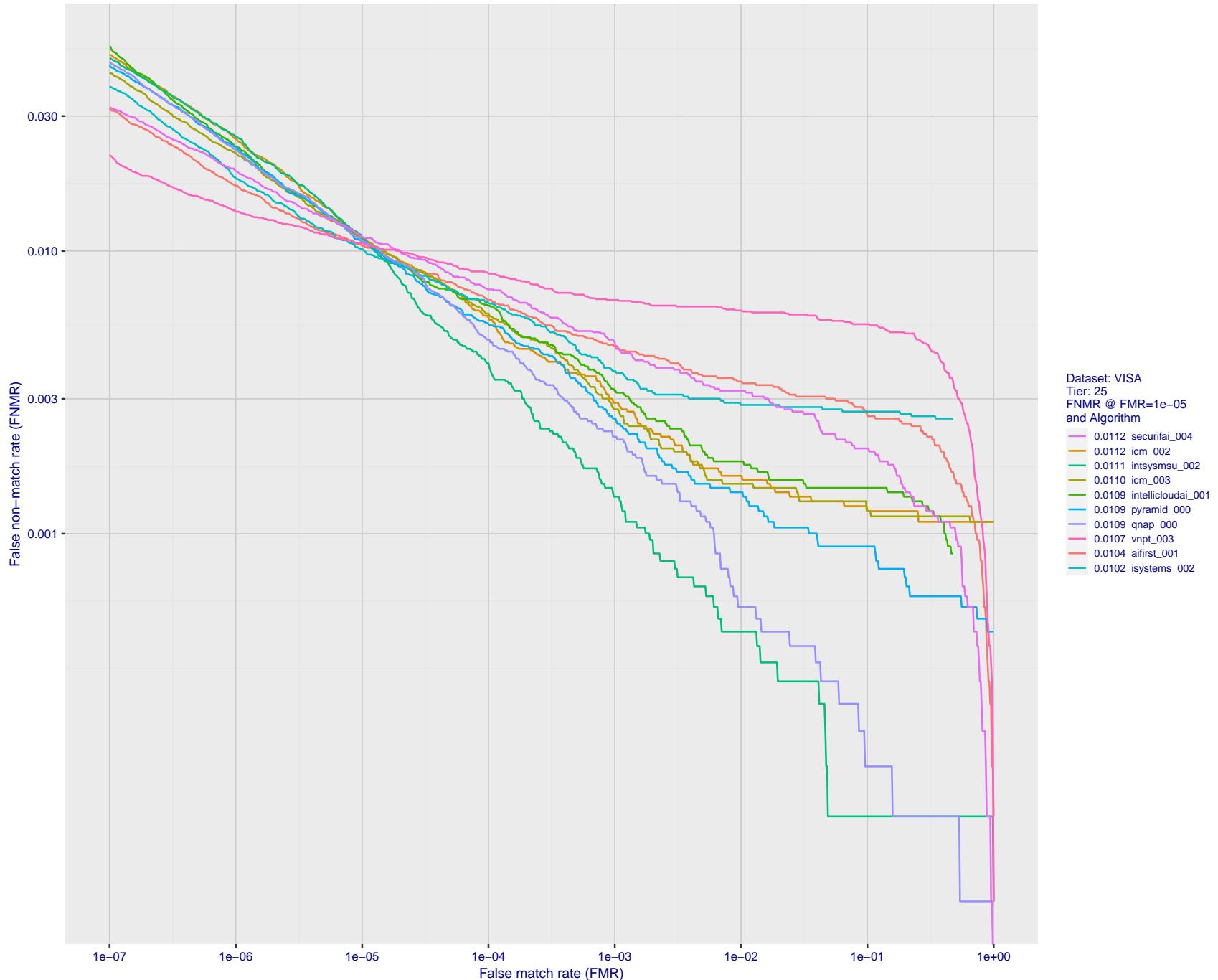


Figure 44: For the visa images, detection error tradeoff (DET) characteristics showing false non-match rate vs. false match rate plotted parametrically on threshold, T . The scales are logarithmic in order to show many decades of FMR.

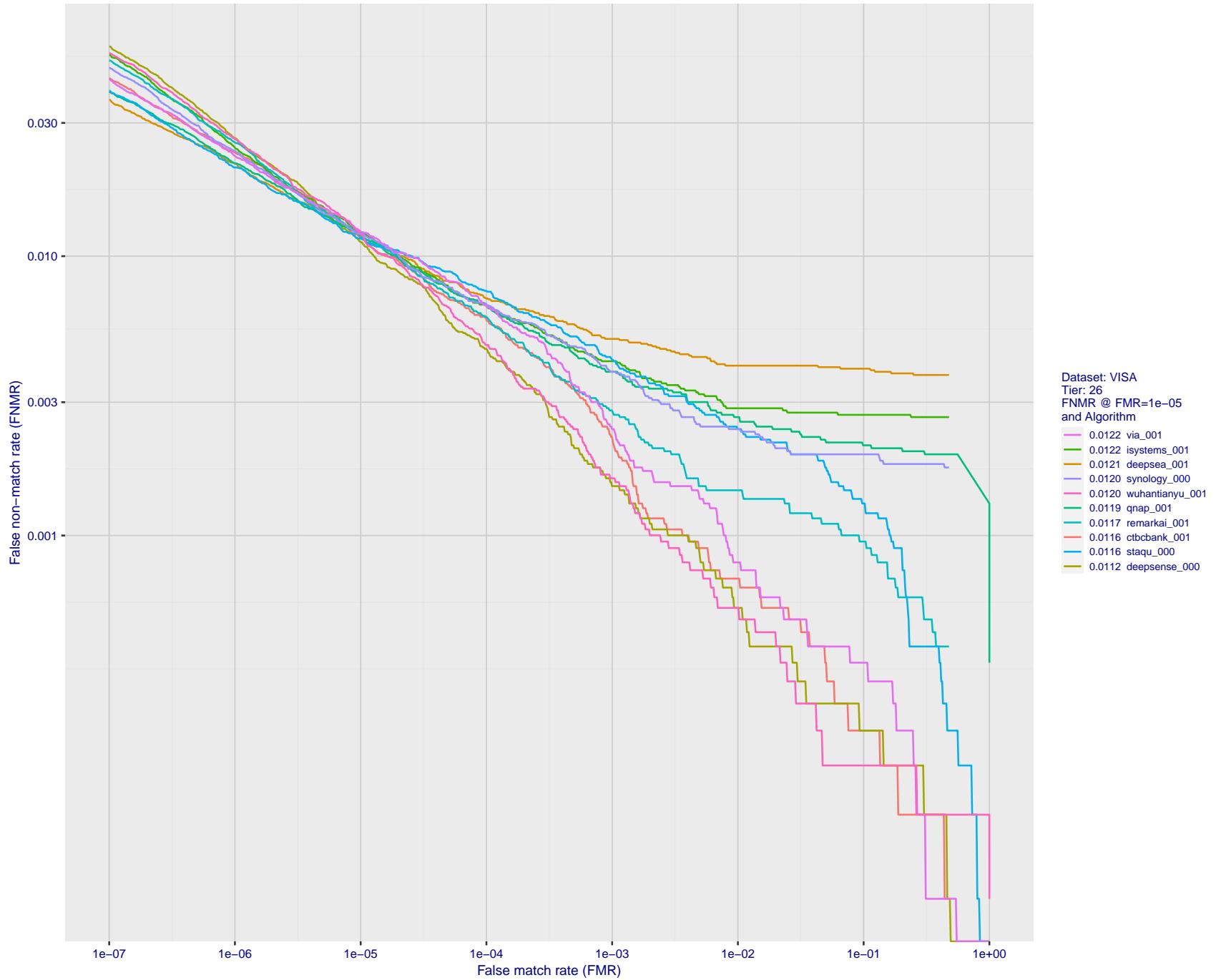


Figure 45: For the visa images, detection error tradeoff (DET) characteristics showing false non-match rate vs. false match rate plotted parametrically on threshold, T . The scales are logarithmic in order to show many decades of FMR.

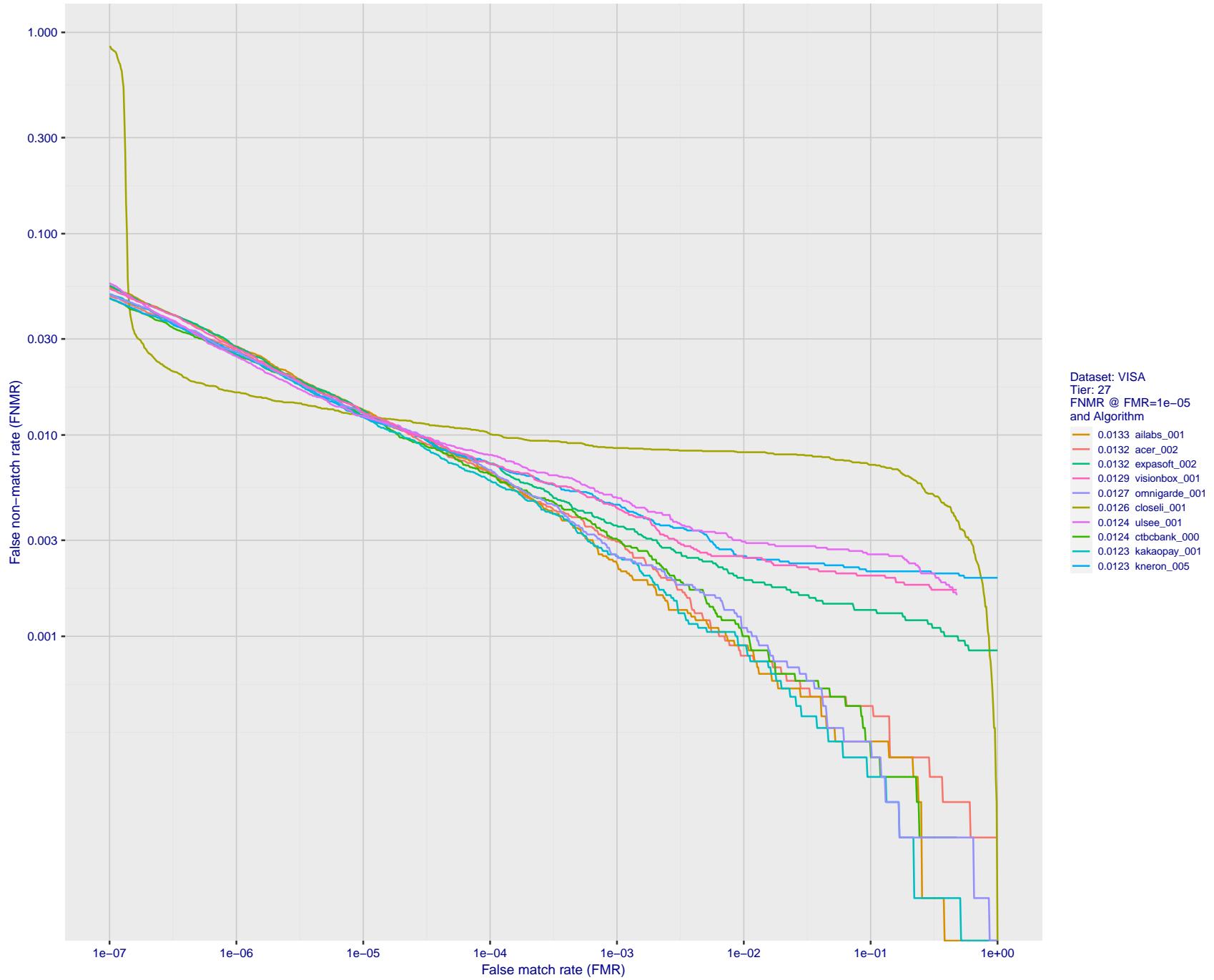


Figure 46: For the visa images, detection error tradeoff (DET) characteristics showing false non-match rate vs. false match rate plotted parametrically on threshold, T . The scales are logarithmic in order to show many decades of FMR.

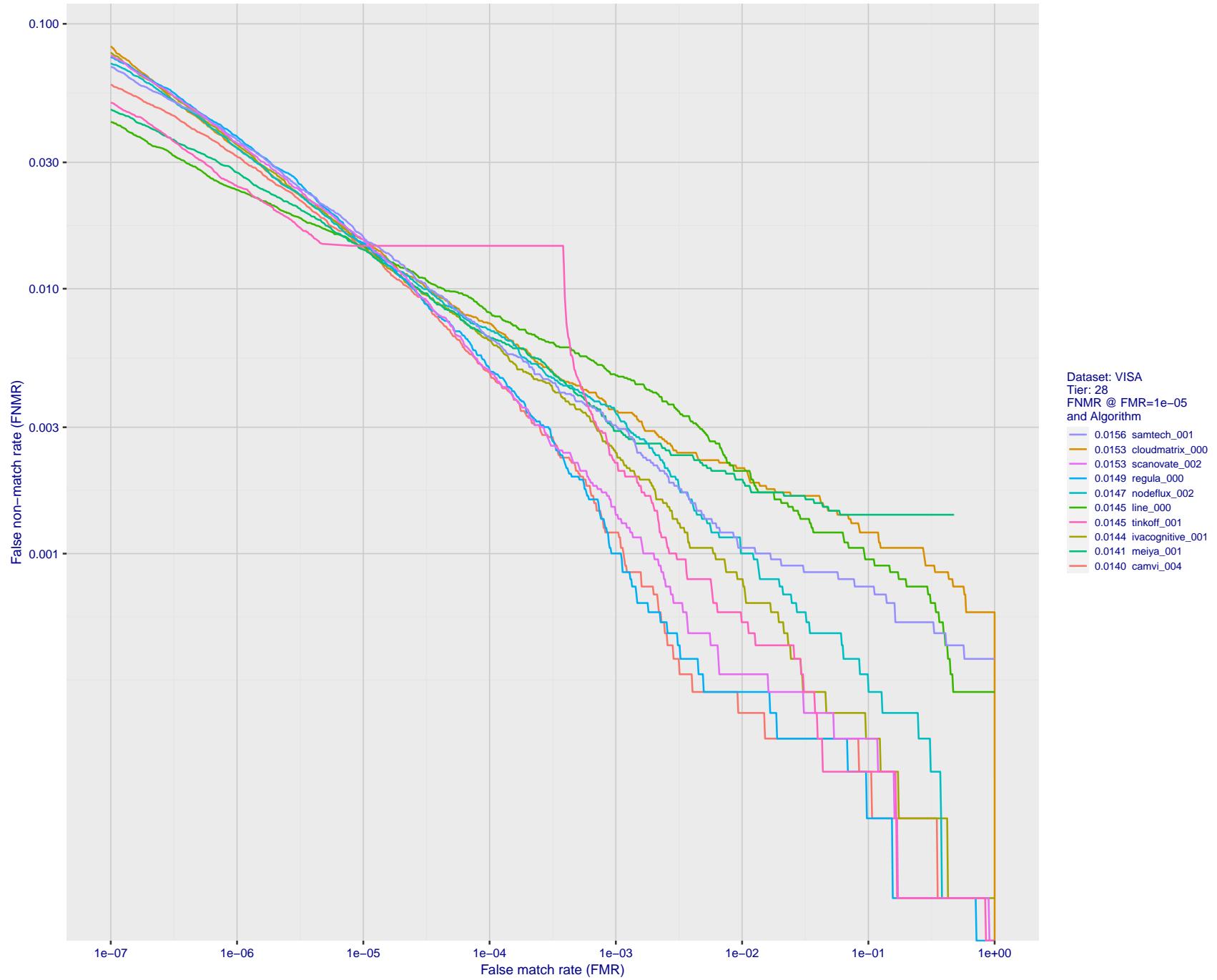


Figure 47: For the visa images, detection error tradeoff (DET) characteristics showing false non-match rate vs. false match rate plotted parametrically on threshold, T . The scales are logarithmic in order to show many decades of FMR.

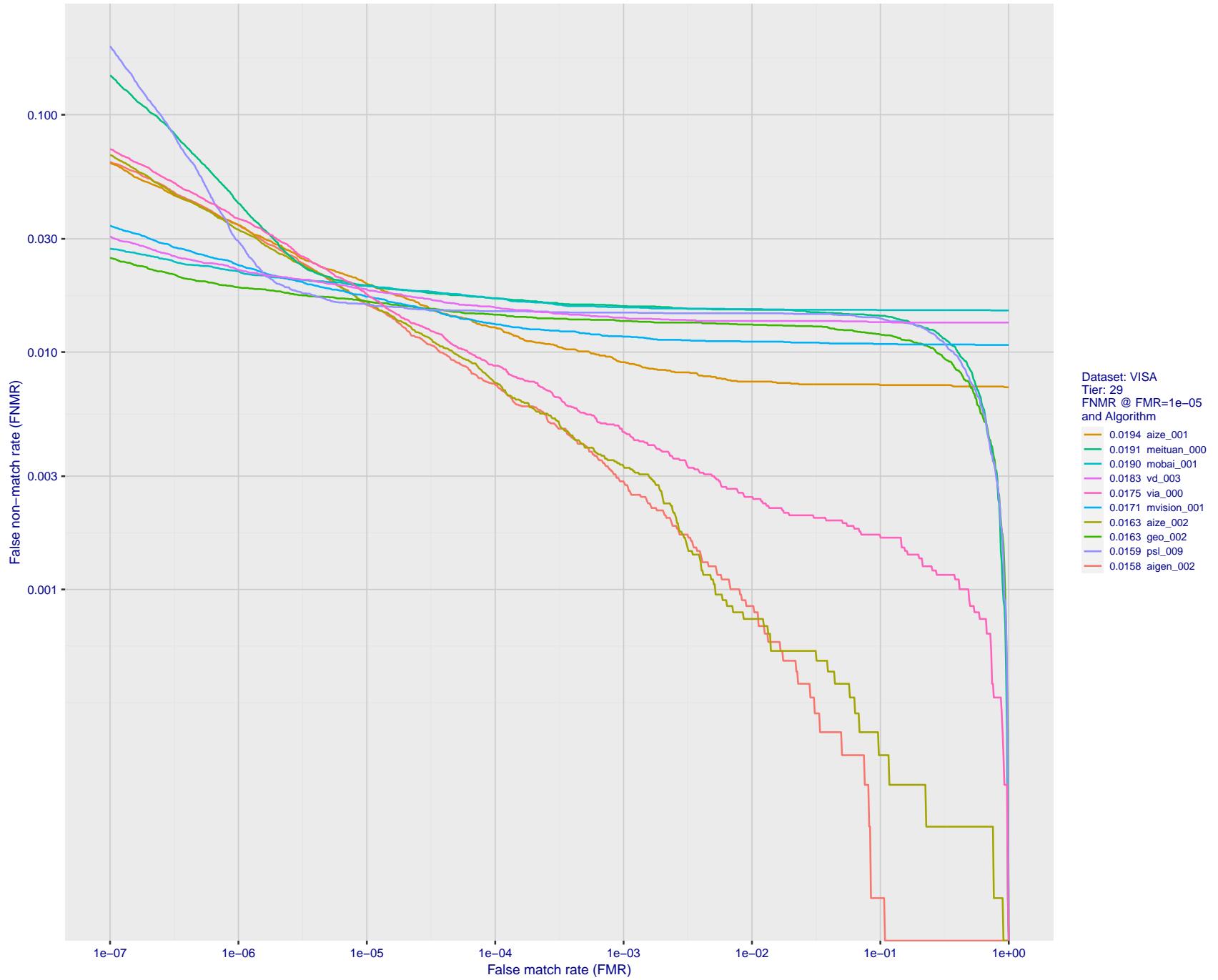


Figure 48: For the visa images, detection error tradeoff (DET) characteristics showing false non-match rate vs. false match rate plotted parametrically on threshold, T . The scales are logarithmic in order to show many decades of FMR.

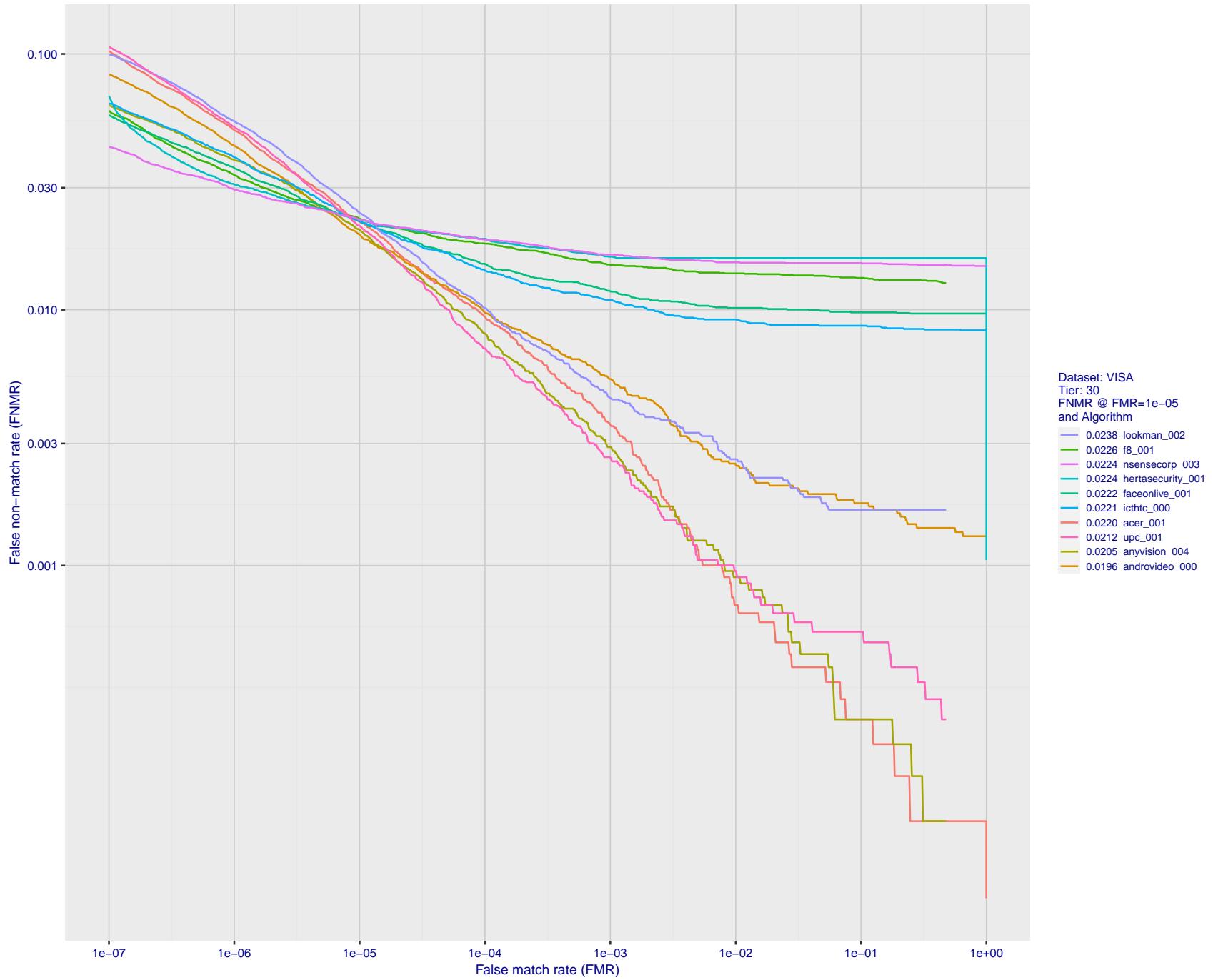


Figure 49: For the visa images, detection error tradeoff (DET) characteristics showing false non-match rate vs. false match rate plotted parametrically on threshold, T . The scales are logarithmic in order to show many decades of FMR.

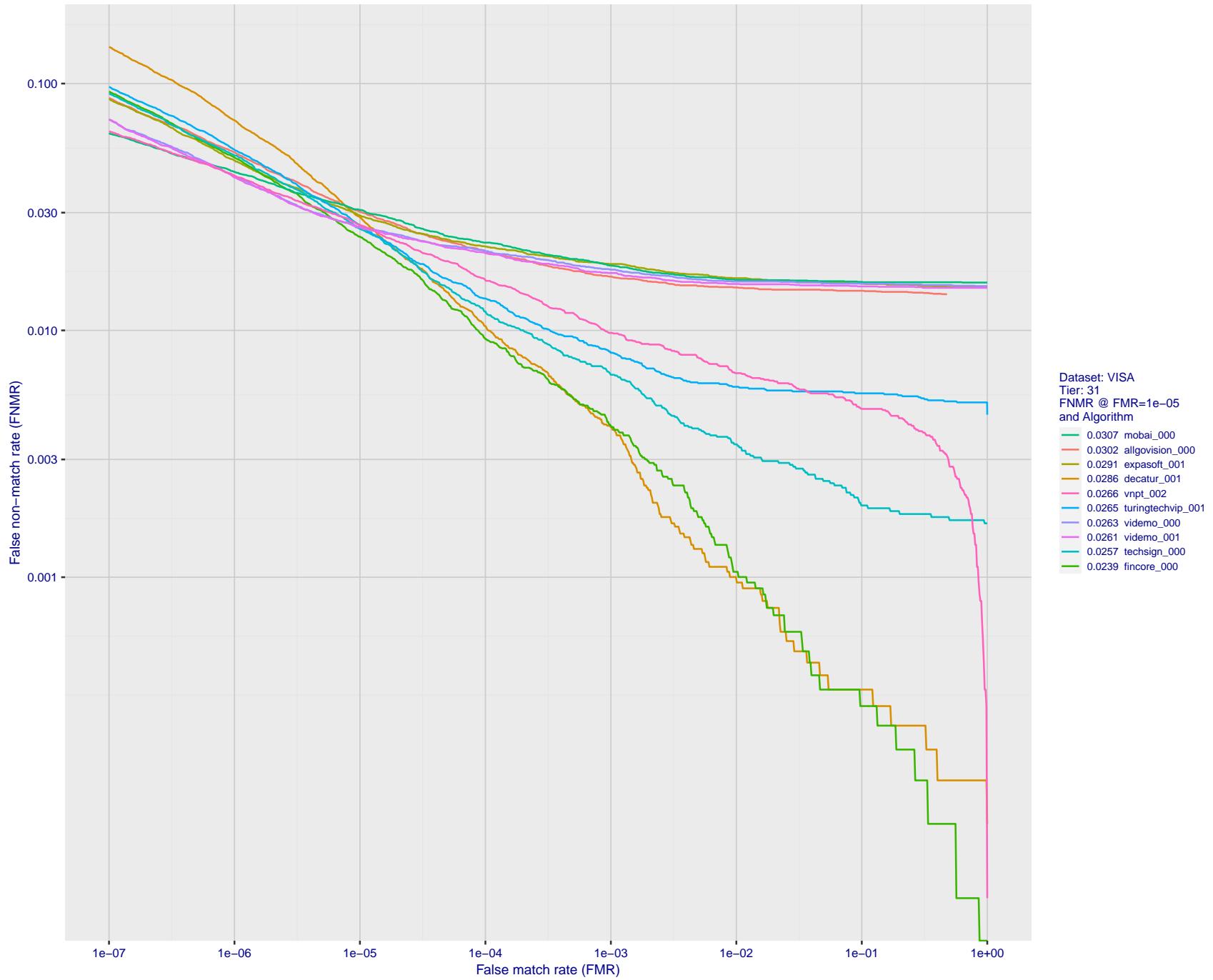


Figure 50: For the visa images, detection error tradeoff (DET) characteristics showing false non-match rate vs. false match rate plotted parametrically on threshold, T . The scales are logarithmic in order to show many decades of FMR.

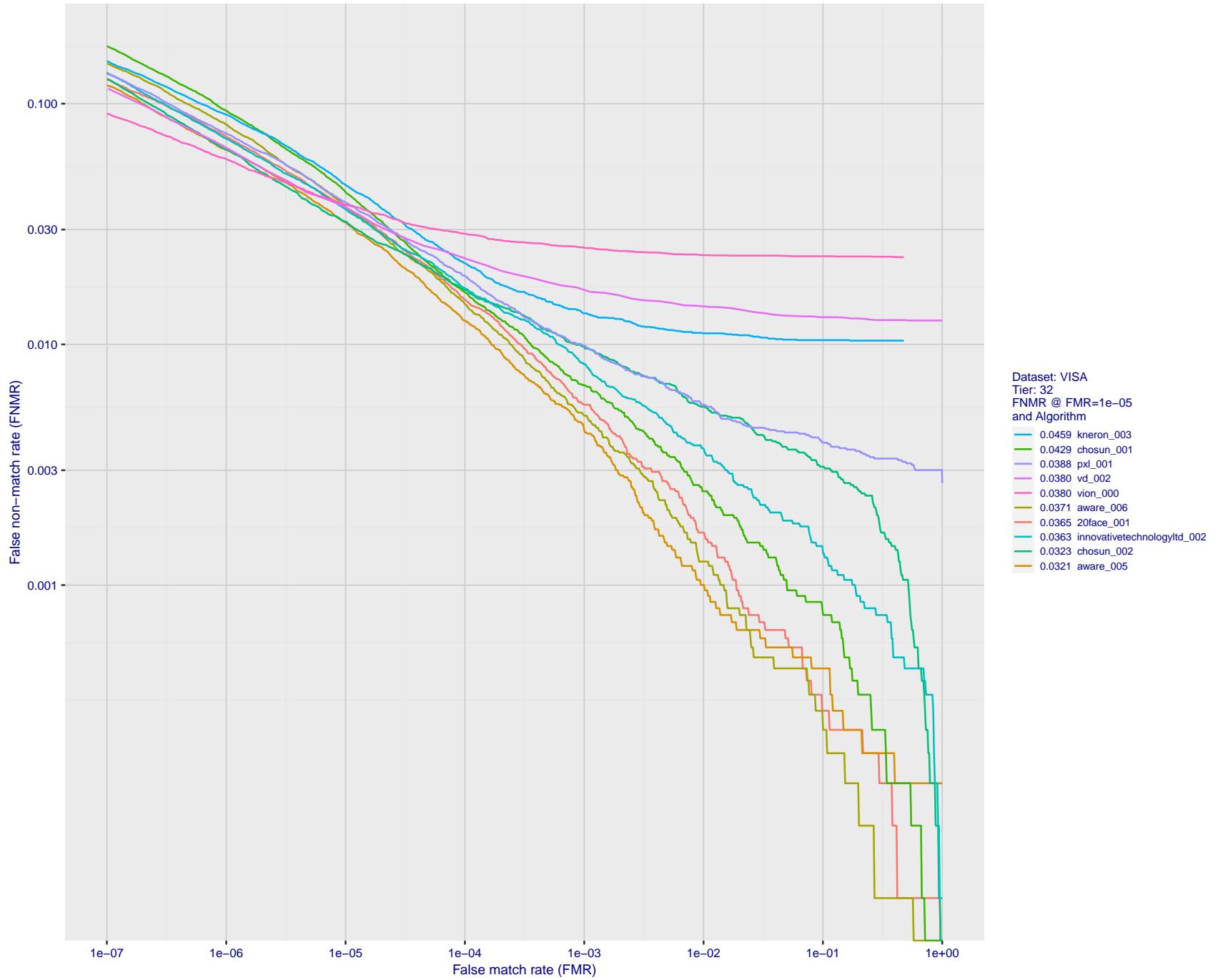


Figure 51: For the visa images, detection error tradeoff (DET) characteristics showing false non-match rate vs. false match rate plotted parametrically on threshold, T . The scales are logarithmic in order to show many decades of FMR.

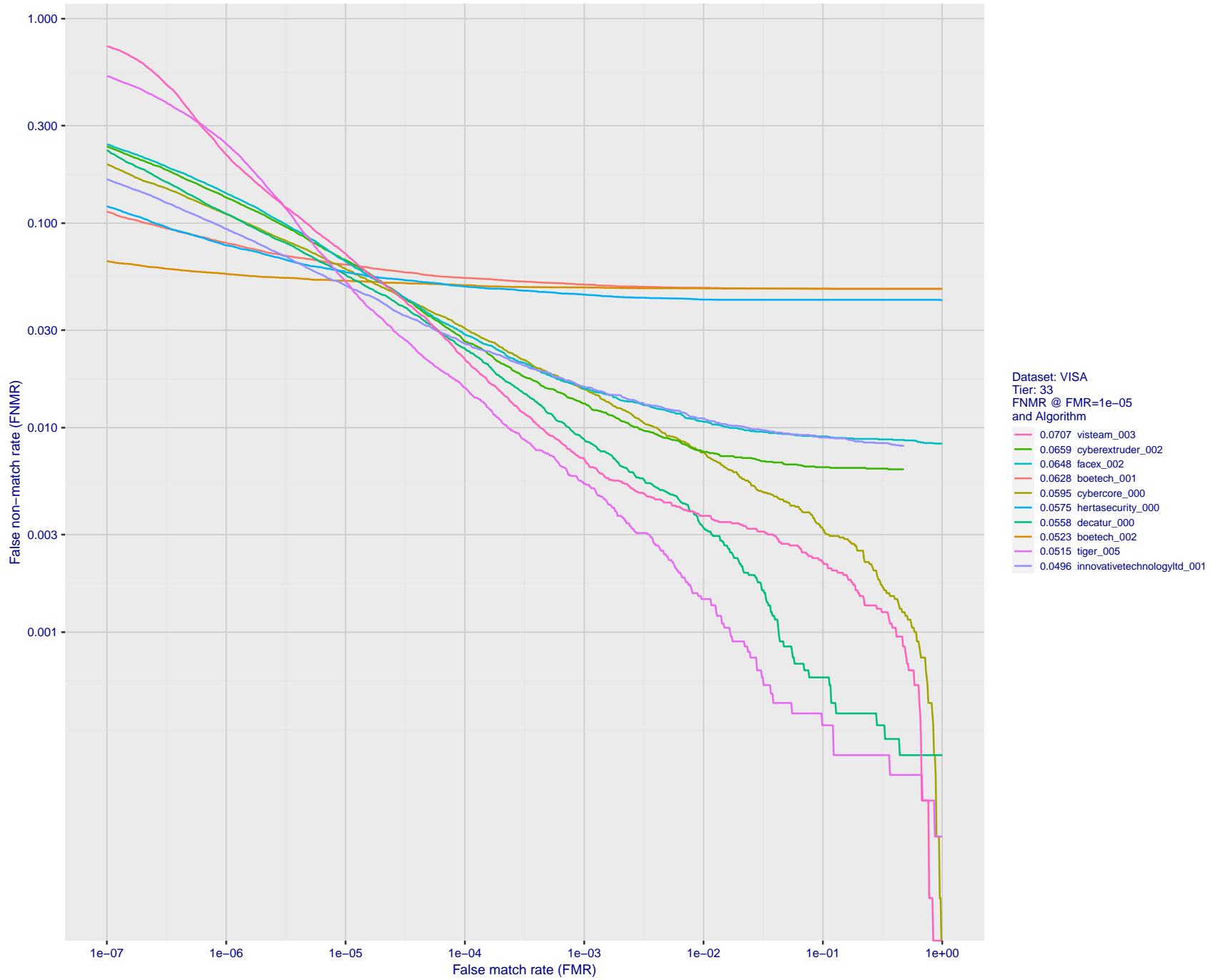


Figure 52: For the visa images, detection error tradeoff (DET) characteristics showing false non-match rate vs. false match rate plotted parametrically on threshold, T . The scales are logarithmic in order to show many decades of FMR.

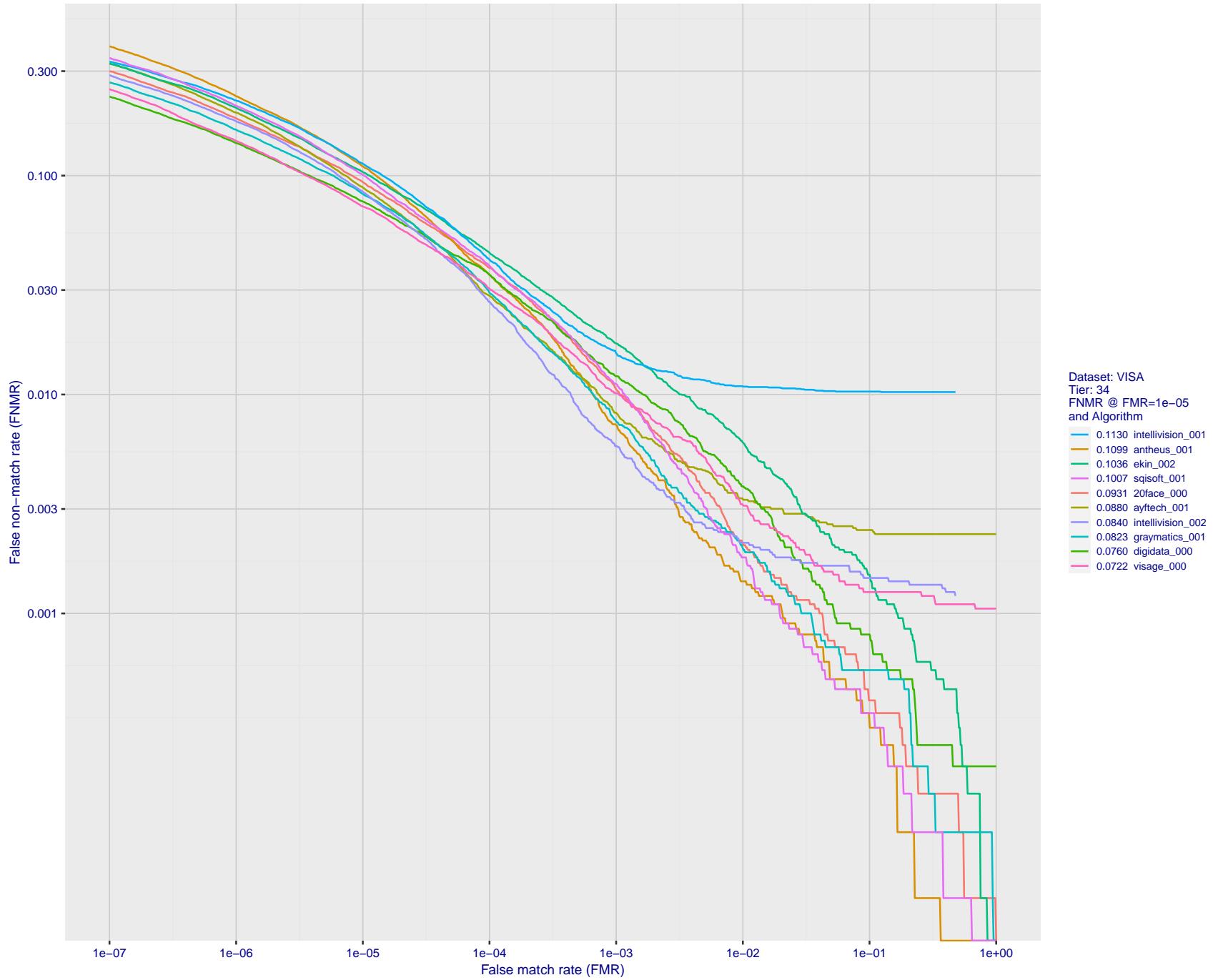


Figure 53: For the visa images, detection error tradeoff (DET) characteristics showing false non-match rate vs. false match rate plotted parametrically on threshold, T . The scales are logarithmic in order to show many decades of FMR.

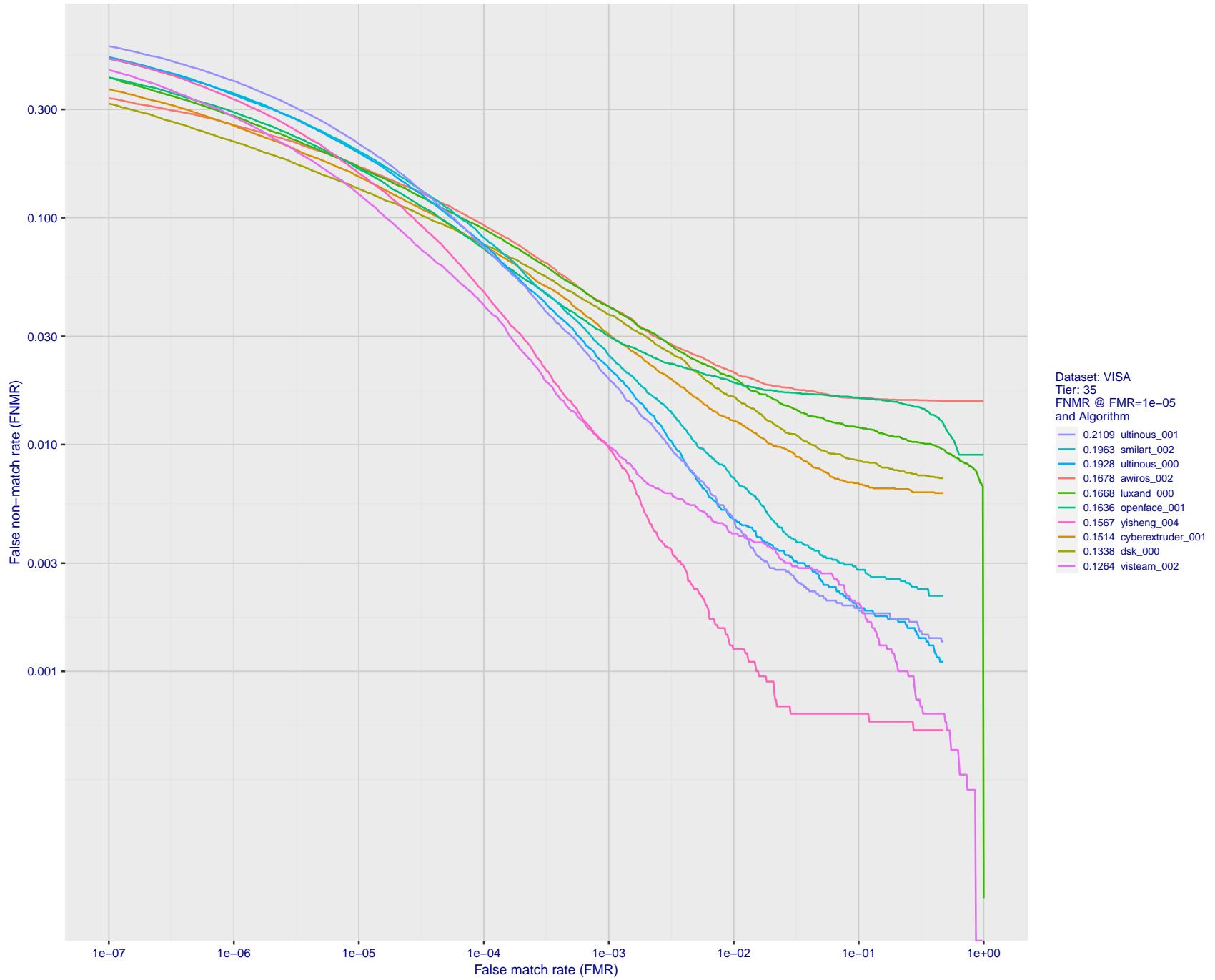


Figure 54: For the visa images, detection error tradeoff (DET) characteristics showing false non-match rate vs. false match rate plotted parametrically on threshold, T . The scales are logarithmic in order to show many decades of FMR.

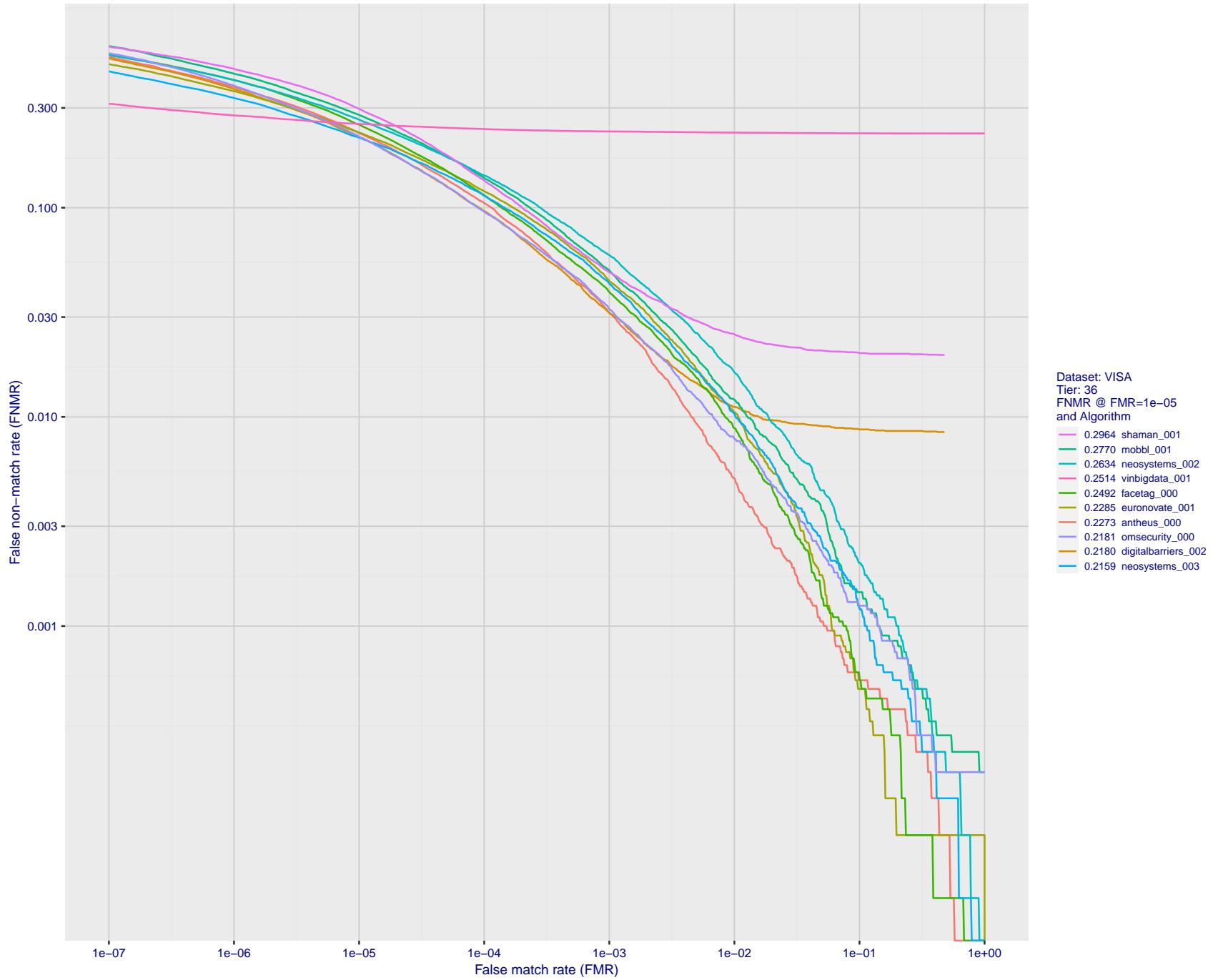


Figure 55: For the visa images, detection error tradeoff (DET) characteristics showing false non-match rate vs. false match rate plotted parametrically on threshold, T . The scales are logarithmic in order to show many decades of FMR.

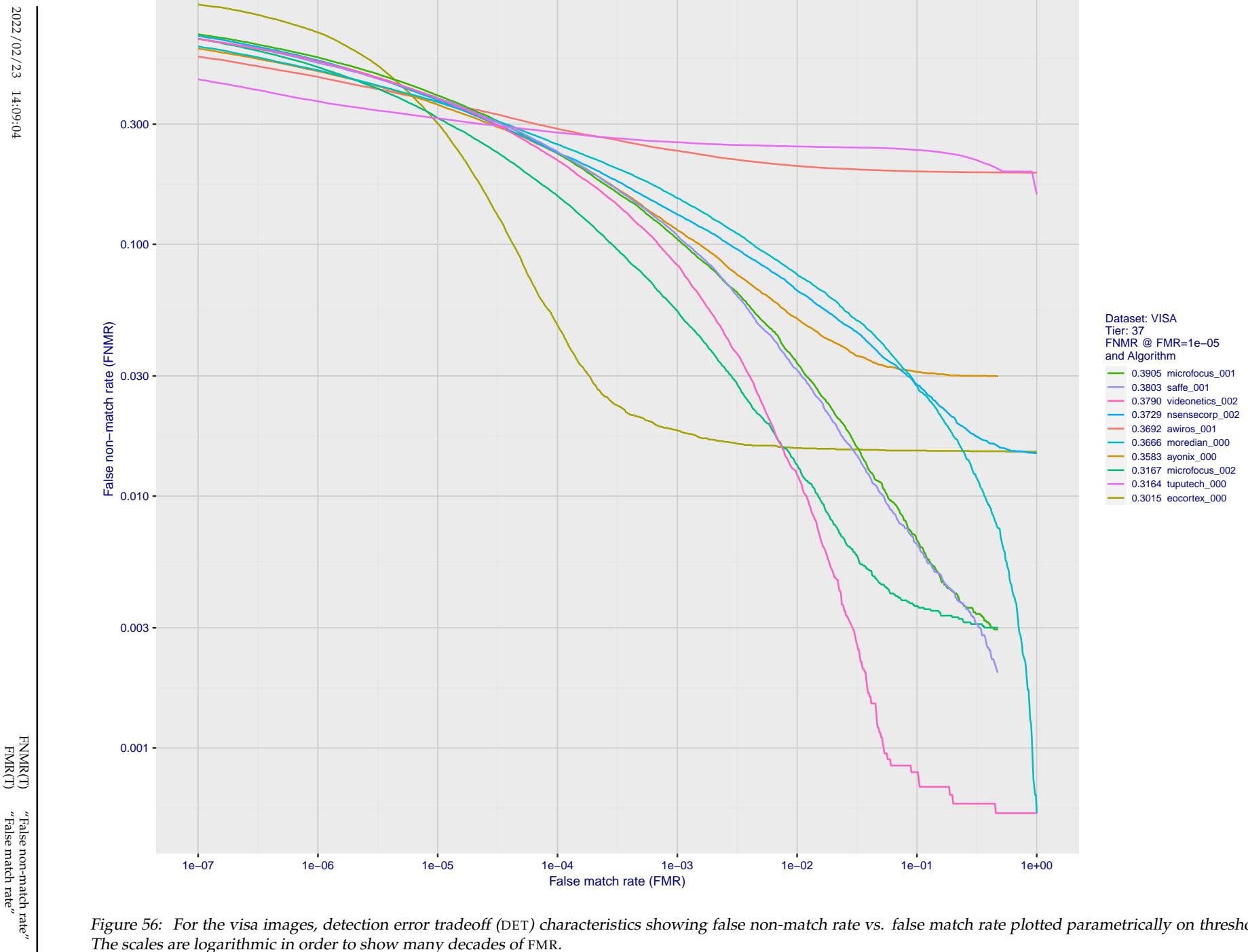


Figure 56: For the visa images, detection error tradeoff (DET) characteristics showing false non-match rate vs. false match rate plotted parametrically on threshold, T . The scales are logarithmic in order to show many decades of FMR.

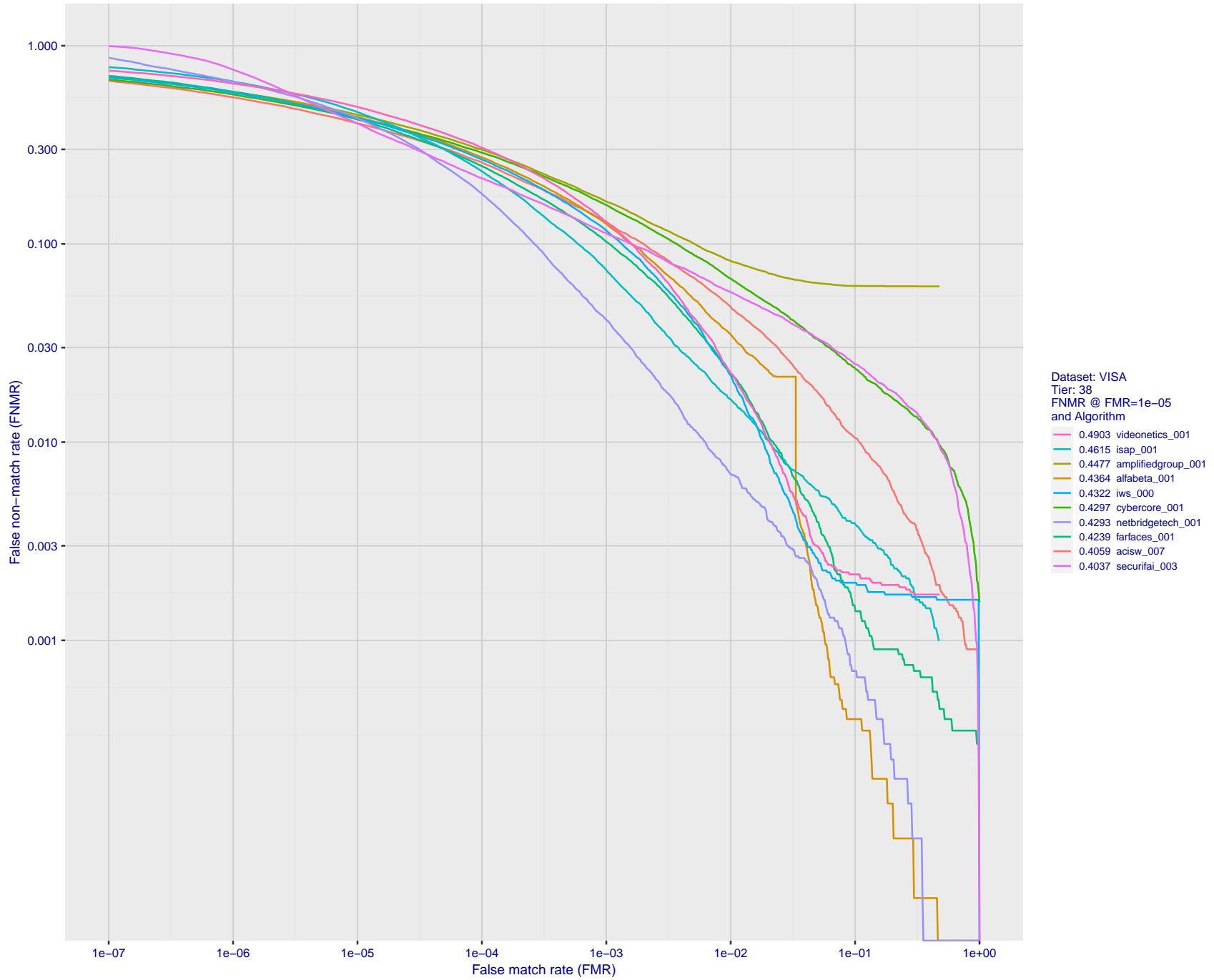


Figure 57: For the visa images, detection error tradeoff (DET) characteristics showing false non-match rate vs. false match rate plotted parametrically on threshold, T . The scales are logarithmic in order to show many decades of FMR.

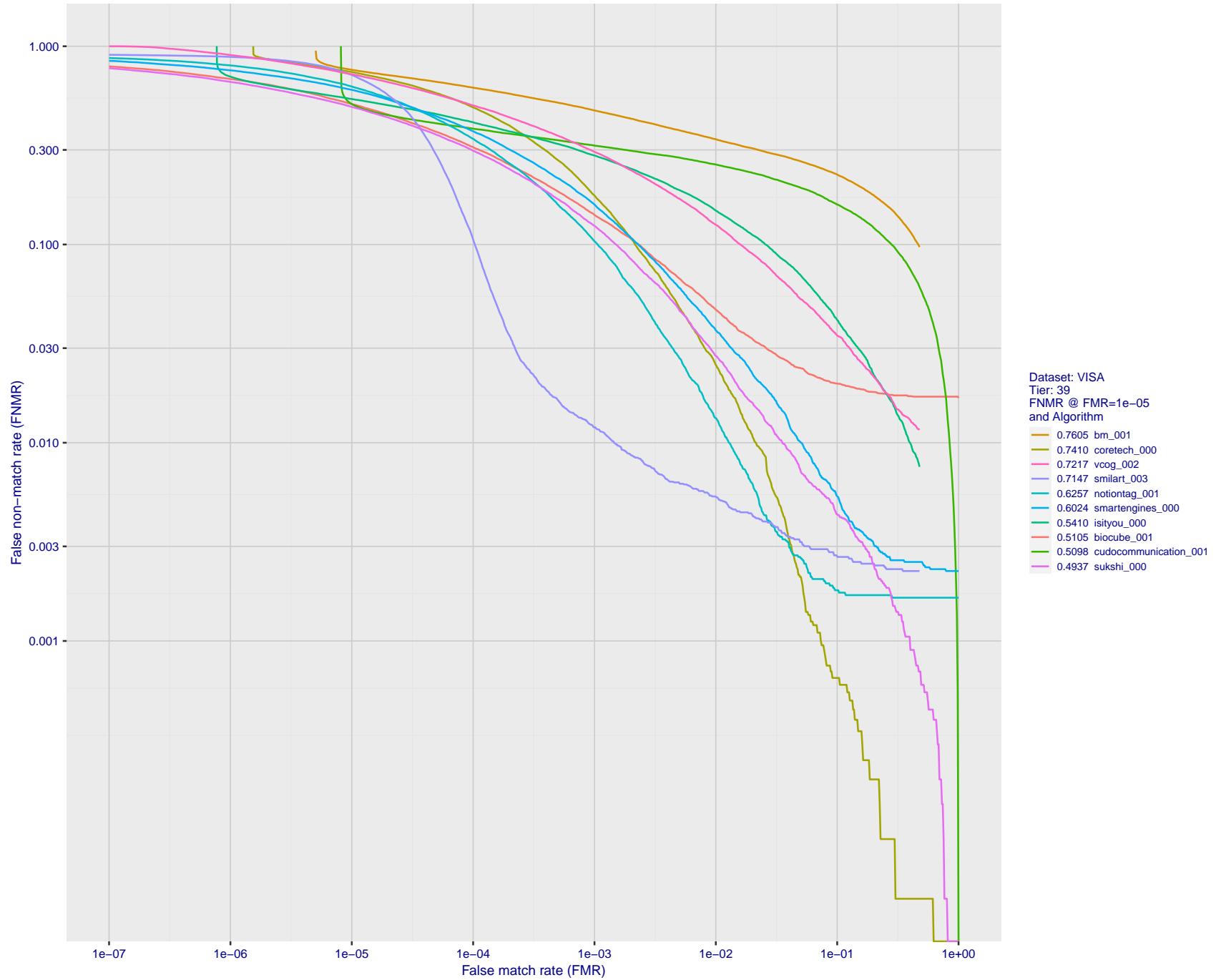


Figure 58: For the visa images, detection error tradeoff (DET) characteristics showing false non-match rate vs. false match rate plotted parametrically on threshold, T . The scales are logarithmic in order to show many decades of FMR.

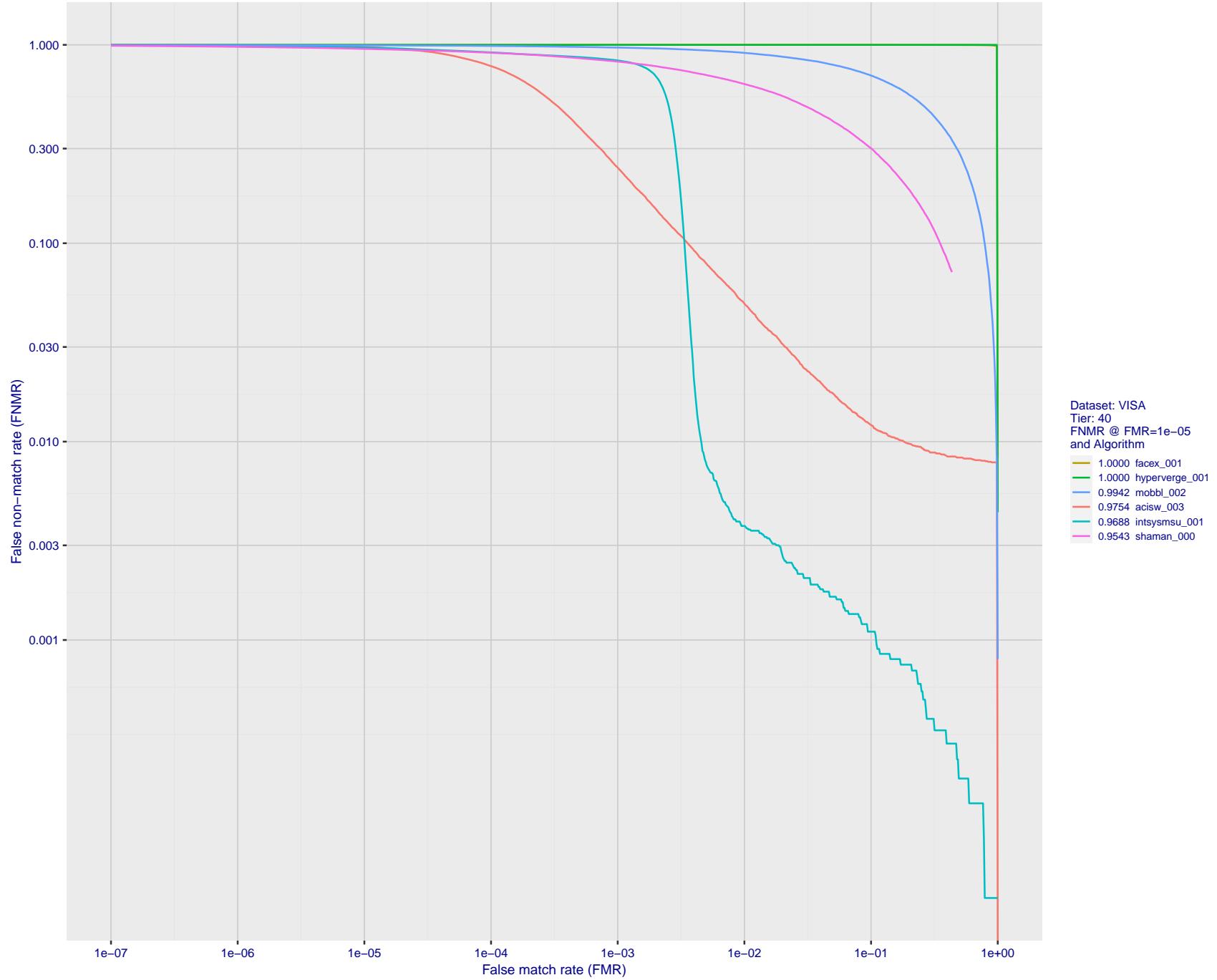


Figure 59: For the visa images, detection error tradeoff (DET) characteristics showing false non-match rate vs. false match rate plotted parametrically on threshold, T . The scales are logarithmic in order to show many decades of FMR.

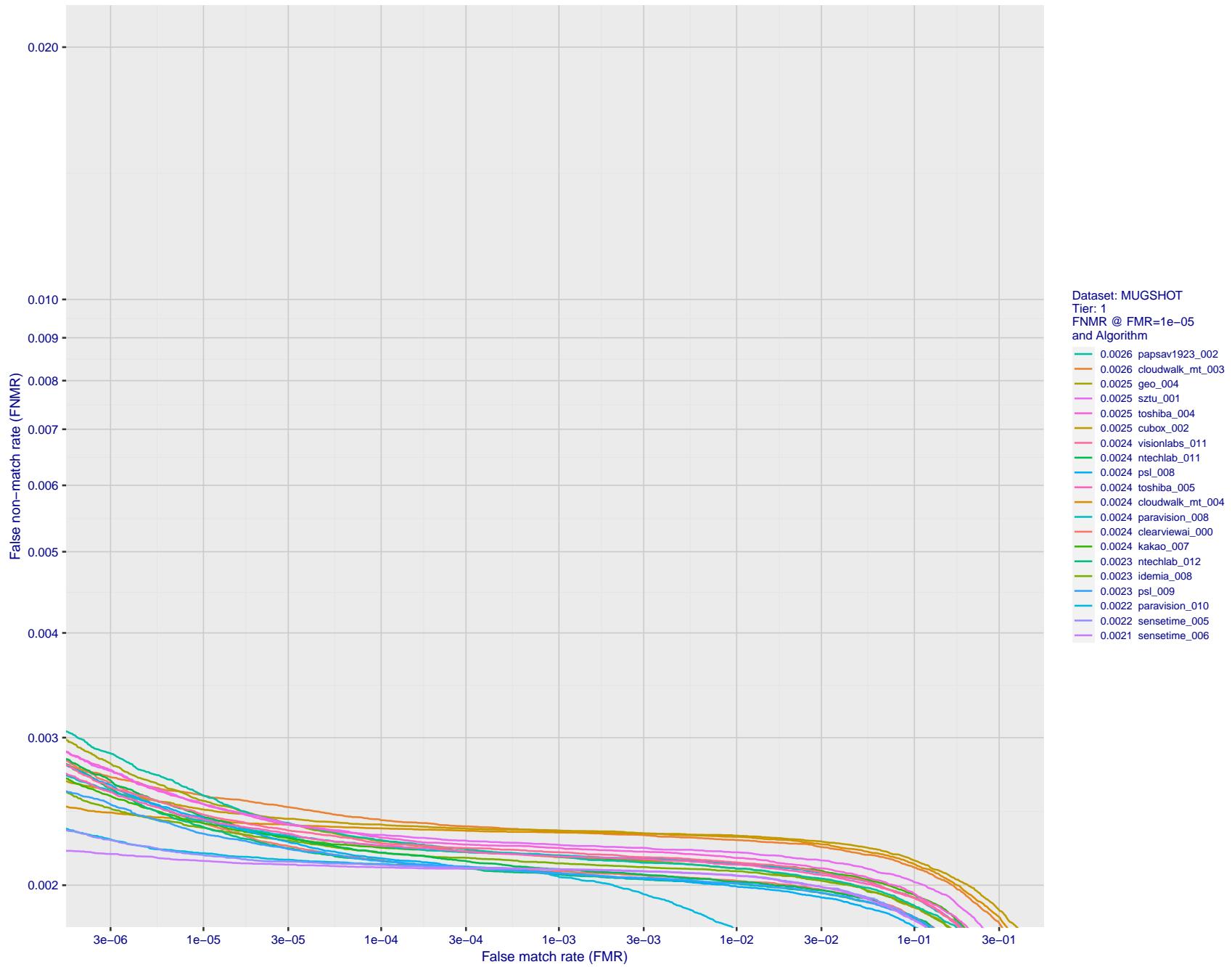


Figure 60: For the mugshot images, detection error tradeoff (DET) characteristics showing false non-match rate vs. false match rate plotted parametrically on threshold, T . The scales are logarithmic in order to show decades of FMR.

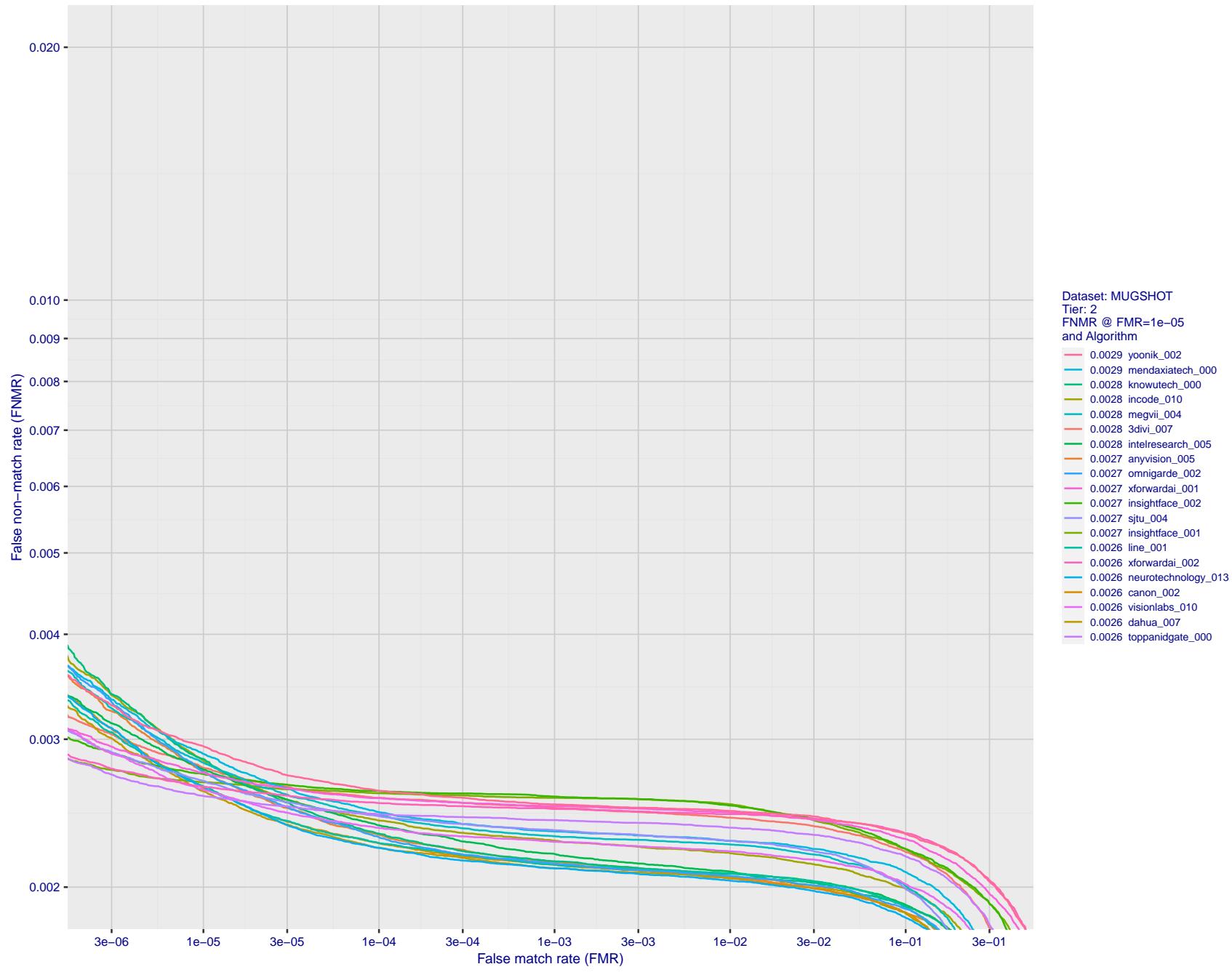


Figure 61: For the mugshot images, detection error tradeoff (DET) characteristics showing false non-match rate vs. false match rate plotted parametrically on threshold, T . The scales are logarithmic in order to show decades of FMR.

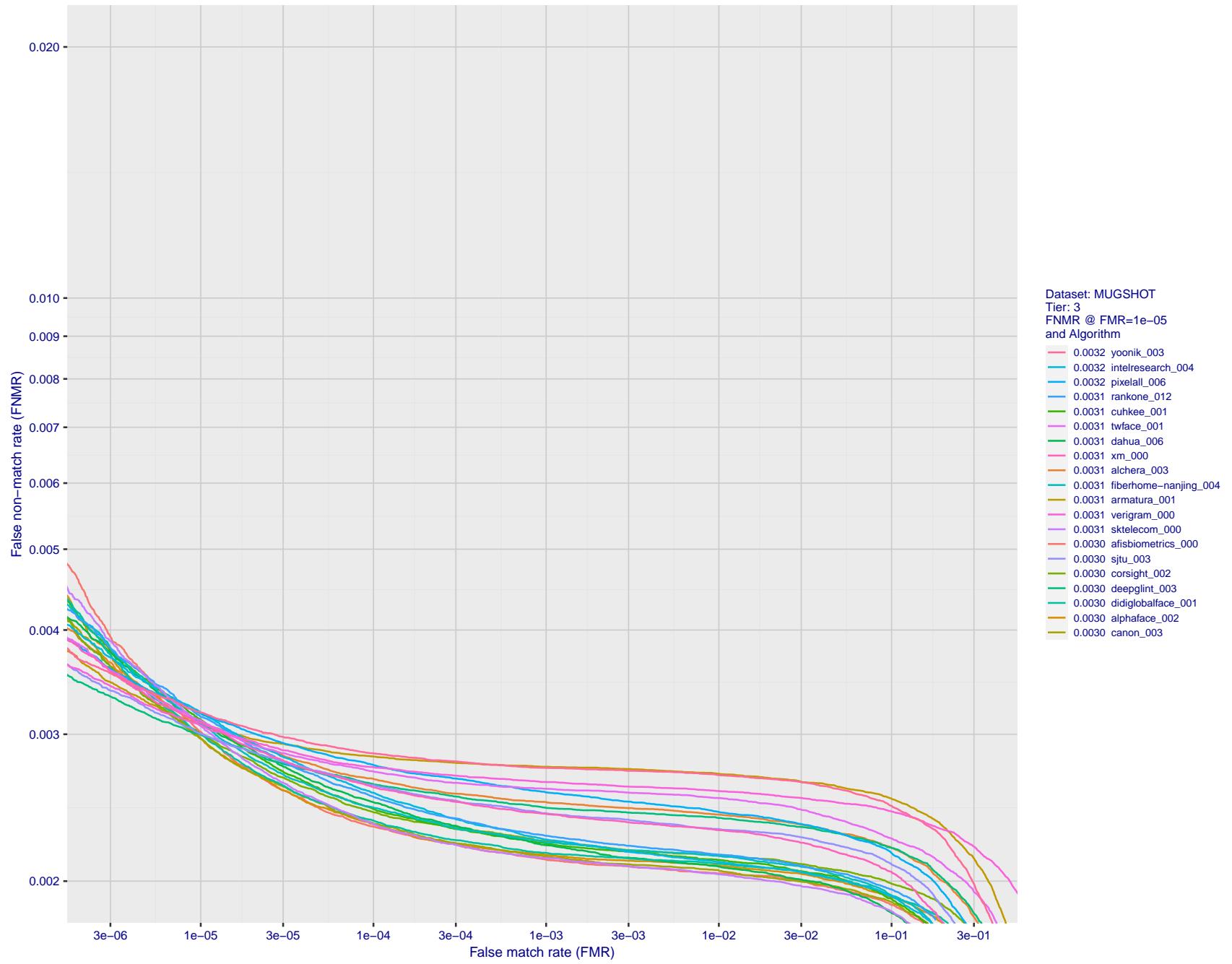


Figure 62: For the mugshot images, detection error tradeoff (DET) characteristics showing false non-match rate vs. false match rate plotted parametrically on threshold, T . The scales are logarithmic in order to show decades of FMR.

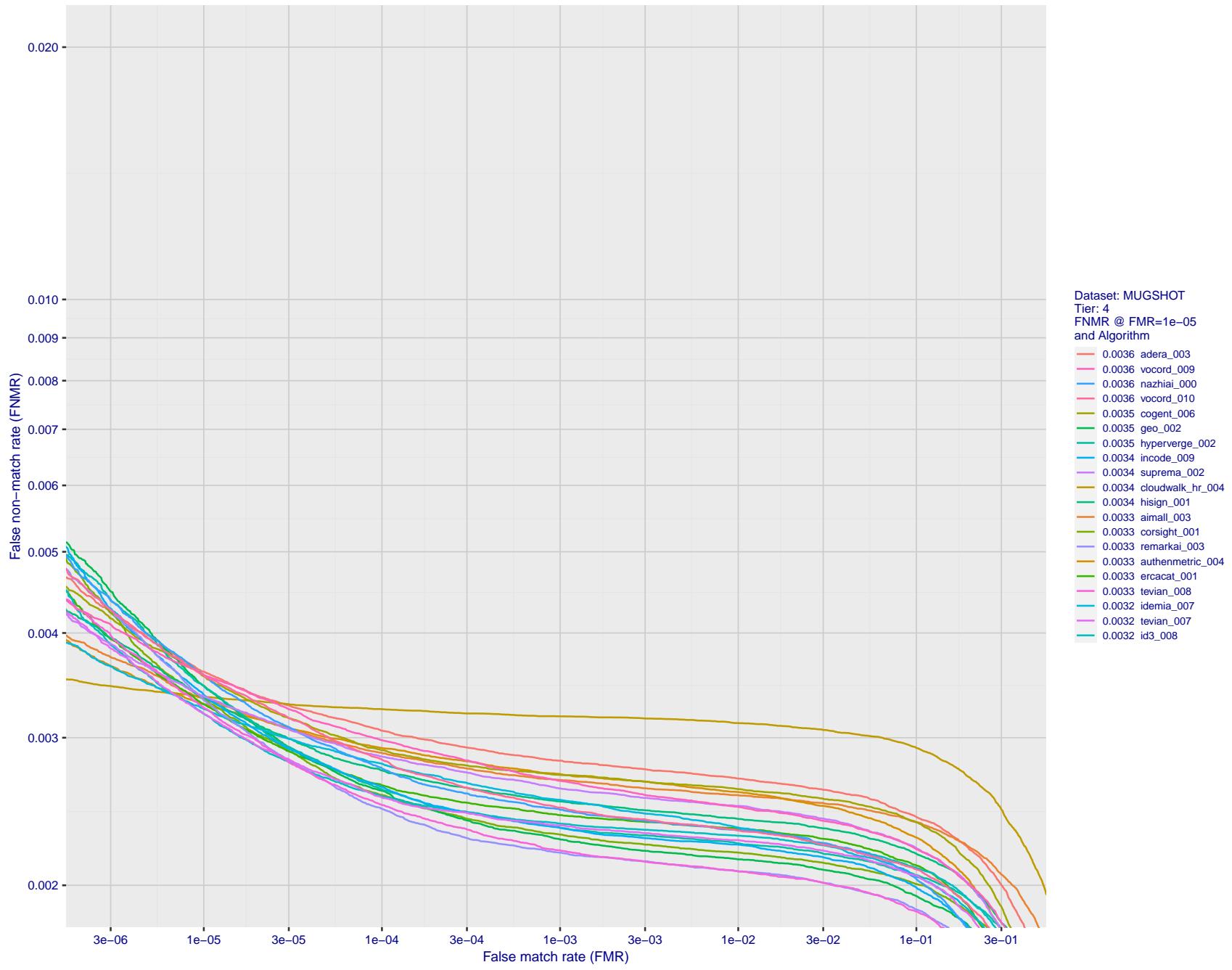


Figure 63: For the mugshot images, detection error tradeoff (DET) characteristics showing false non-match rate vs. false match rate plotted parametrically on threshold, T . The scales are logarithmic in order to show decades of FMR.

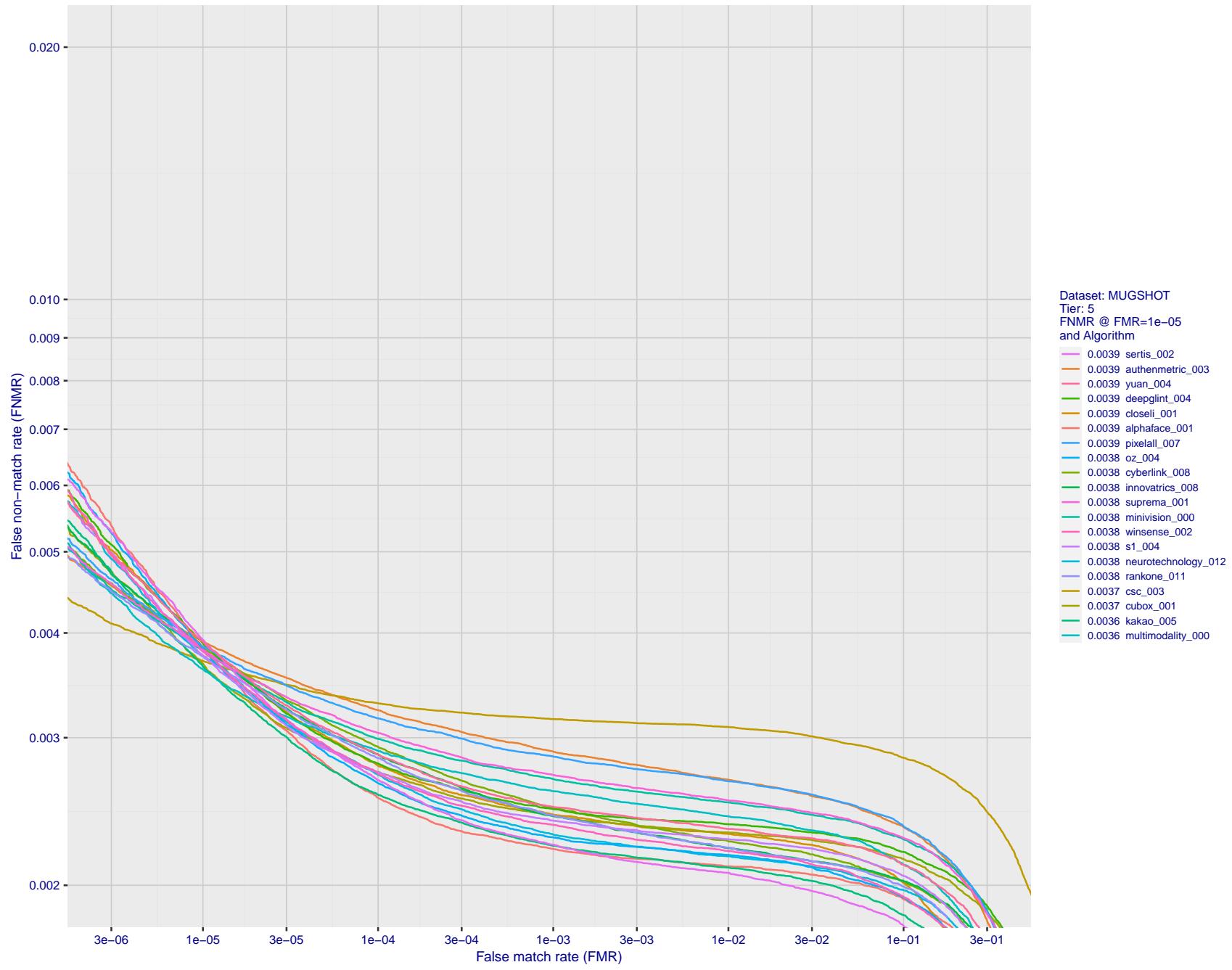


Figure 64: For the mugshot images, detection error tradeoff (DET) characteristics showing false non-match rate vs. false match rate plotted parametrically on threshold, T . The scales are logarithmic in order to show decades of FMR.

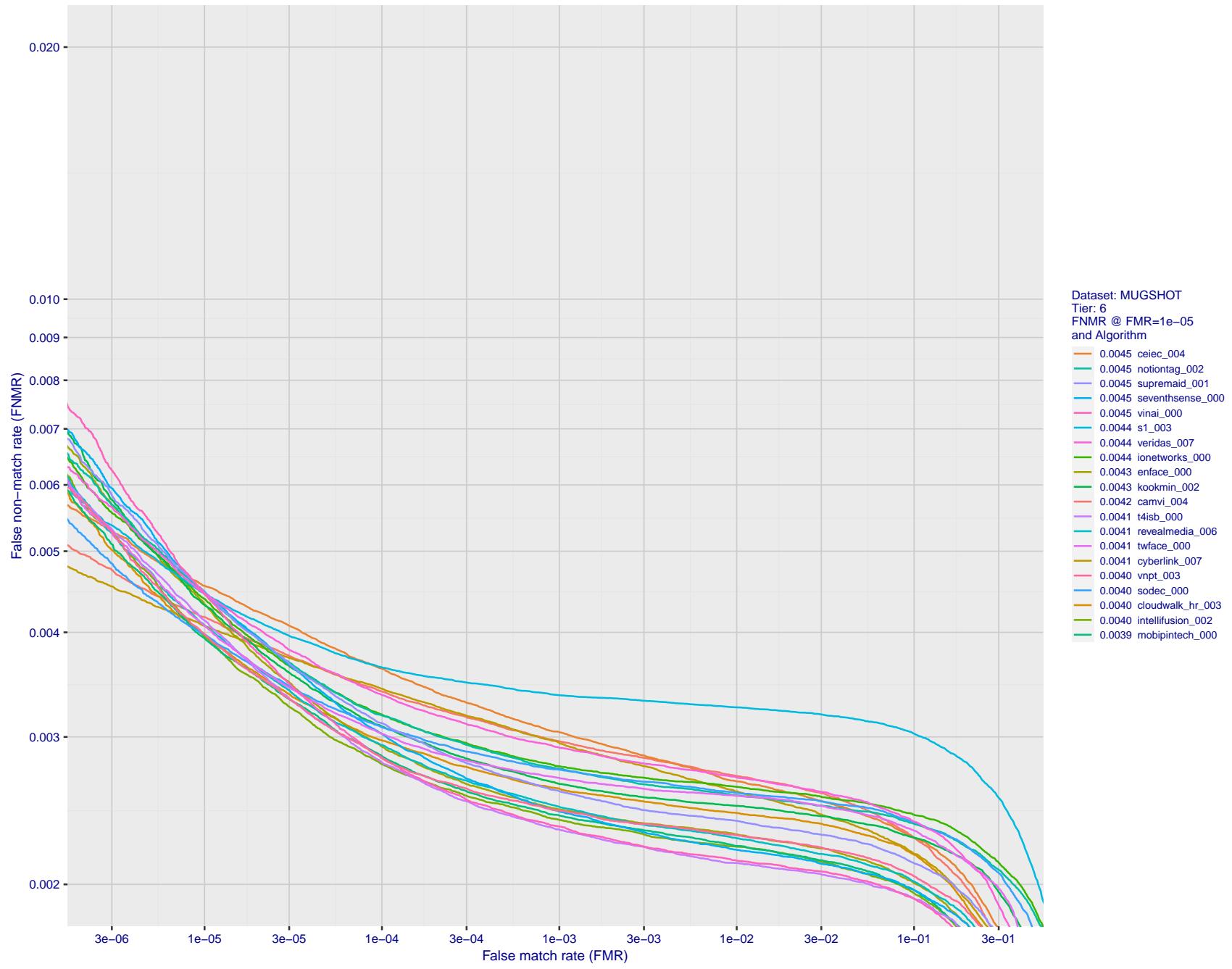


Figure 65: For the mugshot images, detection error tradeoff (DET) characteristics showing false non-match rate vs. false match rate plotted parametrically on threshold, T . The scales are logarithmic in order to show decades of FMR.

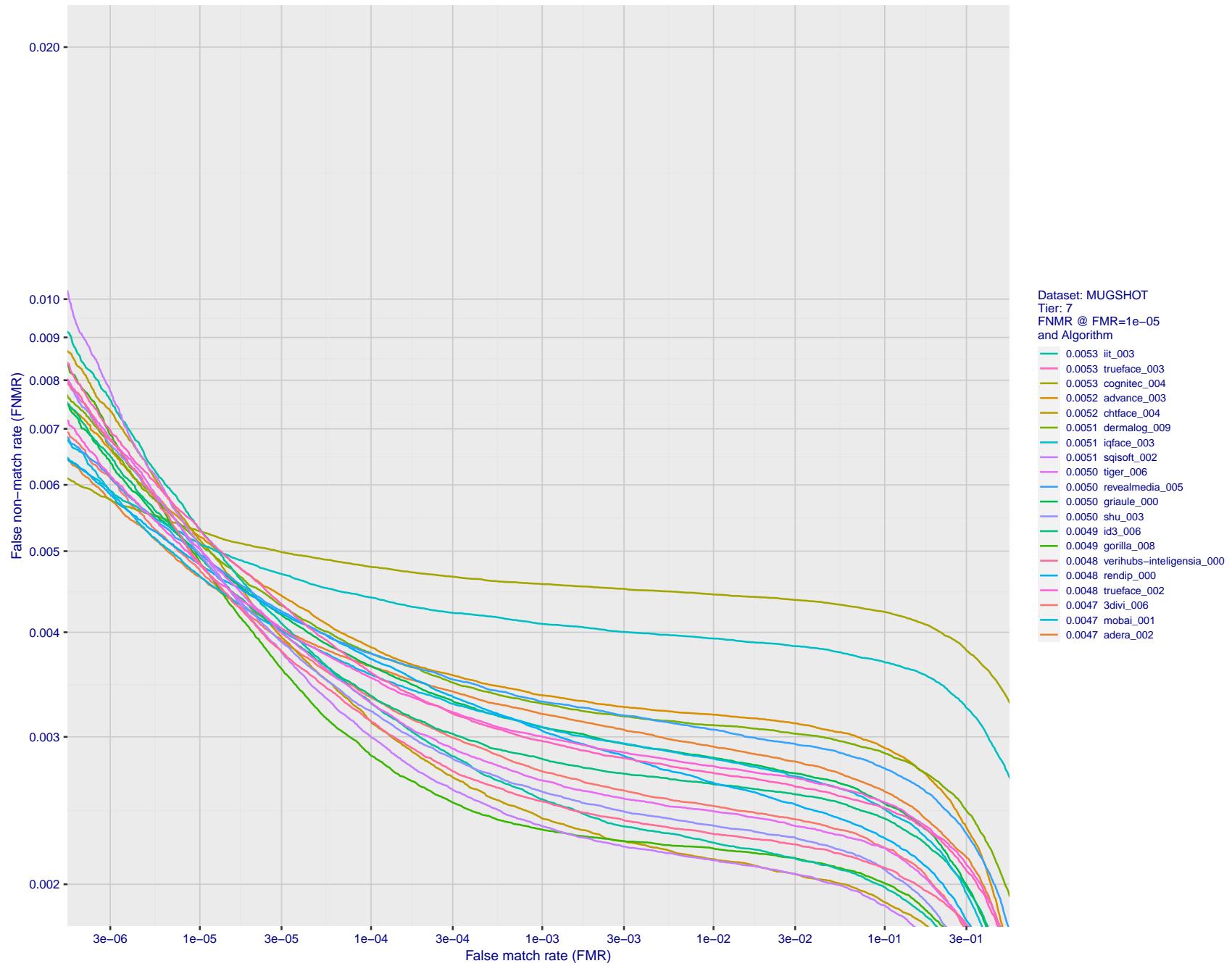


Figure 66: For the mugshot images, detection error tradeoff (DET) characteristics showing false non-match rate vs. false match rate plotted parametrically on threshold, T . The scales are logarithmic in order to show decades of FMR.

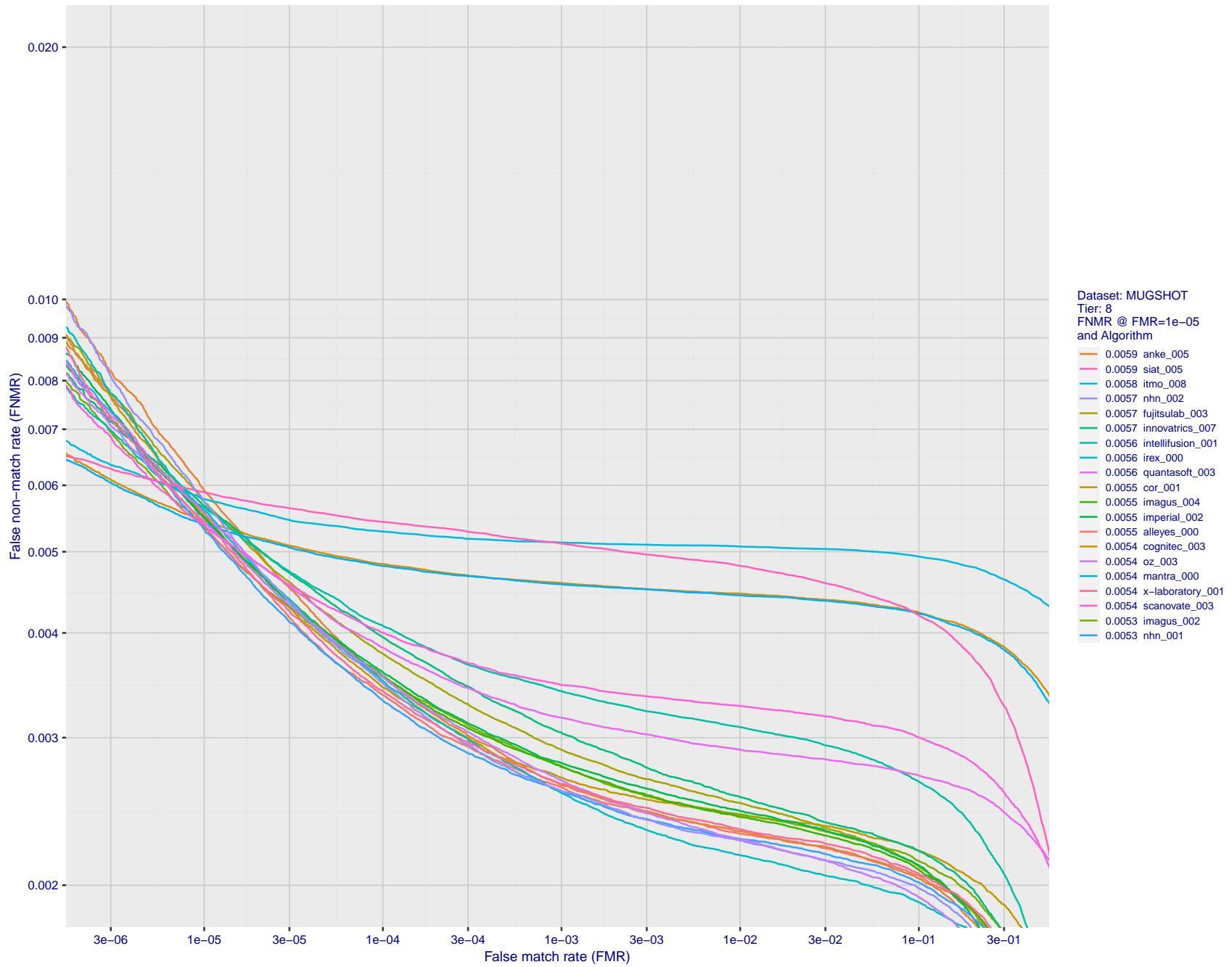


Figure 67: For the mugshot images, detection error tradeoff (DET) characteristics showing false non-match rate vs. false match rate plotted parametrically on threshold, T . The scales are logarithmic in order to show decades of FMR.

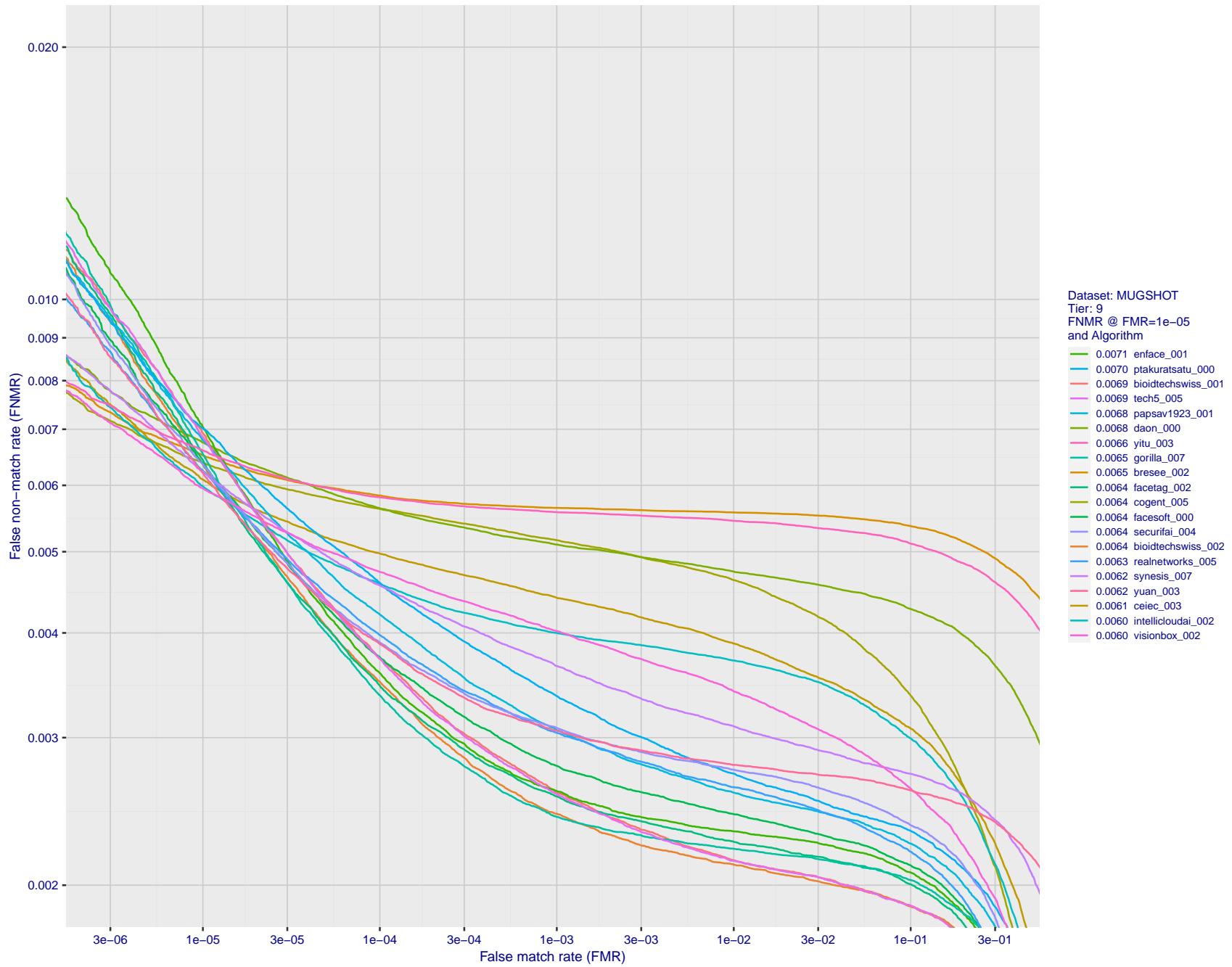


Figure 68: For the mugshot images, detection error tradeoff (DET) characteristics showing false non-match rate vs. false match rate plotted parametrically on threshold, T . The scales are logarithmic in order to show decades of FMR.

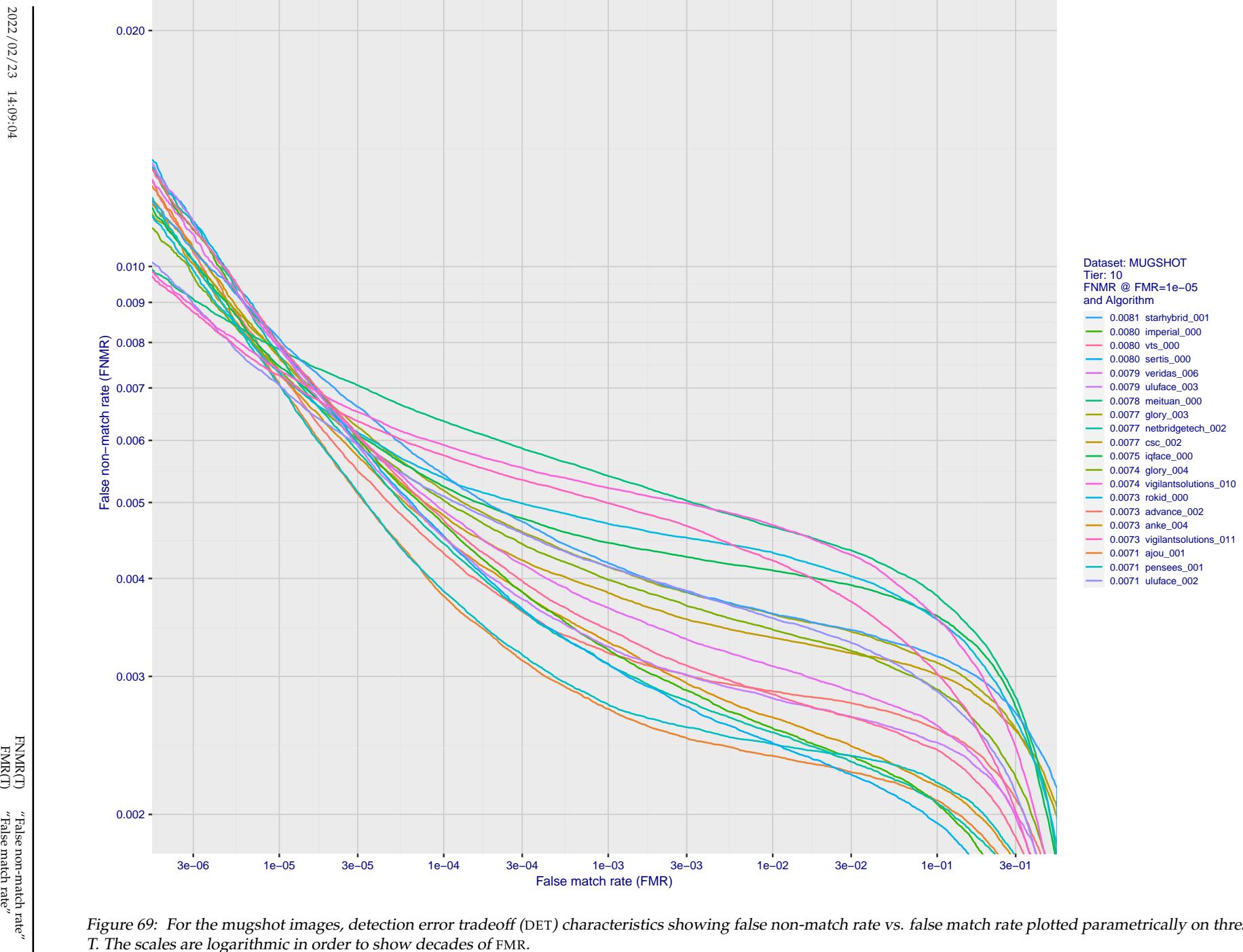


Figure 69: For the mugshot images, detection error tradeoff (DET) characteristics showing false non-match rate vs. false match rate plotted parametrically on threshold, T . The scales are logarithmic in order to show decades of FMR.

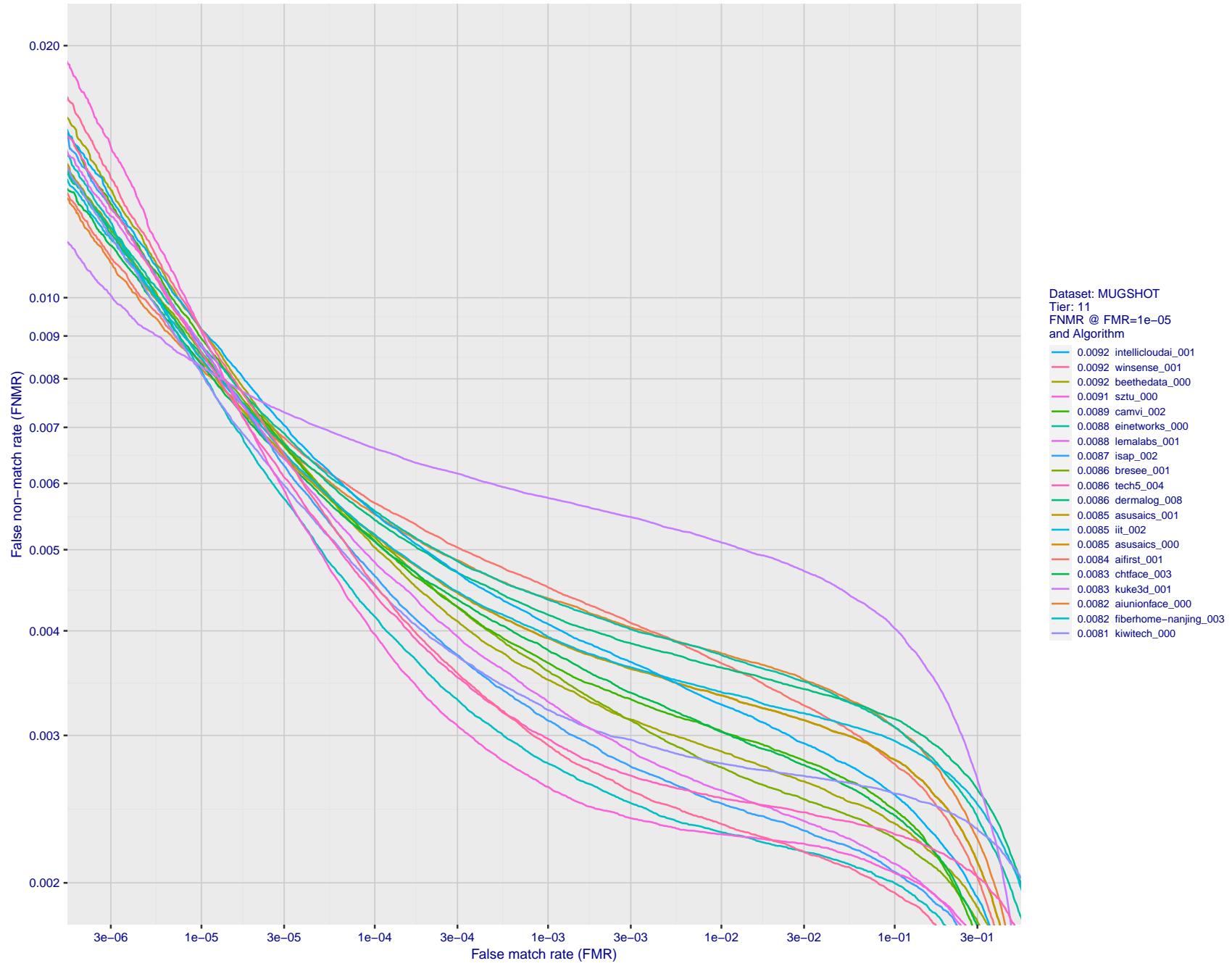


Figure 70: For the mugshot images, detection error tradeoff (DET) characteristics showing false non-match rate vs. false match rate plotted parametrically on threshold, T . The scales are logarithmic in order to show decades of FMR.

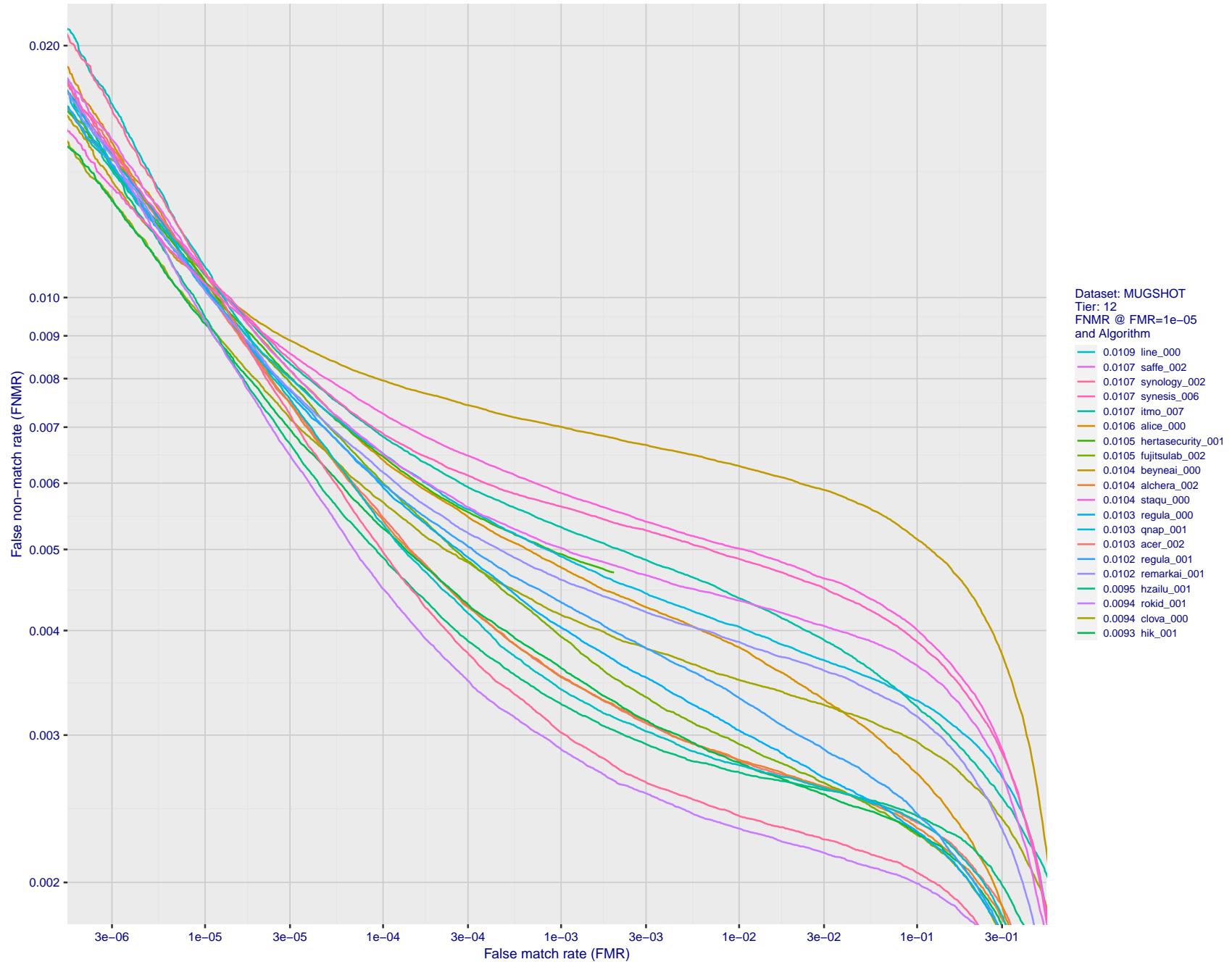


Figure 71: For the mugshot images, detection error tradeoff (DET) characteristics showing false non-match rate vs. false match rate plotted parametrically on threshold, T . The scales are logarithmic in order to show decades of FMR.

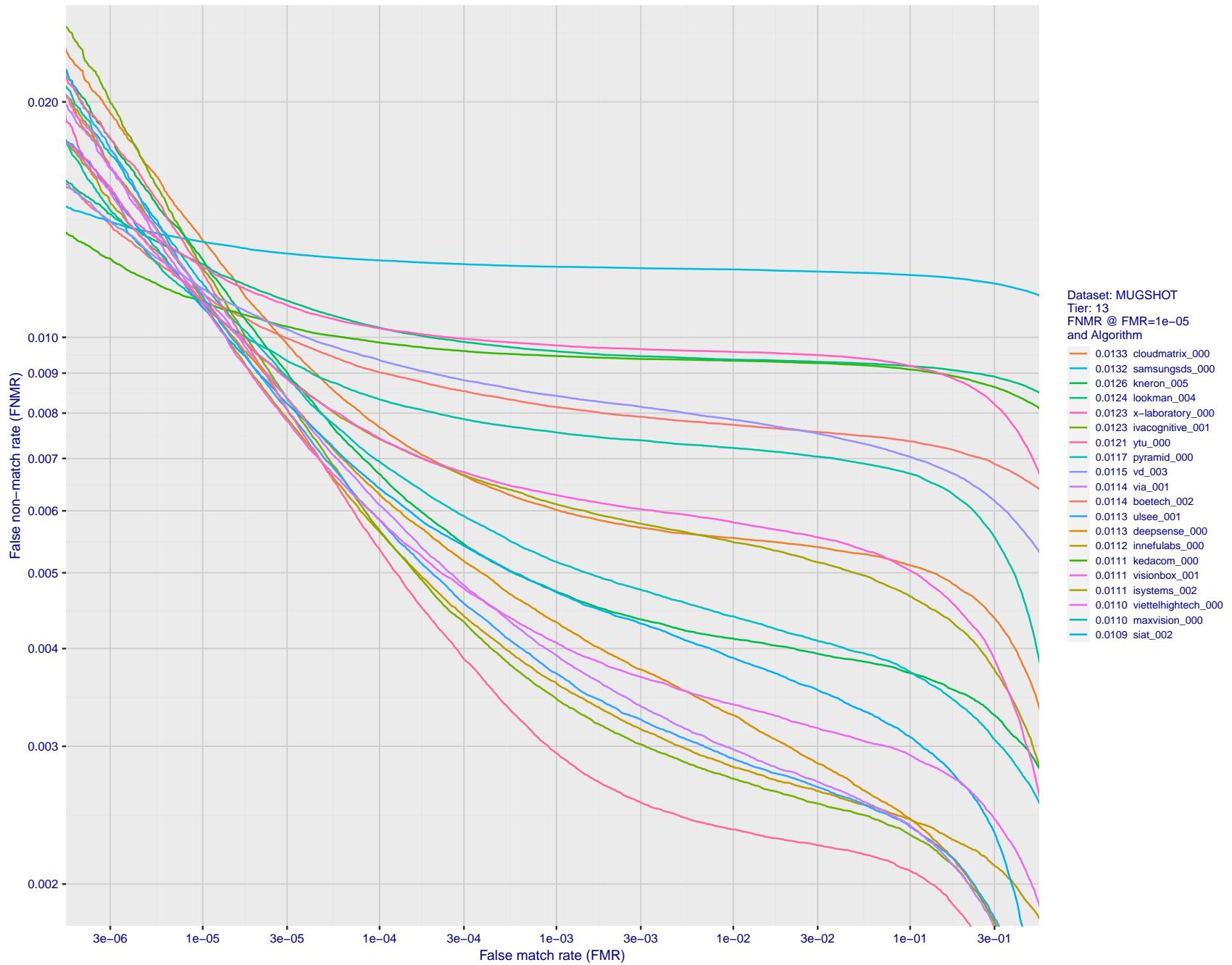


Figure 72: For the mugshot images, detection error tradeoff (DET) characteristics showing false non-match rate vs. false match rate plotted parametrically on threshold, T . The scales are logarithmic in order to show decades of FMR.

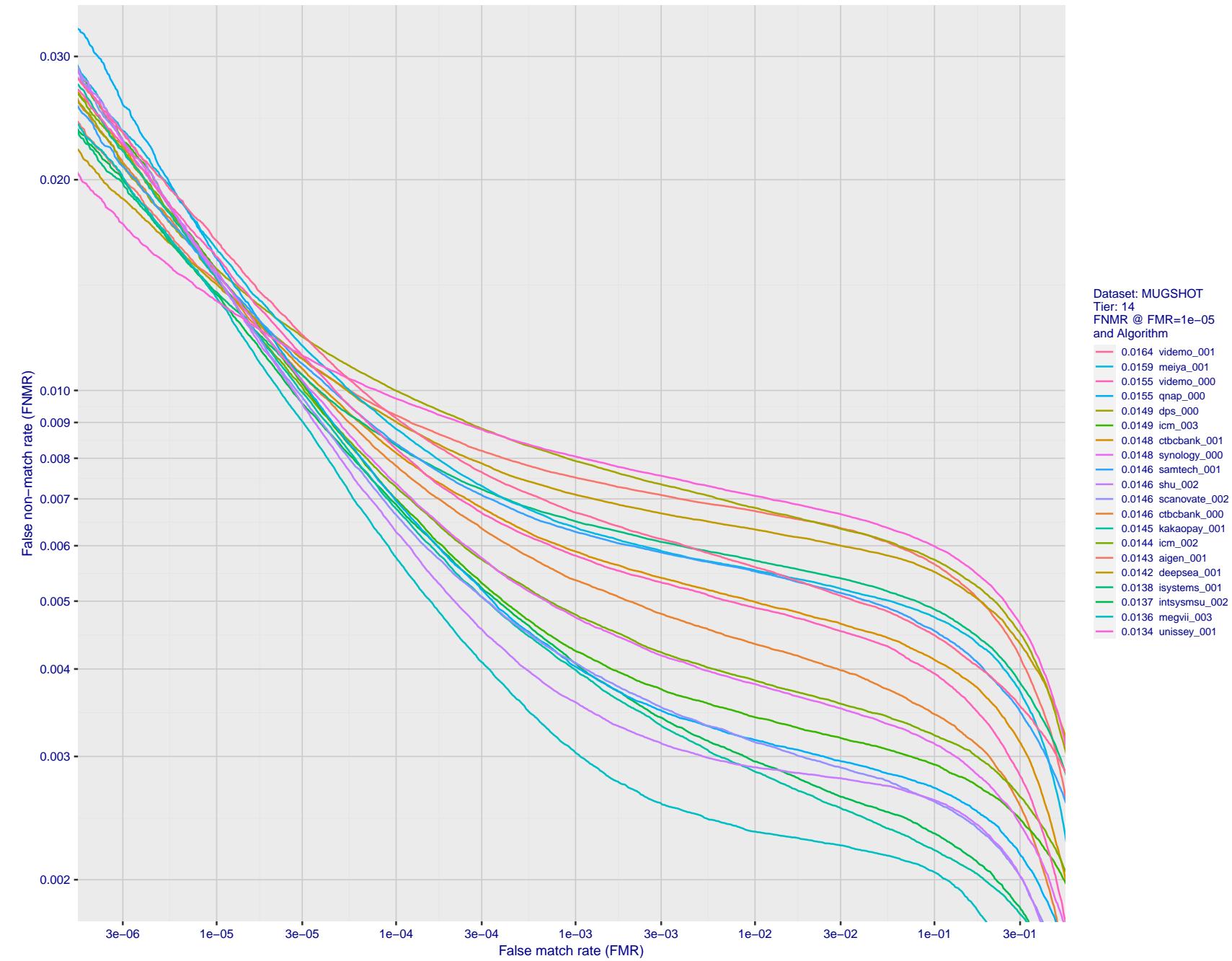


Figure 73: For the mugshot images, detection error tradeoff (DET) characteristics showing false non-match rate vs. false match rate plotted parametrically on threshold, T . The scales are logarithmic in order to show decades of FMR.

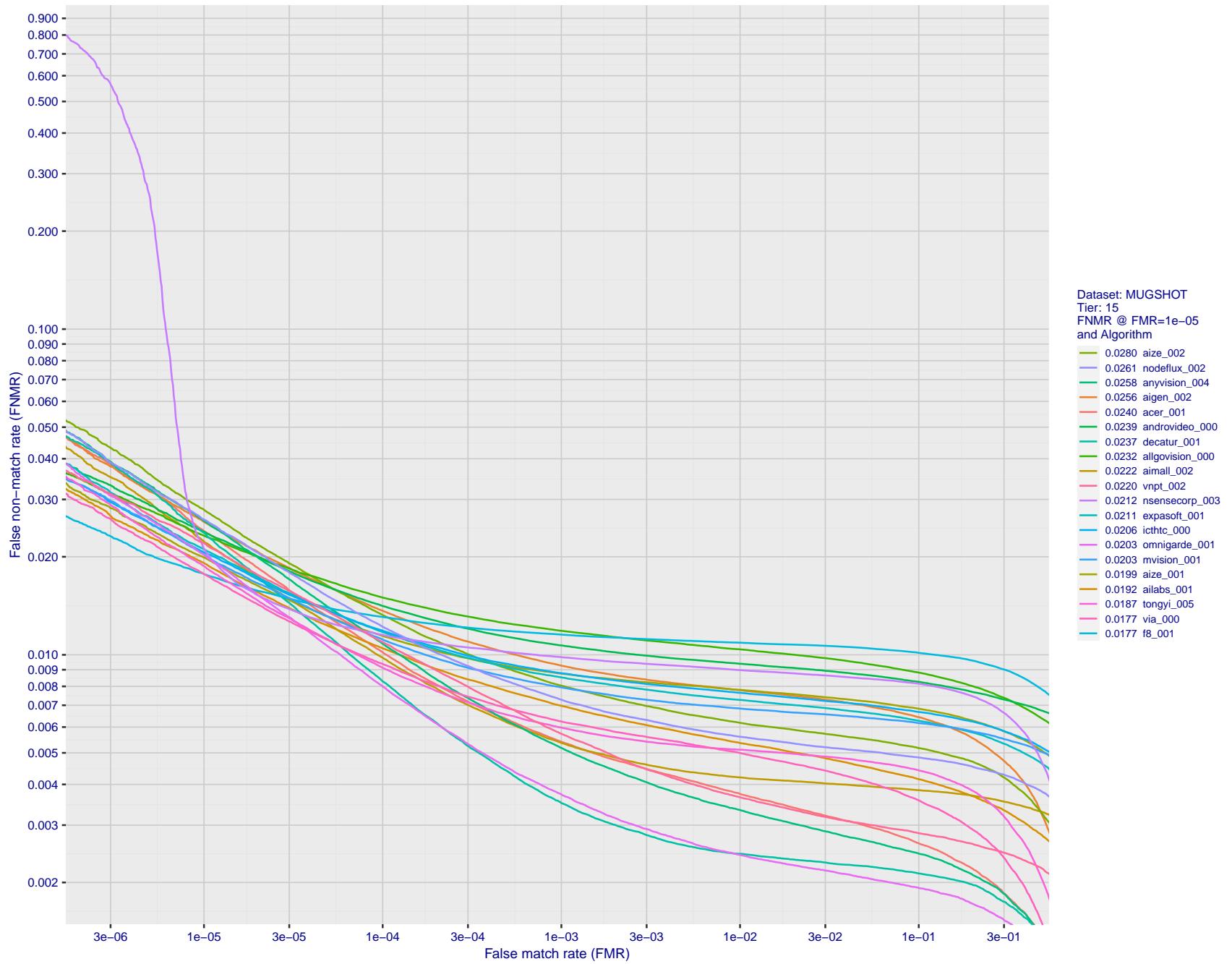


Figure 74: For the mugshot images, detection error tradeoff (DET) characteristics showing false non-match rate vs. false match rate plotted parametrically on threshold, T . The scales are logarithmic in order to show decades of FMR.

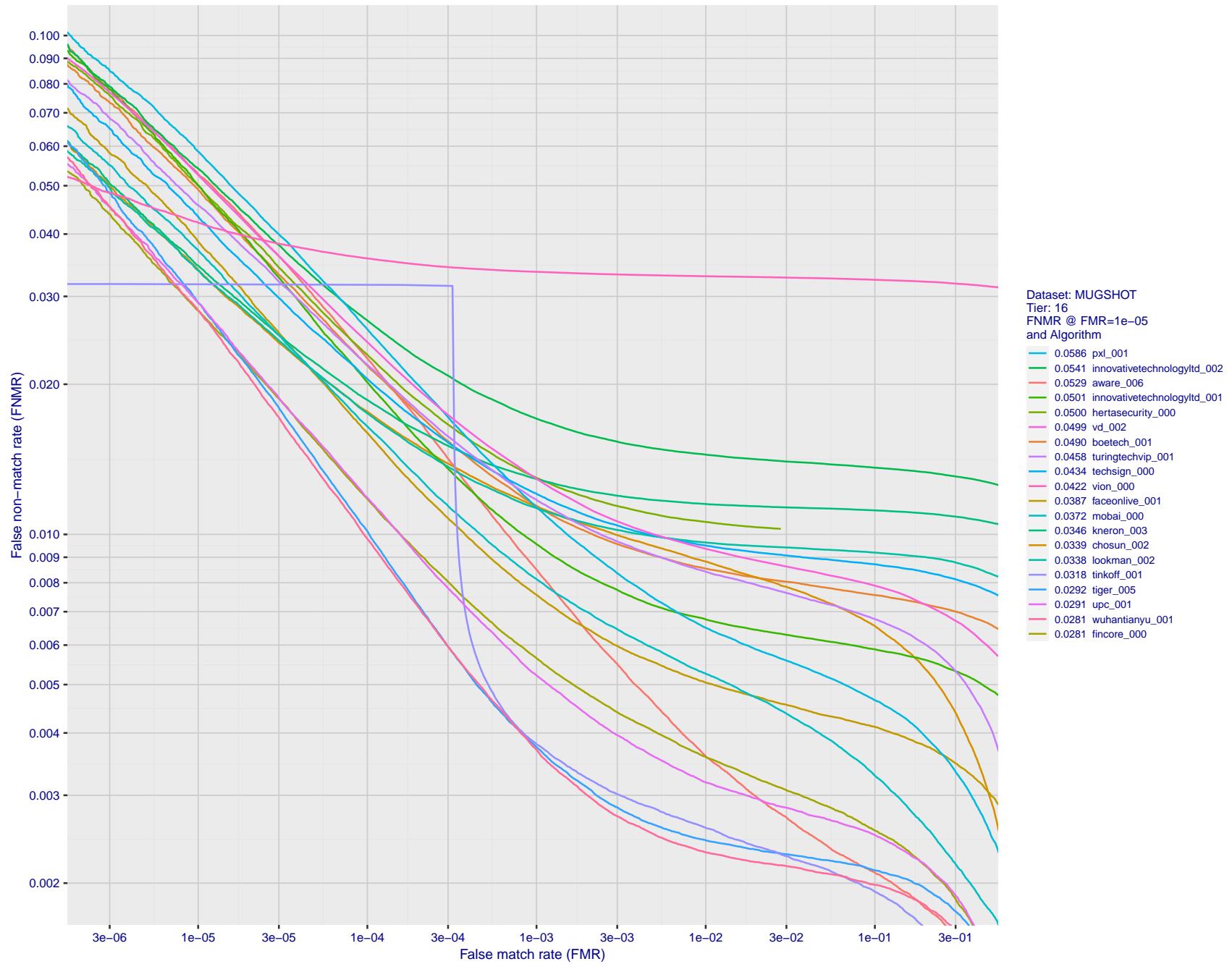


Figure 75: For the mugshot images, detection error tradeoff (DET) characteristics showing false non-match rate vs. false match rate plotted parametrically on threshold, T . The scales are logarithmic in order to show decades of FMR.

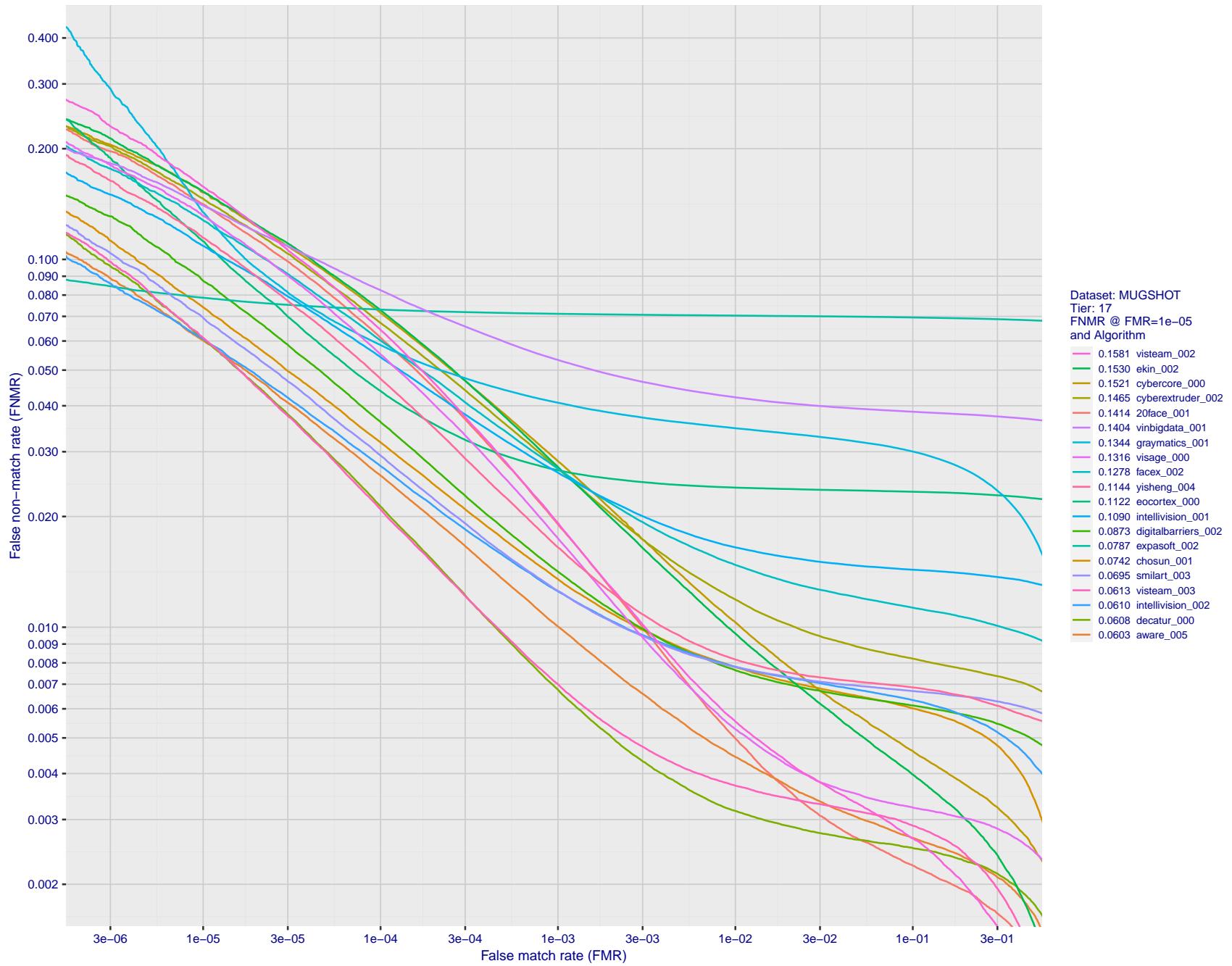


Figure 76: For the mugshot images, detection error tradeoff (DET) characteristics showing false non-match rate vs. false match rate plotted parametrically on threshold, T . The scales are logarithmic in order to show decades of FMR.

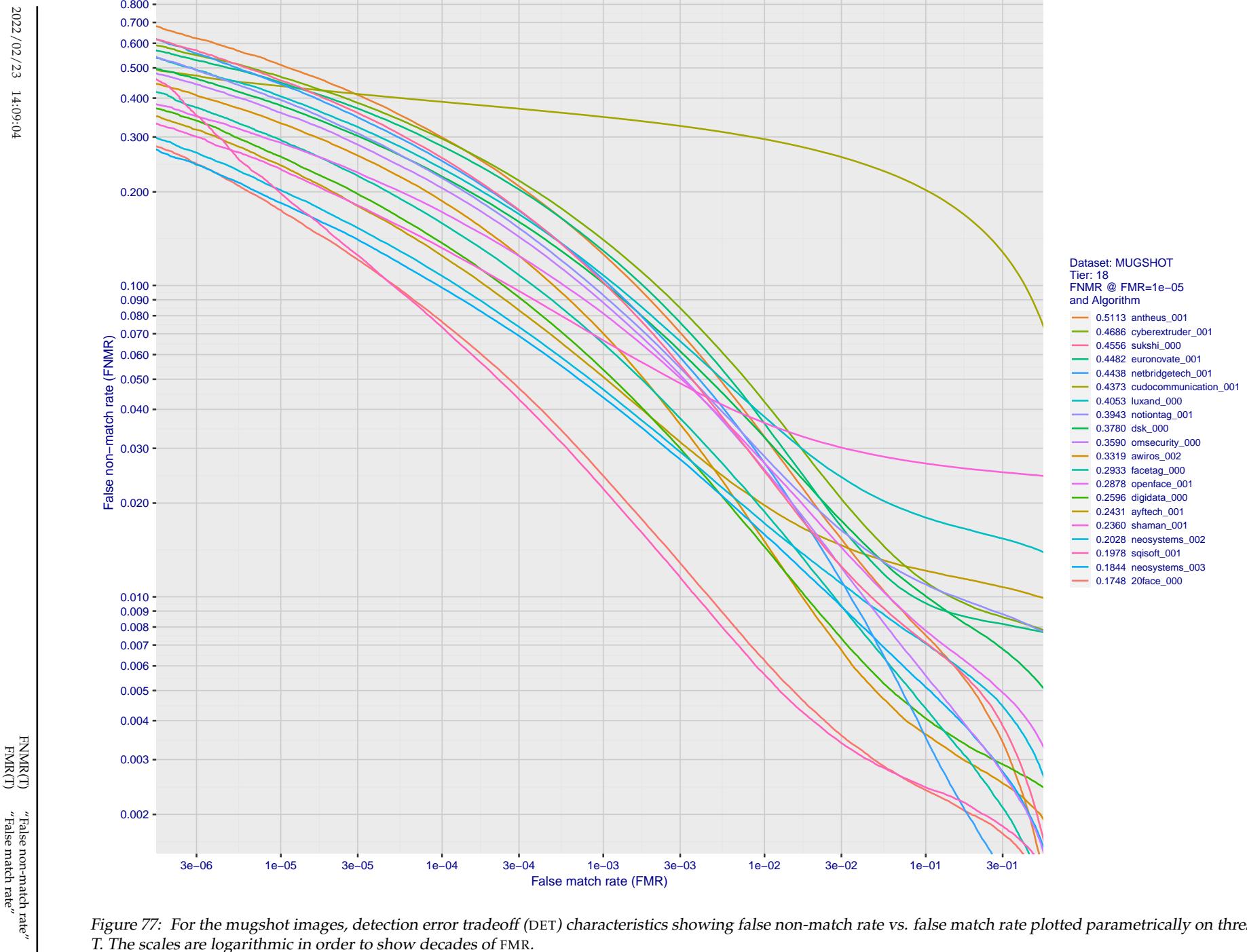


Figure 77: For the mugshot images, detection error tradeoff (DET) characteristics showing false non-match rate vs. false match rate plotted parametrically on threshold, T . The scales are logarithmic in order to show decades of FMR.

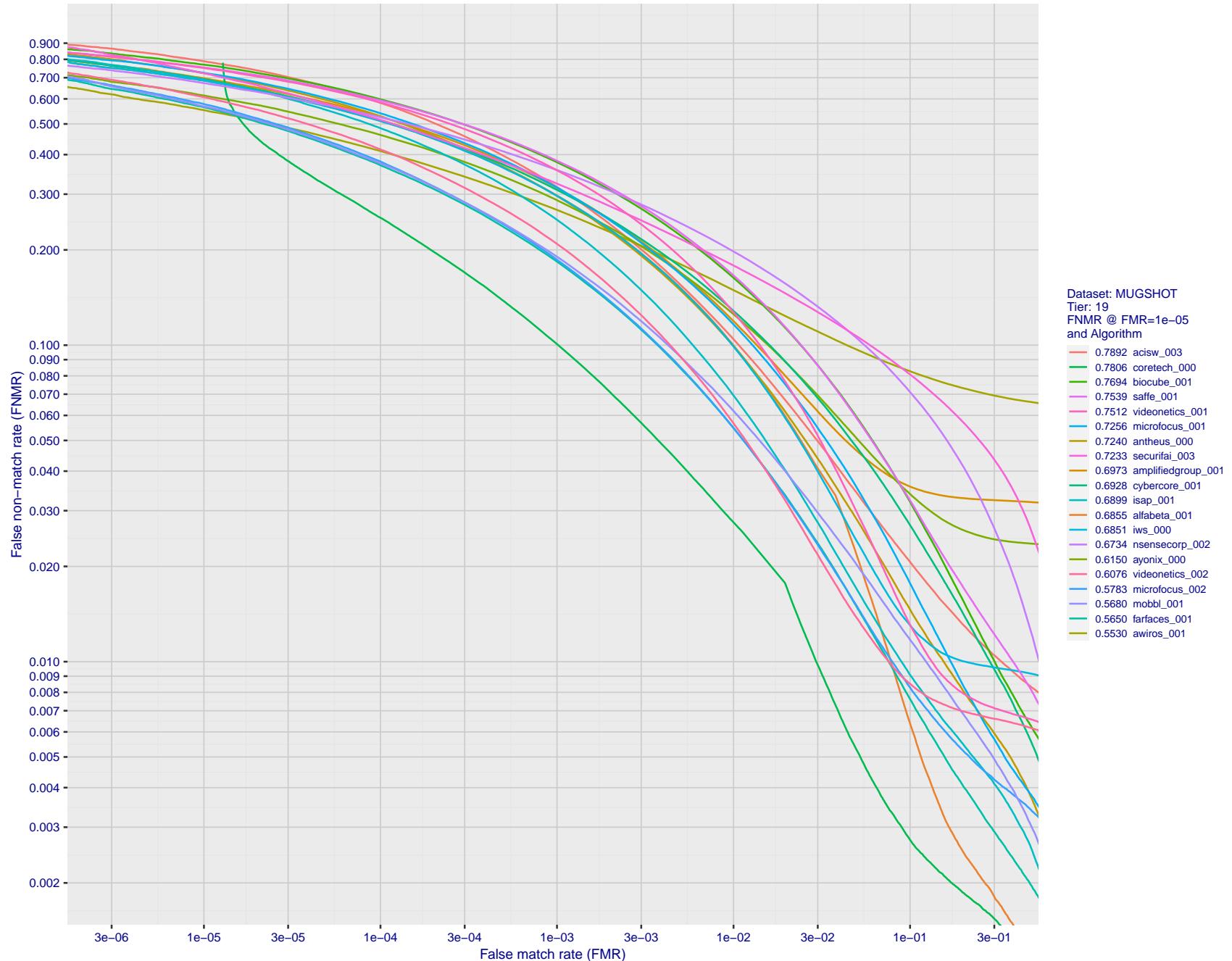


Figure 78: For the mugshot images, detection error tradeoff (DET) characteristics showing false non-match rate vs. false match rate plotted parametrically on threshold, T . The scales are logarithmic in order to show decades of FMR.

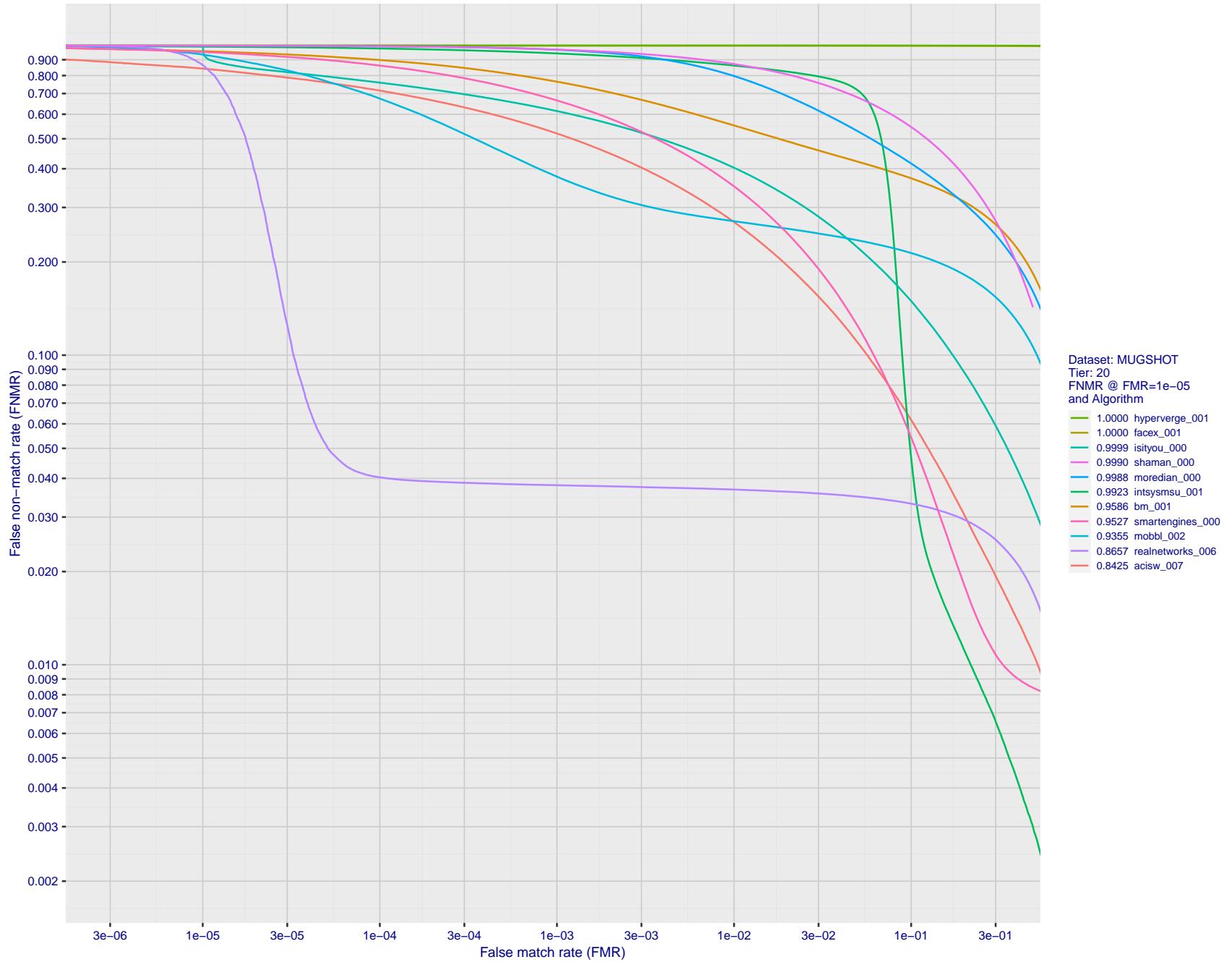


Figure 79: For the mugshot images, detection error tradeoff (DET) characteristics showing false non-match rate vs. false match rate plotted parametrically on threshold, T . The scales are logarithmic in order to show decades of FMR.

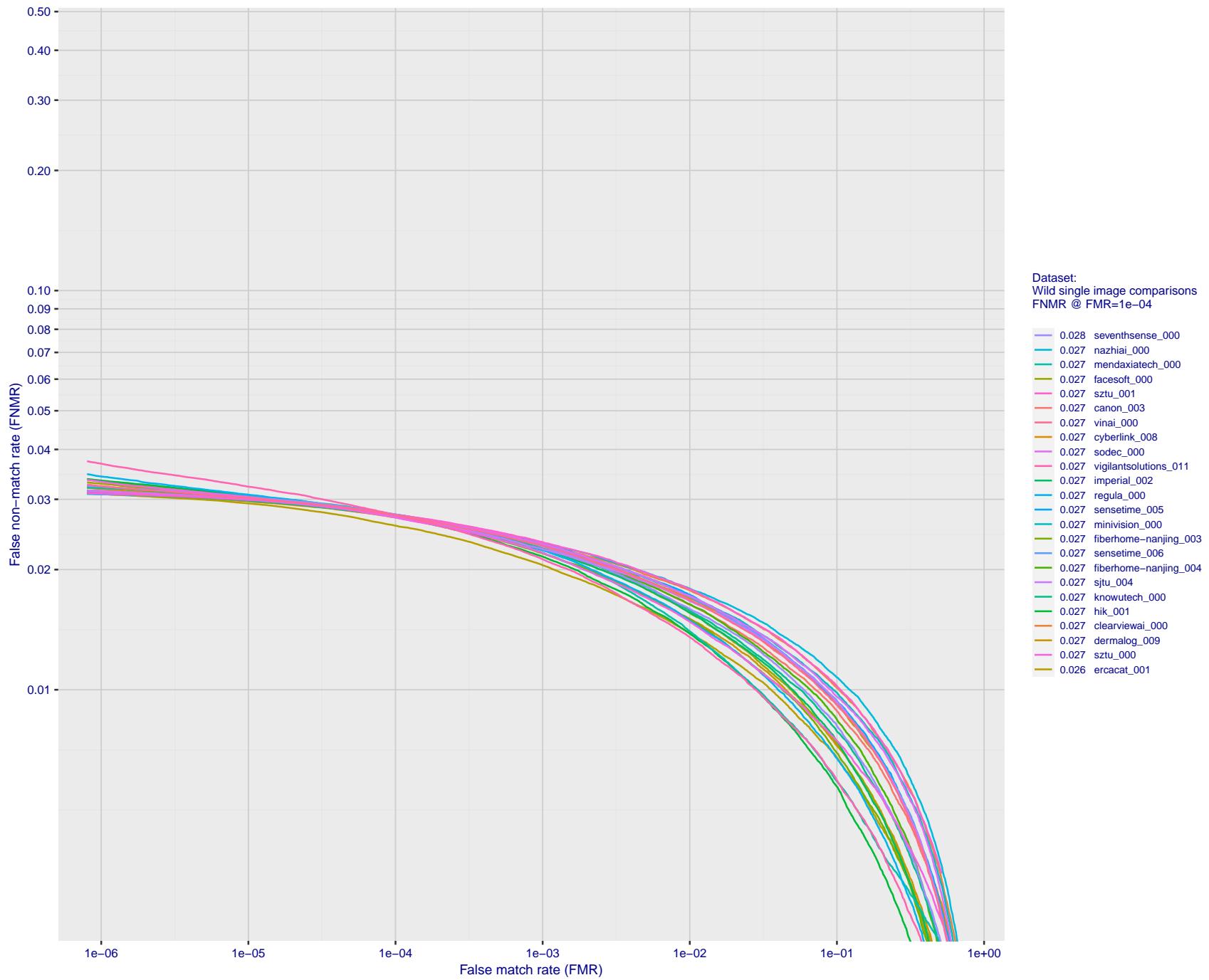


Figure 80: For the 2018 wild image comparisons, detection error tradeoff (DET) characteristics showing false non-match rate vs. false match rate plotted parametrically on threshold, T . The scales are logarithmic in order to show several decades of FMR.

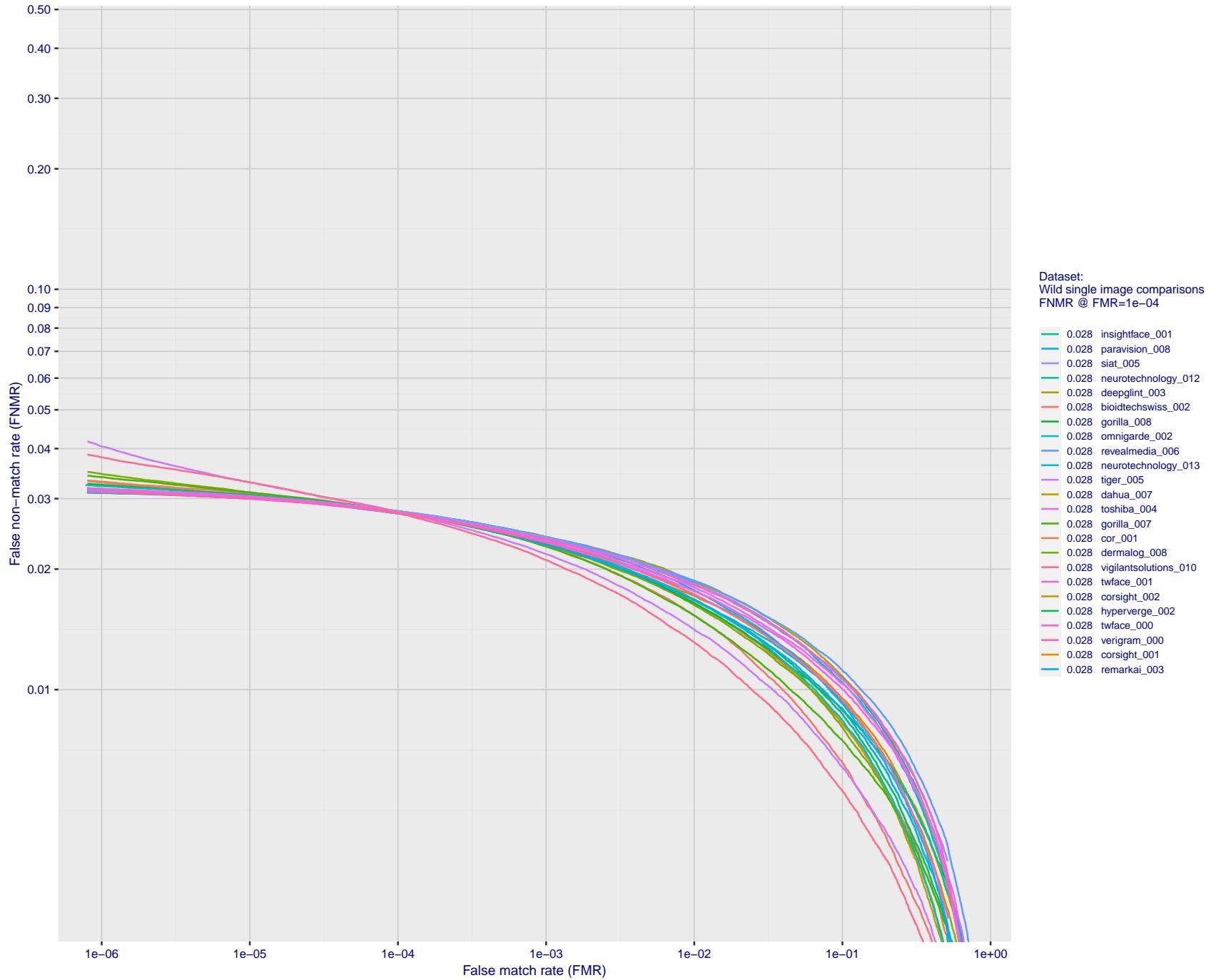


Figure 81: For the 2018 wild image comparisons, detection error tradeoff (DET) characteristics showing false non-match rate vs. false match rate plotted parametrically on threshold, T. The scales are logarithmic in order to show several decades of FMR.

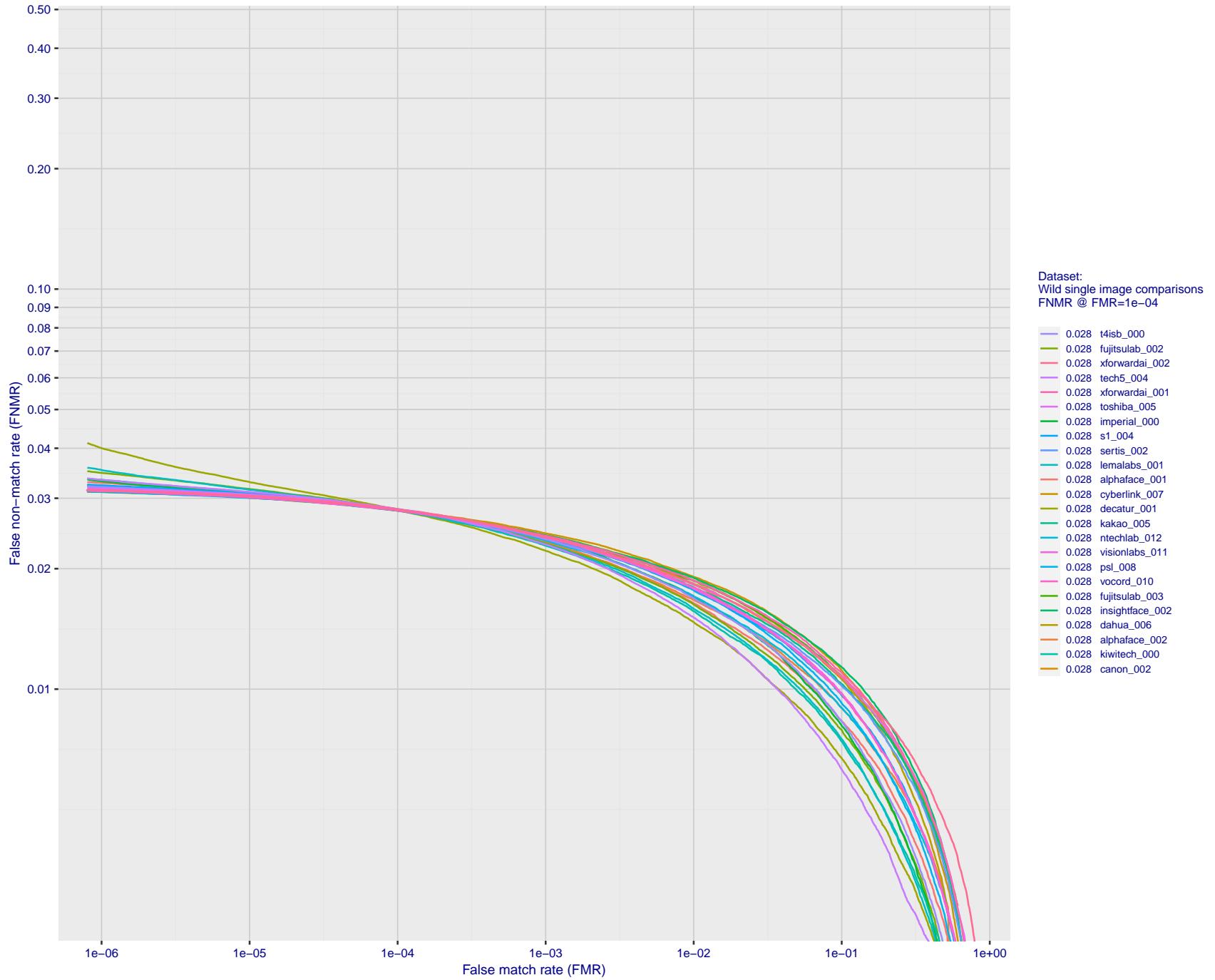


Figure 82: For the 2018 wild image comparisons, detection error tradeoff (DET) characteristics showing false non-match rate vs. false match rate plotted parametrically on threshold, T . The scales are logarithmic in order to show several decades of FMR.

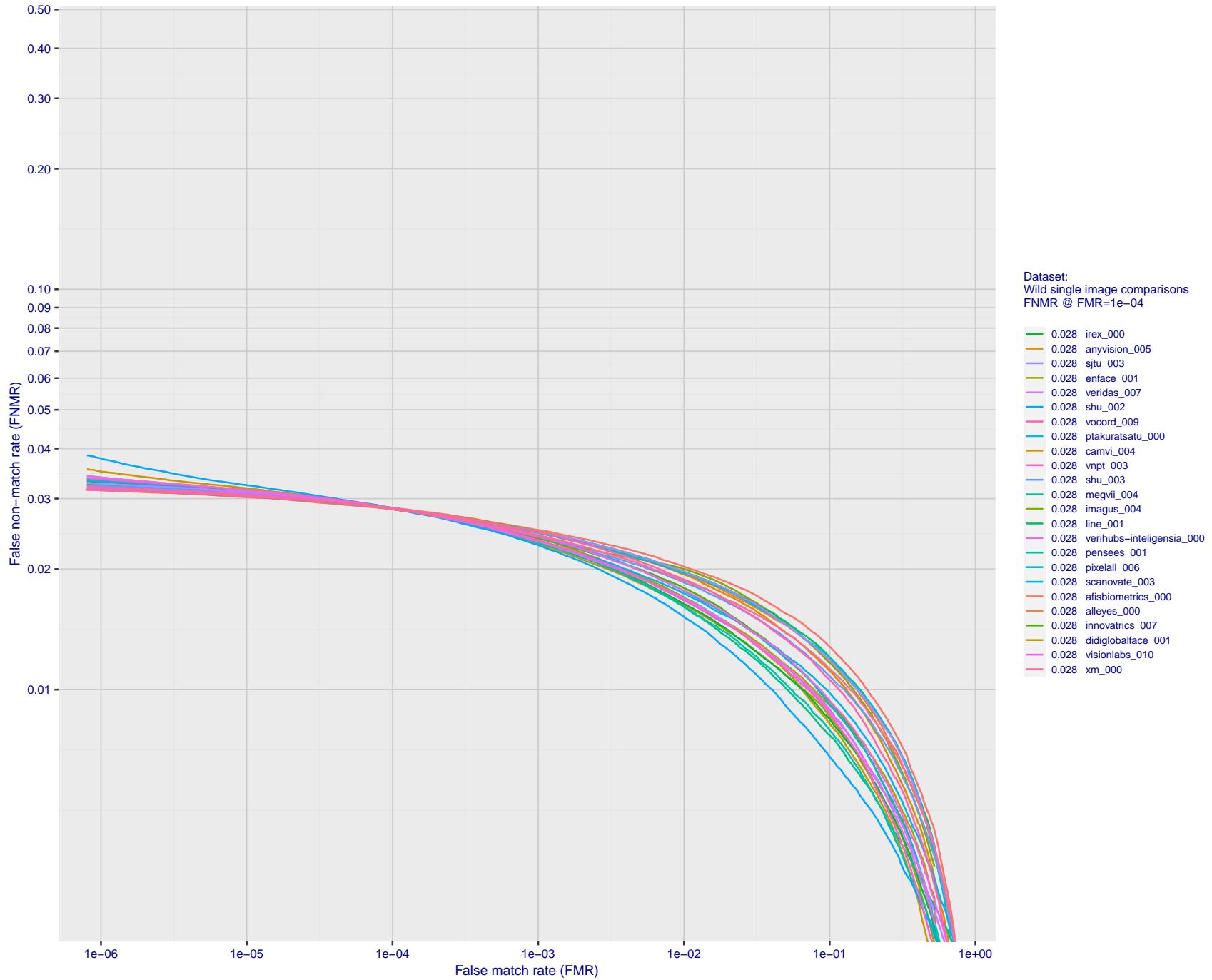


Figure 83: For the 2018 wild image comparisons, detection error tradeoff (DET) characteristics showing false non-match rate vs. false match rate plotted parametrically on threshold, T . The scales are logarithmic in order to show several decades of FMR.

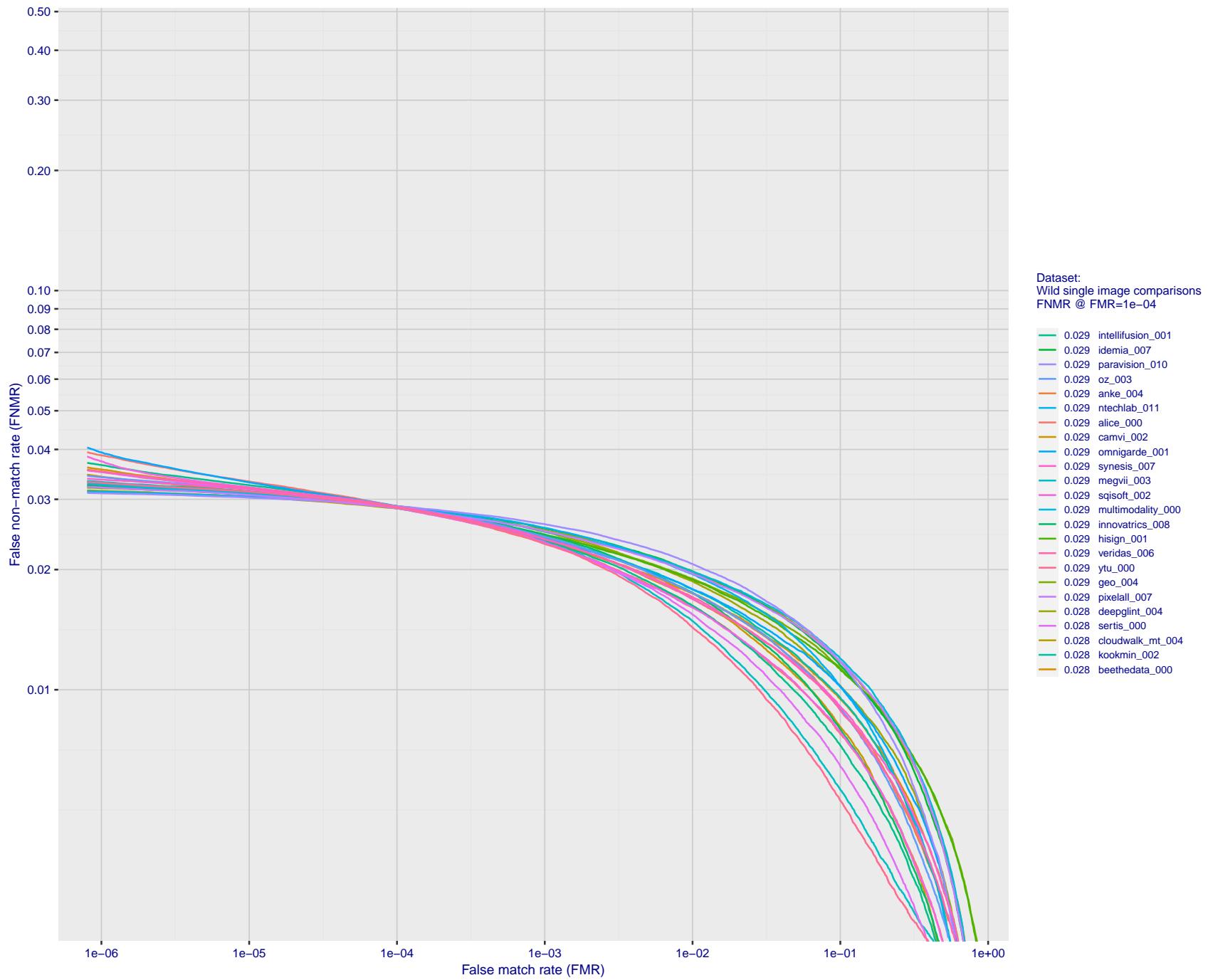


Figure 84: For the 2018 wild image comparisons, detection error tradeoff (DET) characteristics showing false non-match rate vs. false match rate plotted parametrically on threshold, T . The scales are logarithmic in order to show several decades of FMR.

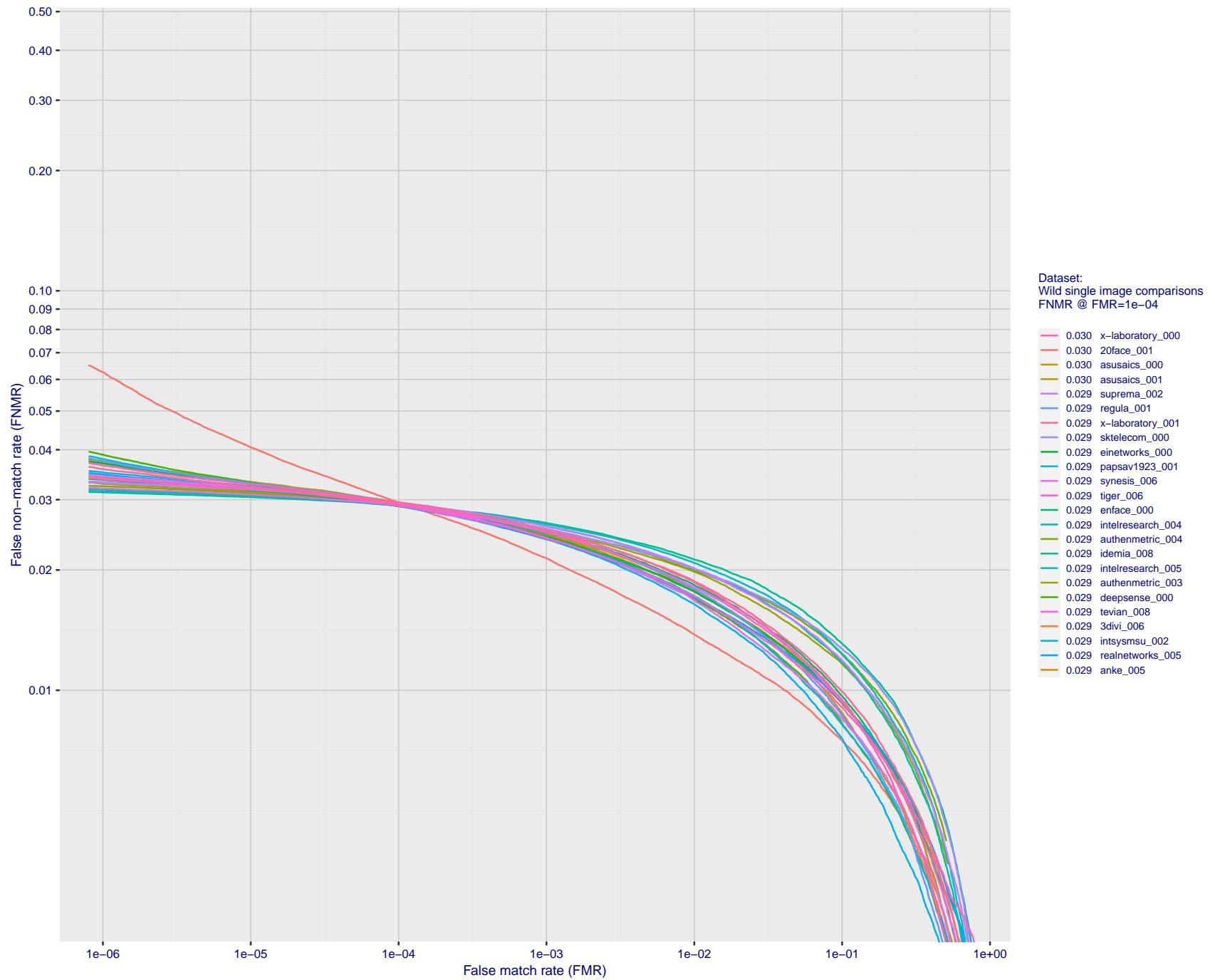


Figure 85: For the 2018 wild image comparisons, detection error tradeoff (DET) characteristics showing false non-match rate vs. false match rate plotted parametrically on threshold, T . The scales are logarithmic in order to show several decades of FMR.

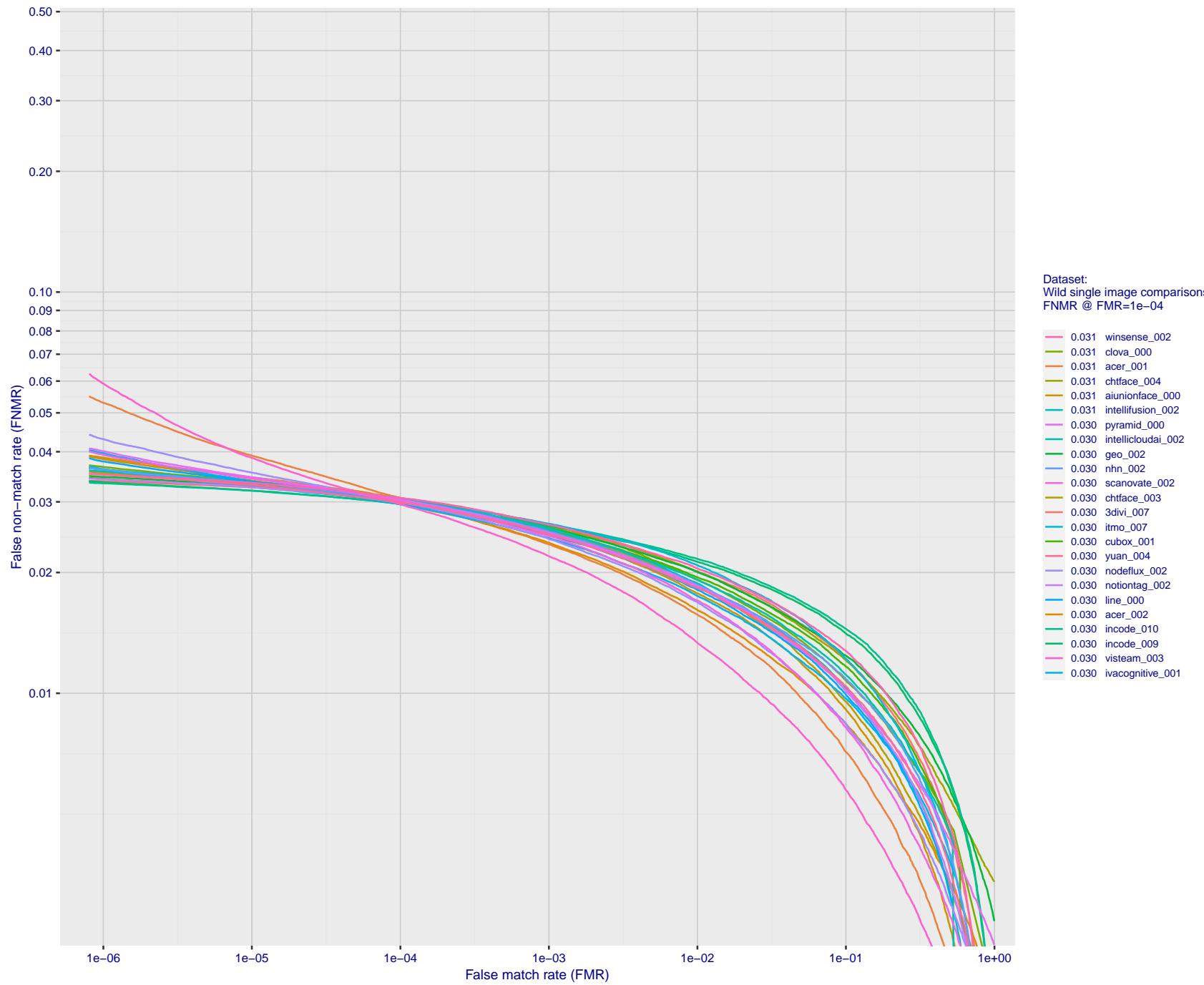


Figure 86: For the 2018 wild image comparisons, detection error tradeoff (DET) characteristics showing false non-match rate vs. false match rate plotted parametrically on threshold, T . The scales are logarithmic in order to show several decades of FMR.

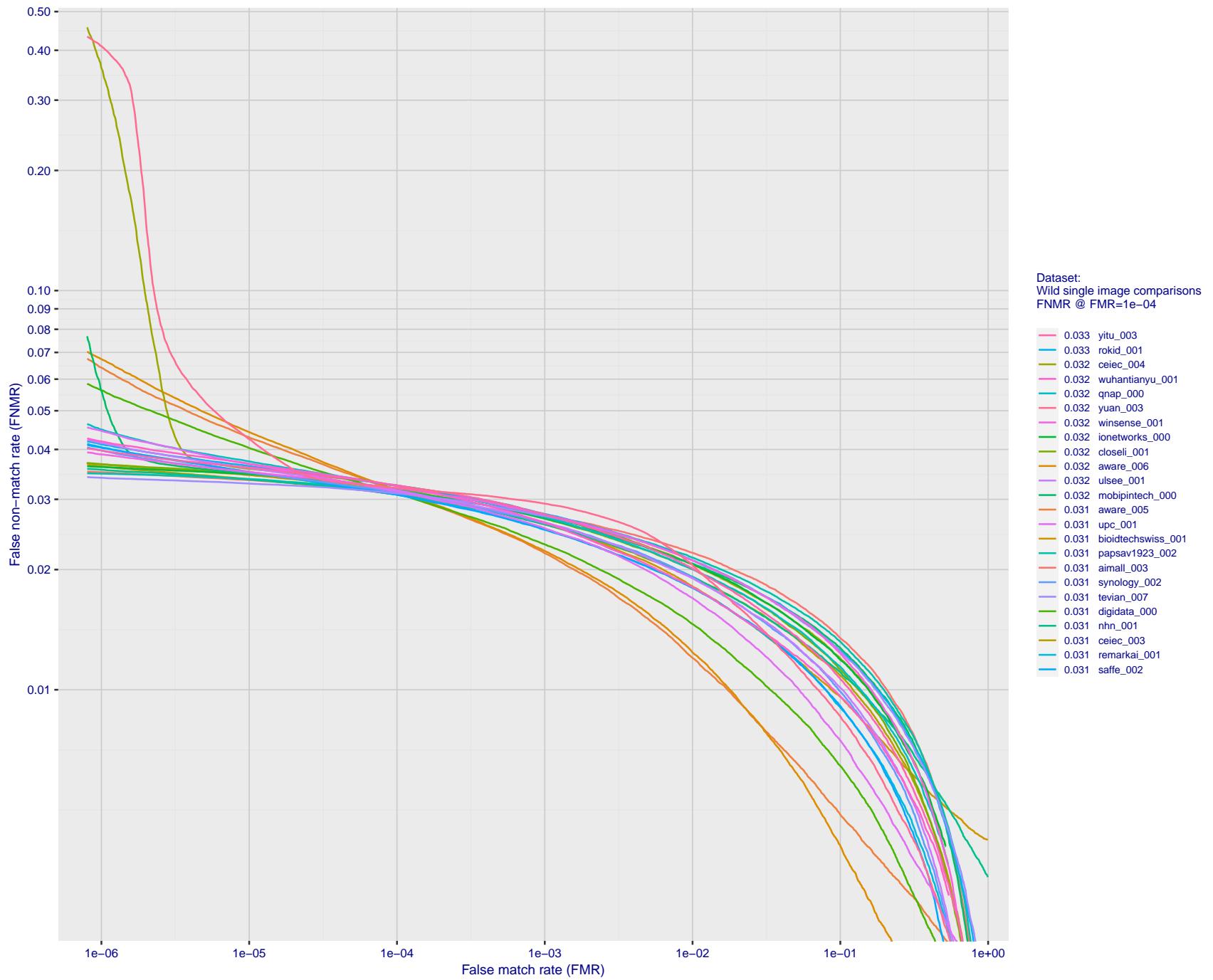


Figure 87: For the 2018 wild image comparisons, detection error tradeoff (DET) characteristics showing false non-match rate vs. false match rate plotted parametrically on threshold, T. The scales are logarithmic in order to show several decades of FMR.

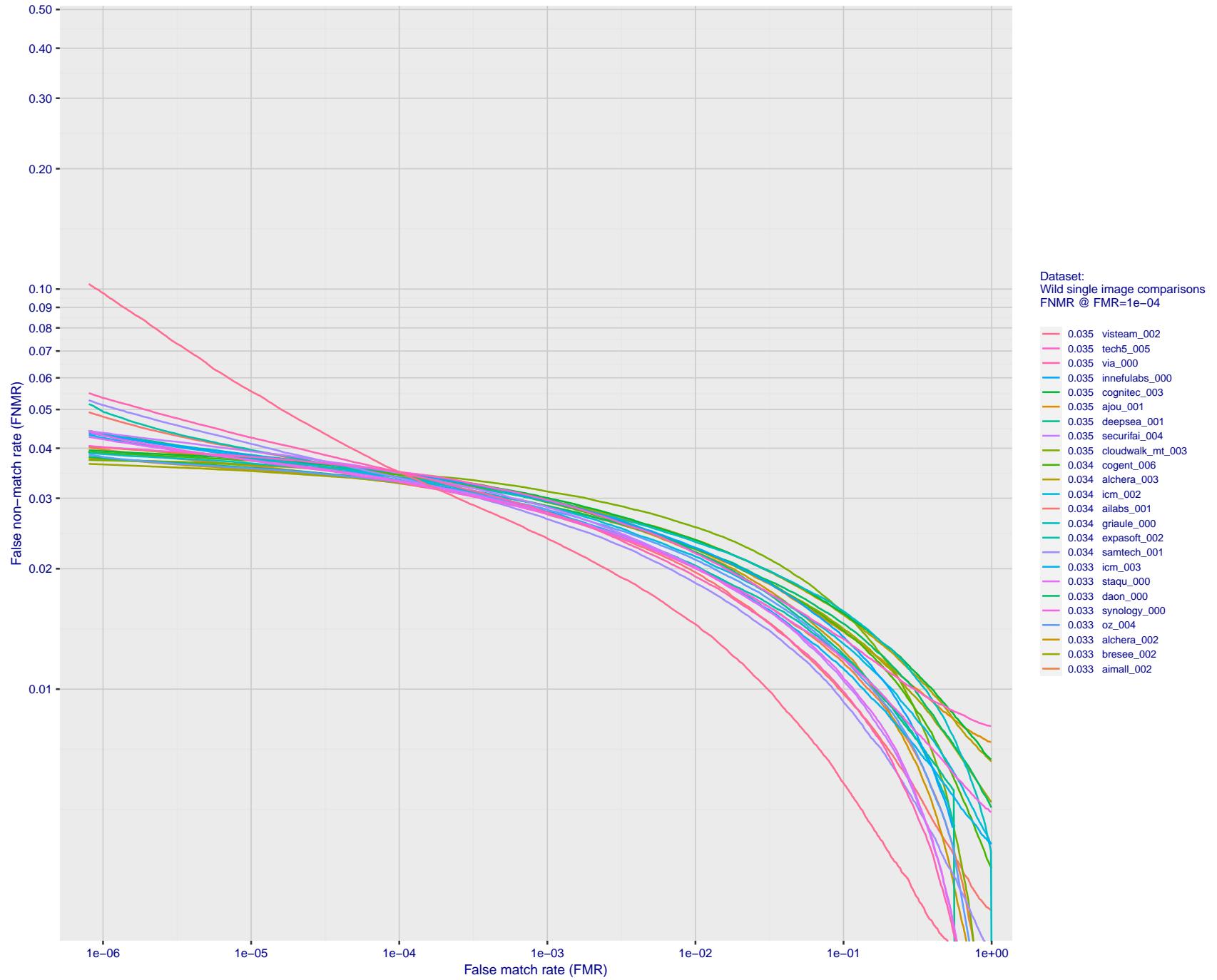


Figure 88: For the 2018 wild image comparisons, detection error tradeoff (DET) characteristics showing false non-match rate vs. false match rate plotted parametrically on threshold, T . The scales are logarithmic in order to show several decades of FMR.

2022/02/23 14:09:04

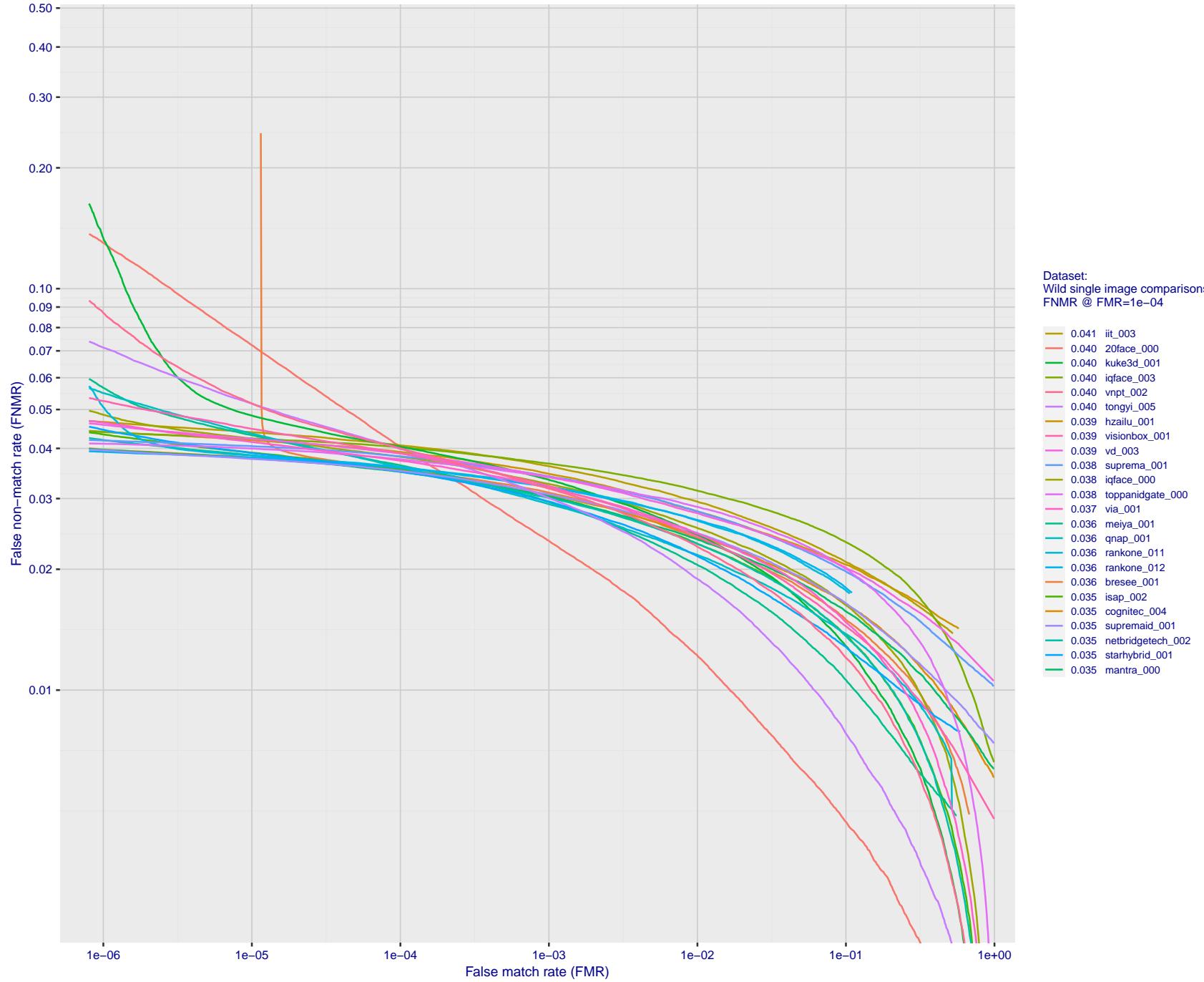


Figure 89: For the 2018 wild image comparisons, detection error tradeoff (DET) characteristics showing false non-match rate vs. false match rate plotted parametrically on threshold, T . The scales are logarithmic in order to show several decades of FMR.

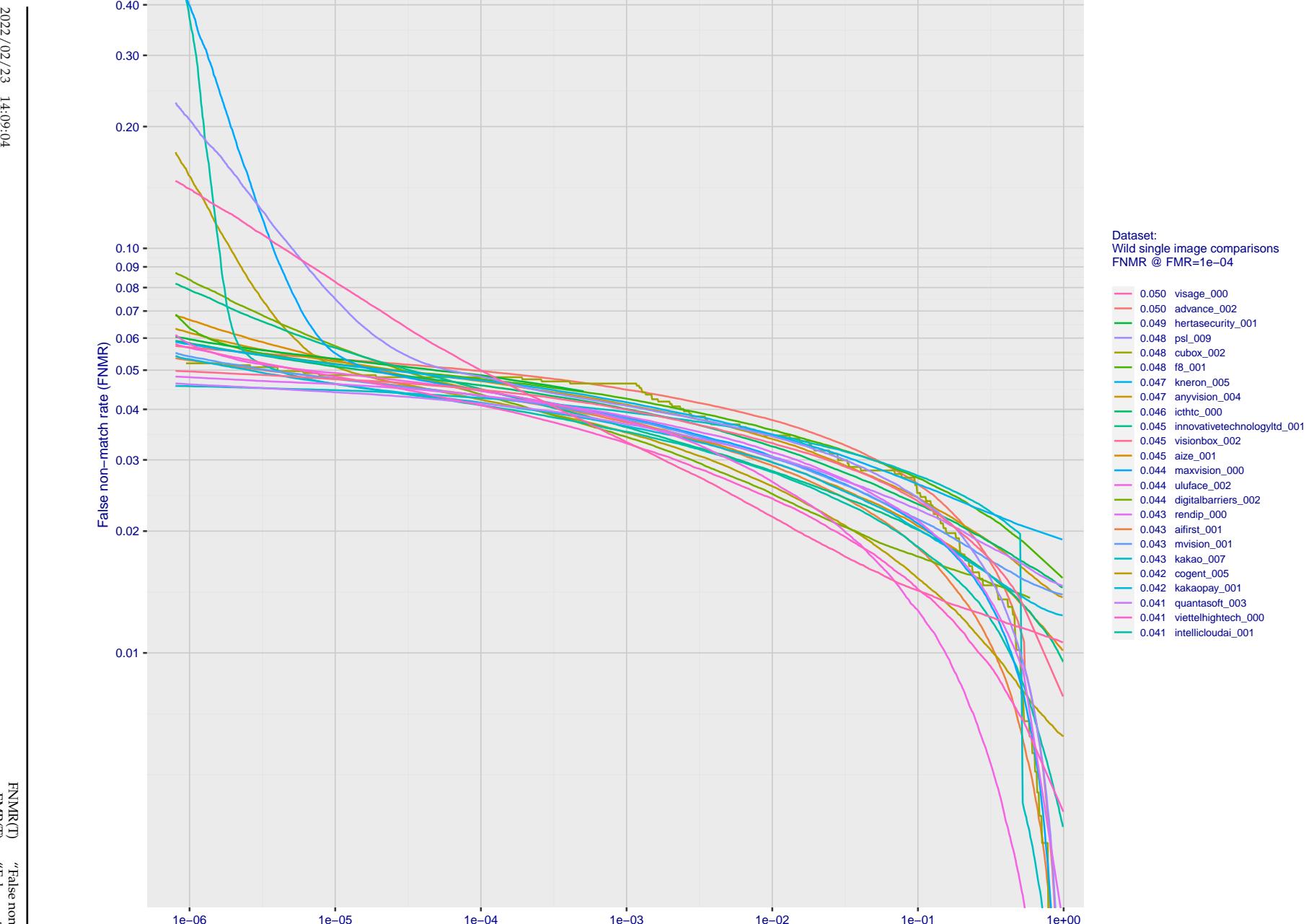


Figure 90: For the 2018 wild image comparisons, detection error tradeoff (DET) characteristics showing false non-match rate vs. false match rate plotted parametrically on threshold, T . The scales are logarithmic in order to show several decades of FMR.

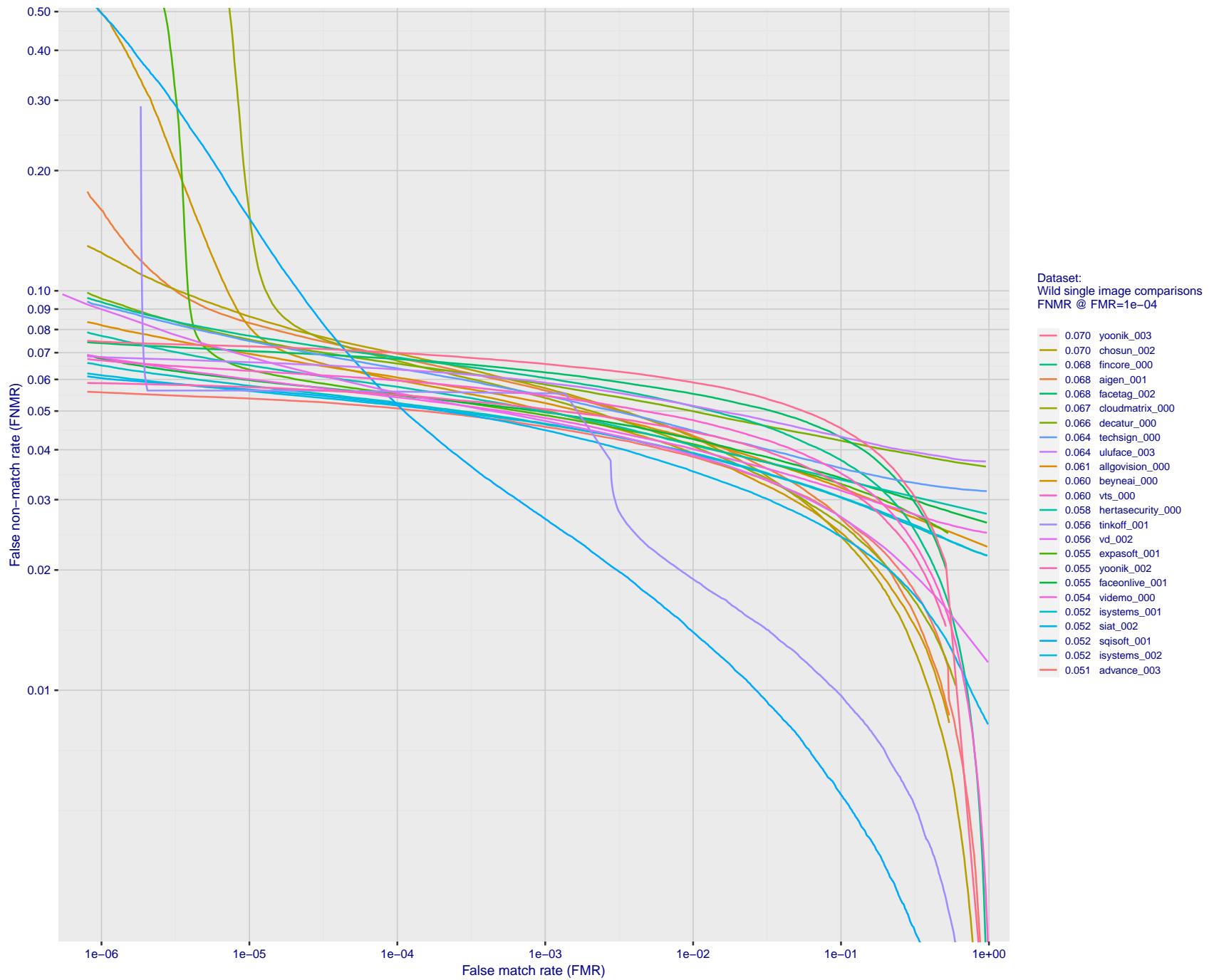


Figure 91: For the 2018 wild image comparisons, detection error tradeoff (DET) characteristics showing false non-match rate vs. false match rate plotted parametrically on threshold, T . The scales are logarithmic in order to show several decades of FMR.

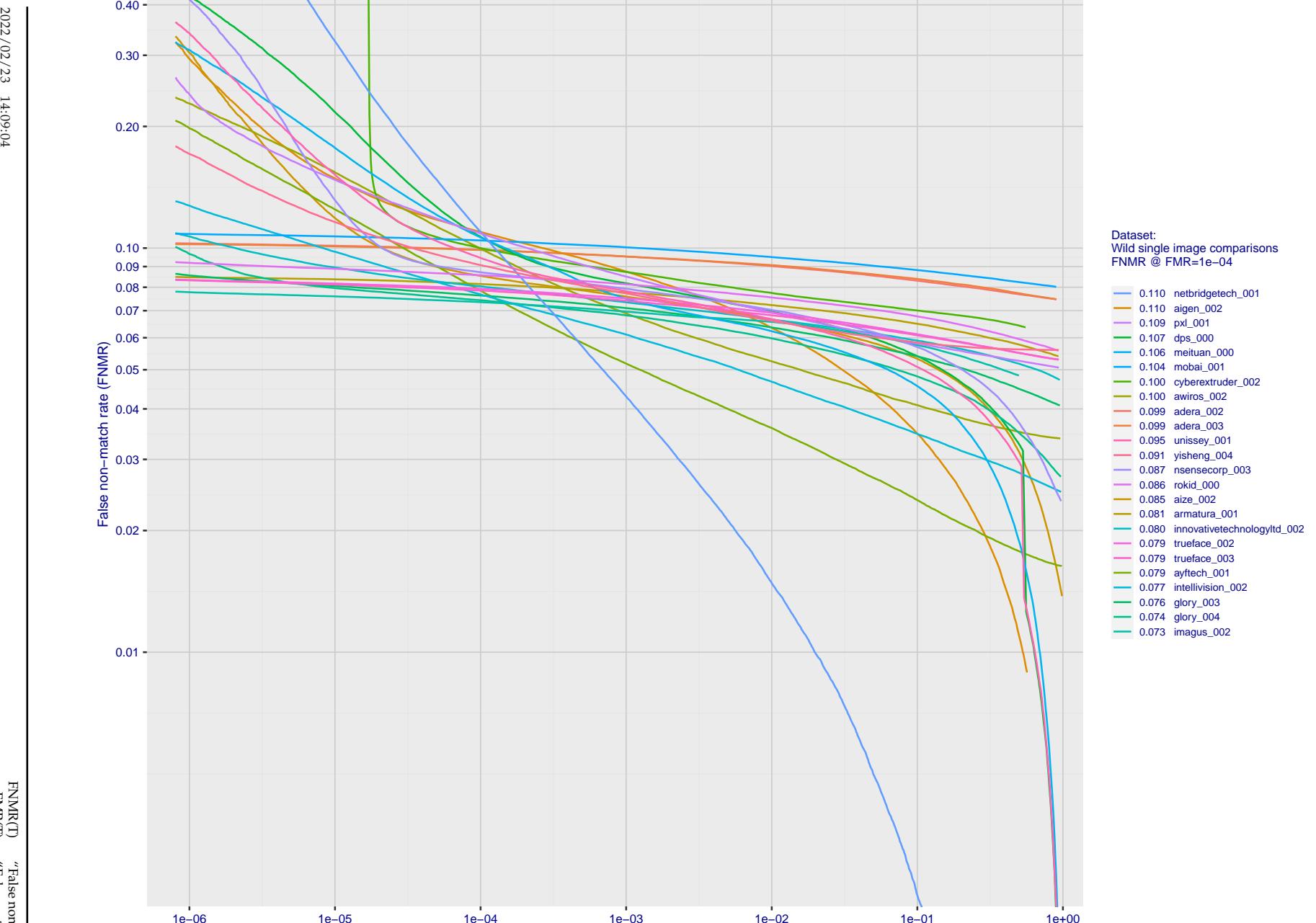


Figure 92: For the 2018 wild image comparisons, detection error tradeoff (DET) characteristics showing false non-match rate vs. false match rate plotted parametrically on threshold, T. The scales are logarithmic in order to show several decades of FMR.

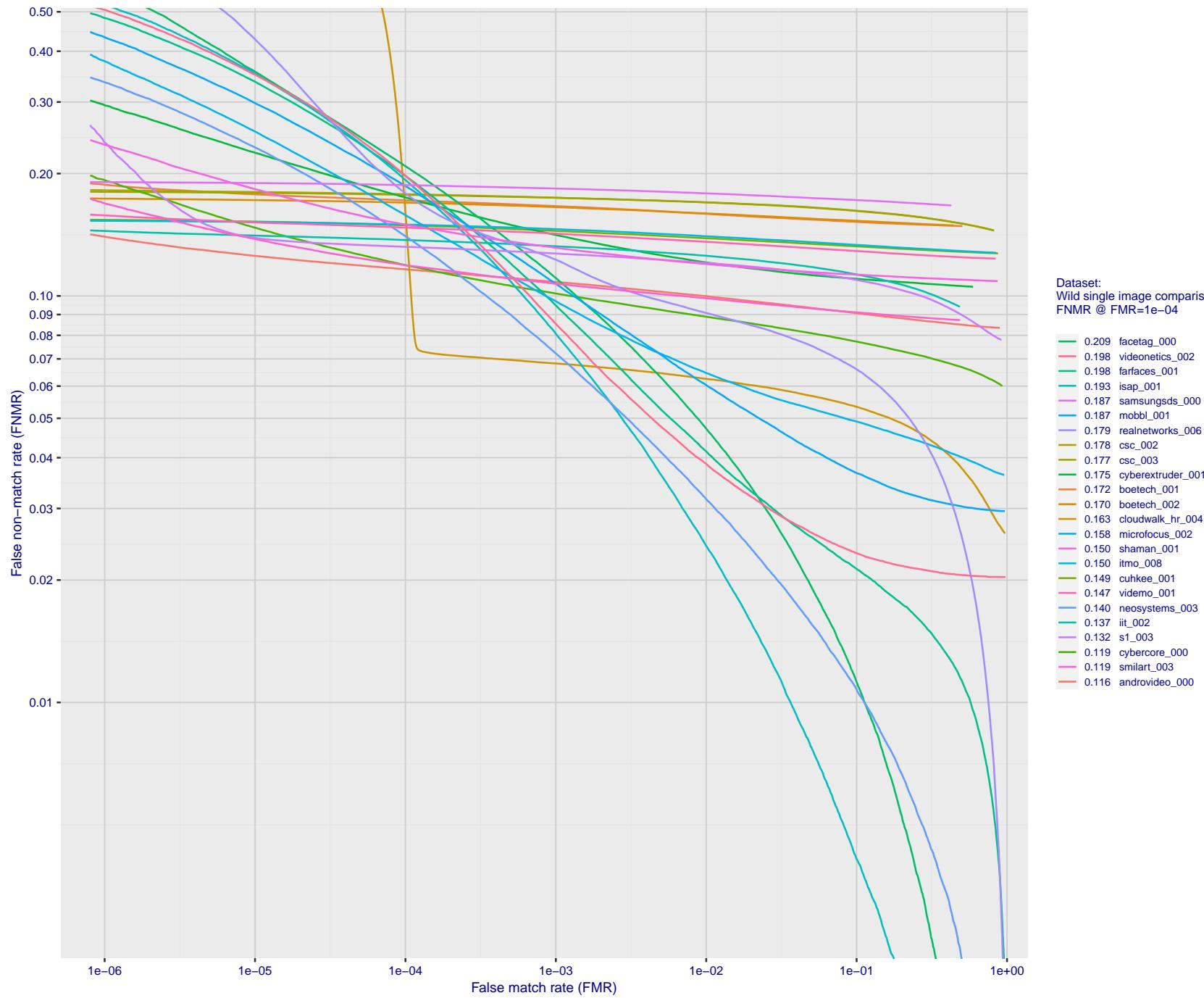


Figure 93: For the 2018 wild image comparisons, detection error tradeoff (DET) characteristics showing false non-match rate vs. false match rate plotted parametrically on threshold, T. The scales are logarithmic in order to show several decades of FMR.

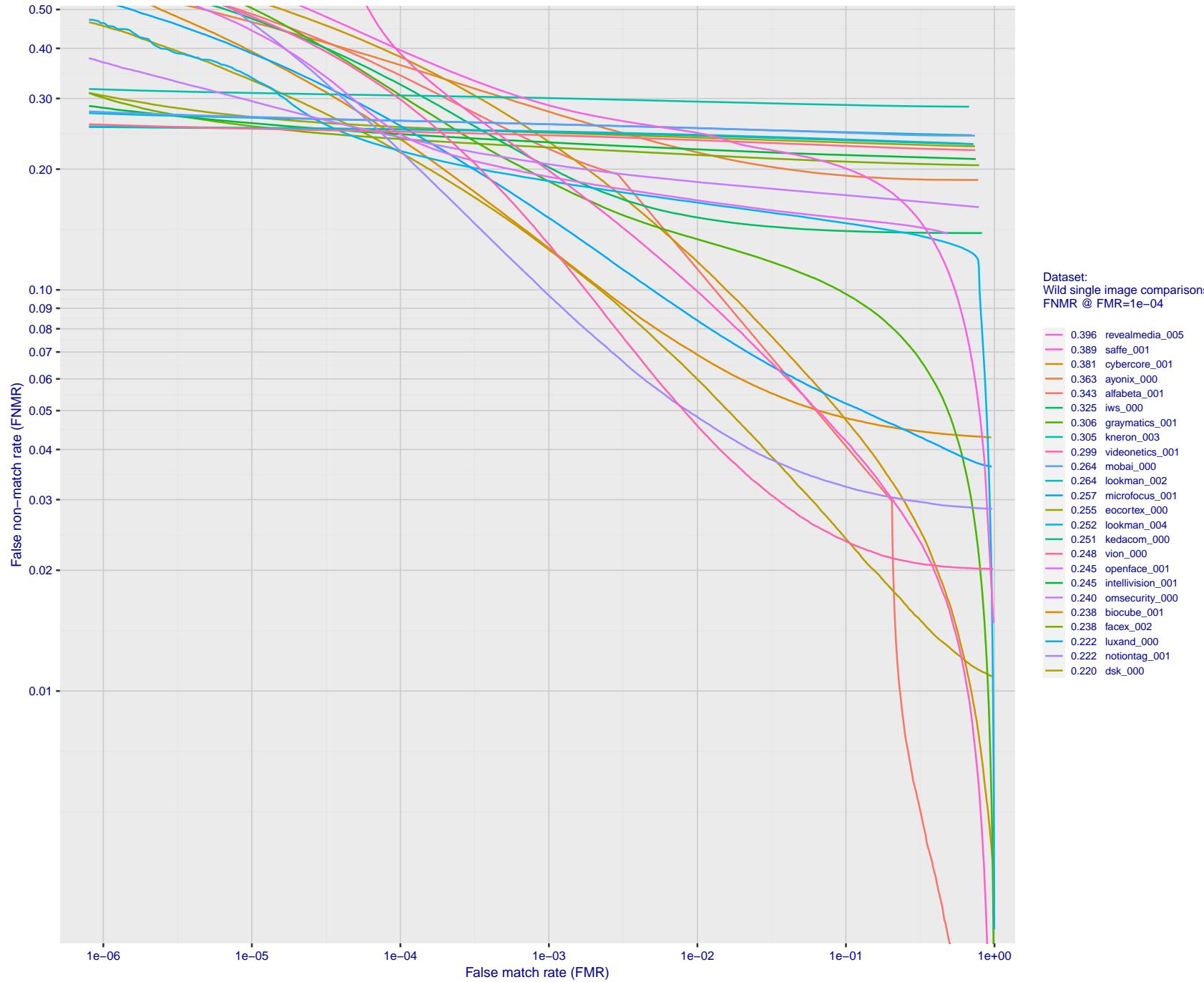


Figure 94: For the 2018 wild image comparisons, detection error tradeoff (DET) characteristics showing false non-match rate vs. false match rate plotted parametrically on threshold, T . The scales are logarithmic in order to show several decades of FMR.

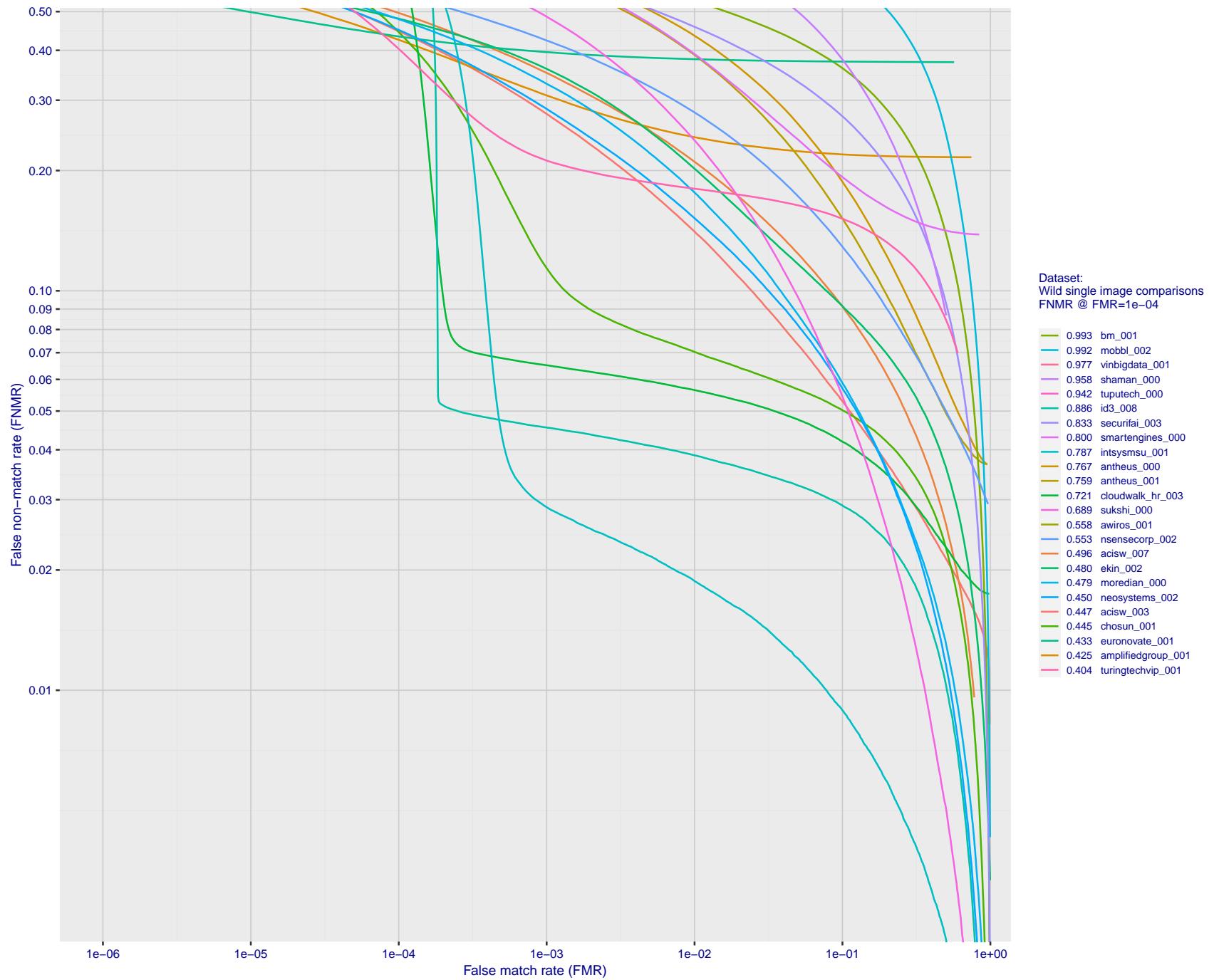


Figure 95: For the 2018 wild image comparisons, detection error tradeoff (DET) characteristics showing false non-match rate vs. false match rate plotted parametrically on threshold, T . The scales are logarithmic in order to show several decades of FMR.

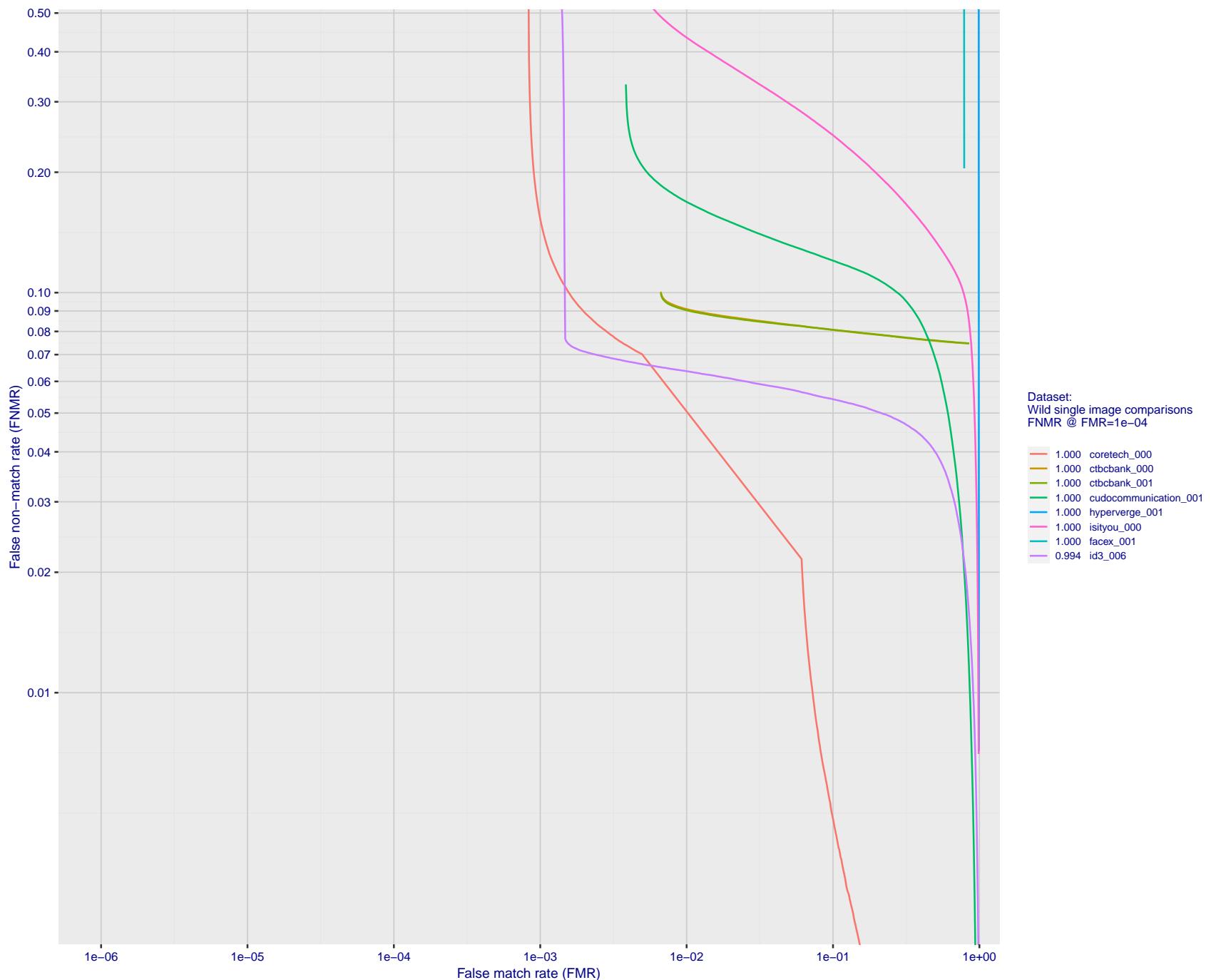


Figure 96: For the 2018 wild image comparisons, detection error tradeoff (DET) characteristics showing false non-match rate vs. false match rate plotted parametrically on threshold, T . The scales are logarithmic in order to show several decades of FMR.

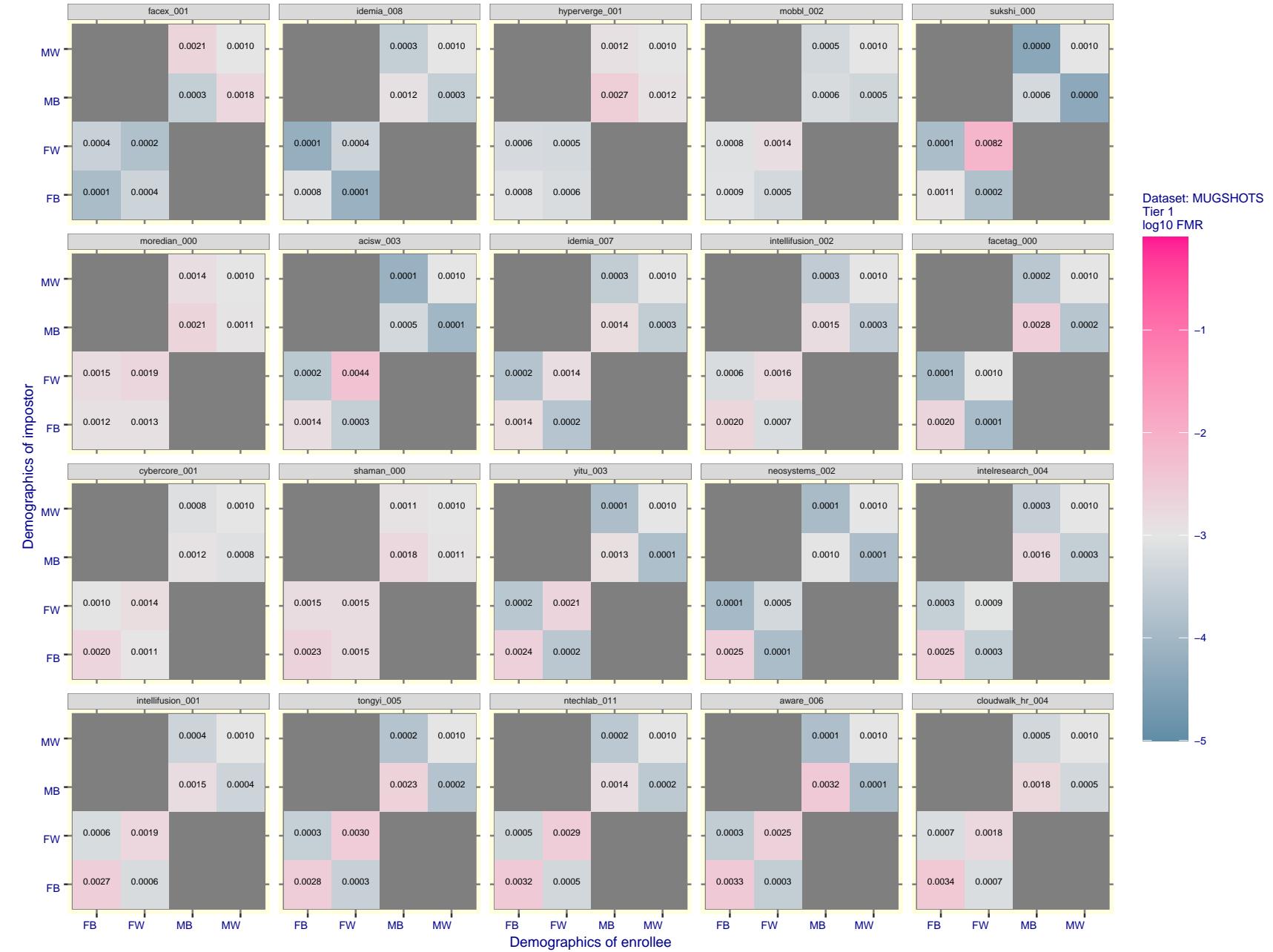


Figure 97: For the mugshot images, FMR for same-sex impostor pairs of images annotated with codes for black female, black male, white female, white male. The threshold is set for each algorithm to give FMR = 0.001 for white males which is the demographic that usually gives the lowest FMR. This means the top right box is the same color in all panels. The panels are sorted over multiple pages in order of FMR on black females, which is the demographic that usually gives the highest FMR.

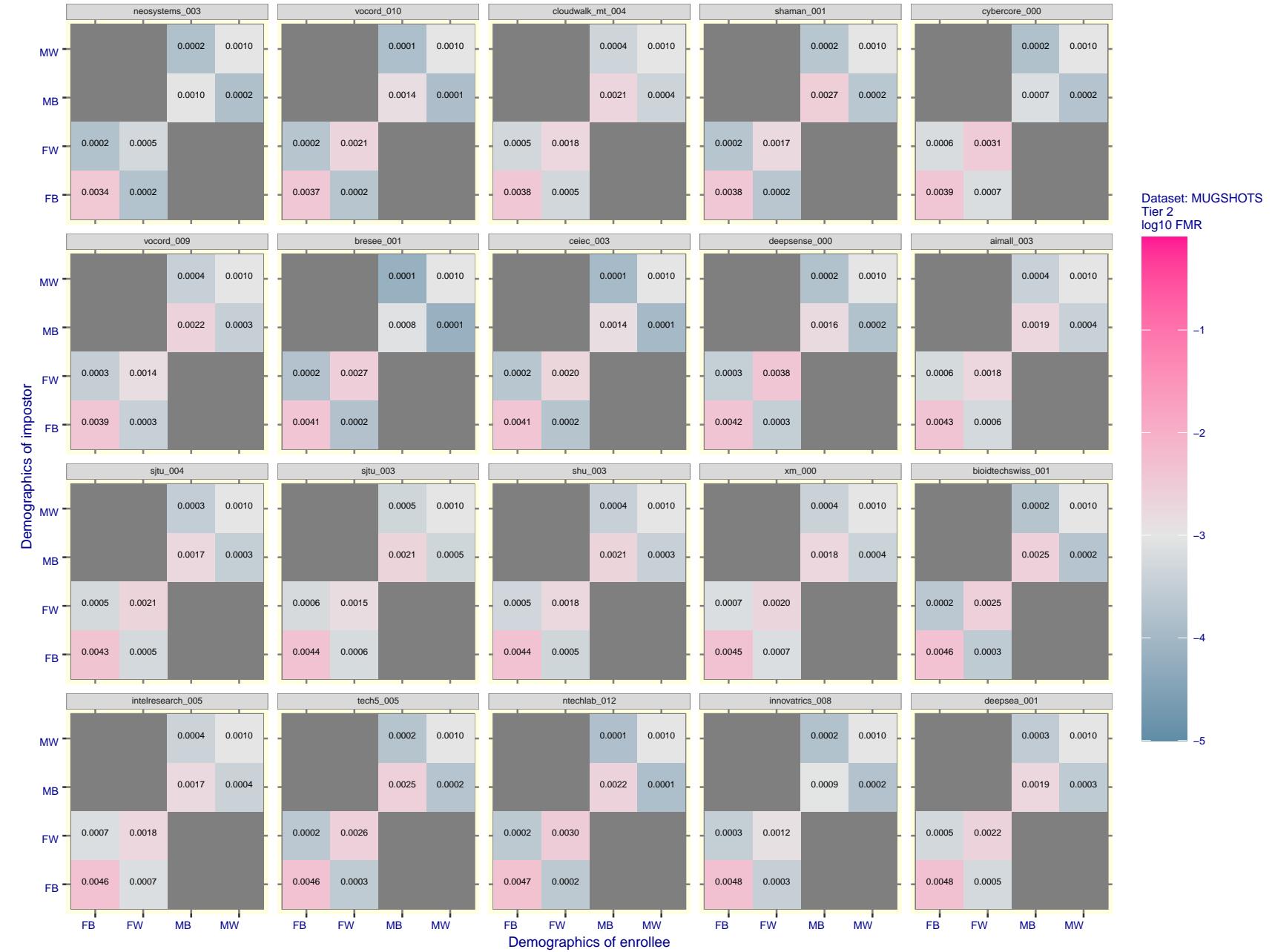


Figure 98: For the mugshot images, FMR for same-sex impostor pairs of images annotated with codes for black female, black male, white female, white male. The threshold is set for each algorithm to give $FMR = 0.001$ for white males which is the demographic that usually gives the lowest FMR. This means the top right box is the same color in all panels. The panels are sorted over multiple pages in order of FMR on black females, which is the demographic that usually gives the highest FMR.

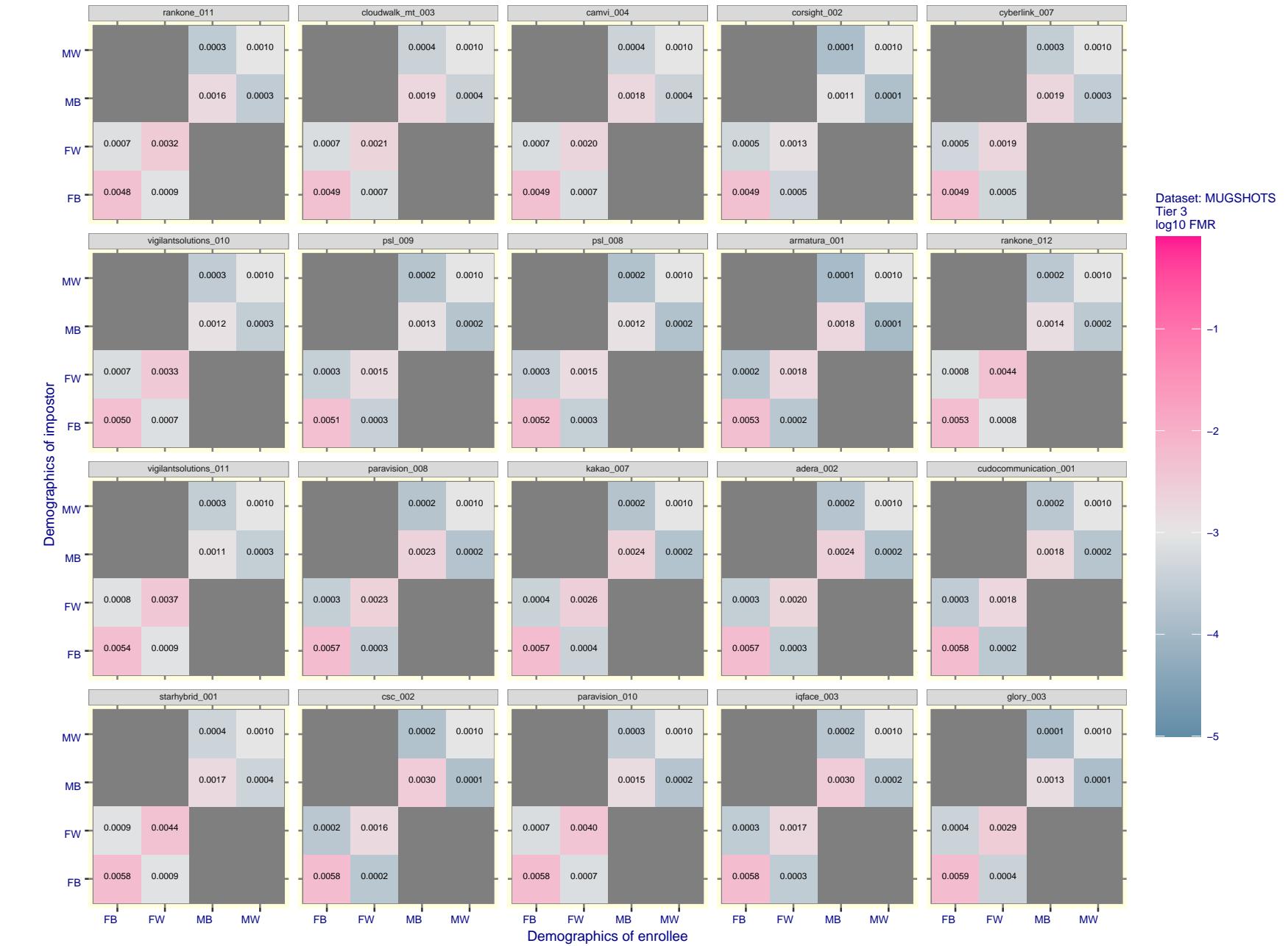


Figure 99: For the mugshot images, FMR for same-sex impostor pairs of images annotated with codes for black female, black male, white female, white male. The threshold is set for each algorithm to give $FMR = 0.001$ for white males which is the demographic that usually gives the lowest FMR. This means the top right box is the same color in all panels. The panels are sorted over multiple pages in order of FMR on black females, which is the demographic that usually gives the highest FMR.

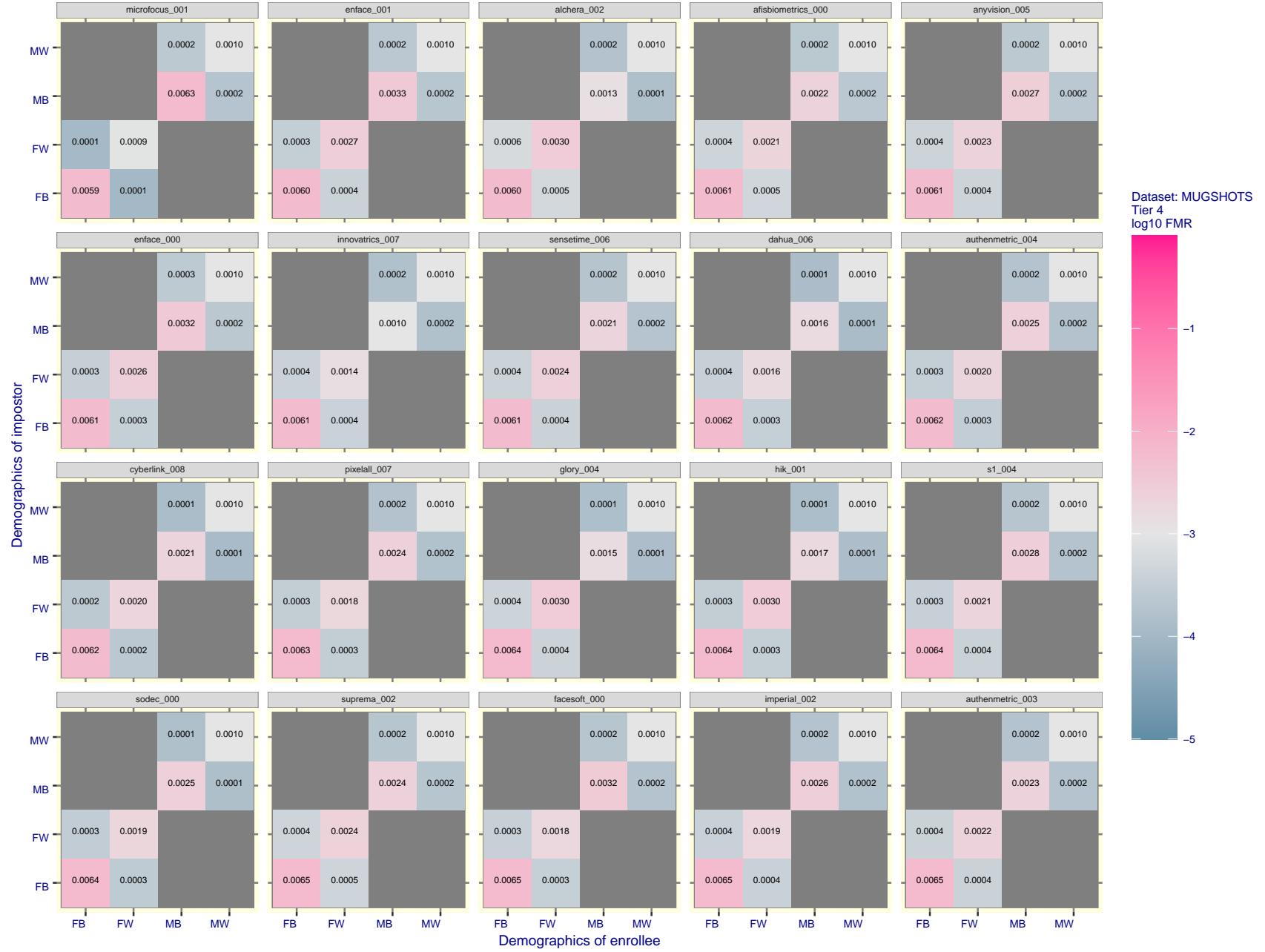


Figure 100: For the mugshot images, FMR for same-sex impostor pairs of images annotated with codes for black female, black male, white female, white male. The threshold is set for each algorithm to give FMR = 0.001 for white males which is the demographic that usually gives the lowest FMR. This means the top right box is the same color in all panels. The panels are sorted over multiple pages in order of FMR on black females, which is the demographic that usually gives the highest FMR.

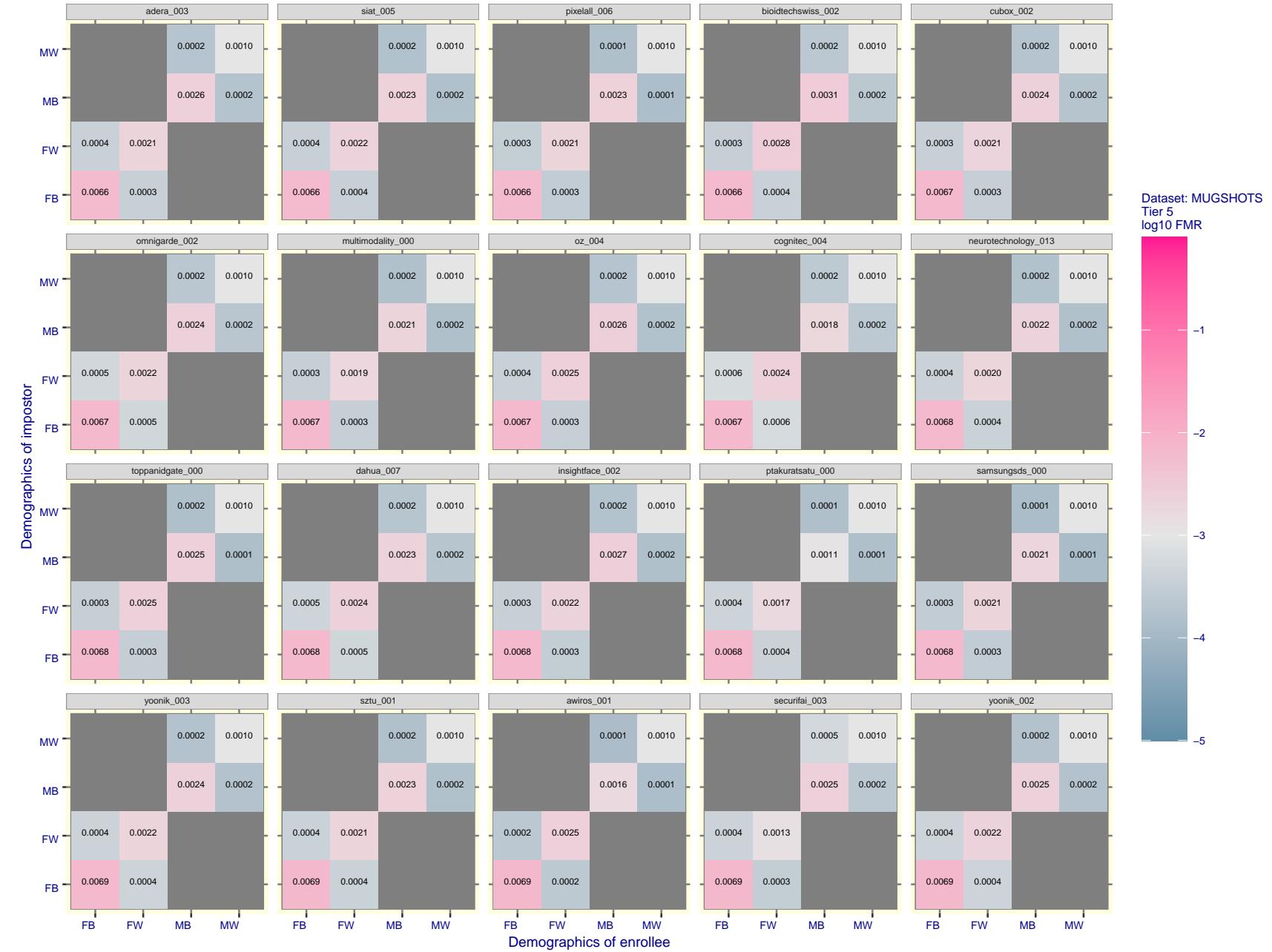


Figure 101: For the mugshot images, FMR for same-sex impostor pairs of images annotated with codes for black female, black male, white female, white male. The threshold is set for each algorithm to give $\text{FMR} = 0.001$ for white males which is the demographic that usually gives the lowest FMR. This means the top right box is the same color in all panels. The panels are sorted over multiple pages in order of FMR on black females, which is the demographic that usually gives the highest FMR.

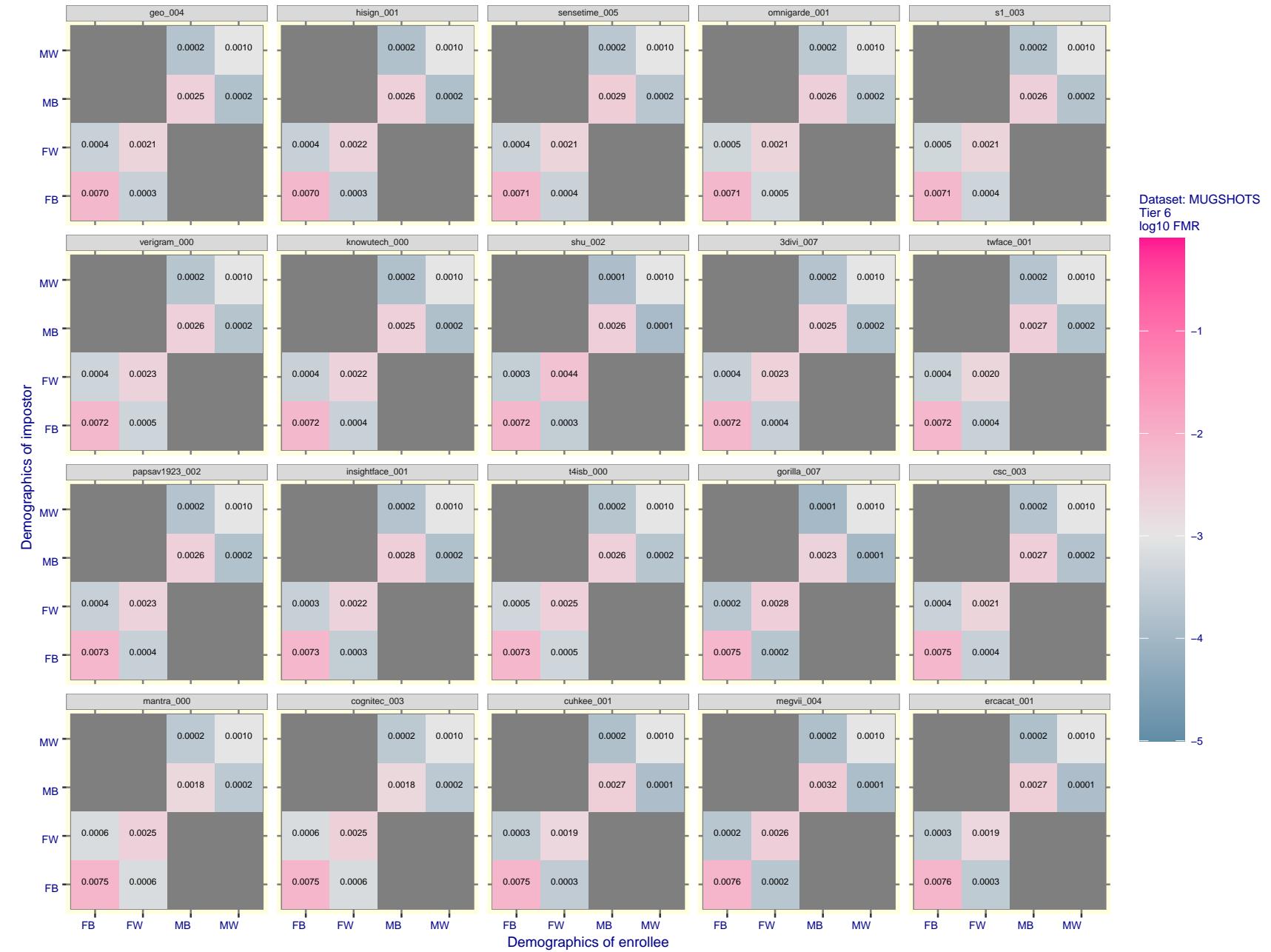


Figure 102: For the mugshot images, FMR for same-sex impostor pairs of images annotated with codes for black female, black male, white female, white male. The threshold is set for each algorithm to give $\text{FMR} = 0.001$ for white males which is the demographic that usually gives the lowest FMR. This means the top right box is the same color in all panels. The panels are sorted over multiple pages in order of FMR on black females, which is the demographic that usually gives the highest FMR.

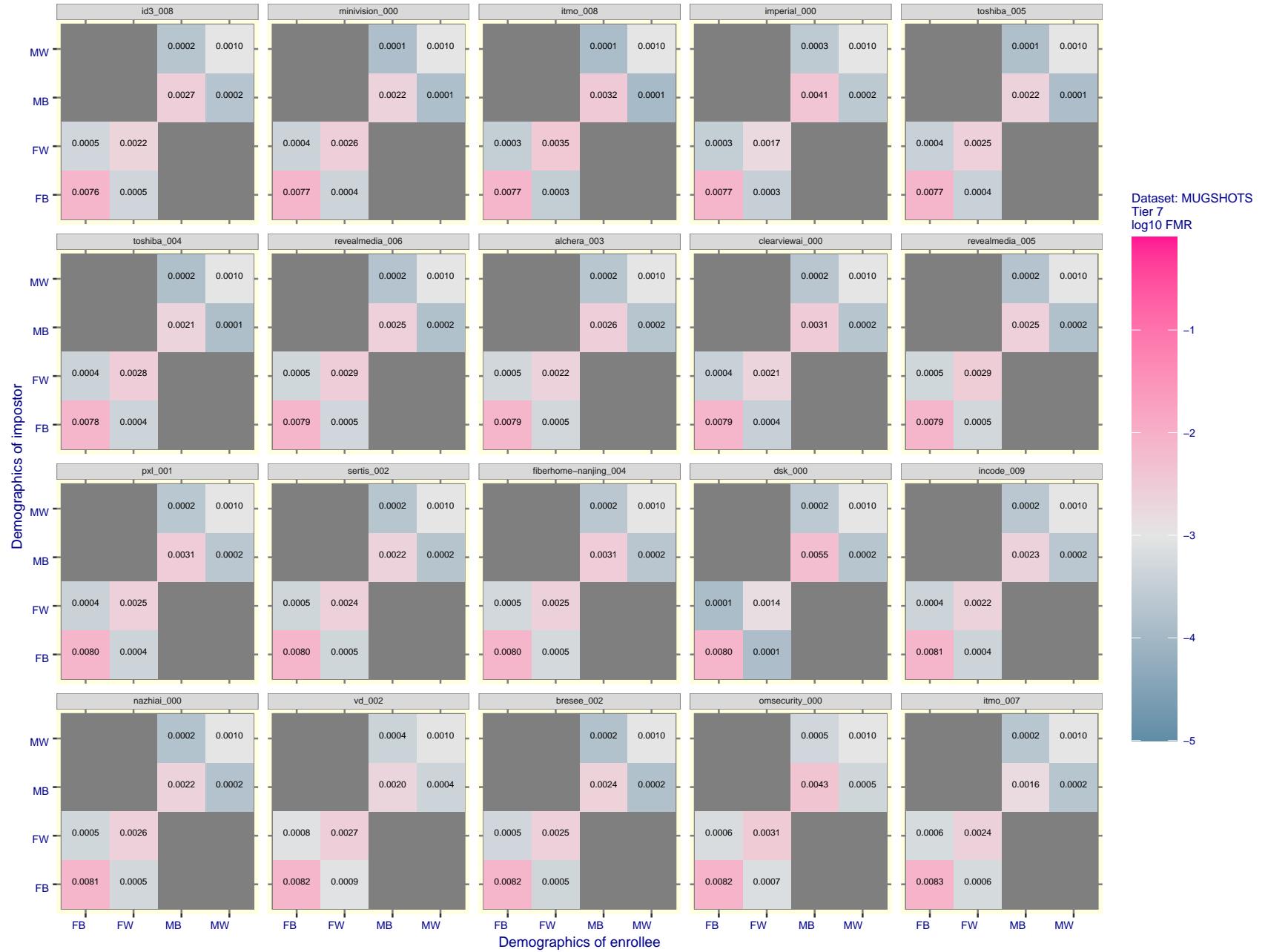


Figure 103: For the mugshot images, FMR for same-sex impostor pairs of images annotated with codes for black female, black male, white female, white male. The threshold is set for each algorithm to give FMR = 0.001 for white males which is the demographic that usually gives the lowest FMR. This means the top right box is the same color in all panels. The panels are sorted over multiple pages in order of FMR on black females, which is the demographic that usually gives the highest FMR.

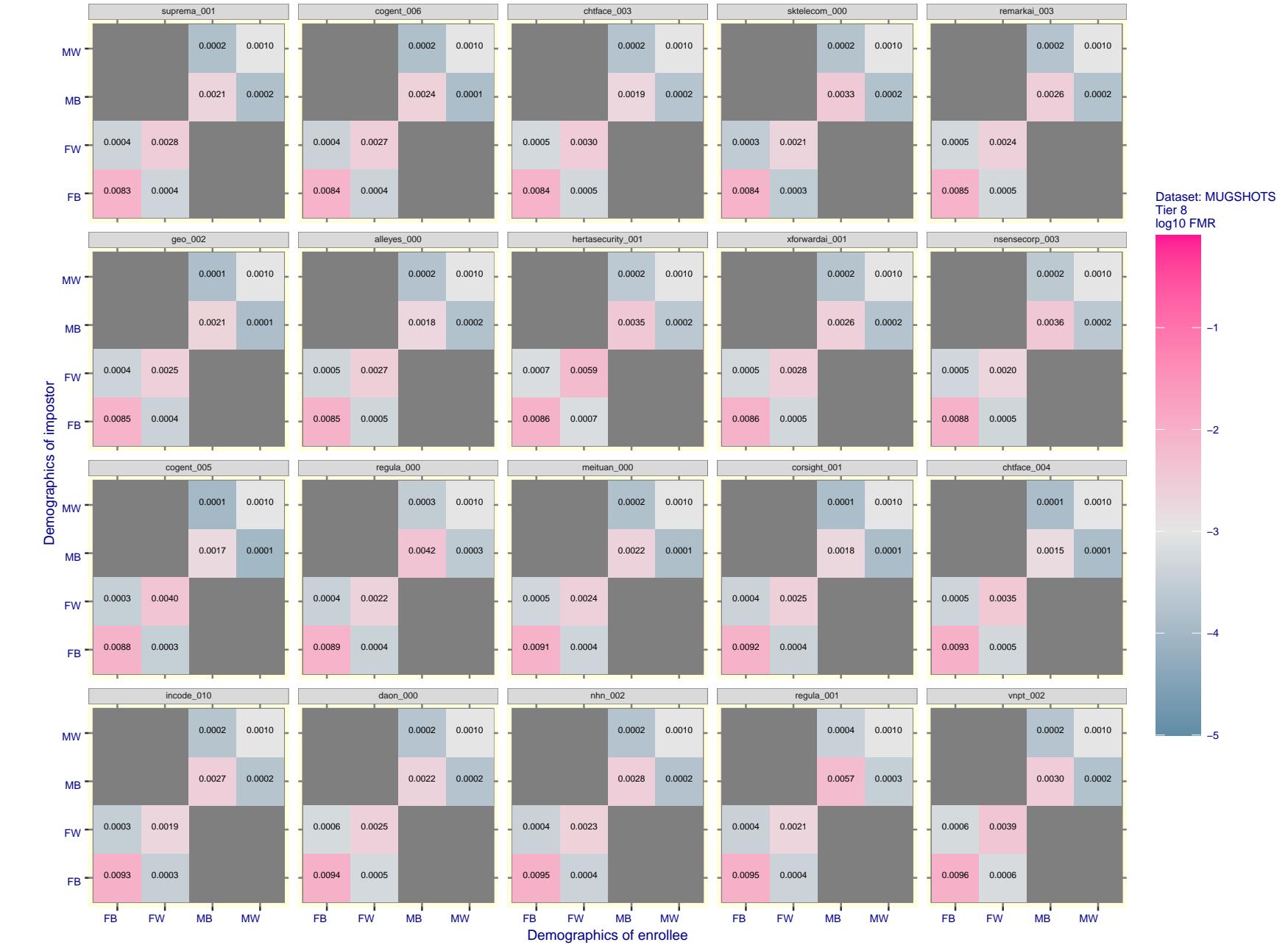


Figure 104: For the mugshot images, FMR for same-sex impostor pairs of images annotated with codes for black female, black male, white female, white male. The threshold is set for each algorithm to give $FMR = 0.001$ for white males which is the demographic that usually gives the lowest FMR. This means the top right box is the same color in all panels. The panels are sorted over multiple pages in order of FMR on black females, which is the demographic that usually gives the highest FMR.

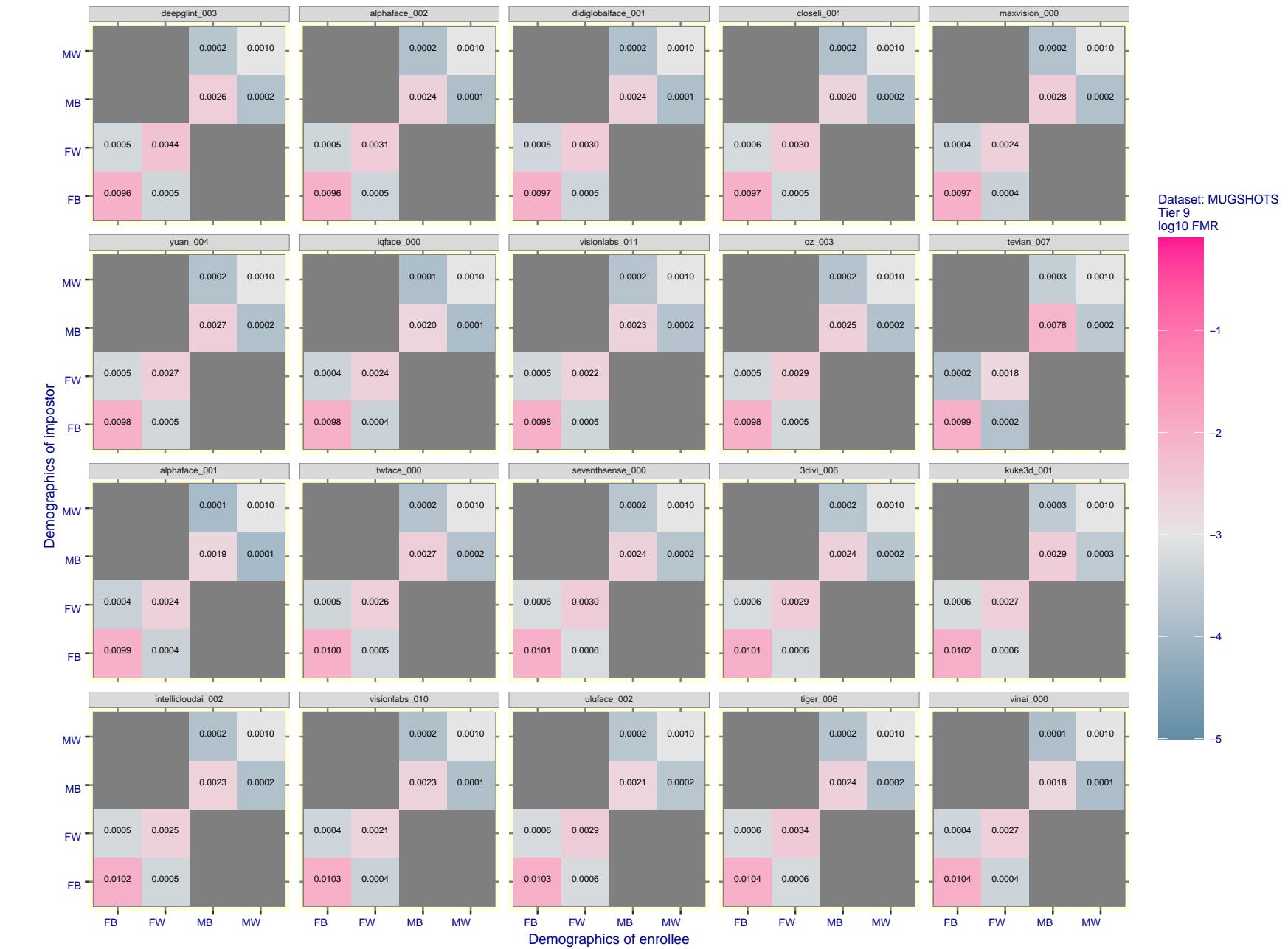


Figure 105: For the mugshot images, FMR for same-sex impostor pairs of images annotated with codes for black female, black male, white female, white male. The threshold is set for each algorithm to give FMR = 0.001 for white males which is the demographic that usually gives the lowest FMR. This means the top right box is the same color in all panels. The panels are sorted over multiple pages in order of FMR on black females, which is the demographic that usually gives the highest FMR.

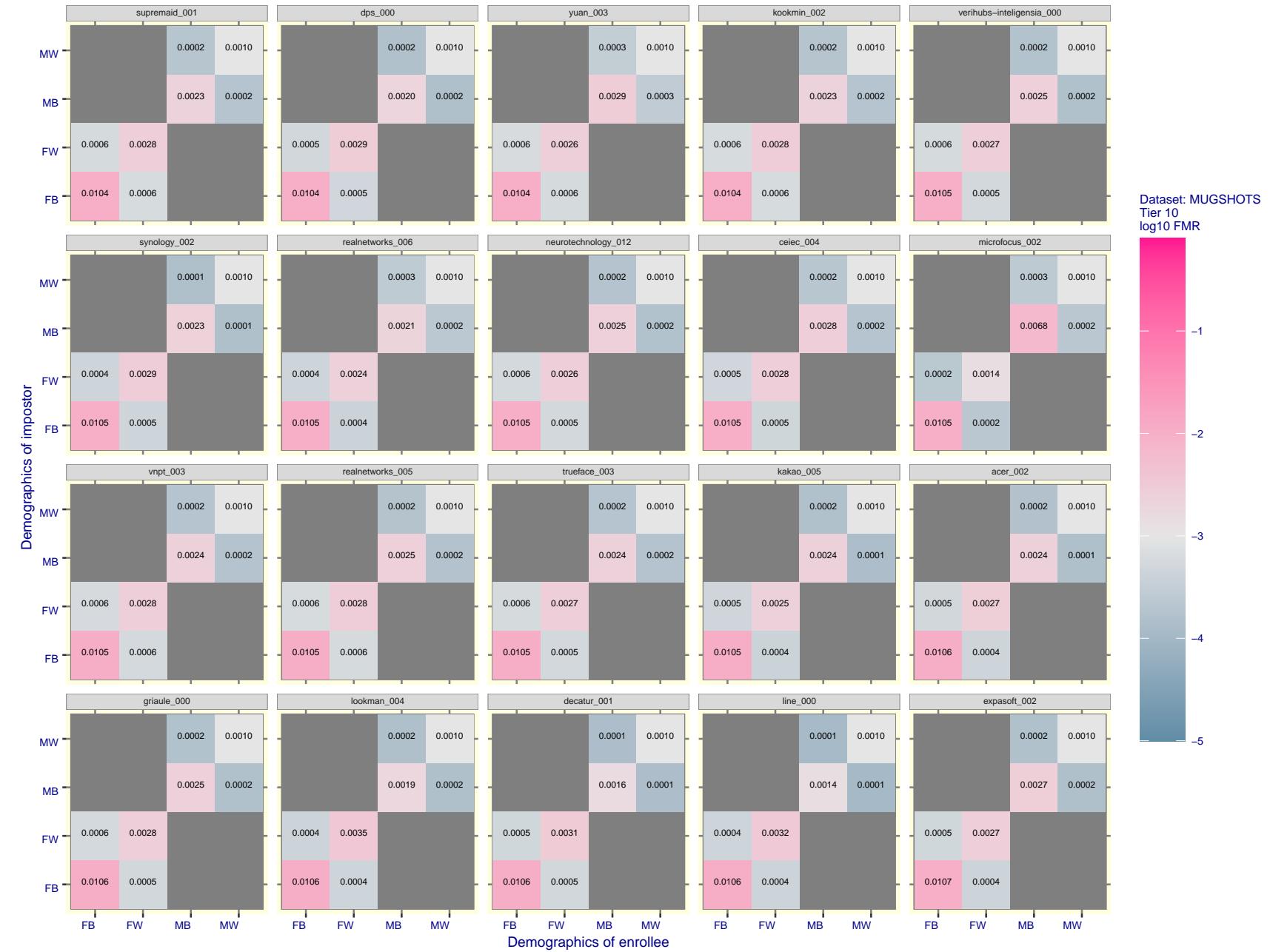


Figure 106: For the mugshot images, FMR for same-sex impostor pairs of images annotated with codes for black female, black male, white female, white male. The threshold is set for each algorithm to give $FMR = 0.001$ for white males which is the demographic that usually gives the lowest FMR. This means the top right box is the same color in all panels. The panels are sorted over multiple pages in order of FMR on black females, which is the demographic that usually gives the highest FMR.

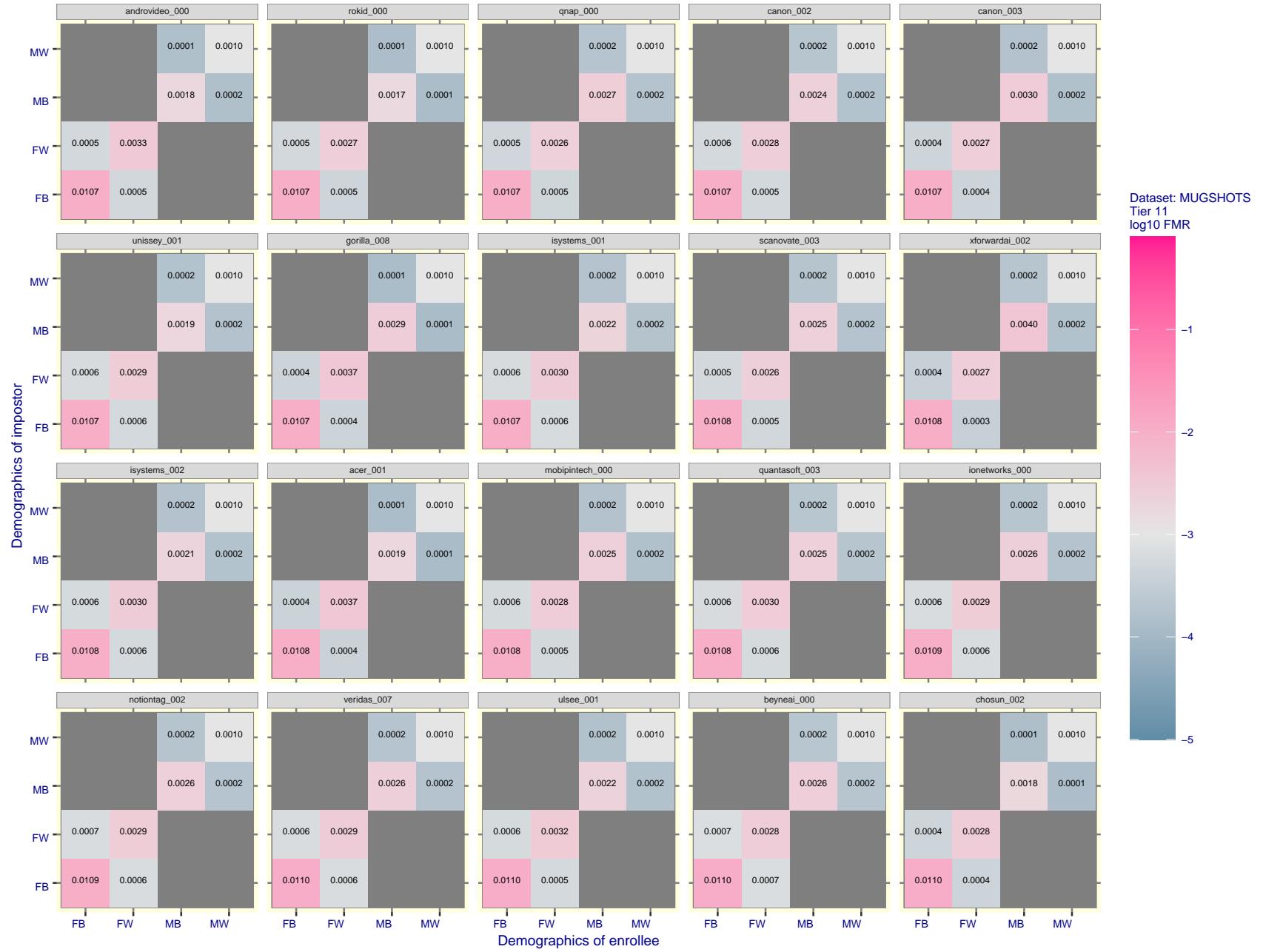


Figure 107: For the mugshot images, FMR for same-sex impostor pairs of images annotated with codes for black female, black male, white female, white male. The threshold is set for each algorithm to give FMR = 0.001 for white males which is the demographic that usually gives the lowest FMR. This means the top right box is the same color in all panels. The panels are sorted over multiple pages in order of FMR on black females, which is the demographic that usually gives the highest FMR.

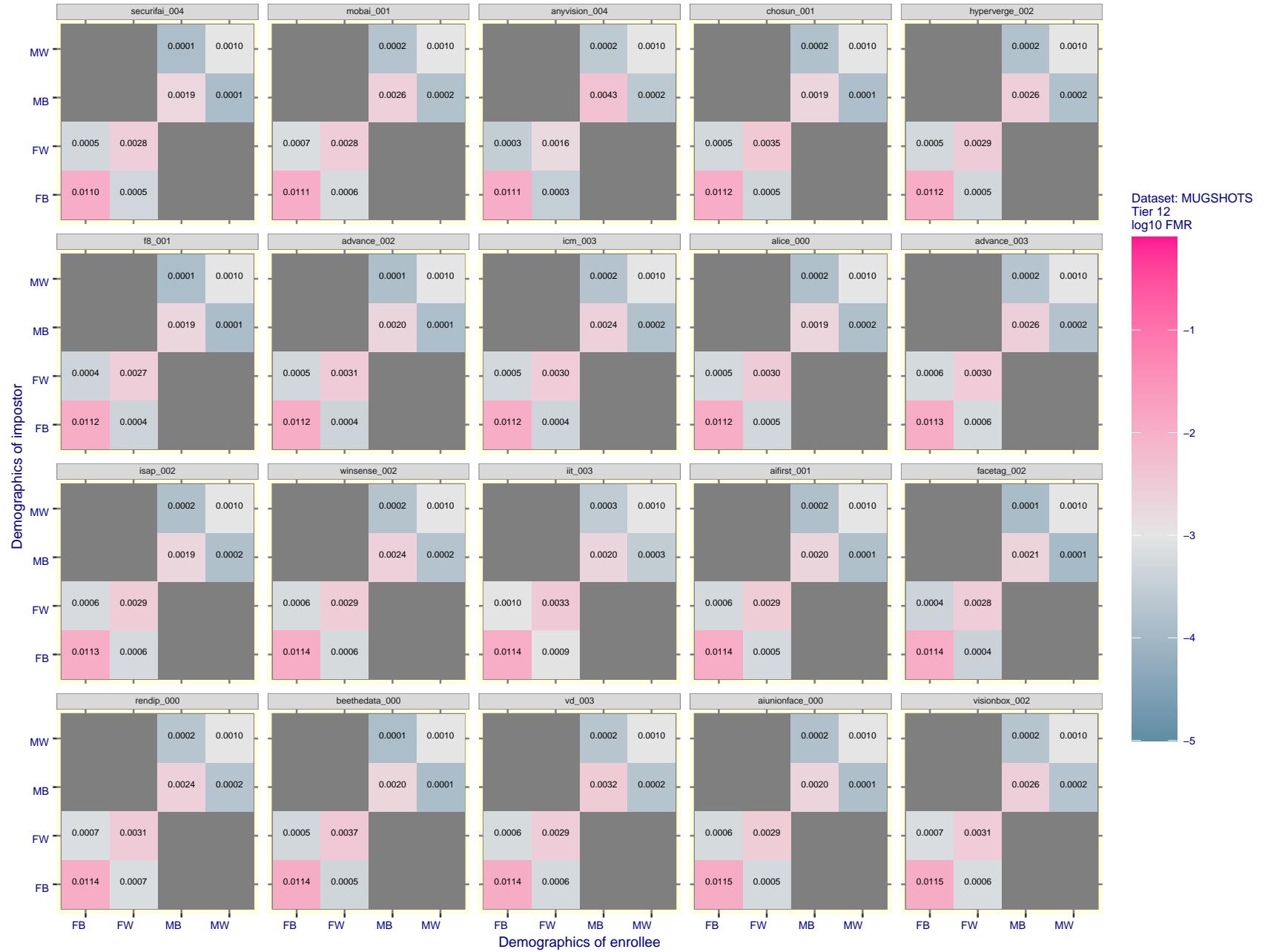


Figure 108: For the mugshot images, FMR for same-sex impostor pairs of images annotated with codes for black female, black male, white female, white male. The threshold is set for each algorithm to give FMR = 0.001 for white males which is the demographic that usually gives the lowest FMR. This means the top right box is the same color in all panels. The panels are sorted over multiple pages in order of FMR on black females, which is the demographic that usually gives the highest FMR.

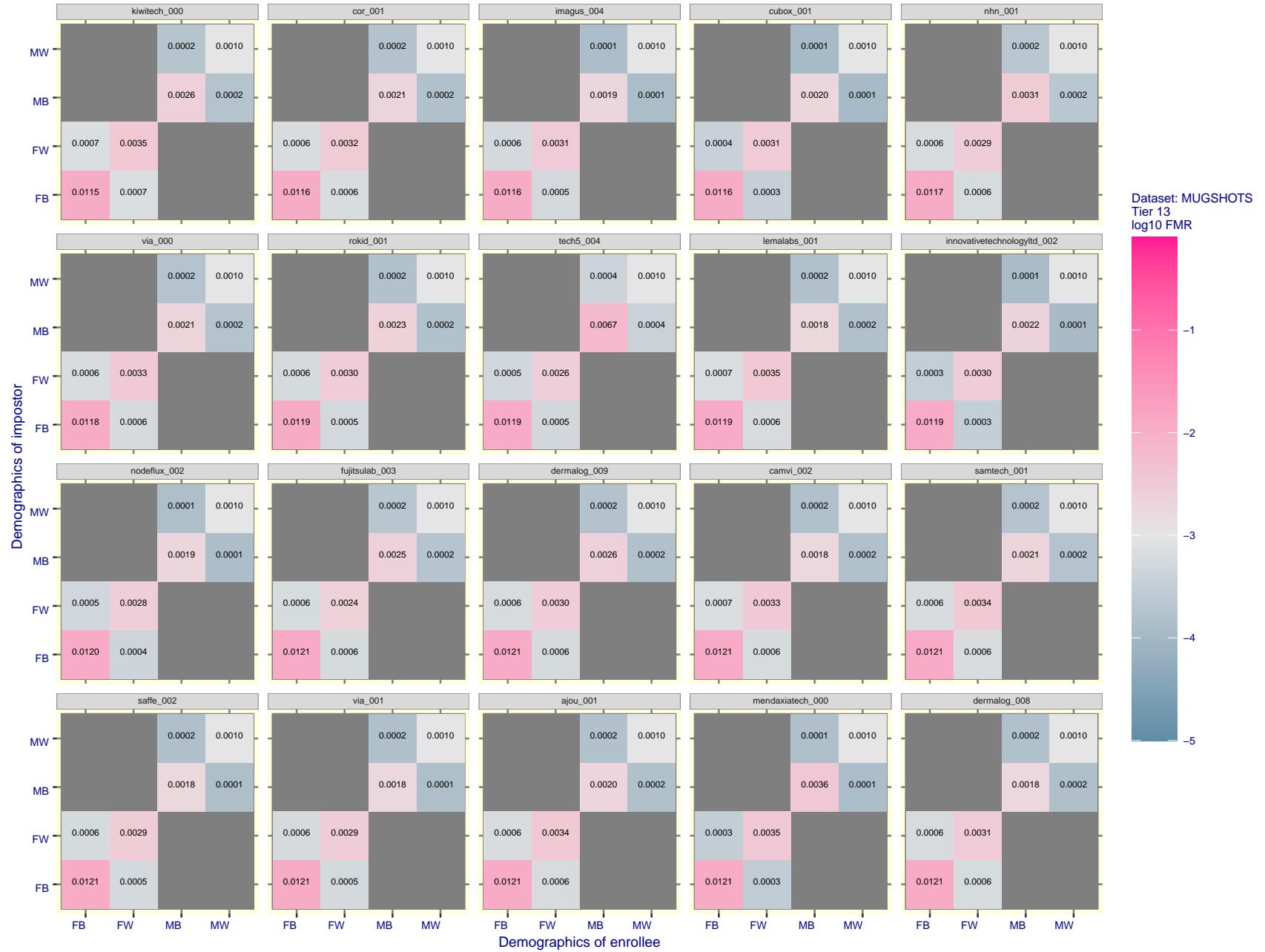


Figure 109: For the mugshot images, FMR for same-sex impostor pairs of images annotated with codes for black female, black male, white female, white male. The threshold is set for each algorithm to give FMR = 0.001 for white males which is the demographic that usually gives the lowest FMR. This means the top right box is the same color in all panels. The panels are sorted over multiple pages in order of FMR on black females, which is the demographic that usually gives the highest FMR.

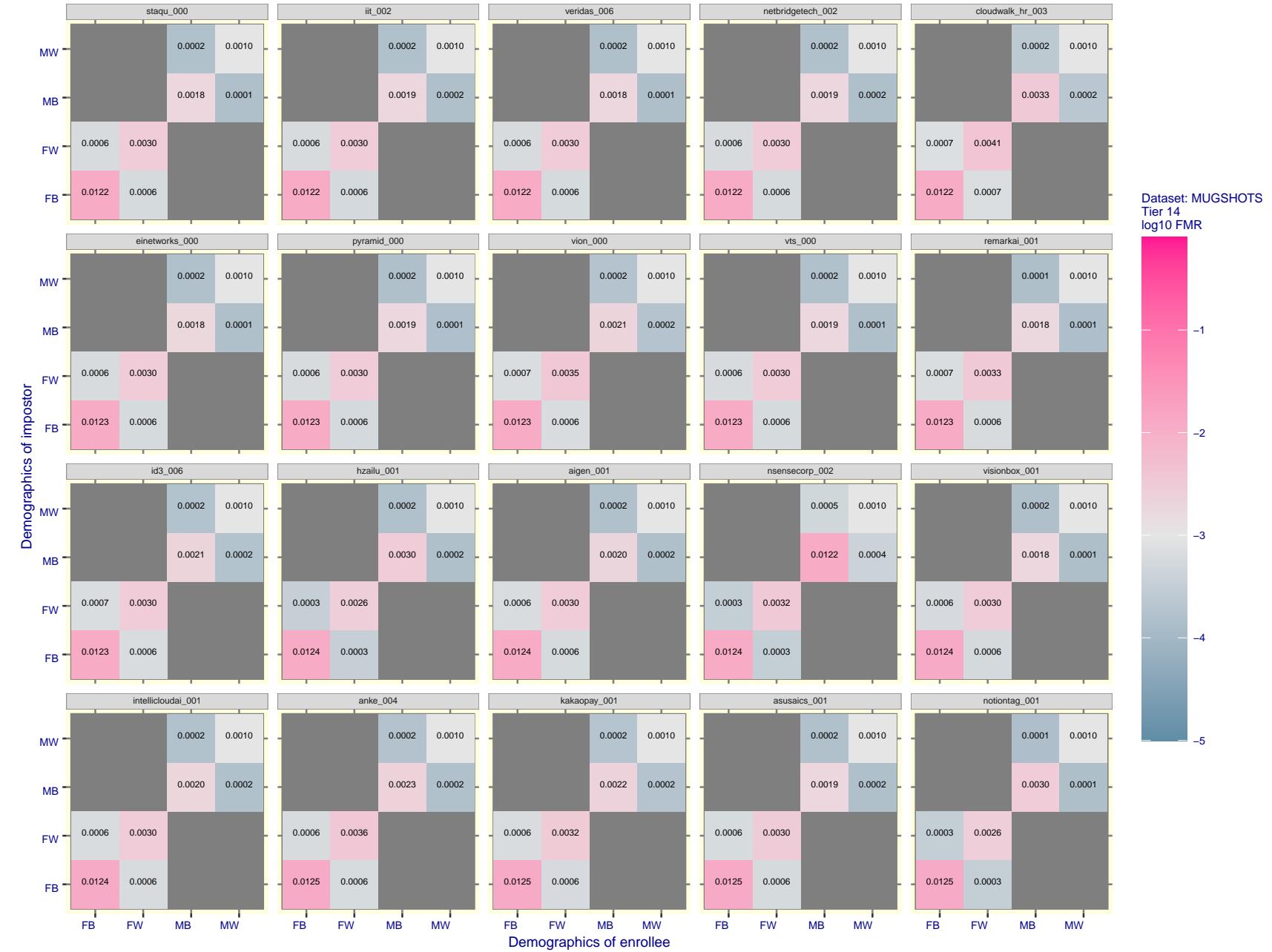


Figure 110: For the mugshot images, FMR for same-sex impostor pairs of images annotated with codes for black female, black male, white female, white male. The threshold is set for each algorithm to give FMR = 0.001 for white males which is the demographic that usually gives the lowest FMR. This means the top right box is the same color in all panels. The panels are sorted over multiple pages in order of FMR on black females, which is the demographic that usually gives the highest FMR.

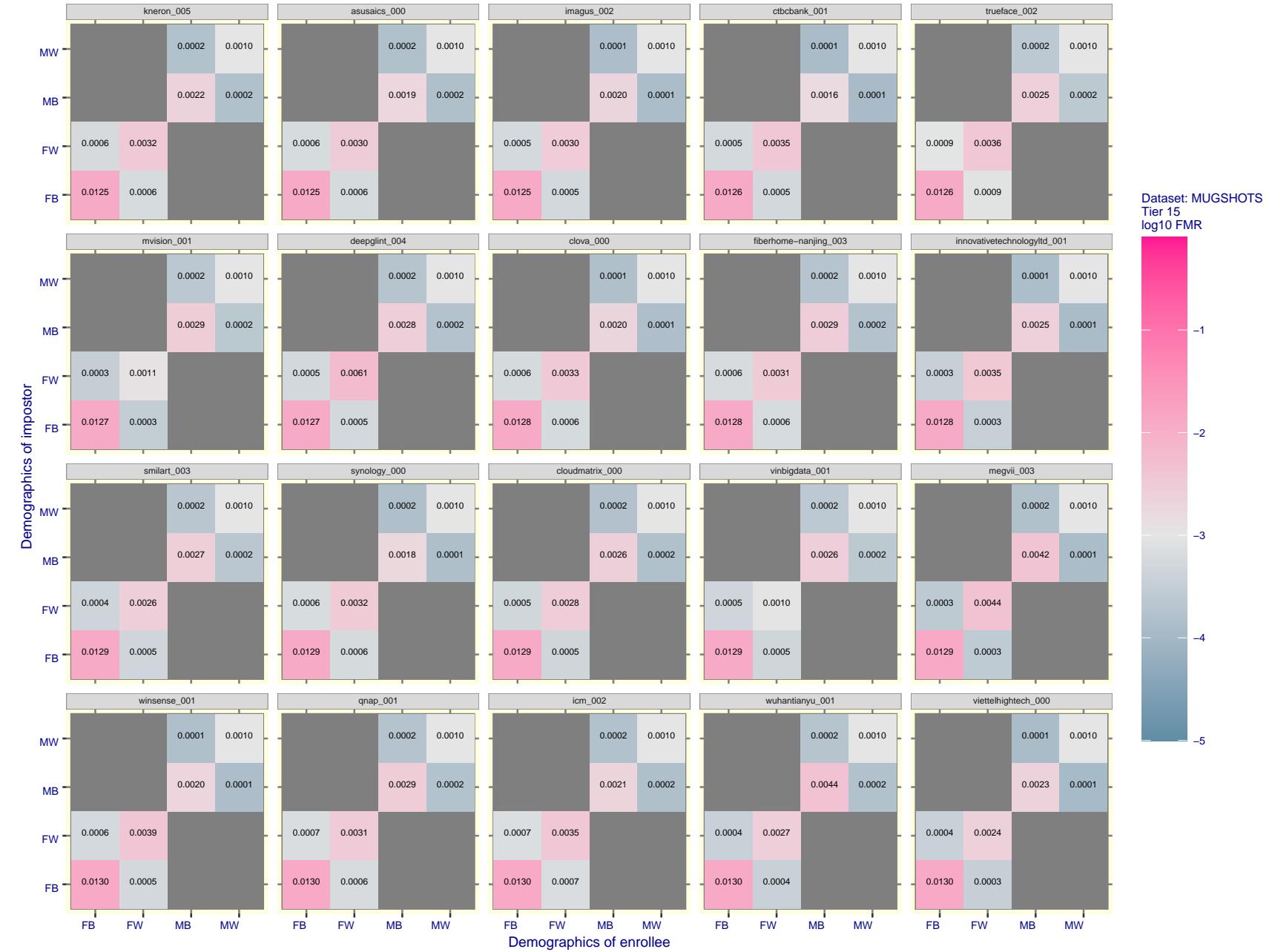


Figure 111: For the mugshot images, FMR for same-sex impostor pairs of images annotated with codes for black female, black male, white female, white male. The threshold is set for each algorithm to give FMR = 0.001 for white males which is the demographic that usually gives the lowest FMR. This means the top right box is the same color in all panels. The panels are sorted over multiple pages in order of FMR on black females, which is the demographic that usually gives the highest FMR.

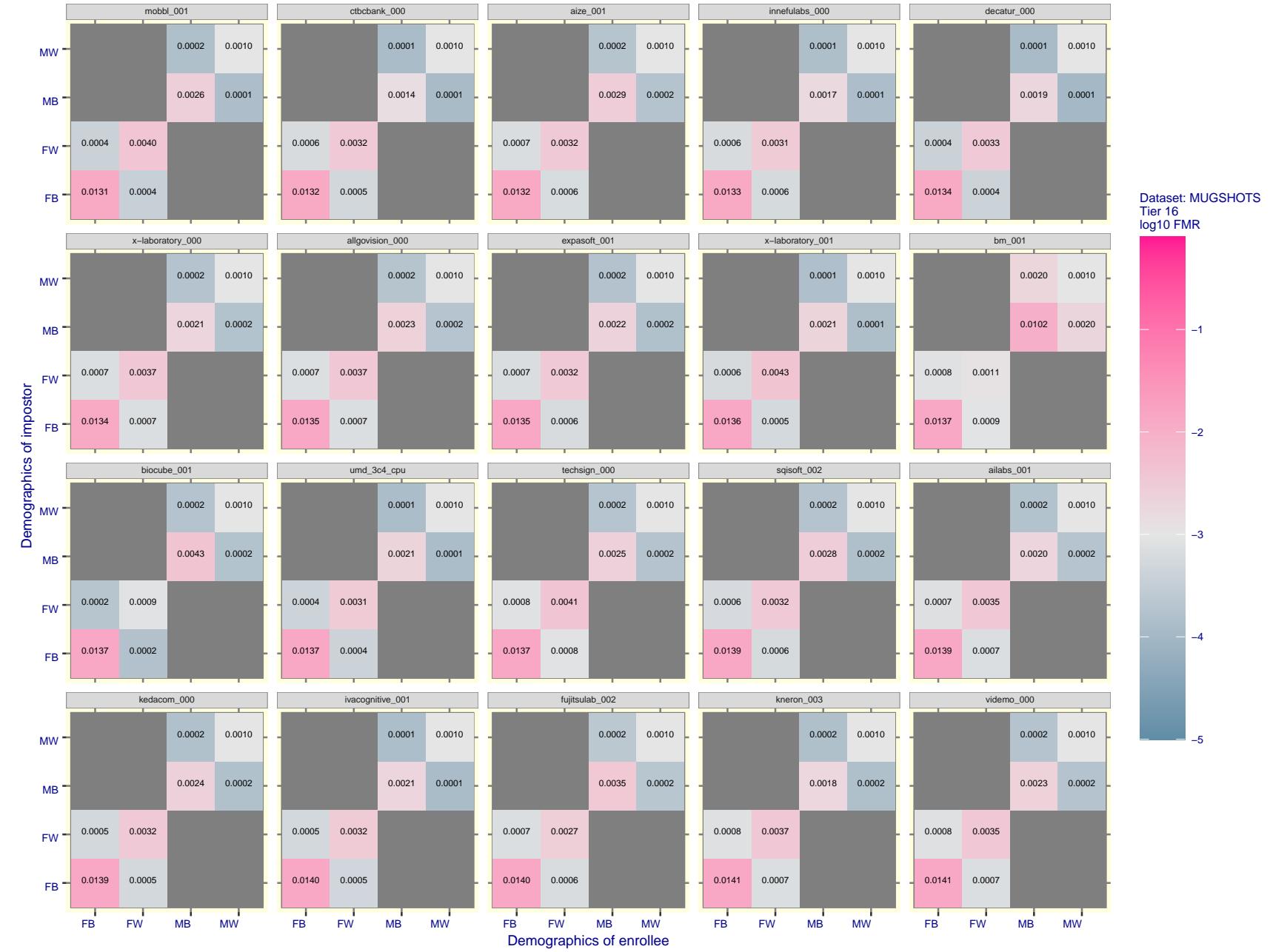


Figure 112: For the mugshot images, FMR for same-sex impostor pairs of images annotated with codes for black female, black male, white female, white male. The threshold is set for each algorithm to give $FMR = 0.001$ for white males which is the demographic that usually gives the lowest FMR. This means the top right box is the same color in all panels. The panels are sorted over multiple pages in order of FMR on black females, which is the demographic that usually gives the highest FMR.

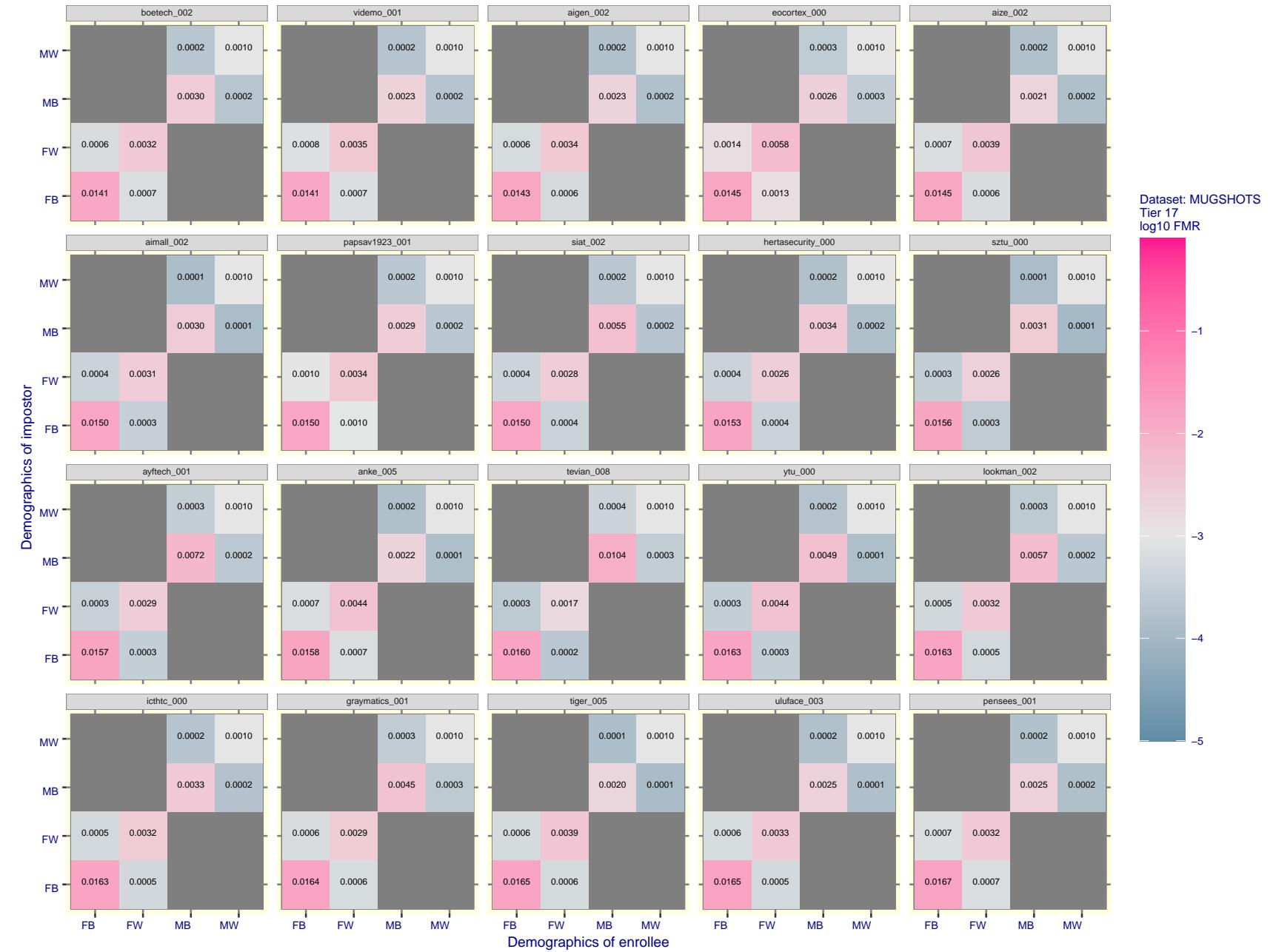


Figure 113: For the mugshot images, FMR for same-sex impostor pairs of images annotated with codes for black female, black male, white female, white male. The threshold is set for each algorithm to give $FMR = 0.001$ for white males which is the demographic that usually gives the lowest FMR. This means the top right box is the same color in all panels. The panels are sorted over multiple pages in order of FMR on black females, which is the demographic that usually gives the highest FMR.

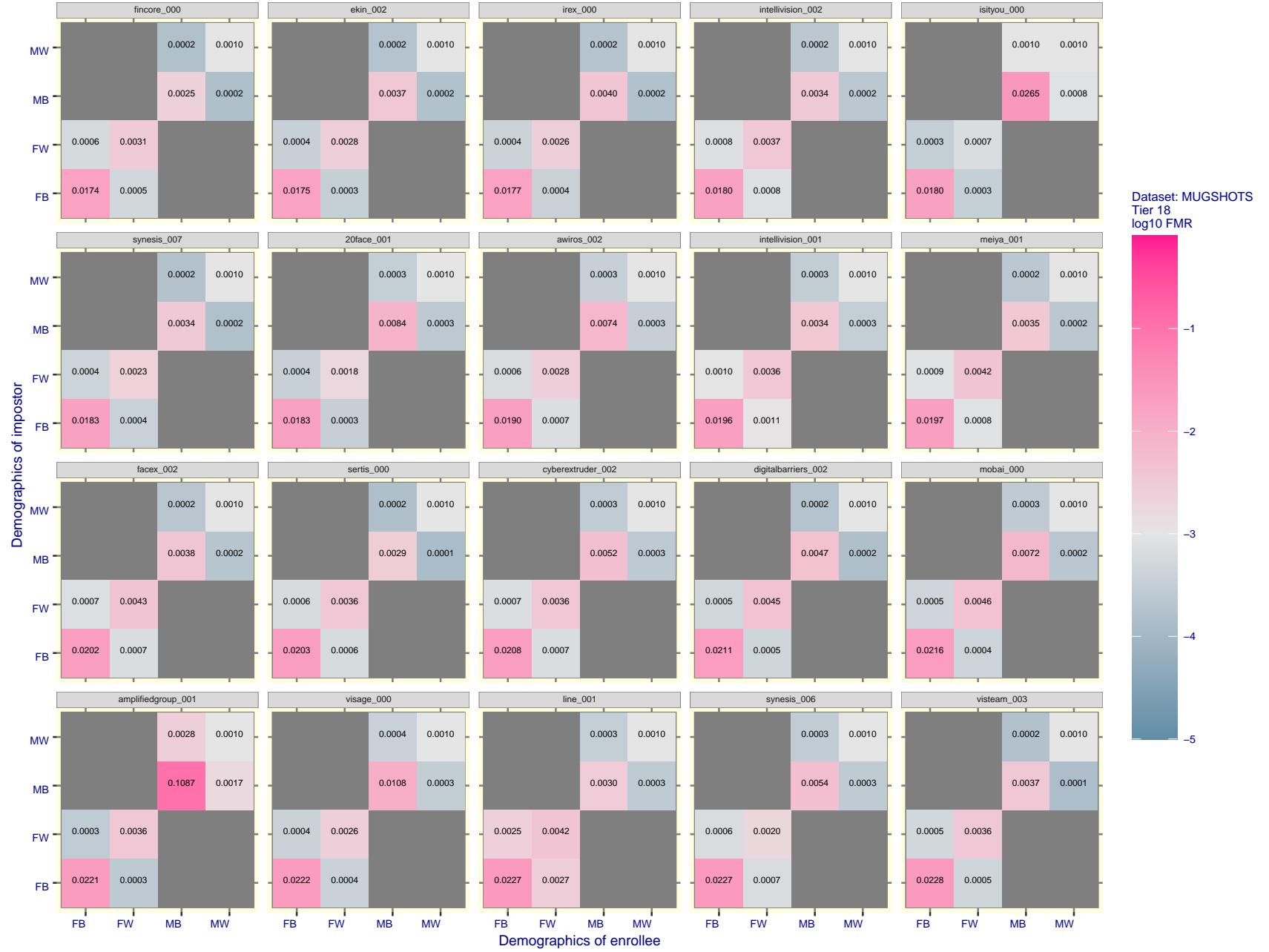


Figure 114: For the mugshot images, FMR for same-sex impostor pairs of images annotated with codes for black female, black male, white female, white male. The threshold is set for each algorithm to give FMR = 0.001 for white males which is the demographic that usually gives the lowest FMR. This means the top right box is the same color in all panels. The panels are sorted over multiple pages in order of FMR on black females, which is the demographic that usually gives the highest FMR.



Figure 115: For the mugshot images, FMR for same-sex impostor pairs of images annotated with codes for black female, black male, white female, white male. The threshold is set for each algorithm to give $FMR = 0.001$ for white males which is the demographic that usually gives the lowest FMR. This means the top right box is the same color in all panels. The panels are sorted over multiple pages in order of FMR on black females, which is the demographic that usually gives the highest FMR.

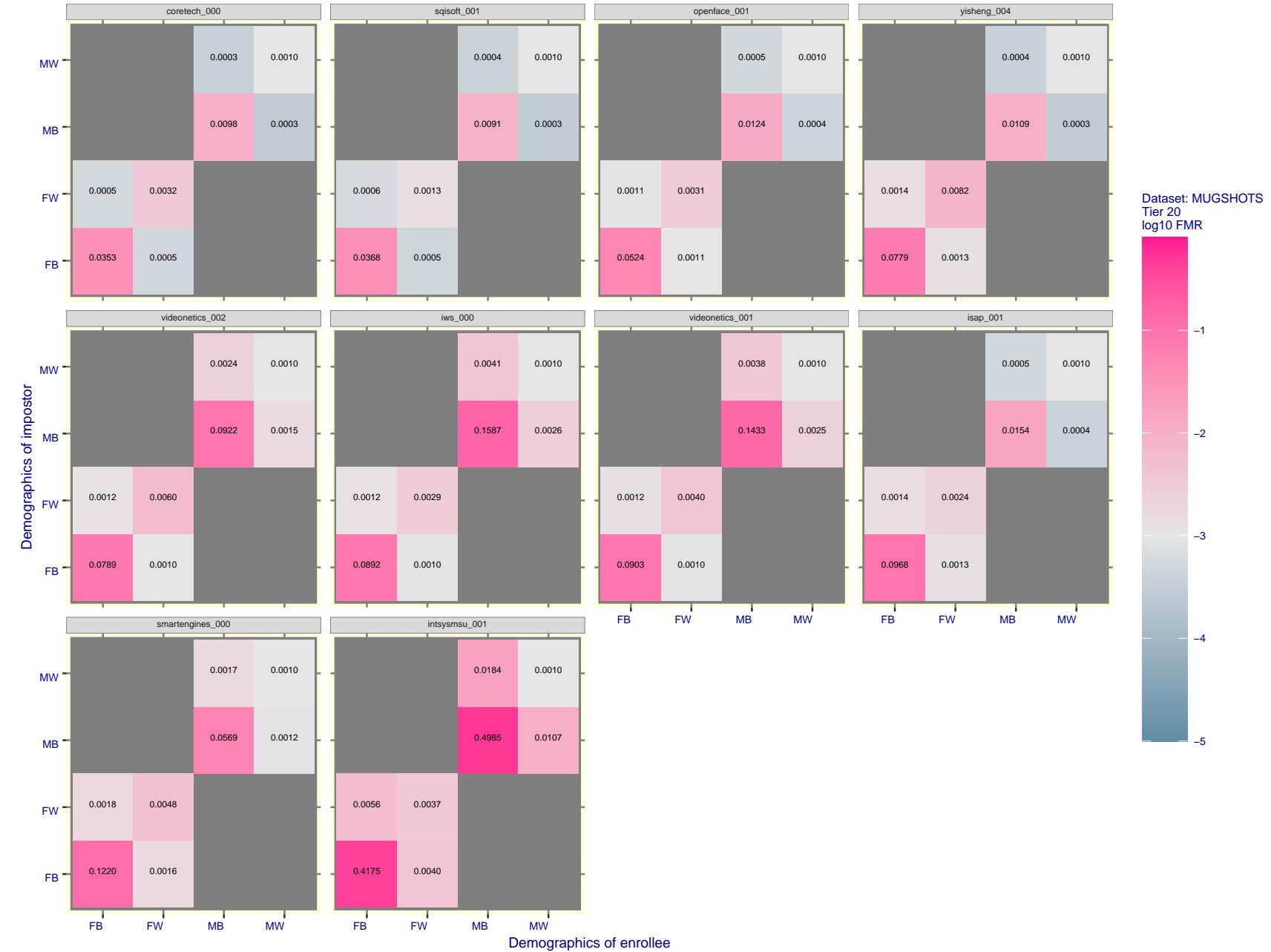


Figure 116: For the mugshot images, FMR for same-sex impostor pairs of images annotated with codes for black female, black male, white female, white male. The threshold is set for each algorithm to give $FMR = 0.001$ for white males which is the demographic that usually gives the lowest FMR. This means the top right box is the same color in all panels. The panels are sorted over multiple pages in order of FMR on black females, which is the demographic that usually gives the highest FMR.

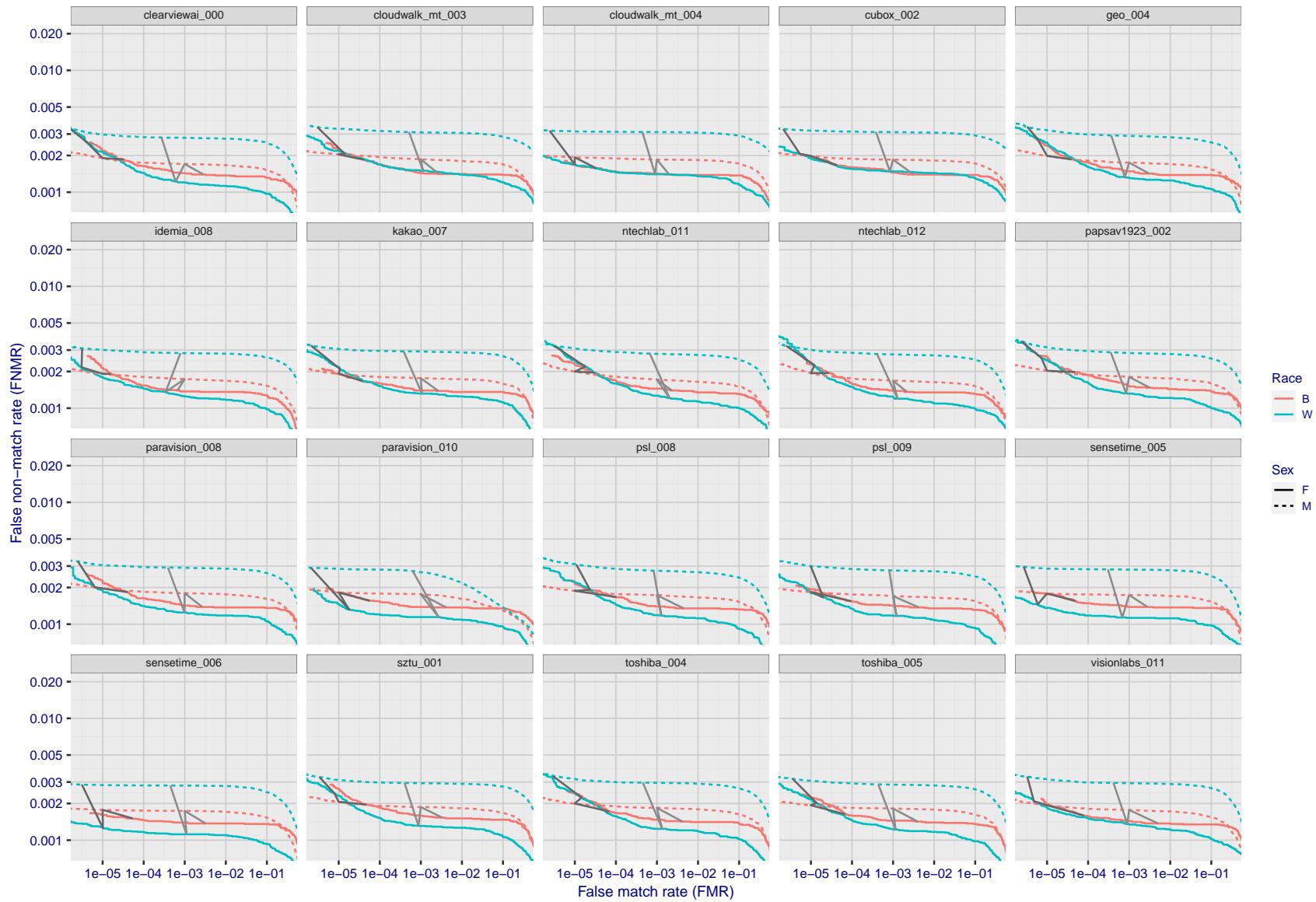


Figure 117: For the mugshot images, error tradeoff characteristics for white females, black females, black males and white males. The Z-shaped grey lines correspond to fixed thresholds, showing both FNMR and FMR vary at one T value. Note: Many of the plots will naively be read as saying women gives worse error rates than men because the solid traces lie above the dotted ones. However, this is misleading and incomplete: The grey lines show the traces reveal horizontal shifts. Thus for the cogent-003 algorithm FNMR for men is higher than for women at a fixed threshold but, at the same time, FMR is higher for women - see Figure 189. As access control systems almost always operate at a fixed threshold, the naive interpretation is incorrect.

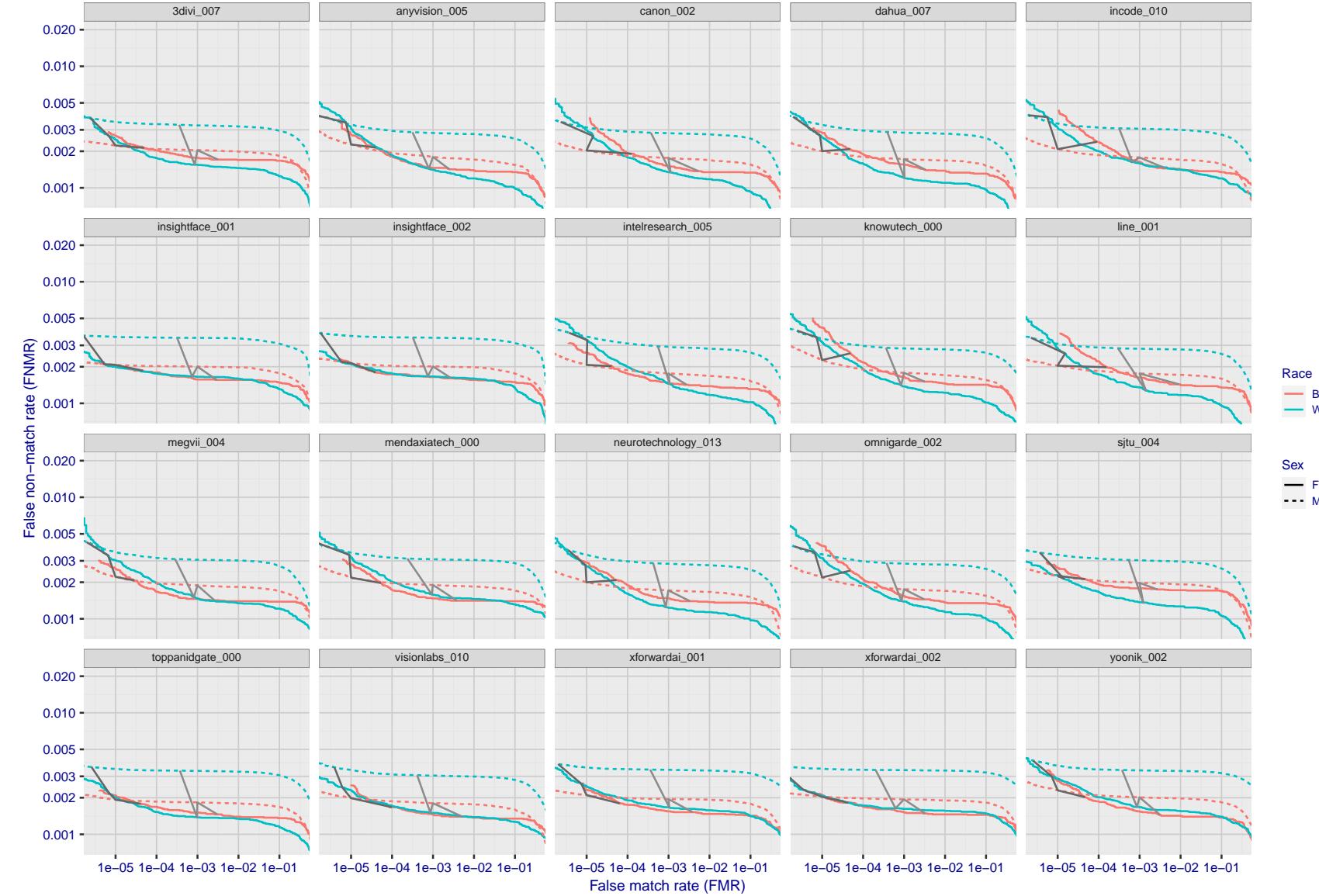


Figure 118: For the mugshot images, error tradeoff characteristics for white females, black females, black males and white males. The Z-shaped grey lines correspond to fixed thresholds, showing both FNMR and FMR vary at one T value. Note: Many of the plots will naively be read as saying women gives worse error rates than men because the solid traces lie above the dotted ones. However, this is misleading and incomplete: The grey lines show the traces reveal horizontal shifts. Thus for the cogent-003 algorithm FNMR for men is higher than for women at a fixed threshold but, at the same time, FMR is higher for women - see Figure 189. As access control systems almost always operate at a fixed threshold, the naive interpretation is incorrect.

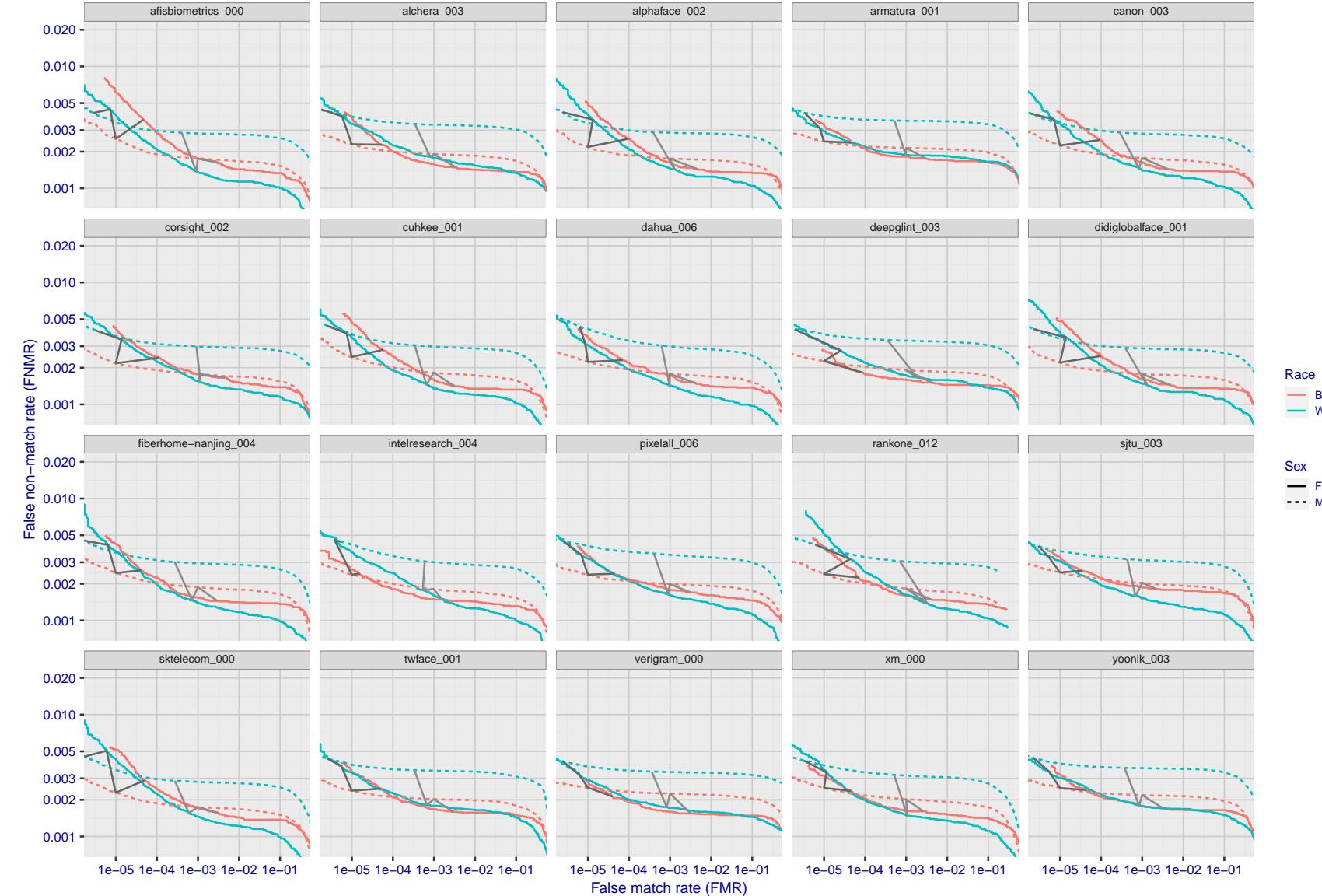


Figure 119: For the mugshot images, error tradeoff characteristics for white females, black females, black males and white males. The Z-shaped grey lines correspond to fixed thresholds, showing both FNMR and FMR vary at one T value. Note: Many of the plots will naively be read as saying women gives worse error rates than men because the solid traces lie above the dotted ones. However, this is misleading and incomplete: The grey lines show the traces reveal horizontal shifts. Thus for the cogent-003 algorithm FNMR for men is higher than for women at a fixed threshold but, at the same time, FMR is higher for women - see Figure 189. As access control systems almost always operate at a fixed threshold, the naive interpretation is incorrect.

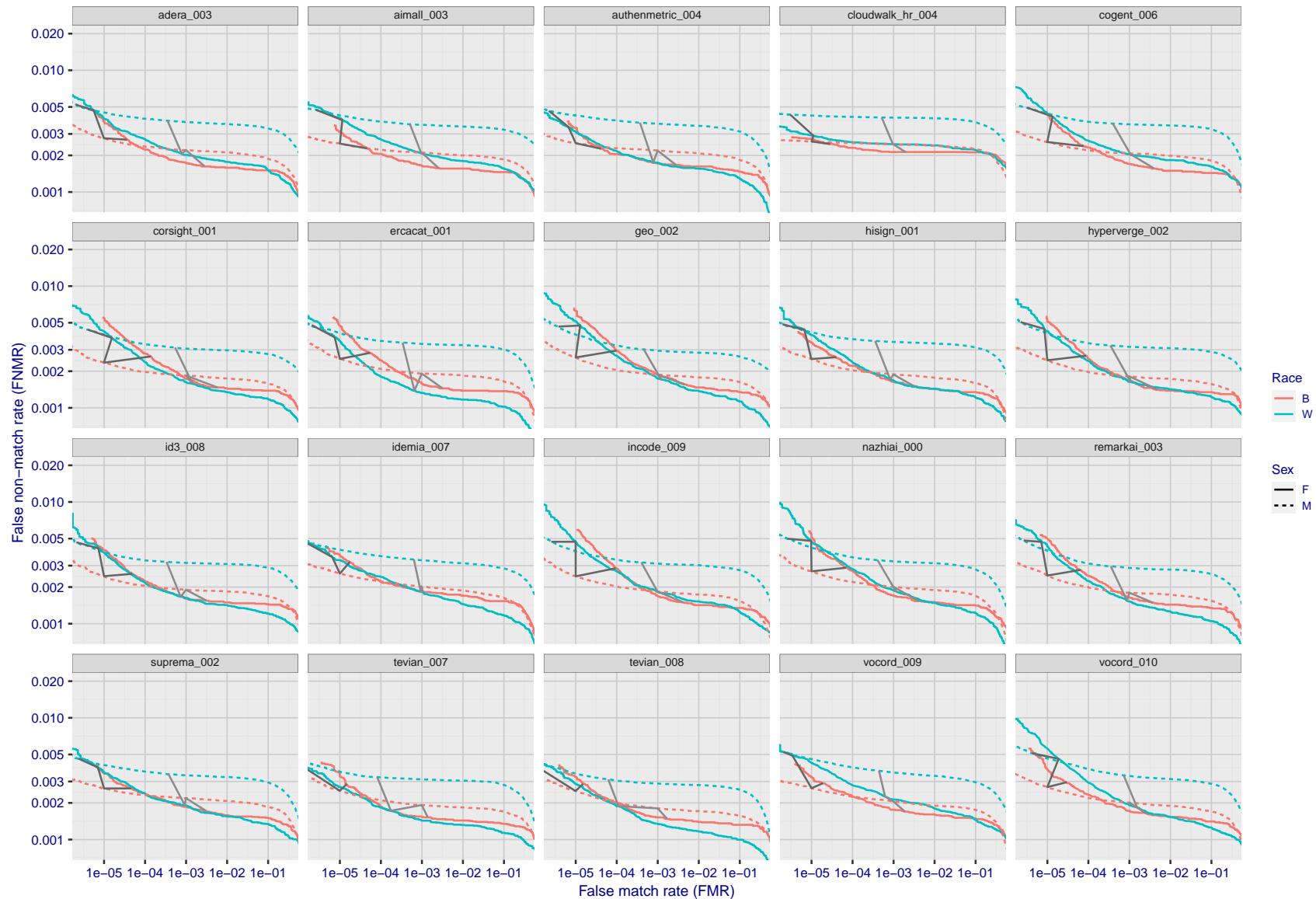


Figure 120: For the mugshot images, error tradeoff characteristics for white females, black females, black males and white males. The Z-shaped grey lines correspond to fixed thresholds, showing both FNMR and FMR vary at one T value. Note: Many of the plots will naively be read as saying women gives worse error rates than men because the solid traces lie above the dotted ones. However, this is misleading and incomplete: The grey lines show the traces reveal horizontal shifts. Thus for the cogent-003 algorithm FNMR for men is higher than for women at a fixed threshold but, at the same time, FMR is higher for women - see Figure 189. As access control systems almost always operate at a fixed threshold, the naive interpretation is incorrect.

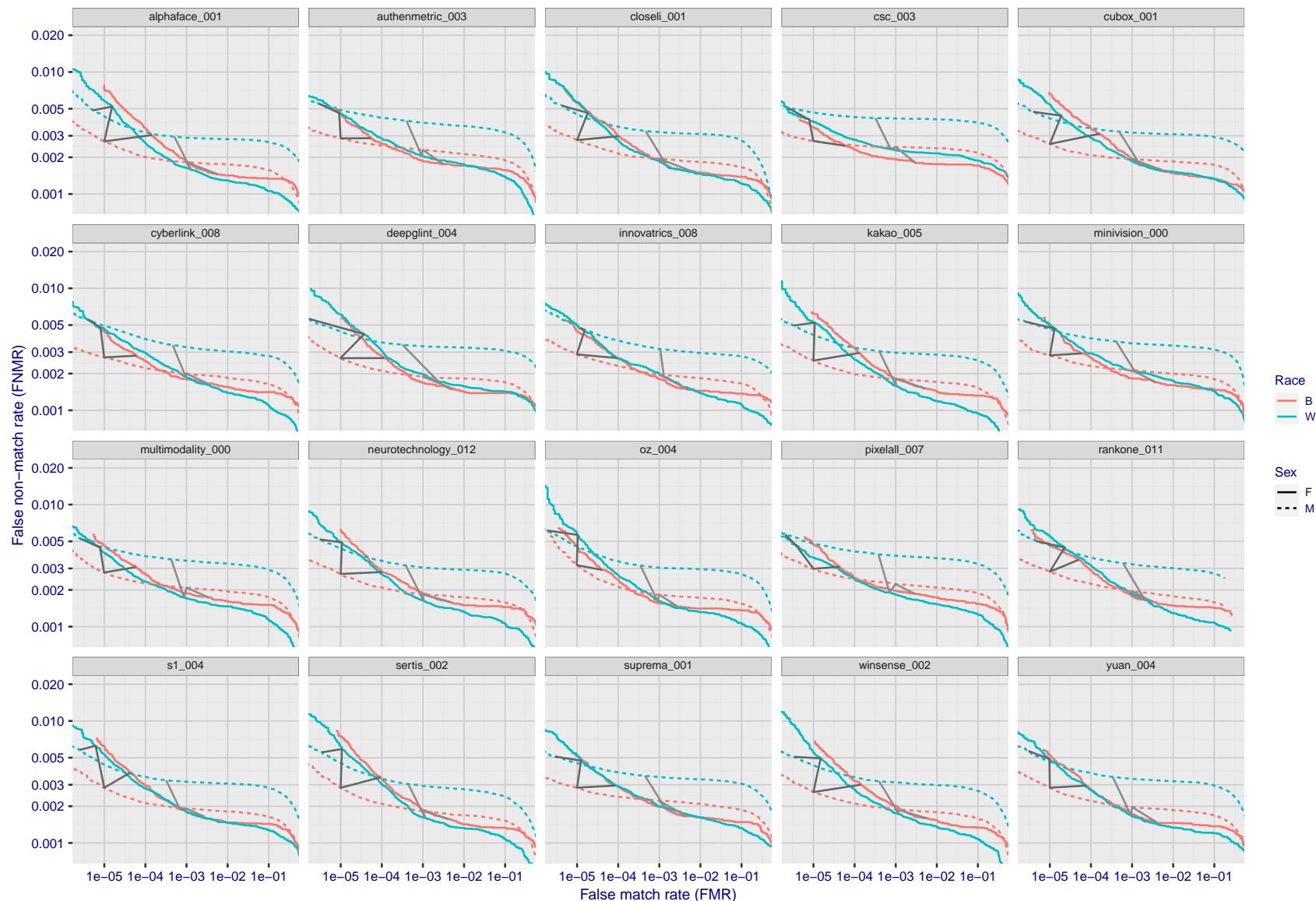


Figure 121: For the mugshot images, error tradeoff characteristics for white females, black females, black males and white males. The Z-shaped grey lines correspond to fixed thresholds, showing both FNMR and FMR vary at one T value. Note: Many of the plots will naively be read as saying women gives worse error rates than men because the solid traces lie above the dotted ones. However, this is misleading and incomplete: The grey lines show the traces reveal horizontal shifts. Thus for the cogent-003 algorithm FNMR for men is higher than for women at a fixed threshold but, at the same time, FMR is higher for women - see Figure 189. As access control systems almost always operate at a fixed threshold, the naive interpretation is incorrect.

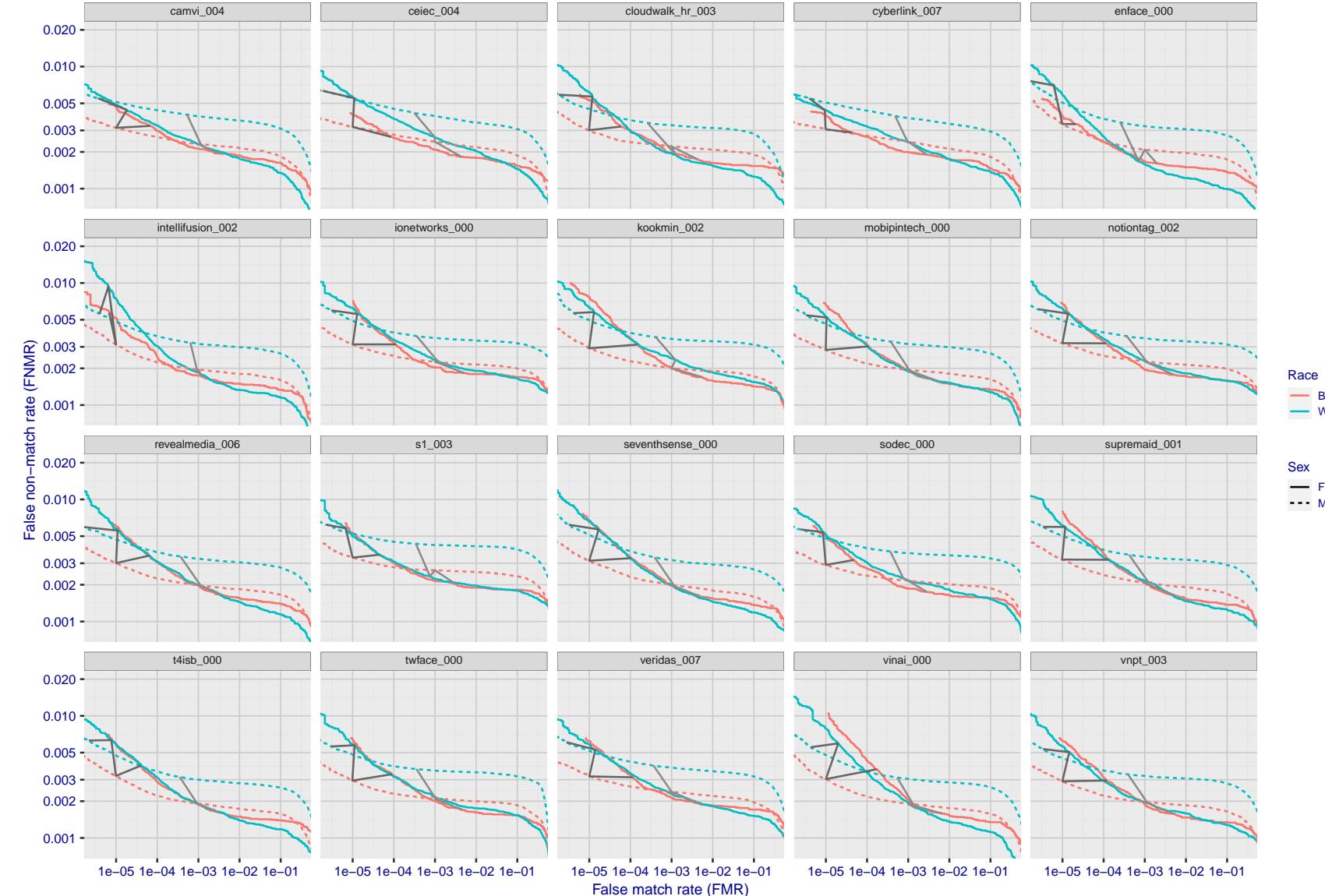


Figure 122: For the mugshot images, error tradeoff characteristics for white females, black females, black males and white males. The Z-shaped grey lines correspond to fixed thresholds, showing both FNMR and FMR vary at one T value. Note: Many of the plots will naively be read as saying women gives worse error rates than men because the solid traces lie above the dotted ones. However, this is misleading and incomplete: The grey lines show the traces reveal horizontal shifts. Thus for the cogent-003 algorithm FNMR for men is higher than for women at a fixed threshold but, at the same time, FMR is higher for women - see Figure 189. As access control systems almost always operate at a fixed threshold, the naive interpretation is incorrect.

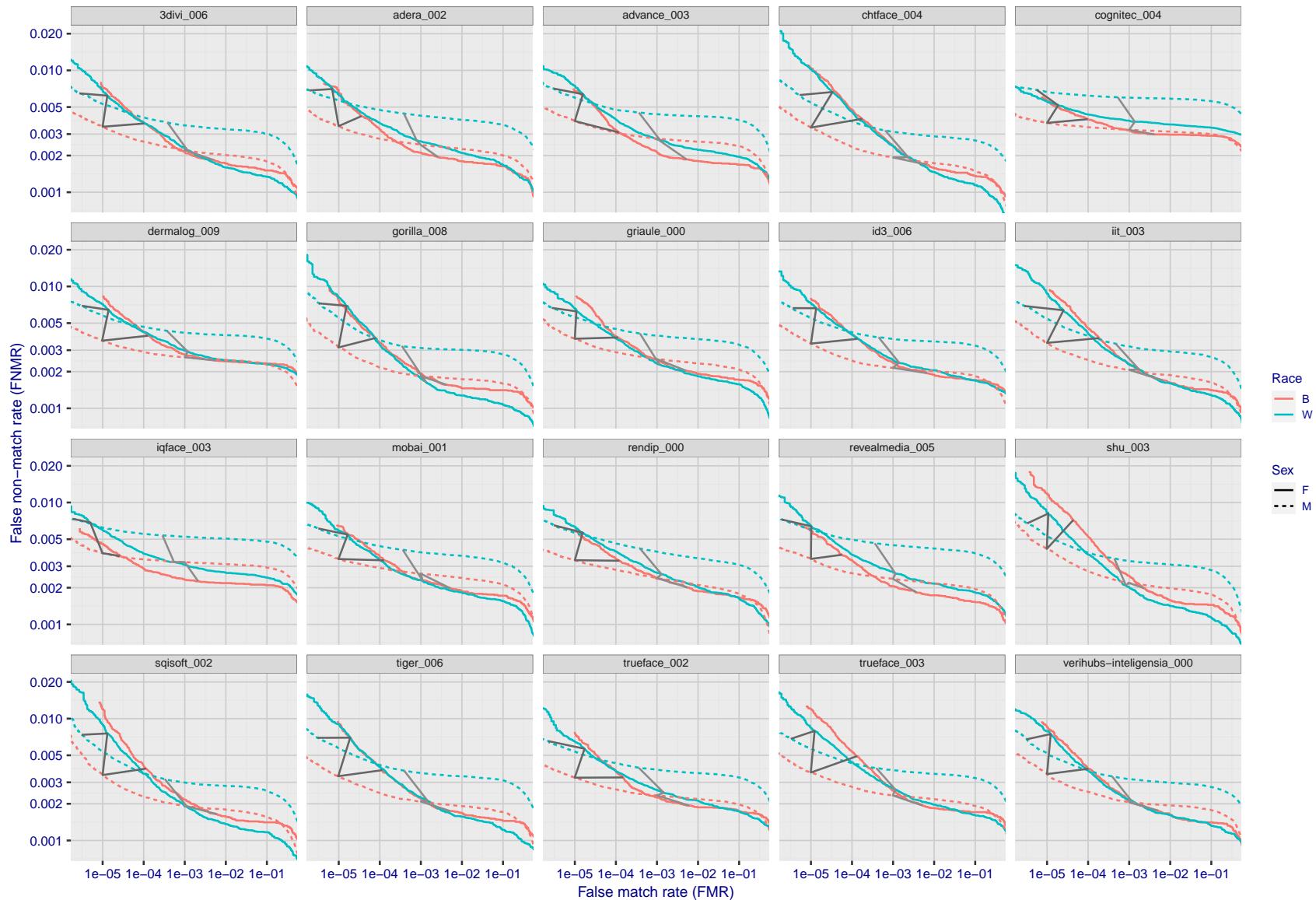


Figure 123: For the mugshot images, error tradeoff characteristics for white females, black females, black males and white males. The Z-shaped grey lines correspond to fixed thresholds, showing both FNMR and FMR vary at one T value. Note: Many of the plots will naively be read as saying women gives worse error rates than men because the solid traces lie above the dotted ones. However, this is misleading and incomplete: The grey lines show the traces reveal horizontal shifts. Thus for the cogent-003 algorithm FNMR for men is higher than for women at a fixed threshold but, at the same time, FMR is higher for women - see Figure 189. As access control systems almost always operate at a fixed threshold, the naive interpretation is incorrect.

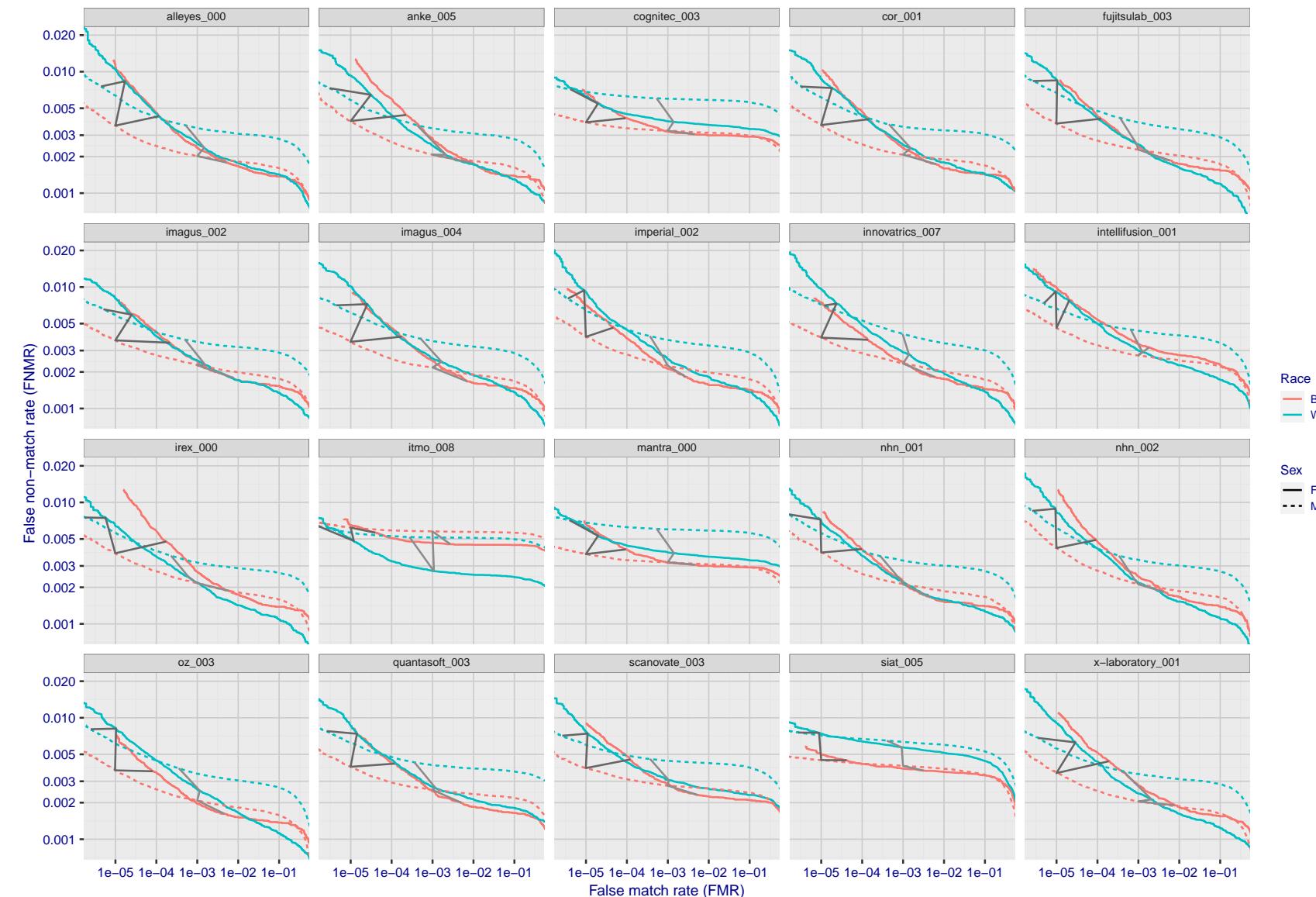


Figure 124: For the mugshot images, error tradeoff characteristics for white females, black females, black males and white males. The Z-shaped grey lines correspond to fixed thresholds, showing both FNMR and FMR vary at one T value. Note: Many of the plots will naively be read as saying women gives worse error rates than men because the solid traces lie above the dotted ones. However, this is misleading and incomplete: The grey lines show the traces reveal horizontal shifts. Thus for the cogent-003 algorithm FNMR for men is higher than for women at a fixed threshold but, at the same time, FMR is higher for women - see Figure 189. As access control systems almost always operate at a fixed threshold, the naive interpretation is incorrect.

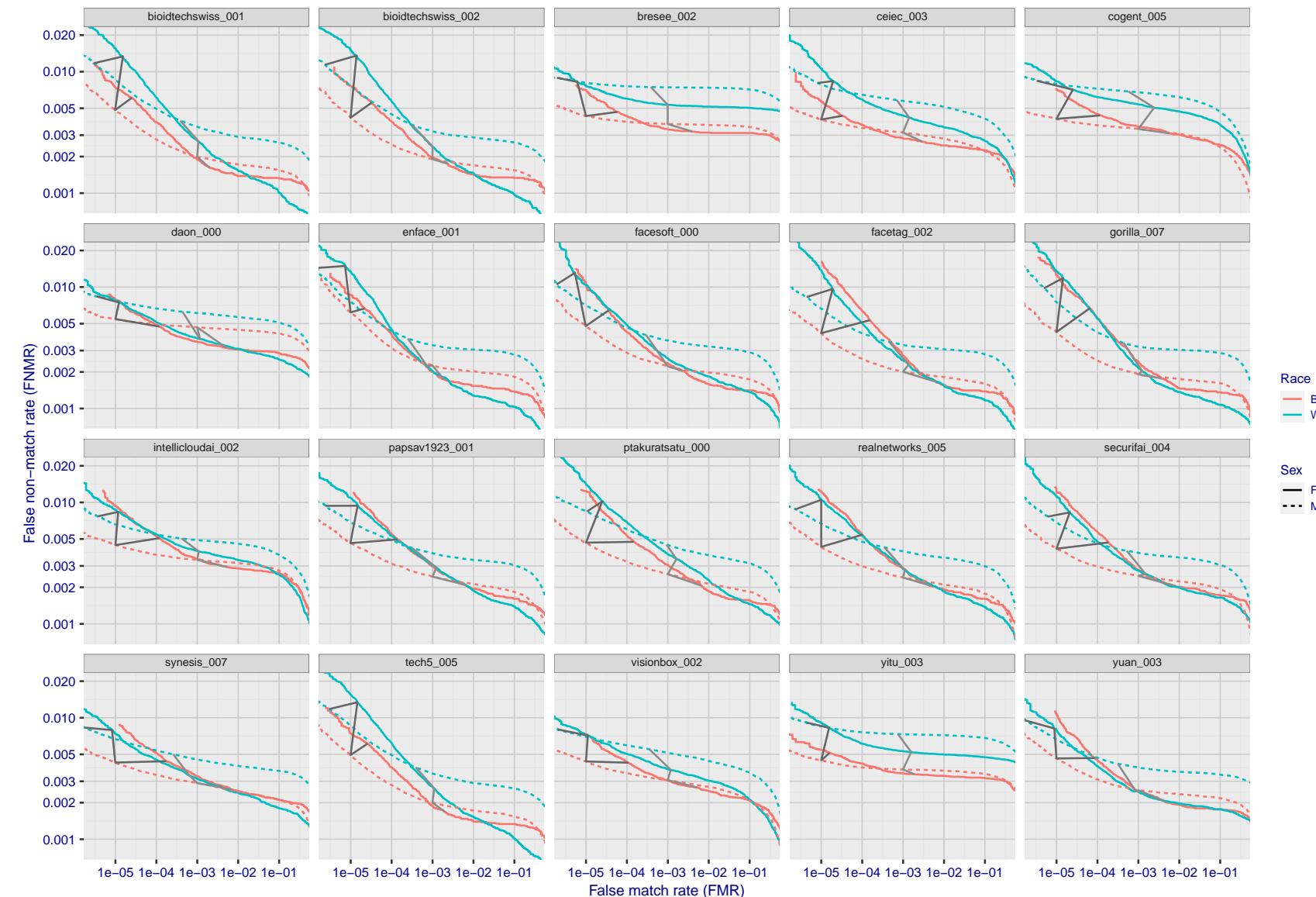


Figure 125: For the mugshot images, error tradeoff characteristics for white females, black females, black males and white males. The Z-shaped grey lines correspond to fixed thresholds, showing both FNMR and FMR vary at one T value. Note: Many of the plots will naively be read as saying women gives worse error rates than men because the solid traces lie above the dotted ones. However, this is misleading and incomplete: The grey lines show the traces reveal horizontal shifts. Thus for the cogent-003 algorithm FNMR for men is higher than for women at a fixed threshold but, at the same time, FMR is higher for women - see Figure 189. As access control systems almost always operate at a fixed threshold, the naive interpretation is incorrect.

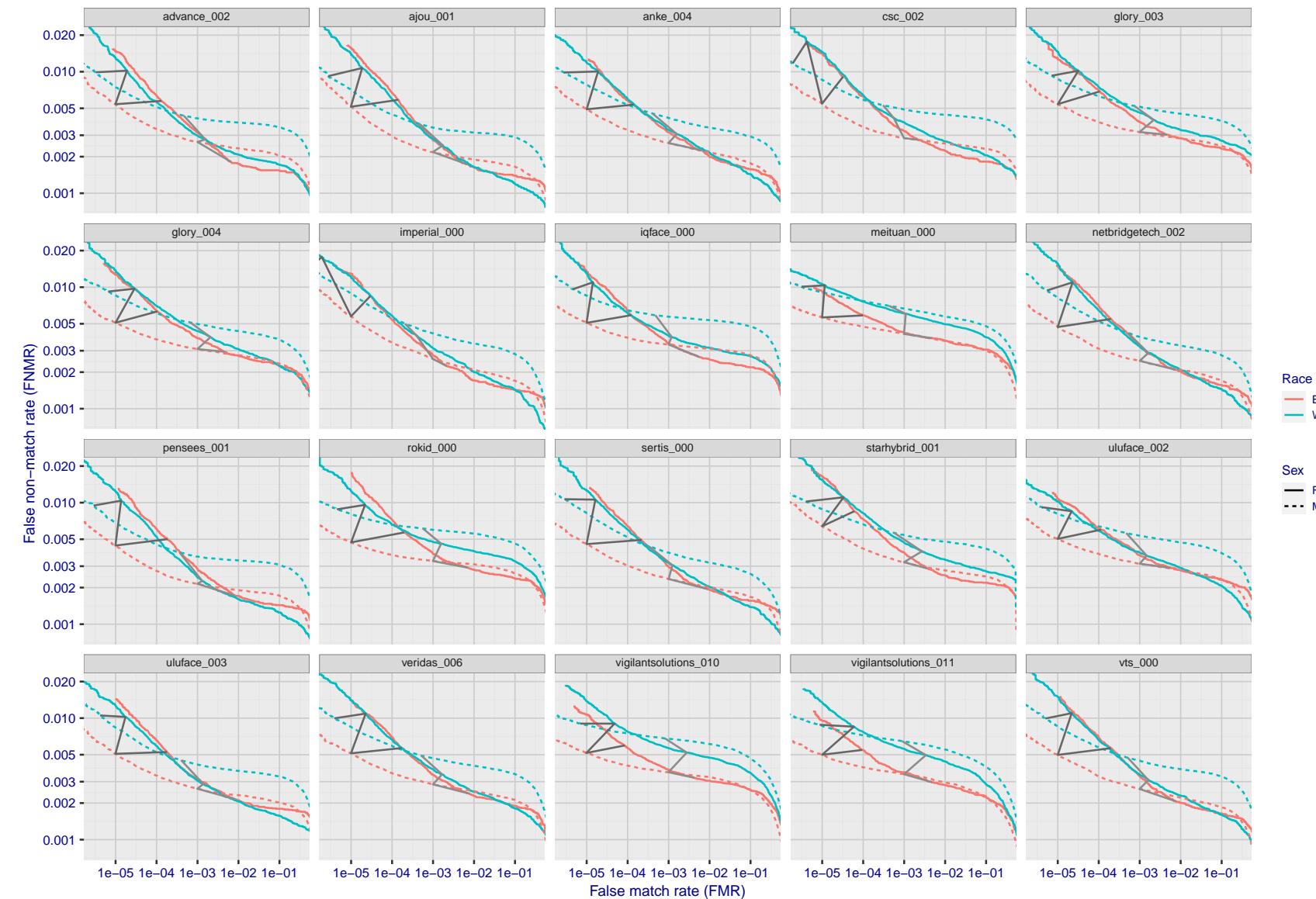


Figure 126: For the mugshot images, error tradeoff characteristics for white females, black females, black males and white males. The Z-shaped grey lines correspond to fixed thresholds, showing both FNMR and FMR vary at one T value. Note: Many of the plots will naively be read as saying women gives worse error rates than men because the solid traces lie above the dotted ones. However, this is misleading and incomplete: The grey lines show the traces reveal horizontal shifts. Thus for the cogent-003 algorithm FNMR for men is higher than for women at a fixed threshold but, at the same time, FMR is higher for women - see Figure 189. As access control systems almost always operate at a fixed threshold, the naive interpretation is incorrect.

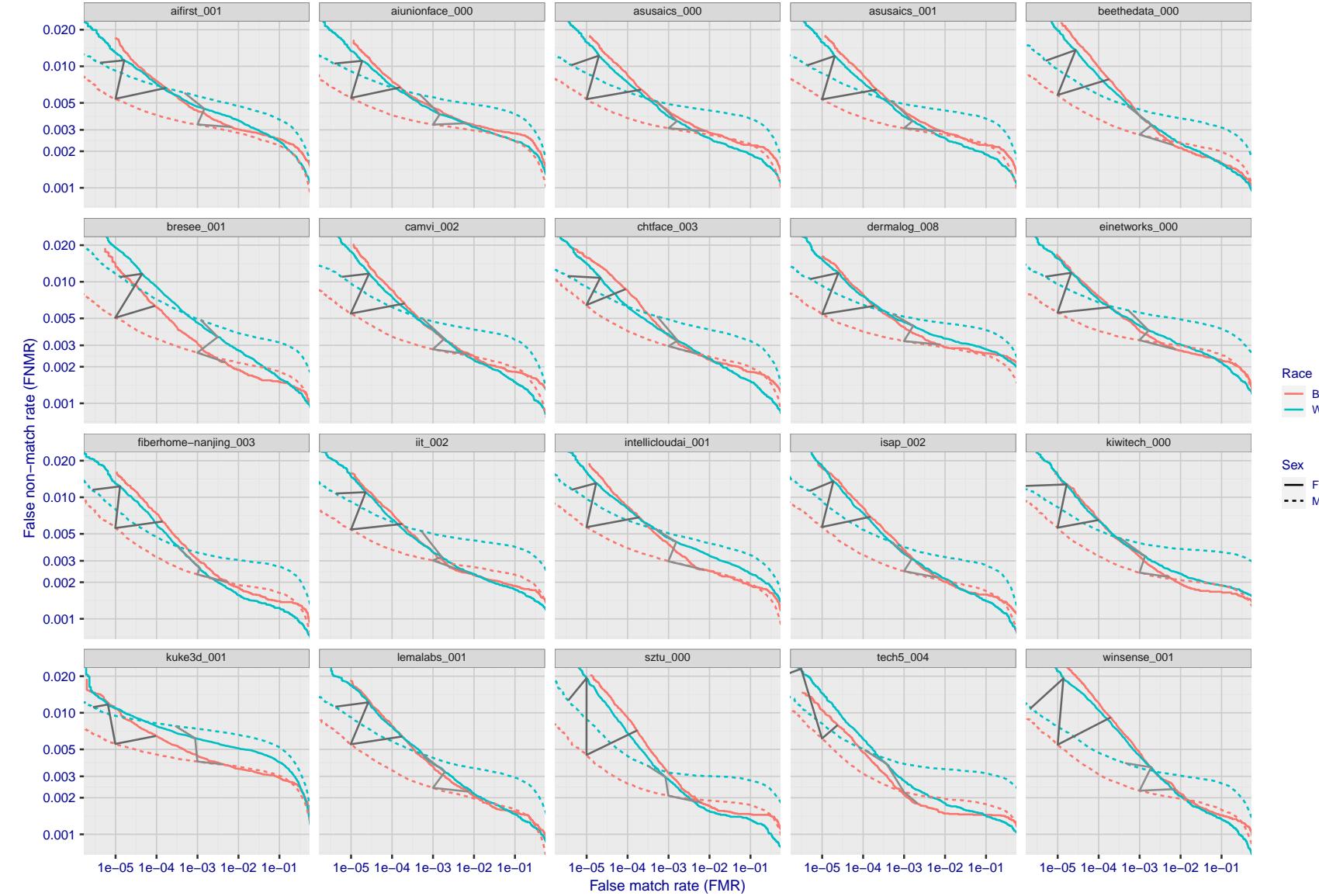


Figure 127: For the mugshot images, error tradeoff characteristics for white females, black females, black males and white males. The Z-shaped grey lines correspond to fixed thresholds, showing both FNMR and FMR vary at one T value. Note: Many of the plots will naively be read as saying women gives worse error rates than men because the solid traces lie above the dotted ones. However, this is misleading and incomplete: The grey lines show the traces reveal horizontal shifts. Thus for the cogent-003 algorithm FNMR for men is higher than for women at a fixed threshold but, at the same time, FMR is higher for women - see Figure 189. As access control systems almost always operate at a fixed threshold, the naive interpretation is incorrect.

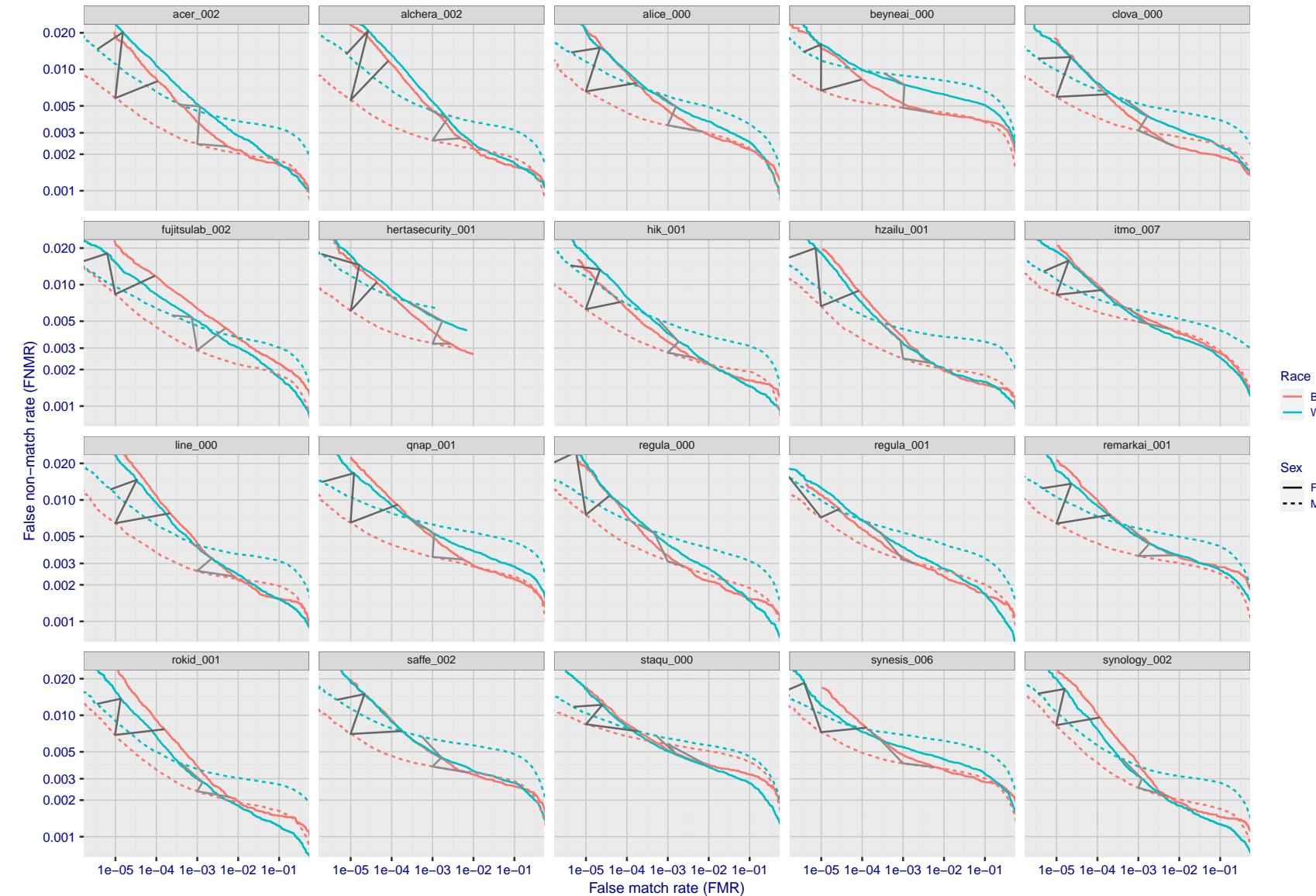


Figure 128: For the mugshot images, error tradeoff characteristics for white females, black females, black males and white males. The Z-shaped grey lines correspond to fixed thresholds, showing both FNMR and FMR vary at one T value. Note: Many of the plots will naively be read as saying women gives worse error rates than men because the solid traces lie above the dotted ones. However, this is misleading and incomplete: The grey lines show the traces reveal horizontal shifts. Thus for the cogent-003 algorithm FNMR for men is higher than for women at a fixed threshold but, at the same time, FMR is higher for women - see Figure 189. As access control systems almost always operate at a fixed threshold, the naive interpretation is incorrect.

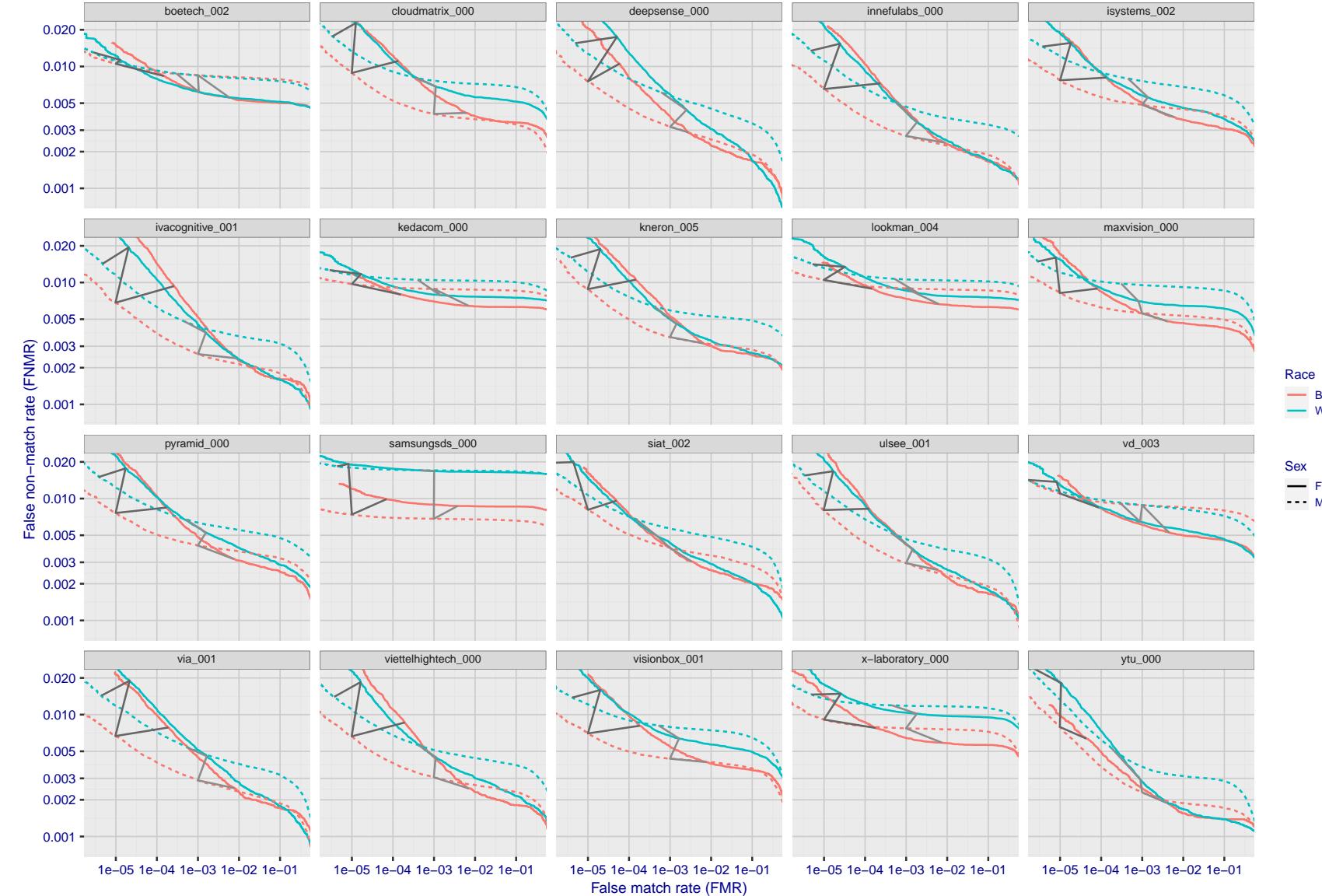


Figure 129: For the mugshot images, error tradeoff characteristics for white females, black females, black males and white males. The Z-shaped grey lines correspond to fixed thresholds, showing both FNMR and FMR vary at one T value. Note: Many of the plots will naively be read as saying women gives worse error rates than men because the solid traces lie above the dotted ones. However, this is misleading and incomplete: The grey lines show the traces reveal horizontal shifts. Thus for the cogent-003 algorithm FNMR for men is higher than for women at a fixed threshold but, at the same time, FMR is higher for women - see Figure 189. As access control systems almost always operate at a fixed threshold, the naive interpretation is incorrect.

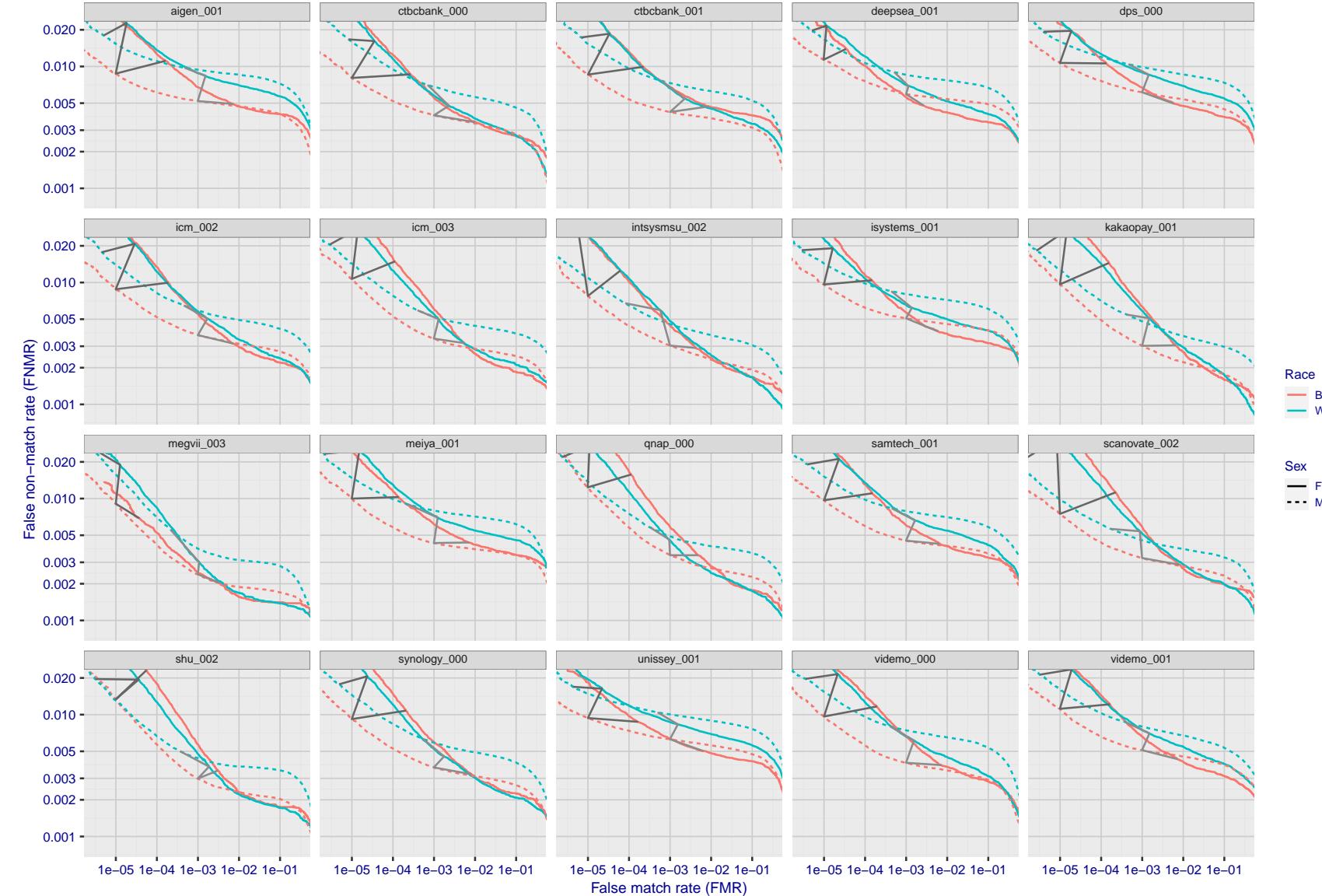


Figure 130: For the mugshot images, error tradeoff characteristics for white females, black females, black males and white males. The Z-shaped grey lines correspond to fixed thresholds, showing both FNMR and FMR vary at one T value. Note: Many of the plots will naively be read as saying women gives worse error rates than men because the solid traces lie above the dotted ones. However, this is misleading and incomplete: The grey lines show the traces reveal horizontal shifts. Thus for the cogent-003 algorithm FNMR for men is higher than for women at a fixed threshold but, at the same time, FMR is higher for women - see Figure 189. As access control systems almost always operate at a fixed threshold, the naive interpretation is incorrect.

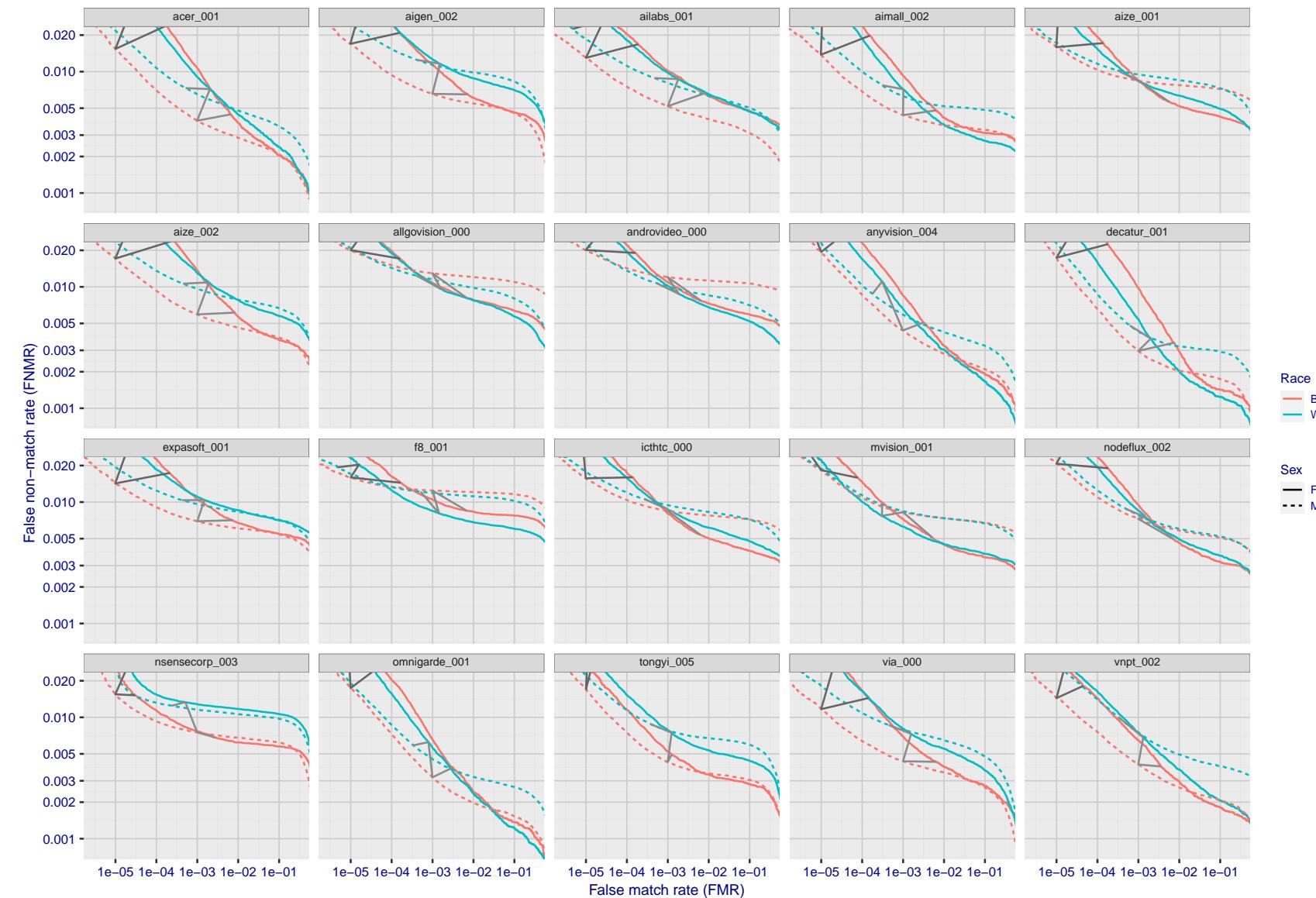


Figure 131: For the mugshot images, error tradeoff characteristics for white females, black females, black males and white males. The Z-shaped grey lines correspond to fixed thresholds, showing both FNMR and FMR vary at one T value. Note: Many of the plots will naively be read as saying women gives worse error rates than men because the solid traces lie above the dotted ones. However, this is misleading and incomplete: The grey lines show the traces reveal horizontal shifts. Thus for the cogent-003 algorithm FNMR for men is higher than for women at a fixed threshold but, at the same time, FMR is higher for women - see Figure 189. As access control systems almost always operate at a fixed threshold, the naive interpretation is incorrect.

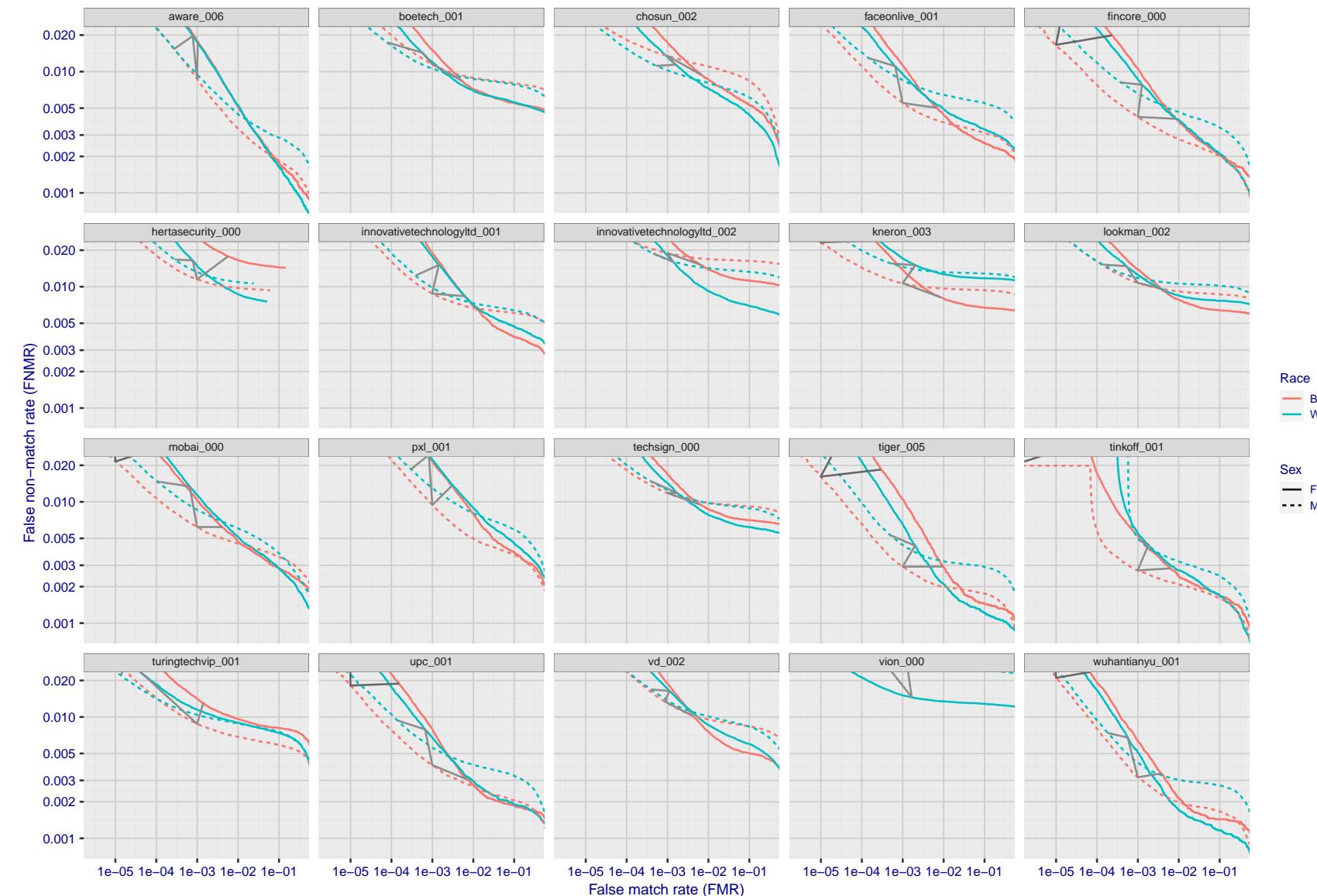


Figure 132: For the mugshot images, error tradeoff characteristics for white females, black females, black males and white males. The Z-shaped grey lines correspond to fixed thresholds, showing both FNMR and FMR vary at one T value. Note: Many of the plots will naively be read as saying women gives worse error rates than men because the solid traces lie above the dotted ones. However, this is misleading and incomplete: The grey lines show the traces reveal horizontal shifts. Thus for the cogent-003 algorithm FNMR for men is higher than for women at a fixed threshold but, at the same time, FMR is higher for women - see Figure 189. As access control systems almost always operate at a fixed threshold, the naive interpretation is incorrect.

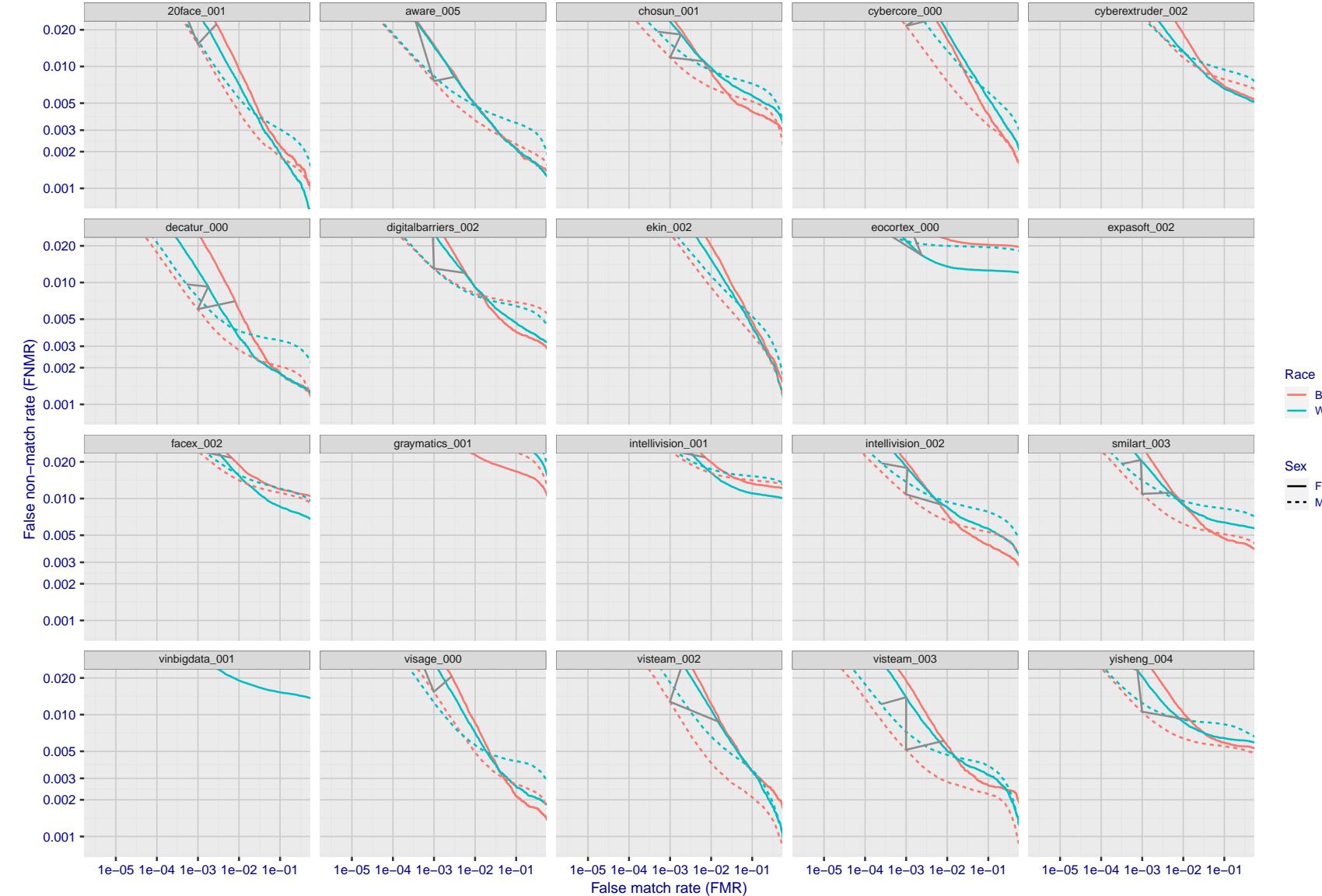


Figure 133: For the mugshot images, error tradeoff characteristics for white females, black females, black males and white males. The Z-shaped grey lines correspond to fixed thresholds, showing both FNMR and FMR vary at one T value. Note: Many of the plots will naively be read as saying women gives worse error rates than men because the solid traces lie above the dotted ones. However, this is misleading and incomplete: The grey lines show the traces reveal horizontal shifts. Thus for the cogent-003 algorithm FNMR for men is higher than for women at a fixed threshold but, at the same time, FMR is higher for women - see Figure 189. As access control systems almost always operate at a fixed threshold, the naive interpretation is incorrect.

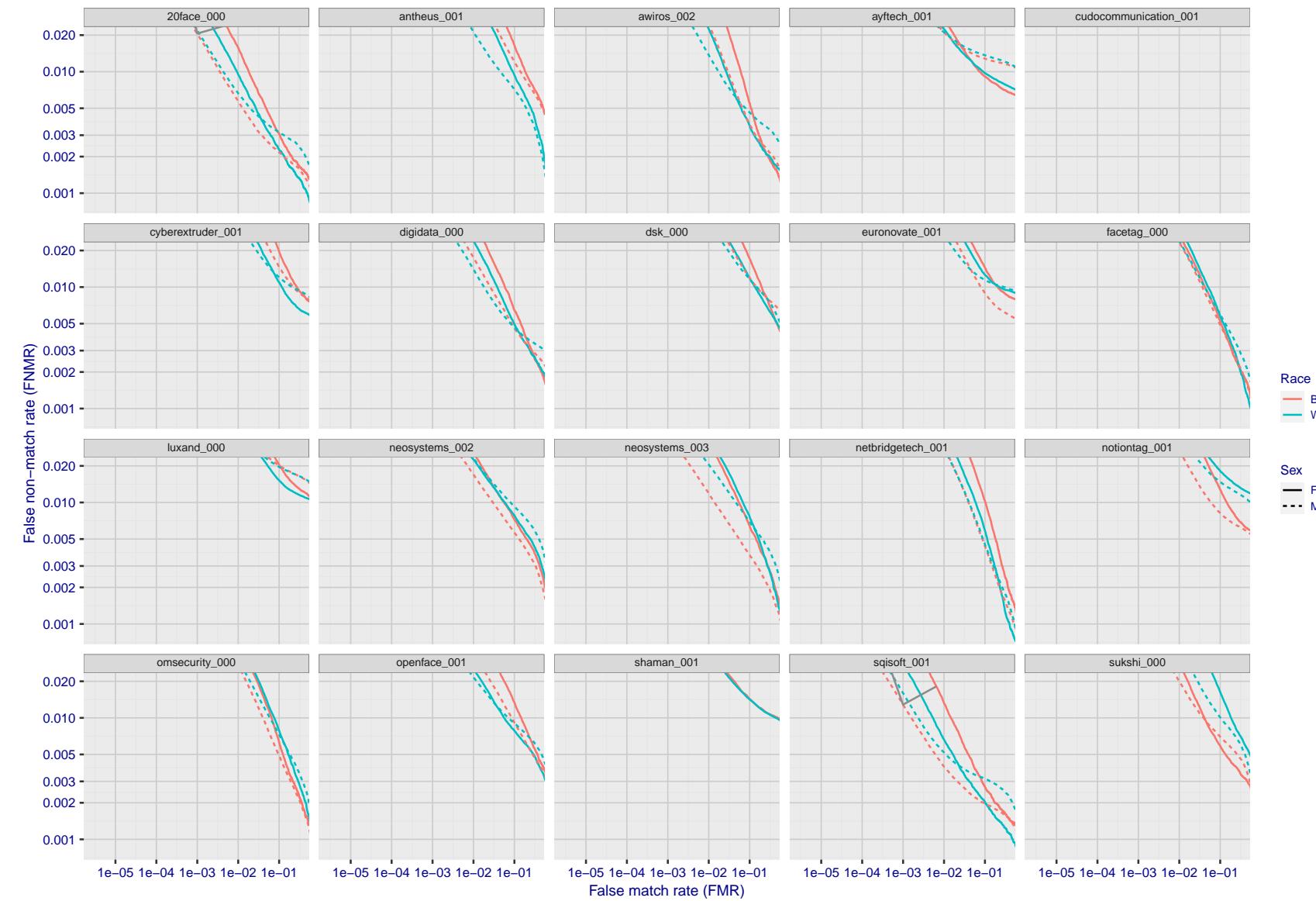


Figure 134: For the mugshot images, error tradeoff characteristics for white females, black females, black males and white males. The Z-shaped grey lines correspond to fixed thresholds, showing both FNMR and FMR vary at one T value. Note: Many of the plots will naively be read as saying women gives worse error rates than men because the solid traces lie above the dotted ones. However, this is misleading and incomplete: The grey lines show the traces reveal horizontal shifts. Thus for the cogent-003 algorithm FNMR for men is higher than for women at a fixed threshold but, at the same time, FMR is higher for women - see Figure 189. As access control systems almost always operate at a fixed threshold, the naive interpretation is incorrect.

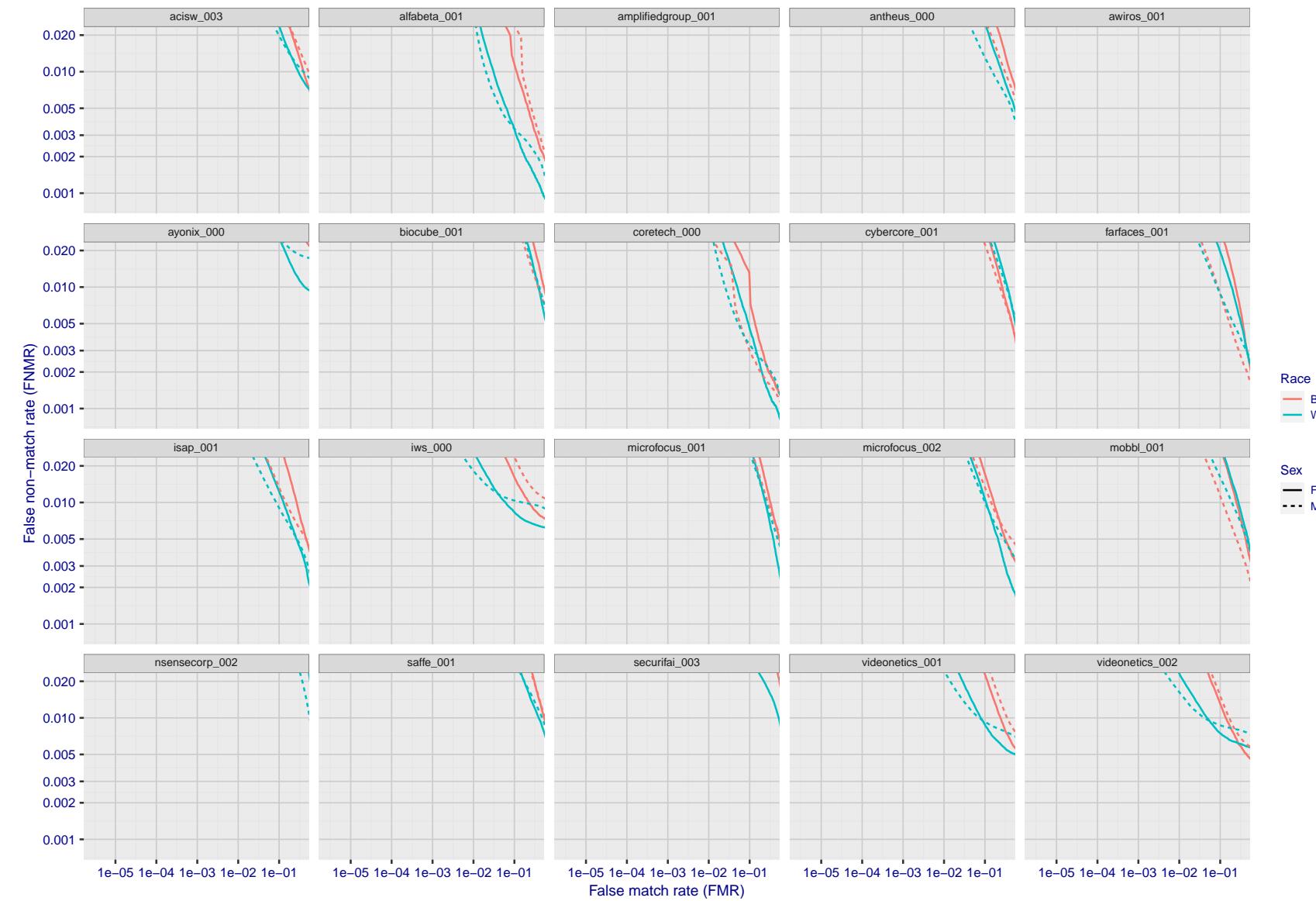


Figure 135: For the mugshot images, error tradeoff characteristics for white females, black females, black males and white males. The Z-shaped grey lines correspond to fixed thresholds, showing both FNMR and FMR vary at one T value. Note: Many of the plots will naively be read as saying women gives worse error rates than men because the solid traces lie above the dotted ones. However, this is misleading and incomplete: The grey lines show the traces reveal horizontal shifts. Thus for the cogent-003 algorithm FNMR for men is higher than for women at a fixed threshold but, at the same time, FMR is higher for women - see Figure 189. As access control systems almost always operate at a fixed threshold, the naive interpretation is incorrect.

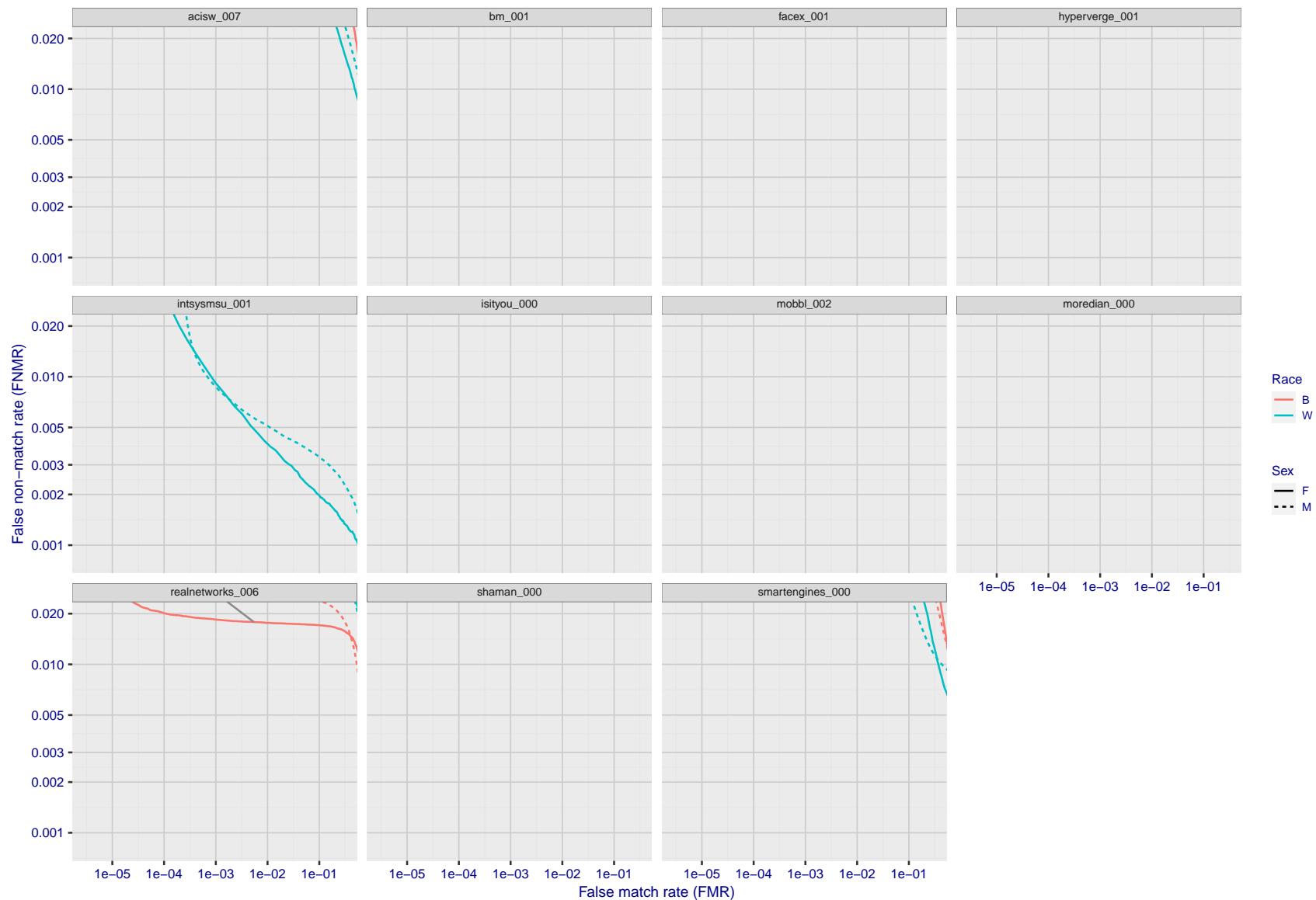


Figure 136: For the mugshot images, error tradeoff characteristics for white females, black females, black males and white males. The Z-shaped grey lines correspond to fixed thresholds, showing both FNMR and FMR vary at one T value. Note: Many of the plots will naively be read as saying women gives worse error rates than men because the solid traces lie above the dotted ones. However, this is misleading and incomplete: The grey lines show the traces reveal horizontal shifts. Thus for the cogent-003 algorithm FNMR for men is higher than for women at a fixed threshold but, at the same time, FMR is higher for women - see Figure 189. As access control systems almost always operate at a fixed threshold, the naive interpretation is incorrect.

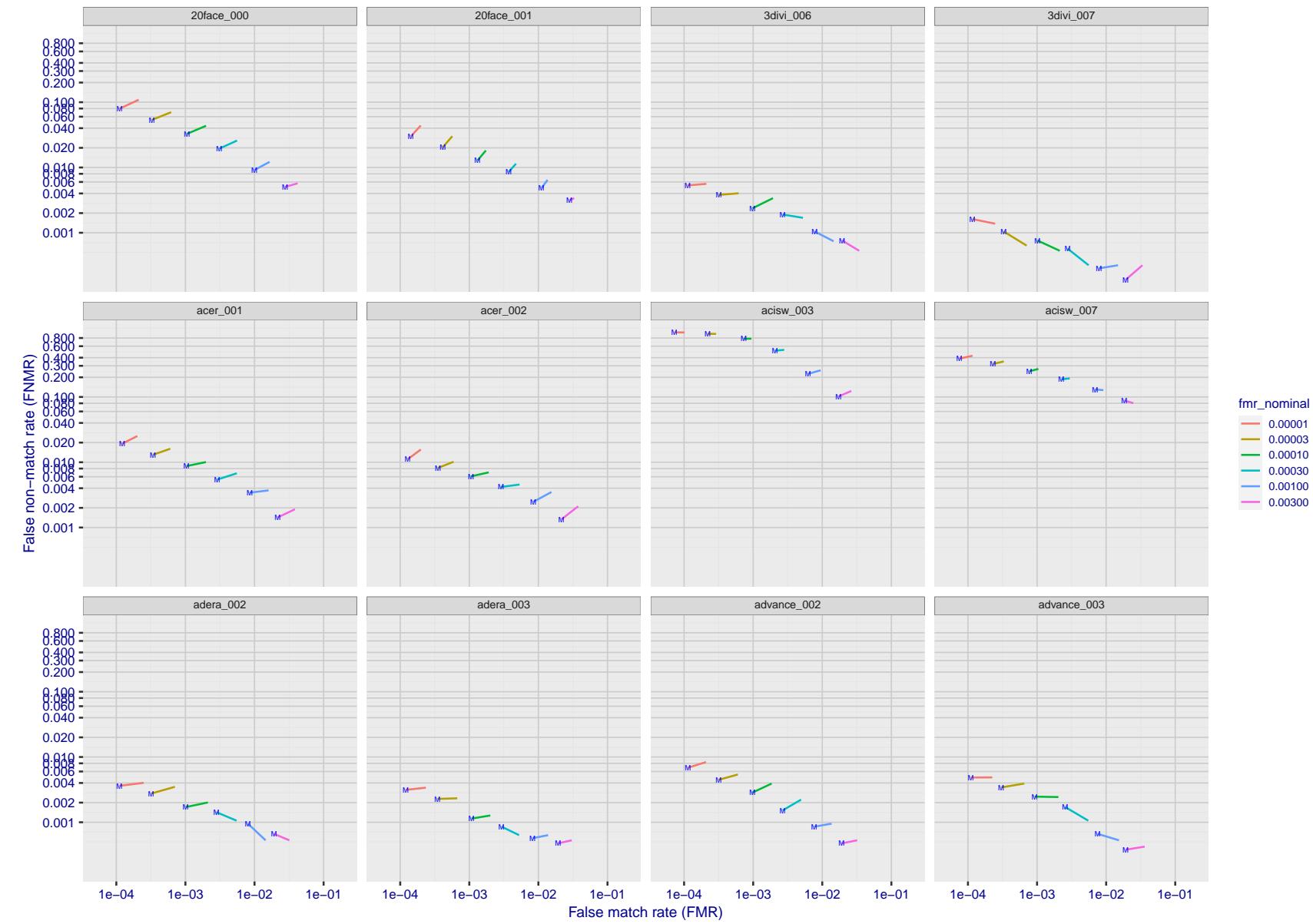


Figure 137: For the visa images, FNMR and FMR at six operating points along the DET characteristic. At each point a line is drawn between $(FMR, FNMR)_{MALE}$ and $(FMR, FNMR)_{FEMALE}$ showing how which sex has lower FMR and/or FNMR. The "M" label denotes male, the other end of the line corresponds to female. The six operating thresholds are selected to give the nominal false match rates given in the legend, and are computed over all impostor pairs regardless of age, sex, and place of birth. The plotted FMR values are broadly an order of magnitude larger than the nominal rates because FMR is computed over demographically-matched impostor pairs i.e individuals of the same sex, from the same geographic region (see section 3.6.1), and the same age group (see section 3.6.2).

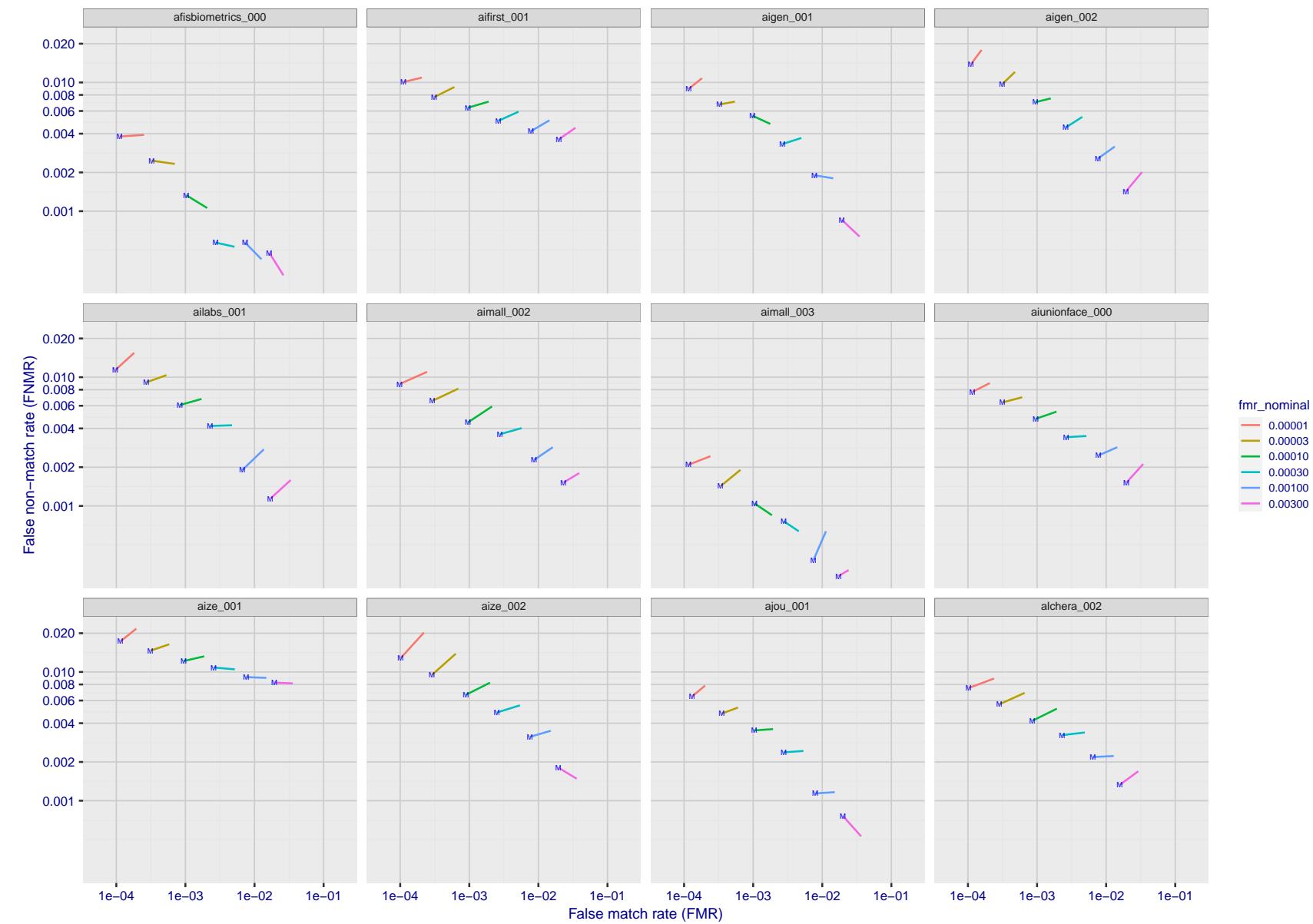


Figure 138: For the visa images, FNMR and FMR at six operating points along the DET characteristic. At each point a line is drawn between $(FMR, FNMR)_{MALE}$ and $(FMR, FNMR)_{FEMALE}$ showing how which sex has lower FMR and/or FNMR. The "M" label denotes male, the other end of the line corresponds to female. The six operating thresholds are selected to give the nominal false match rates given in the legend, and are computed over all impostor pairs regardless of age, sex, and place of birth. The plotted FMR values are broadly an order of magnitude larger than the nominal rates because FMR is computed over demographically-matched impostor pairs i.e individuals of the same sex, from the same geographic region (see section 3.6.1), and the same age group (see section 3.6.2).

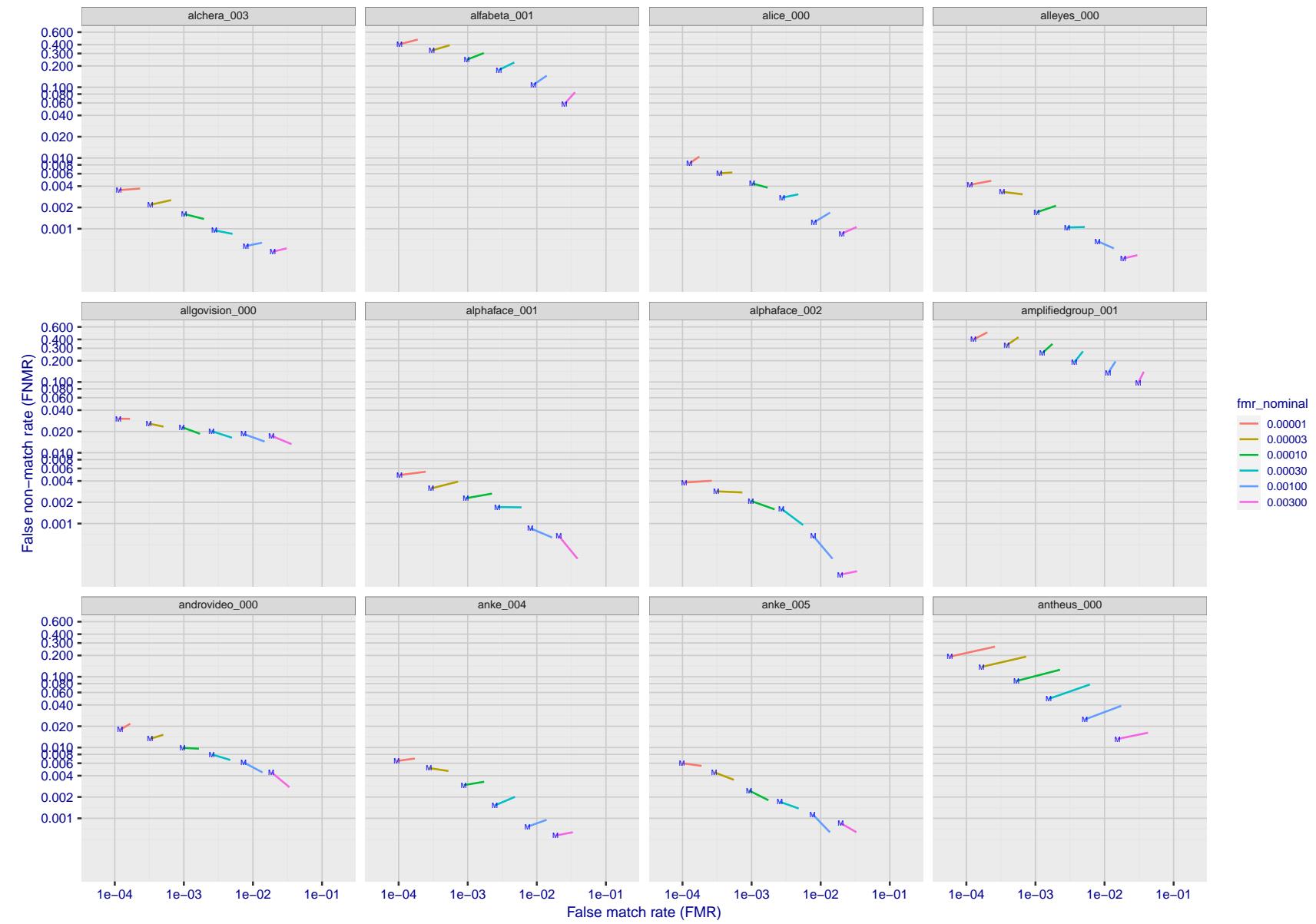


Figure 139: For the visa images, FNMR and FMR at six operating points along the DET characteristic. At each point a line is drawn between $(FMR, FNMR)_{MALE}$ and $(FMR, FNMR)_{FEMALE}$ showing how which sex has lower FMR and/or FNMR. The "M" label denotes male, the other end of the line corresponds to female. The six operating thresholds are selected to give the nominal false match rates given in the legend, and are computed over all impostor pairs regardless of age, sex, and place of birth. The plotted FMR values are broadly an order of magnitude larger than the nominal rates because FMR is computed over demographically-matched impostor pairs i.e individuals of the same sex, from the same geographic region (see section 3.6.1), and the same age group (see section 3.6.2).

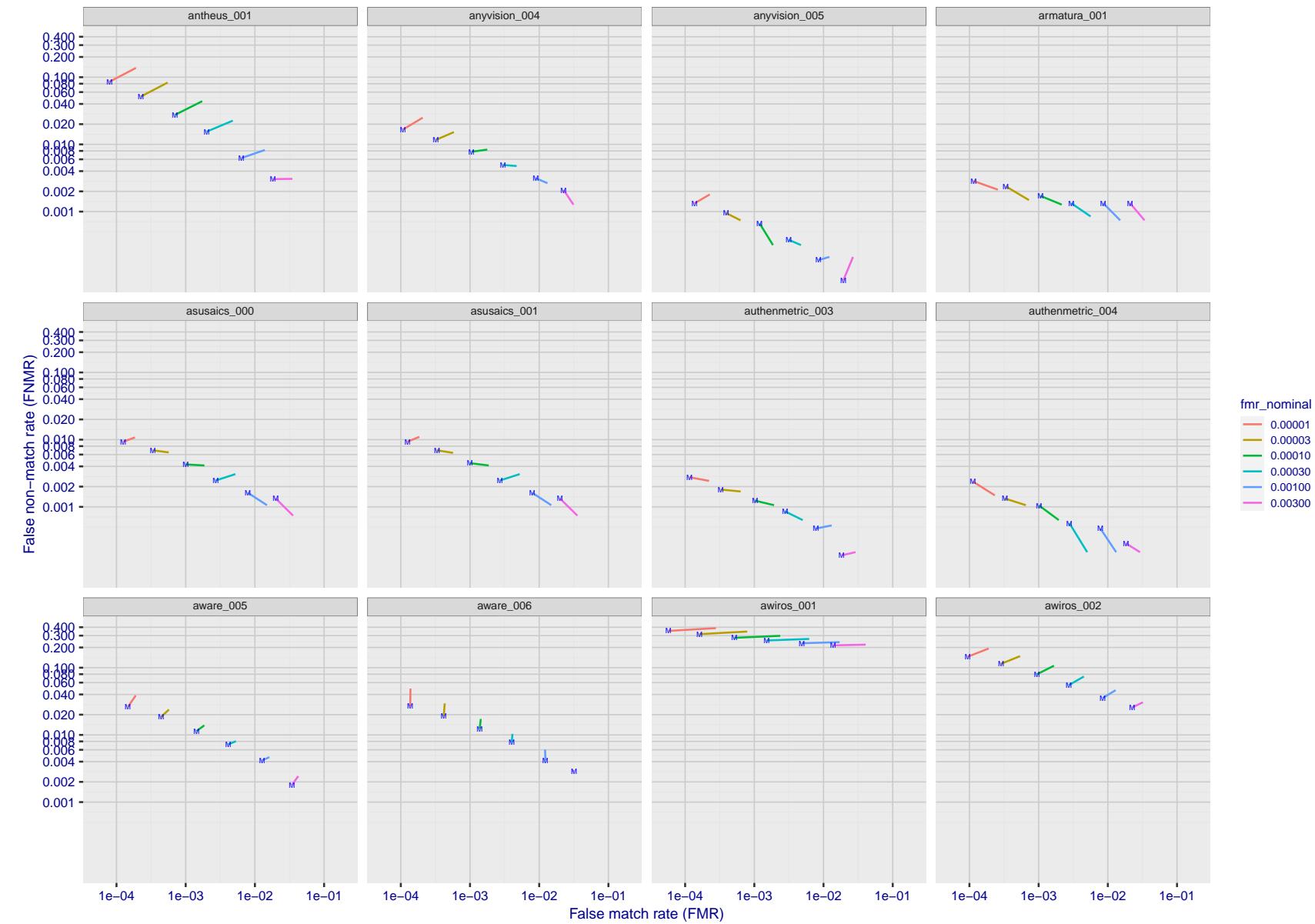


Figure 140: For the visa images, FNMR and FMR at six operating points along the DET characteristic. At each point a line is drawn between $(FMR, FNMR)_{MALE}$ and $(FMR, FNMR)_{FEMALE}$ showing how which sex has lower FMR and/or FNMR. The "M" label denotes male, the other end of the line corresponds to female. The six operating thresholds are selected to give the nominal false match rates given in the legend, and are computed over all impostor pairs regardless of age, sex, and place of birth. The plotted FMR values are broadly an order of magnitude larger than the nominal rates because FMR is computed over demographically-matched impostor pairs i.e individuals of the same sex, from the same geographic region (see section 3.6.1), and the same age group (see section 3.6.2).

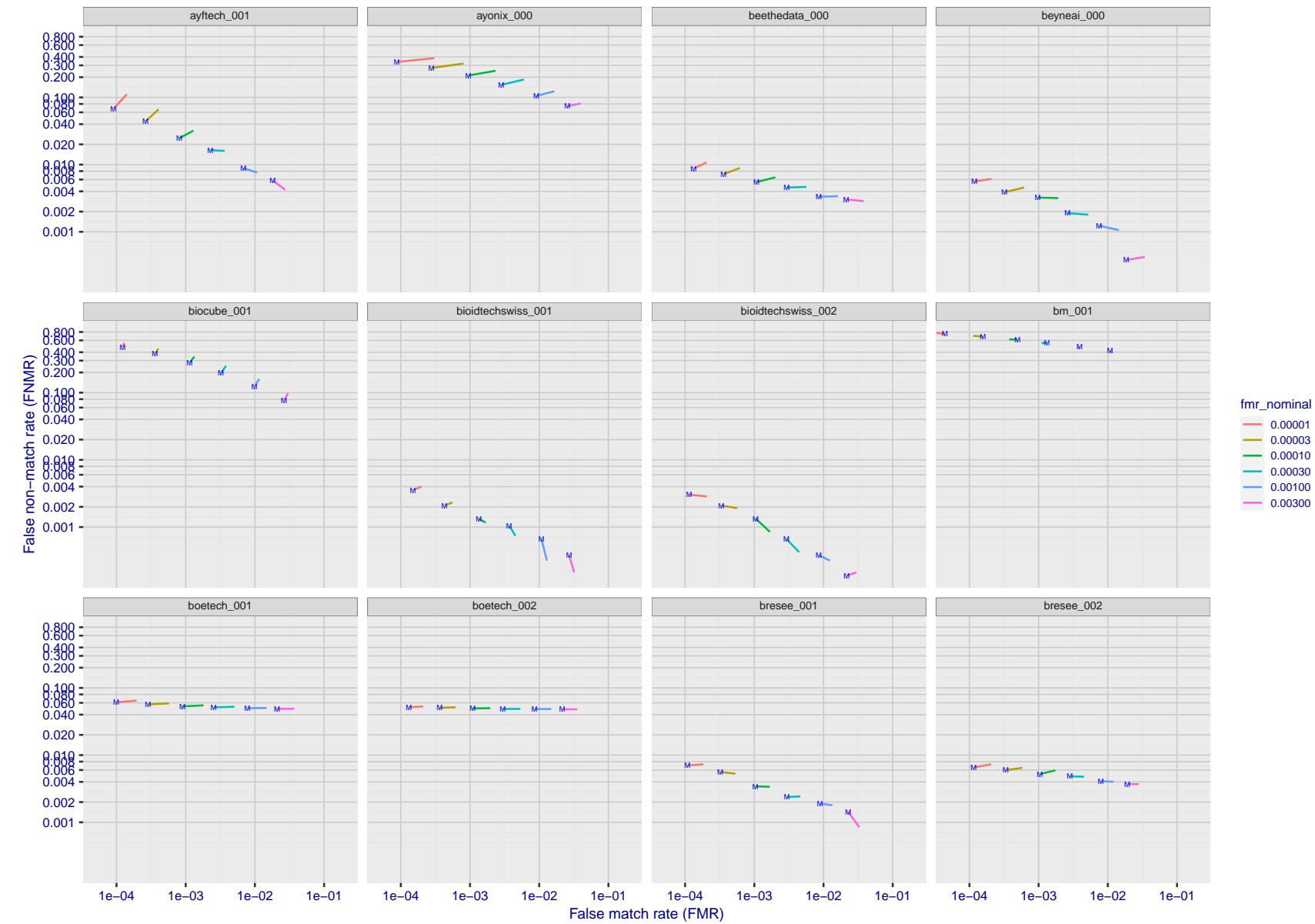


Figure 141: For the visa images, FNMR and FMR at six operating points along the DET characteristic. At each point a line is drawn between $(FMR, FNMR)_{MALE}$ and $(FMR, FNMR)_{FEMALE}$ showing how which sex has lower FMR and/or FNMR. The "M" label denotes male, the other end of the line corresponds to female. The six operating thresholds are selected to give the nominal false match rates given in the legend, and are computed over all impostor pairs regardless of age, sex, and place of birth. The plotted FMR values are broadly an order of magnitude larger than the nominal rates because FMR is computed over demographically-matched impostor pairs i.e individuals of the same sex, from the same geographic region (see section 3.6.1), and the same age group (see section 3.6.2).

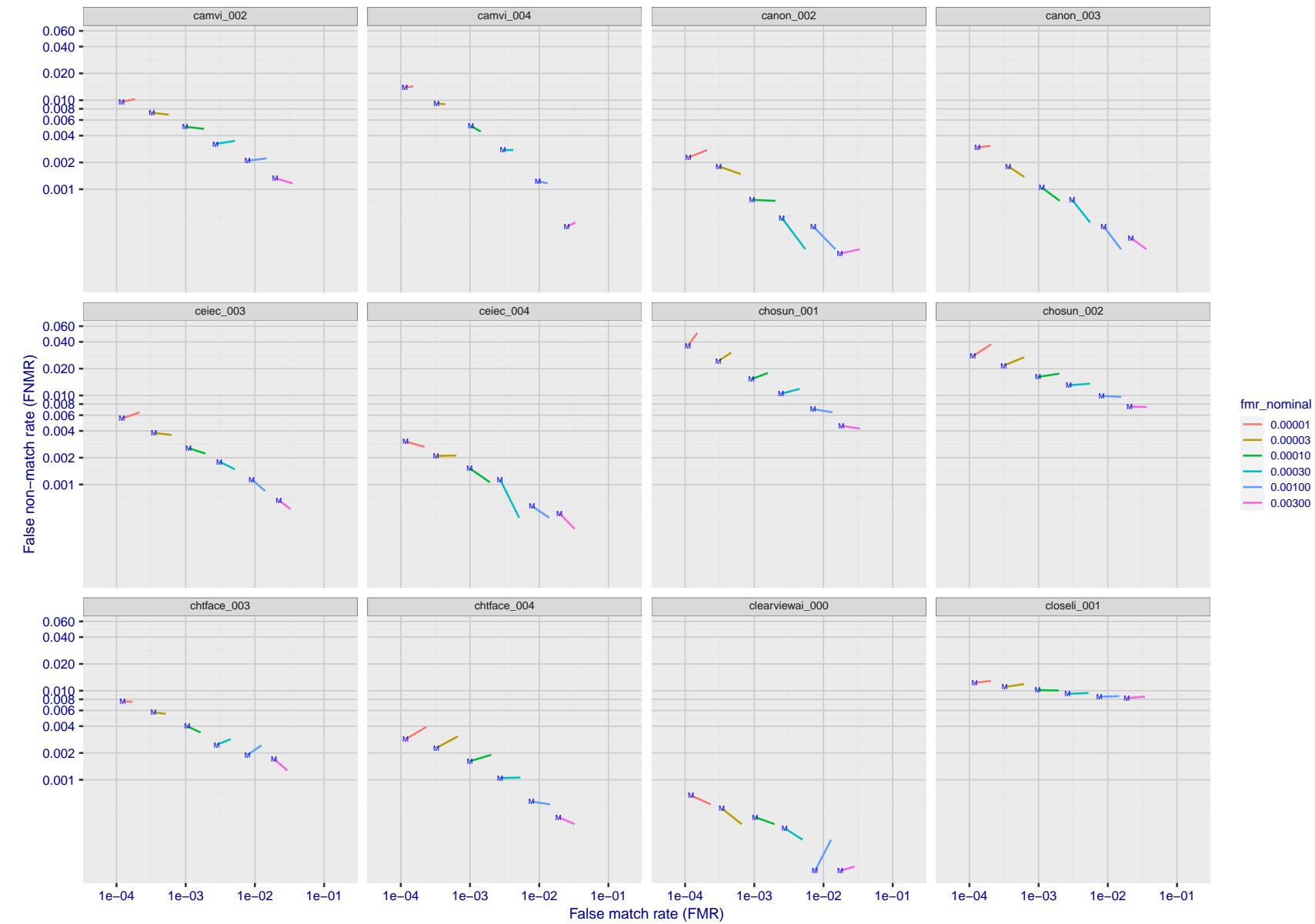


Figure 142: For the visa images, FNMR and FMR at six operating points along the DET characteristic. At each point a line is drawn between $(FMR, FNMR)_{MALE}$ and $(FMR, FNMR)_{FEMALE}$ showing how which sex has lower FMR and/or FNMR. The "M" label denotes male, the other end of the line corresponds to female. The six operating thresholds are selected to give the nominal false match rates given in the legend, and are computed over all impostor pairs regardless of age, sex, and place of birth. The plotted FMR values are broadly an order of magnitude larger than the nominal rates because FMR is computed over demographically-matched impostor pairs i.e individuals of the same sex, from the same geographic region (see section 3.6.1), and the same age group (see section 3.6.2).

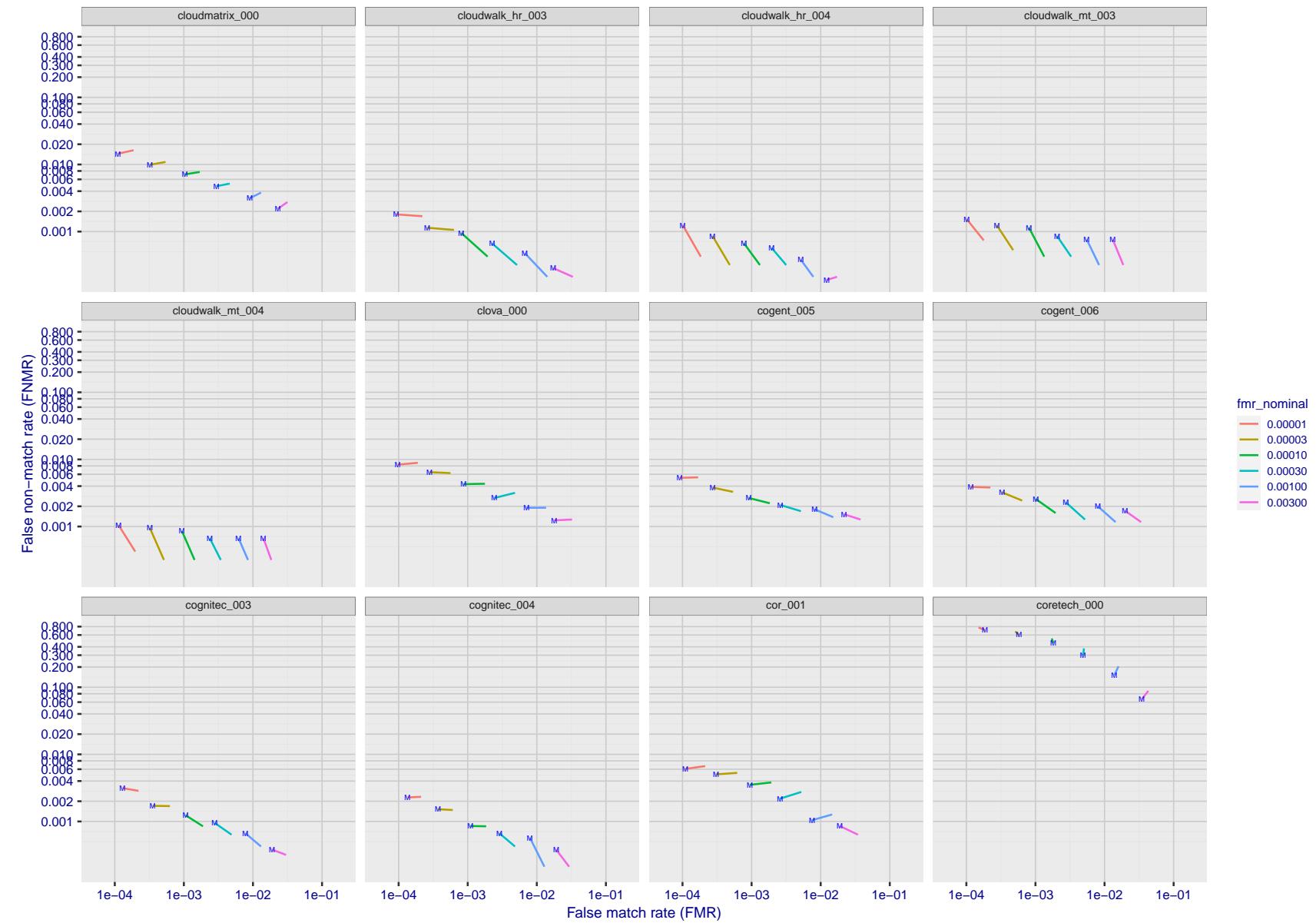


Figure 143: For the visa images, FNMR and FMR at six operating points along the DET characteristic. At each point a line is drawn between $(FMR, FNMR)_{MALE}$ and $(FMR, FNMR)_{FEMALE}$ showing how which sex has lower FMR and/or FNMR. The "M" label denotes male, the other end of the line corresponds to female. The six operating thresholds are selected to give the nominal false match rates given in the legend, and are computed over all impostor pairs regardless of age, sex, and place of birth. The plotted FMR values are broadly an order of magnitude larger than the nominal rates because FMR is computed over demographically-matched impostor pairs i.e individuals of the same sex, from the same geographic region (see section 3.6.1), and the same age group (see section 3.6.2).

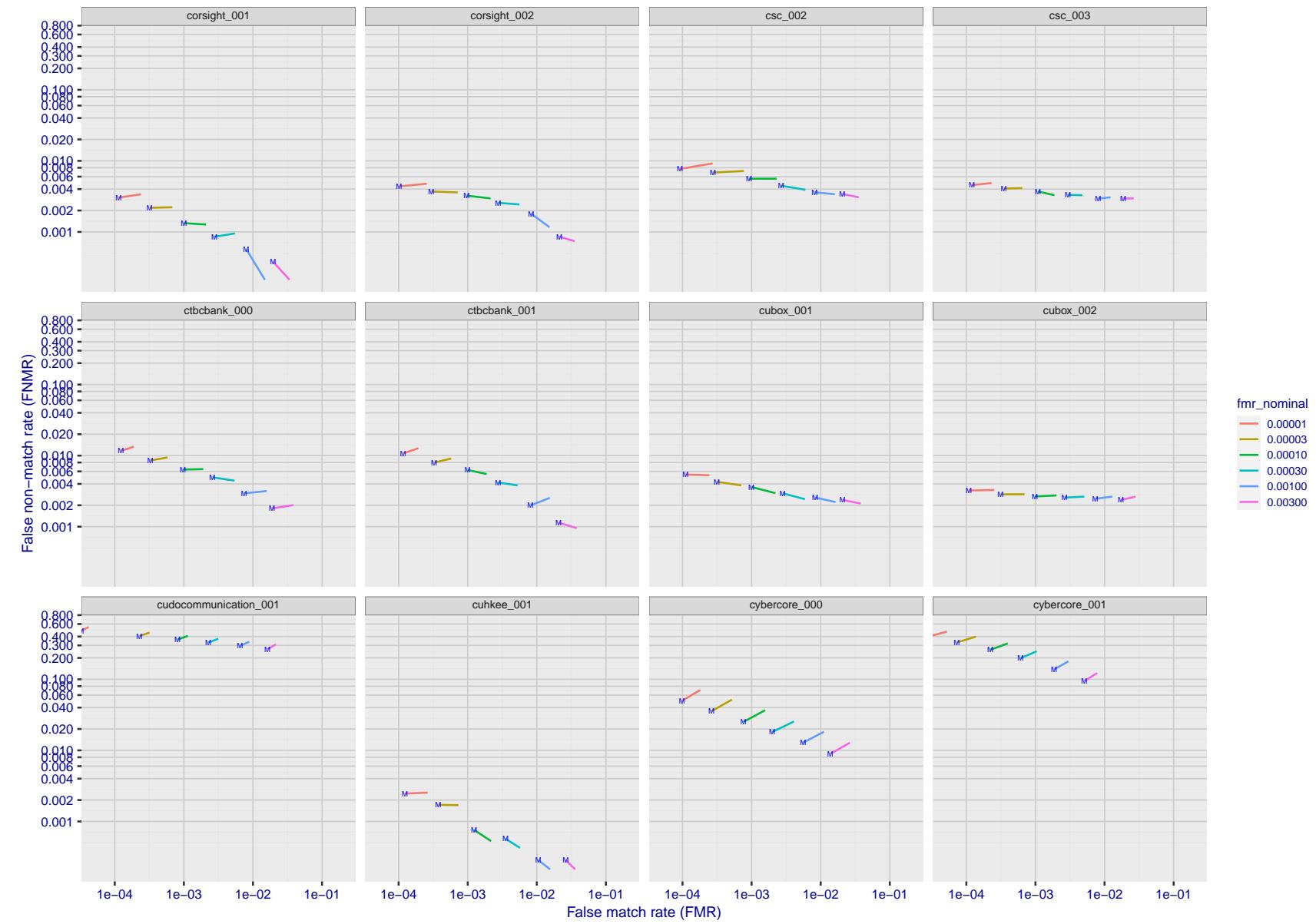


Figure 144: For the visa images, FNMR and FMR at six operating points along the DET characteristic. At each point a line is drawn between $(FMR, FNMR)_{MALE}$ and $(FMR, FNMR)_{FEMALE}$ showing how which sex has lower FMR and/or FNMR. The "M" label denotes male, the other end of the line corresponds to female. The six operating thresholds are selected to give the nominal false match rates given in the legend, and are computed over all impostor pairs regardless of age, sex, and place of birth. The plotted FMR values are broadly an order of magnitude larger than the nominal rates because FMR is computed over demographically-matched impostor pairs i.e individuals of the same sex, from the same geographic region (see section 3.6.1), and the same age group (see section 3.6.2).

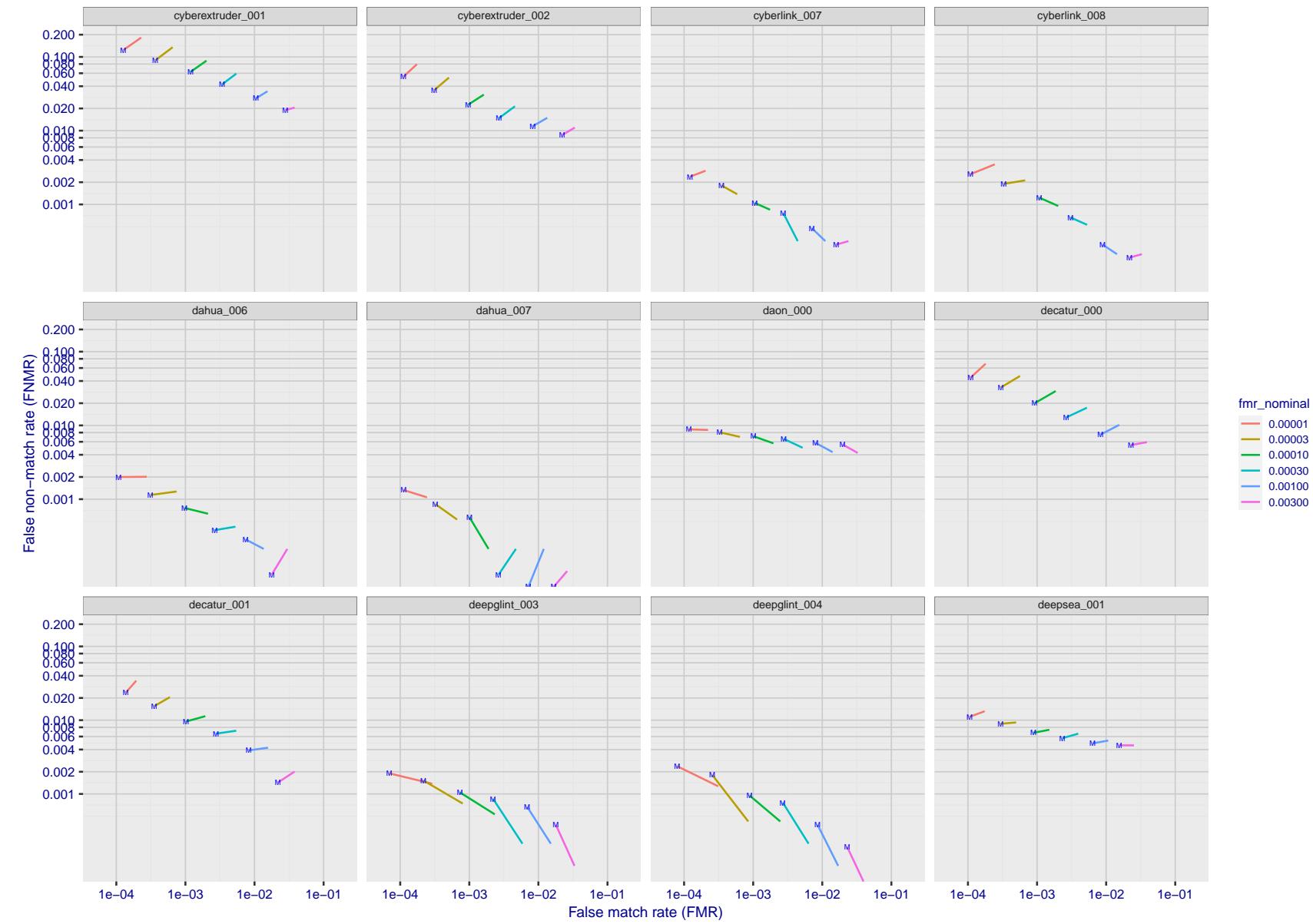


Figure 145: For the visa images, FNMR and FMR at six operating points along the DET characteristic. At each point a line is drawn between $(FMR, FNMR)_{MALE}$ and $(FMR, FNMR)_{FEMALE}$ showing how which sex has lower FMR and/or FNMR. The "M" label denotes male, the other end of the line corresponds to female. The six operating thresholds are selected to give the nominal false match rates given in the legend, and are computed over all impostor pairs regardless of age, sex, and place of birth. The plotted FMR values are broadly an order of magnitude larger than the nominal rates because FMR is computed over demographically-matched impostor pairs i.e individuals of the same sex, from the same geographic region (see section 3.6.1), and the same age group (see section 3.6.2).

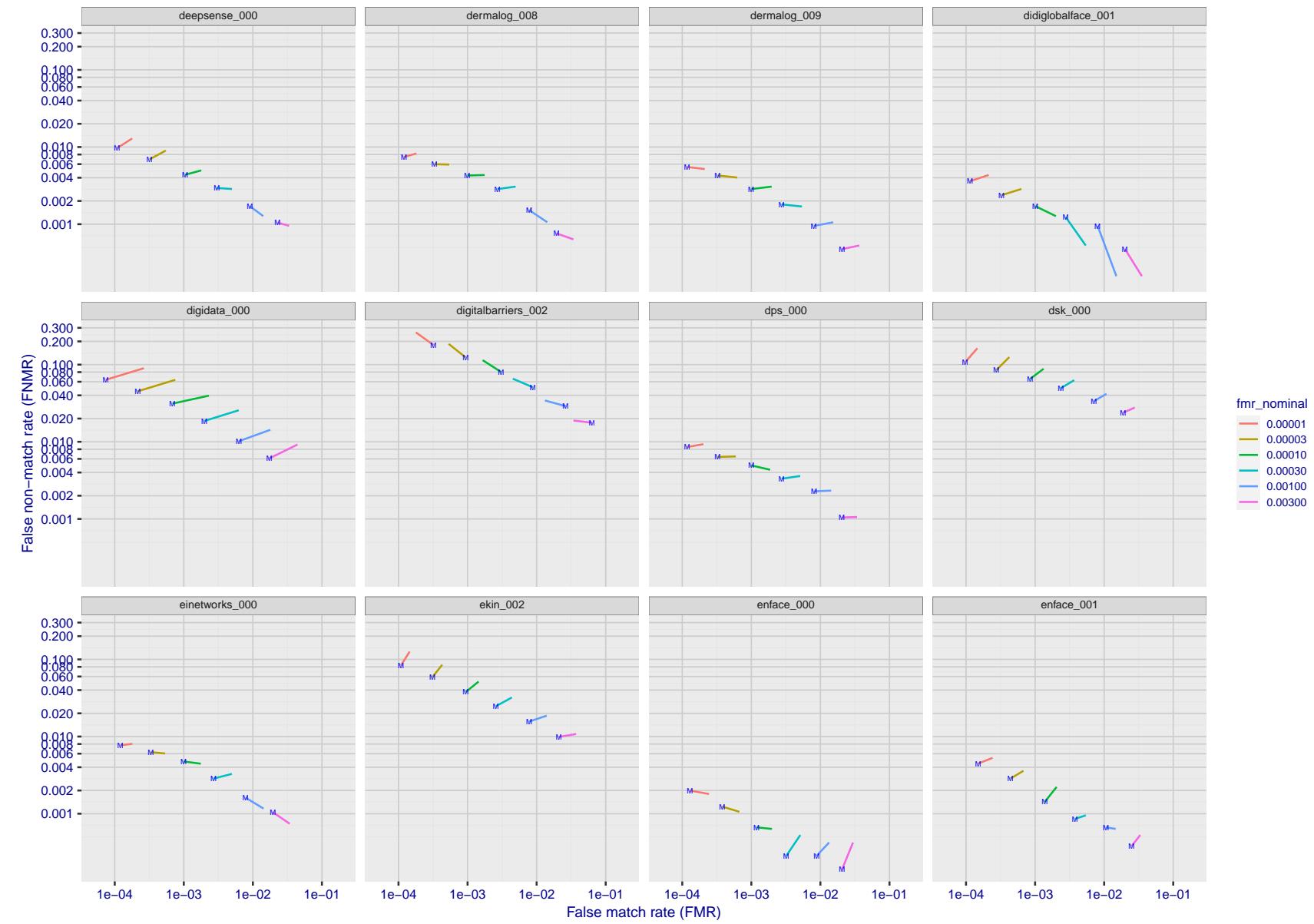


Figure 146: For the visa images, FNMR and FMR at six operating points along the DET characteristic. At each point a line is drawn between $(FMR, FNMR)_{MALE}$ and $(FMR, FNMR)_{FEMALE}$ showing how which sex has lower FMR and/or FNMR. The "M" label denotes male, the other end of the line corresponds to female. The six operating thresholds are selected to give the nominal false match rates given in the legend, and are computed over all impostor pairs regardless of age, sex, and place of birth. The plotted FMR values are broadly an order of magnitude larger than the nominal rates because FMR is computed over demographically-matched impostor pairs i.e individuals of the same sex, from the same geographic region (see section 3.6.1), and the same age group (see section 3.6.2).

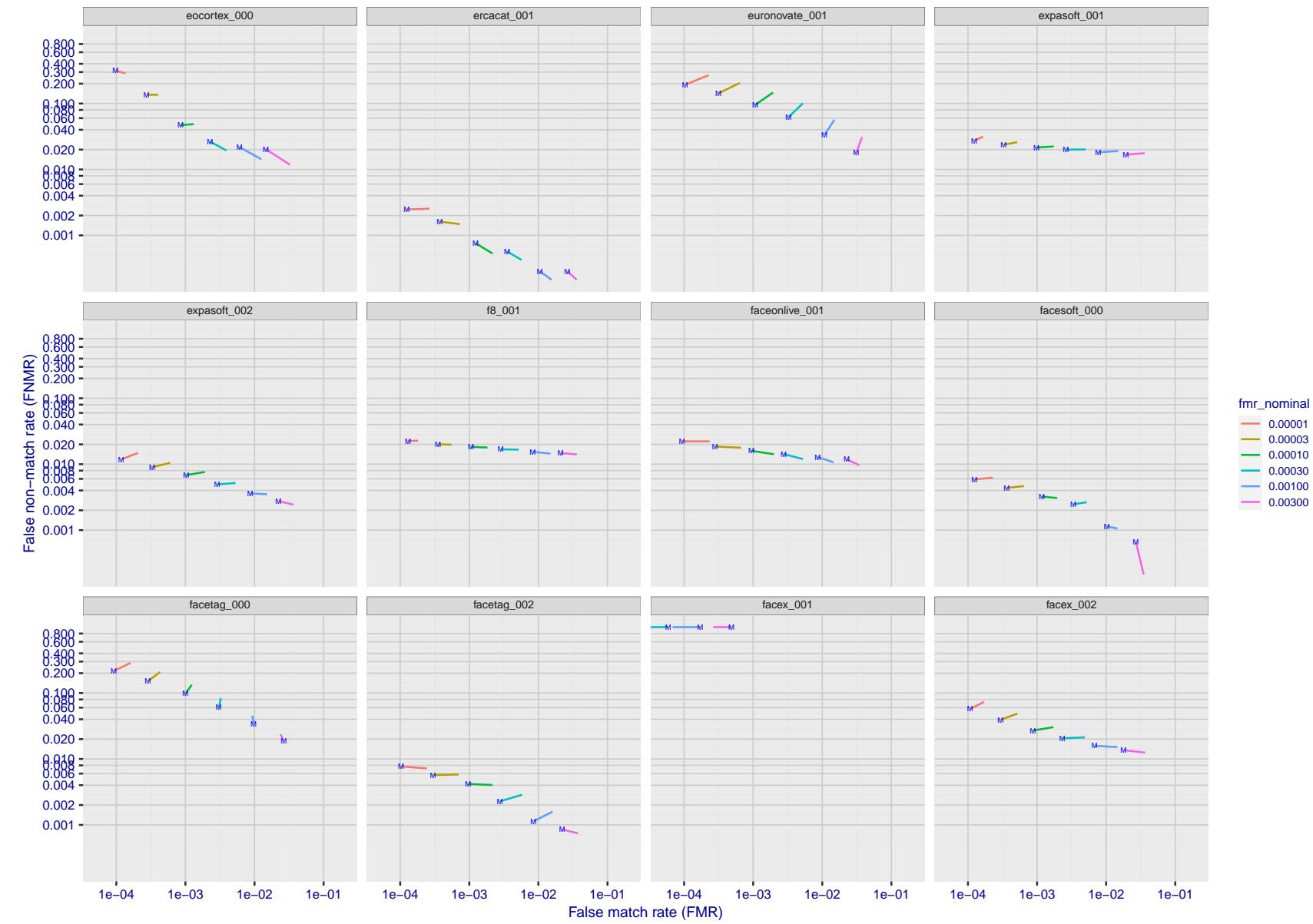


Figure 147: For the visa images, FNMR and FMR at six operating points along the DET characteristic. At each point a line is drawn between $(FMR, FNMR)_{MALE}$ and $(FMR, FNMR)_{FEMALE}$ showing how which sex has lower FMR and/or FNMR. The "M" label denotes male, the other end of the line corresponds to female. The six operating thresholds are selected to give the nominal false match rates given in the legend, and are computed over all impostor pairs regardless of age, sex, and place of birth. The plotted FMR values are broadly an order of magnitude larger than the nominal rates because FMR is computed over demographically-matched impostor pairs i.e individuals of the same sex, from the same geographic region (see section 3.6.1), and the same age group (see section 3.6.2).

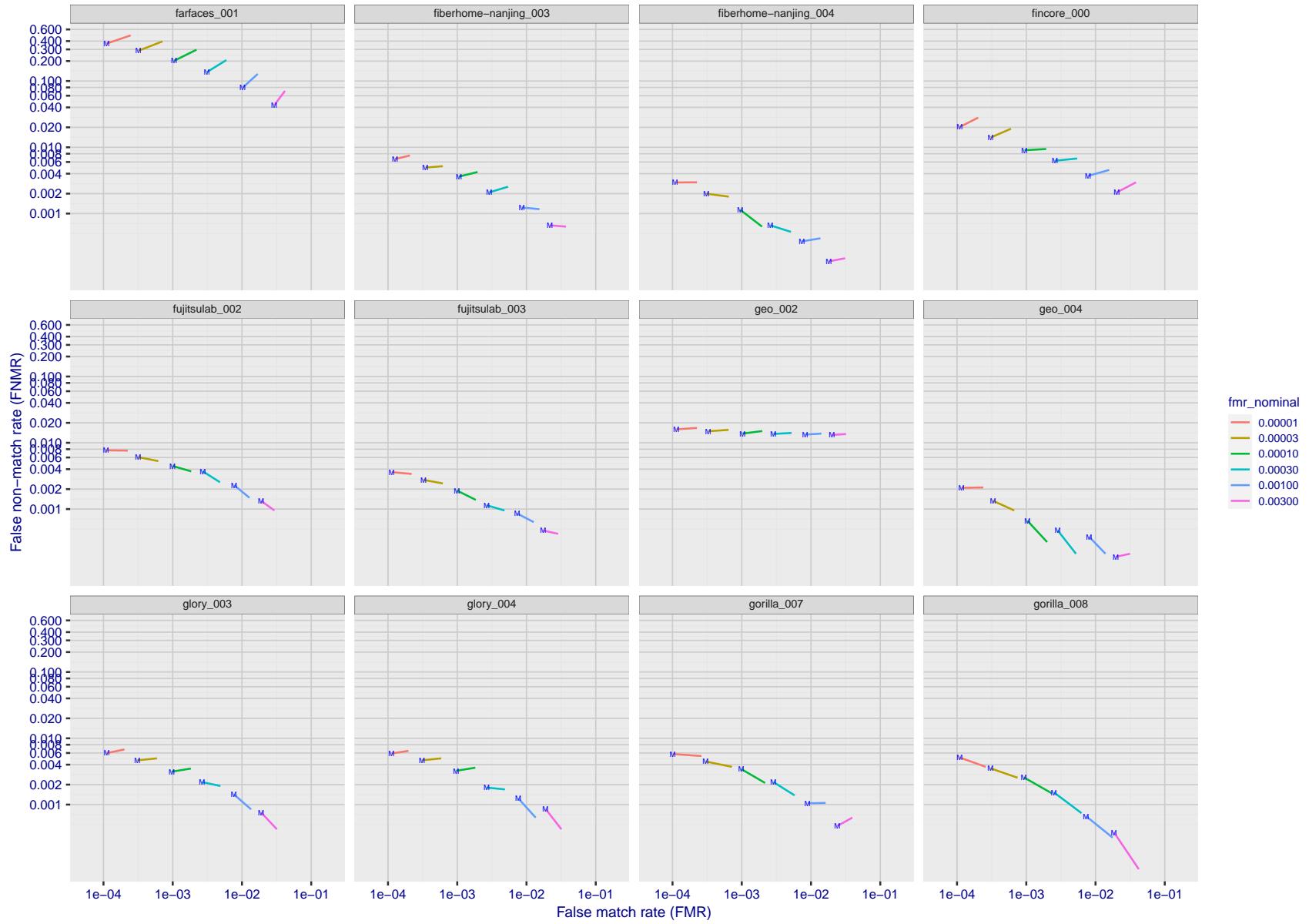


Figure 148: For the visa images, FNMR and FMR at six operating points along the DET characteristic. At each point a line is drawn between $(FMR, FNMR)_{MALE}$ and $(FMR, FNMR)_{FEMALE}$ showing how which sex has lower FMR and/or FNMR. The "M" label denotes male, the other end of the line corresponds to female. The six operating thresholds are selected to give the nominal false match rates given in the legend, and are computed over all impostor pairs regardless of age, sex, and place of birth. The plotted FMR values are broadly an order of magnitude larger than the nominal rates because FMR is computed over demographically-matched impostor pairs i.e individuals of the same sex, from the same geographic region (see section 3.6.1), and the same age group (see section 3.6.2).

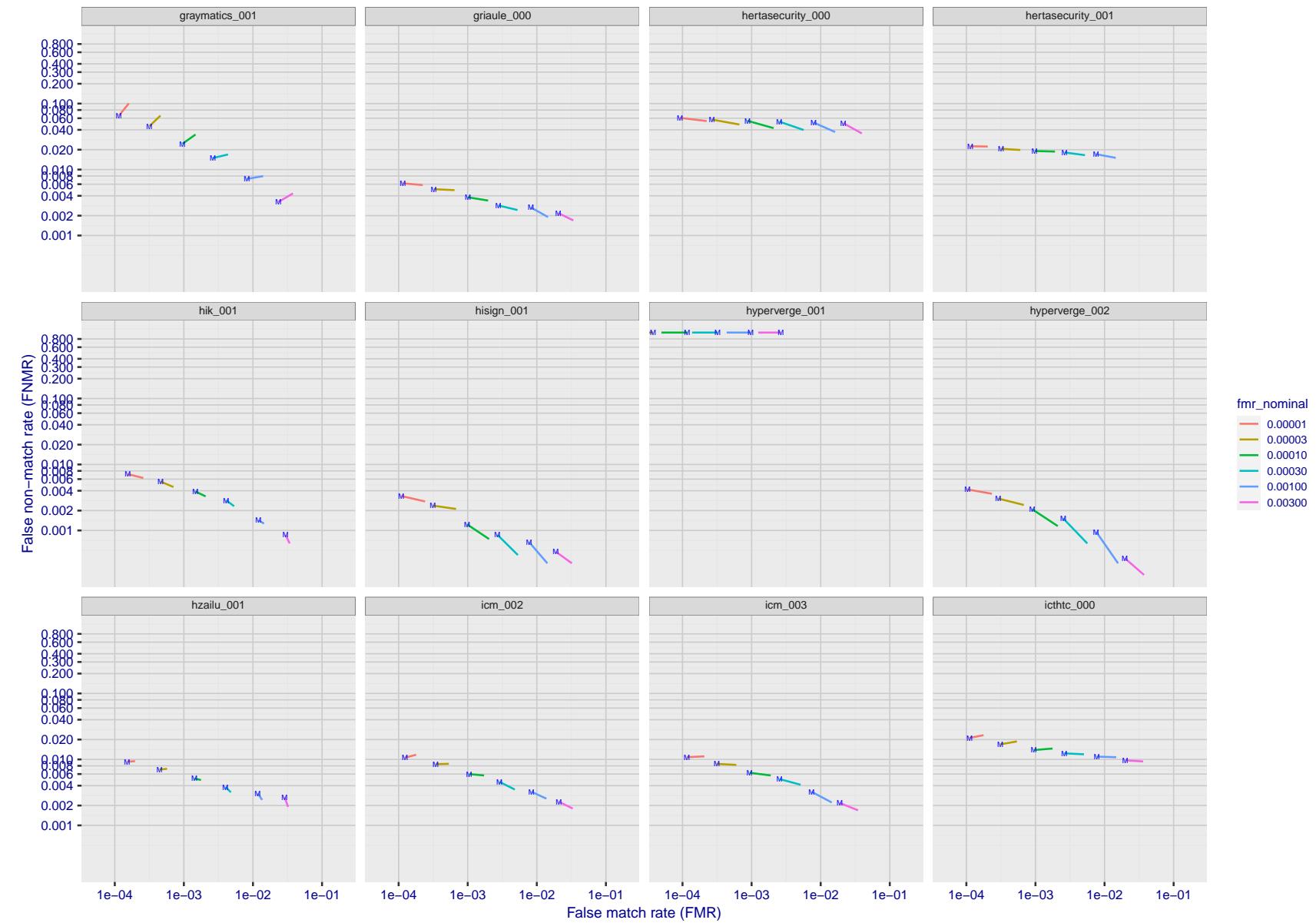


Figure 149: For the visa images, FNMR and FMR at six operating points along the DET characteristic. At each point a line is drawn between $(FMR, FNMR)_{MALE}$ and $(FMR, FNMR)_{FEMALE}$ showing how which sex has lower FMR and/or FNMR. The "M" label denotes male, the other end of the line corresponds to female. The six operating thresholds are selected to give the nominal false match rates given in the legend, and are computed over all impostor pairs regardless of age, sex, and place of birth. The plotted FMR values are broadly an order of magnitude larger than the nominal rates because FMR is computed over demographically-matched impostor pairs i.e individuals of the same sex, from the same geographic region (see section 3.6.1), and the same age group (see section 3.6.2).

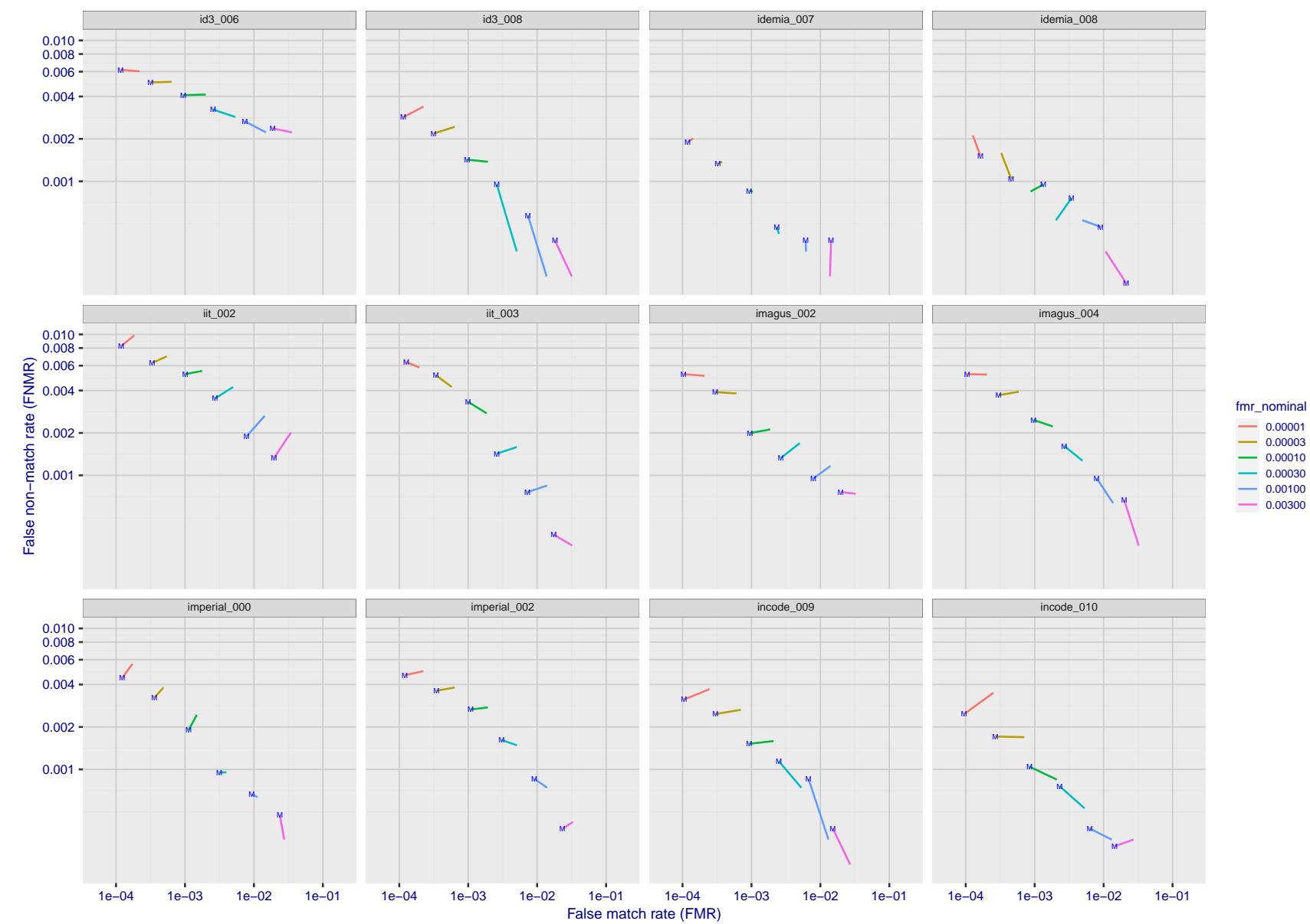


Figure 150: For the visa images, FNMR and FMR at six operating points along the DET characteristic. At each point a line is drawn between $(FMR, FNMR)_{MALE}$ and $(FMR, FNMR)_{FEMALE}$ showing how which sex has lower FMR and/or FNMR. The "M" label denotes male, the other end of the line corresponds to female. The six operating thresholds are selected to give the nominal false match rates given in the legend, and are computed over all impostor pairs regardless of age, sex, and place of birth. The plotted FMR values are broadly an order of magnitude larger than the nominal rates because FMR is computed over demographically-matched impostor pairs i.e individuals of the same sex, from the same geographic region (see section 3.6.1), and the same age group (see section 3.6.2).

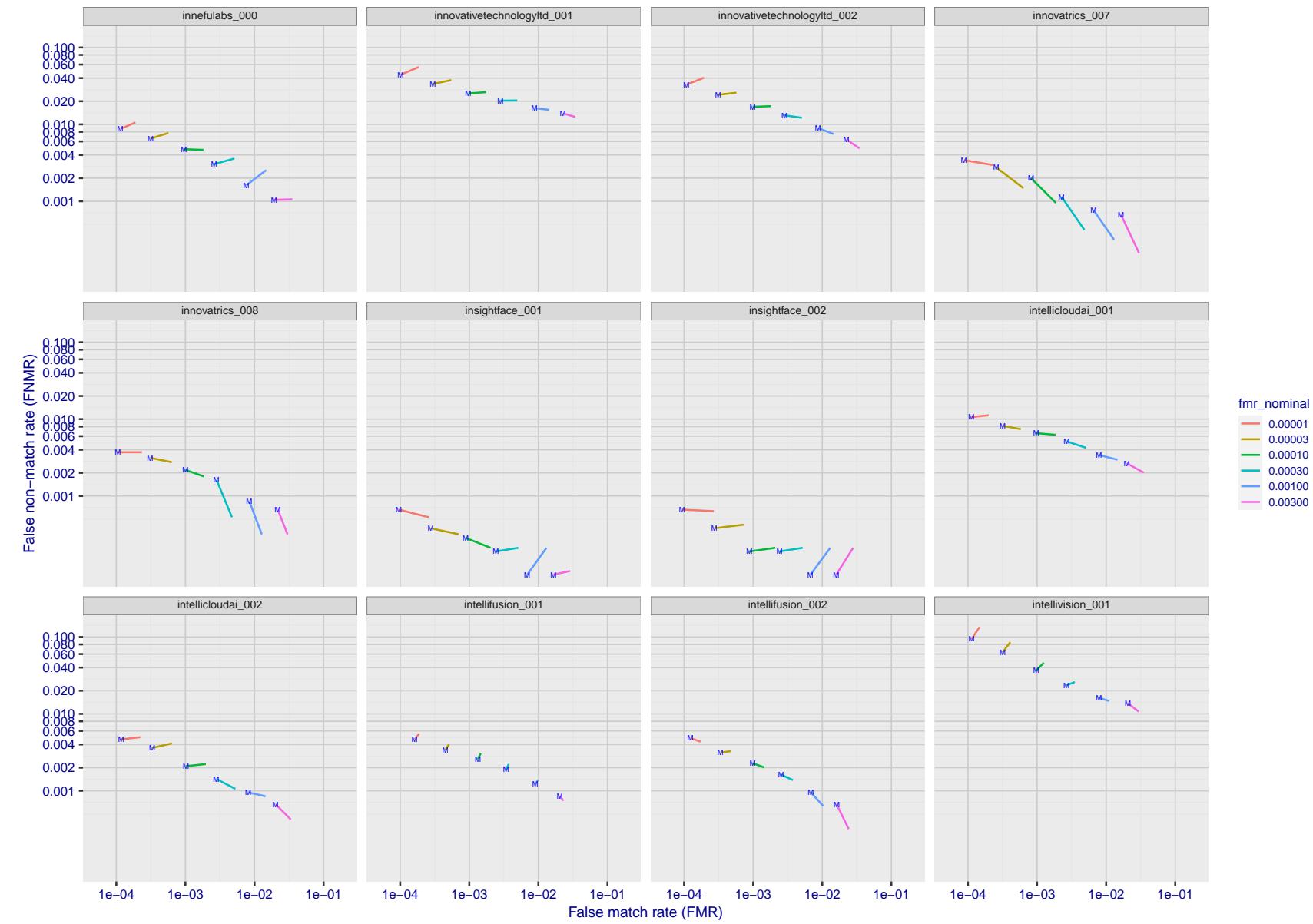


Figure 151: For the visa images, FNMR and FMR at six operating points along the DET characteristic. At each point a line is drawn between $(FMR, FNMR)_{MALE}$ and $(FMR, FNMR)_{FEMALE}$ showing how which sex has lower FMR and/or FNMR. The "M" label denotes male, the other end of the line corresponds to female. The six operating thresholds are selected to give the nominal false match rates given in the legend, and are computed over all impostor pairs regardless of age, sex, and place of birth. The plotted FMR values are broadly an order of magnitude larger than the nominal rates because FMR is computed over demographically-matched impostor pairs i.e individuals of the same sex, from the same geographic region (see section 3.6.1), and the same age group (see section 3.6.2).

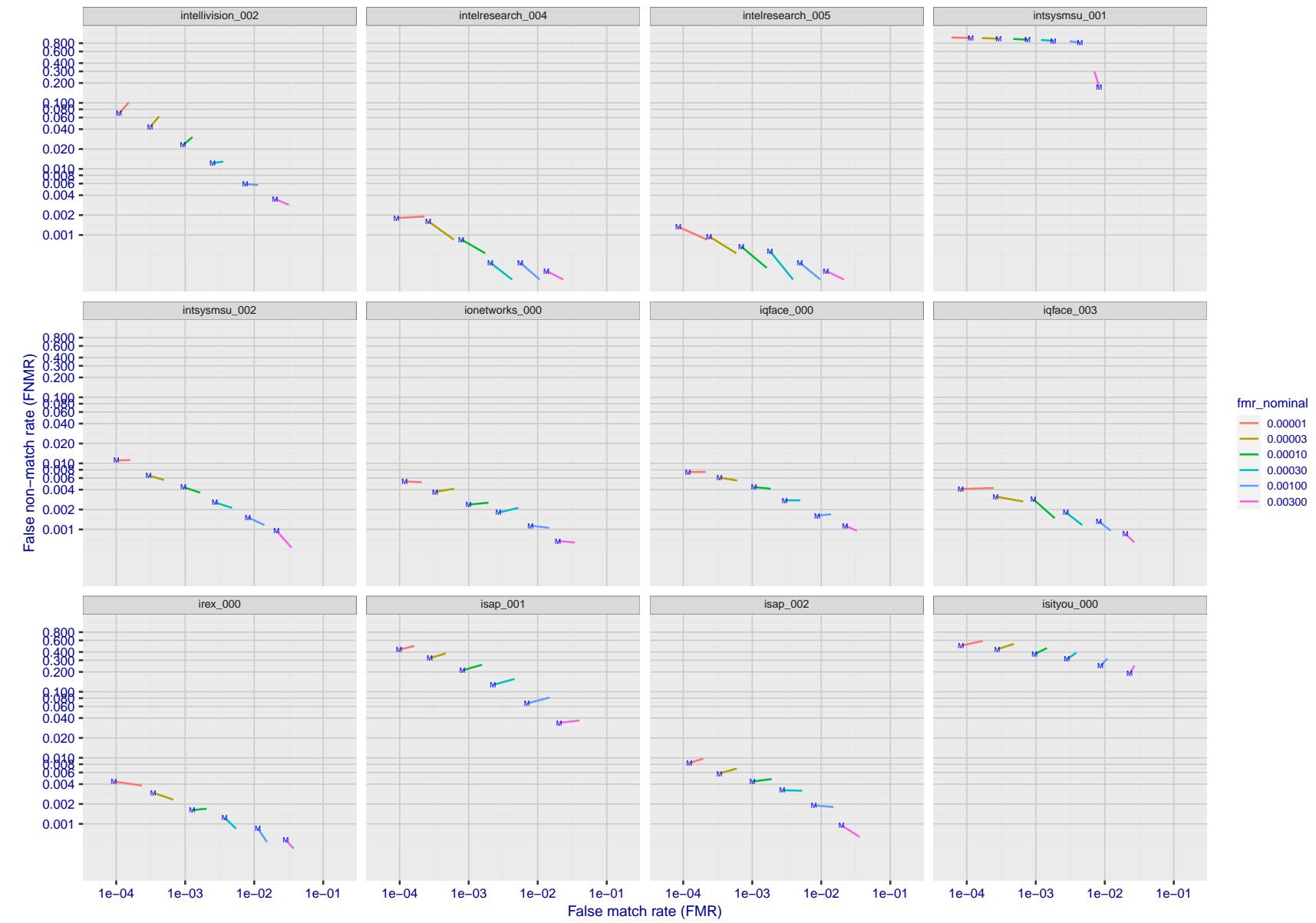


Figure 152: For the visa images, FNMR and FMR at six operating points along the DET characteristic. At each point a line is drawn between $(FMR, FNMR)_{MALE}$ and $(FMR, FNMR)_{FEMALE}$ showing how which sex has lower FMR and/or FNMR. The "M" label denotes male, the other end of the line corresponds to female. The six operating thresholds are selected to give the nominal false match rates given in the legend, and are computed over all impostor pairs regardless of age, sex, and place of birth. The plotted FMR values are broadly an order of magnitude larger than the nominal rates because FMR is computed over demographically-matched impostor pairs i.e individuals of the same sex, from the same geographic region (see section 3.6.1), and the same age group (see section 3.6.2).

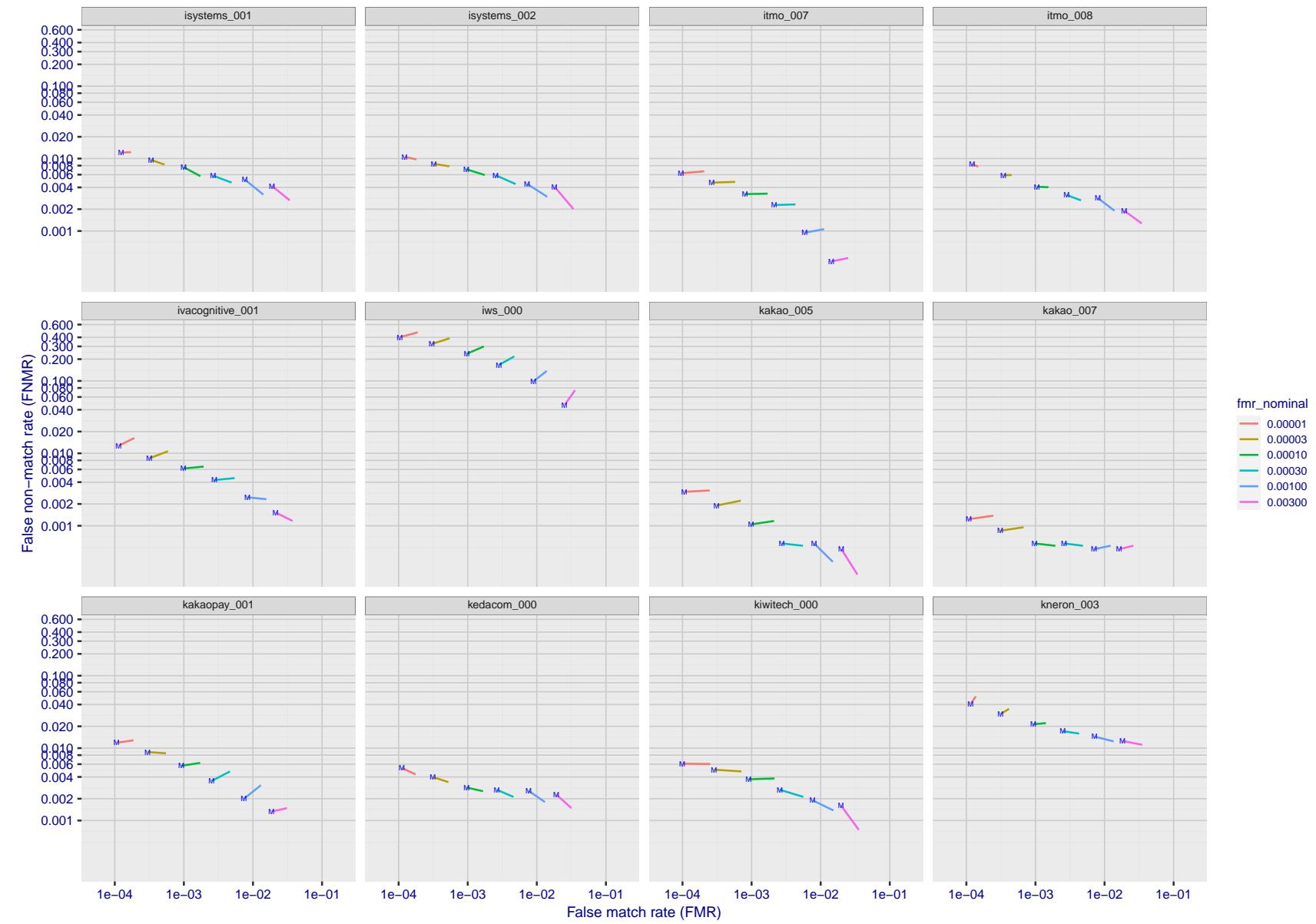


Figure 153: For the visa images, FNMR and FMR at six operating points along the DET characteristic. At each point a line is drawn between $(FMR, FNMR)_{MALE}$ and $(FMR, FNMR)_{FEMALE}$ showing how which sex has lower FMR and/or FNMR. The "M" label denotes male, the other end of the line corresponds to female. The six operating thresholds are selected to give the nominal false match rates given in the legend, and are computed over all impostor pairs regardless of age, sex, and place of birth. The plotted FMR values are broadly an order of magnitude larger than the nominal rates because FMR is computed over demographically-matched impostor pairs i.e individuals of the same sex, from the same geographic region (see section 3.6.1), and the same age group (see section 3.6.2).

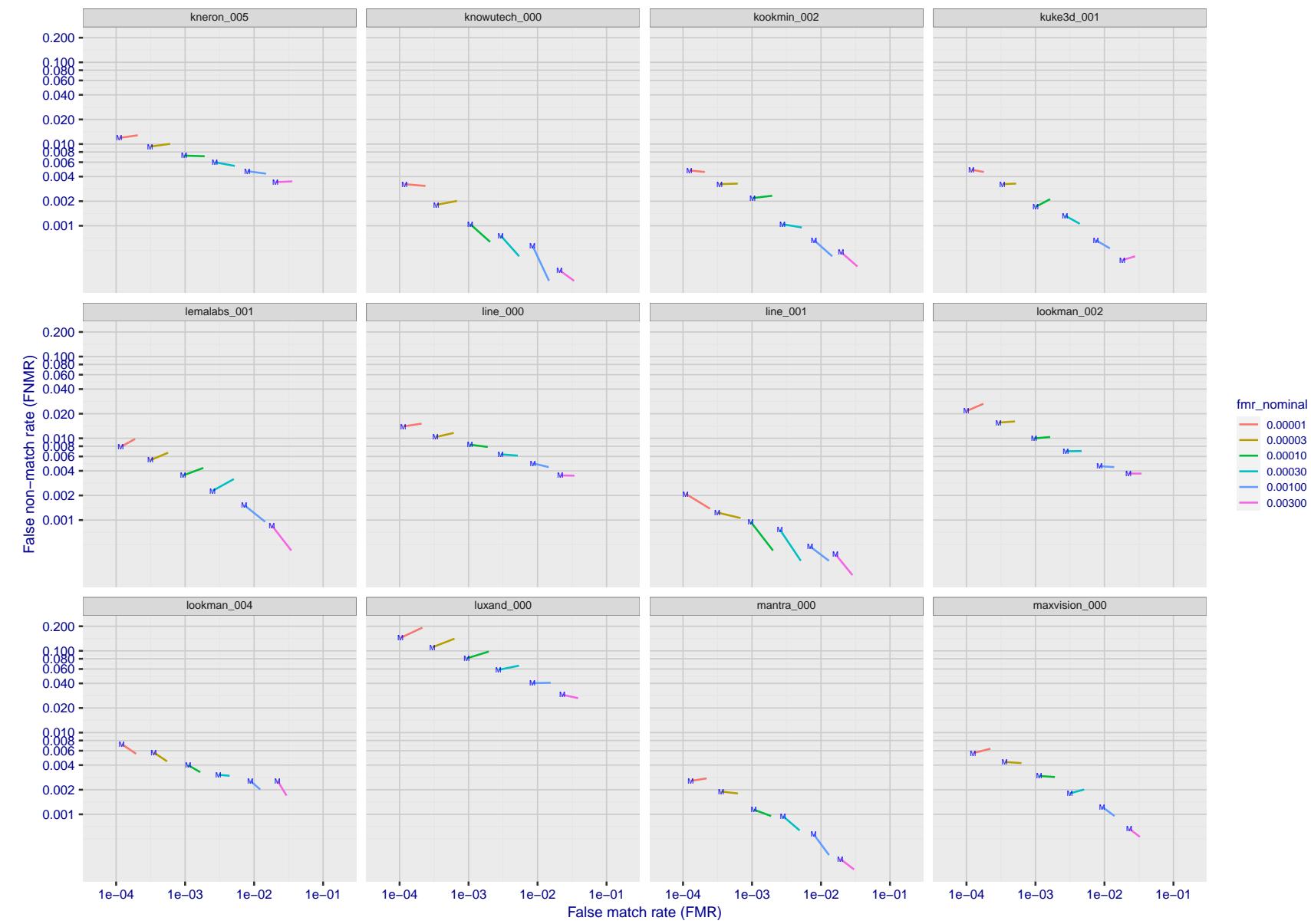


Figure 154: For the visa images, FNMR and FMR at six operating points along the DET characteristic. At each point a line is drawn between $(FMR, FNMR)_{MALE}$ and $(FMR, FNMR)_{FEMALE}$ showing how which sex has lower FMR and/or FNMR. The "M" label denotes male, the other end of the line corresponds to female. The six operating thresholds are selected to give the nominal false match rates given in the legend, and are computed over all impostor pairs regardless of age, sex, and place of birth. The plotted FMR values are broadly an order of magnitude larger than the nominal rates because FMR is computed over demographically-matched impostor pairs i.e individuals of the same sex, from the same geographic region (see section 3.6.1), and the same age group (see section 3.6.2).

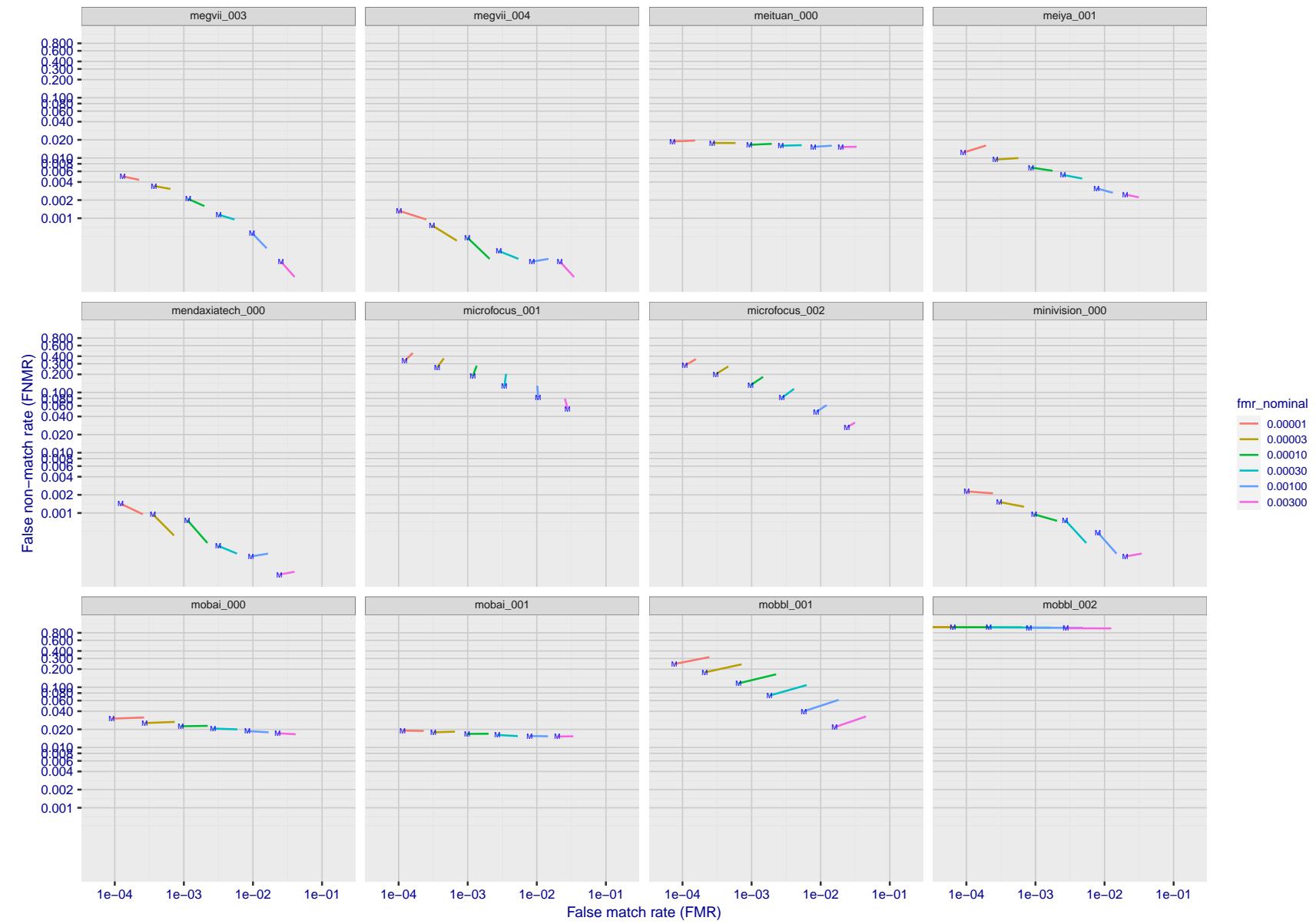


Figure 155: For the visa images, FNMR and FMR at six operating points along the DET characteristic. At each point a line is drawn between $(FMR, FNMR)_{MALE}$ and $(FMR, FNMR)_{FEMALE}$ showing how which sex has lower FMR and/or FNMR. The "M" label denotes male, the other end of the line corresponds to female. The six operating thresholds are selected to give the nominal false match rates given in the legend, and are computed over all impostor pairs regardless of age, sex, and place of birth. The plotted FMR values are broadly an order of magnitude larger than the nominal rates because FMR is computed over demographically-matched impostor pairs i.e individuals of the same sex, from the same geographic region (see section 3.6.1), and the same age group (see section 3.6.2).

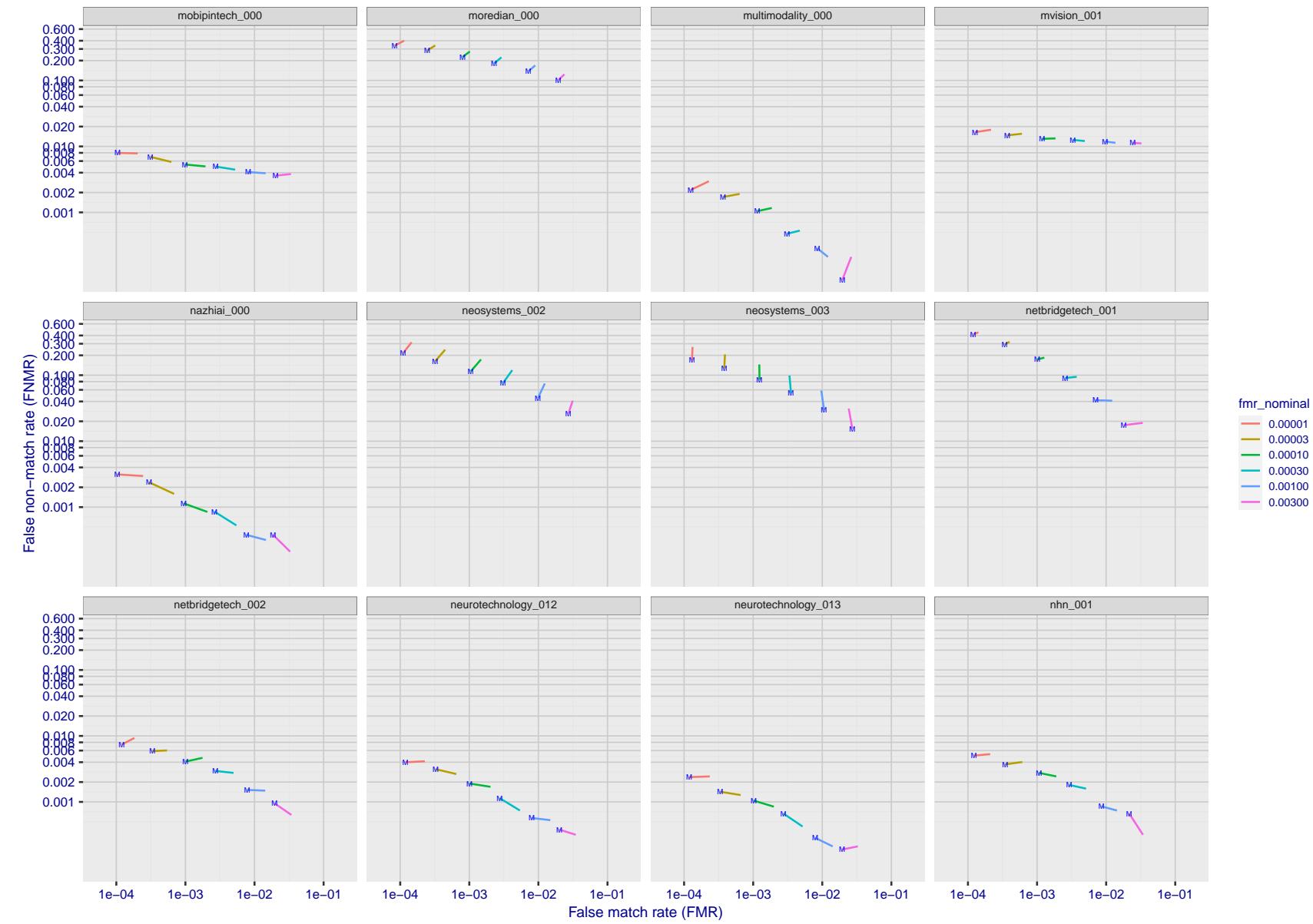


Figure 156: For the visa images, FNMR and FMR at six operating points along the DET characteristic. At each point a line is drawn between $(FMR, FNMR)_{MALE}$ and $(FMR, FNMR)_{FEMALE}$ showing how which sex has lower FMR and/or FNMR. The "M" label denotes male, the other end of the line corresponds to female. The six operating thresholds are selected to give the nominal false match rates given in the legend, and are computed over all impostor pairs regardless of age, sex, and place of birth. The plotted FMR values are broadly an order of magnitude larger than the nominal rates because FMR is computed over demographically-matched impostor pairs i.e individuals of the same sex, from the same geographic region (see section 3.6.1), and the same age group (see section 3.6.2).

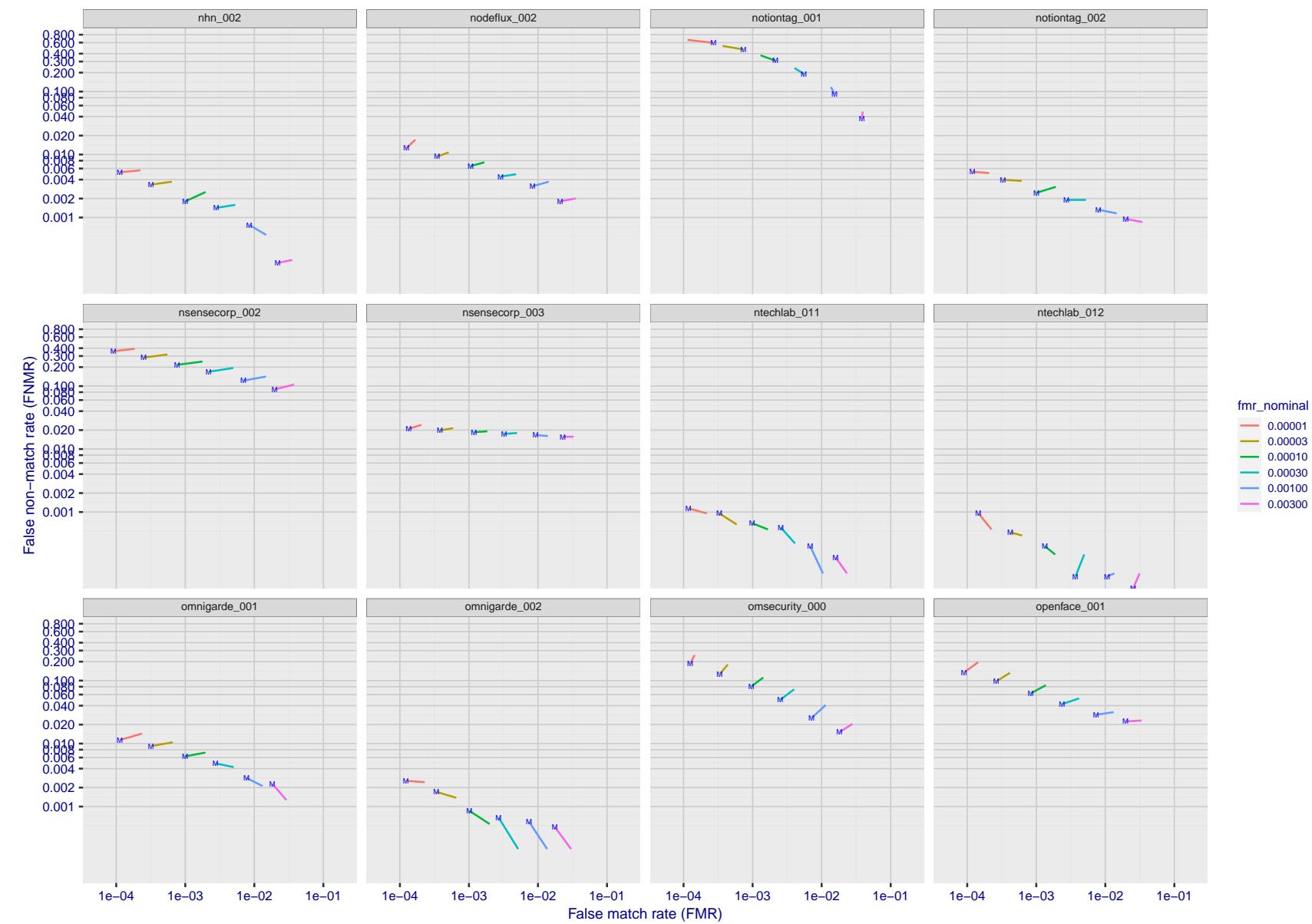


Figure 157: For the visa images, FNMR and FMR at six operating points along the DET characteristic. At each point a line is drawn between $(FMR, FNMR)_{MALE}$ and $(FMR, FNMR)_{FEMALE}$ showing how which sex has lower FMR and/or FNMR. The "M" label denotes male, the other end of the line corresponds to female. The six operating thresholds are selected to give the nominal false match rates given in the legend, and are computed over all impostor pairs regardless of age, sex, and place of birth. The plotted FMR values are broadly an order of magnitude larger than the nominal rates because FMR is computed over demographically-matched impostor pairs i.e individuals of the same sex, from the same geographic region (see section 3.6.1), and the same age group (see section 3.6.2).

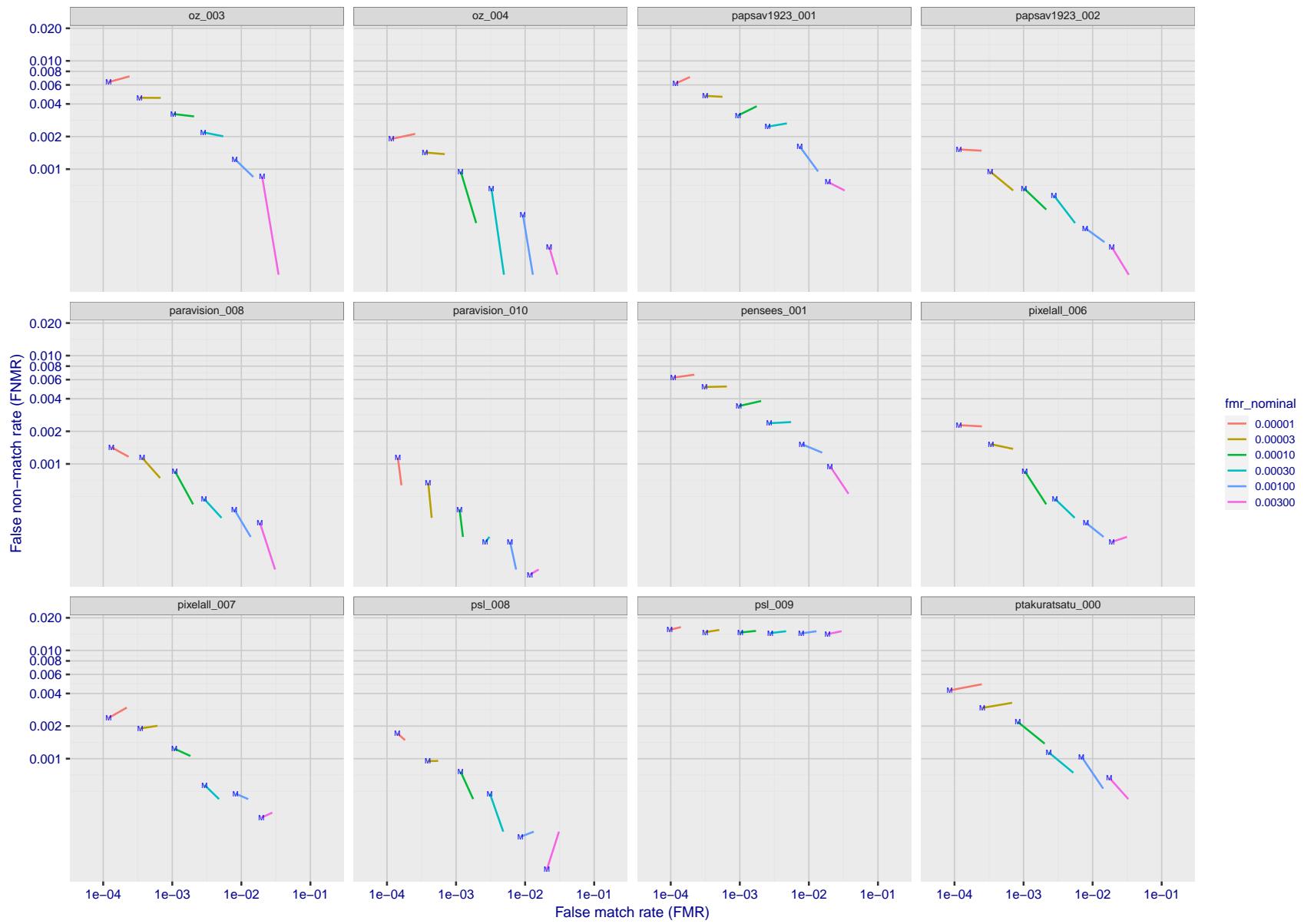


Figure 158: For the visa images, FNMR and FMR at six operating points along the DET characteristic. At each point a line is drawn between $(FMR, FNMR)_{MALE}$ and $(FMR, FNMR)_{FEMALE}$ showing how which sex has lower FMR and/or FNMR. The "M" label denotes male, the other end of the line corresponds to female. The six operating thresholds are selected to give the nominal false match rates given in the legend, and are computed over all impostor pairs regardless of age, sex, and place of birth. The plotted FMR values are broadly an order of magnitude larger than the nominal rates because FMR is computed over demographically-matched impostor pairs i.e individuals of the same sex, from the same geographic region (see section 3.6.1), and the same age group (see section 3.6.2).

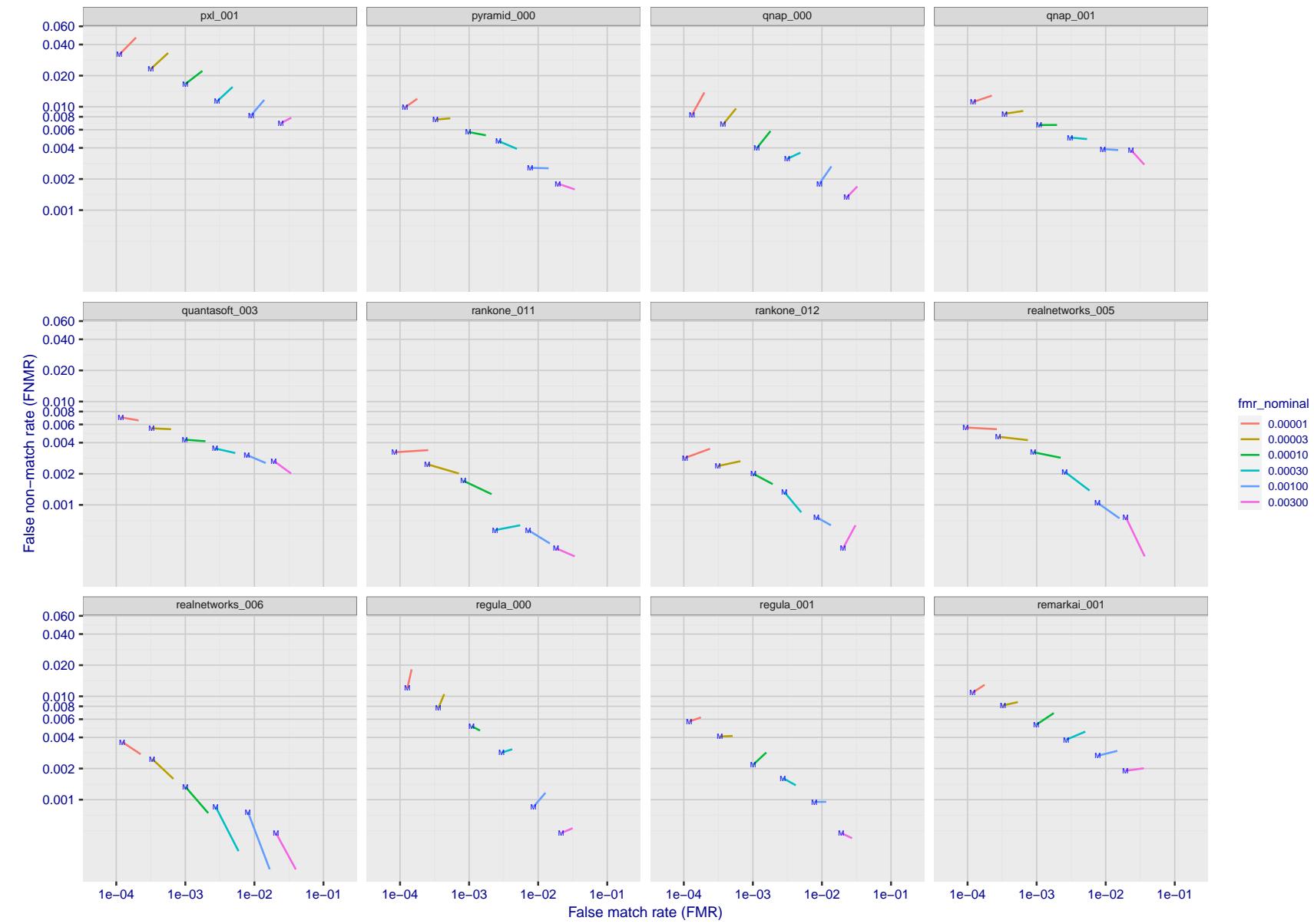


Figure 159: For the visa images, FNMR and FMR at six operating points along the DET characteristic. At each point a line is drawn between $(FMR, FNMR)_{MALE}$ and $(FMR, FNMR)_{FEMALE}$ showing how which sex has lower FMR and/or FNMR. The "M" label denotes male, the other end of the line corresponds to female. The six operating thresholds are selected to give the nominal false match rates given in the legend, and are computed over all impostor pairs regardless of age, sex, and place of birth. The plotted FMR values are broadly an order of magnitude larger than the nominal rates because FMR is computed over demographically-matched impostor pairs i.e individuals of the same sex, from the same geographic region (see section 3.6.1), and the same age group (see section 3.6.2).

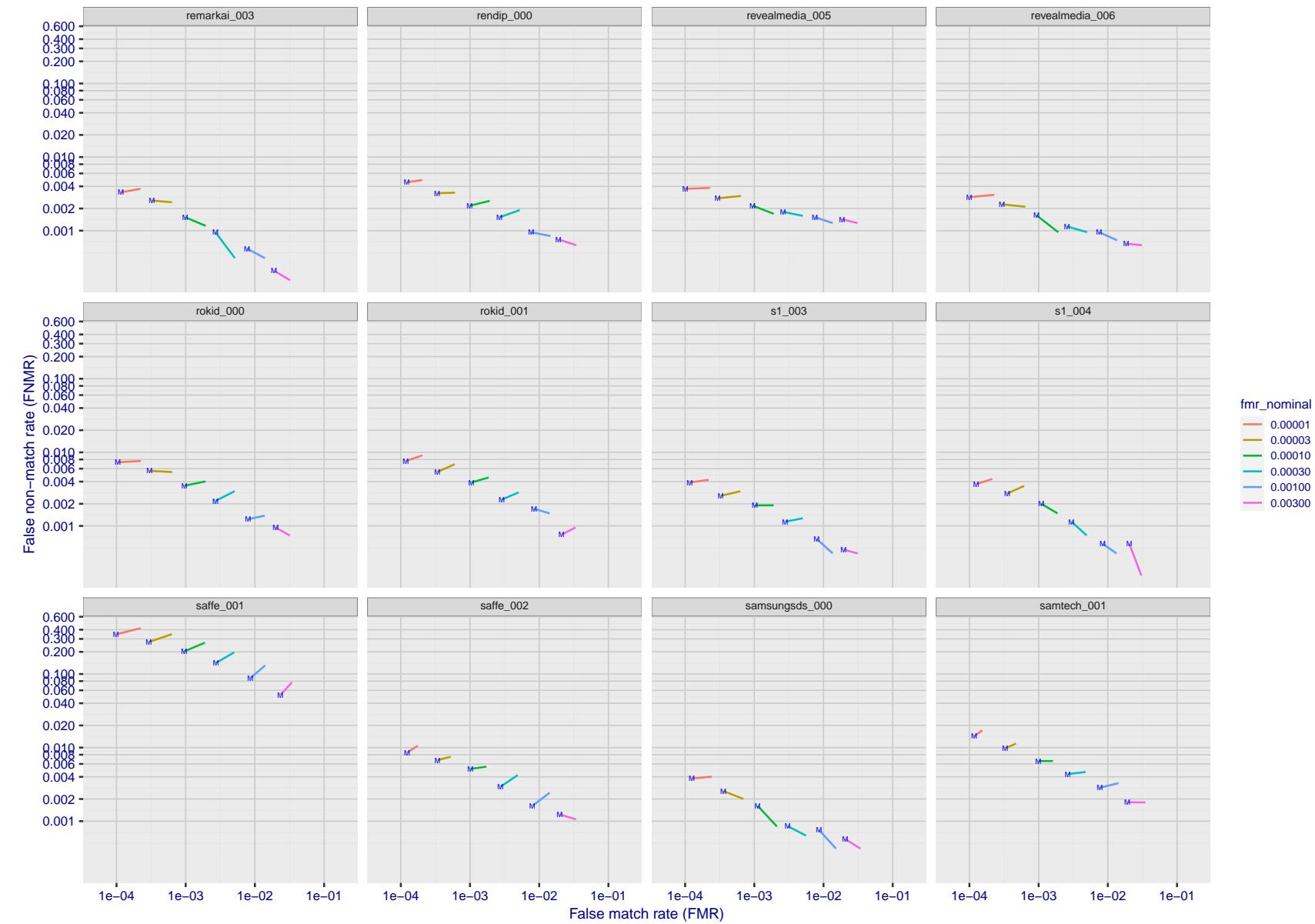


Figure 160: For the visa images, FNMR and FMR at six operating points along the DET characteristic. At each point a line is drawn between $(FMR, FNMR)_{MALE}$ and $(FMR, FNMR)_{FEMALE}$ showing how which sex has lower FMR and/or FNMR. The "M" label denotes male, the other end of the line corresponds to female. The six operating thresholds are selected to give the nominal false match rates given in the legend, and are computed over all impostor pairs regardless of age, sex, and place of birth. The plotted FMR values are broadly an order of magnitude larger than the nominal rates because FMR is computed over demographically-matched impostor pairs i.e individuals of the same sex, from the same geographic region (see section 3.6.1), and the same age group (see section 3.6.2).

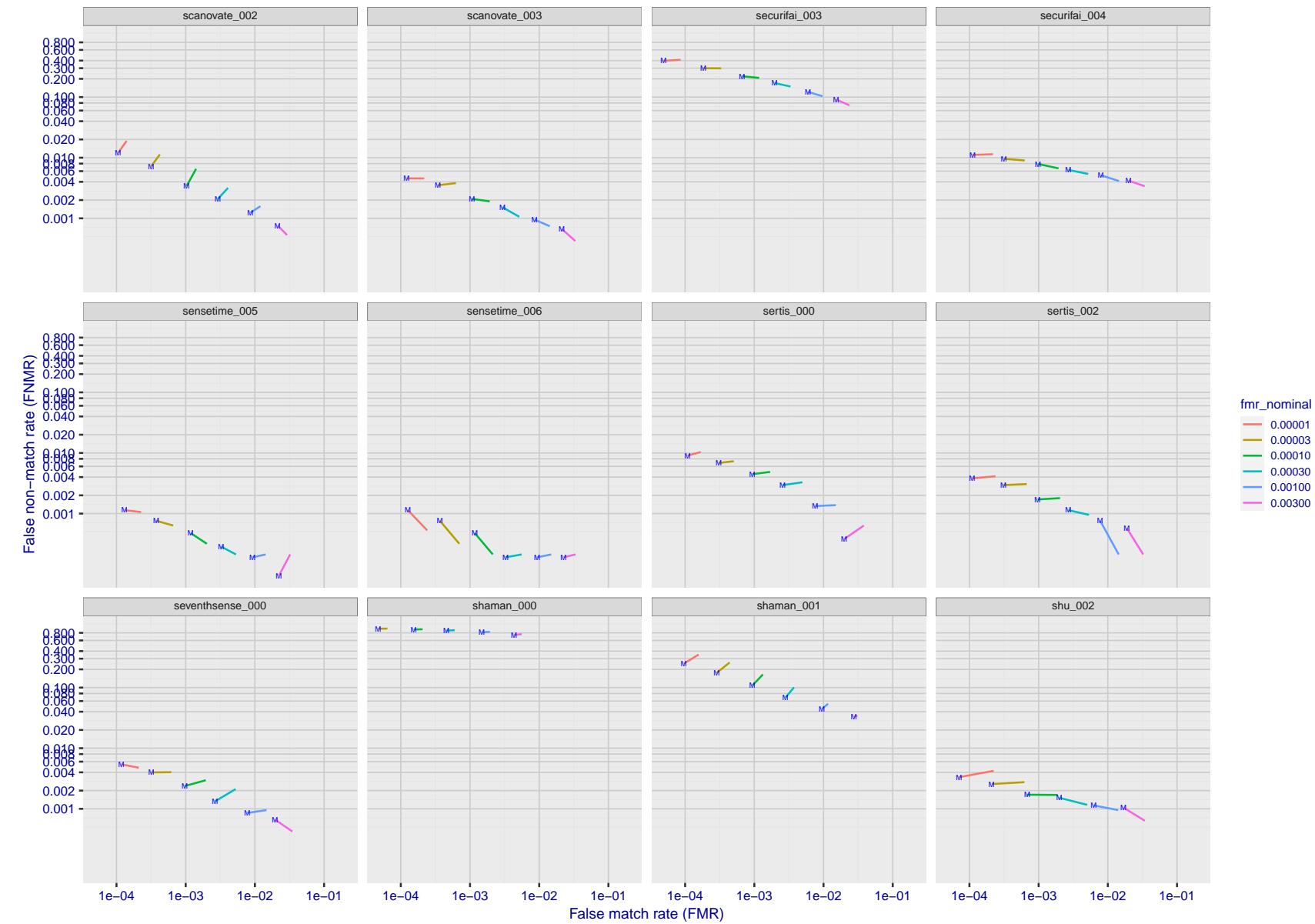


Figure 161: For the visa images, FNMR and FMR at six operating points along the DET characteristic. At each point a line is drawn between $(FMR, FNMR)_{MALE}$ and $(FMR, FNMR)_{FEMALE}$ showing how which sex has lower FMR and/or FNMR. The "M" label denotes male, the other end of the line corresponds to female. The six operating thresholds are selected to give the nominal false match rates given in the legend, and are computed over all impostor pairs regardless of age, sex, and place of birth. The plotted FMR values are broadly an order of magnitude larger than the nominal rates because FMR is computed over demographically-matched impostor pairs i.e individuals of the same sex, from the same geographic region (see section 3.6.1), and the same age group (see section 3.6.2).

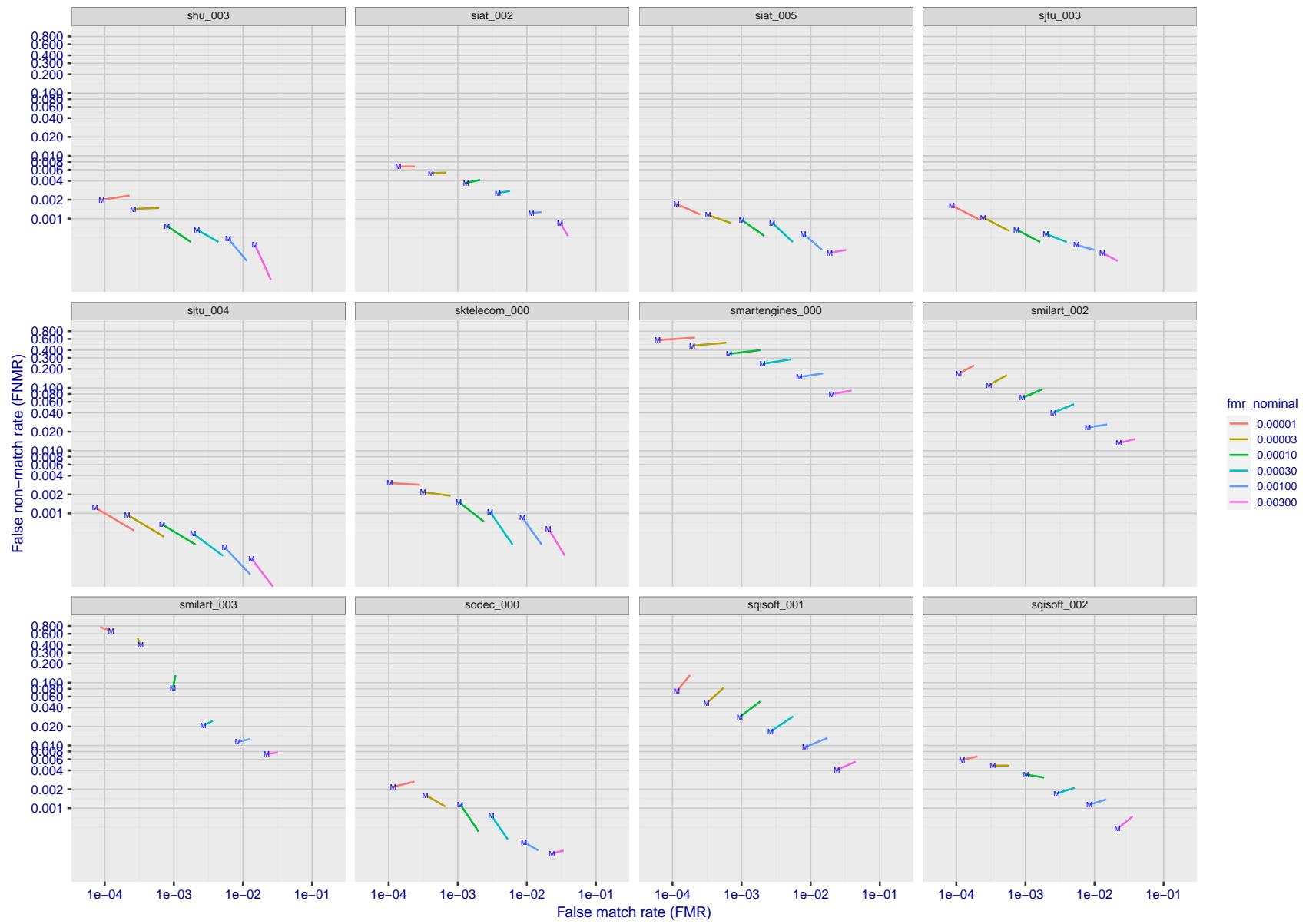


Figure 162: For the visa images, FNMR and FMR at six operating points along the DET characteristic. At each point a line is drawn between $(FMR, FNMR)_{MALE}$ and $(FMR, FNMR)_{FEMALE}$ showing how which sex has lower FMR and/or FNMR. The "M" label denotes male, the other end of the line corresponds to female. The six operating thresholds are selected to give the nominal false match rates given in the legend, and are computed over all impostor pairs regardless of age, sex, and place of birth. The plotted FMR values are broadly an order of magnitude larger than the nominal rates because FMR is computed over demographically-matched impostor pairs i.e individuals of the same sex, from the same geographic region (see section 3.6.1), and the same age group (see section 3.6.2).

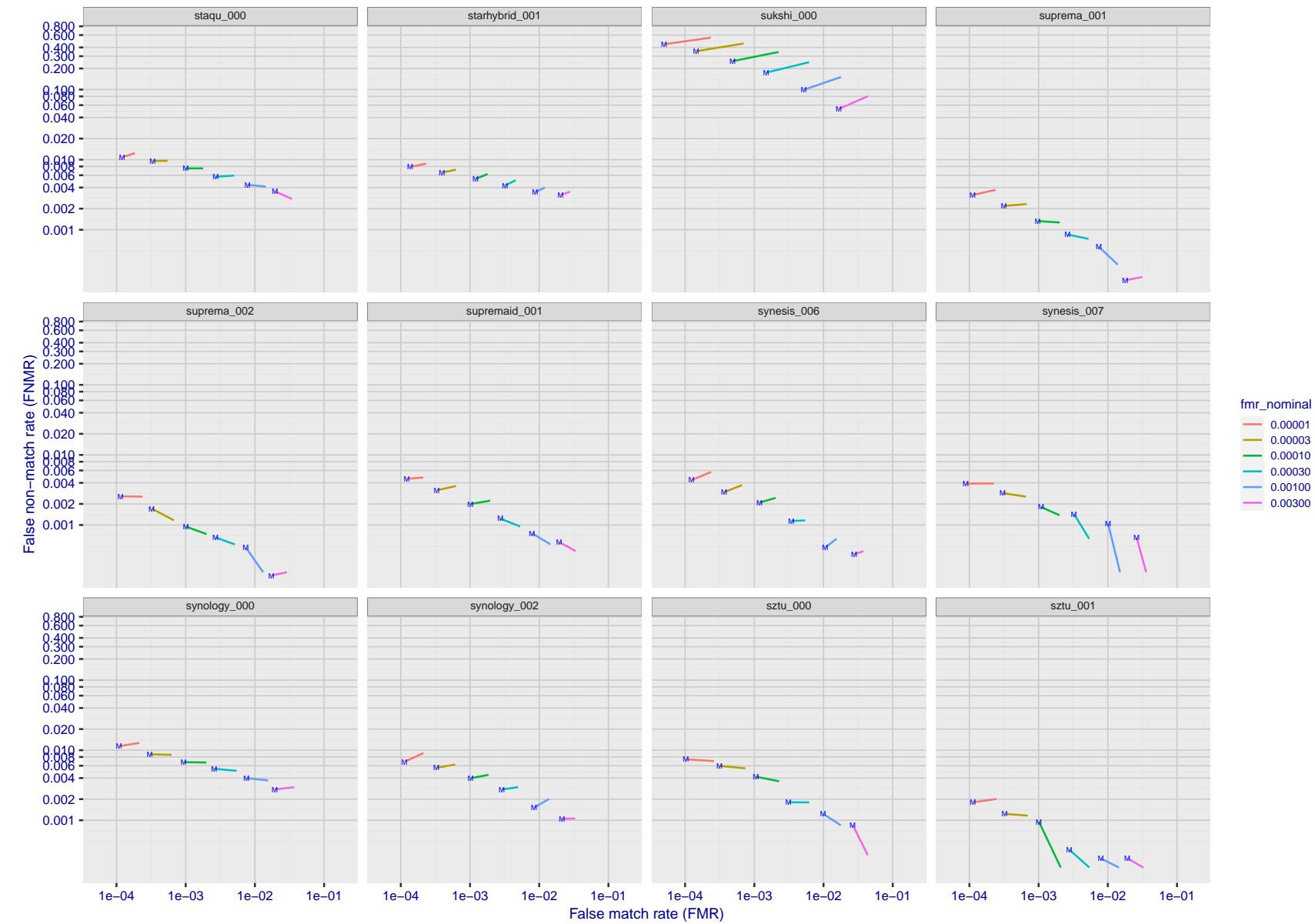


Figure 163: For the visa images, FNMR and FMR at six operating points along the DET characteristic. At each point a line is drawn between $(FMR, FNMR)_{MALE}$ and $(FMR, FNMR)_{FEMALE}$ showing how which sex has lower FMR and/or FNMR. The "M" label denotes male, the other end of the line corresponds to female. The six operating thresholds are selected to give the nominal false match rates given in the legend, and are computed over all impostor pairs regardless of age, sex, and place of birth. The plotted FMR values are broadly an order of magnitude larger than the nominal rates because FMR is computed over demographically-matched impostor pairs i.e individuals of the same sex, from the same geographic region (see section 3.6.1), and the same age group (see section 3.6.2).

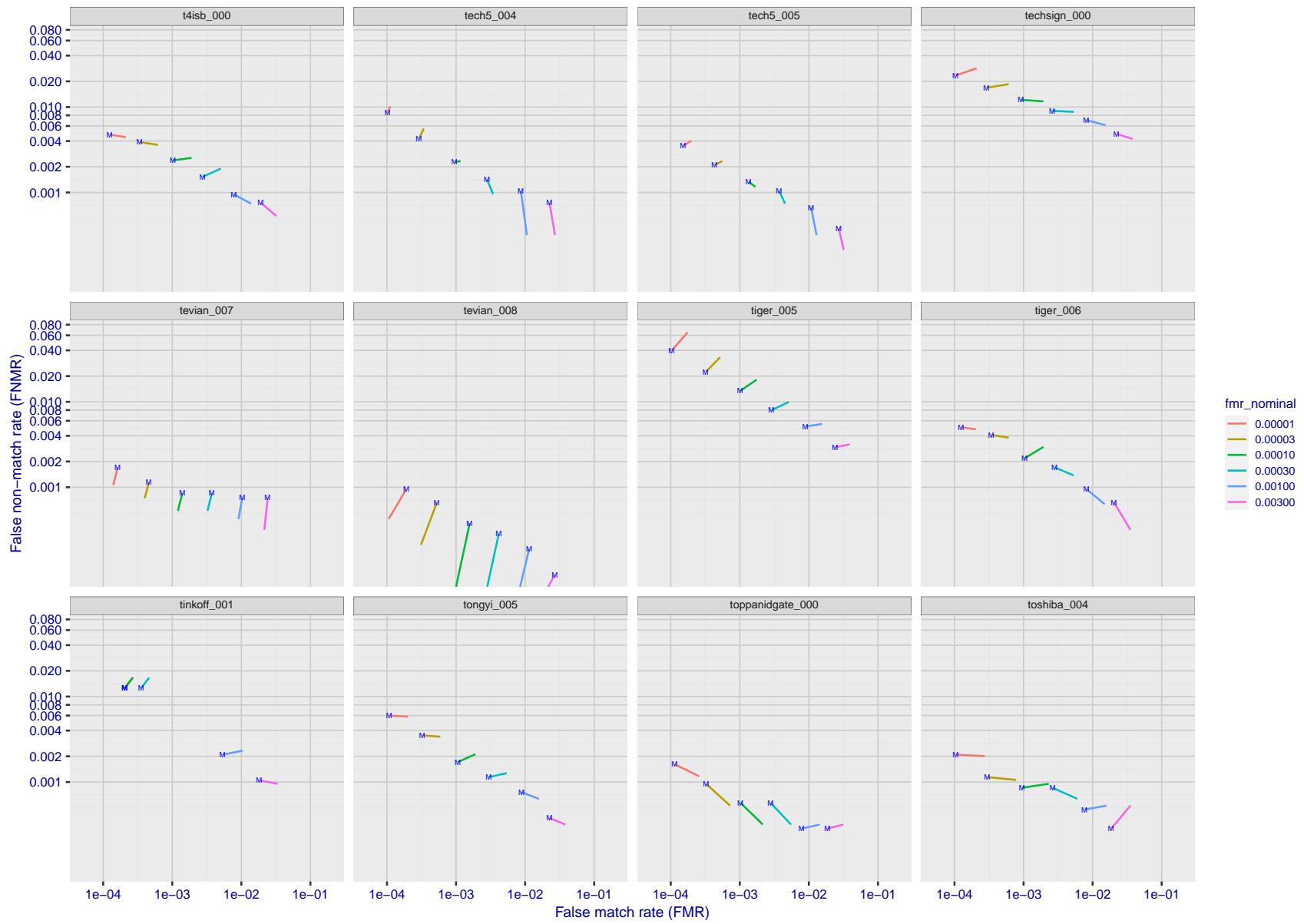


Figure 164: For the visa images, FNMR and FMR at six operating points along the DET characteristic. At each point a line is drawn between $(FMR, FNMR)_{MALE}$ and $(FMR, FNMR)_{FEMALE}$ showing how which sex has lower FMR and/or FNMR. The "M" label denotes male, the other end of the line corresponds to female. The six operating thresholds are selected to give the nominal false match rates given in the legend, and are computed over all impostor pairs regardless of age, sex, and place of birth. The plotted FMR values are broadly an order of magnitude larger than the nominal rates because FMR is computed over demographically-matched impostor pairs i.e individuals of the same sex, from the same geographic region (see section 3.6.1), and the same age group (see section 3.6.2).

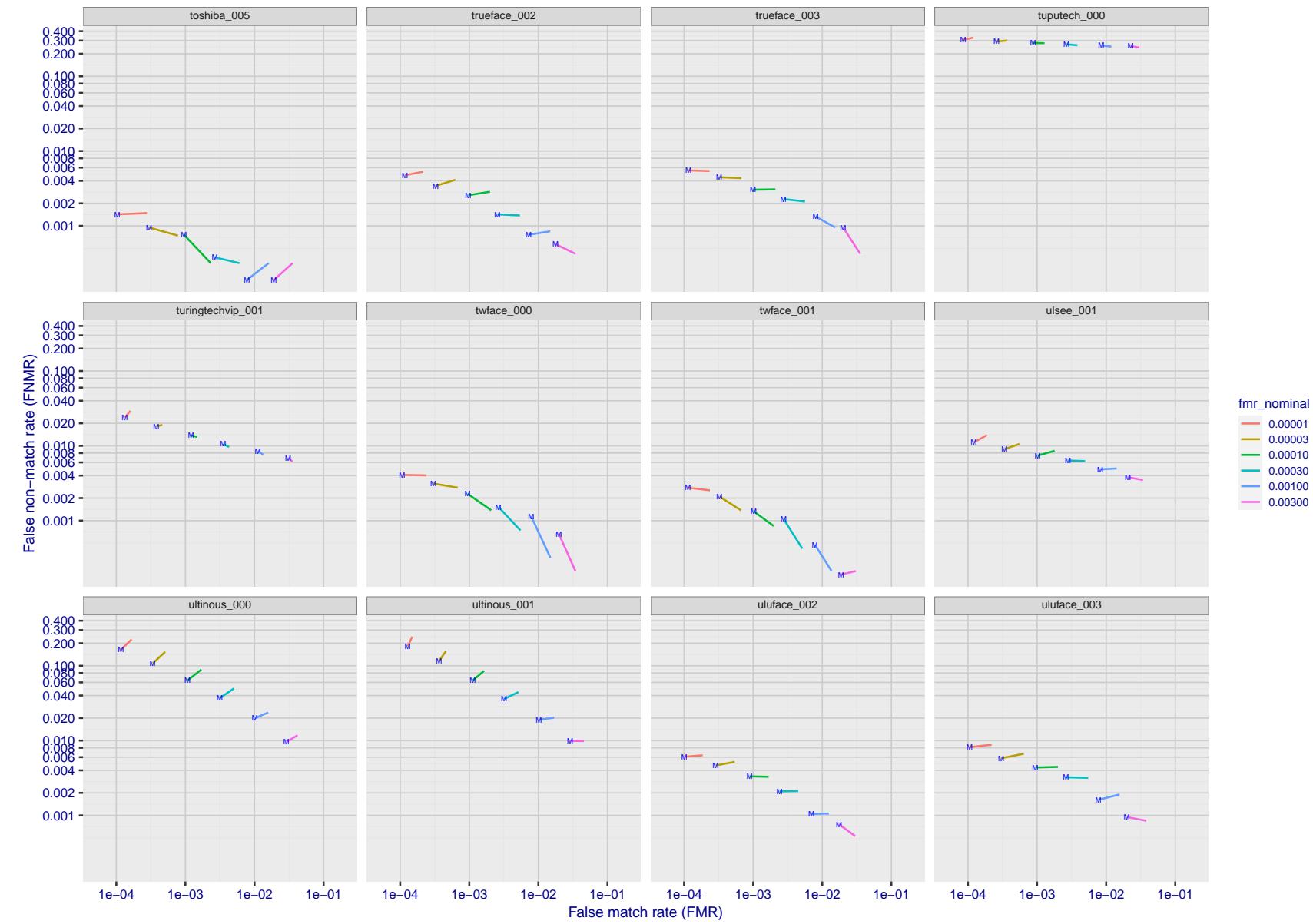


Figure 165: For the visa images, FNMR and FMR at six operating points along the DET characteristic. At each point a line is drawn between $(FMR, FNMR)_{MALE}$ and $(FMR, FNMR)_{FEMALE}$ showing how which sex has lower FMR and/or FNMR. The "M" label denotes male, the other end of the line corresponds to female. The six operating thresholds are selected to give the nominal false match rates given in the legend, and are computed over all impostor pairs regardless of age, sex, and place of birth. The plotted FMR values are broadly an order of magnitude larger than the nominal rates because FMR is computed over demographically-matched impostor pairs i.e individuals of the same sex, from the same geographic region (see section 3.6.1), and the same age group (see section 3.6.2).

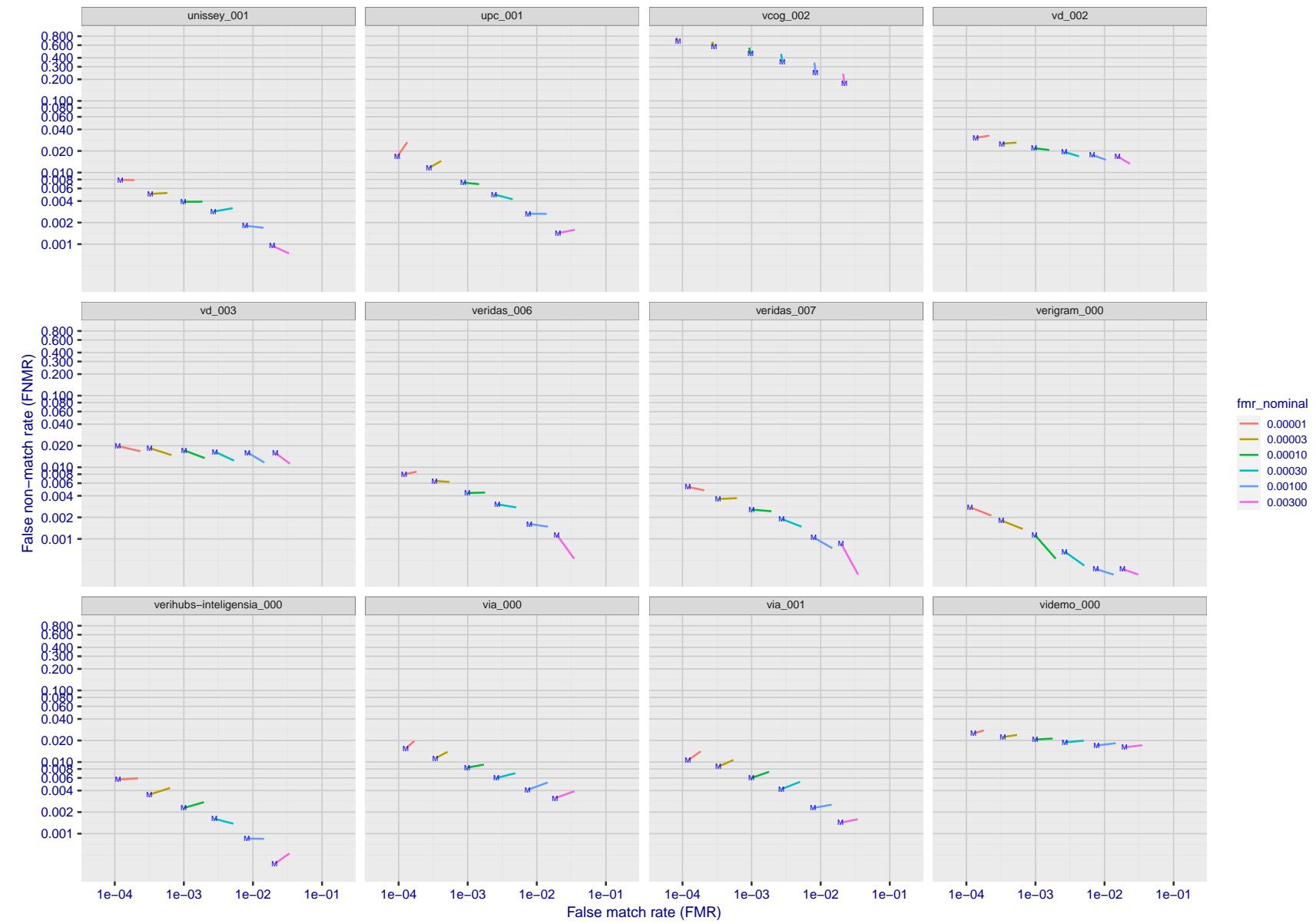


Figure 166: For the visa images, FNMR and FMR at six operating points along the DET characteristic. At each point a line is drawn between $(FMR, FNMR)_{MALE}$ and $(FMR, FNMR)_{FEMALE}$ showing how which sex has lower FMR and/or FNMR. The "M" label denotes male, the other end of the line corresponds to female. The six operating thresholds are selected to give the nominal false match rates given in the legend, and are computed over all impostor pairs regardless of age, sex, and place of birth. The plotted FMR values are broadly an order of magnitude larger than the nominal rates because FMR is computed over demographically-matched impostor pairs i.e individuals of the same sex, from the same geographic region (see section 3.6.1), and the same age group (see section 3.6.2).

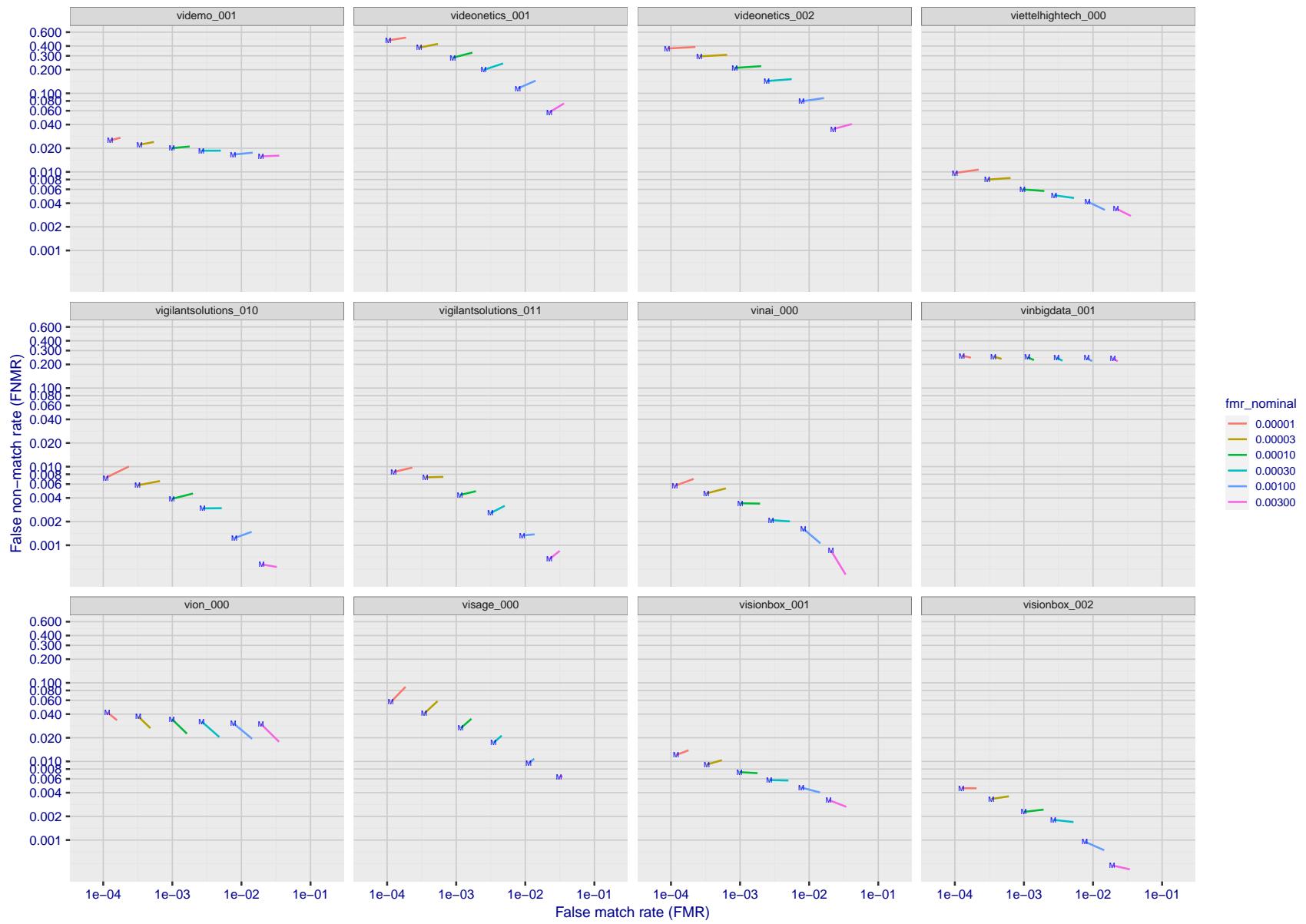


Figure 167: For the visa images, FNMR and FMR at six operating points along the DET characteristic. At each point a line is drawn between $(FMR, FNMR)_{MALE}$ and $(FMR, FNMR)_{FEMALE}$ showing how which sex has lower FMR and/or FNMR. The "M" label denotes male, the other end of the line corresponds to female. The six operating thresholds are selected to give the nominal false match rates given in the legend, and are computed over all impostor pairs regardless of age, sex, and place of birth. The plotted FMR values are broadly an order of magnitude larger than the nominal rates because FMR is computed over demographically-matched impostor pairs i.e individuals of the same sex, from the same geographic region (see section 3.6.1), and the same age group (see section 3.6.2).

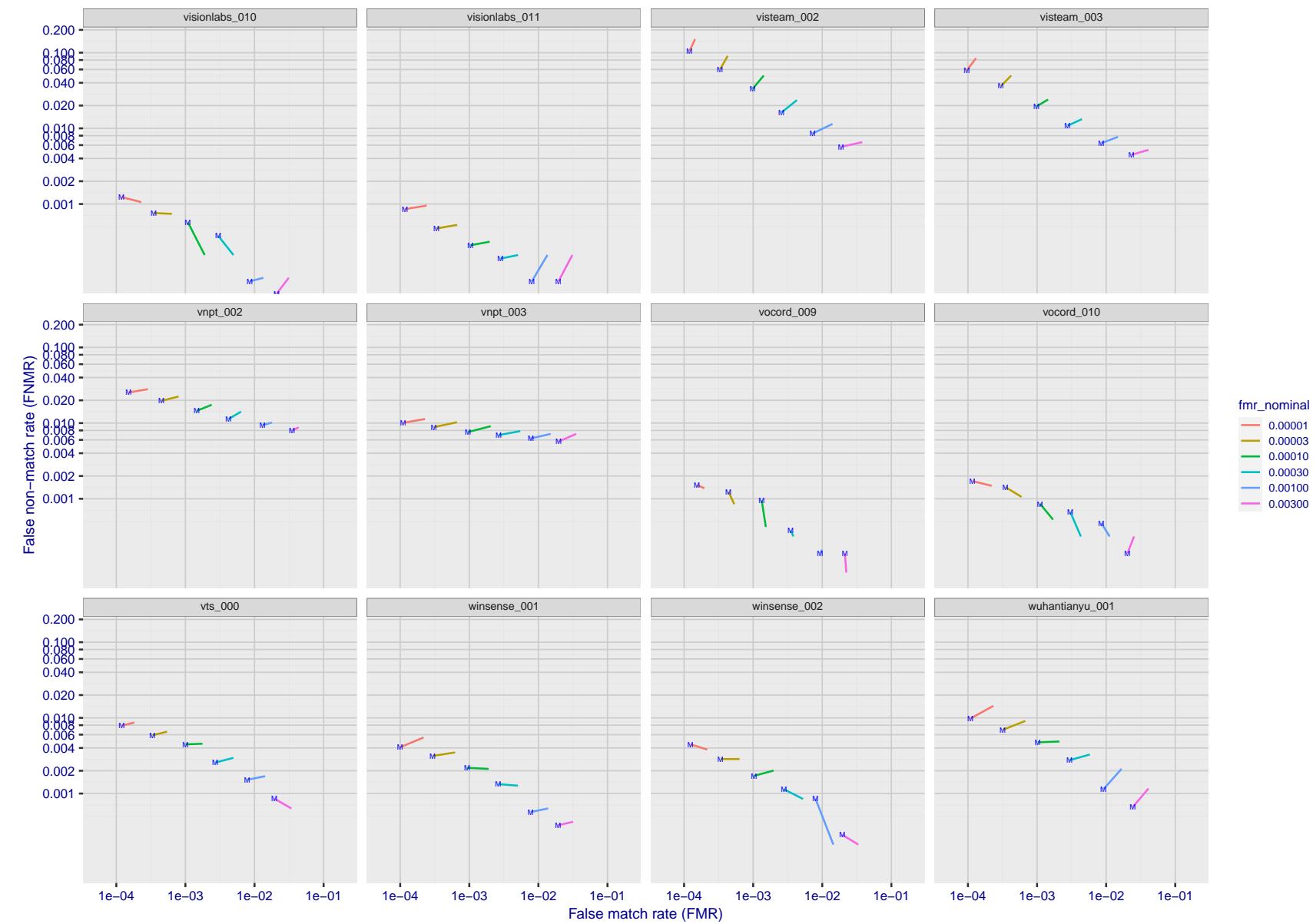


Figure 168: For the visa images, FNMR and FMR at six operating points along the DET characteristic. At each point a line is drawn between $(FMR, FNMR)_{MALE}$ and $(FMR, FNMR)_{FEMALE}$ showing how which sex has lower FMR and/or FNMR. The "M" label denotes male, the other end of the line corresponds to female. The six operating thresholds are selected to give the nominal false match rates given in the legend, and are computed over all impostor pairs regardless of age, sex, and place of birth. The plotted FMR values are broadly an order of magnitude larger than the nominal rates because FMR is computed over demographically-matched impostor pairs i.e individuals of the same sex, from the same geographic region (see section 3.6.1), and the same age group (see section 3.6.2).

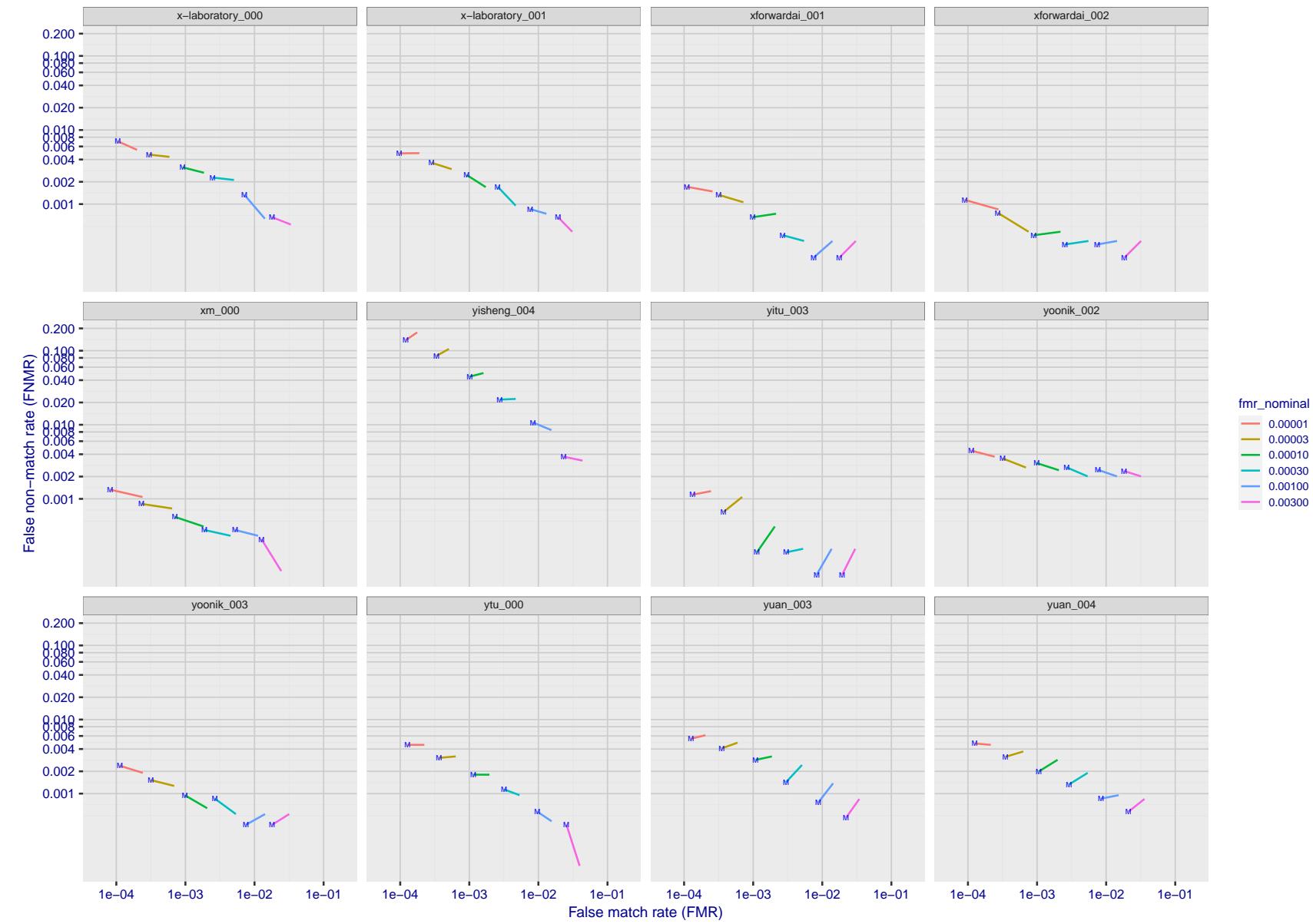


Figure 169: For the visa images, FNMR and FMR at six operating points along the DET characteristic. At each point a line is drawn between $(FMR, FNMR)_{MALE}$ and $(FMR, FNMR)_{FEMALE}$ showing how which sex has lower FMR and/or FNMR. The "M" label denotes male, the other end of the line corresponds to female. The six operating thresholds are selected to give the nominal false match rates given in the legend, and are computed over all impostor pairs regardless of age, sex, and place of birth. The plotted FMR values are broadly an order of magnitude larger than the nominal rates because FMR is computed over demographically-matched impostor pairs i.e individuals of the same sex, from the same geographic region (see section 3.6.1), and the same age group (see section 3.6.2).

2022/02/23 14:09:04

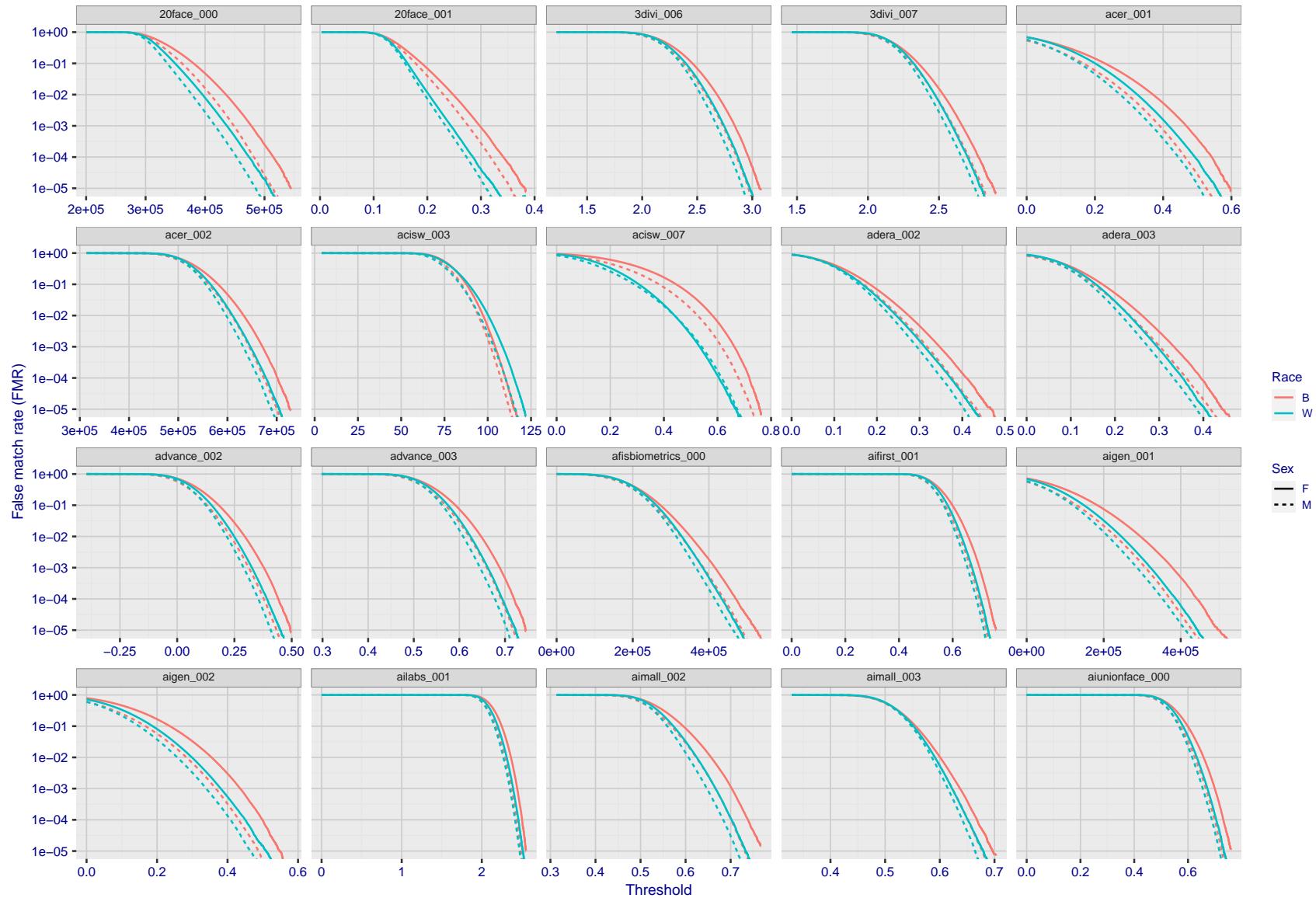


Figure 170: For the mugshot images, the false match calibration curves show false match rate vs. threshold. Separate curves appear for white females, black females, black males and white males.

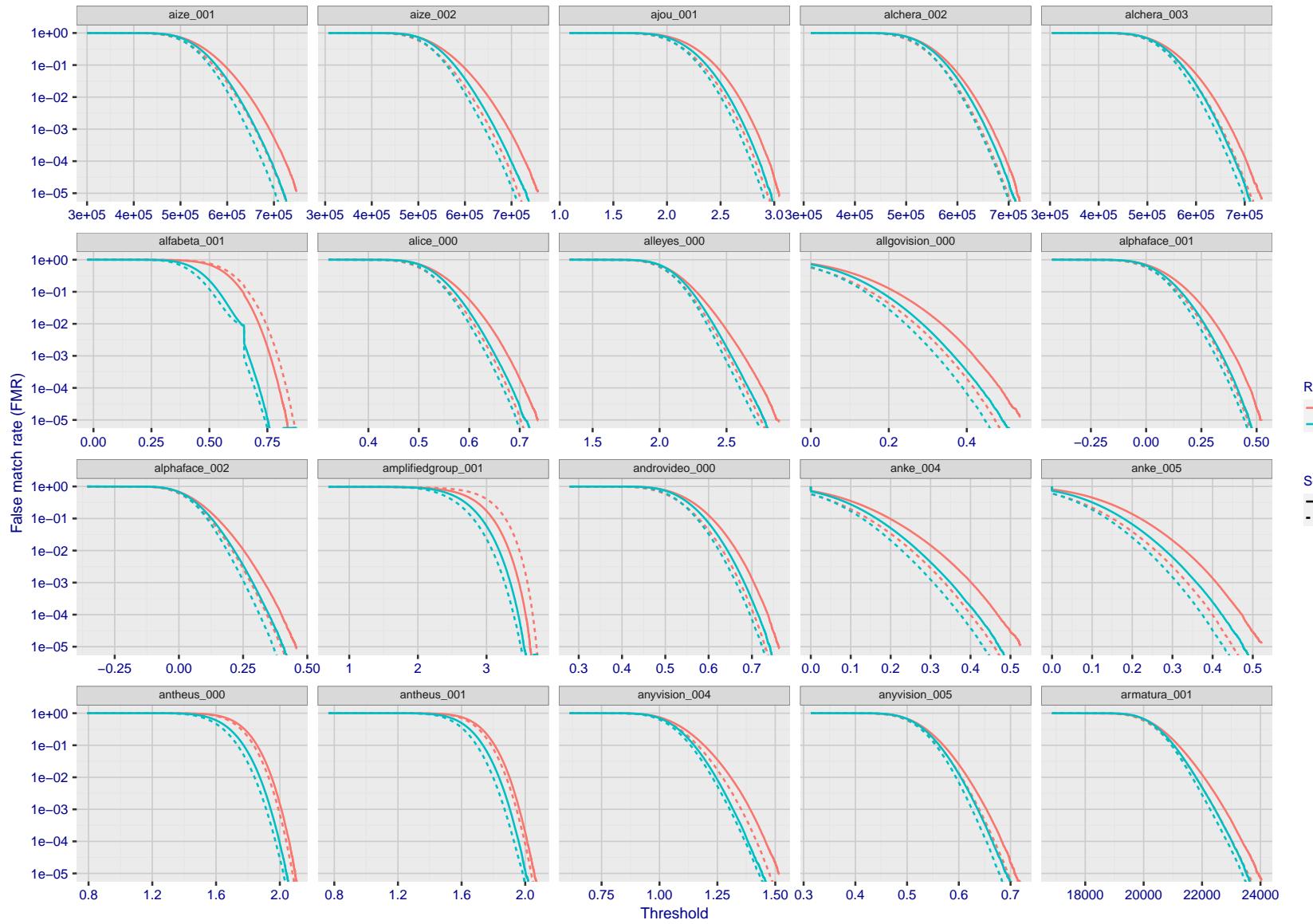


Figure 171: For the mugshot images, the false match calibration curves show false match rate vs. threshold. Separate curves appear for white females, black females, black males and white males.

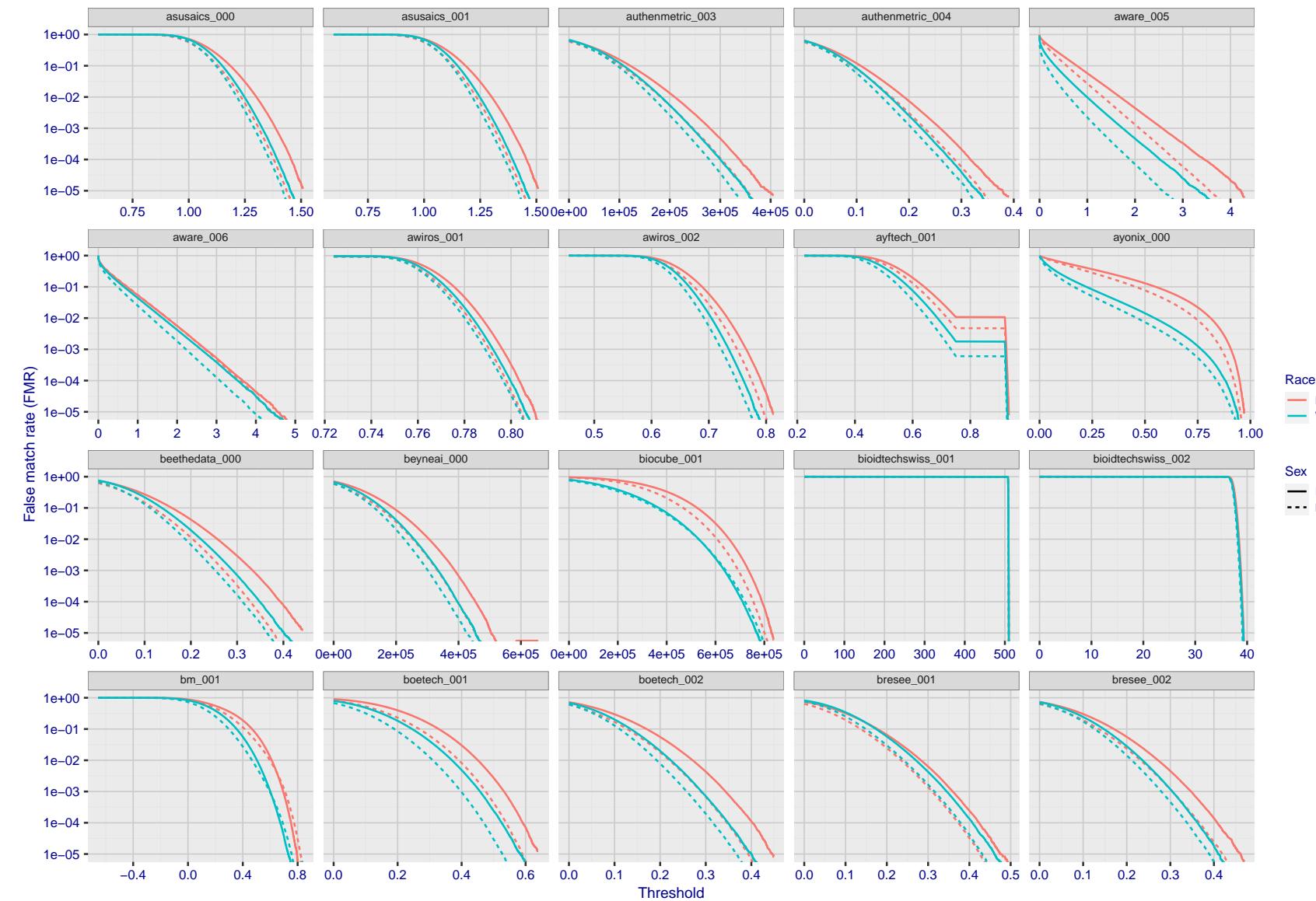


Figure 172: For the mugshot images, the false match calibration curves show false match rate vs. threshold. Separate curves appear for white females, black females, black males and white males.

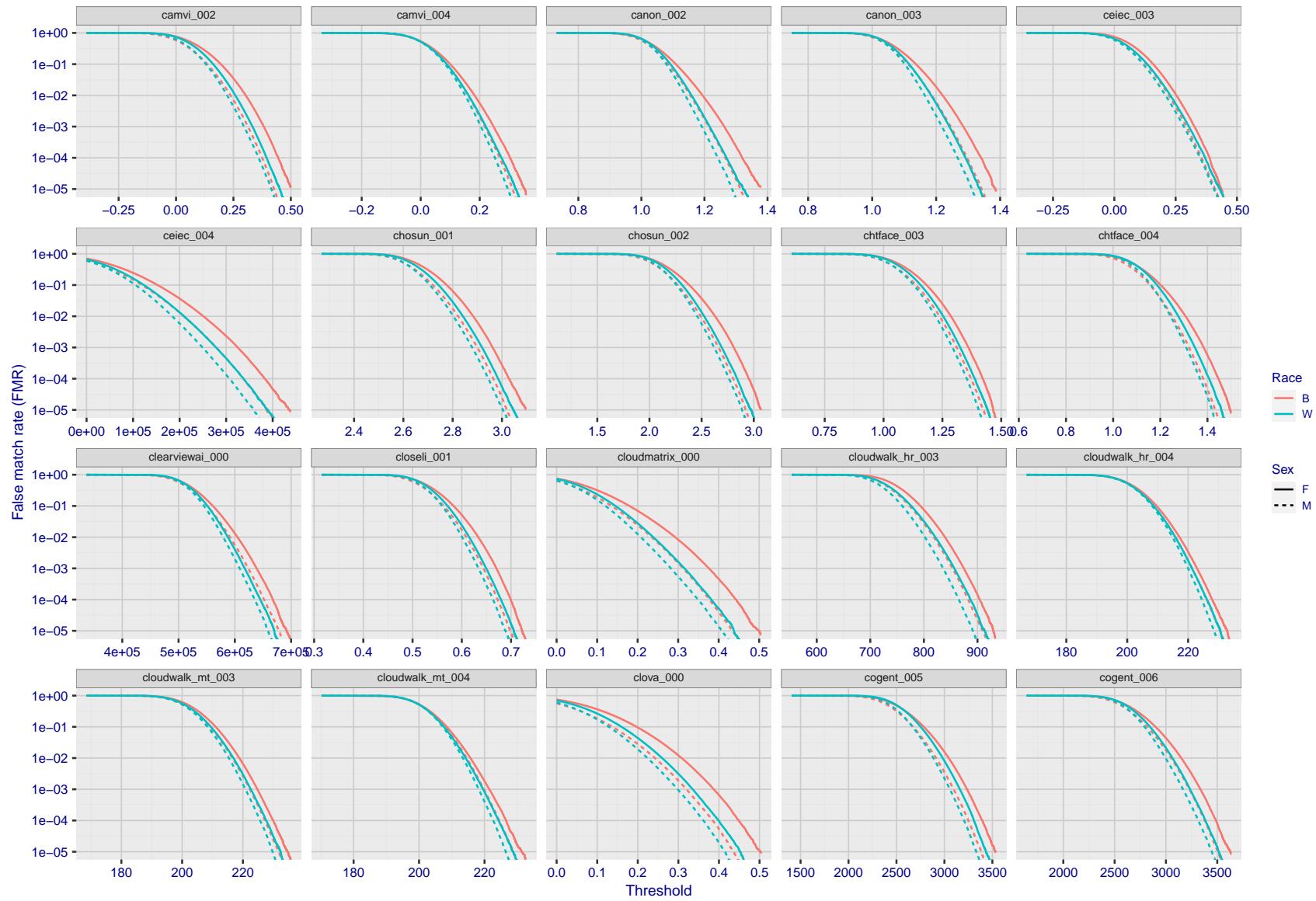


Figure 173: For the mugshot images, the false match calibration curves show false match rate vs. threshold. Separate curves appear for white females, black females, black males and white males.

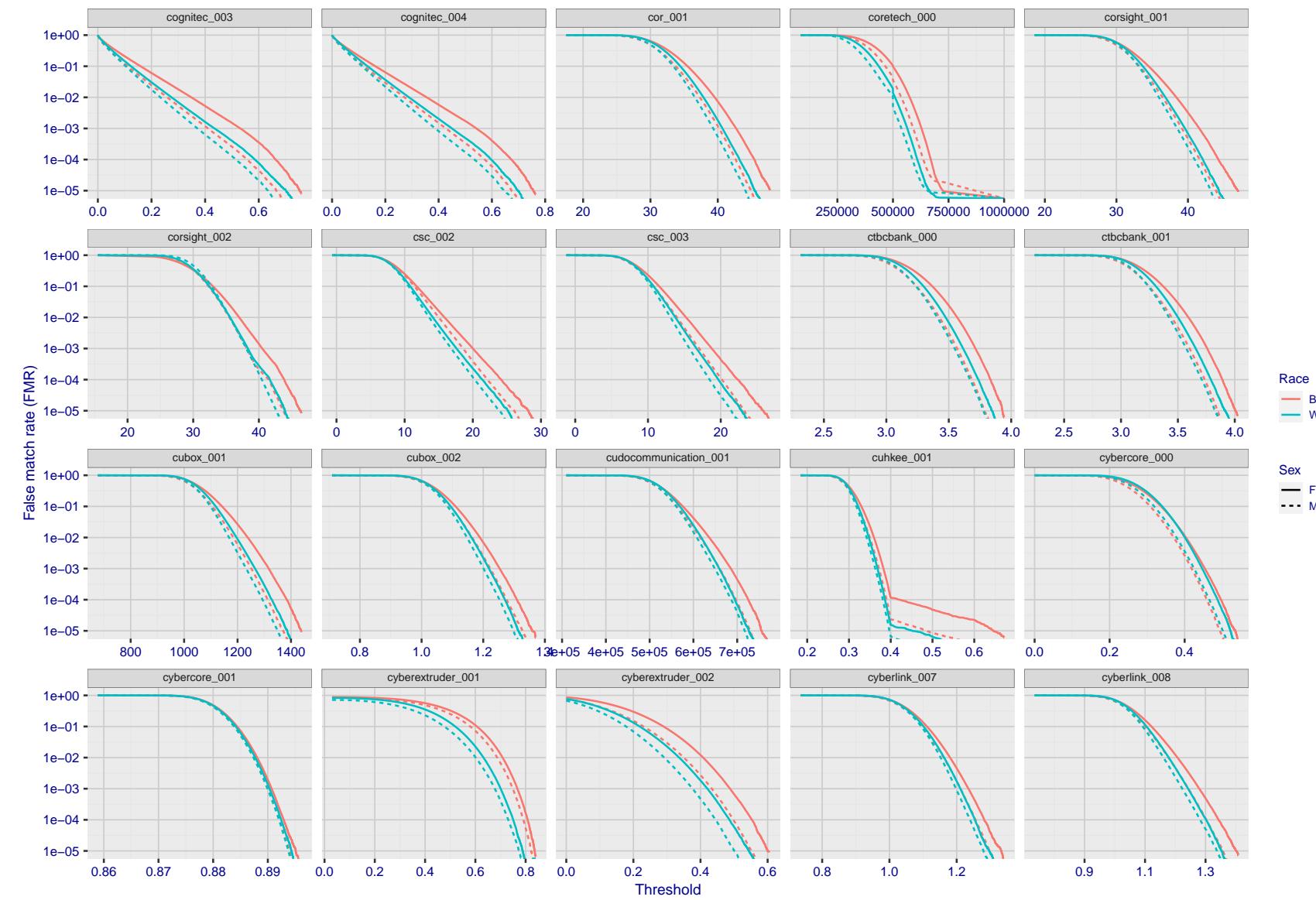


Figure 174: For the mugshot images, the false match calibration curves show false match rate vs. threshold. Separate curves appear for white females, black females, black males and white males.

2022/02/23 14:09:04

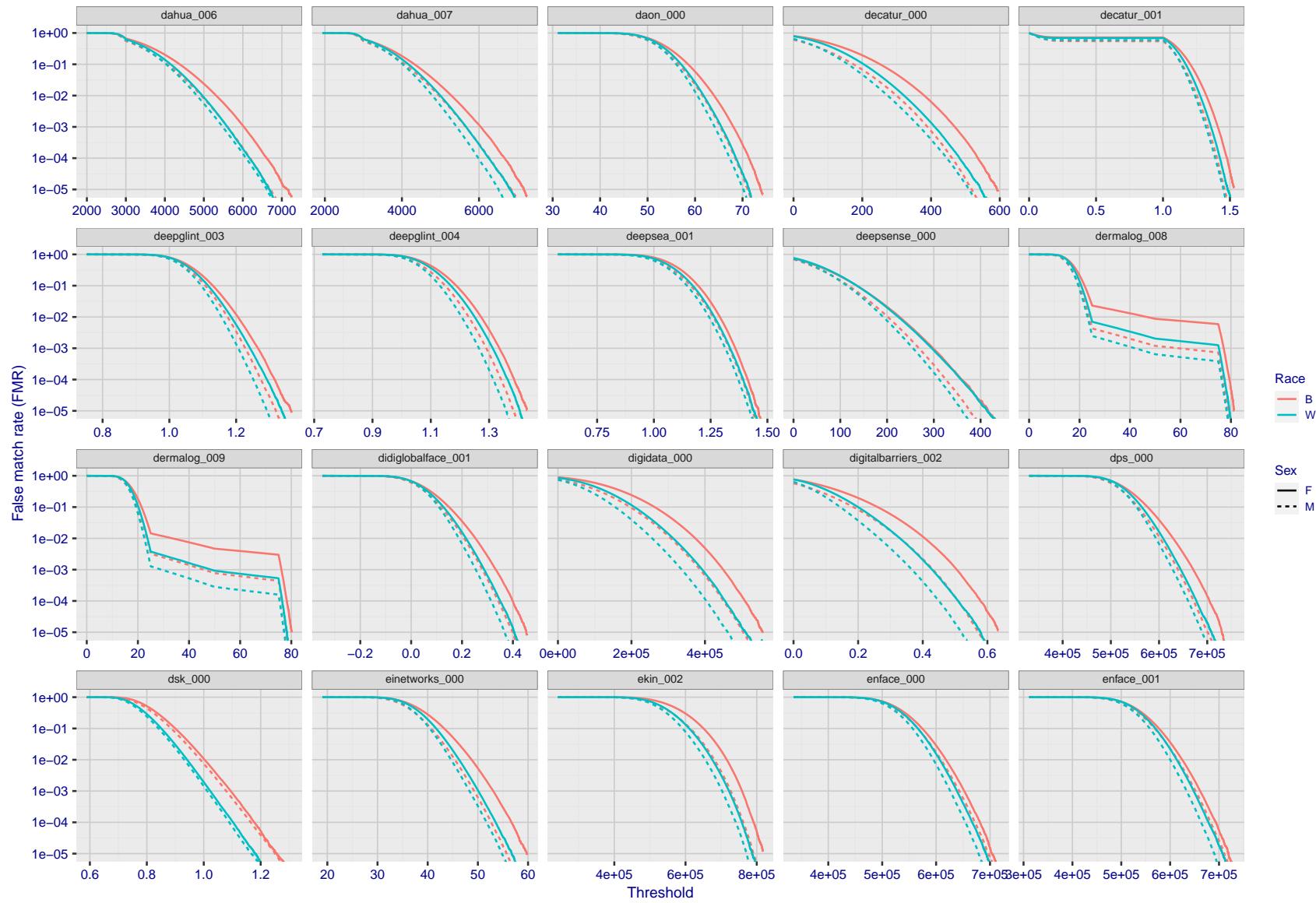


Figure 175: For the mugshot images, the false match calibration curves show false match rate vs. threshold. Separate curves appear for white females, black females, black males and white males.

2022/02/23 14:09:04

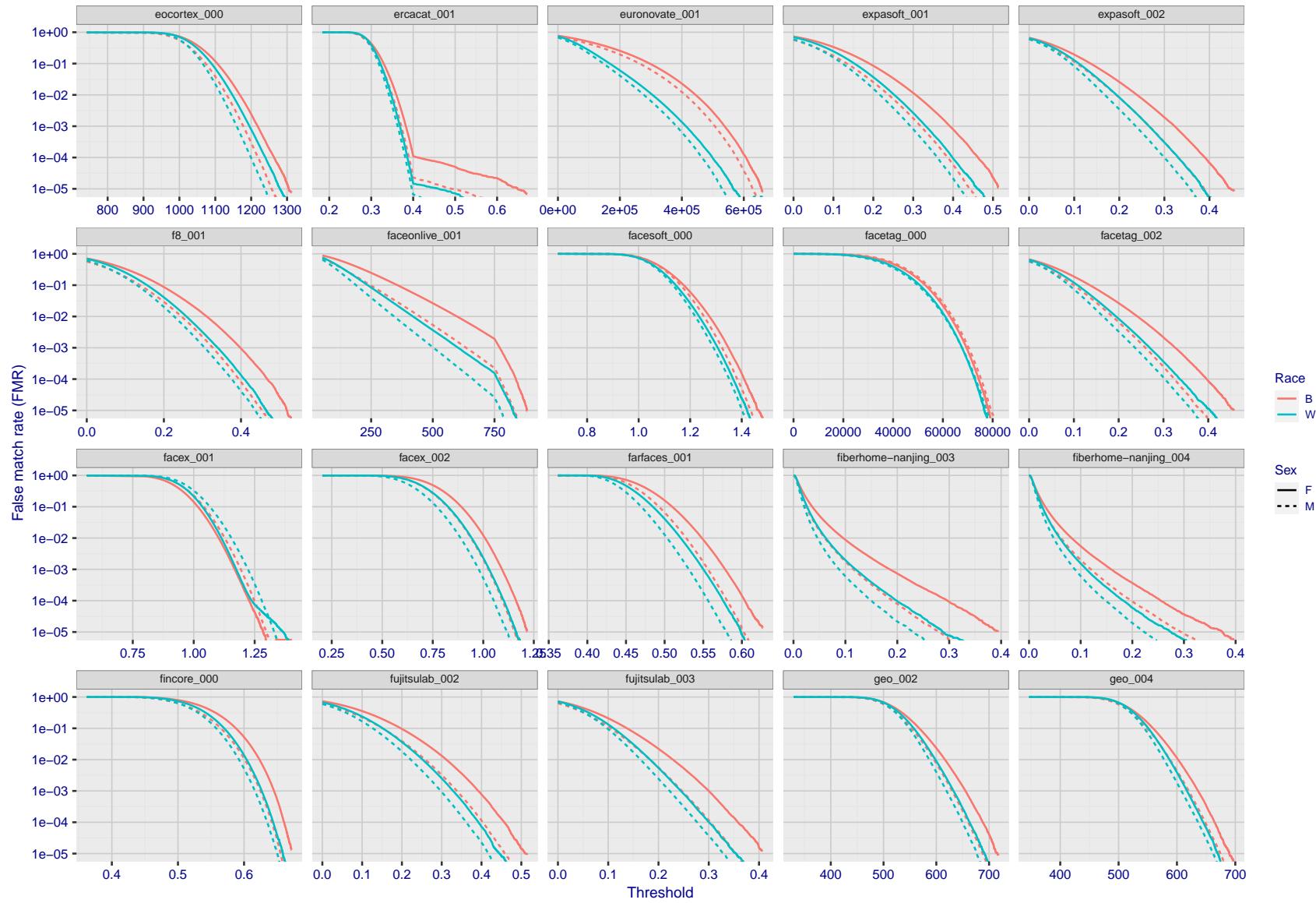


Figure 176: For the mugshot images, the false match calibration curves show false match rate vs. threshold. Separate curves appear for white females, black females, black males and white males.

2022/02/23 14:09:04

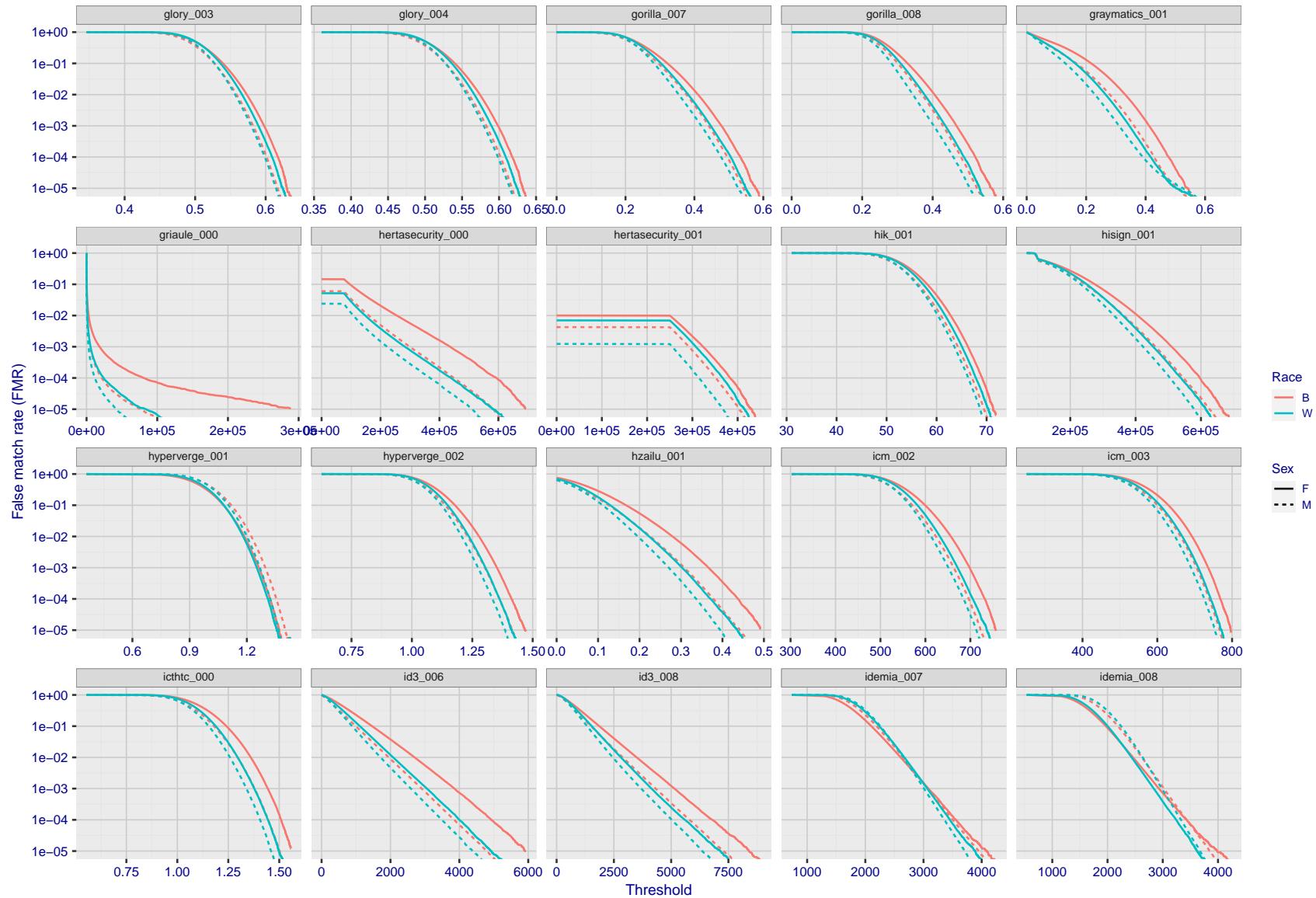


Figure 177: For the mugshot images, the false match calibration curves show false match rate vs. threshold. Separate curves appear for white females, black females, black males and white males.

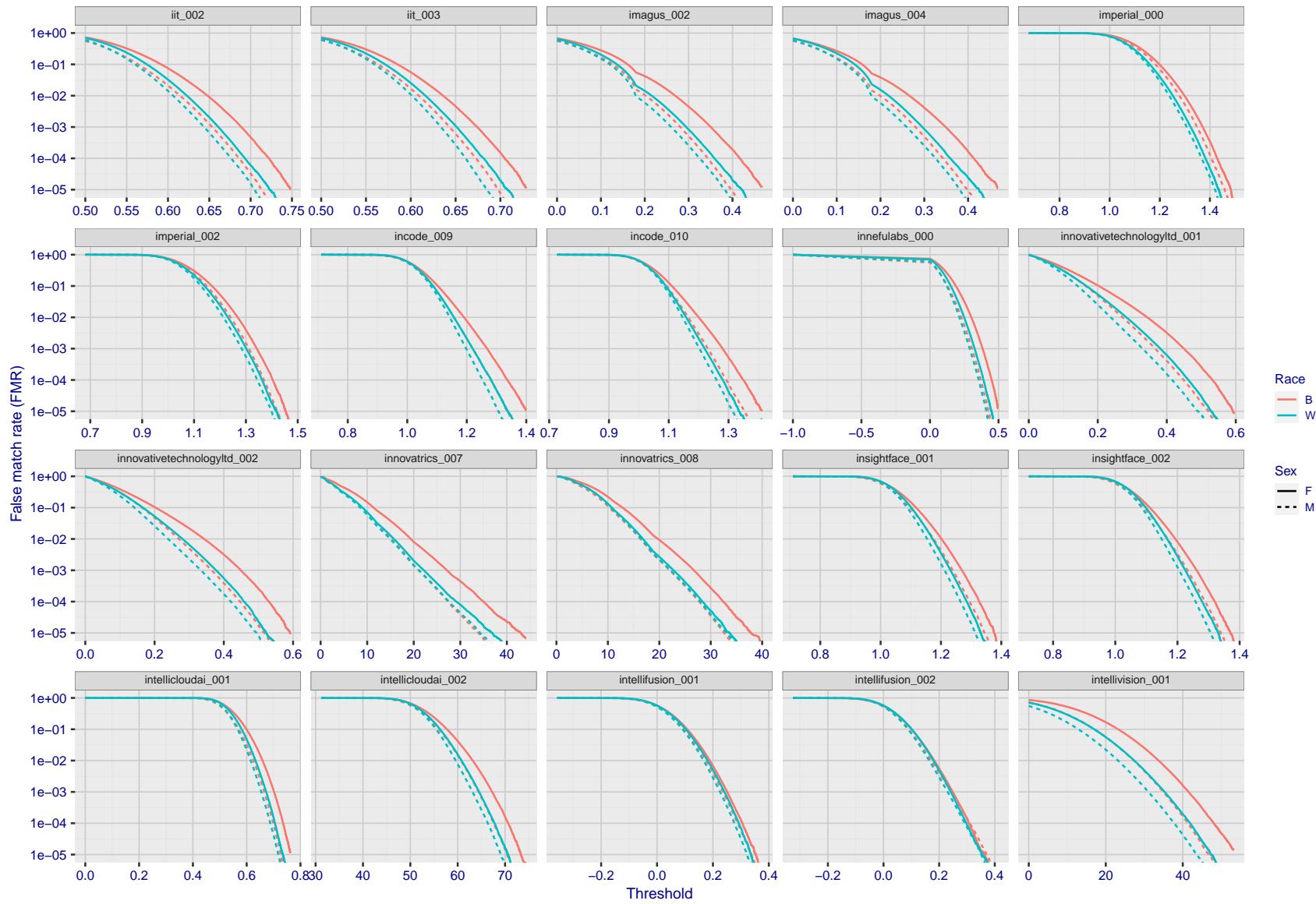


Figure 178: For the mugshot images, the false match calibration curves show false match rate vs. threshold. Separate curves appear for white females, black females, black males and white males.

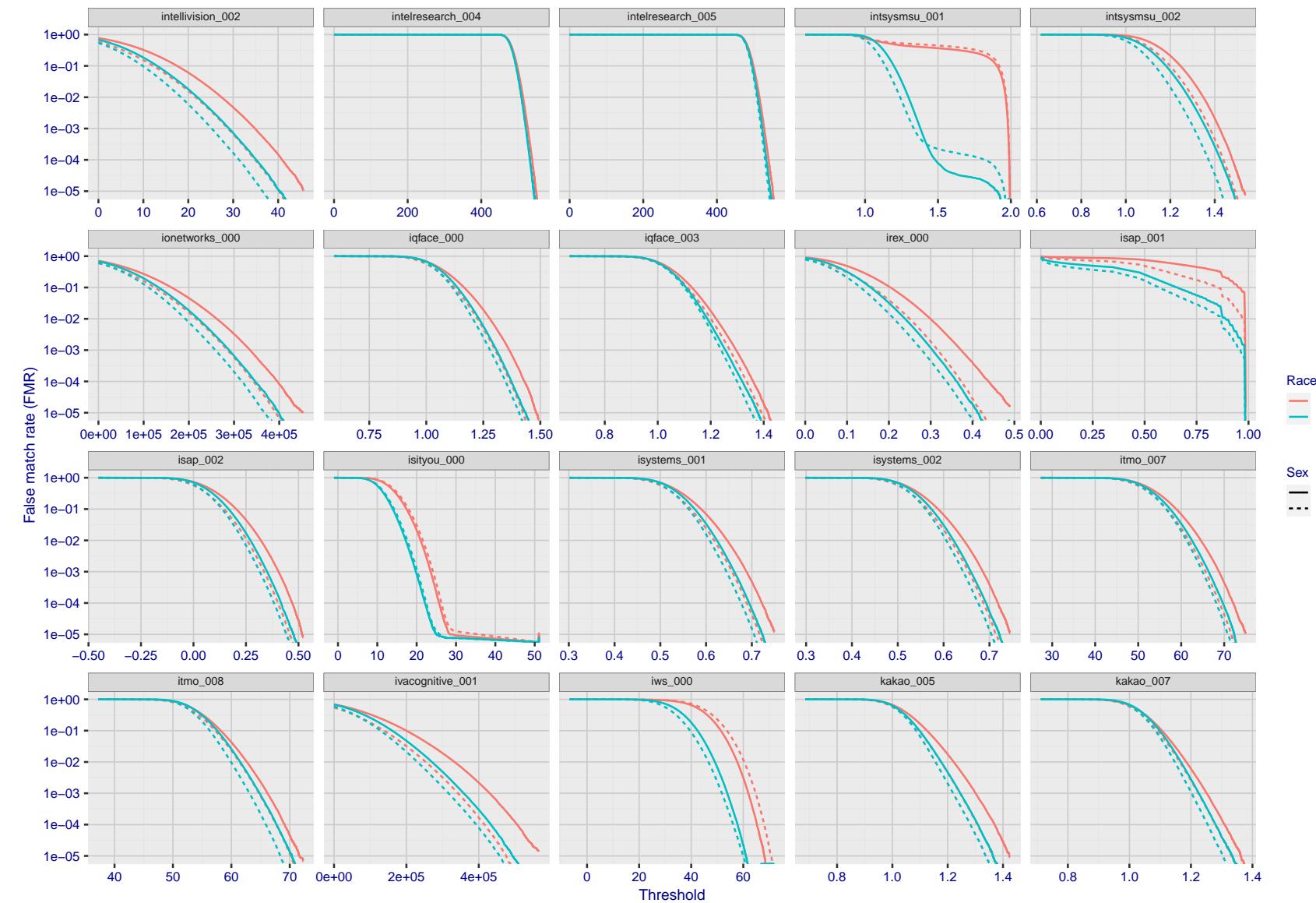


Figure 179: For the mugshot images, the false match calibration curves show false match rate vs. threshold. Separate curves appear for white females, black females, black males and white males.

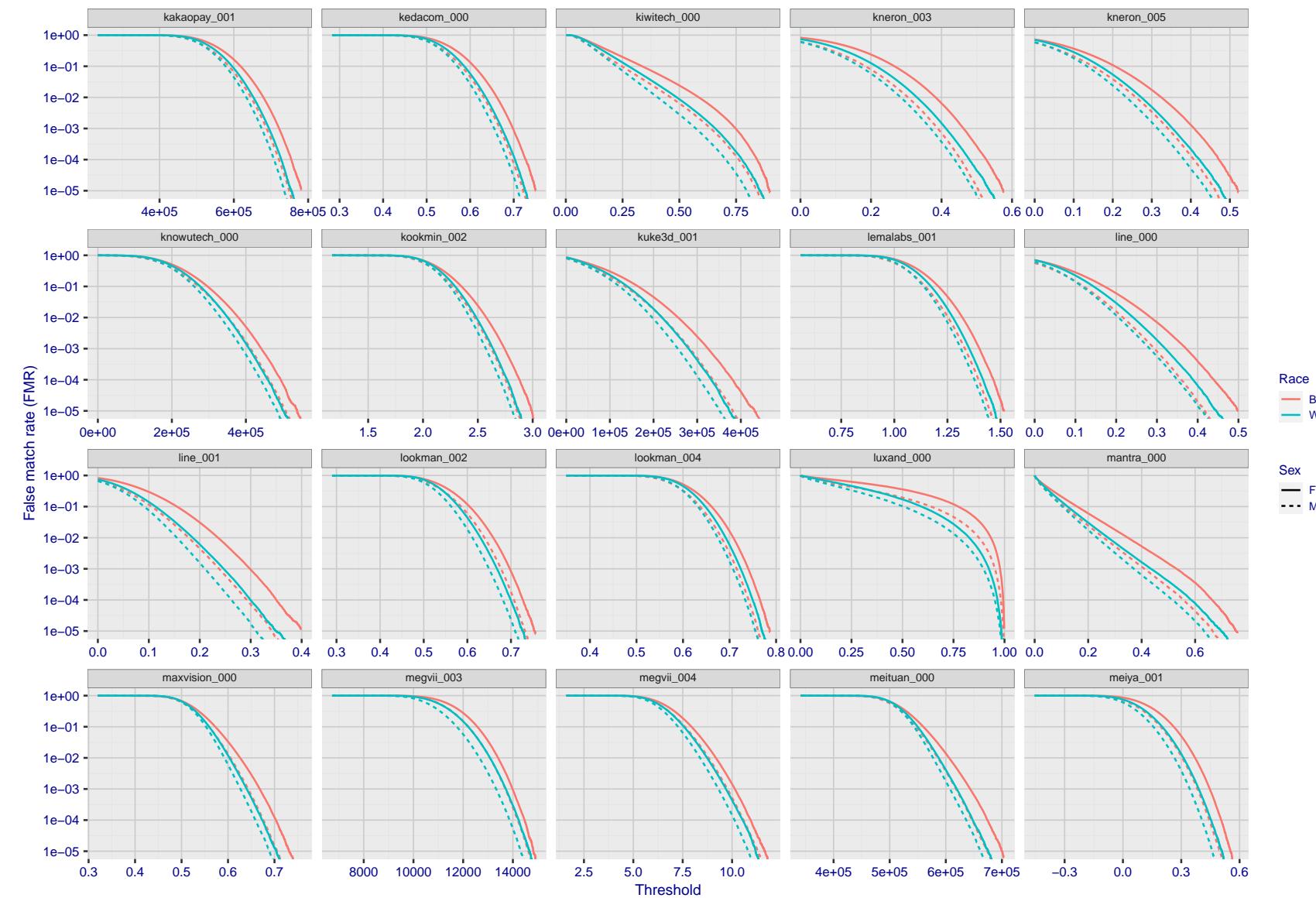


Figure 180: For the mugshot images, the false match calibration curves show false match rate vs. threshold. Separate curves appear for white females, black females, black males and white males.

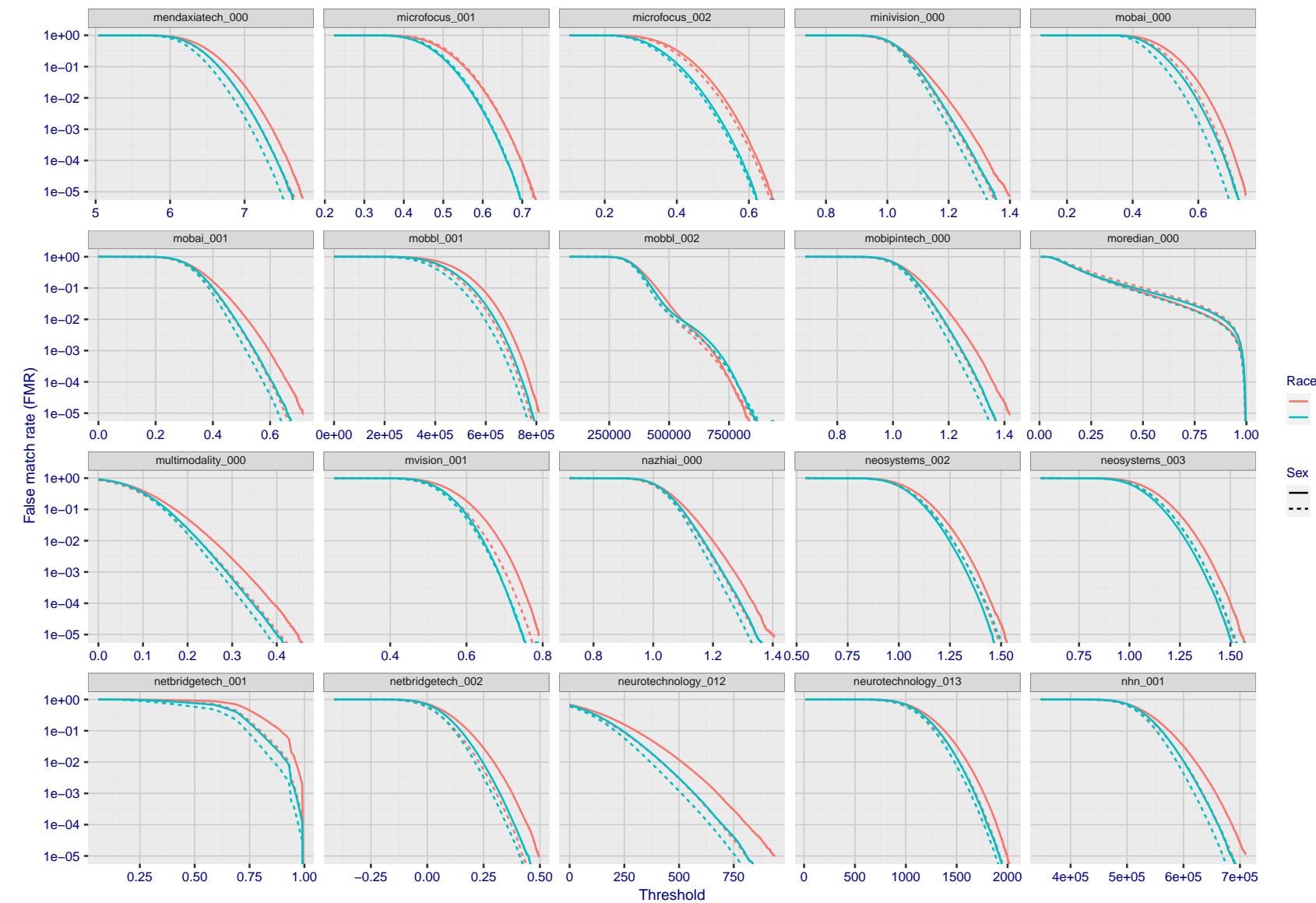


Figure 181: For the mugshot images, the false match calibration curves show false match rate vs. threshold. Separate curves appear for white females, black females, black males and white males.

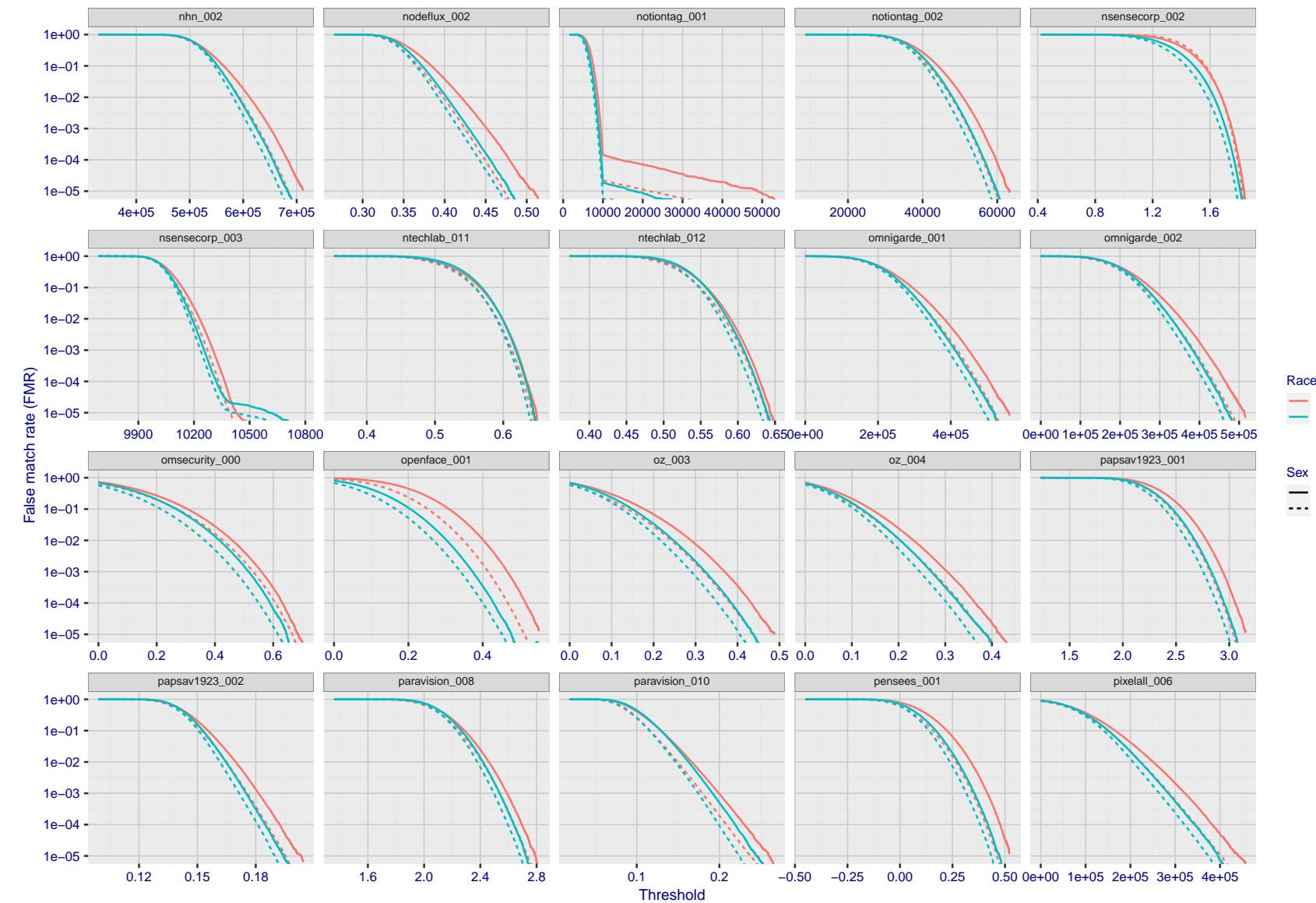


Figure 182: For the mugshot images, the false match calibration curves show false match rate vs. threshold. Separate curves appear for white females, black females, black males and white males.

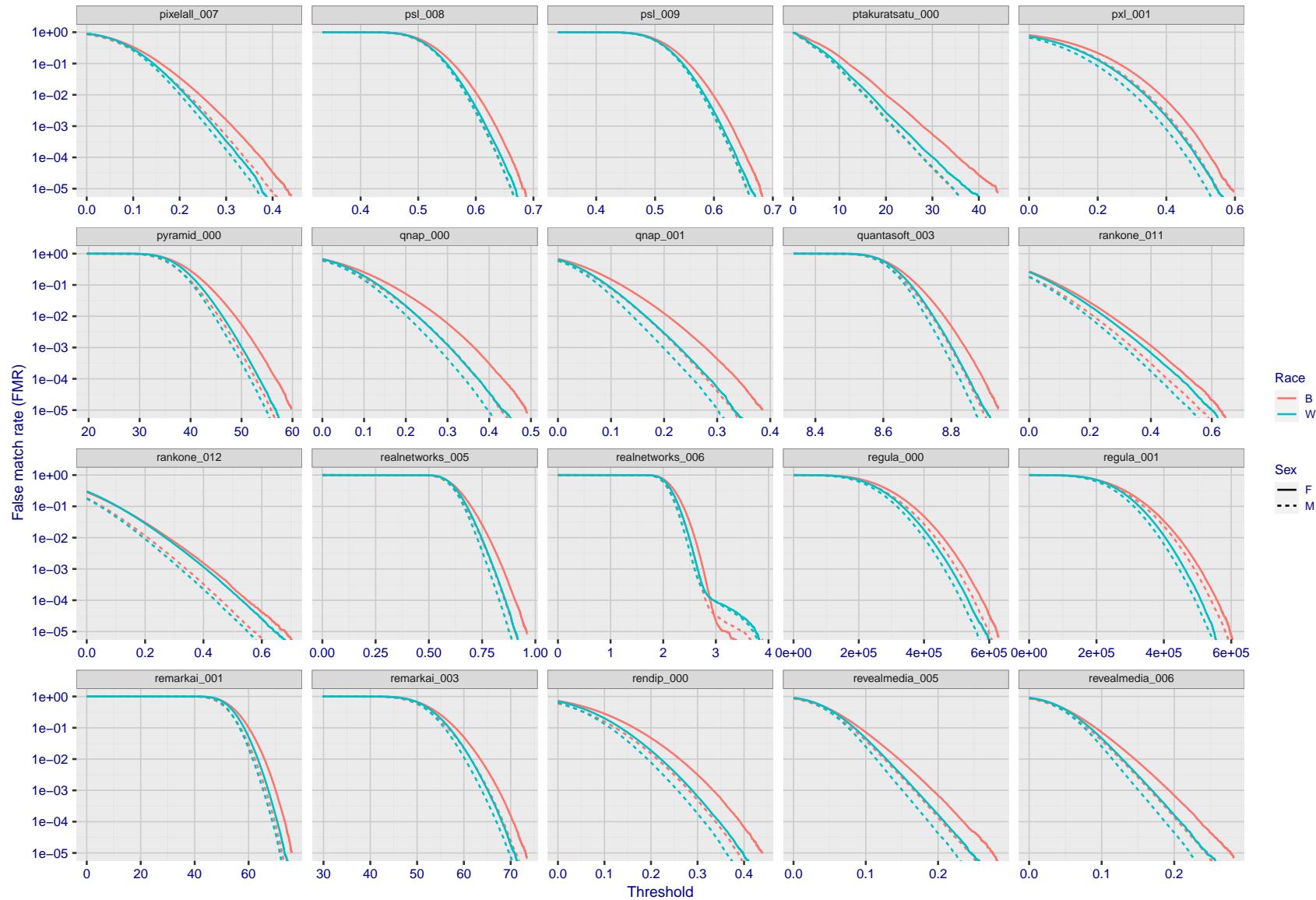


Figure 183: For the mugshot images, the false match calibration curves show false match rate vs. threshold. Separate curves appear for white females, black females, black males and white males.

2022/02/23 14:09:04

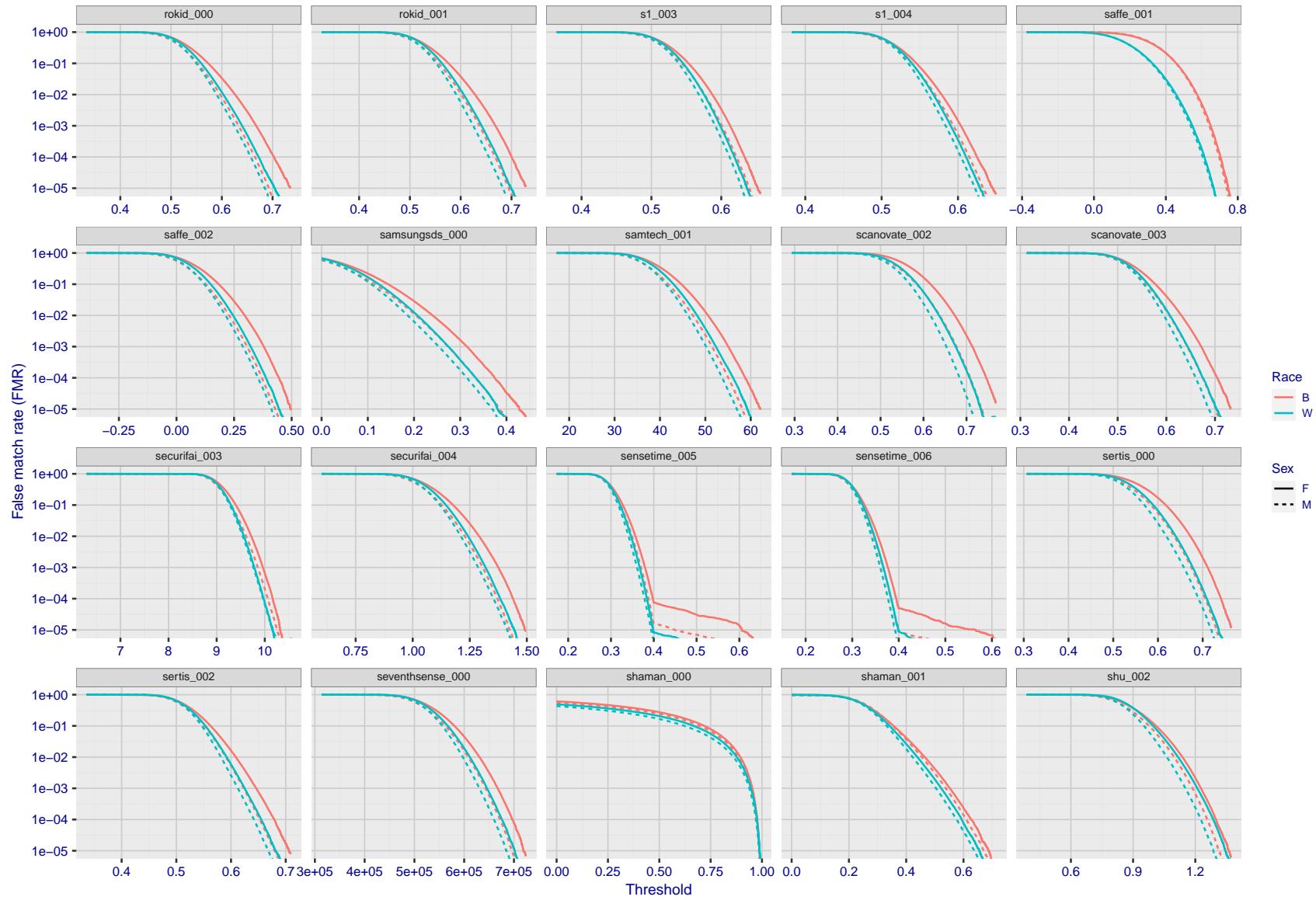


Figure 184: For the mugshot images, the false match calibration curves show false match rate vs. threshold. Separate curves appear for white females, black females, black males and white males.

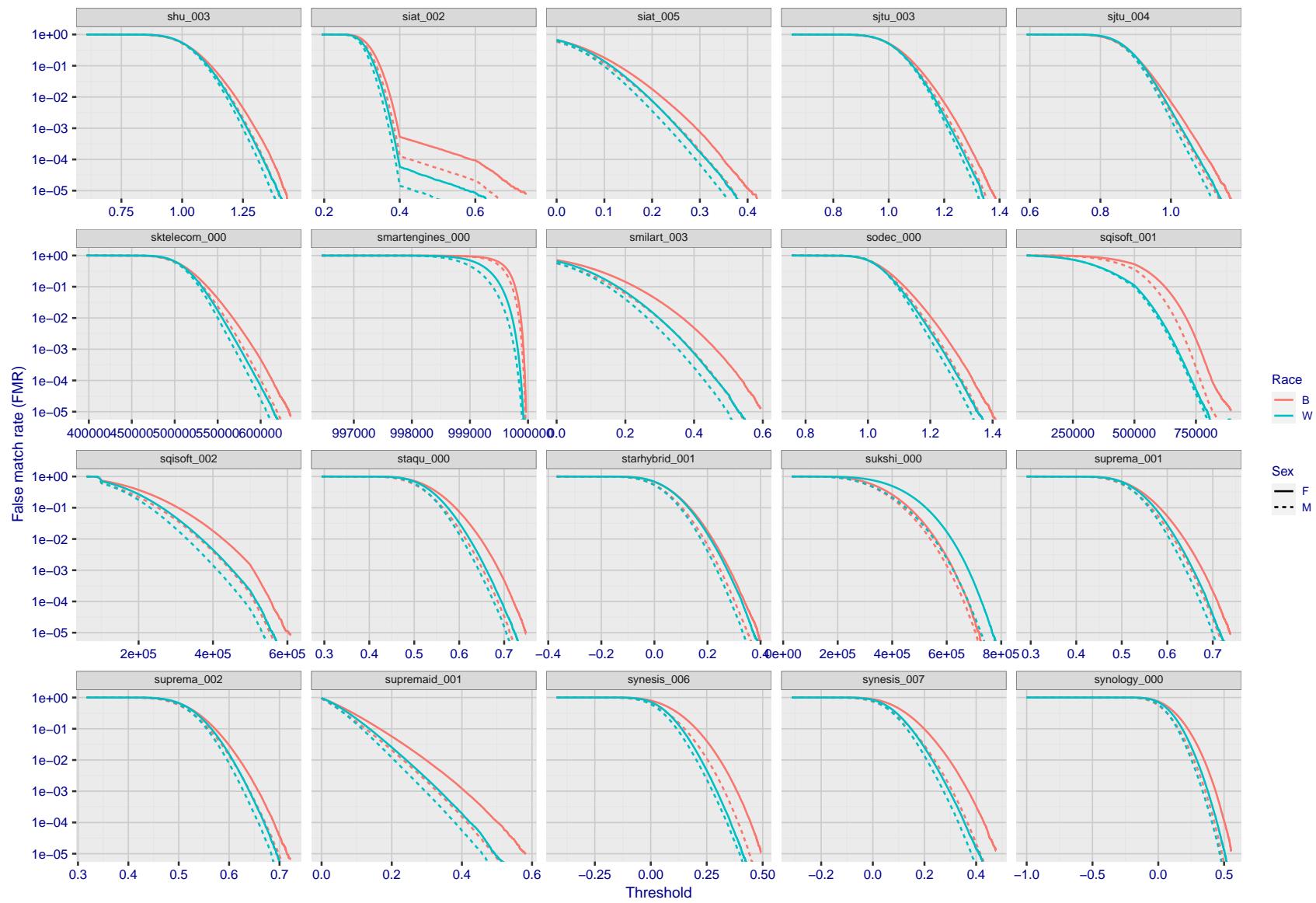


Figure 185: For the mugshot images, the false match calibration curves show false match rate vs. threshold. Separate curves appear for white females, black females, black males and white males.

2022/02/23 14:09:04

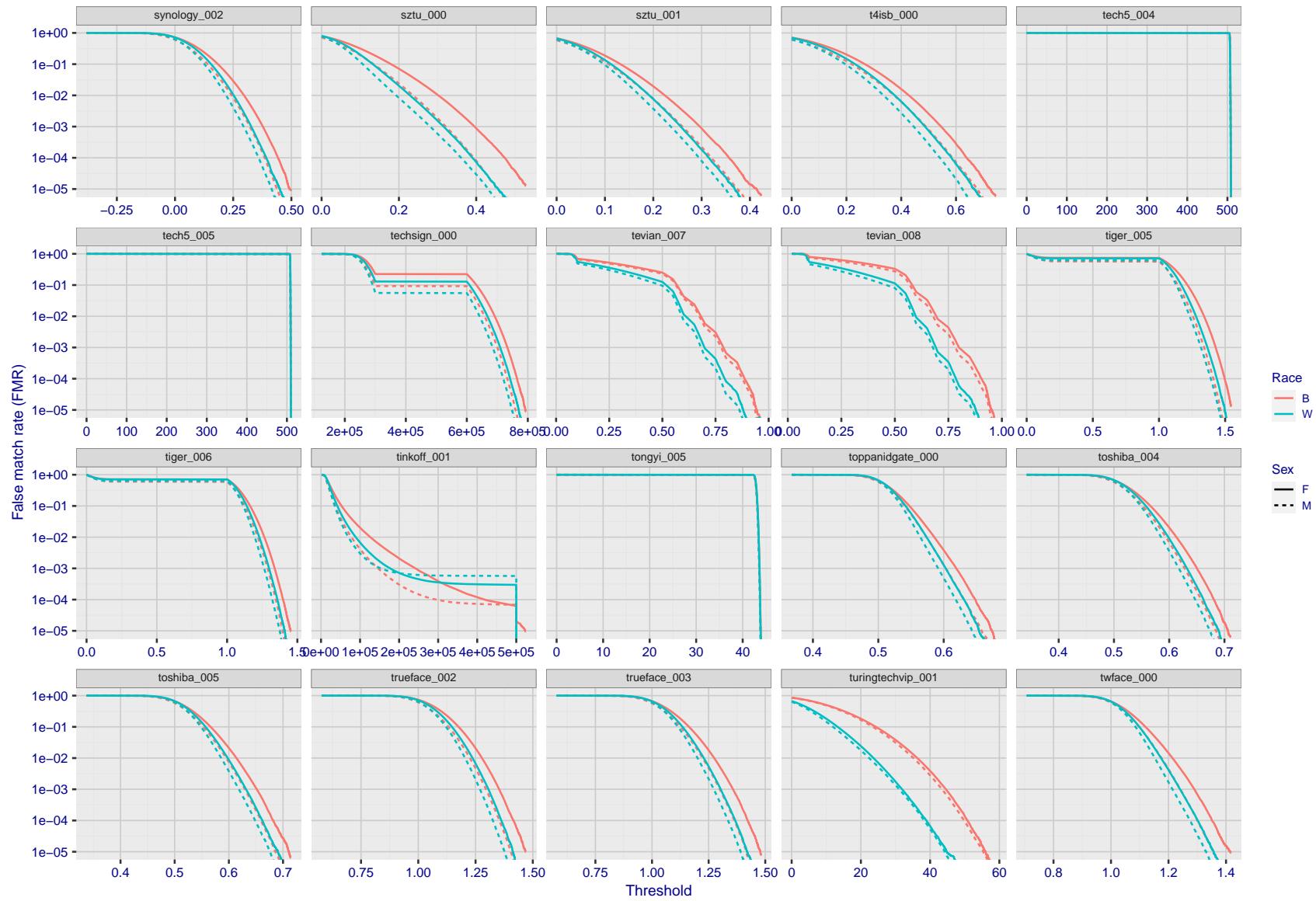


Figure 186: For the mugshot images, the false match calibration curves show false match rate vs. threshold. Separate curves appear for white females, black females, black males and white males.

2022/02/23 14:09:04

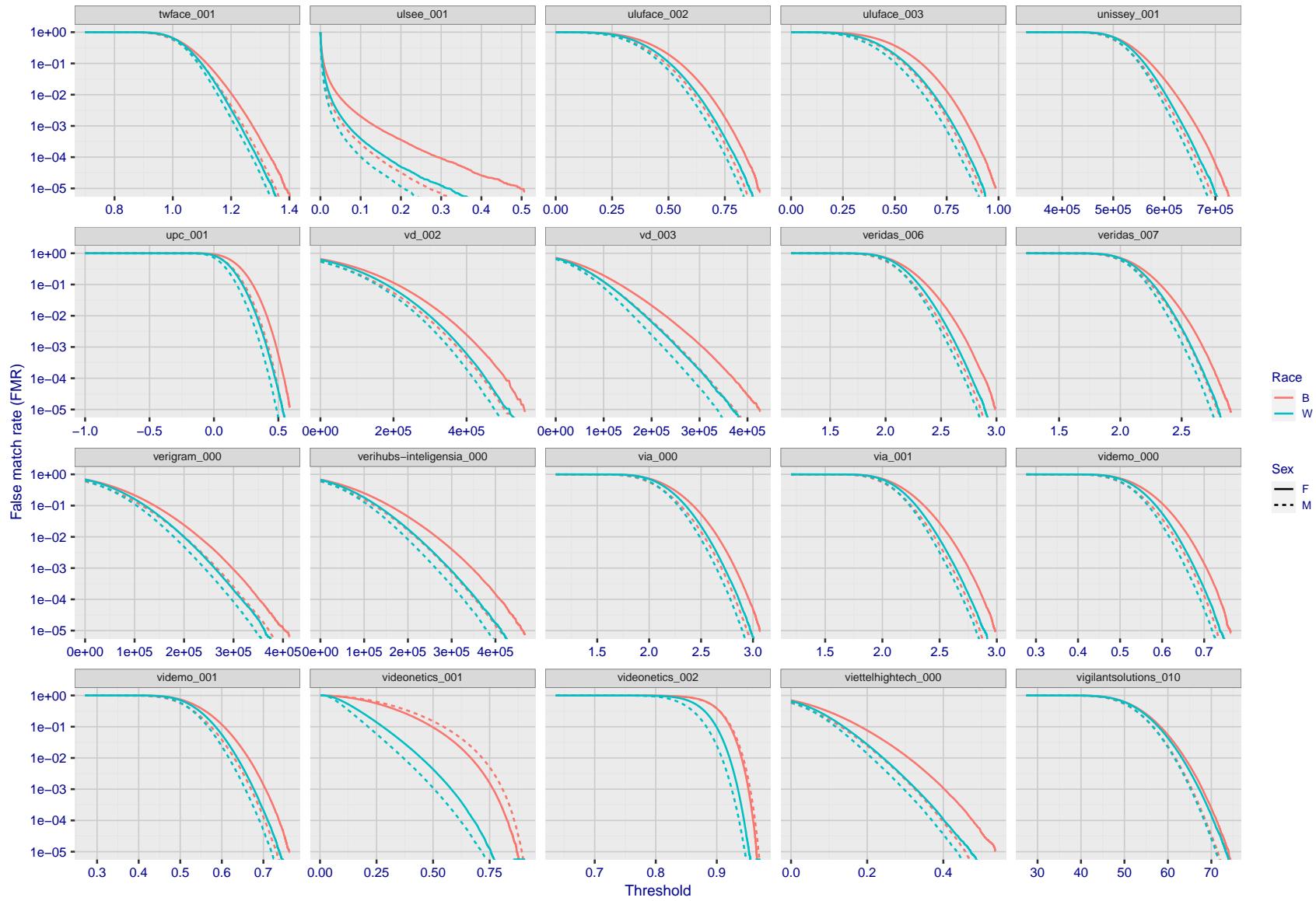


Figure 187: For the mugshot images, the false match calibration curves show false match rate vs. threshold. Separate curves appear for white females, black females, black males and white males.

2022/02/23 14:09:04

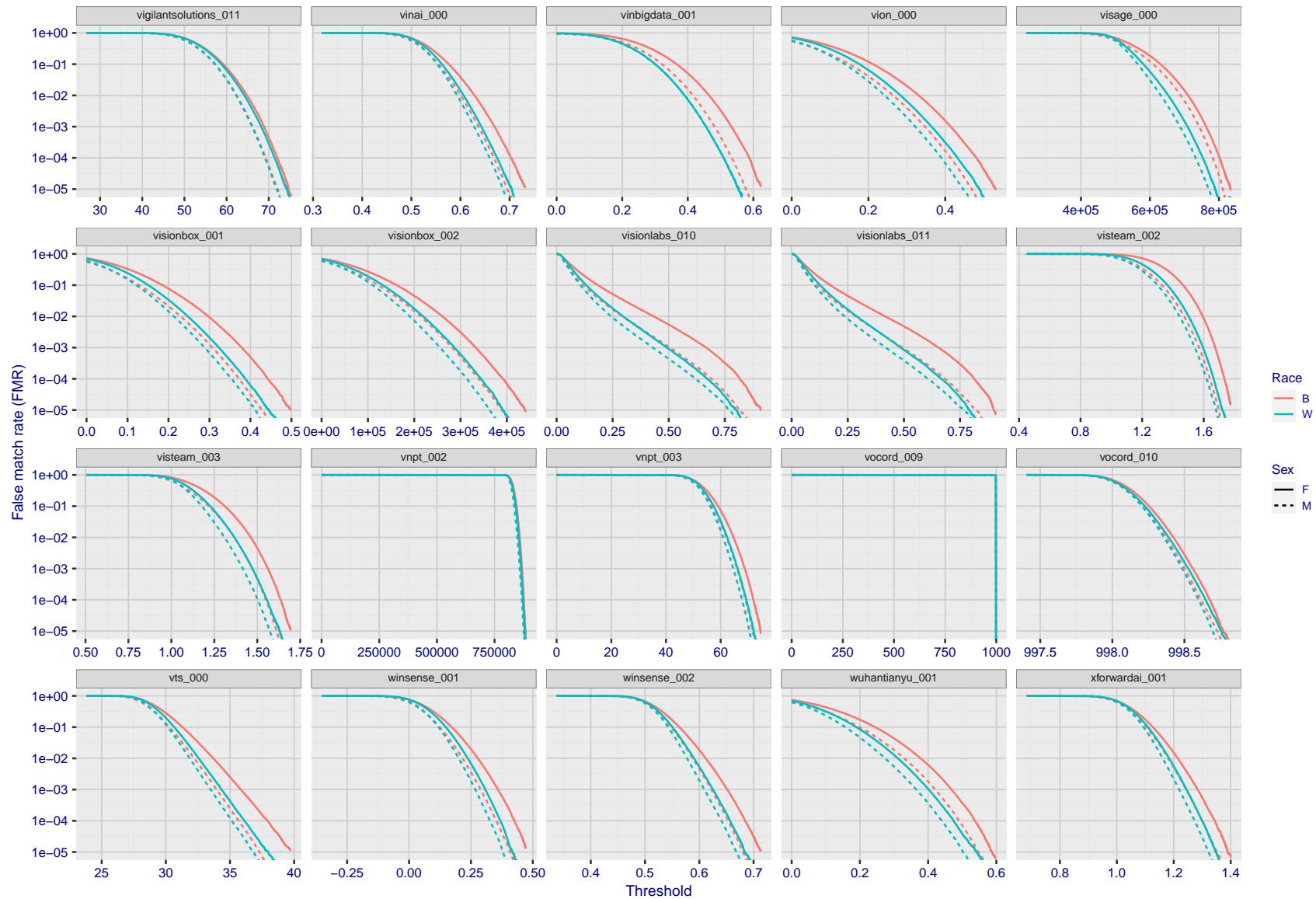


Figure 188: For the mugshot images, the false match calibration curves show false match rate vs. threshold. Separate curves appear for white females, black females, black males and white males.

FNMR(T)
"False non-match rate"
"False match rate"

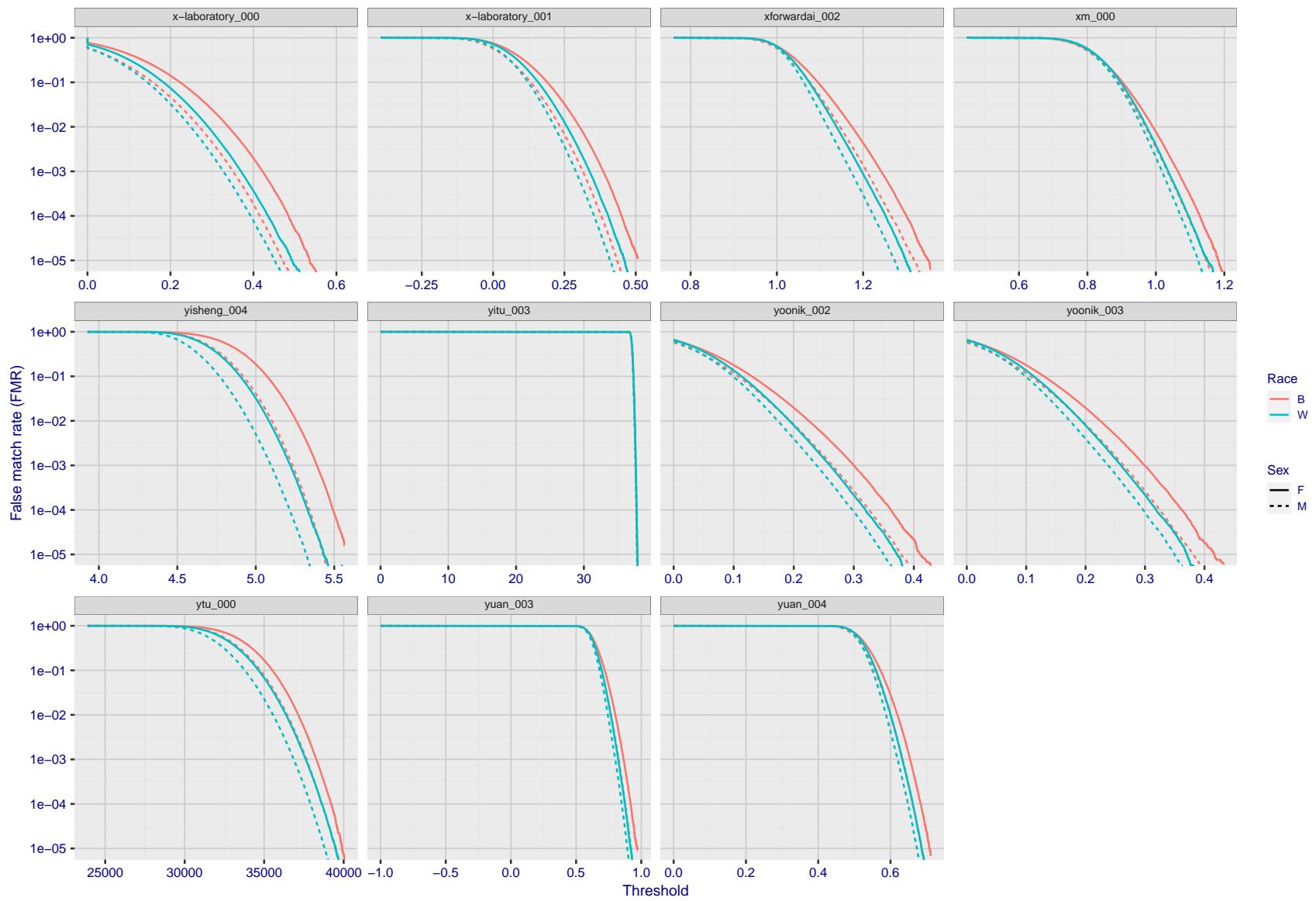


Figure 189: For the mugshot images, the false match calibration curves show false match rate vs. threshold. Separate curves appear for white females, black females, black males and white males.

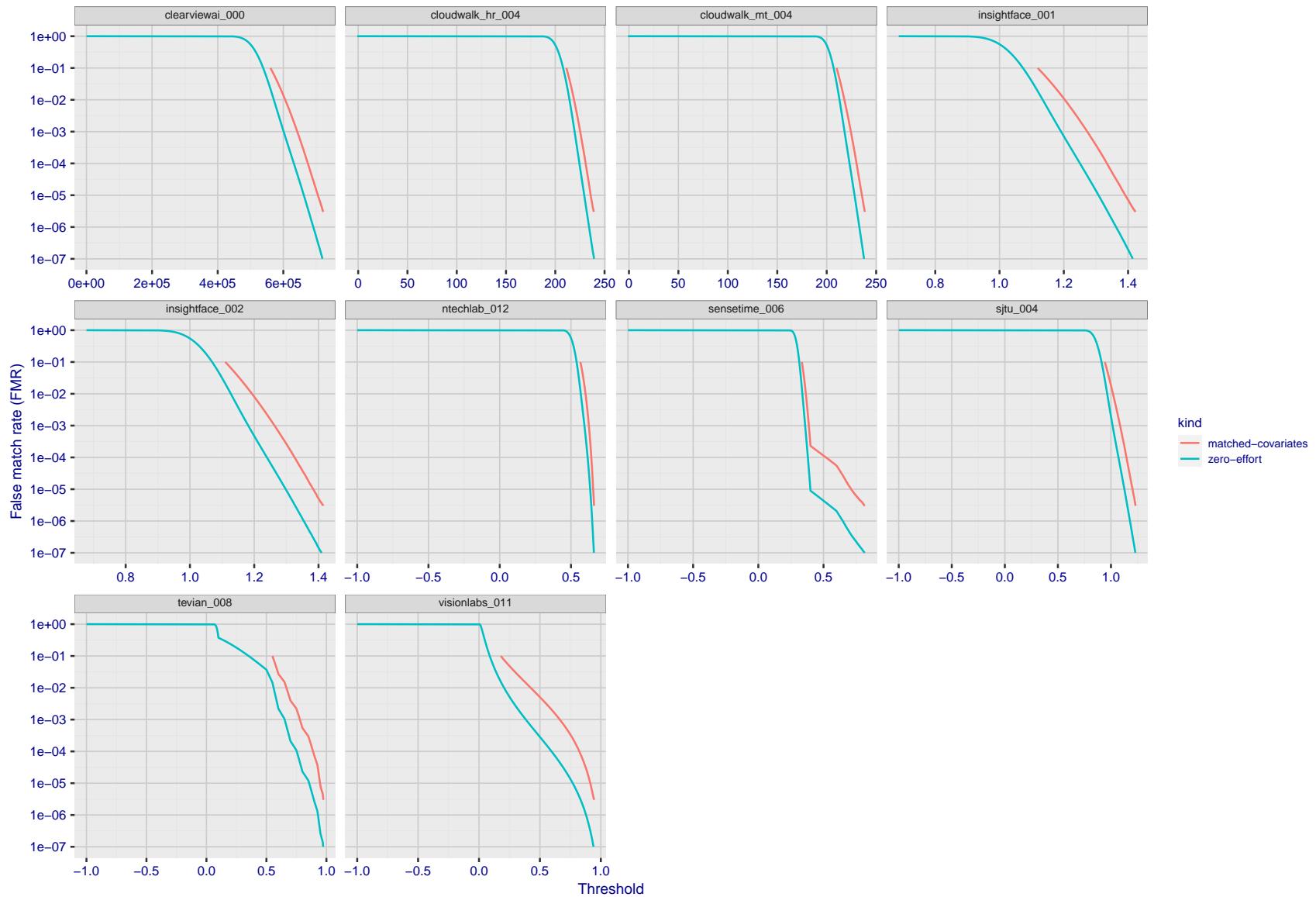


Figure 190: For the visa images, the false match calibration curves show FMR vs. threshold, T . The blue (lower) curves are for zero-effort impostors (i.e. comparing all images against all). The red (upper) curves are for persons of the same-sex, same-age, and same national-origin. This shows that FMR is underestimated (by a factor of 10 or more) by using a zero-effort impostor calculation to calibrate T . As shown later (sec. 3.6), FMR is higher for demographic-matched impostors.

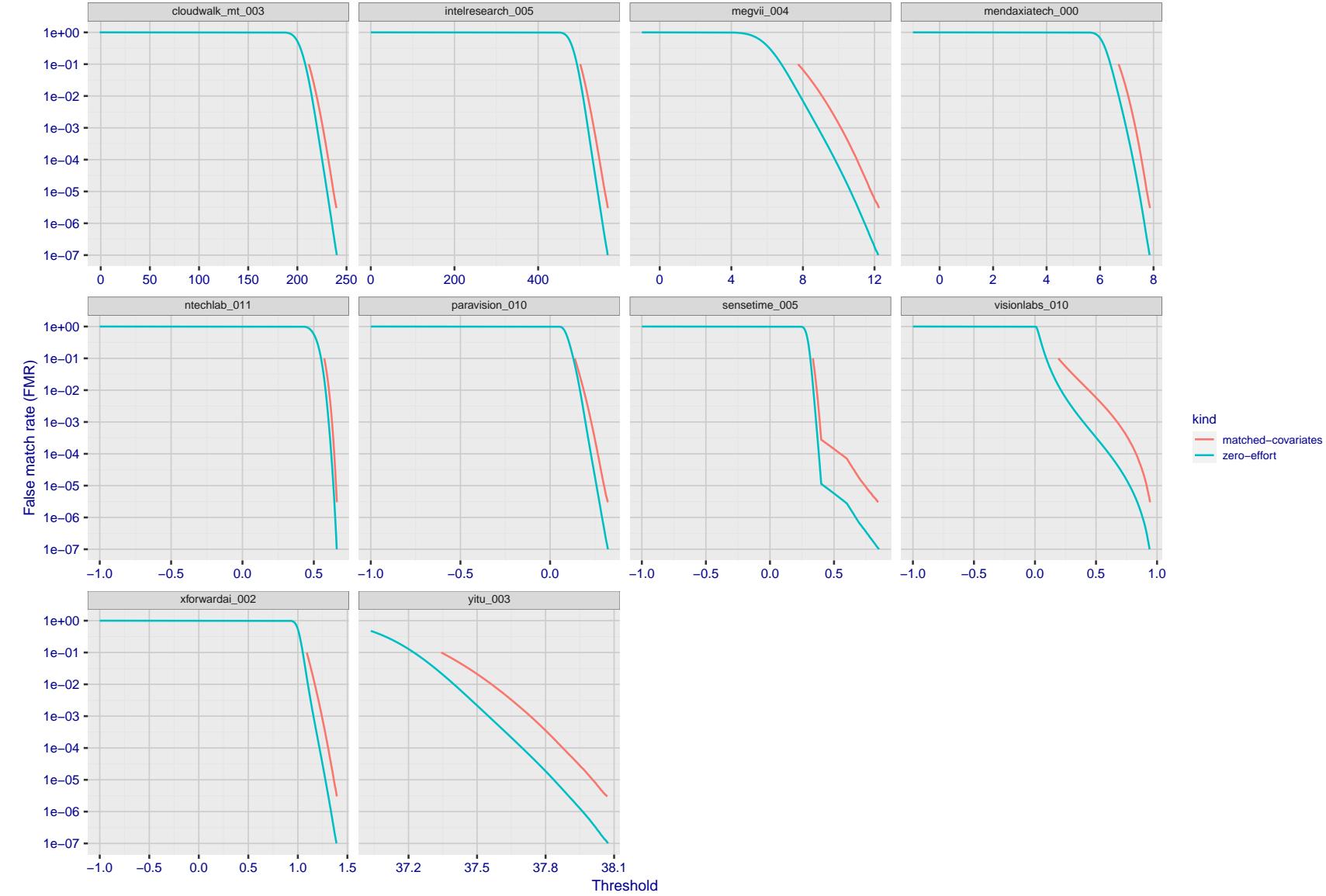


Figure 191: For the visa images, the false match calibration curves show FMR vs. threshold, T . The blue (lower) curves are for zero-effort impostors (i.e. comparing all images against all). The red (upper) curves are for persons of the same-sex, same-age, and same national-origin. This shows that FMR is underestimated (by a factor of 10 or more) by using a zero-effort impostor calculation to calibrate T . As shown later (sec. 3.6), FMR is higher for demographic-matched impostors.

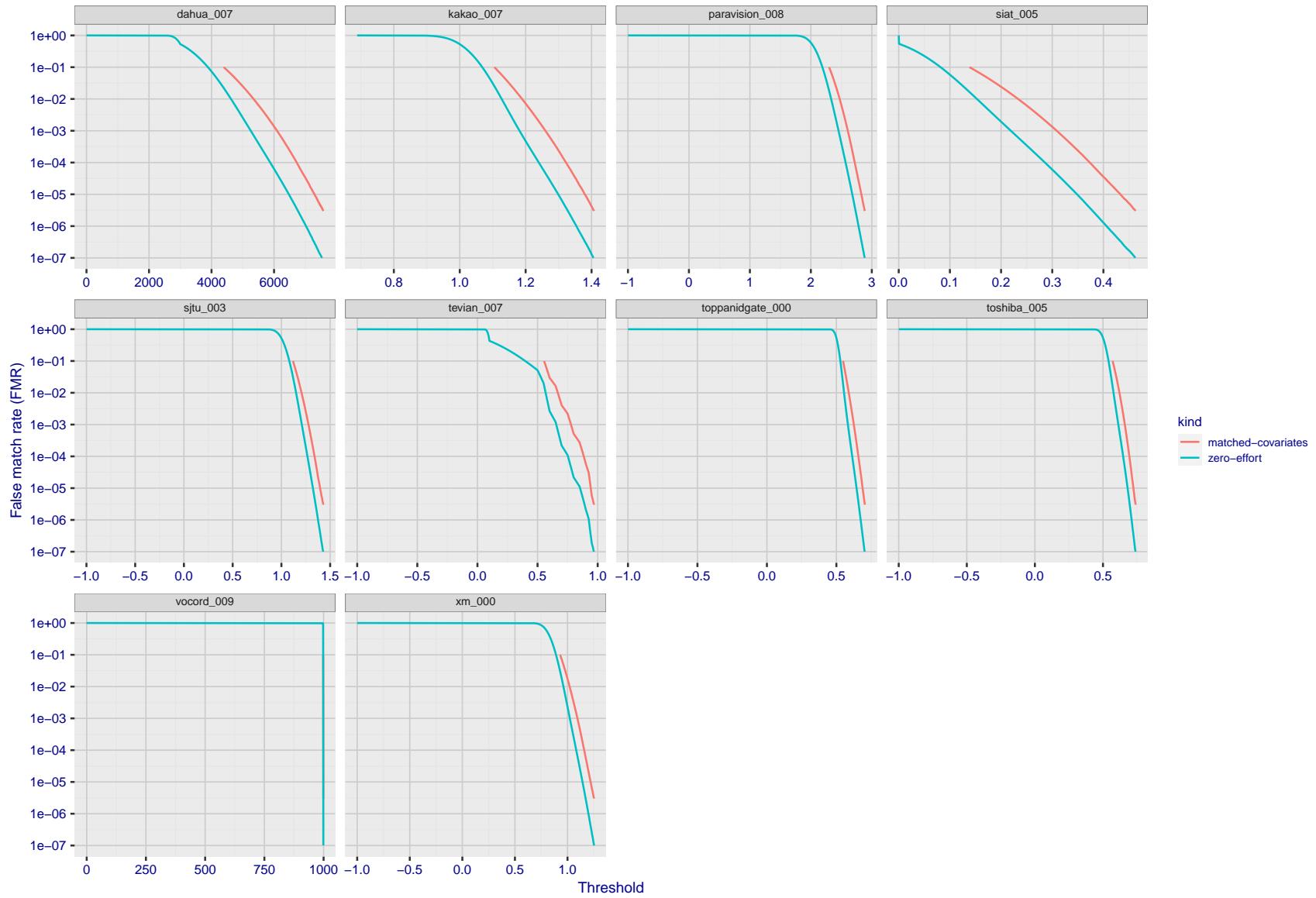


Figure 192: For the visa images, the false match calibration curves show FMR vs. threshold, T . The blue (lower) curves are for zero-effort impostors (i.e. comparing all images against all). The red (upper) curves are for persons of the same-sex, same-age, and same national-origin. This shows that FMR is underestimated (by a factor of 10 or more) by using a zero-effort impostor calculation to calibrate T . As shown later (sec. 3.6), FMR is higher for demographic-matched impostors.

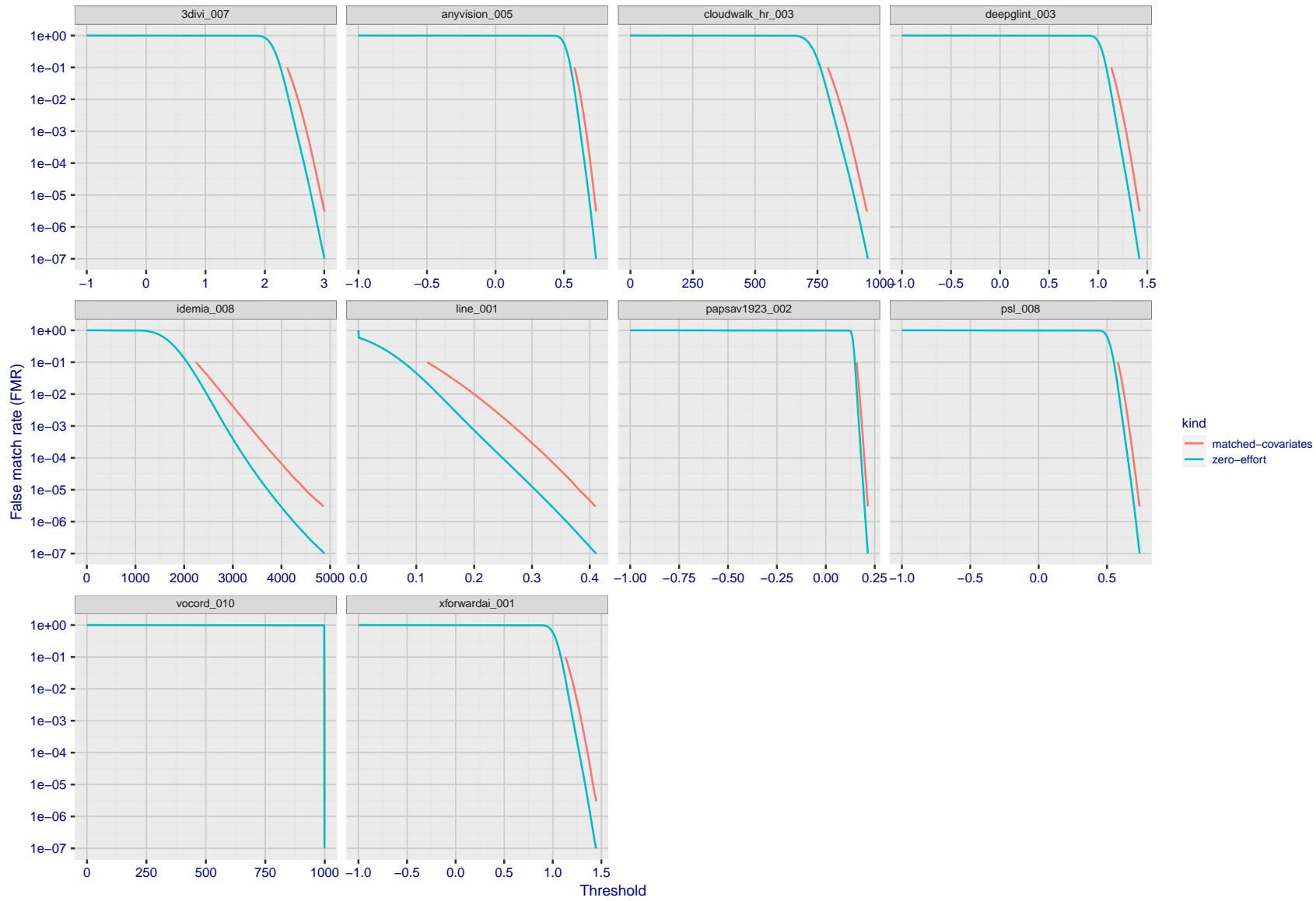


Figure 193: For the visa images, the false match calibration curves show FMR vs. threshold, T . The blue (lower) curves are for zero-effort impostors (i.e. comparing all images against all). The red (upper) curves are for persons of the same-sex, same-age, and same national-origin. This shows that FMR is underestimated (by a factor of 10 or more) by using a zero-effort impostor calculation to calibrate T . As shown later (sec. 3.6), FMR is higher for demographic-matched impostors.

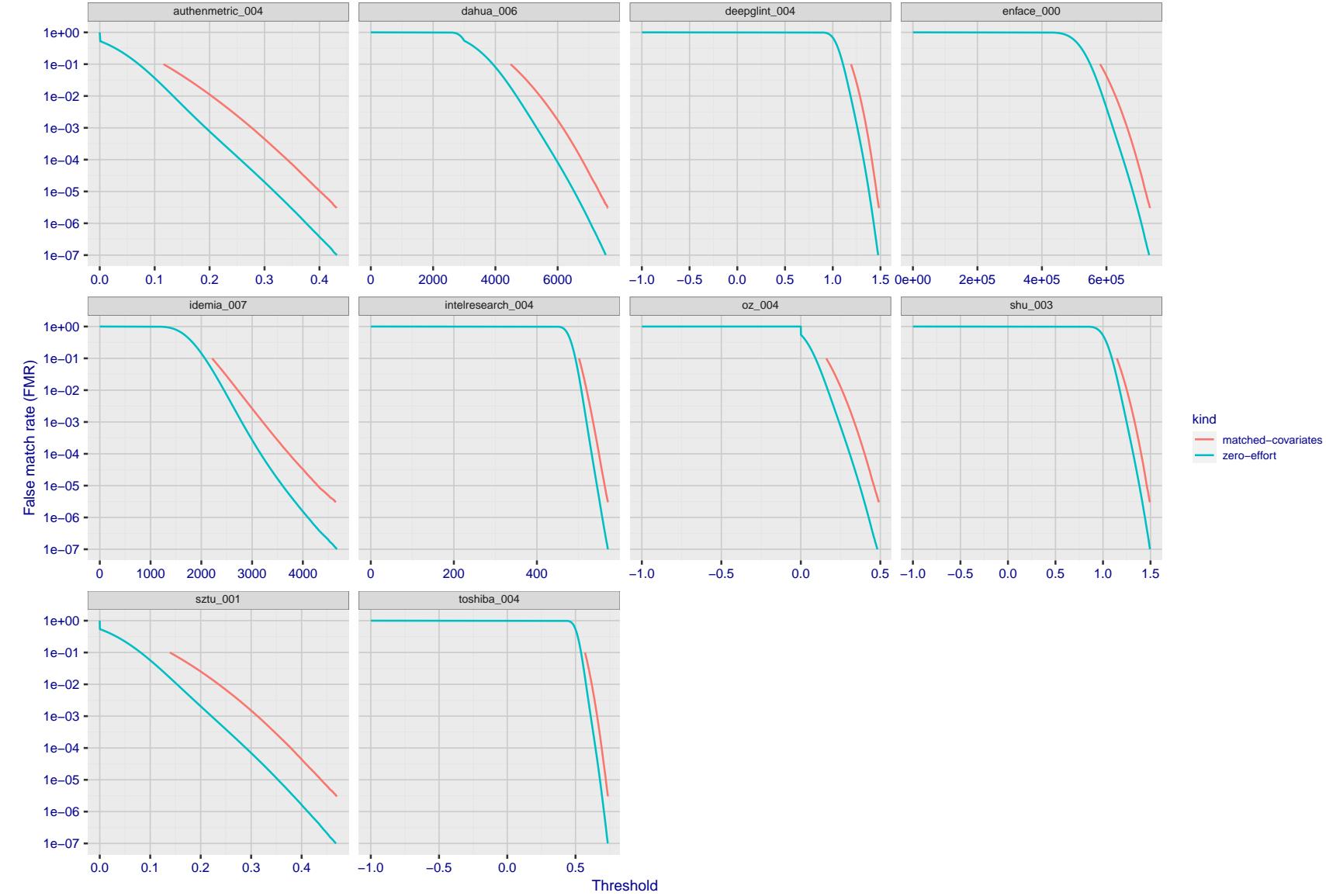


Figure 194: For the visa images, the false match calibration curves show FMR vs. threshold, T . The blue (lower) curves are for zero-effort impostors (i.e. comparing all images against all). The red (upper) curves are for persons of the same-sex, same-age, and same national-origin. This shows that FMR is underestimated (by a factor of 10 or more) by using a zero-effort impostor calculation to calibrate T . As shown later (sec. 3.6), FMR is higher for demographic-matched impostors.

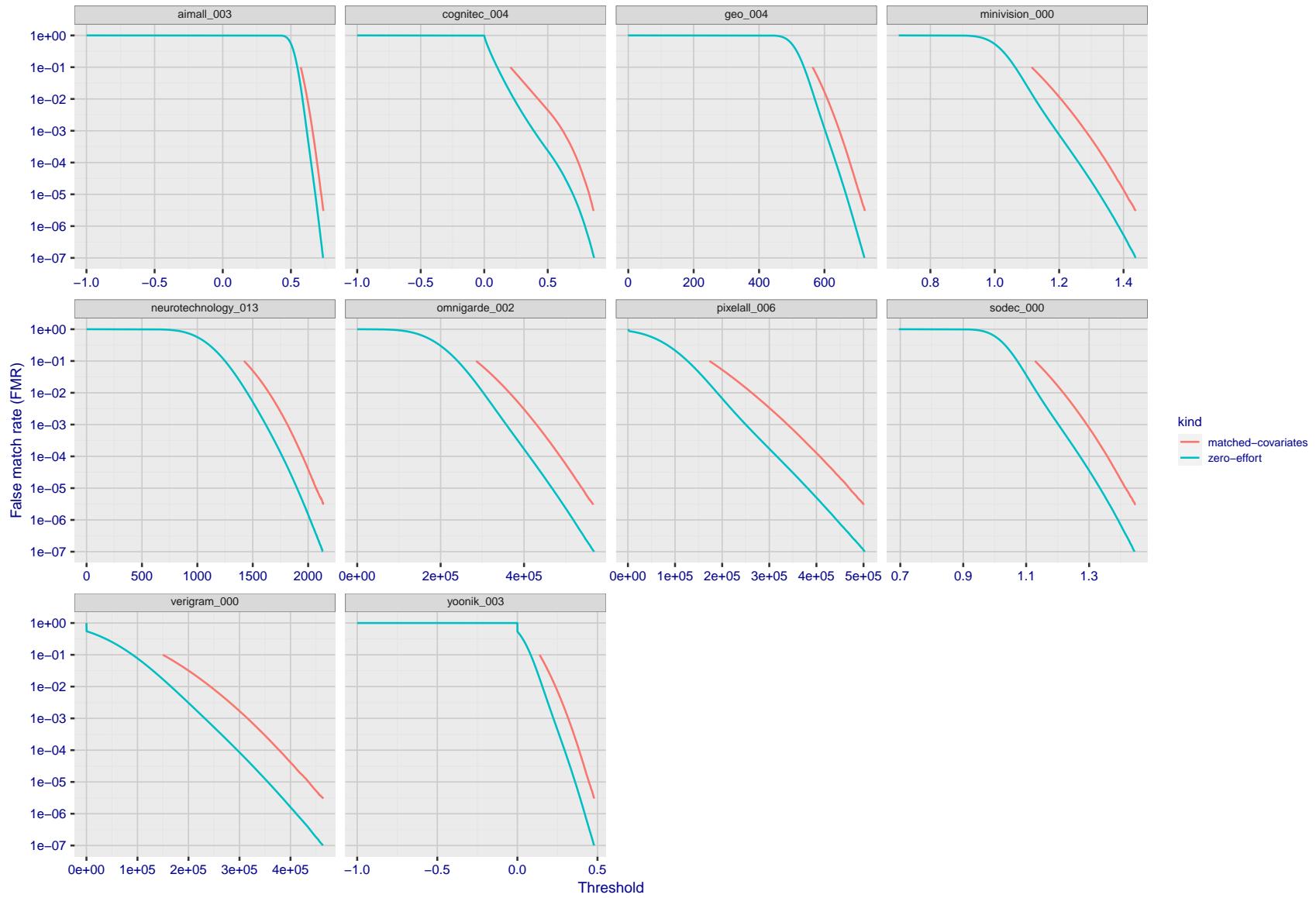


Figure 195: For the visa images, the false match calibration curves show FMR vs. threshold, T . The blue (lower) curves are for zero-effort impostors (i.e. comparing all images against all). The red (upper) curves are for persons of the same-sex, same-age, and same national-origin. This shows that FMR is underestimated (by a factor of 10 or more) by using a zero-effort impostor calculation to calibrate T . As shown later (sec. 3.6), FMR is higher for demographic-matched impostors.

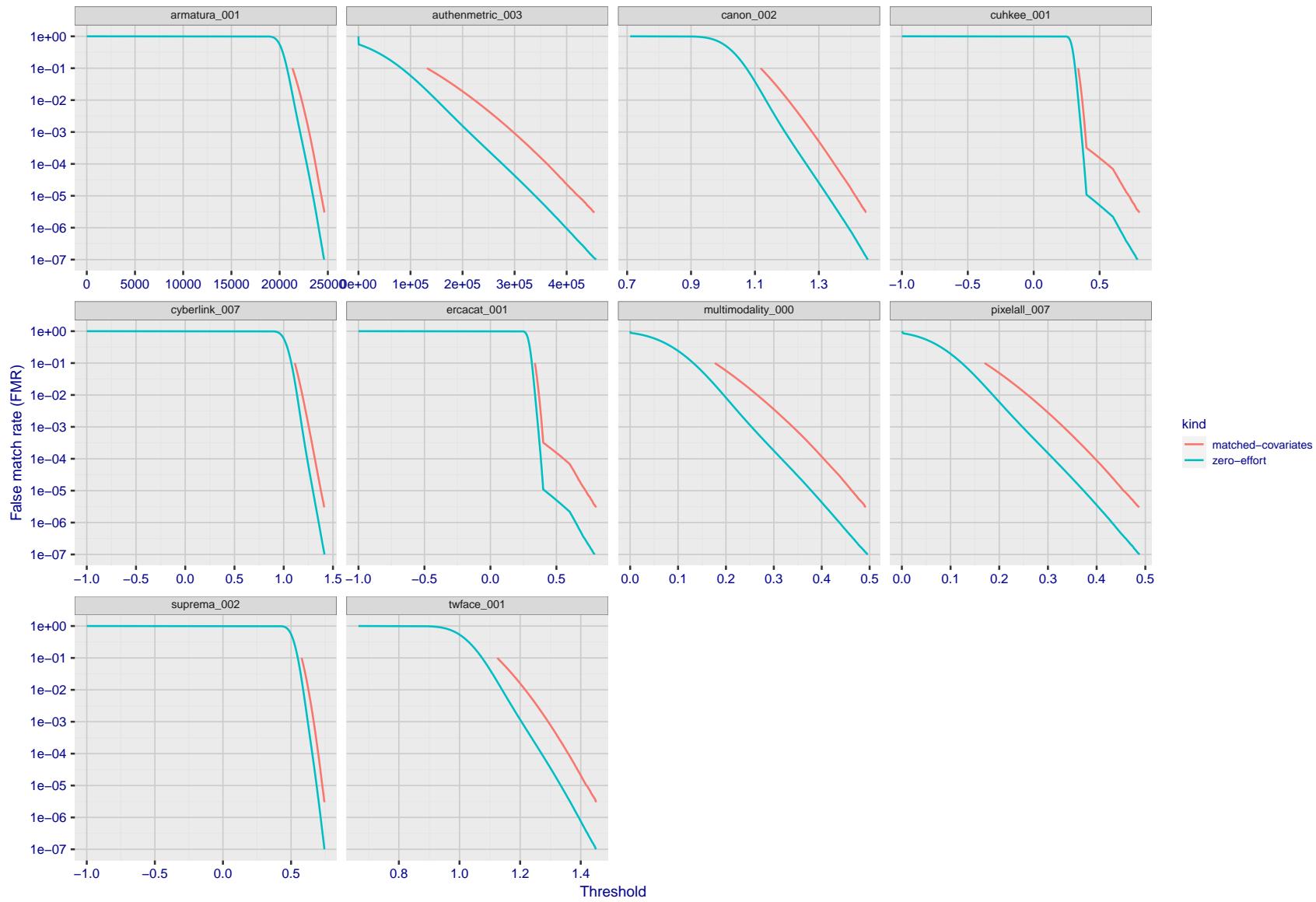


Figure 196: For the visa images, the false match calibration curves show FMR vs. threshold, T . The blue (lower) curves are for zero-effort impostors (i.e. comparing all images against all). The red (upper) curves are for persons of the same-sex, same-age, and same national-origin. This shows that FMR is underestimated (by a factor of 10 or more) by using a zero-effort impostor calculation to calibrate T . As shown later (sec. 3.6), FMR is higher for demographic-matched impostors.

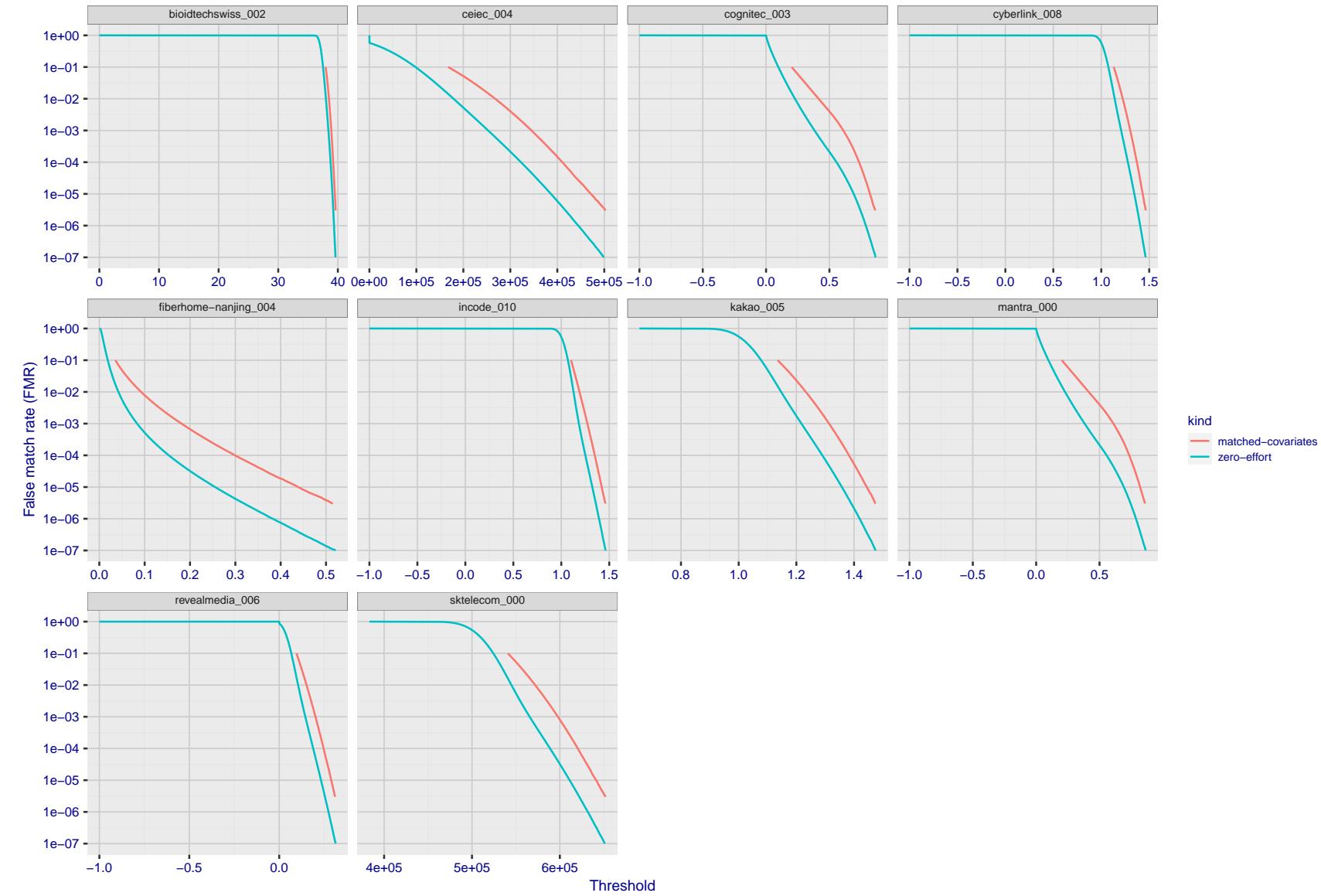


Figure 197: For the visa images, the false match calibration curves show FMR vs. threshold, T . The blue (lower) curves are for zero-effort impostors (i.e. comparing all images against all). The red (upper) curves are for persons of the same-sex, same-age, and same national-origin. This shows that FMR is underestimated (by a factor of 10 or more) by using a zero-effort impostor calculation to calibrate T . As shown later (sec. 3.6), FMR is higher for demographic-matched impostors.

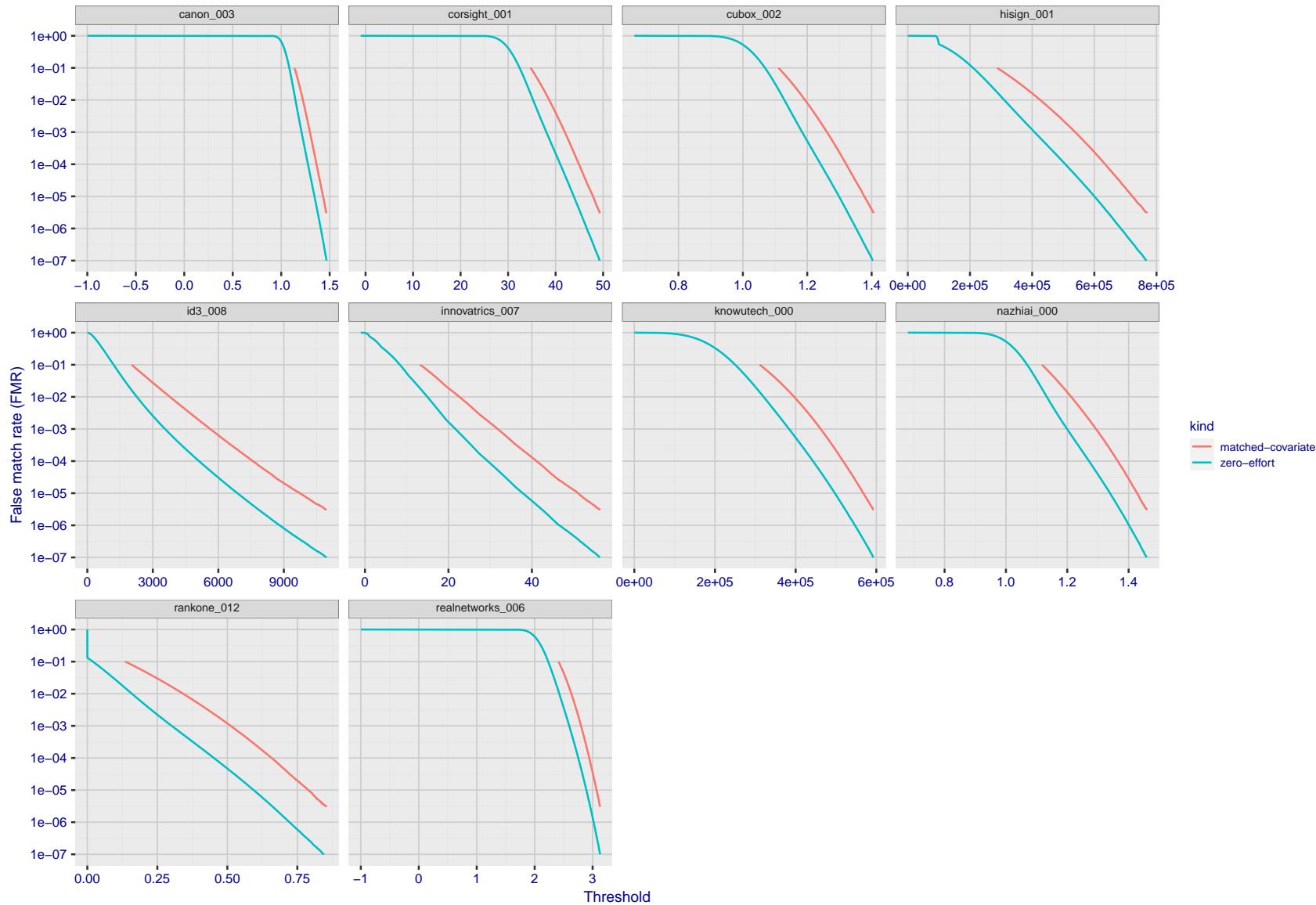


Figure 198: For the visa images, the false match calibration curves show FMR vs. threshold, T . The blue (lower) curves are for zero-effort impostors (i.e. comparing all images against all). The red (upper) curves are for persons of the same-sex, same-age, and same national-origin. This shows that FMR is underestimated (by a factor of 10 or more) by using a zero-effort impostor calculation to calibrate T . As shown later (sec. 3.6), FMR is higher for demographic-matched impostors.

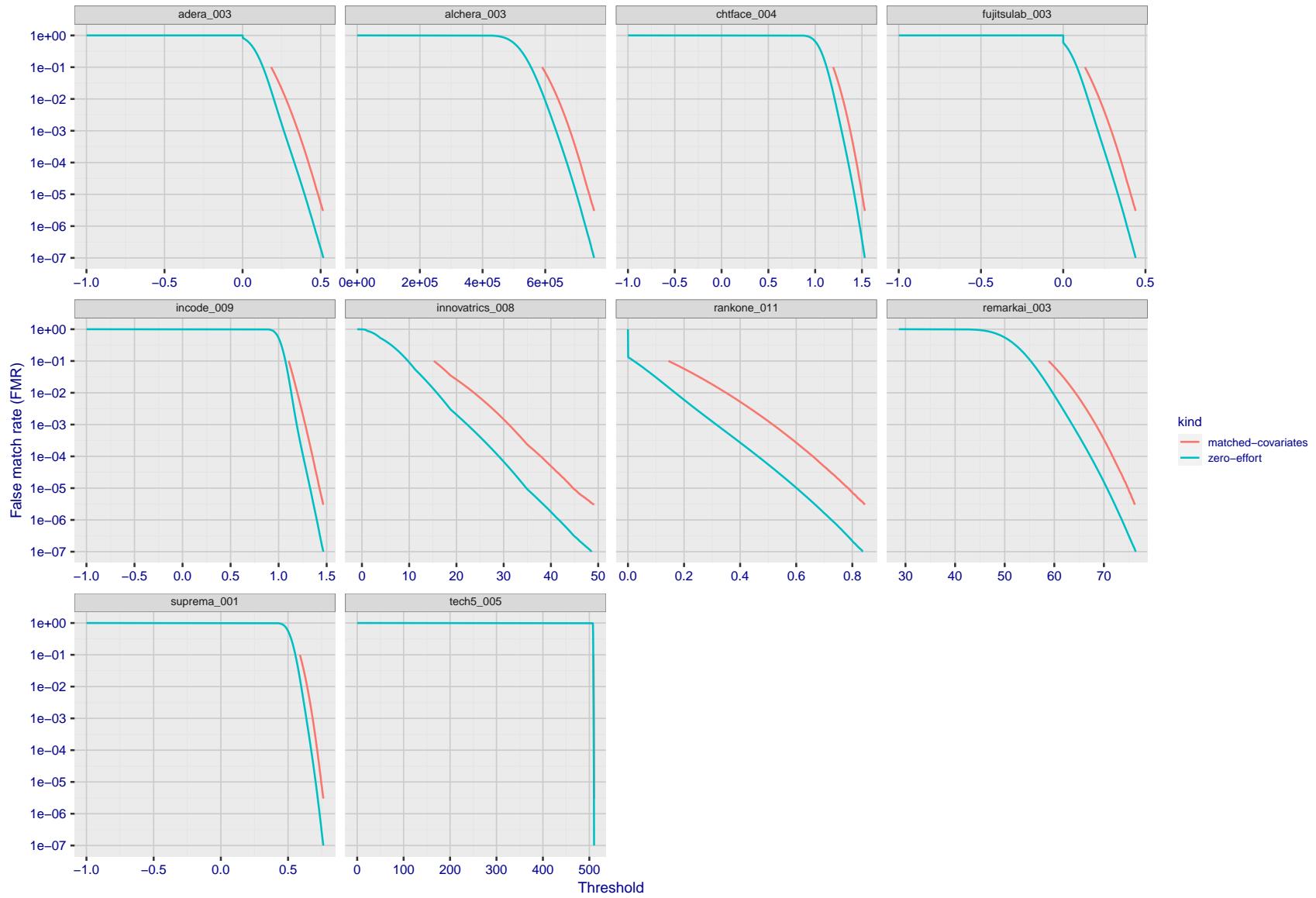


Figure 199: For the visa images, the false match calibration curves show FMR vs. threshold, T . The blue (lower) curves are for zero-effort impostors (i.e. comparing all images against all). The red (upper) curves are for persons of the same-sex, same-age, and same national-origin. This shows that FMR is underestimated (by a factor of 10 or more) by using a zero-effort impostor calculation to calibrate T . As shown later (sec. 3.6), FMR is higher for demographic-matched impostors.

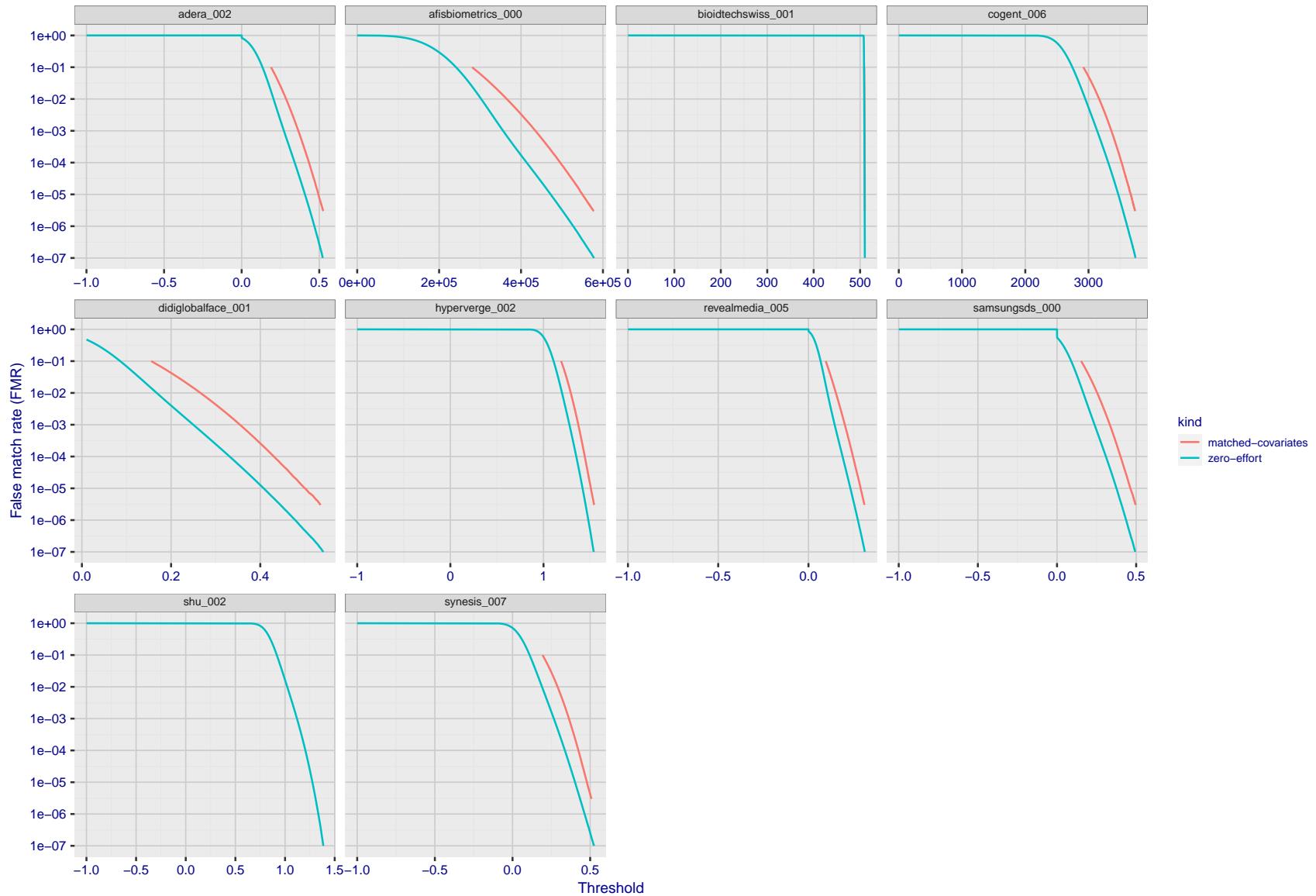


Figure 200: For the visa images, the false match calibration curves show FMR vs. threshold, T . The blue (lower) curves are for zero-effort impostors (i.e. comparing all images against all). The red (upper) curves are for persons of the same-sex, same-age, and same national-origin. This shows that FMR is underestimated (by a factor of 10 or more) by using a zero-effort impostor calculation to calibrate T . As shown later (sec. 3.6), FMR is higher for demographic-matched impostors.

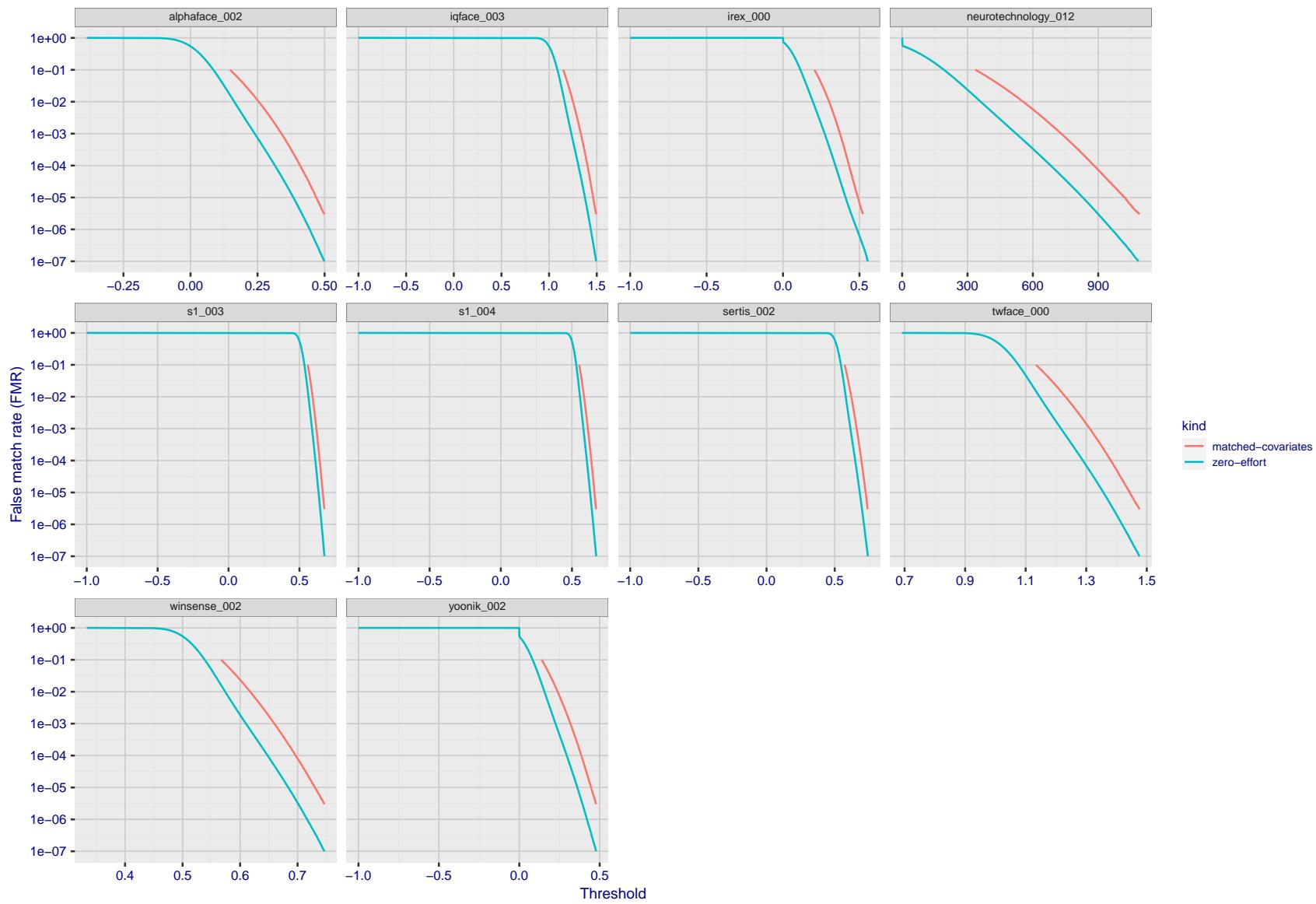


Figure 201: For the visa images, the false match calibration curves show FMR vs. threshold, T . The blue (lower) curves are for zero-effort impostors (i.e. comparing all images against all). The red (upper) curves are for persons of the same-sex, same-age, and same national-origin. This shows that FMR is underestimated (by a factor of 10 or more) by using a zero-effort impostor calculation to calibrate T . As shown later (sec. 3.6), FMR is higher for demographic-matched impostors.

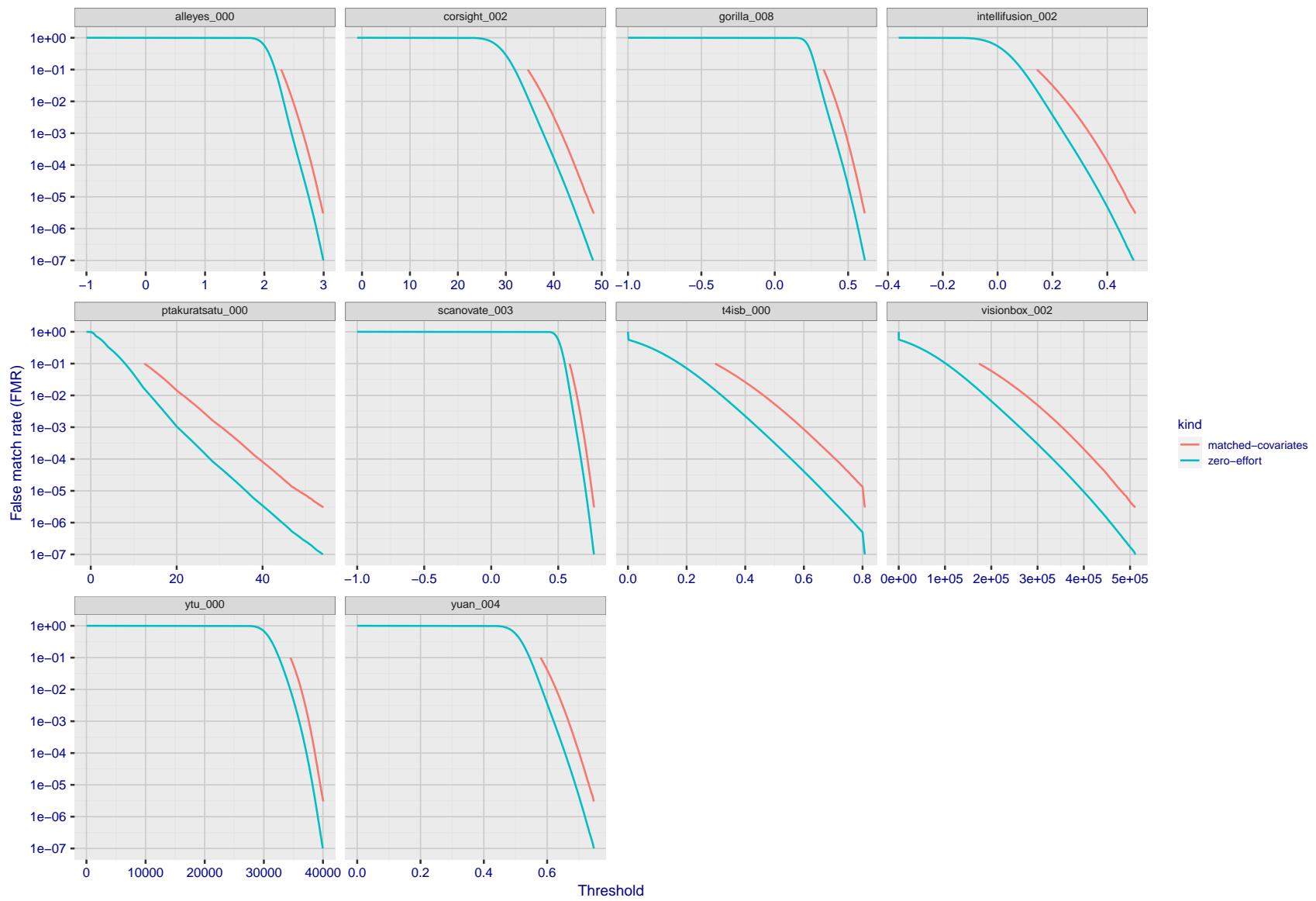


Figure 202: For the visa images, the false match calibration curves show FMR vs. threshold, T . The blue (lower) curves are for zero-effort impostors (i.e. comparing all images against all). The red (upper) curves are for persons of the same-sex, same-age, and same national-origin. This shows that FMR is underestimated (by a factor of 10 or more) by using a zero-effort impostor calculation to calibrate T . As shown later (sec. 3.6), FMR is higher for demographic-matched impostors.

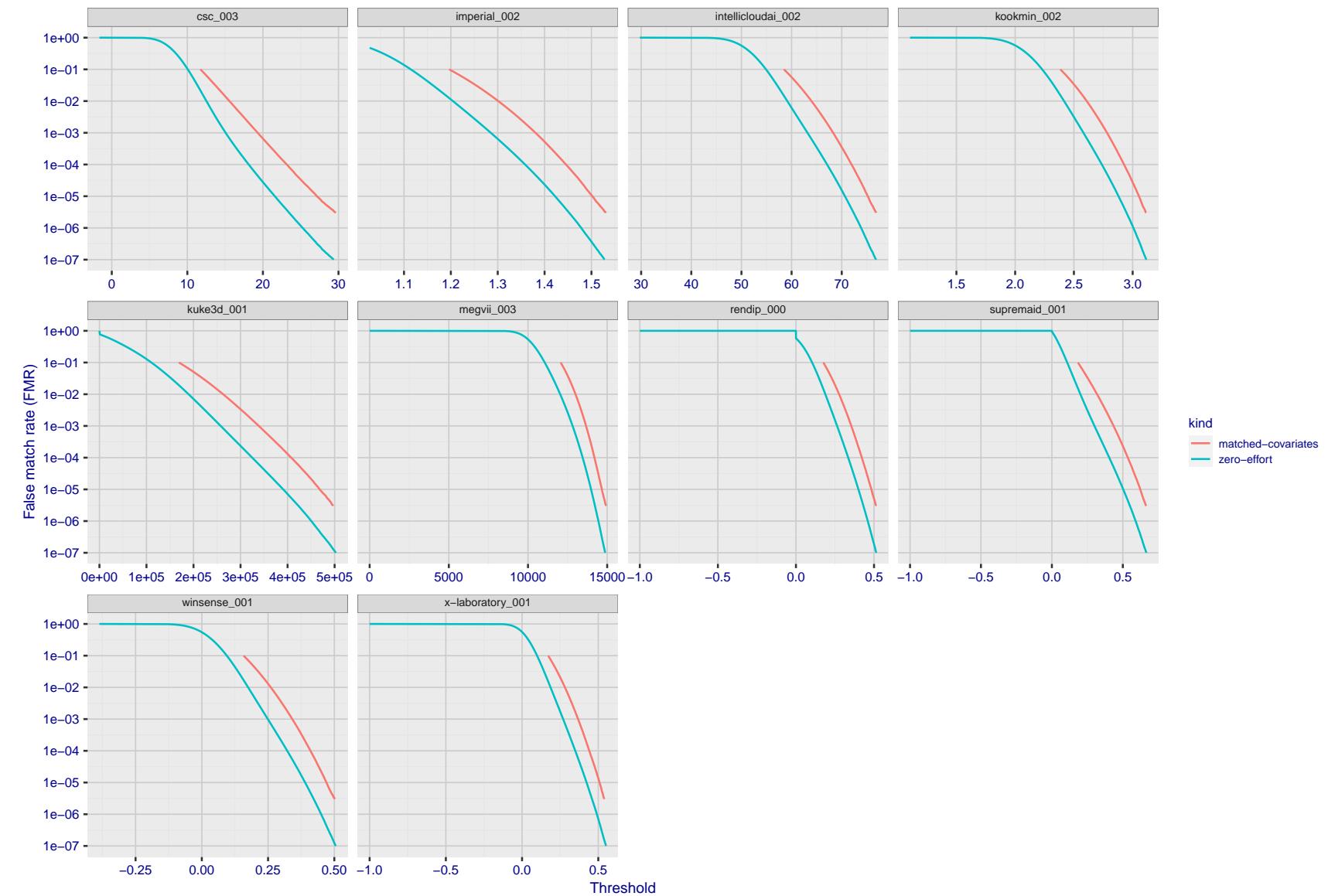


Figure 203: For the visa images, the false match calibration curves show FMR vs. threshold, T . The blue (lower) curves are for zero-effort impostors (i.e. comparing all images against all). The red (upper) curves are for persons of the same-sex, same-age, and same national-origin. This shows that FMR is underestimated (by a factor of 10 or more) by using a zero-effort impostor calculation to calibrate T . As shown later (sec. 3.6), FMR is higher for demographic-matched impostors.

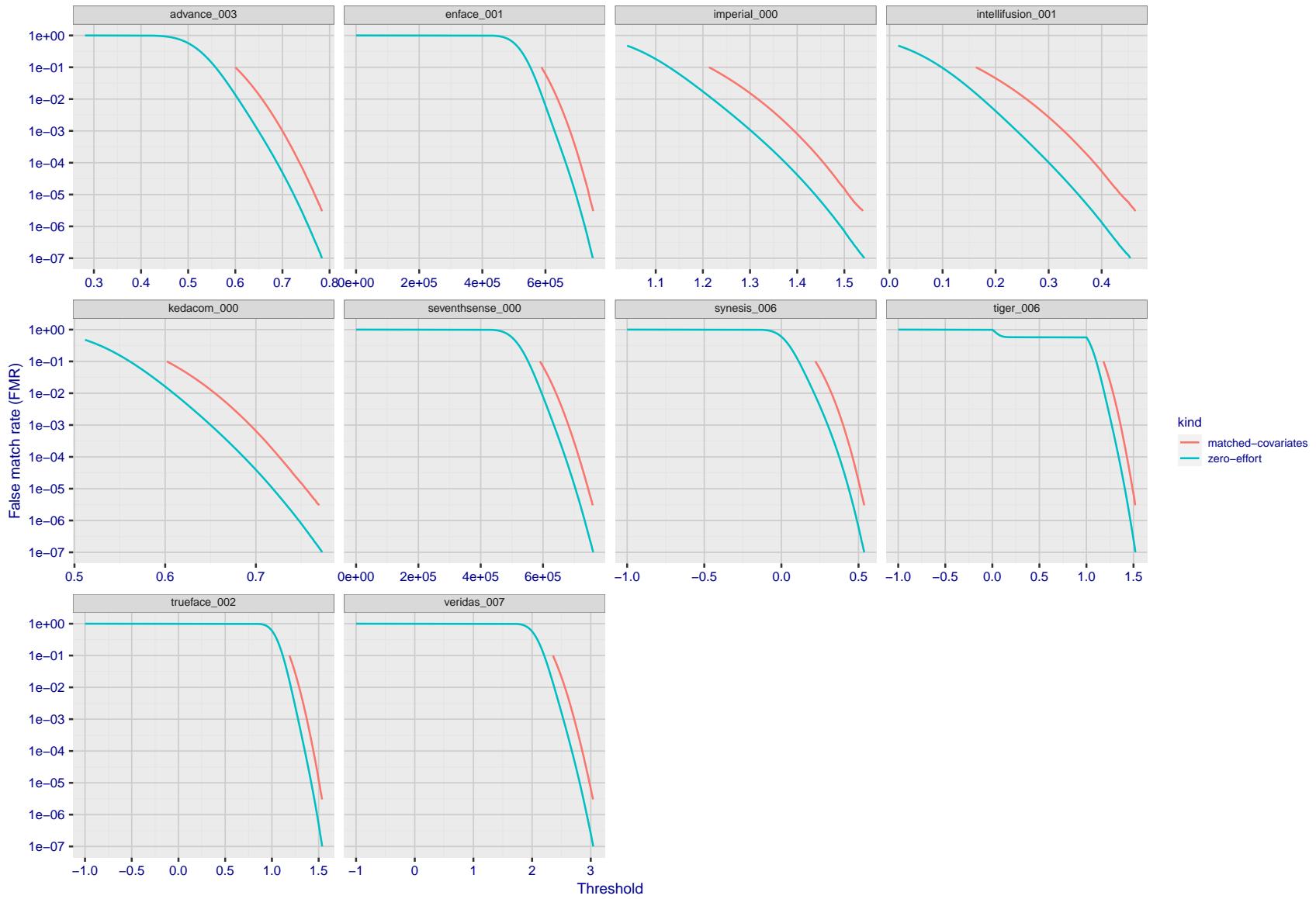


Figure 204: For the visa images, the false match calibration curves show FMR vs. threshold, T . The blue (lower) curves are for zero-effort impostors (i.e. comparing all images against all). The red (upper) curves are for persons of the same-sex, same-age, and same national-origin. This shows that FMR is underestimated (by a factor of 10 or more) by using a zero-effort impostor calculation to calibrate T . As shown later (sec. 3.6), FMR is higher for demographic-matched impostors.

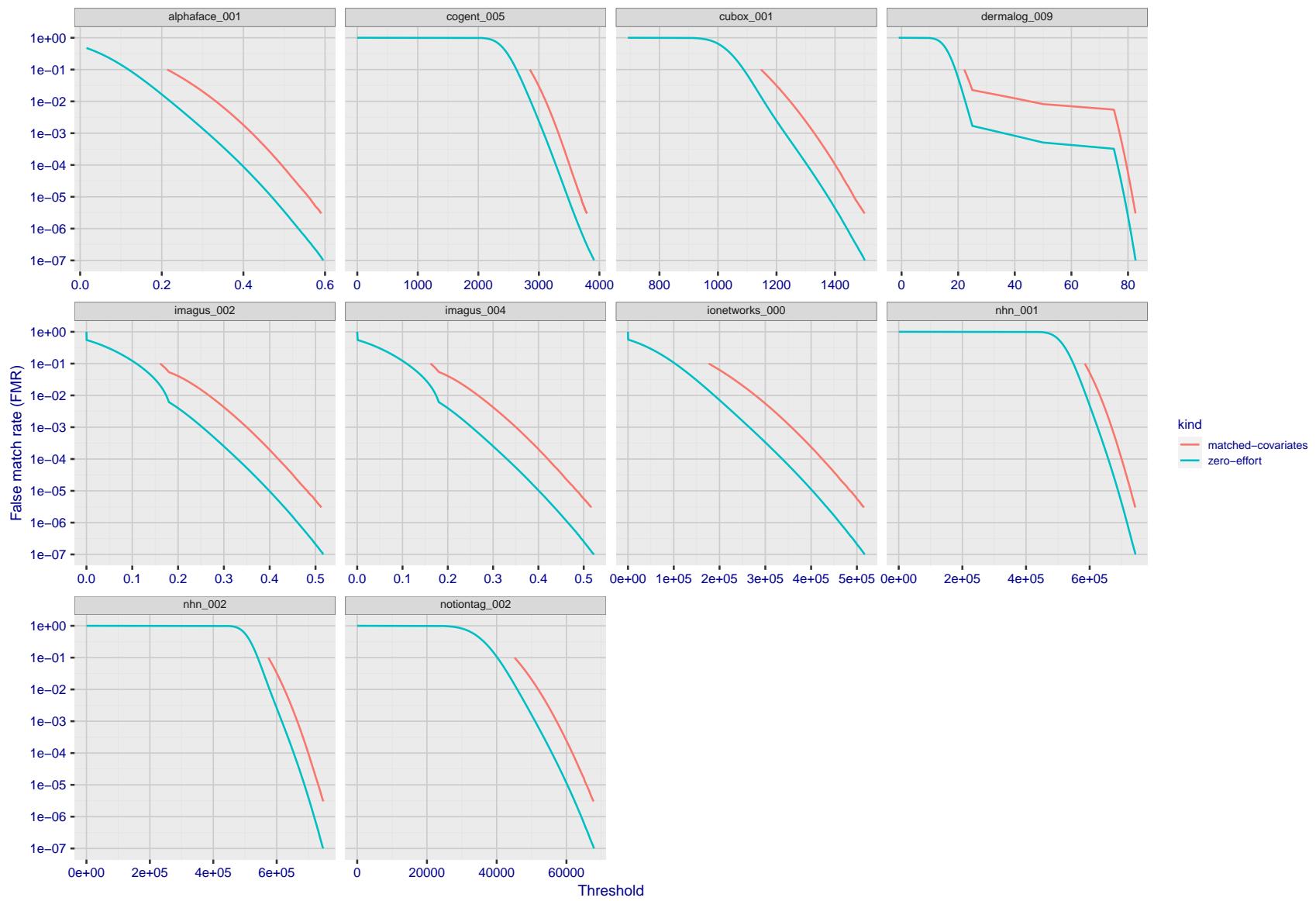


Figure 205: For the visa images, the false match calibration curves show FMR vs. threshold, T . The blue (lower) curves are for zero-effort impostors (i.e. comparing all images against all). The red (upper) curves are for persons of the same-sex, same-age, and same national-origin. This shows that FMR is underestimated (by a factor of 10 or more) by using a zero-effort impostor calculation to calibrate T . As shown later (sec. 3.6), FMR is higher for demographic-matched impostors.

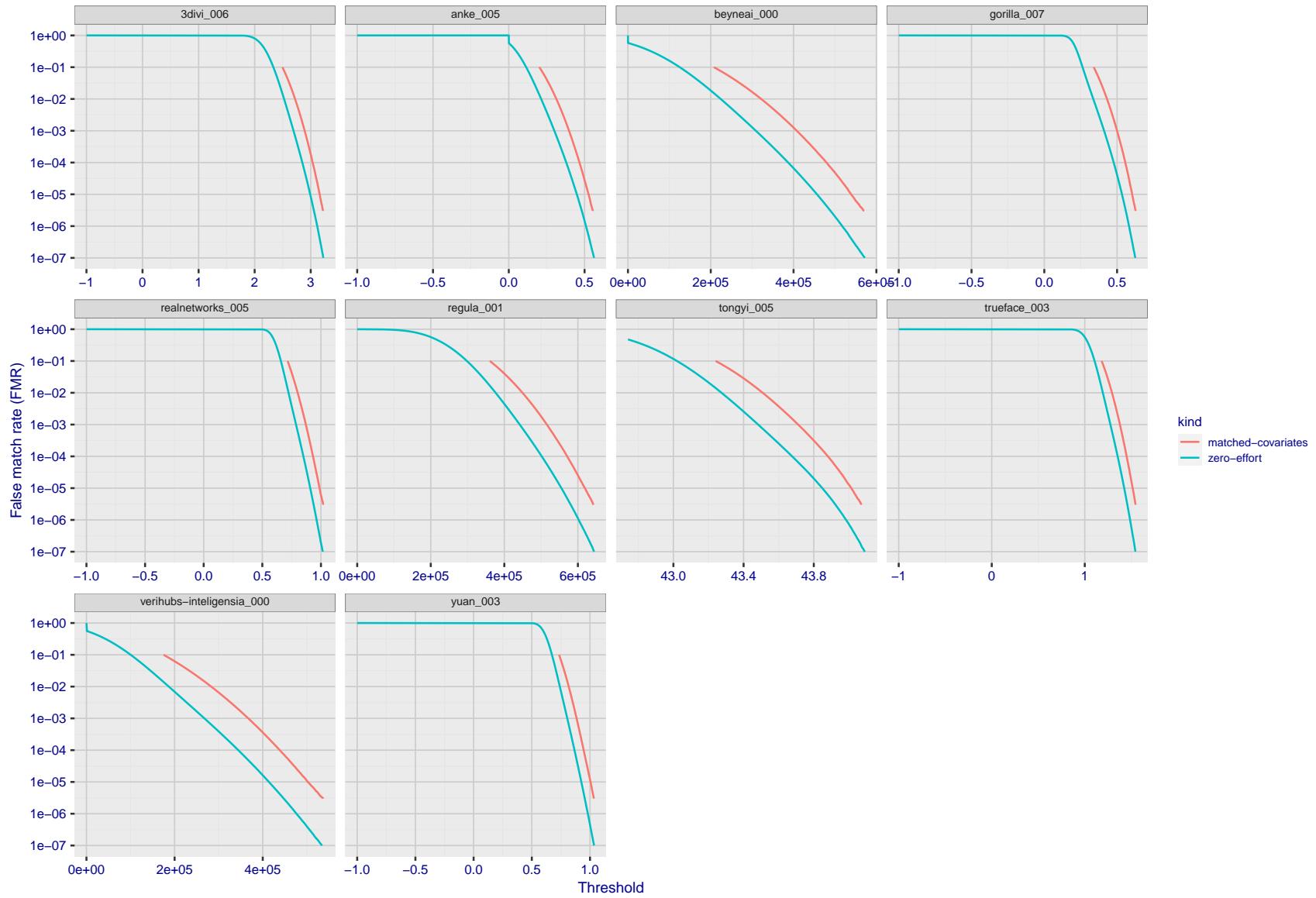


Figure 206: For the visa images, the false match calibration curves show FMR vs. threshold, T . The blue (lower) curves are for zero-effort impostors (i.e. comparing all images against all). The red (upper) curves are for persons of the same-sex, same-age, and same national-origin. This shows that FMR is underestimated (by a factor of 10 or more) by using a zero-effort impostor calculation to calibrate T . As shown later (sec. 3.6), FMR is higher for demographic-matched impostors.

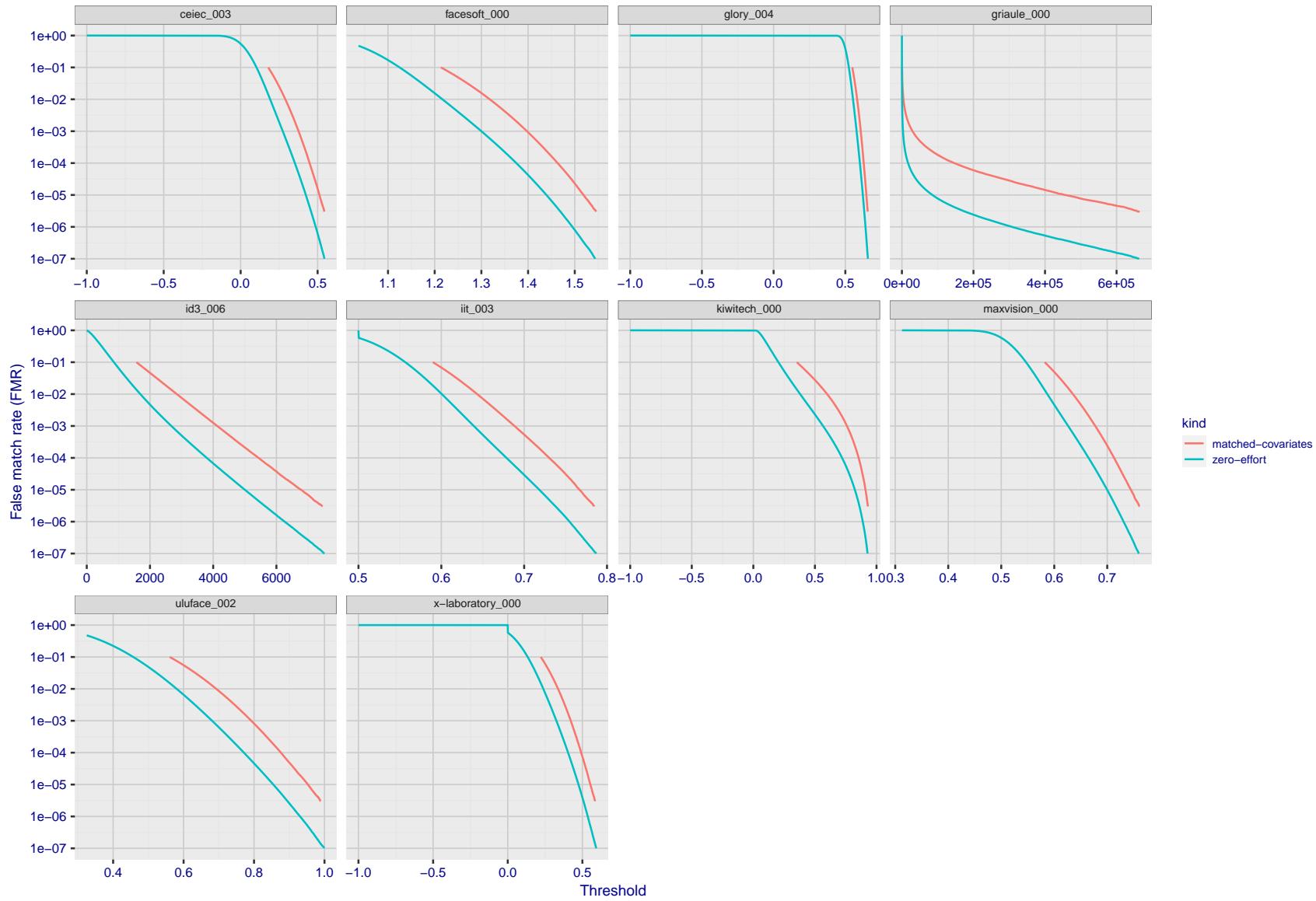


Figure 207: For the visa images, the false match calibration curves show FMR vs. threshold, T . The blue (lower) curves are for zero-effort impostors (i.e. comparing all images against all). The red (upper) curves are for persons of the same-sex, same-age, and same national-origin. This shows that FMR is underestimated (by a factor of 10 or more) by using a zero-effort impostor calculation to calibrate T . As shown later (sec. 3.6), FMR is higher for demographic-matched impostors.

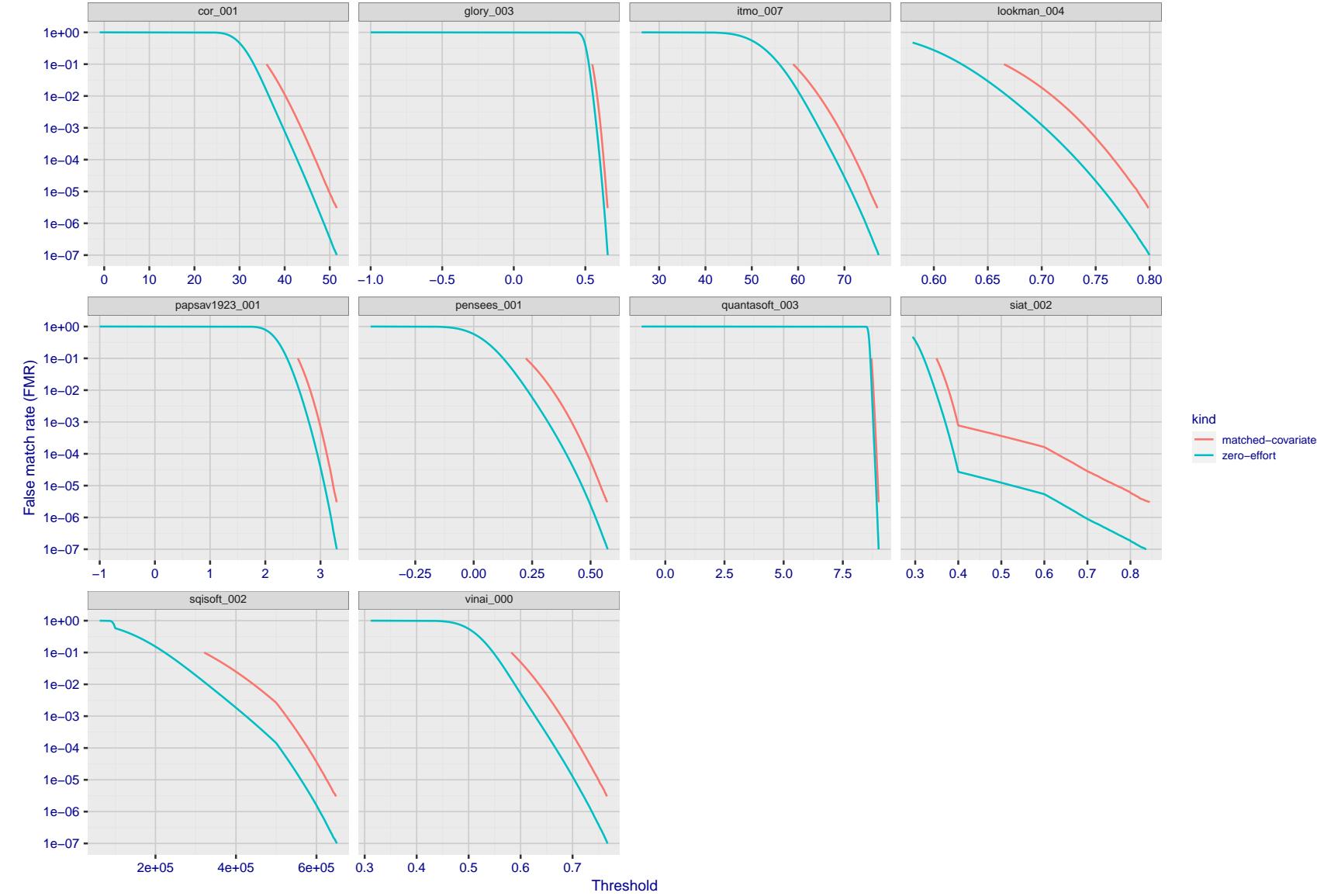


Figure 208: For the visa images, the false match calibration curves show FMR vs. threshold, T . The blue (lower) curves are for zero-effort impostors (i.e. comparing all images against all). The red (upper) curves are for persons of the same-sex, same-age, and same national-origin. This shows that FMR is underestimated (by a factor of 10 or more) by using a zero-effort impostor calculation to calibrate T . As shown later (sec. 3.6), FMR is higher for demographic-matched impostors.

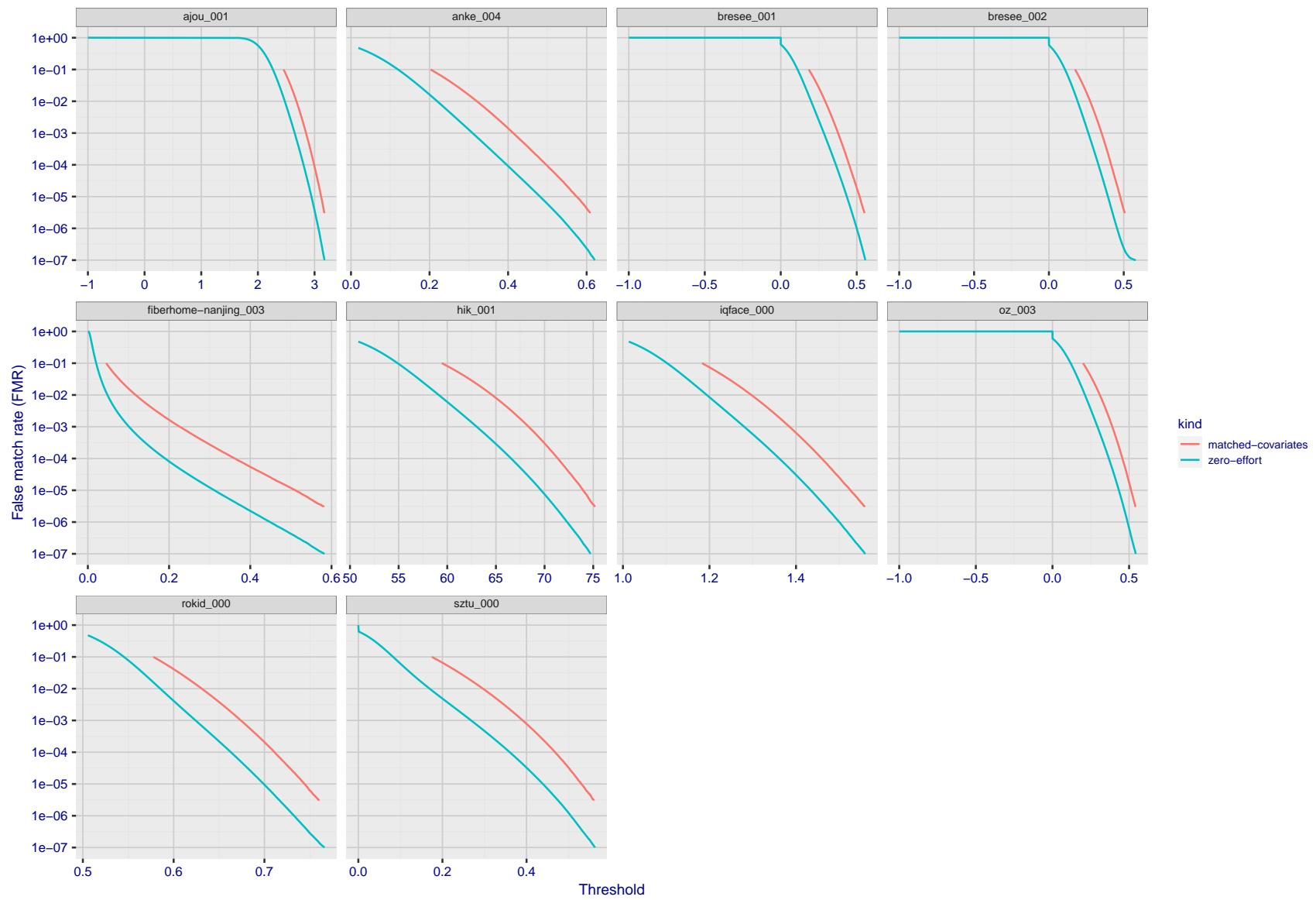


Figure 209: For the visa images, the false match calibration curves show FMR vs. threshold, T . The blue (lower) curves are for zero-effort impostors (i.e. comparing all images against all). The red (upper) curves are for persons of the same-sex, same-age, and same national-origin. This shows that FMR is underestimated (by a factor of 10 or more) by using a zero-effort impostor calculation to calibrate T . As shown later (sec. 3.6), FMR is higher for demographic-matched impostors.

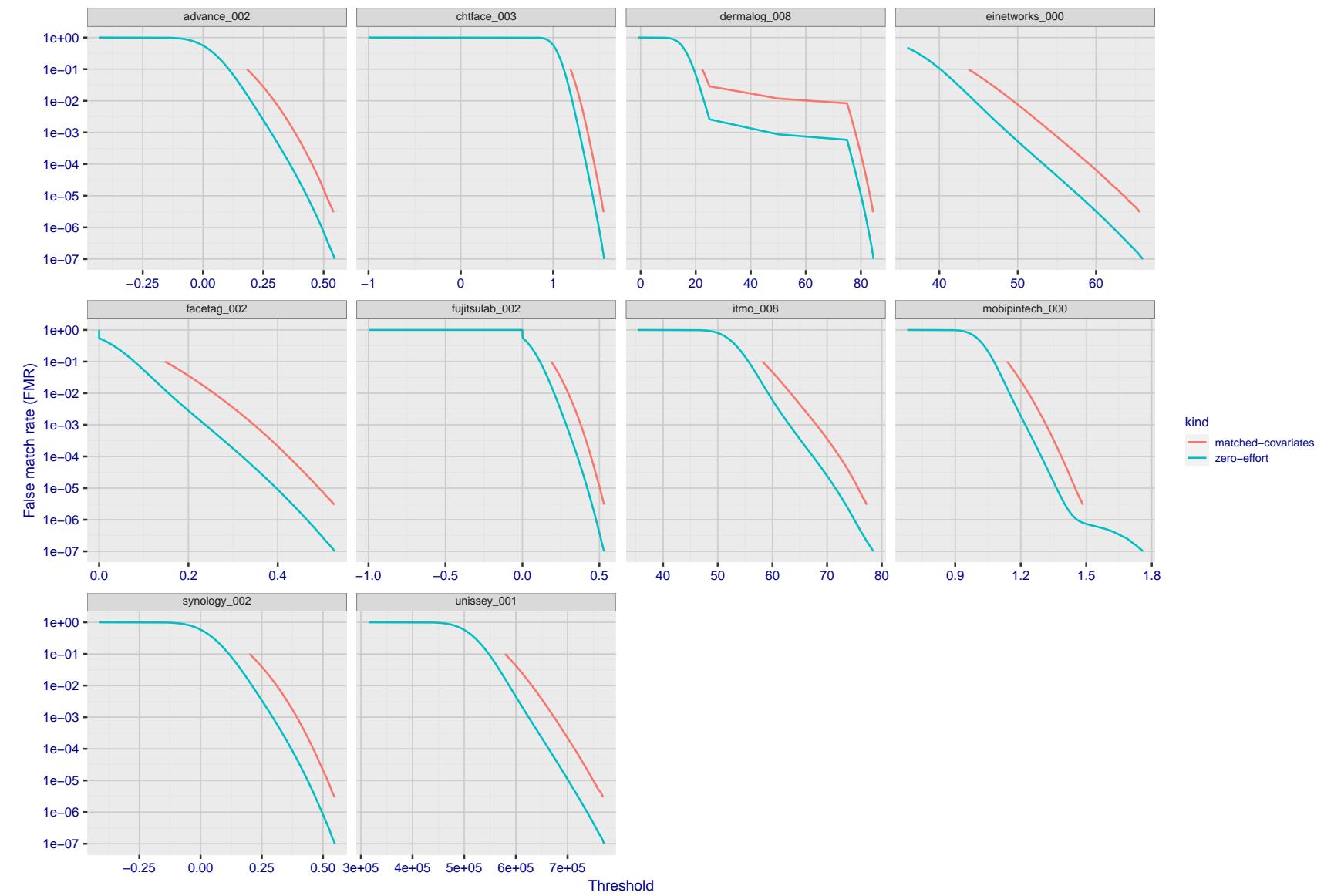


Figure 210: For the visa images, the false match calibration curves show FMR vs. threshold, T . The blue (lower) curves are for zero-effort impostors (i.e. comparing all images against all). The red (upper) curves are for persons of the same-sex, same-age, and same national-origin. This shows that FMR is underestimated (by a factor of 10 or more) by using a zero-effort impostor calculation to calibrate T . As shown later (sec. 3.6), FMR is higher for demographic-matched impostors.

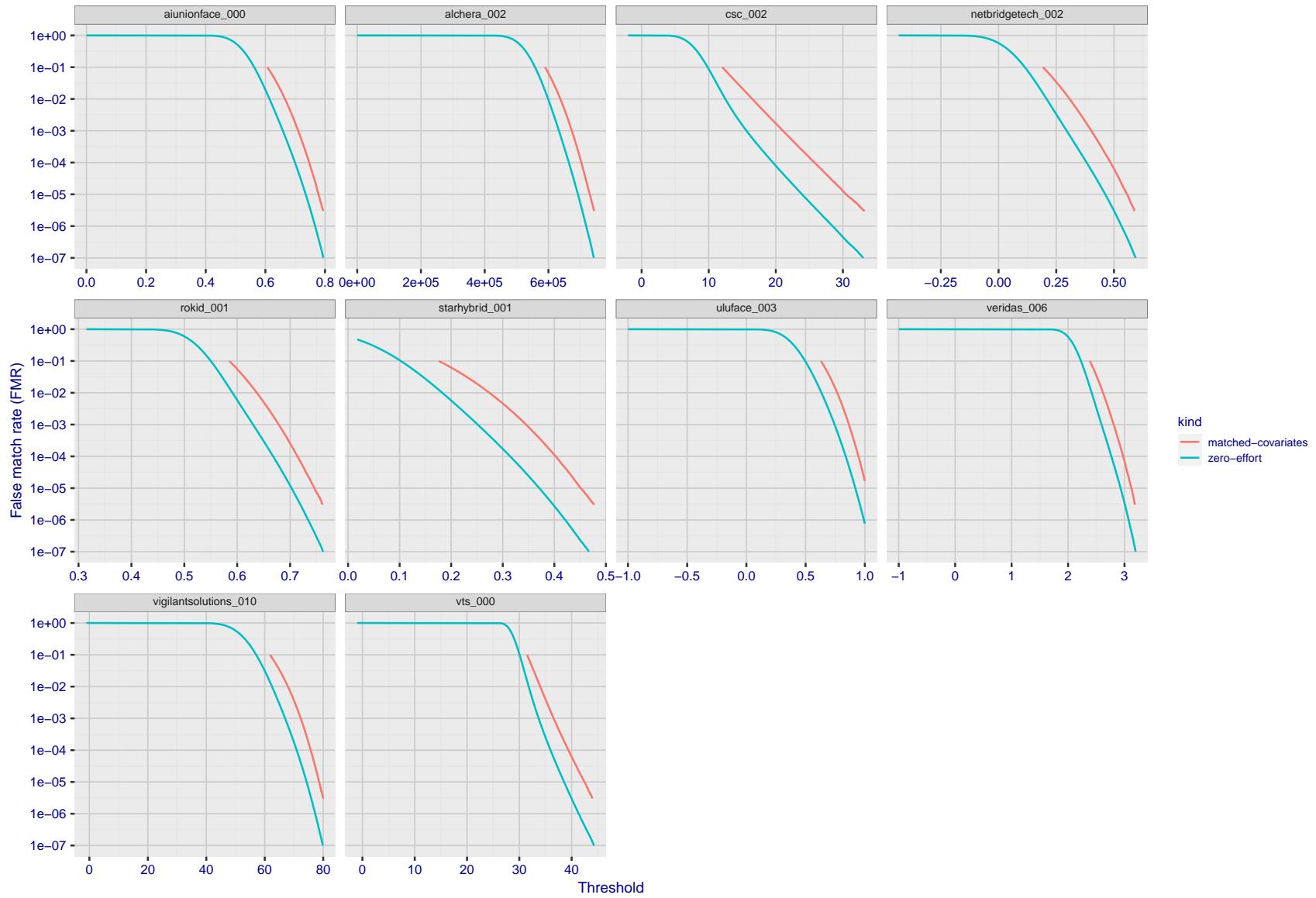


Figure 211: For the visa images, the false match calibration curves show FMR vs. threshold, T . The blue (lower) curves are for zero-effort impostors (i.e. comparing all images against all). The red (upper) curves are for persons of the same-sex, same-age, and same national-origin. This shows that FMR is underestimated (by a factor of 10 or more) by using a zero-effort impostor calculation to calibrate T . As shown later (sec. 3.6), FMR is higher for demographic-matched impostors.

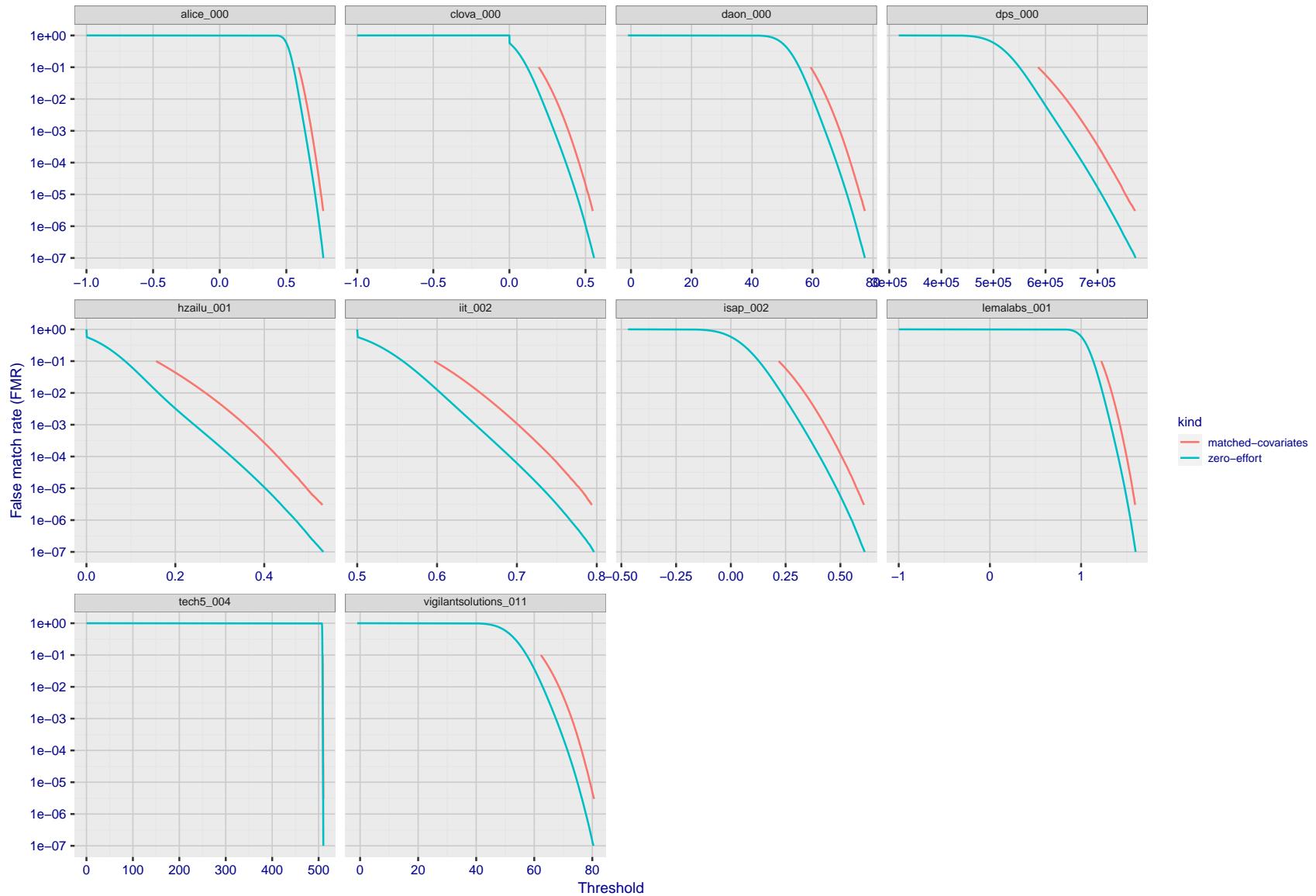


Figure 212: For the visa images, the false match calibration curves show FMR vs. threshold, T . The blue (lower) curves are for zero-effort impostors (i.e. comparing all images against all). The red (upper) curves are for persons of the same-sex, same-age, and same national-origin. This shows that FMR is underestimated (by a factor of 10 or more) by using a zero-effort impostor calculation to calibrate T . As shown later (sec. 3.6), FMR is higher for demographic-matched impostors.

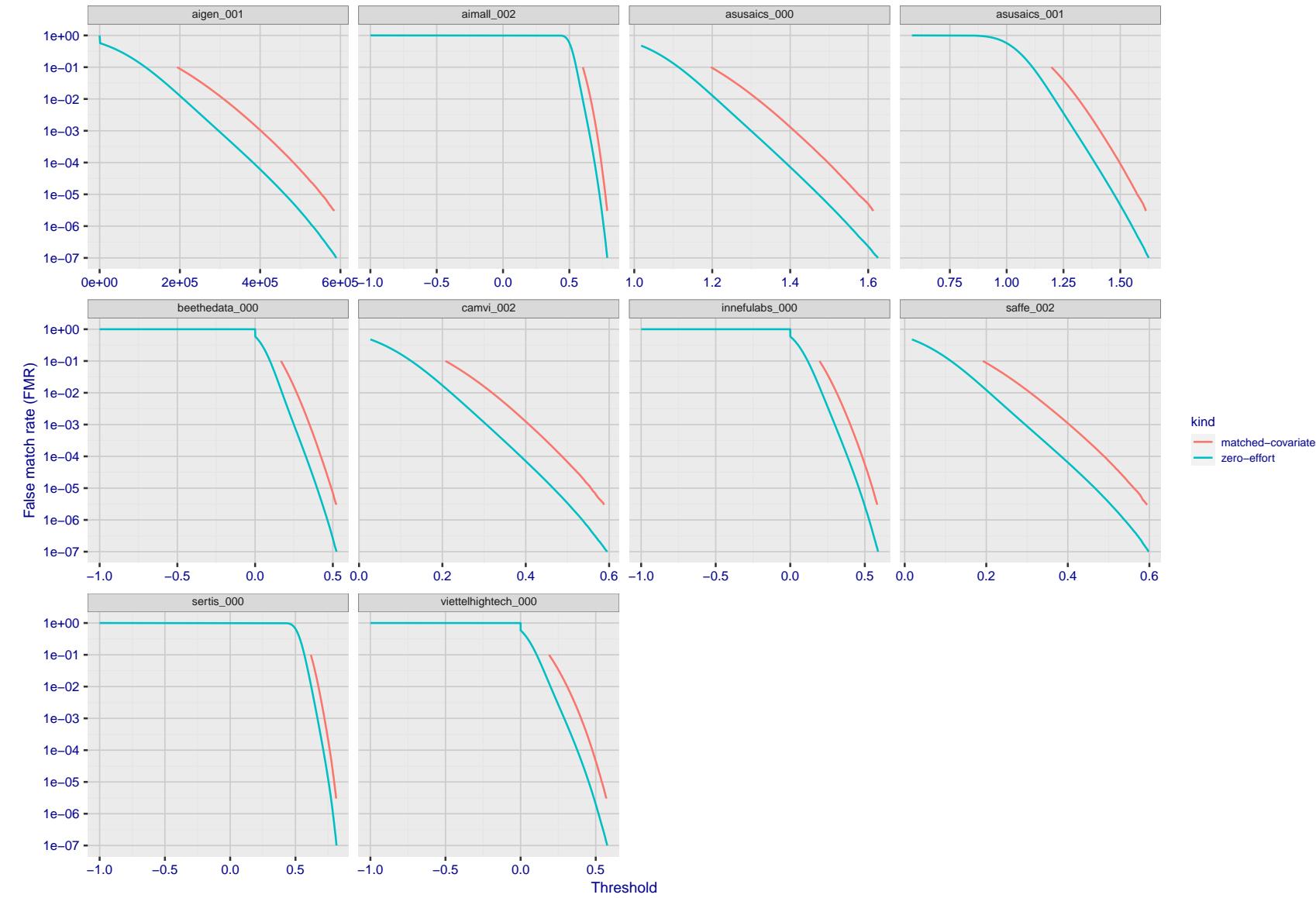


Figure 213: For the visa images, the false match calibration curves show FMR vs. threshold, T . The blue (lower) curves are for zero-effort impostors (i.e. comparing all images against all). The red (upper) curves are for persons of the same-sex, same-age, and same national-origin. This shows that FMR is underestimated (by a factor of 10 or more) by using a zero-effort impostor calculation to calibrate T . As shown later (sec. 3.6), FMR is higher for demographic-matched impostors.

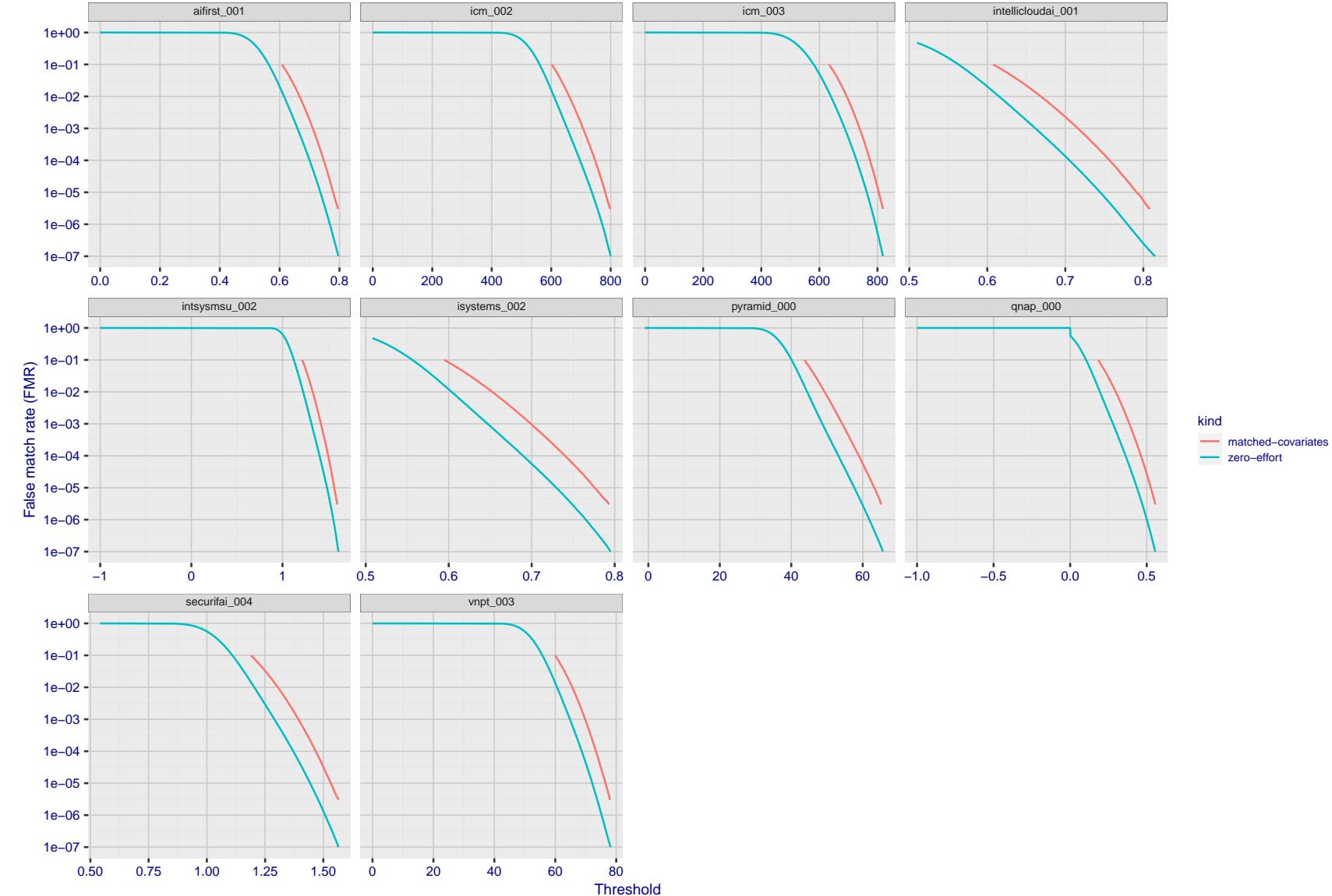


Figure 214: For the visa images, the false match calibration curves show FMR vs. threshold, T . The blue (lower) curves are for zero-effort impostors (i.e. comparing all images against all). The red (upper) curves are for persons of the same-sex, same-age, and same national-origin. This shows that FMR is underestimated (by a factor of 10 or more) by using a zero-effort impostor calculation to calibrate T . As shown later (sec. 3.6), FMR is higher for demographic-matched impostors.

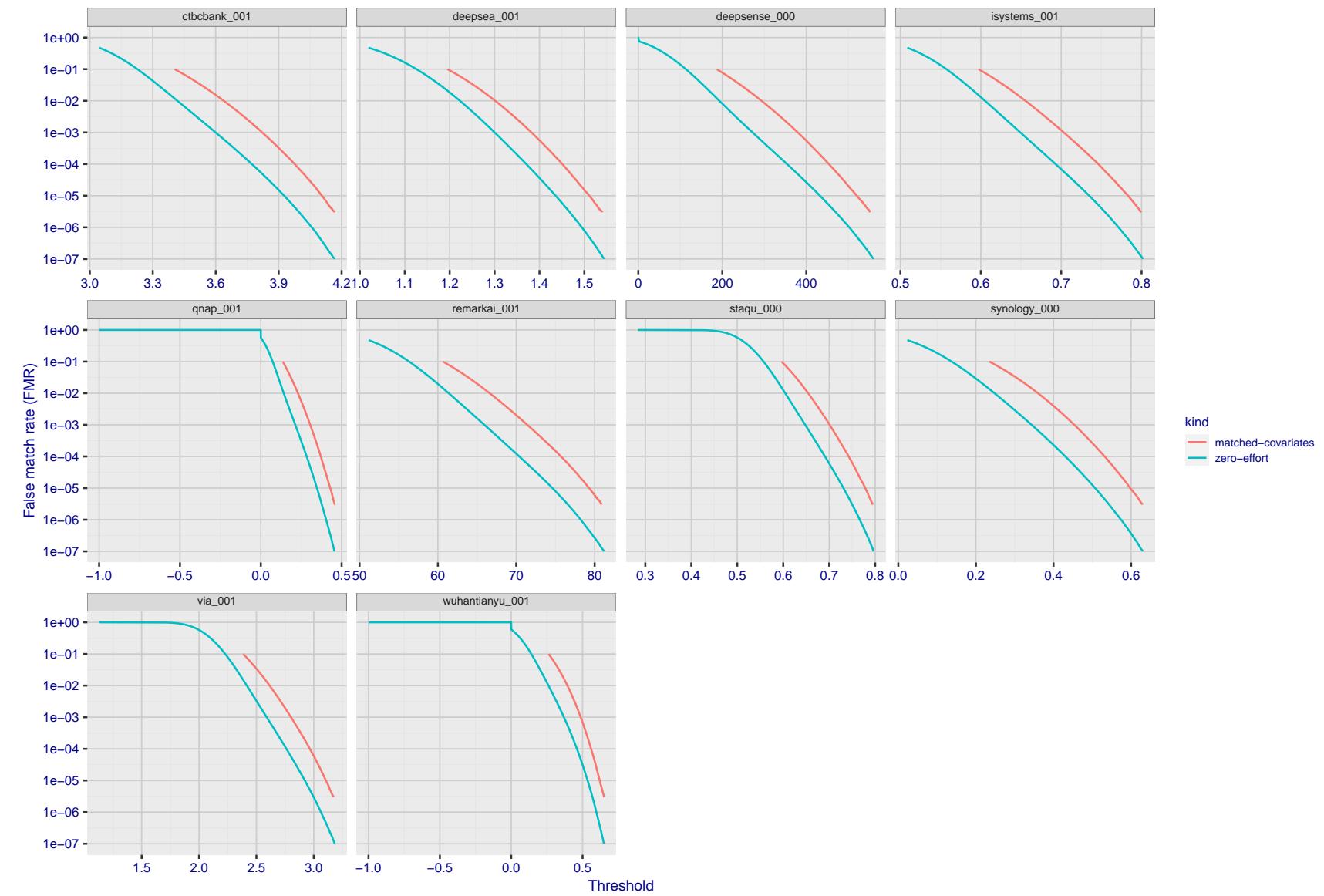


Figure 215: For the visa images, the false match calibration curves show FMR vs. threshold, T . The blue (lower) curves are for zero-effort impostors (i.e. comparing all images against all). The red (upper) curves are for persons of the same-sex, same-age, and same national-origin. This shows that FMR is underestimated (by a factor of 10 or more) by using a zero-effort impostor calculation to calibrate T . As shown later (sec. 3.6), FMR is higher for demographic-matched impostors.

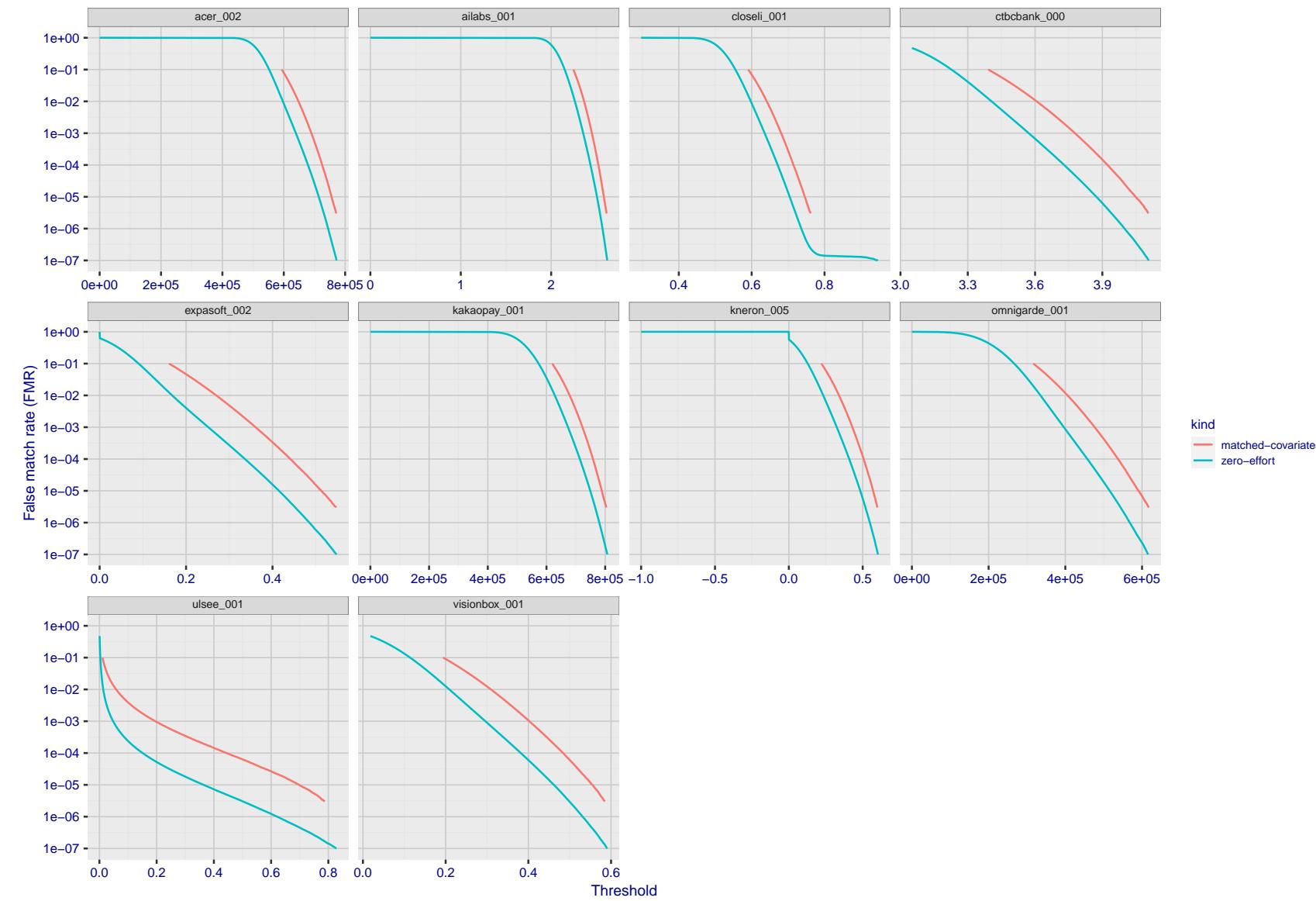


Figure 216: For the visa images, the false match calibration curves show FMR vs. threshold, T . The blue (lower) curves are for zero-effort impostors (i.e. comparing all images against all). The red (upper) curves are for persons of the same-sex, same-age, and same national-origin. This shows that FMR is underestimated (by a factor of 10 or more) by using a zero-effort impostor calculation to calibrate T . As shown later (sec. 3.6), FMR is higher for demographic-matched impostors.

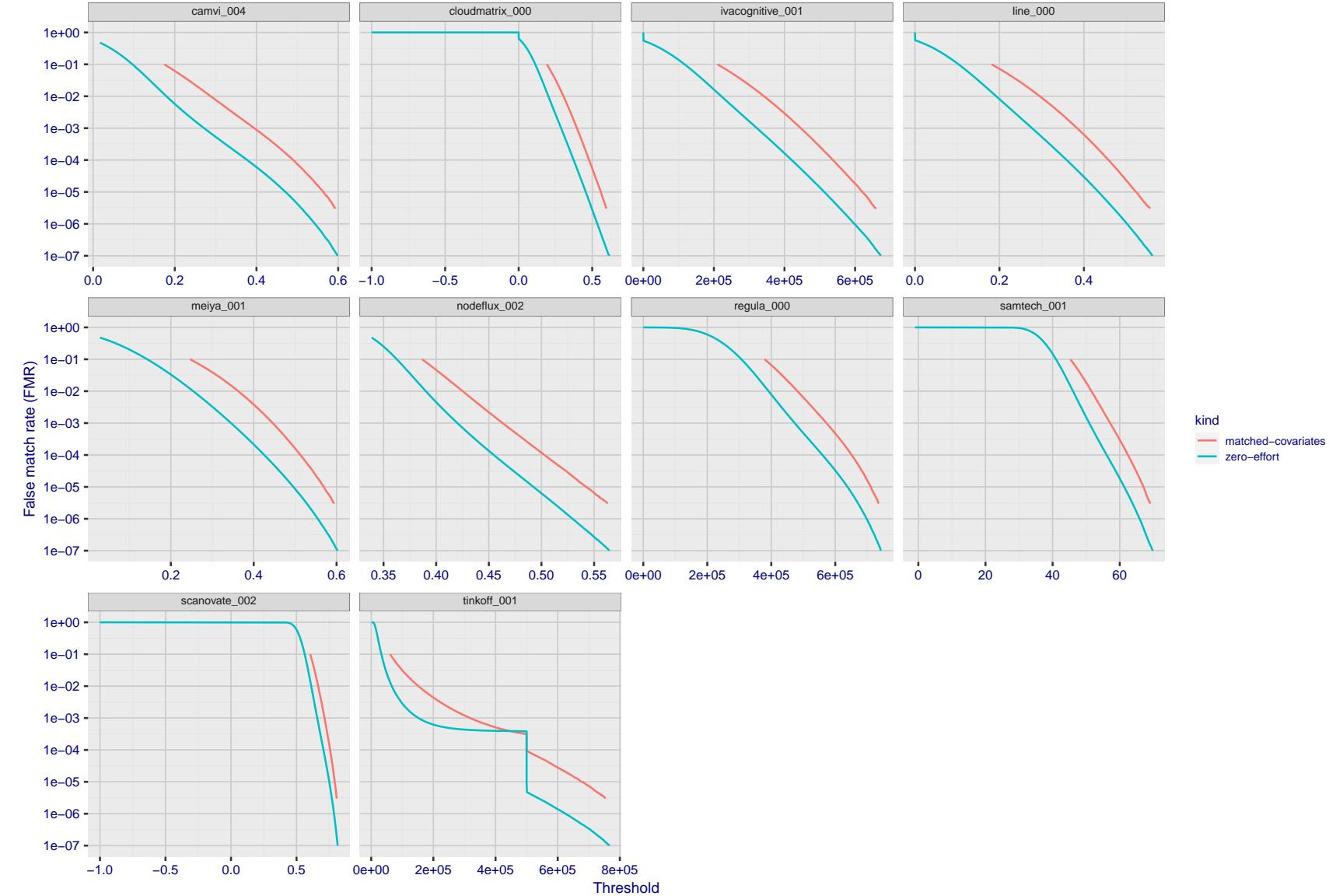


Figure 217: For the visa images, the false match calibration curves show FMR vs. threshold, T . The blue (lower) curves are for zero-effort impostors (i.e. comparing all images against all). The red (upper) curves are for persons of the same-sex, same-age, and same national-origin. This shows that FMR is underestimated (by a factor of 10 or more) by using a zero-effort impostor calculation to calibrate T . As shown later (sec. 3.6), FMR is higher for demographic-matched impostors.

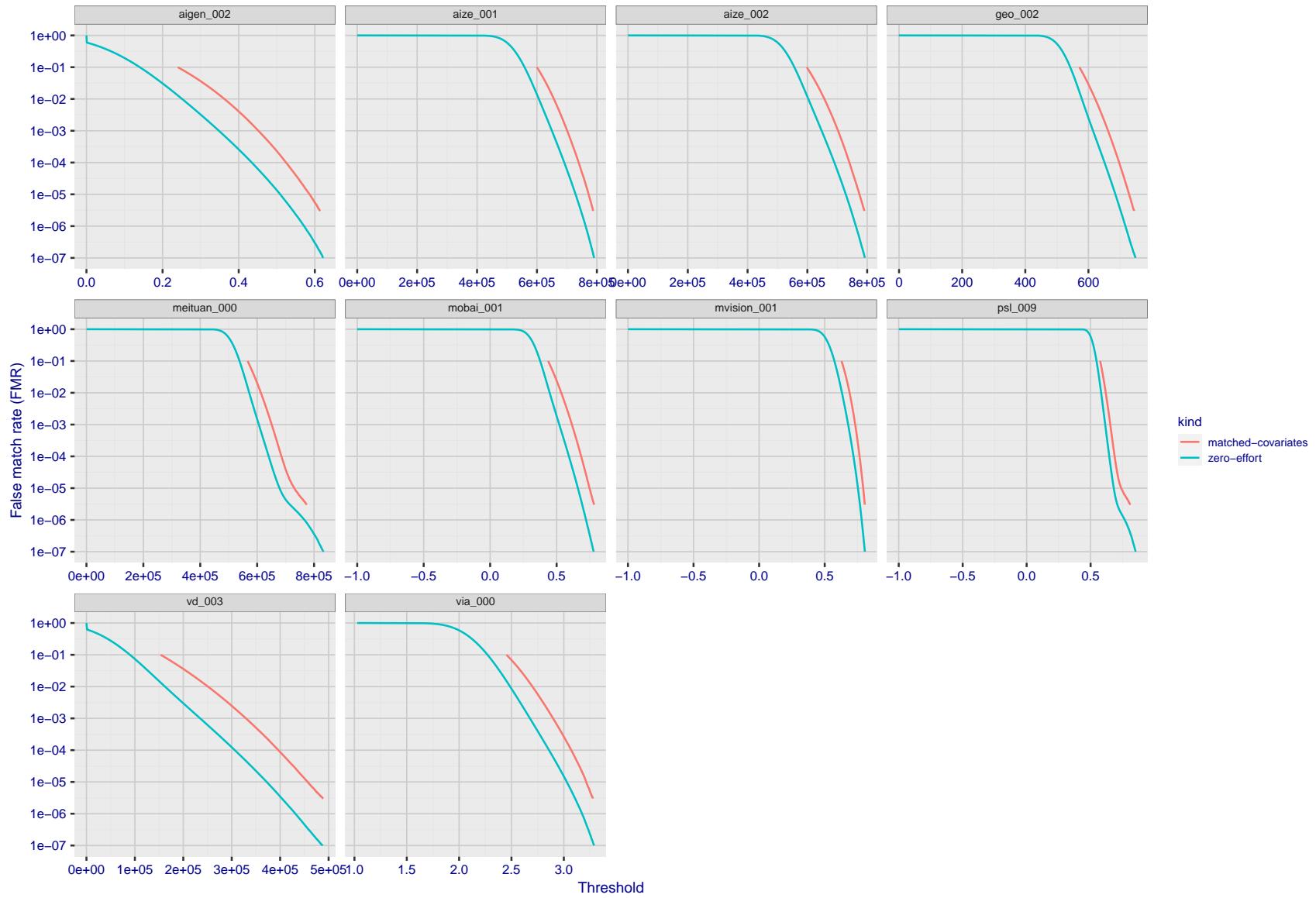


Figure 218: For the visa images, the false match calibration curves show FMR vs. threshold, T . The blue (lower) curves are for zero-effort impostors (i.e. comparing all images against all). The red (upper) curves are for persons of the same-sex, same-age, and same national-origin. This shows that FMR is underestimated (by a factor of 10 or more) by using a zero-effort impostor calculation to calibrate T . As shown later (sec. 3.6), FMR is higher for demographic-matched impostors.

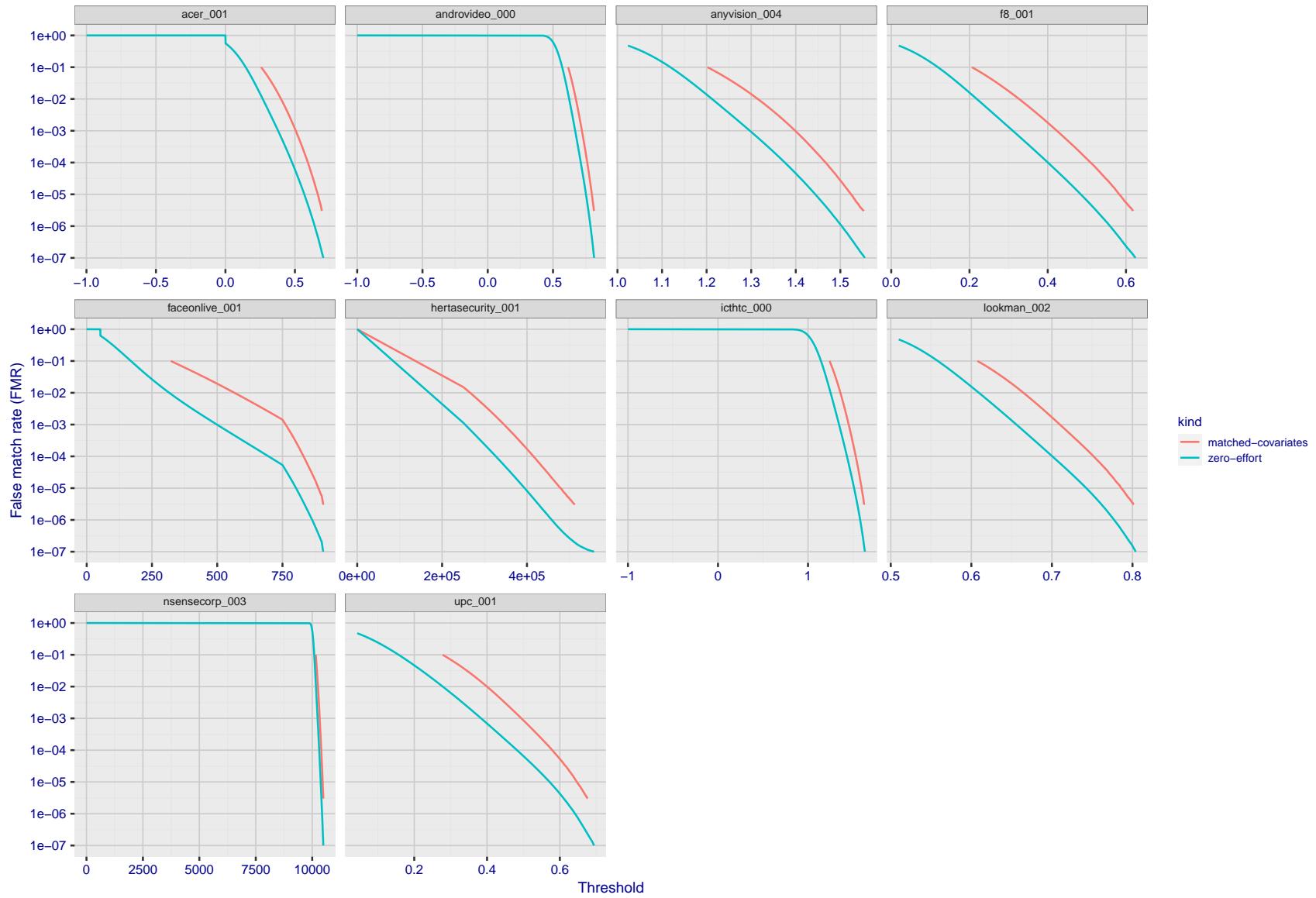


Figure 219: For the visa images, the false match calibration curves show FMR vs. threshold, T . The blue (lower) curves are for zero-effort impostors (i.e. comparing all images against all). The red (upper) curves are for persons of the same-sex, same-age, and same national-origin. This shows that FMR is underestimated (by a factor of 10 or more) by using a zero-effort impostor calculation to calibrate T . As shown later (sec. 3.6), FMR is higher for demographic-matched impostors.

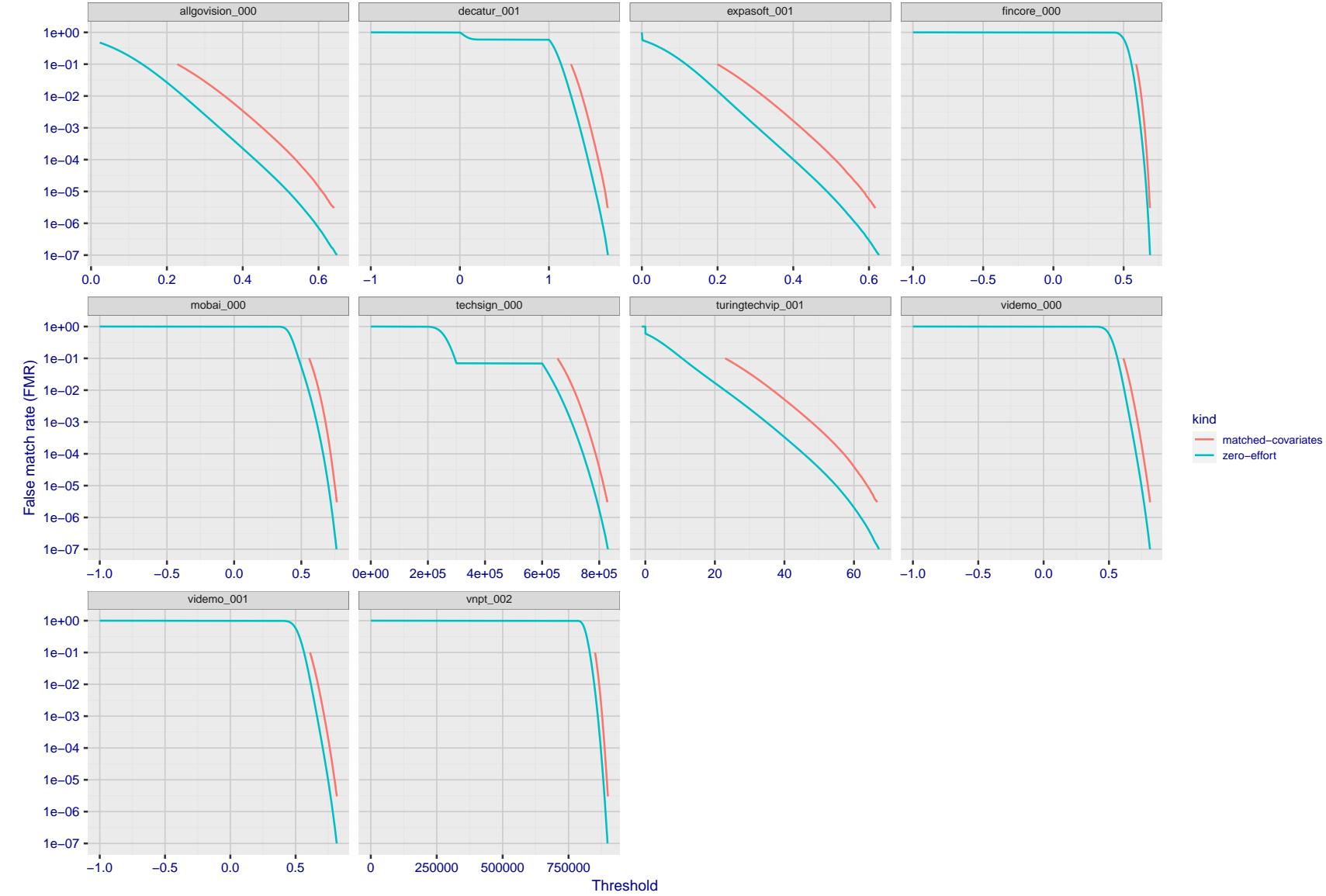


Figure 220: For the visa images, the false match calibration curves show FMR vs. threshold, T . The blue (lower) curves are for zero-effort impostors (i.e. comparing all images against all). The red (upper) curves are for persons of the same-sex, same-age, and same national-origin. This shows that FMR is underestimated (by a factor of 10 or more) by using a zero-effort impostor calculation to calibrate T . As shown later (sec. 3.6), FMR is higher for demographic-matched impostors.

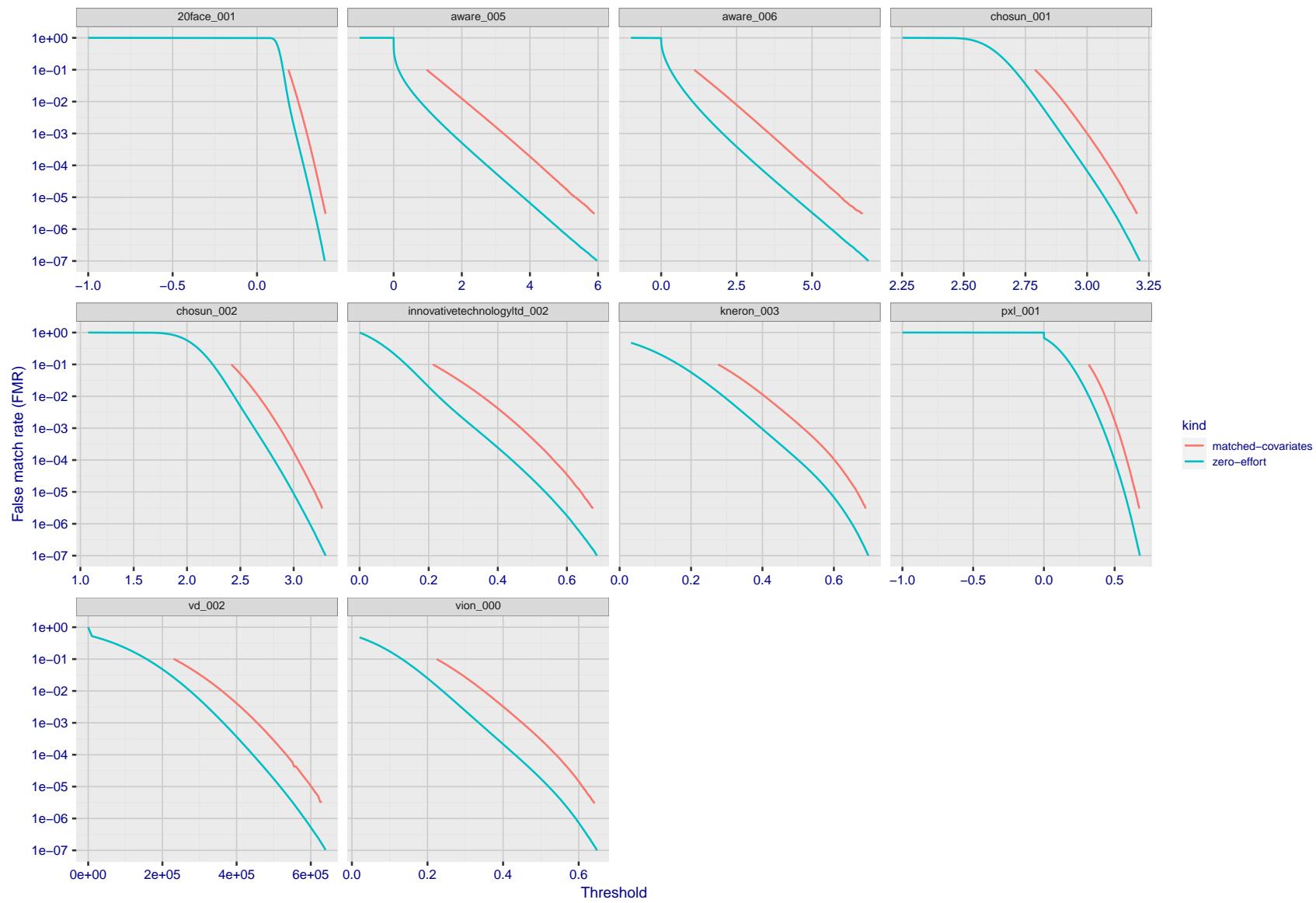


Figure 221: For the visa images, the false match calibration curves show FMR vs. threshold, T . The blue (lower) curves are for zero-effort impostors (i.e. comparing all images against all). The red (upper) curves are for persons of the same-sex, same-age, and same national-origin. This shows that FMR is underestimated (by a factor of 10 or more) by using a zero-effort impostor calculation to calibrate T . As shown later (sec. 3.6), FMR is higher for demographic-matched impostors.

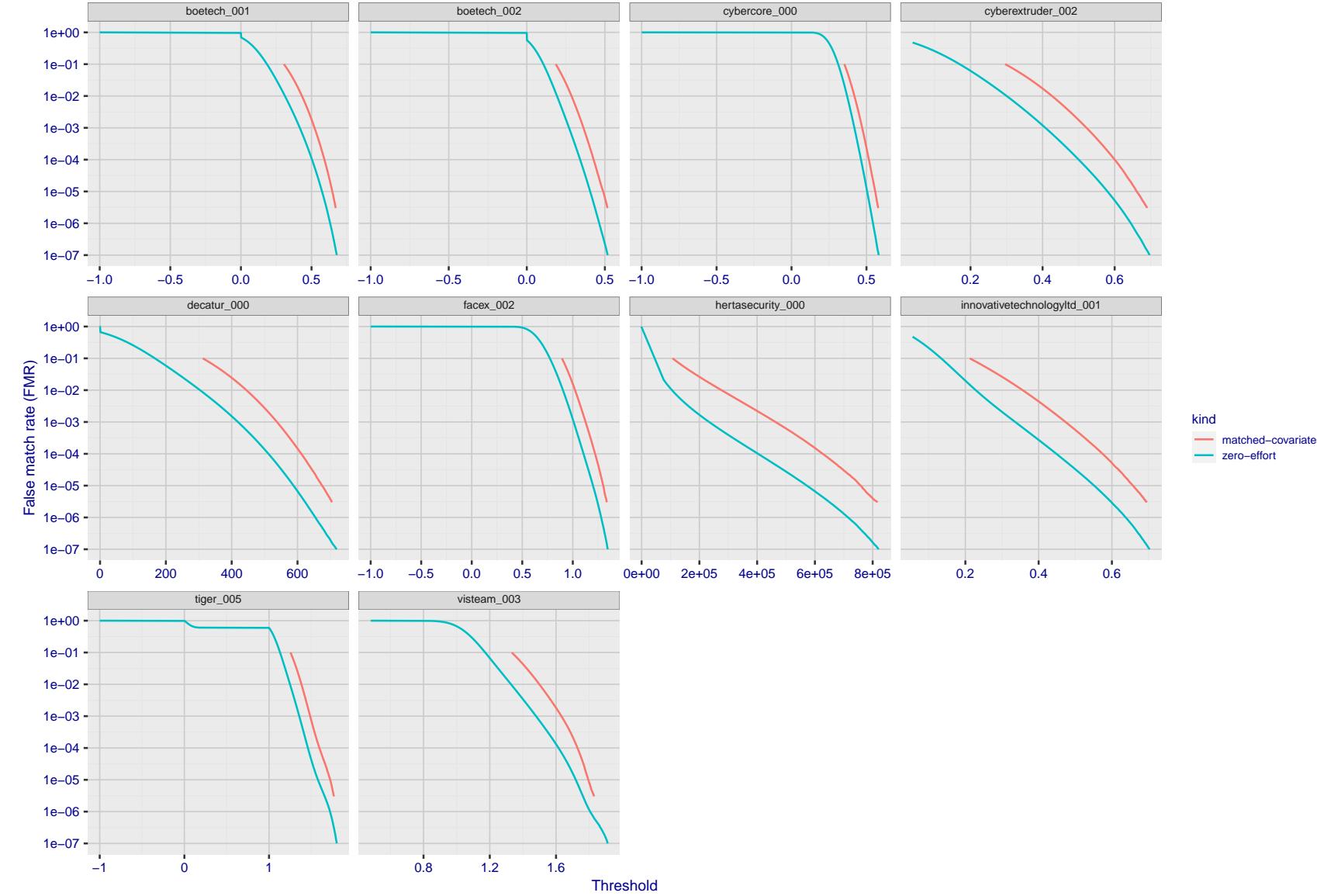


Figure 222: For the visa images, the false match calibration curves show FMR vs. threshold, T . The blue (lower) curves are for zero-effort impostors (i.e. comparing all images against all). The red (upper) curves are for persons of the same-sex, same-age, and same national-origin. This shows that FMR is underestimated (by a factor of 10 or more) by using a zero-effort impostor calculation to calibrate T . As shown later (sec. 3.6), FMR is higher for demographic-matched impostors.

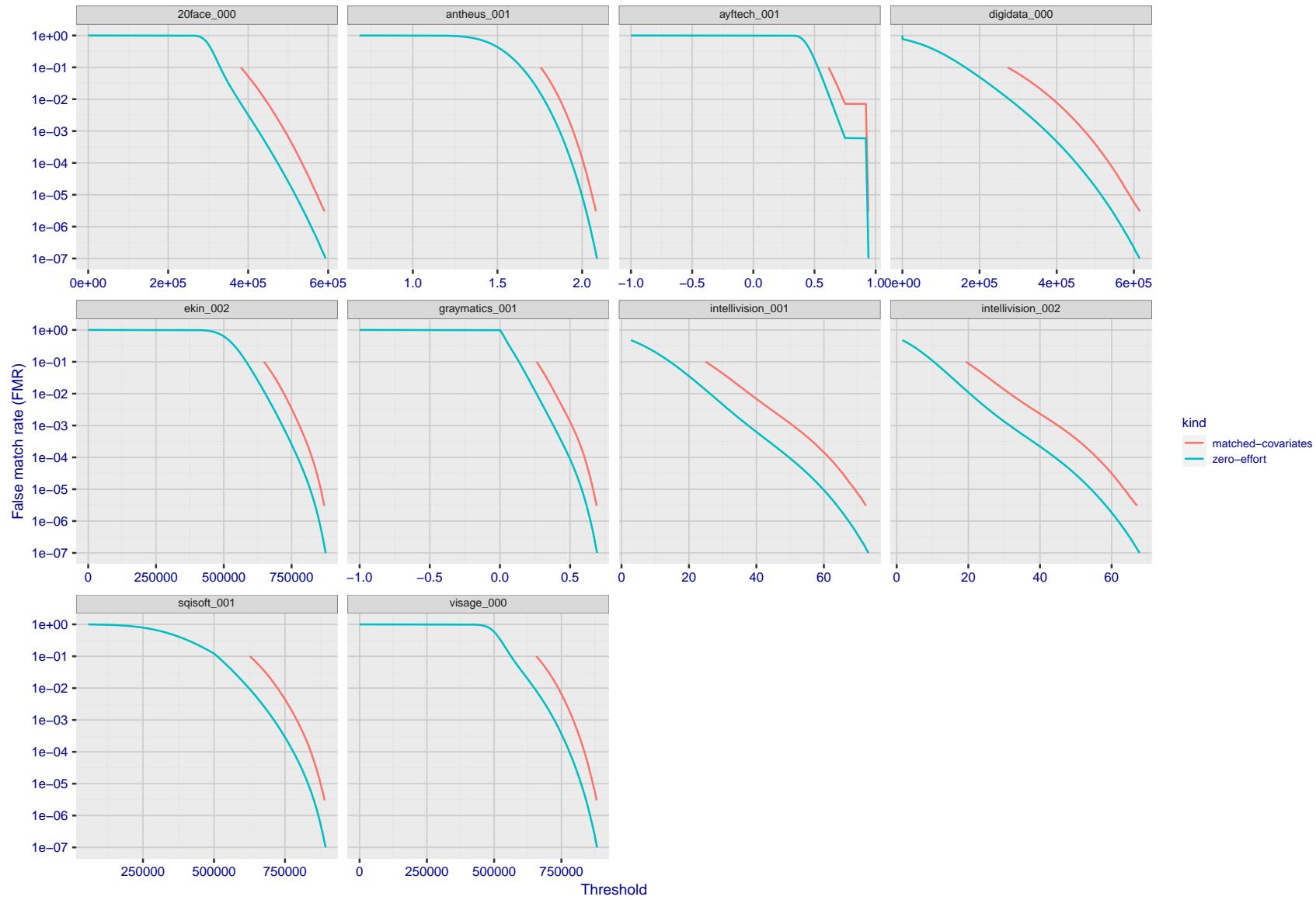


Figure 223: For the visa images, the false match calibration curves show FMR vs. threshold, T . The blue (lower) curves are for zero-effort impostors (i.e. comparing all images against all). The red (upper) curves are for persons of the same-sex, same-age, and same national-origin. This shows that FMR is underestimated (by a factor of 10 or more) by using a zero-effort impostor calculation to calibrate T . As shown later (sec. 3.6), FMR is higher for demographic-matched impostors.

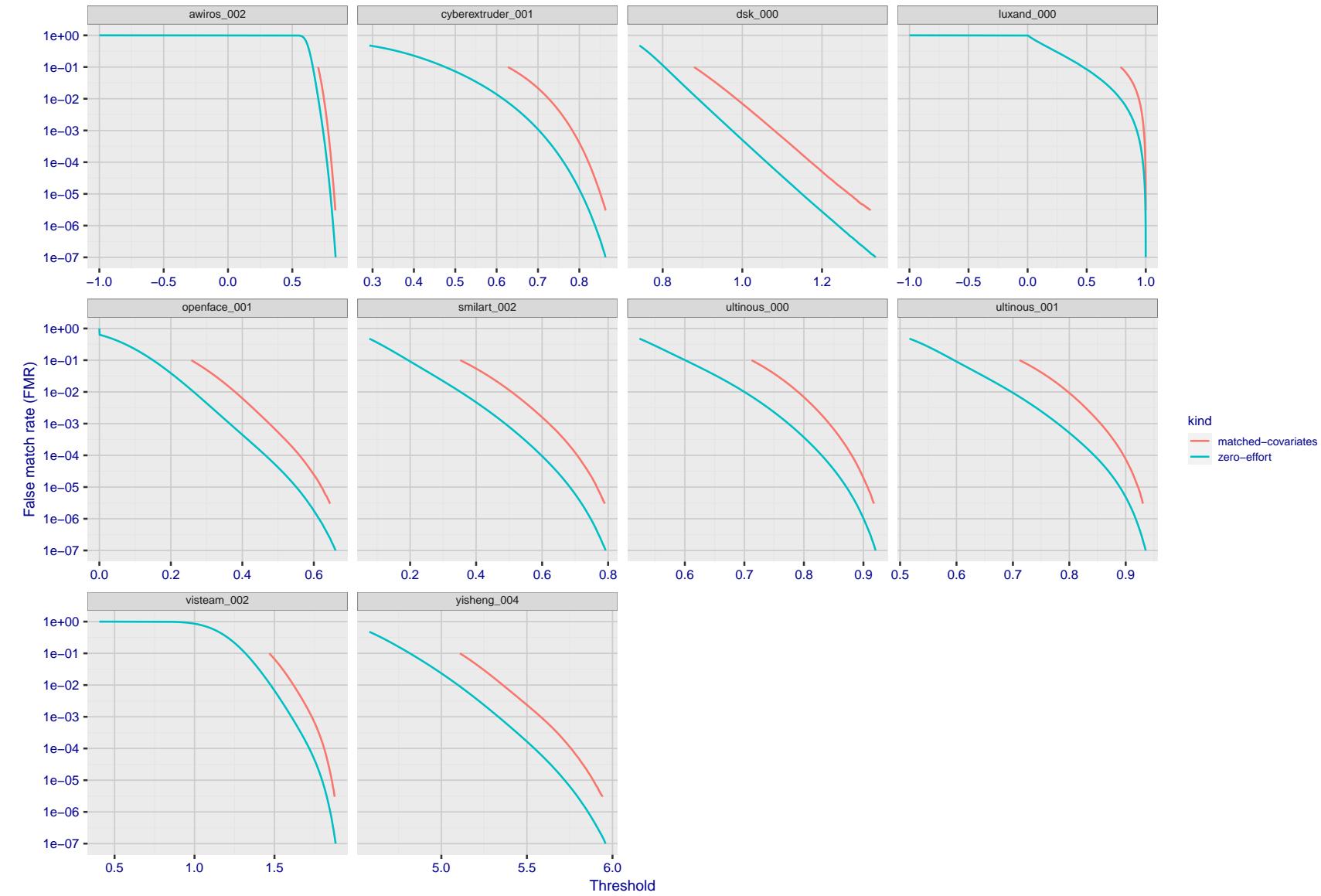


Figure 224: For the visa images, the false match calibration curves show FMR vs. threshold, T . The blue (lower) curves are for zero-effort impostors (i.e. comparing all images against all). The red (upper) curves are for persons of the same-sex, same-age, and same national-origin. This shows that FMR is underestimated (by a factor of 10 or more) by using a zero-effort impostor calculation to calibrate T . As shown later (sec. 3.6), FMR is higher for demographic-matched impostors.

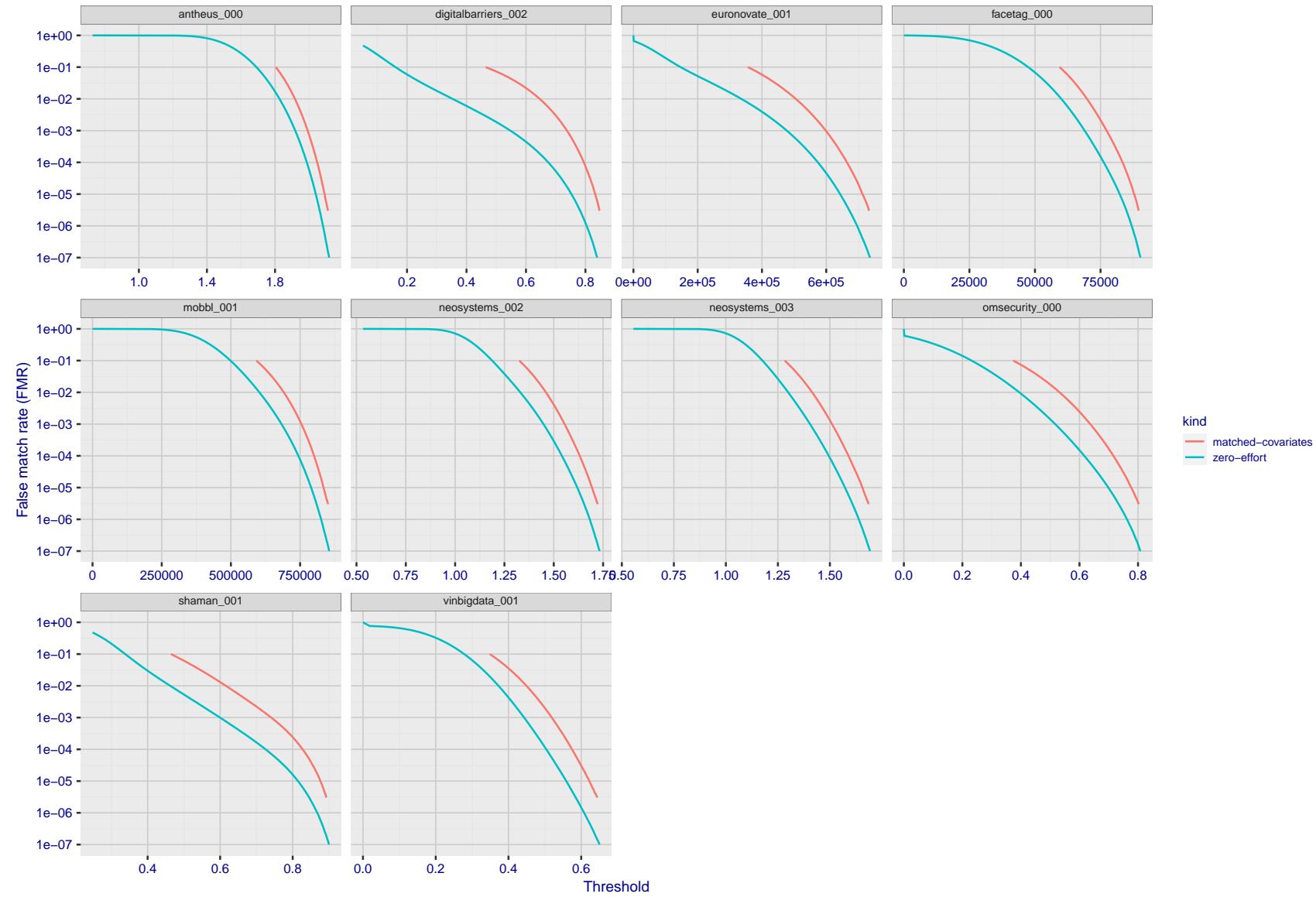


Figure 225: For the visa images, the false match calibration curves show FMR vs. threshold, T . The blue (lower) curves are for zero-effort impostors (i.e. comparing all images against all). The red (upper) curves are for persons of the same-sex, same-age, and same national-origin. This shows that FMR is underestimated (by a factor of 10 or more) by using a zero-effort impostor calculation to calibrate T . As shown later (sec. 3.6), FMR is higher for demographic-matched impostors.

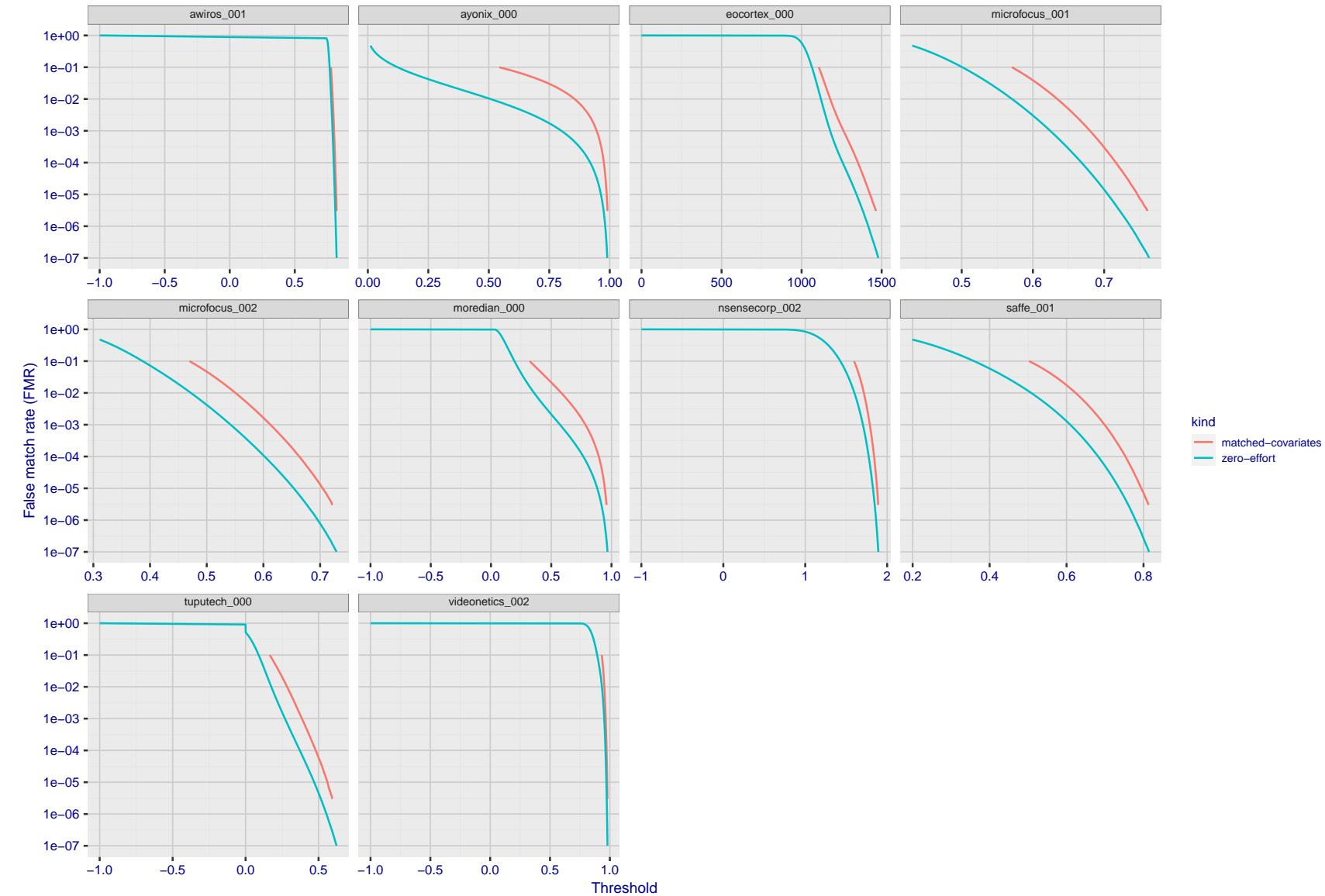


Figure 226: For the visa images, the false match calibration curves show FMR vs. threshold, T . The blue (lower) curves are for zero-effort impostors (i.e. comparing all images against all). The red (upper) curves are for persons of the same-sex, same-age, and same national-origin. This shows that FMR is underestimated (by a factor of 10 or more) by using a zero-effort impostor calculation to calibrate T . As shown later (sec. 3.6), FMR is higher for demographic-matched impostors.

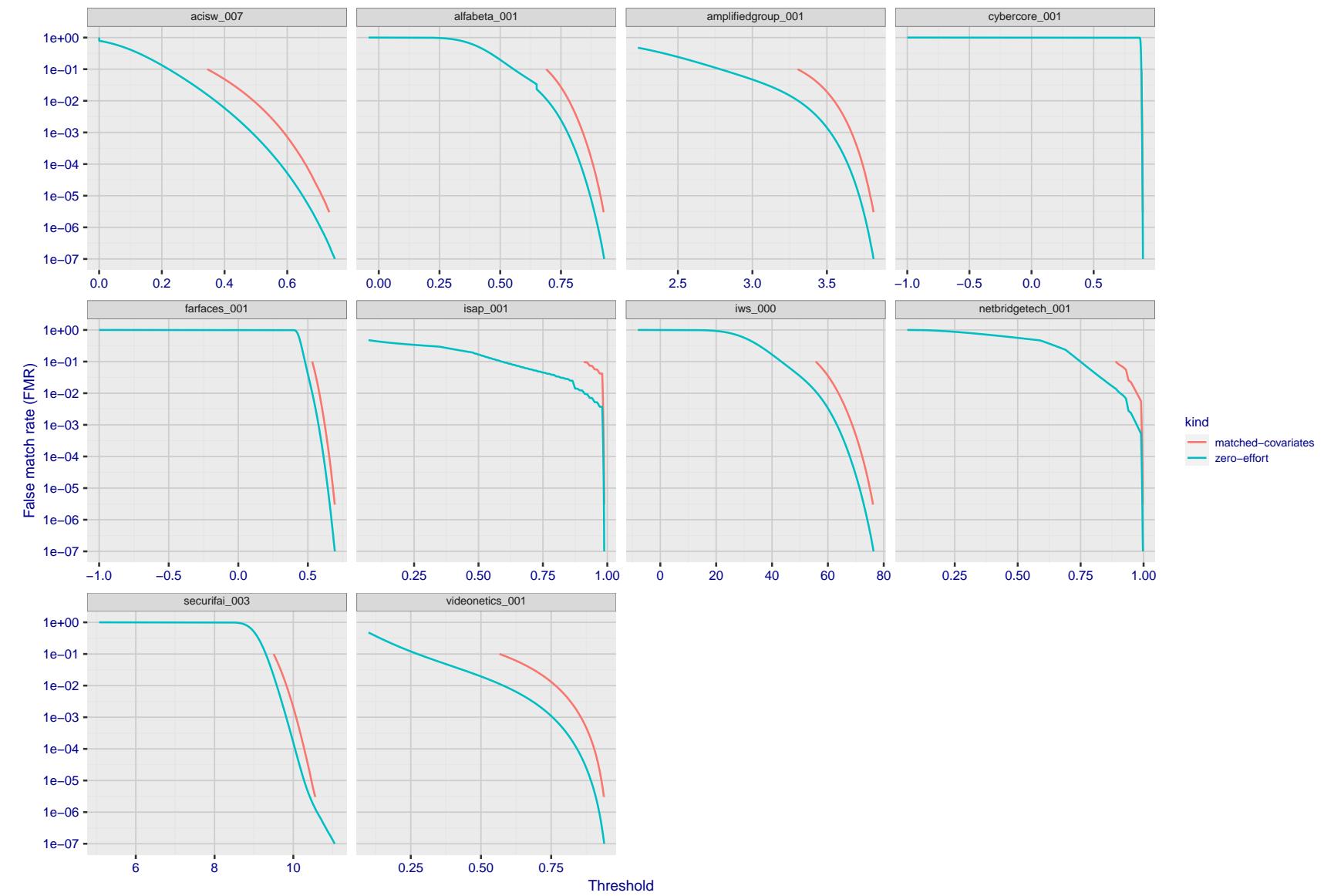


Figure 227: For the visa images, the false match calibration curves show FMR vs. threshold, T . The blue (lower) curves are for zero-effort impostors (i.e. comparing all images against all). The red (upper) curves are for persons of the same-sex, same-age, and same national-origin. This shows that FMR is underestimated (by a factor of 10 or more) by using a zero-effort impostor calculation to calibrate T . As shown later (sec. 3.6), FMR is higher for demographic-matched impostors.

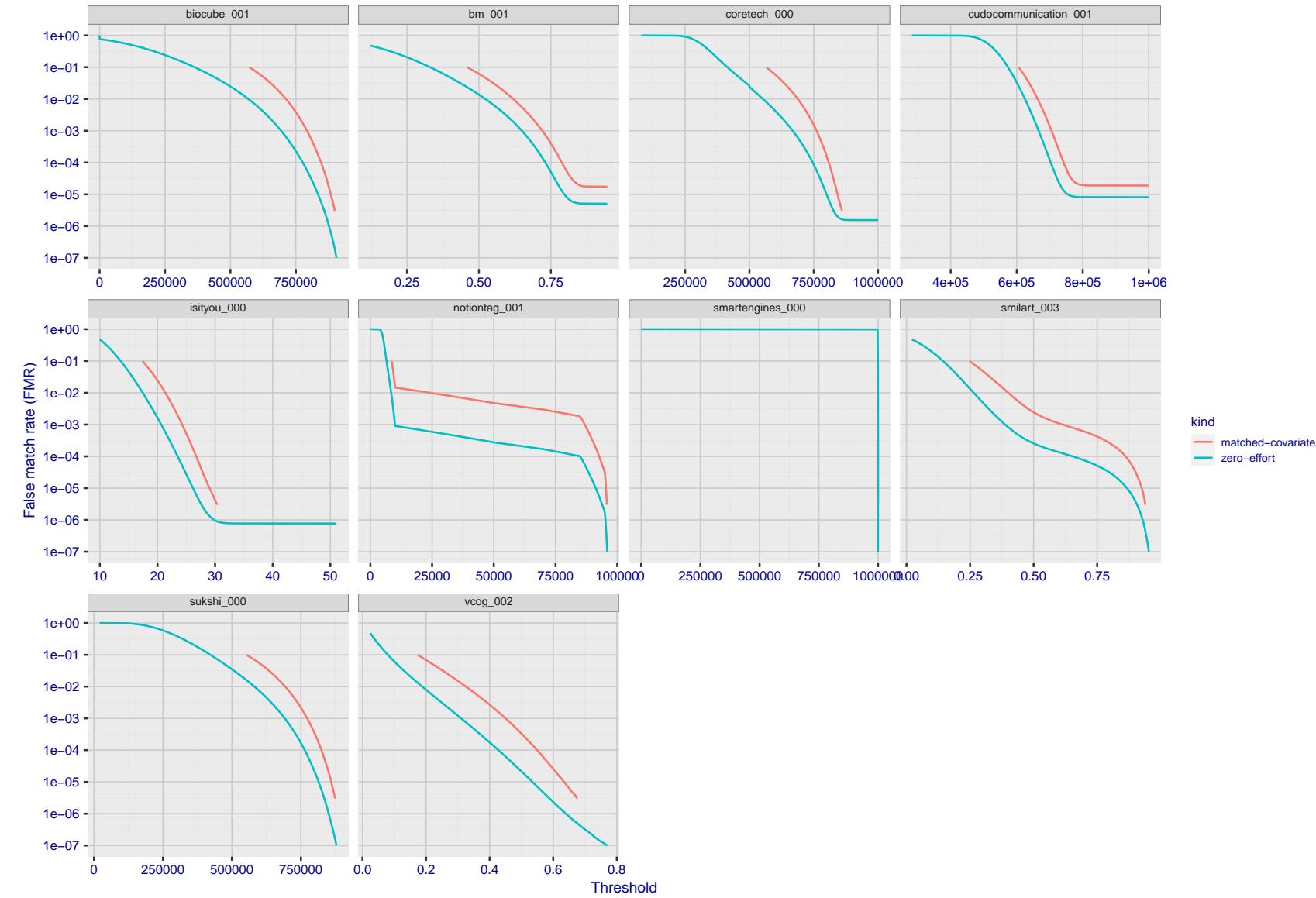


Figure 228: For the visa images, the false match calibration curves show FMR vs. threshold, T . The blue (lower) curves are for zero-effort impostors (i.e. comparing all images against all). The red (upper) curves are for persons of the same-sex, same-age, and same national-origin. This shows that FMR is underestimated (by a factor of 10 or more) by using a zero-effort impostor calculation to calibrate T . As shown later (sec. 3.6), FMR is higher for demographic-matched impostors.

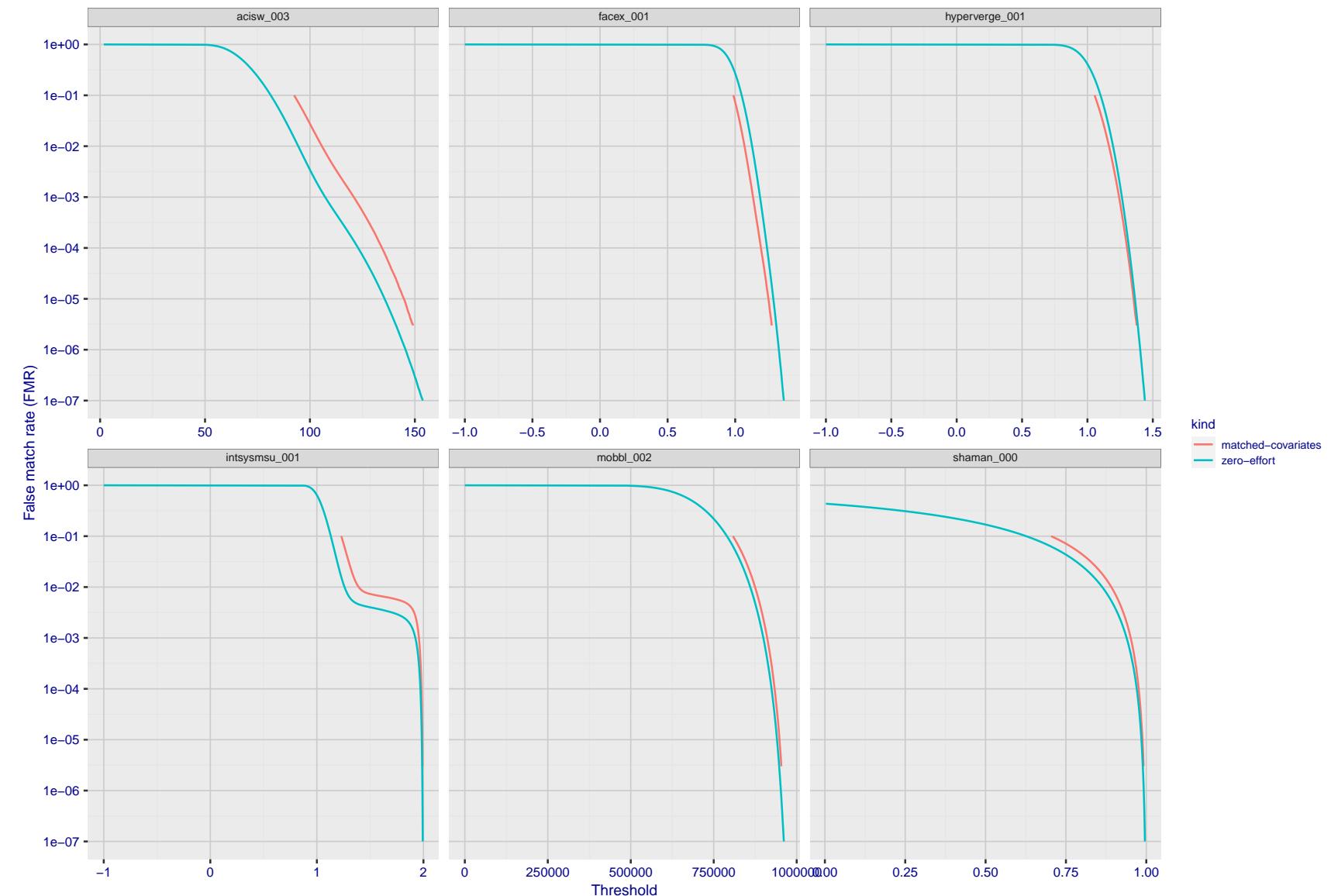


Figure 229: For the visa images, the false match calibration curves show FMR vs. threshold, T . The blue (lower) curves are for zero-effort impostors (i.e. comparing all images against all). The red (upper) curves are for persons of the same-sex, same-age, and same national-origin. This shows that FMR is underestimated (by a factor of 10 or more) by using a zero-effort impostor calculation to calibrate T . As shown later (sec. 3.6), FMR is higher for demographic-matched impostors.

3.5 Genuine distribution stability

3.5.1 Effect of birth place on the genuine distribution

Background: Both skin tone and bone structure vary geographically. Prior studies have reported variations in FNMR and FMR.

Goal: To measure false non-match rate (FNMR) variation with country of birth.

Methods: Thresholds are determined that give $FMR = \{0.001, 0.0001\}$ over the entire impostor set. Then FNMR is measured over 1000 bootstrap replications of the genuine scores. Only those countries with at least 140 individuals are included in the analysis.

Results: Figure 262 shows FNMR by country of birth for the two thresholds.

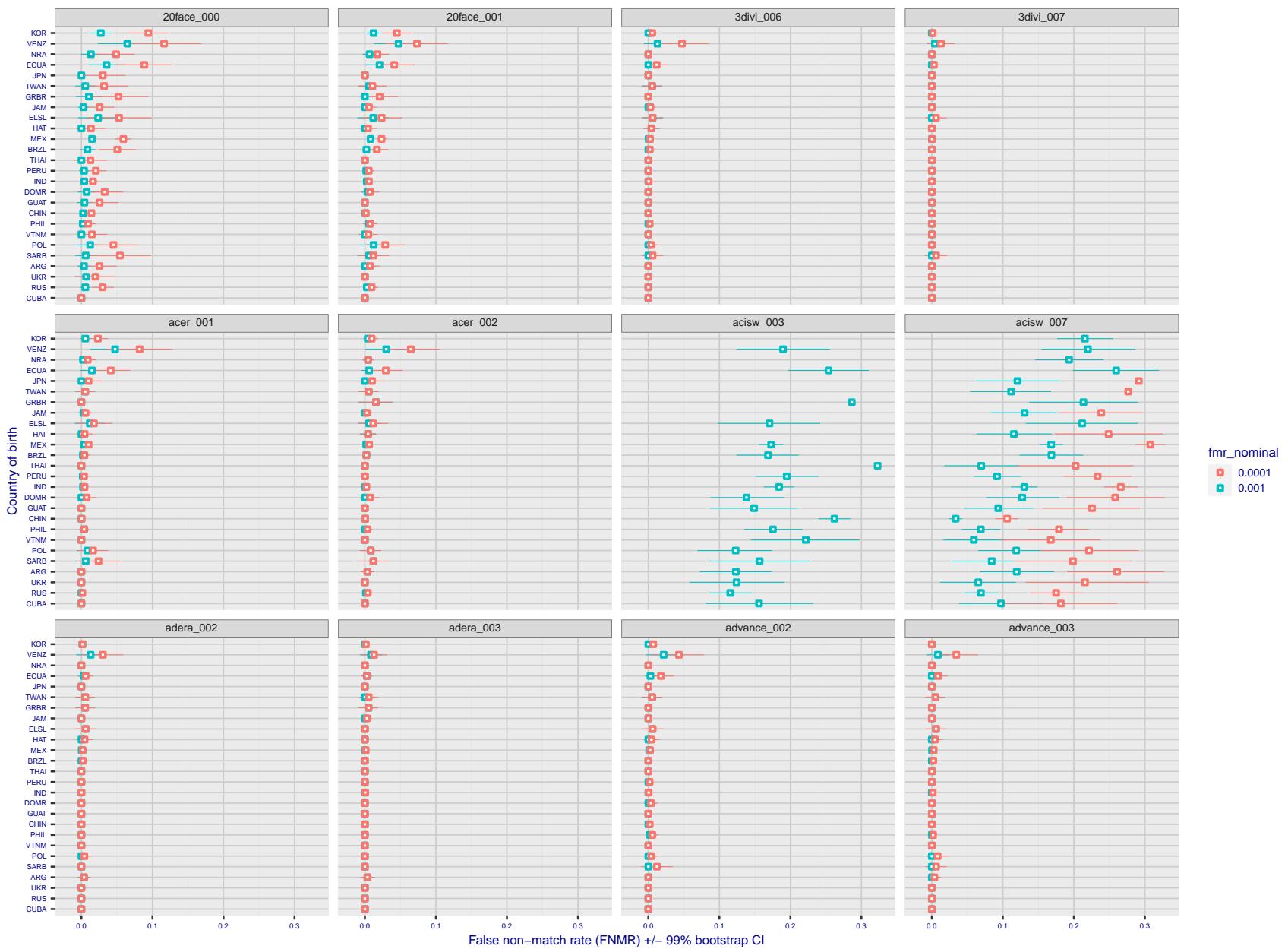


Figure 230: For the visa images, the dots show FNMR by country of birth for two globally set operating thresholds corresponding to $FMR = \{0.001, 0.0001\}$ computed over all on the order of 10^{10} impostor scores. The FMR in each bin will vary also - see subsequent impostor heatmaps in sec. 3.6.1. The figures shows an order of magnitude variation in FNMR across country of birth; these effects are likely due quality variations, then demographics like age and race. The error rates in some cases are zero, and in others the DET is flat so the error rates at the two thresholds are identical. The lines span 1% and 99% of bootstrap replicated FNMR estimates.

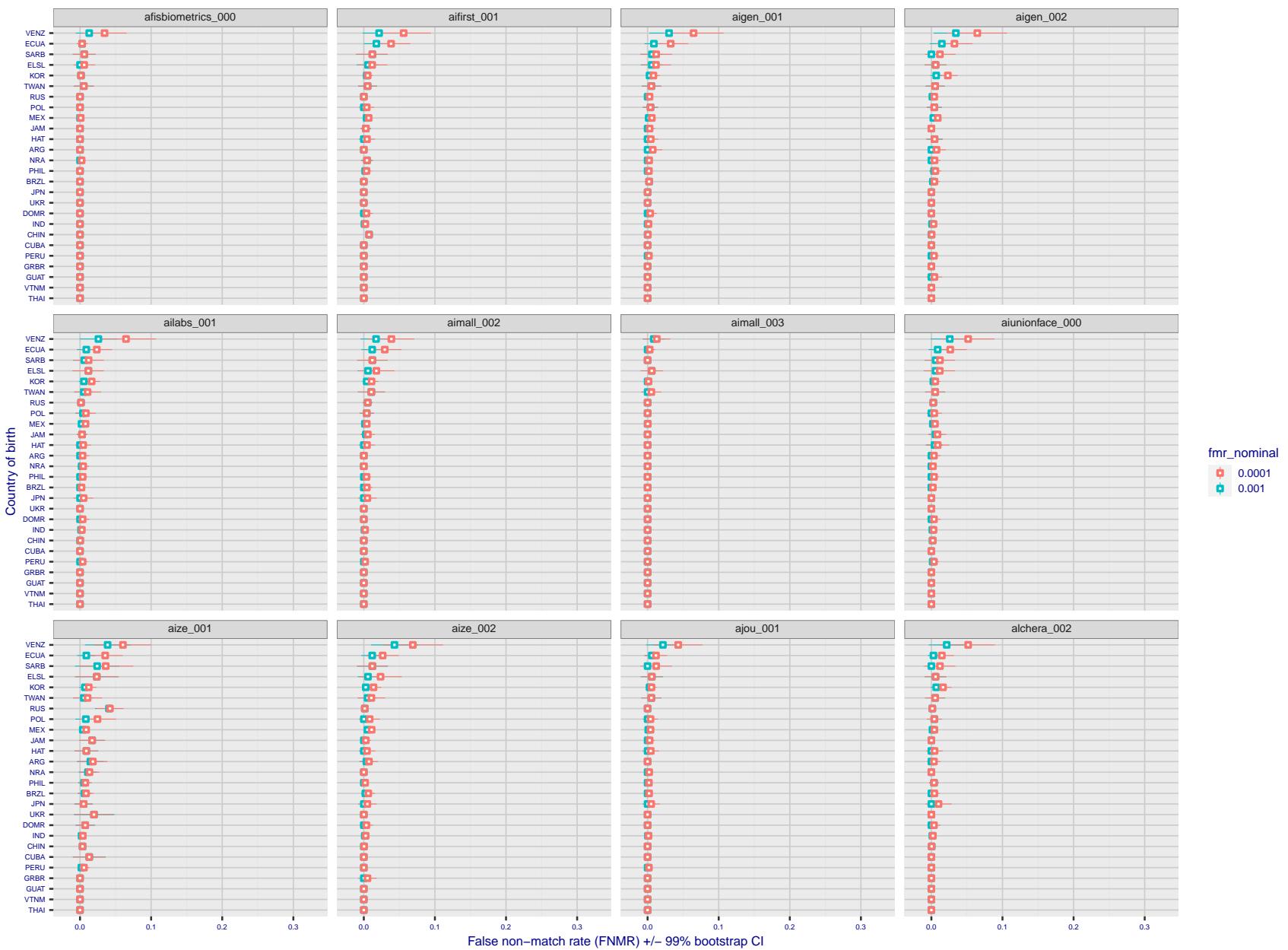


Figure 231: For the visa images, the dots show FNMR by country of birth for two globally set operating thresholds corresponding to $FMR = \{0.001, 0.0001\}$ computed over all on the order of 10^{10} impostor scores. The FMR in each bin will vary also - see subsequent impostor heatmaps in sec. 3.6.1. The figures shows an order of magnitude variation in FNMR across country of birth; these effects are likely due quality variations, then demographics like age and race. The error rates in some cases are zero, and in others the DET is flat so the error rates at the two thresholds are identical. The lines span 1% and 99% of bootstrap replicated FNMR estimates.

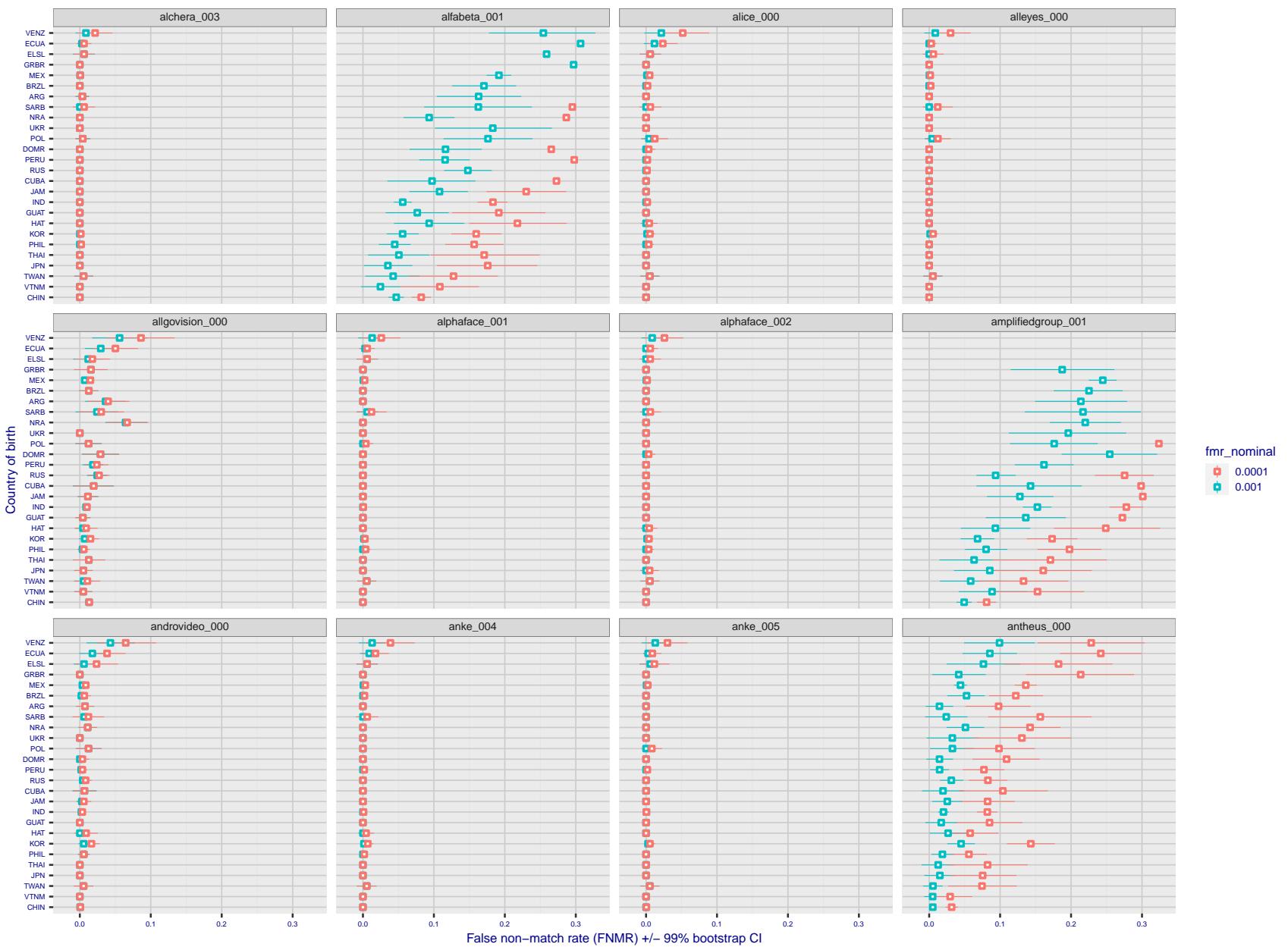


Figure 232: For the visa images, the dots show FNMR by country of birth for two globally set operating thresholds corresponding to $FMR = \{0.001, 0.0001\}$ computed over all on the order of 10^{10} impostor scores. The FMR in each bin will vary also - see subsequent impostor heatmaps in sec. 3.6.1. The figures shows an order of magnitude variation in FNMR across country of birth; these effects are likely due quality variations, then demographics like age and race. The error rates in some cases are zero, and in others the DET is flat so the error rates at the two thresholds are identical. The lines span 1% and 99% of bootstrap replicated FNMR estimates.

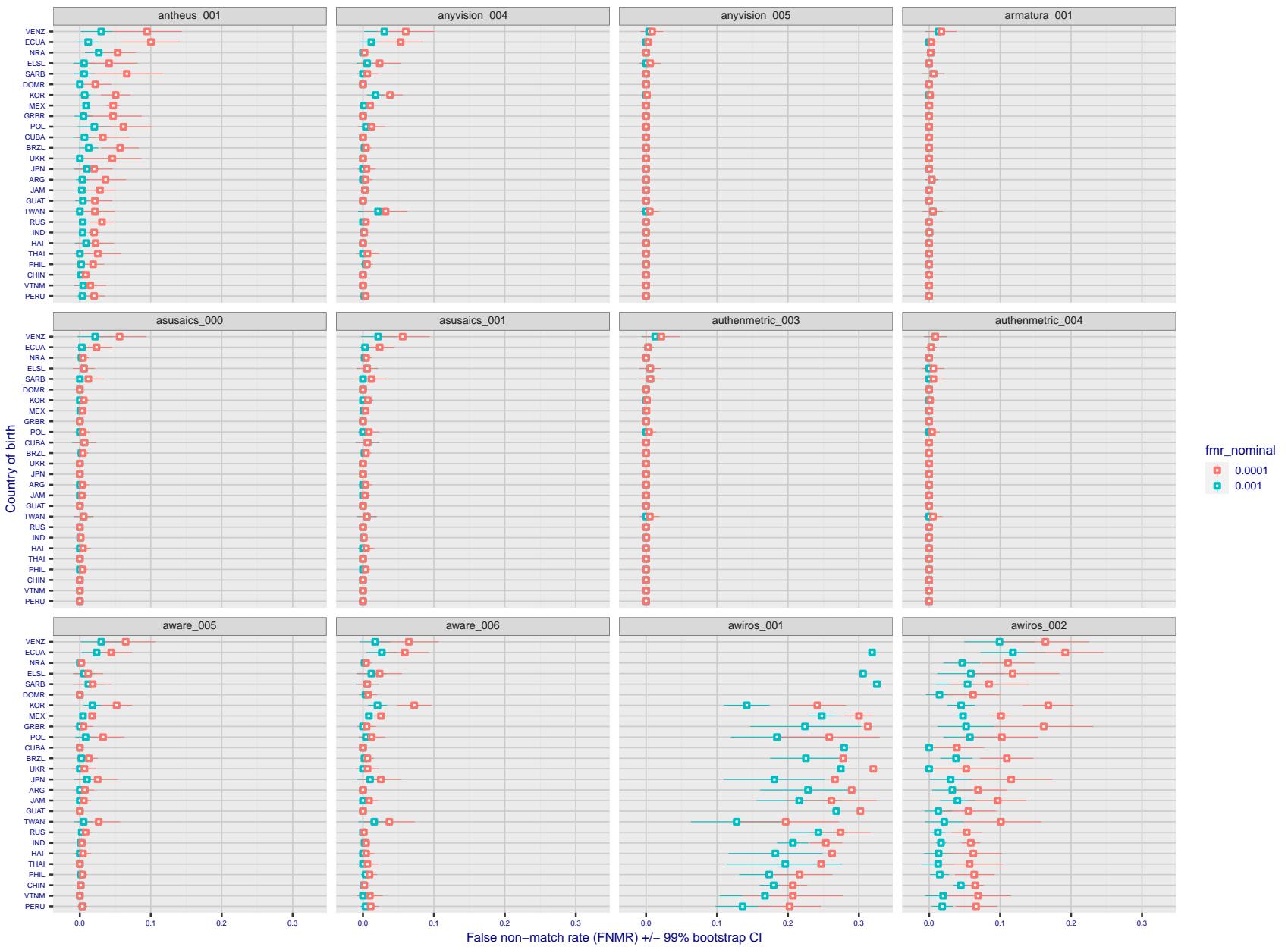


Figure 233: For the visa images, the dots show FNMR by country of birth for two globally set operating thresholds corresponding to $FMR = \{0.001, 0.0001\}$ computed over all on the order of 10^{10} impostor scores. The FMR in each bin will vary also - see subsequent impostor heatmaps in sec. 3.6.1. The figures shows an order of magnitude variation in FNMR across country of birth; these effects are likely due quality variations, then demographics like age and race. The error rates in some cases are zero, and in others the DET is flat so the error rates at the two thresholds are identical. The lines span 1% and 99% of bootstrap replicated FNMR estimates.

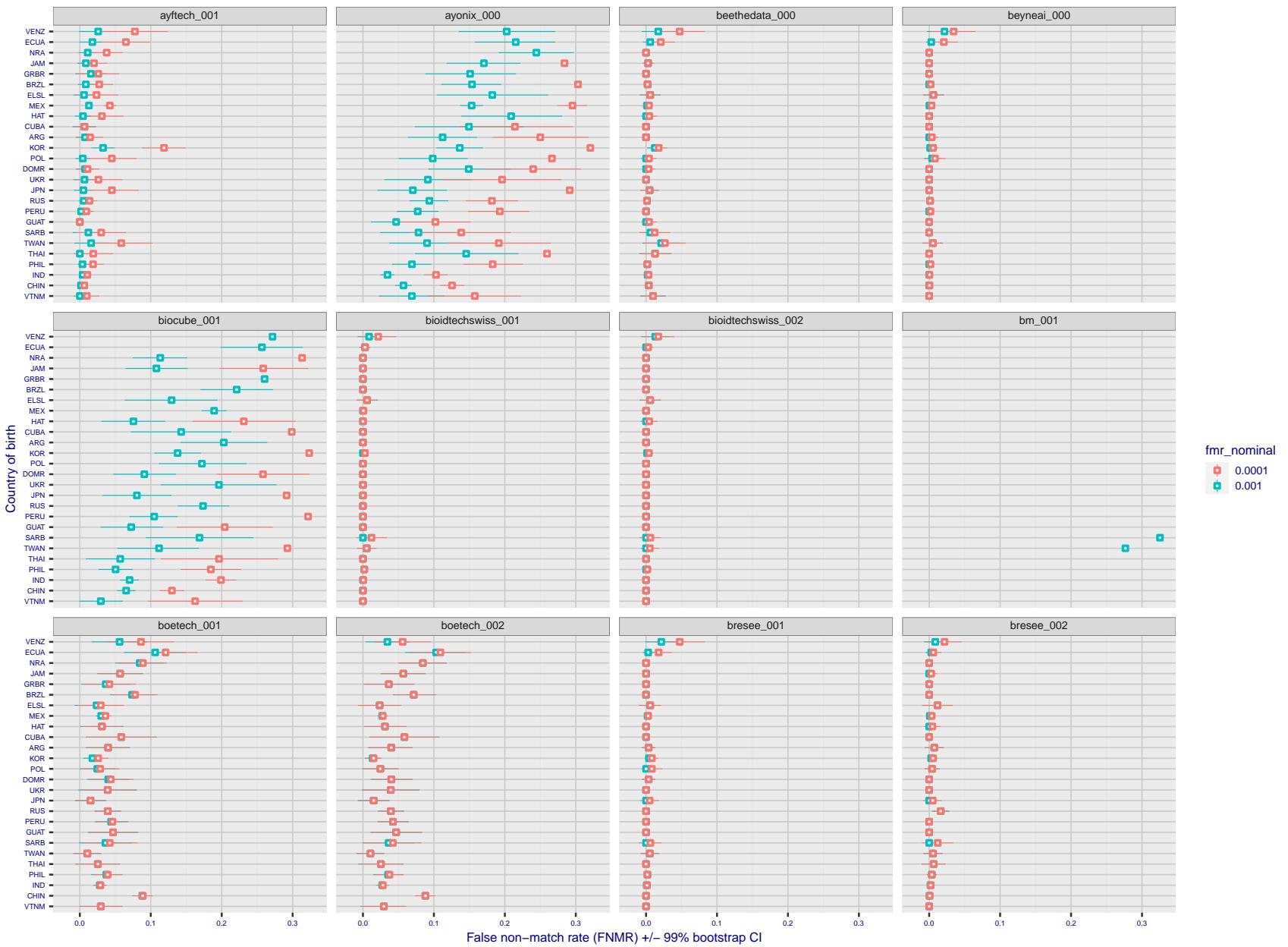


Figure 234: For the visa images, the dots show FNMR by country of birth for two globally set operating thresholds corresponding to $FMR = \{0.001, 0.0001\}$ computed over all on the order of 10^{10} impostor scores. The FMR in each bin will vary also - see subsequent impostor heatmaps in sec. 3.6.1. The figures shows an order of magnitude variation in FNMR across country of birth; these effects are likely due quality variations, then demographics like age and race. The error rates in some cases are zero, and in others the DET is flat so the error rates at the two thresholds are identical. The lines span 1% and 99% of bootstrap replicated FNMR estimates.

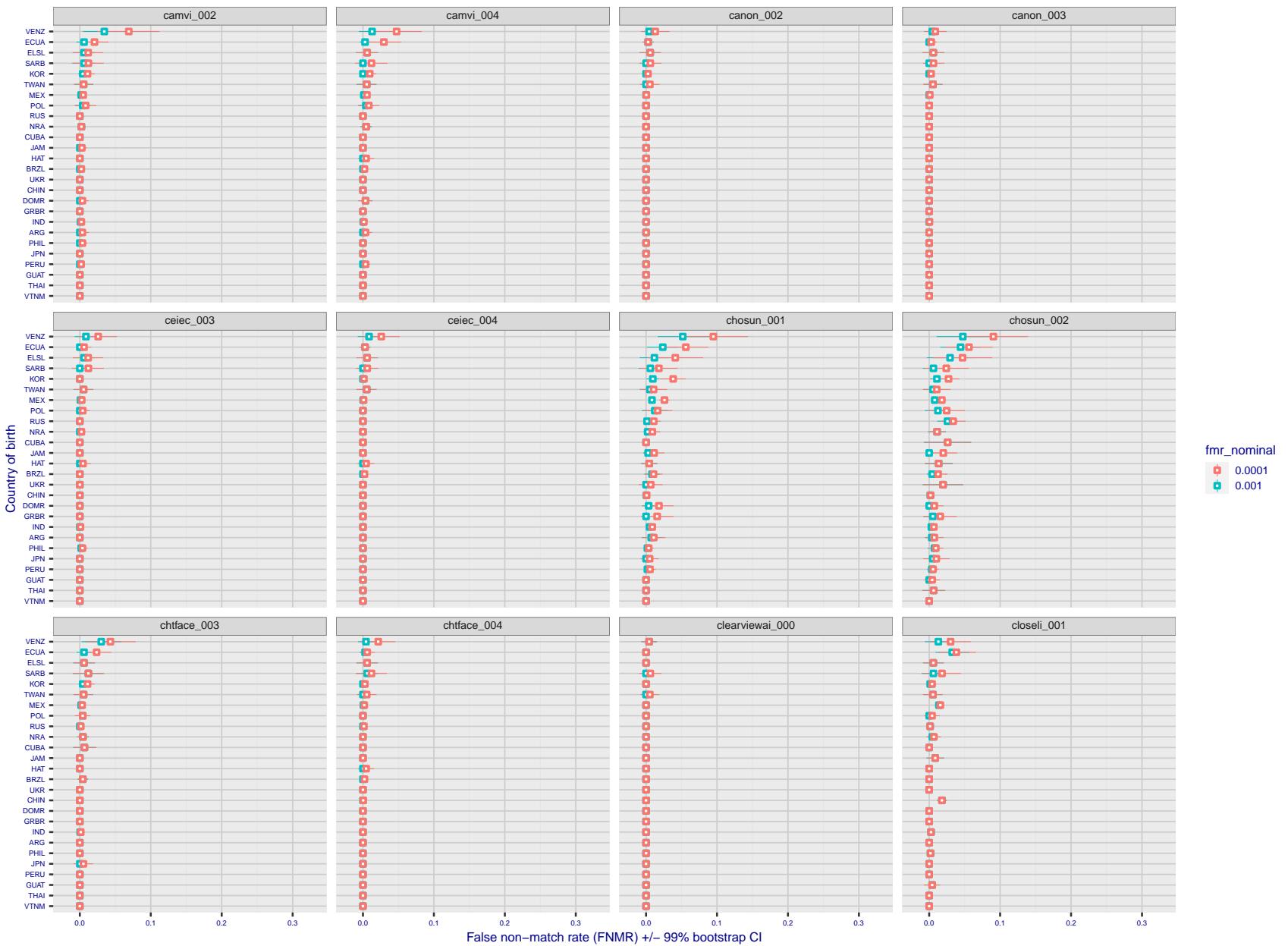


Figure 235: For the visa images, the dots show FNMR by country of birth for two globally set operating thresholds corresponding to $FMR = \{0.001, 0.0001\}$ computed over all on the order of 10^{10} impostor scores. The FMR in each bin will vary also - see subsequent impostor heatmaps in sec. 3.6.1. The figures shows an order of magnitude variation in FNMR across country of birth; these effects are likely due quality variations, then demographics like age and race. The error rates in some cases are zero, and in others the DET is flat so the error rates at the two thresholds are identical. The lines span 1% and 99% of bootstrap replicated FNMR estimates.

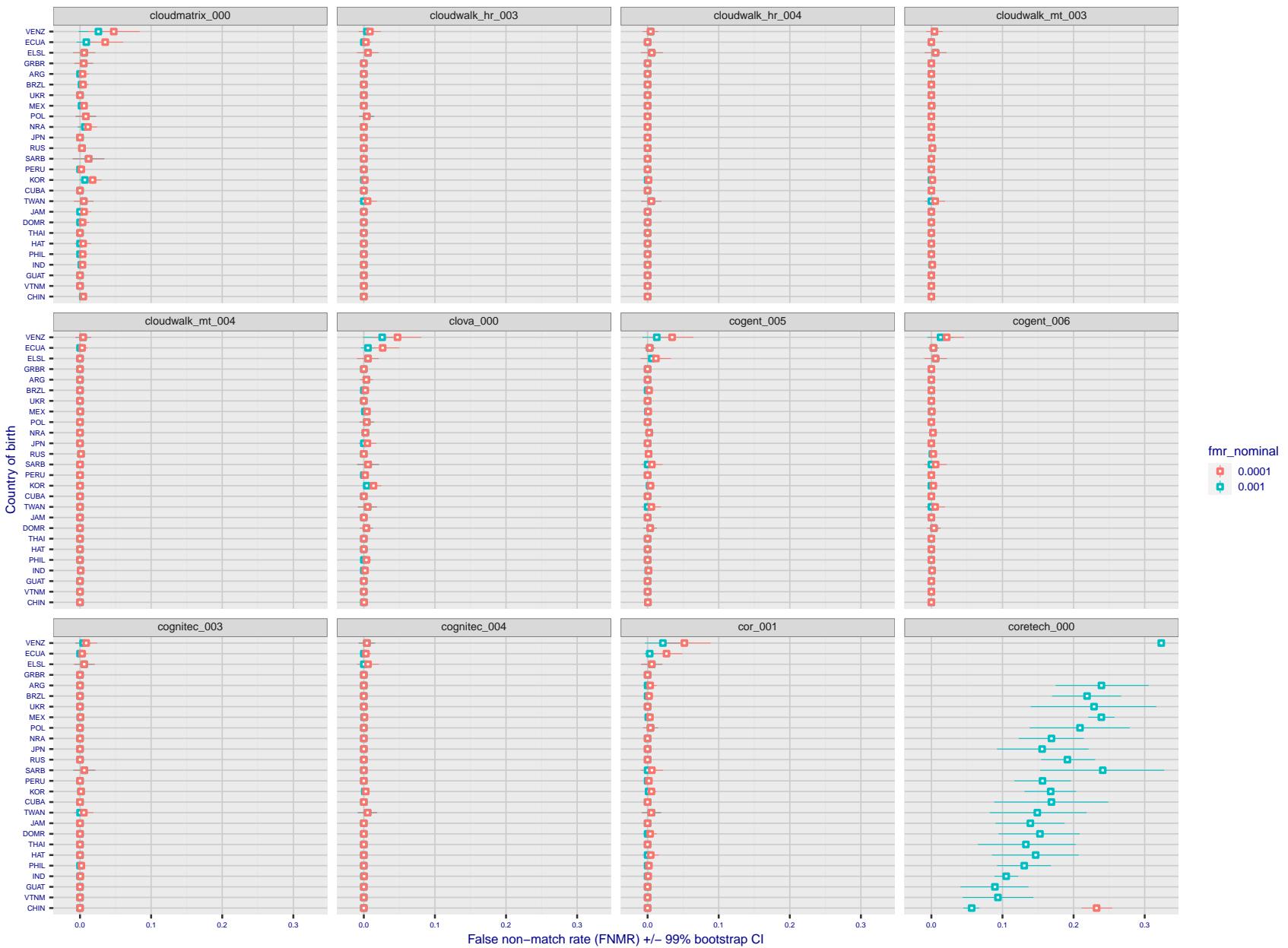


Figure 236: For the visa images, the dots show FNMR by country of birth for two globally set operating thresholds corresponding to $FMR = \{0.001, 0.0001\}$ computed over all on the order of 10^{10} impostor scores. The FMR in each bin will vary also - see subsequent impostor heatmaps in sec. 3.6.1. The figures shows an order of magnitude variation in FNMR across country of birth; these effects are likely due quality variations, then demographics like age and race. The error rates in some cases are zero, and in others the DET is flat so the error rates at the two thresholds are identical. The lines span 1% and 99% of bootstrap replicated FNMR estimates.

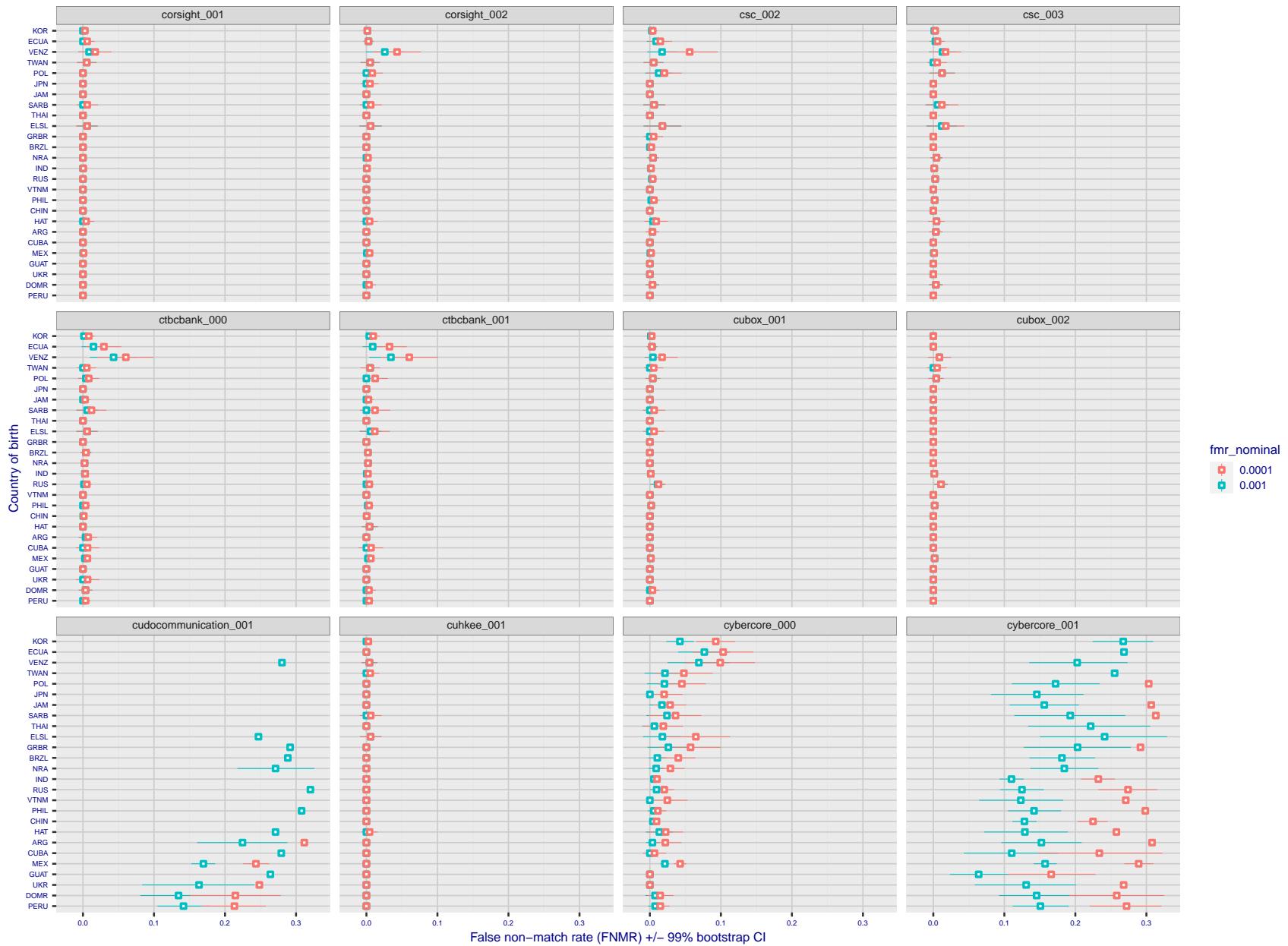


Figure 237: For the visa images, the dots show FNMR by country of birth for two globally set operating thresholds corresponding to $FMR = \{0.001, 0.0001\}$ computed over all on the order of 10^{10} impostor scores. The FMR in each bin will vary also - see subsequent impostor heatmaps in sec. 3.6.1. The figures shows an order of magnitude variation in FNMR across country of birth; these effects are likely due quality variations, then demographics like age and race. The error rates in some cases are zero, and in others the DET is flat so the error rates at the two thresholds are identical. The lines span 1% and 99% of bootstrap replicated FNMR estimates.

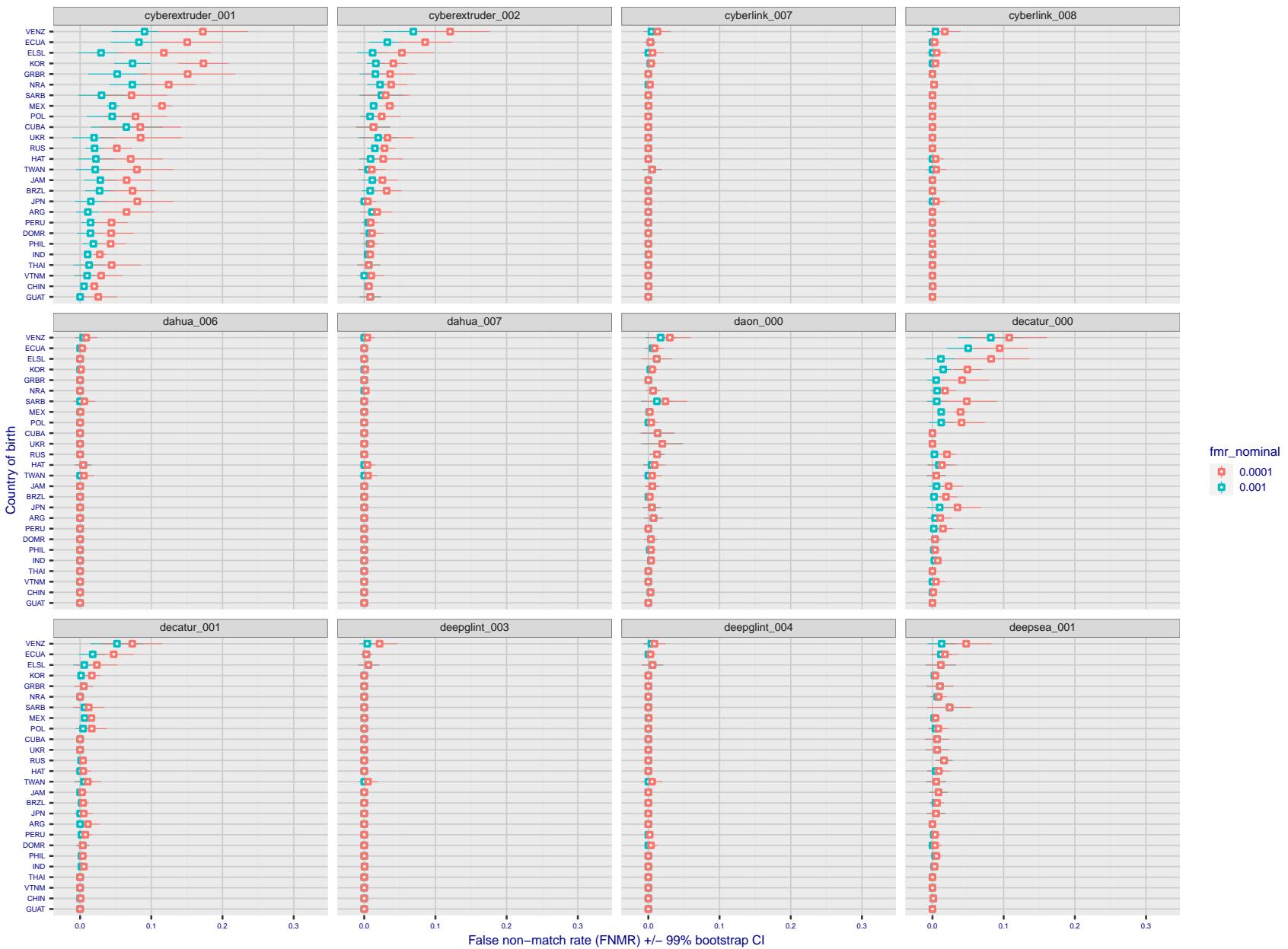


Figure 238: For the visa images, the dots show FNMR by country of birth for two globally set operating thresholds corresponding to $FMR = \{0.001, 0.0001\}$ computed over all on the order of 10^{10} impostor scores. The FMR in each bin will vary also - see subsequent impostor heatmaps in sec. 3.6.1. The figures shows an order of magnitude variation in FNMR across country of birth; these effects are likely due quality variations, then demographics like age and race. The error rates in some cases are zero, and in others the DET is flat so the error rates at the two thresholds are identical. The lines span 1% and 99% of bootstrap replicated FNMR estimates.

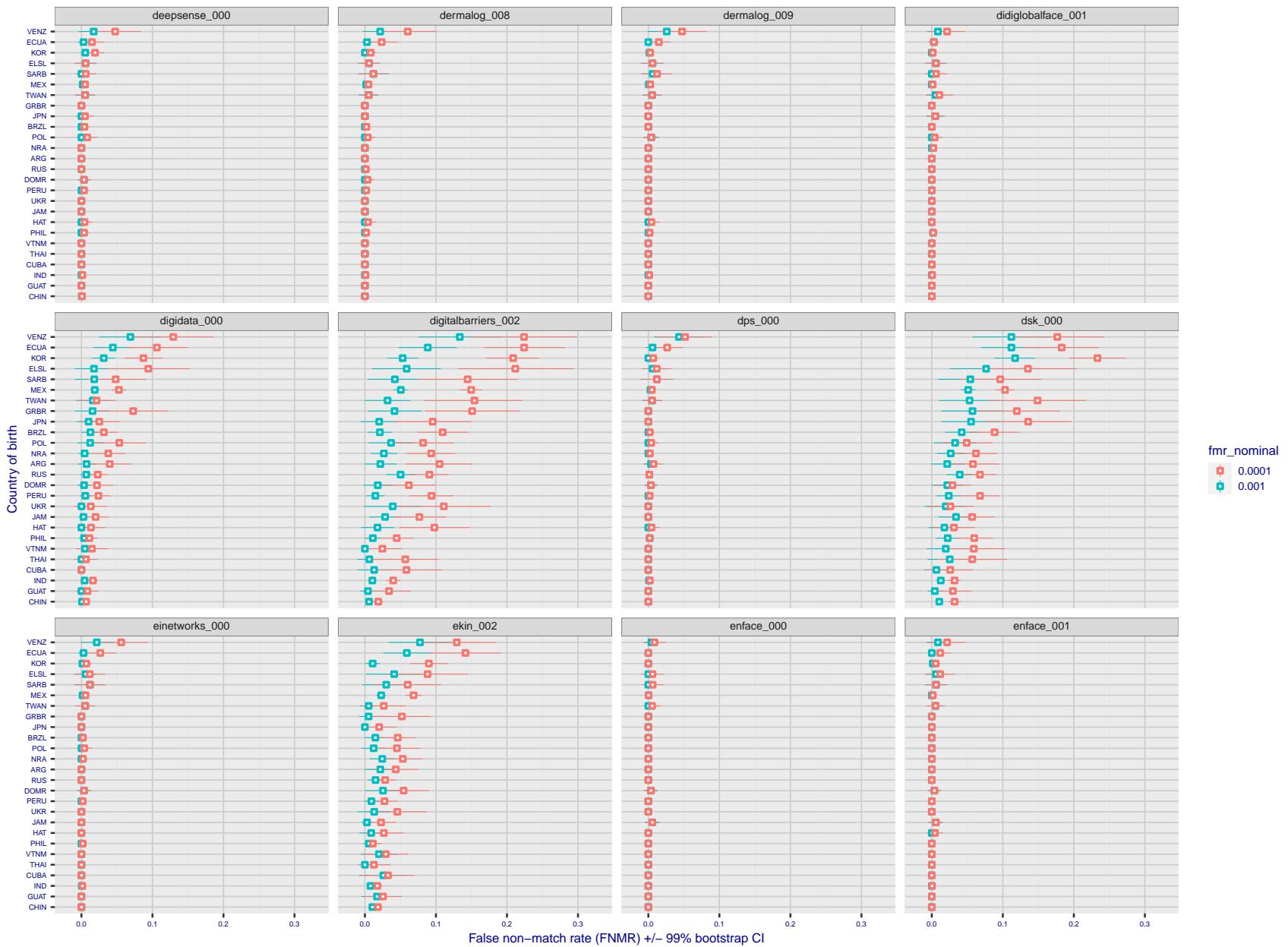


Figure 239: For the visa images, the dots show FNMR by country of birth for two globally set operating thresholds corresponding to $FMR = \{0.001, 0.0001\}$ computed over all on the order of 10^{10} impostor scores. The FMR in each bin will vary also - see subsequent impostor heatmaps in sec. 3.6.1. The figures shows an order of magnitude variation in FNMR across country of birth; these effects are likely due quality variations, then demographics like age and race. The error rates in some cases are zero, and in others the DET is flat so the error rates at the two thresholds are identical. The lines span 1% and 99% of bootstrap replicated FNMR estimates.

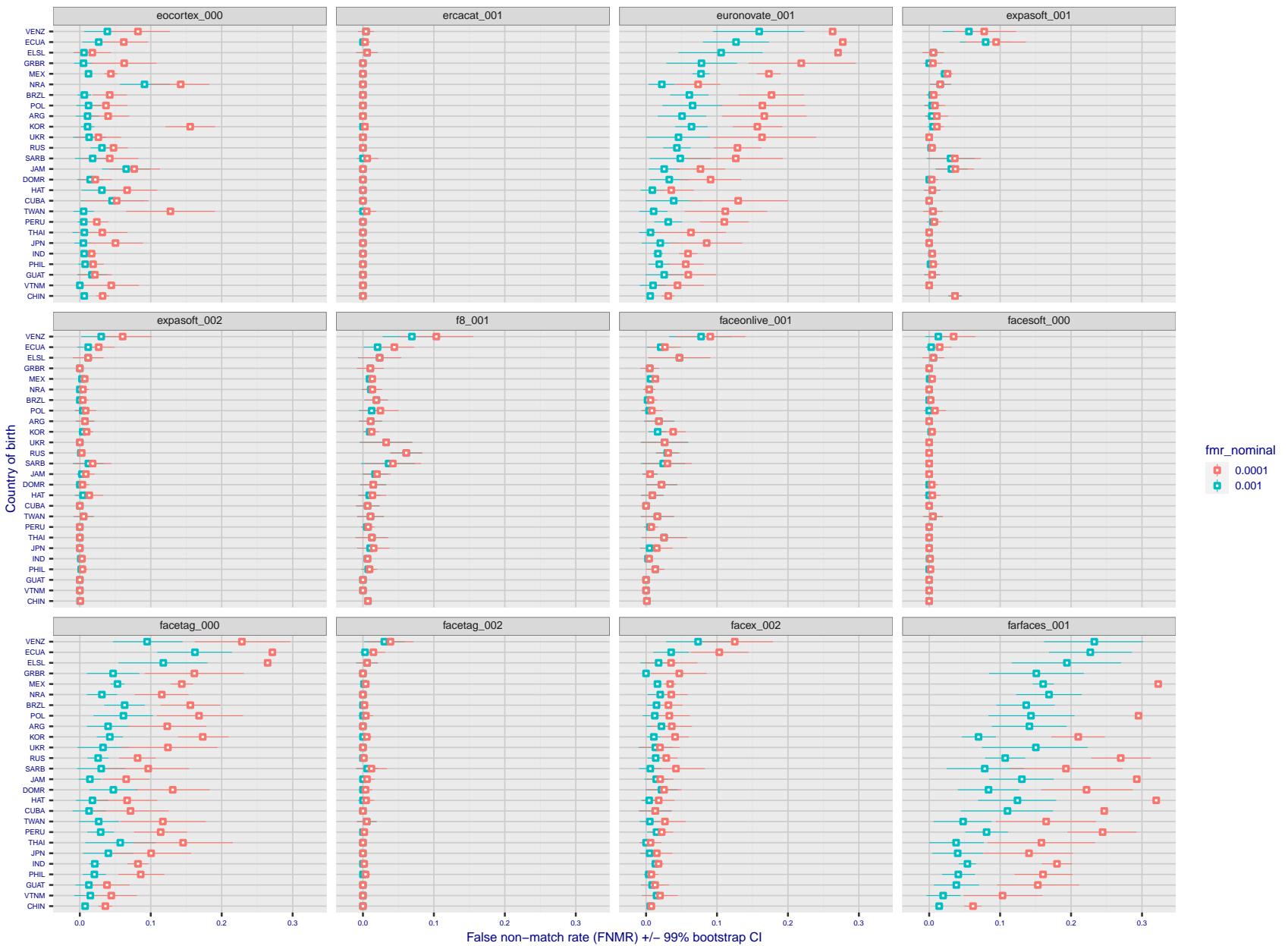


Figure 240: For the visa images, the dots show FNMR by country of birth for two globally set operating thresholds corresponding to $FMR = \{0.001, 0.0001\}$ computed over all on the order of 10^{10} impostor scores. The FMR in each bin will vary also - see subsequent impostor heatmaps in sec. 3.6.1. The figures shows an order of magnitude variation in FNMR across country of birth; these effects are likely due quality variations, then demographics like age and race. The error rates in some cases are zero, and in others the DET is flat so the error rates at the two thresholds are identical. The lines span 1% and 99% of bootstrap replicated FNMR estimates.

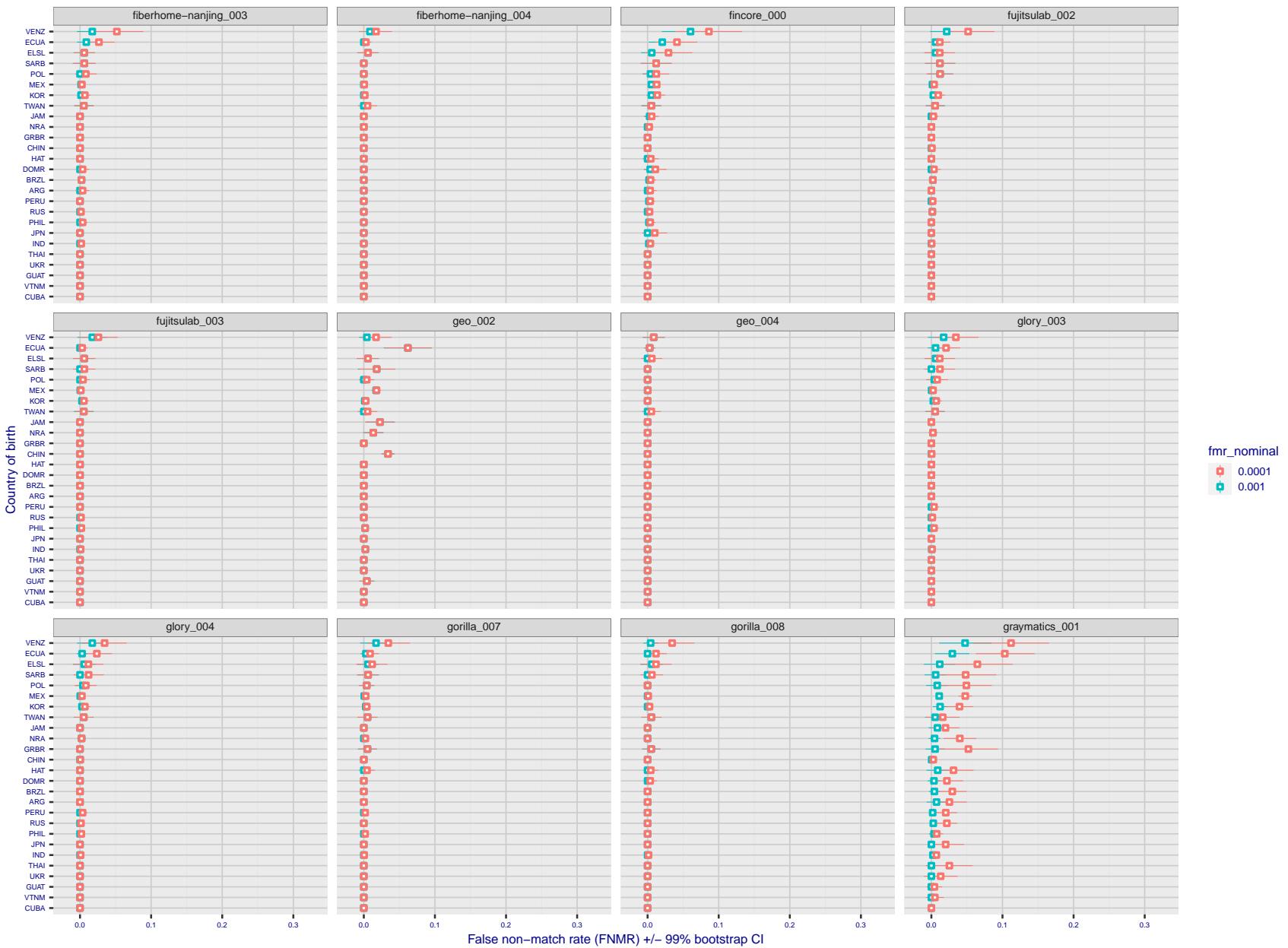


Figure 241: For the visa images, the dots show FNMR by country of birth for two globally set operating thresholds corresponding to $FMR = \{0.001, 0.0001\}$ computed over all on the order of 10^{10} impostor scores. The FMR in each bin will vary also - see subsequent impostor heatmaps in sec. 3.6.1. The figures shows an order of magnitude variation in FNMR across country of birth; these effects are likely due quality variations, then demographics like age and race. The error rates in some cases are zero, and in others the DET is flat so the error rates at the two thresholds are identical. The lines span 1% and 99% of bootstrap replicated FNMR estimates.

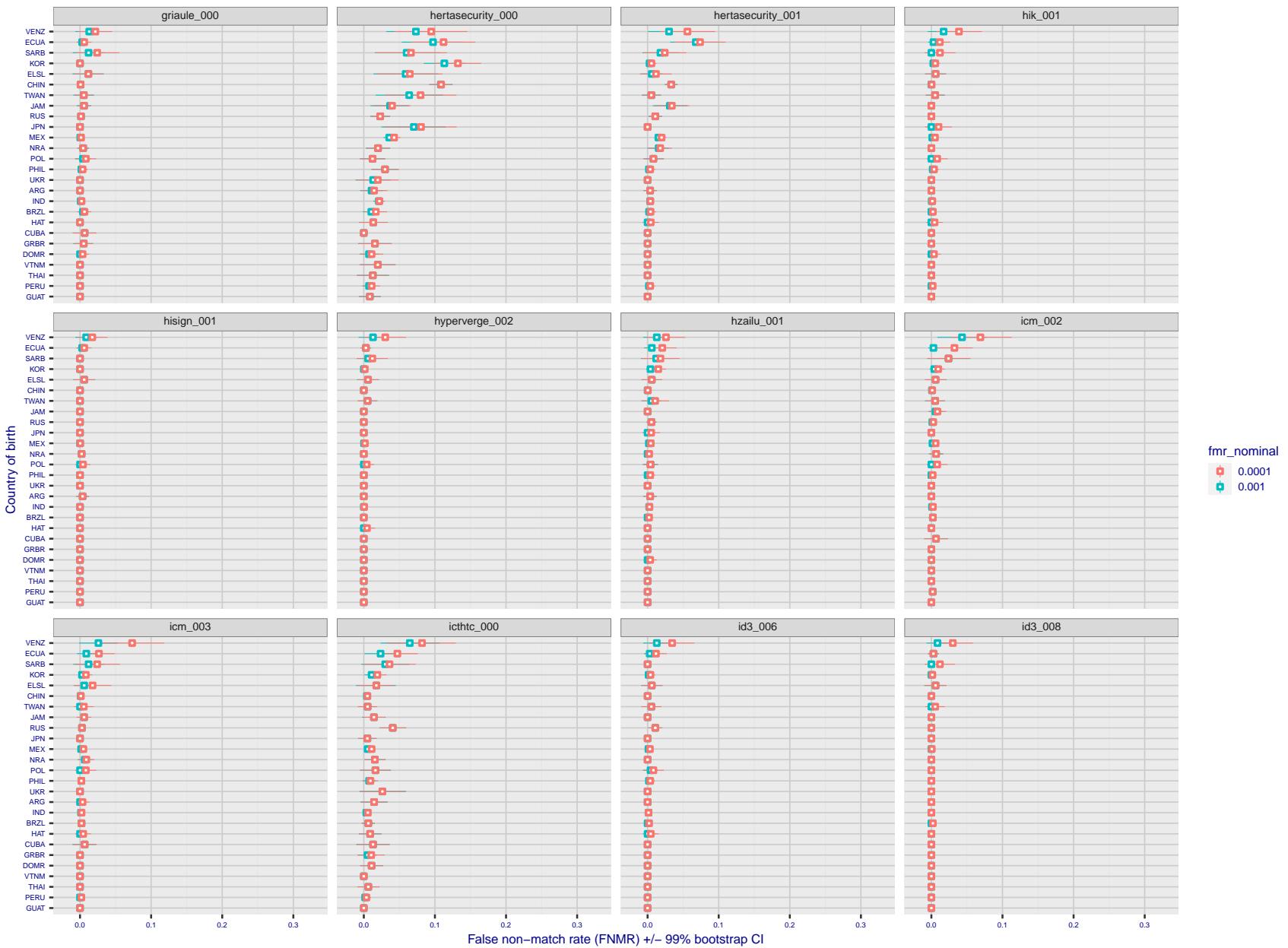


Figure 242: For the visa images, the dots show FNMR by country of birth for two globally set operating thresholds corresponding to $FMR = \{0.001, 0.0001\}$ computed over all on the order of 10^{10} impostor scores. The FMR in each bin will vary also - see subsequent impostor heatmaps in sec. 3.6.1. The figures shows an order of magnitude variation in FNMR across country of birth; these effects are likely due quality variations, then demographics like age and race. The error rates in some cases are zero, and in others the DET is flat so the error rates at the two thresholds are identical. The lines span 1% and 99% of bootstrap replicated FNMR estimates.

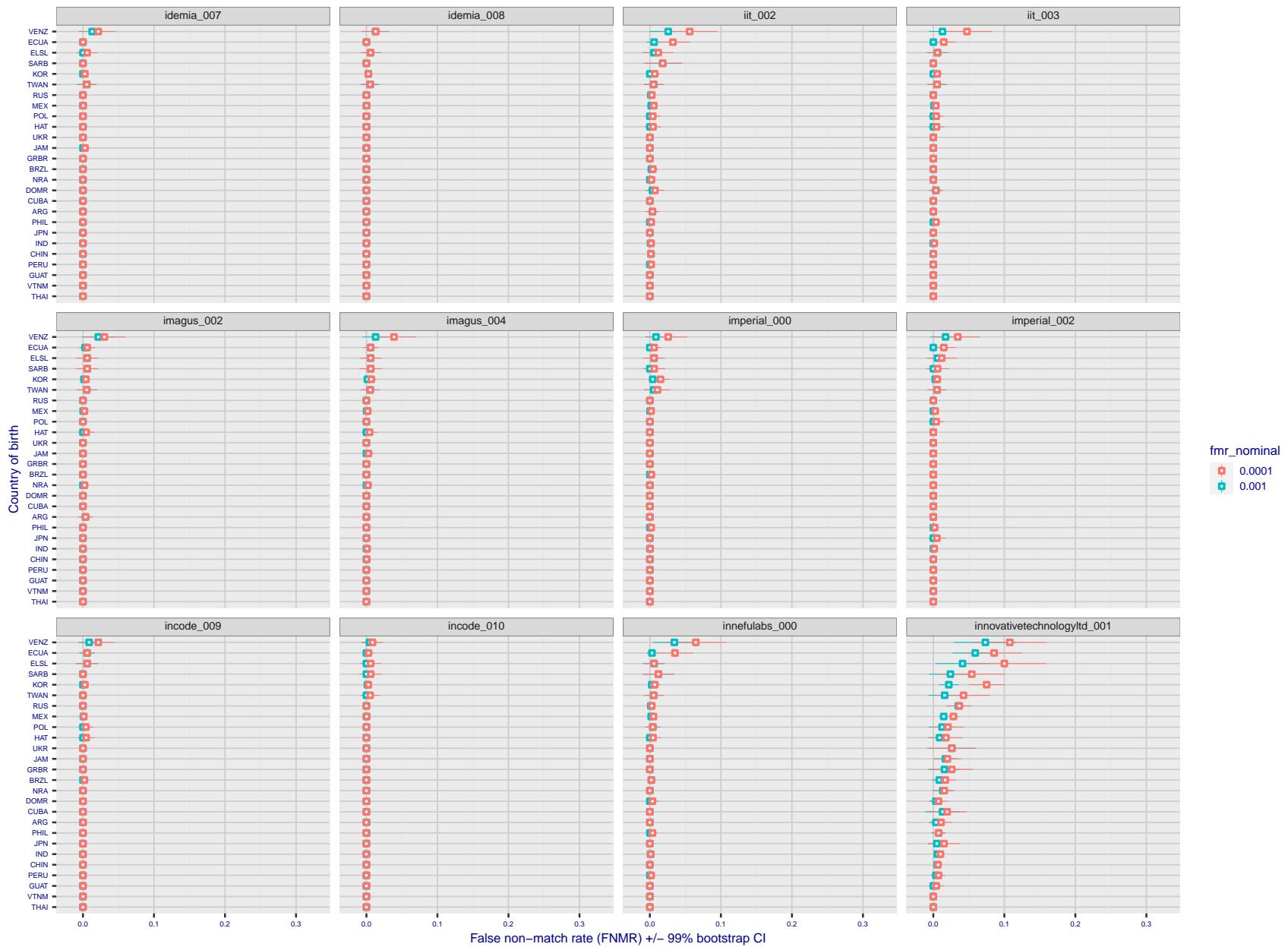


Figure 243: For the visa images, the dots show FNMR by country of birth for two globally set operating thresholds corresponding to $FMR = \{0.001, 0.0001\}$ computed over all on the order of 10^{10} impostor scores. The FMR in each bin will vary also - see subsequent impostor heatmaps in sec. 3.6.1. The figures shows an order of magnitude variation in FNMR across country of birth; these effects are likely due quality variations, then demographics like age and race. The error rates in some cases are zero, and in others the DET is flat so the error rates at the two thresholds are identical. The lines span 1% and 99% of bootstrap replicated FNMR estimates.

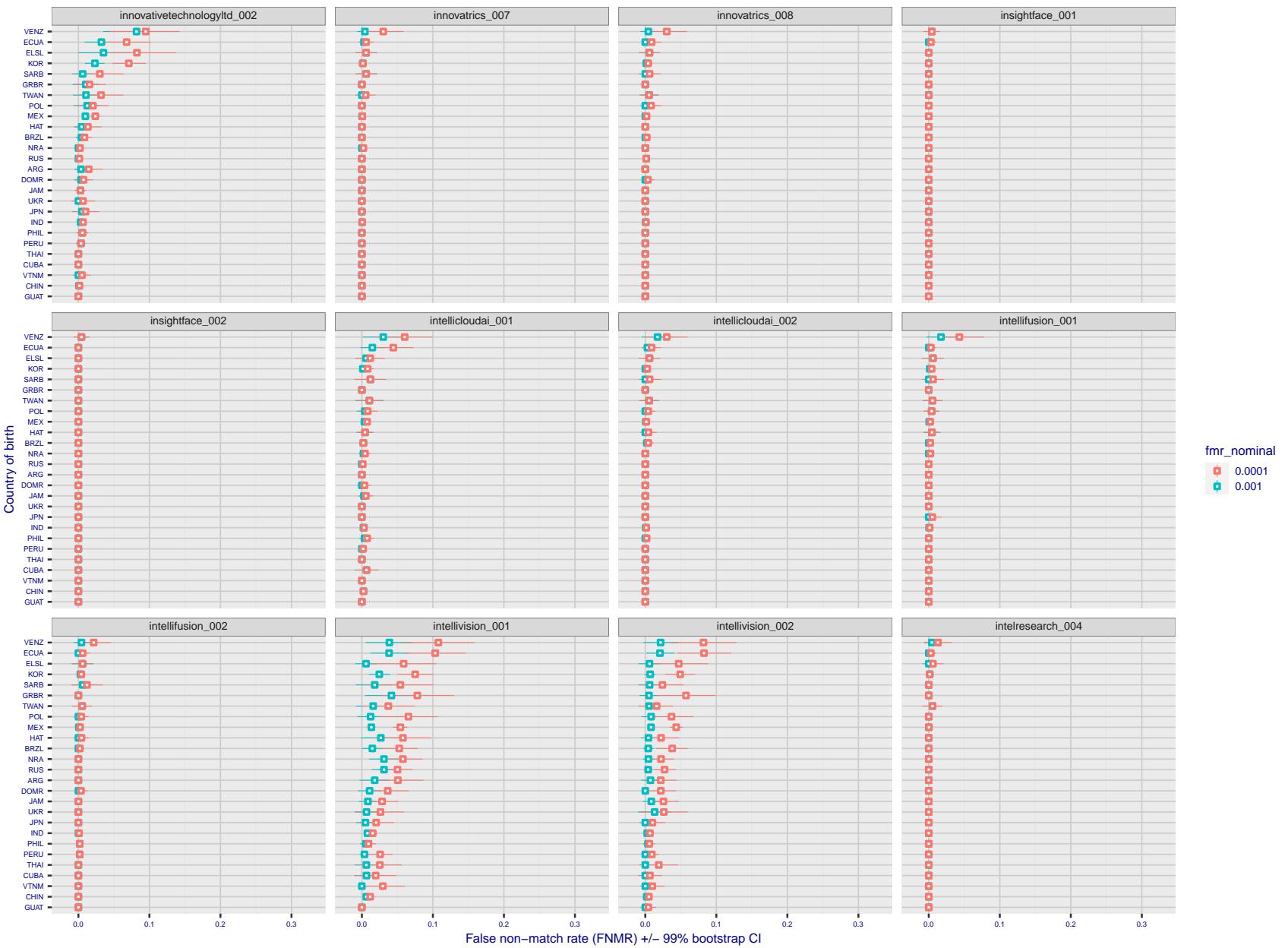


Figure 244: For the visa images, the dots show FNMR by country of birth for two globally set operating thresholds corresponding to $FMR = \{0.001, 0.0001\}$ computed over all on the order of 10^{10} impostor scores. The FMR in each bin will vary also - see subsequent impostor heatmaps in sec. 3.6.1. The figures shows an order of magnitude variation in FNMR across country of birth; these effects are likely due quality variations, then demographics like age and race. The error rates in some cases are zero, and in others the DET is flat so the error rates at the two thresholds are identical. The lines span 1% and 99% of bootstrap replicated FNMR estimates.

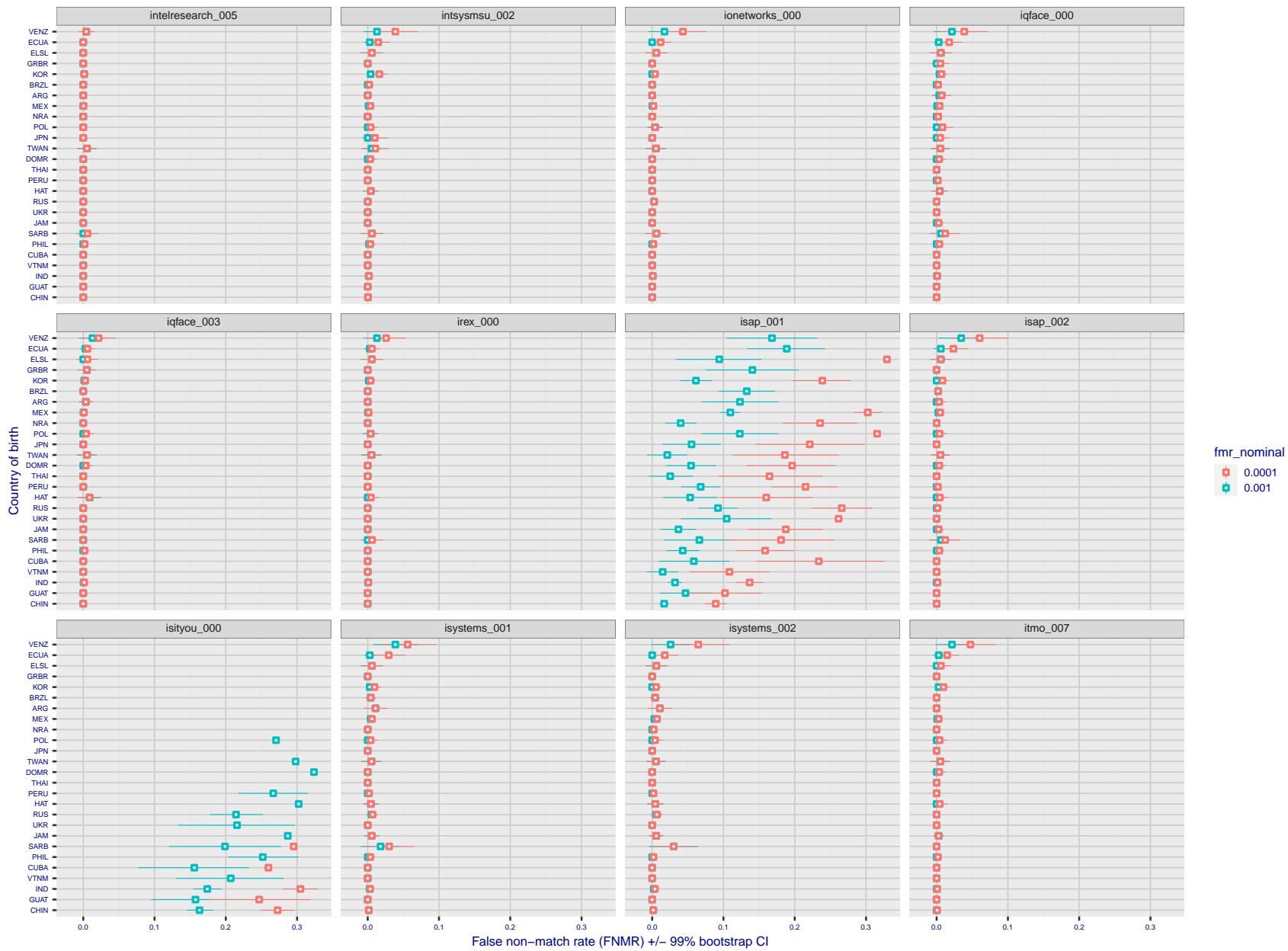


Figure 245: For the visa images, the dots show FNMR by country of birth for two globally set operating thresholds corresponding to $FMR = \{0.001, 0.0001\}$ computed over all on the order of 10^{10} impostor scores. The FMR in each bin will vary also - see subsequent impostor heatmaps in sec. 3.6.1. The figures shows an order of magnitude variation in FNMR across country of birth; these effects are likely due quality variations, then demographics like age and race. The error rates in some cases are zero, and in others the DET is flat so the error rates at the two thresholds are identical. The lines span 1% and 99% of bootstrap replicated FNMR estimates.

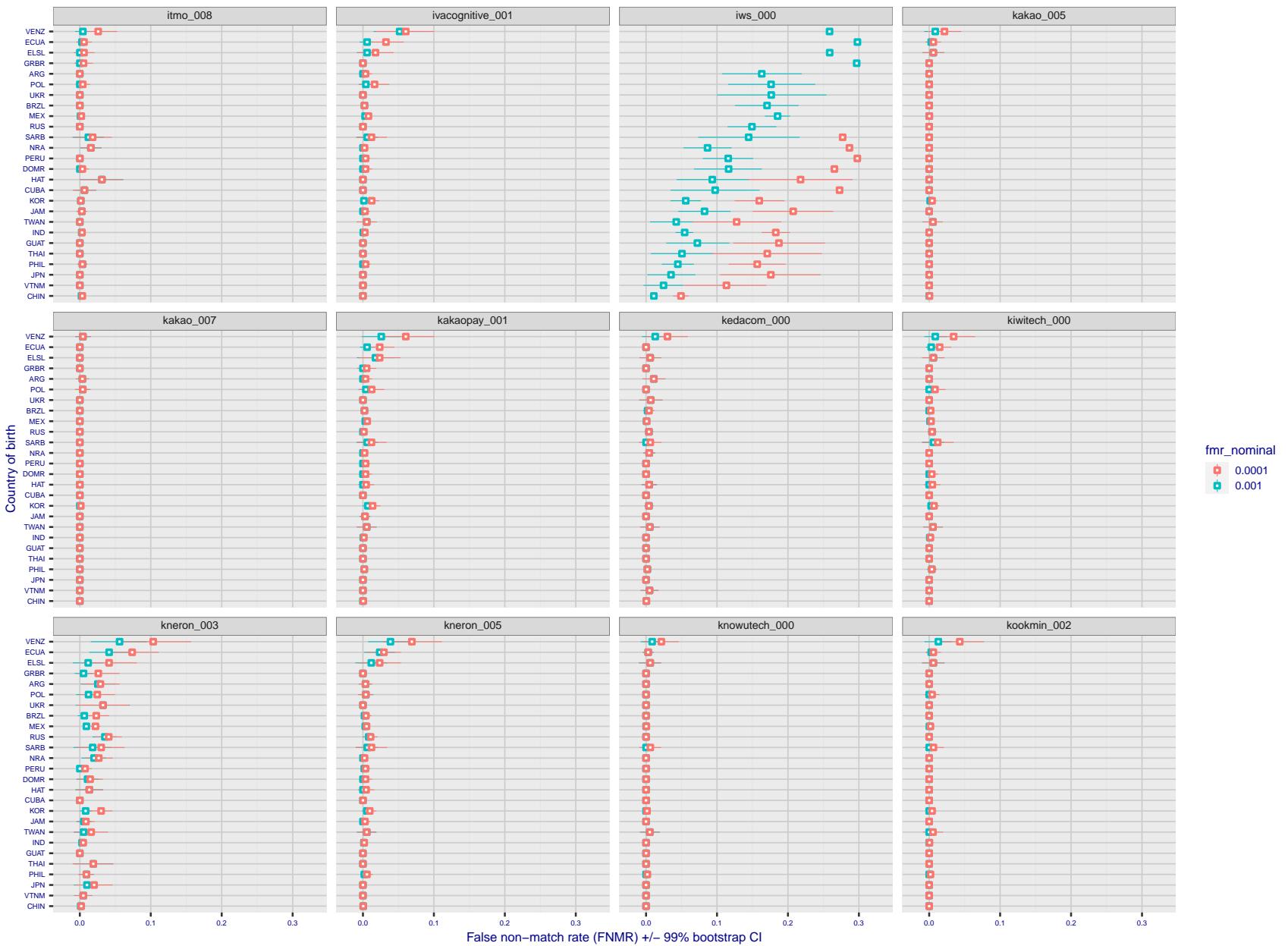


Figure 246: For the visa images, the dots show FNMR by country of birth for two globally set operating thresholds corresponding to $FMR = \{0.001, 0.0001\}$ computed over all on the order of 10^{10} impostor scores. The FMR in each bin will vary also - see subsequent impostor heatmaps in sec. 3.6.1. The figures shows an order of magnitude variation in FNMR across country of birth; these effects are likely due quality variations, then demographics like age and race. The error rates in some cases are zero, and in others the DET is flat so the error rates at the two thresholds are identical. The lines span 1% and 99% of bootstrap replicated FNMR estimates.

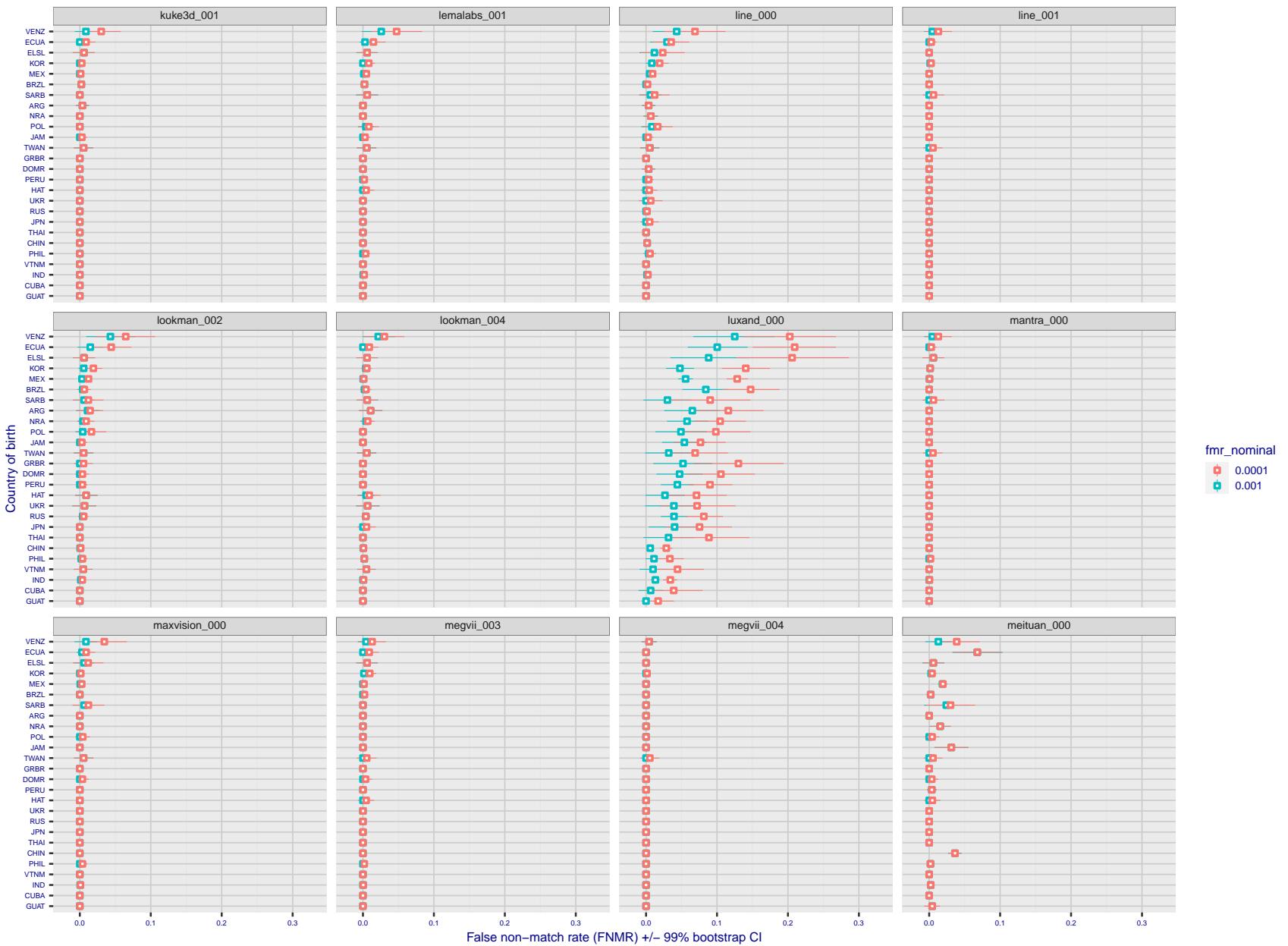


Figure 247: For the visa images, the dots show FNMR by country of birth for two globally set operating thresholds corresponding to $FMR = \{0.001, 0.0001\}$ computed over all on the order of 10^{10} impostor scores. The FMR in each bin will vary also - see subsequent impostor heatmaps in sec. 3.6.1. The figures shows an order of magnitude variation in FNMR across country of birth; these effects are likely due quality variations, then demographics like age and race. The error rates in some cases are zero, and in others the DET is flat so the error rates at the two thresholds are identical. The lines span 1% and 99% of bootstrap replicated FNMR estimates.

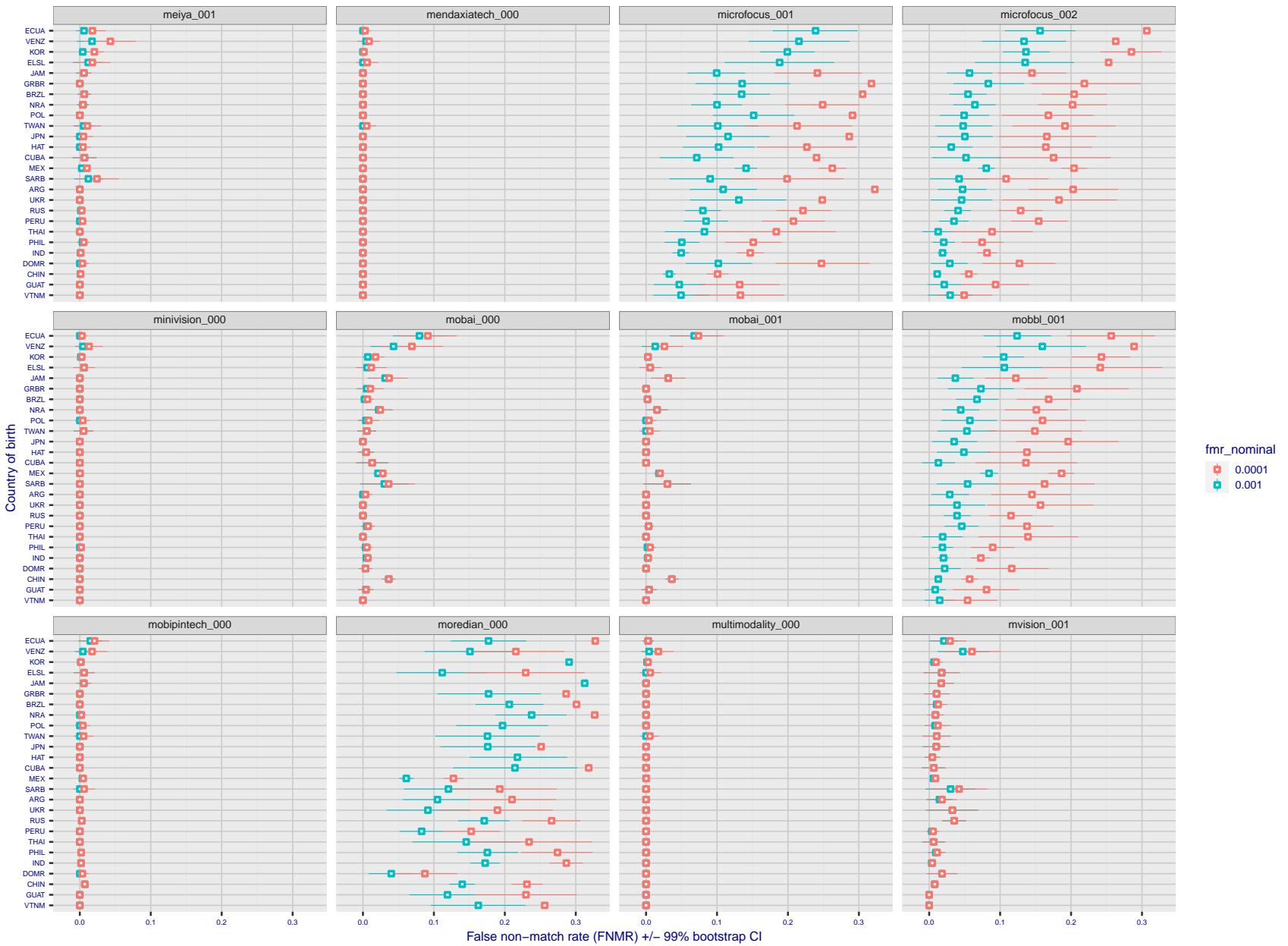


Figure 248: For the visa images, the dots show FNMR by country of birth for two globally set operating thresholds corresponding to $FMR = \{0.001, 0.0001\}$ computed over all on the order of 10^{10} impostor scores. The FMR in each bin will vary also - see subsequent impostor heatmaps in sec. 3.6.1. The figures shows an order of magnitude variation in FNMR across country of birth; these effects are likely due quality variations, then demographics like age and race. The error rates in some cases are zero, and in others the DET is flat so the error rates at the two thresholds are identical. The lines span 1% and 99% of bootstrap replicated FNMR estimates.

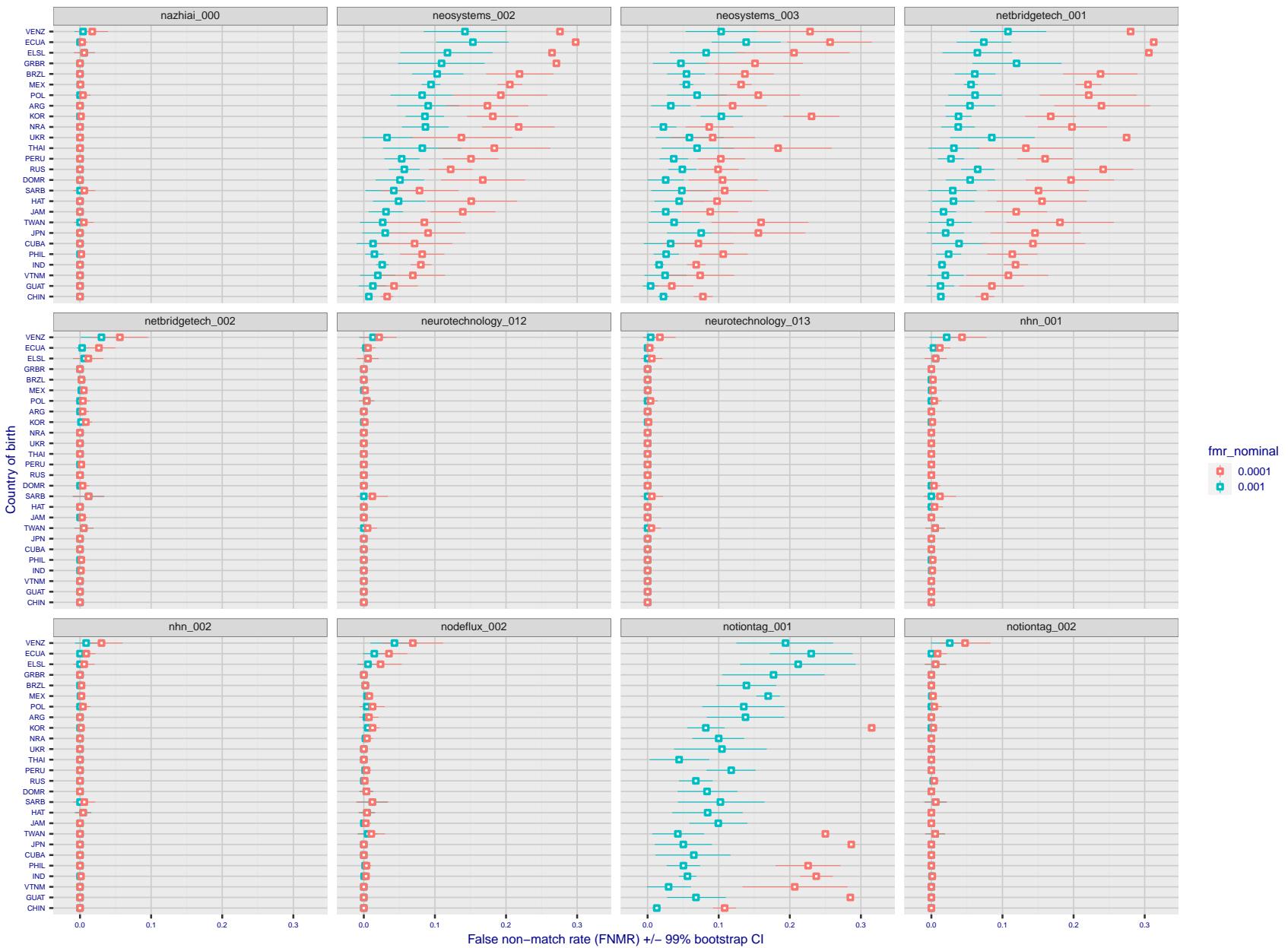


Figure 249: For the visa images, the dots show FNMR by country of birth for two globally set operating thresholds corresponding to $FMR = \{0.001, 0.0001\}$ computed over all on the order of 10^{10} impostor scores. The FMR in each bin will vary also - see subsequent impostor heatmaps in sec. 3.6.1. The figures shows an order of magnitude variation in FNMR across country of birth; these effects are likely due quality variations, then demographics like age and race. The error rates in some cases are zero, and in others the DET is flat so the error rates at the two thresholds are identical. The lines span 1% and 99% of bootstrap replicated FNMR estimates.

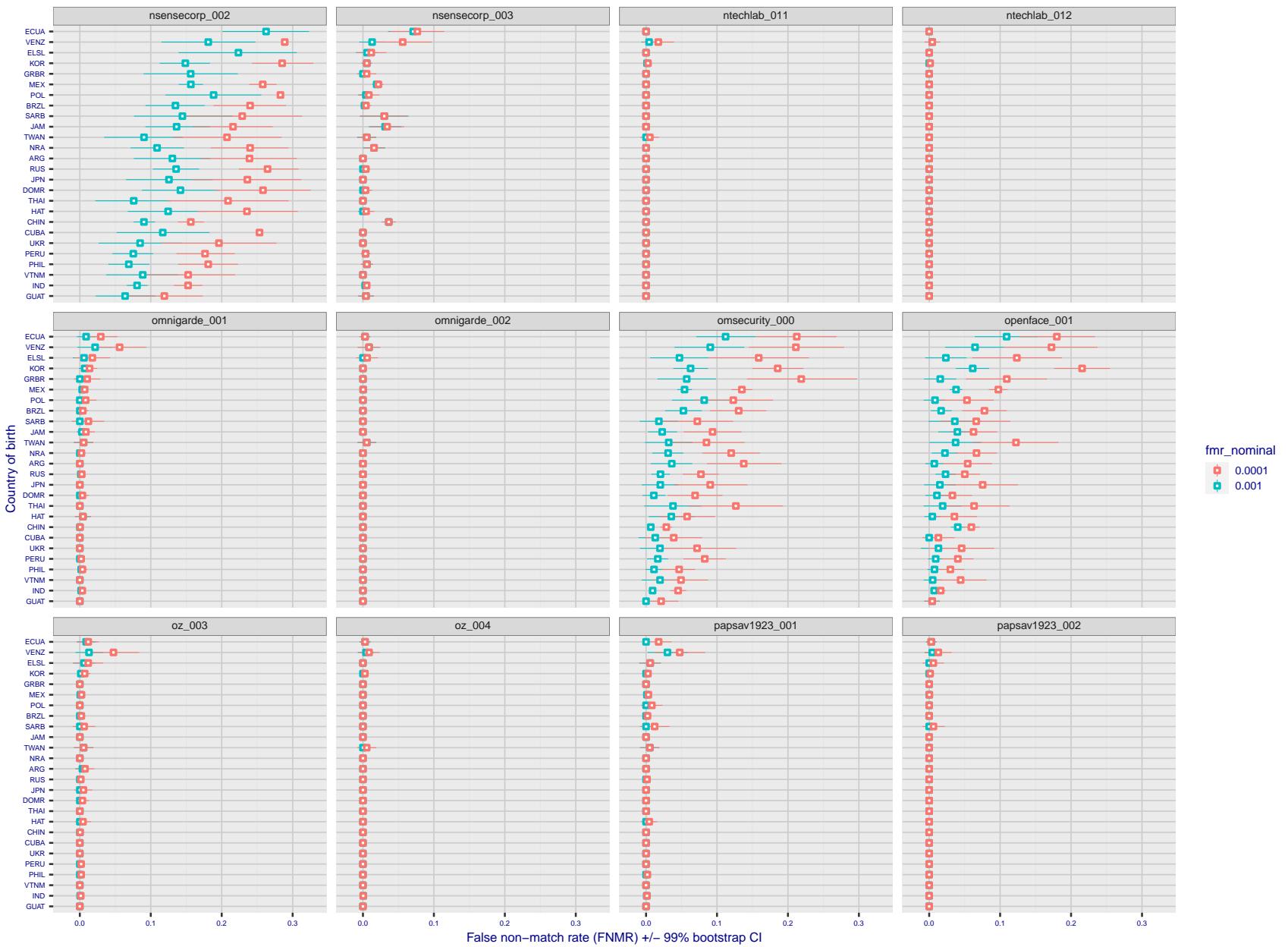


Figure 250: For the visa images, the dots show FNMR by country of birth for two globally set operating thresholds corresponding to $FMR = \{0.001, 0.0001\}$ computed over all on the order of 10^{10} impostor scores. The FMR in each bin will vary also - see subsequent impostor heatmaps in sec. 3.6.1. The figures shows an order of magnitude variation in FNMR across country of birth; these effects are likely due quality variations, then demographics like age and race. The error rates in some cases are zero, and in others the DET is flat so the error rates at the two thresholds are identical. The lines span 1% and 99% of bootstrap replicated FNMR estimates.

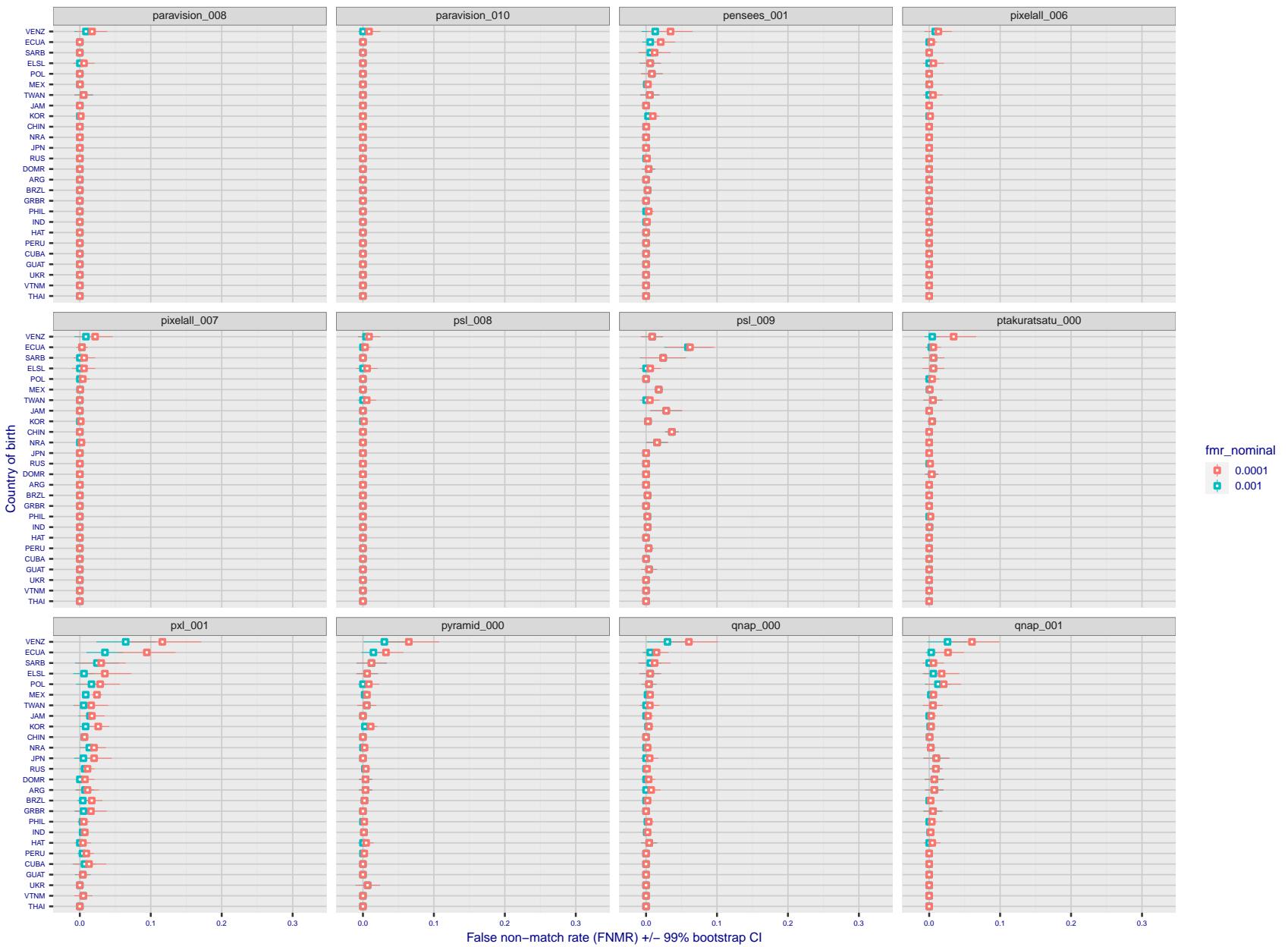


Figure 251: For the visa images, the dots show FNMR by country of birth for two globally set operating thresholds corresponding to $FMR = \{0.001, 0.0001\}$ computed over all on the order of 10^{10} impostor scores. The FMR in each bin will vary also - see subsequent impostor heatmaps in sec. 3.6.1. The figures shows an order of magnitude variation in FNMR across country of birth; these effects are likely due quality variations, then demographics like age and race. The error rates in some cases are zero, and in others the DET is flat so the error rates at the two thresholds are identical. The lines span 1% and 99% of bootstrap replicated FNMR estimates.

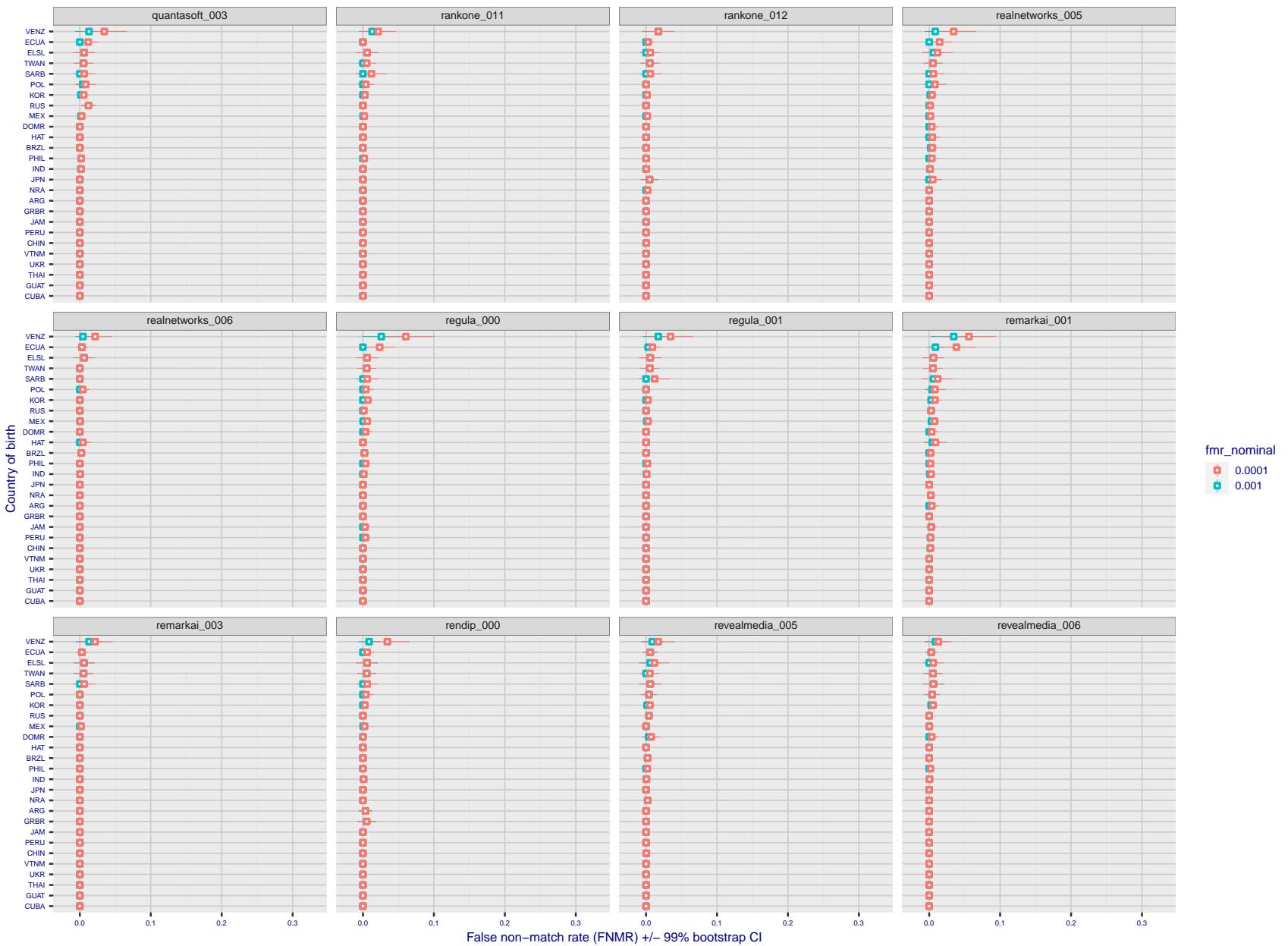


Figure 252: For the visa images, the dots show FNMR by country of birth for two globally set operating thresholds corresponding to $FMR = \{0.001, 0.0001\}$ computed over all on the order of 10^{10} impostor scores. The FMR in each bin will vary also - see subsequent impostor heatmaps in sec. 3.6.1. The figures shows an order of magnitude variation in FNMR across country of birth; these effects are likely due quality variations, then demographics like age and race. The error rates in some cases are zero, and in others the DET is flat so the error rates at the two thresholds are identical. The lines span 1% and 99% of bootstrap replicated FNMR estimates.

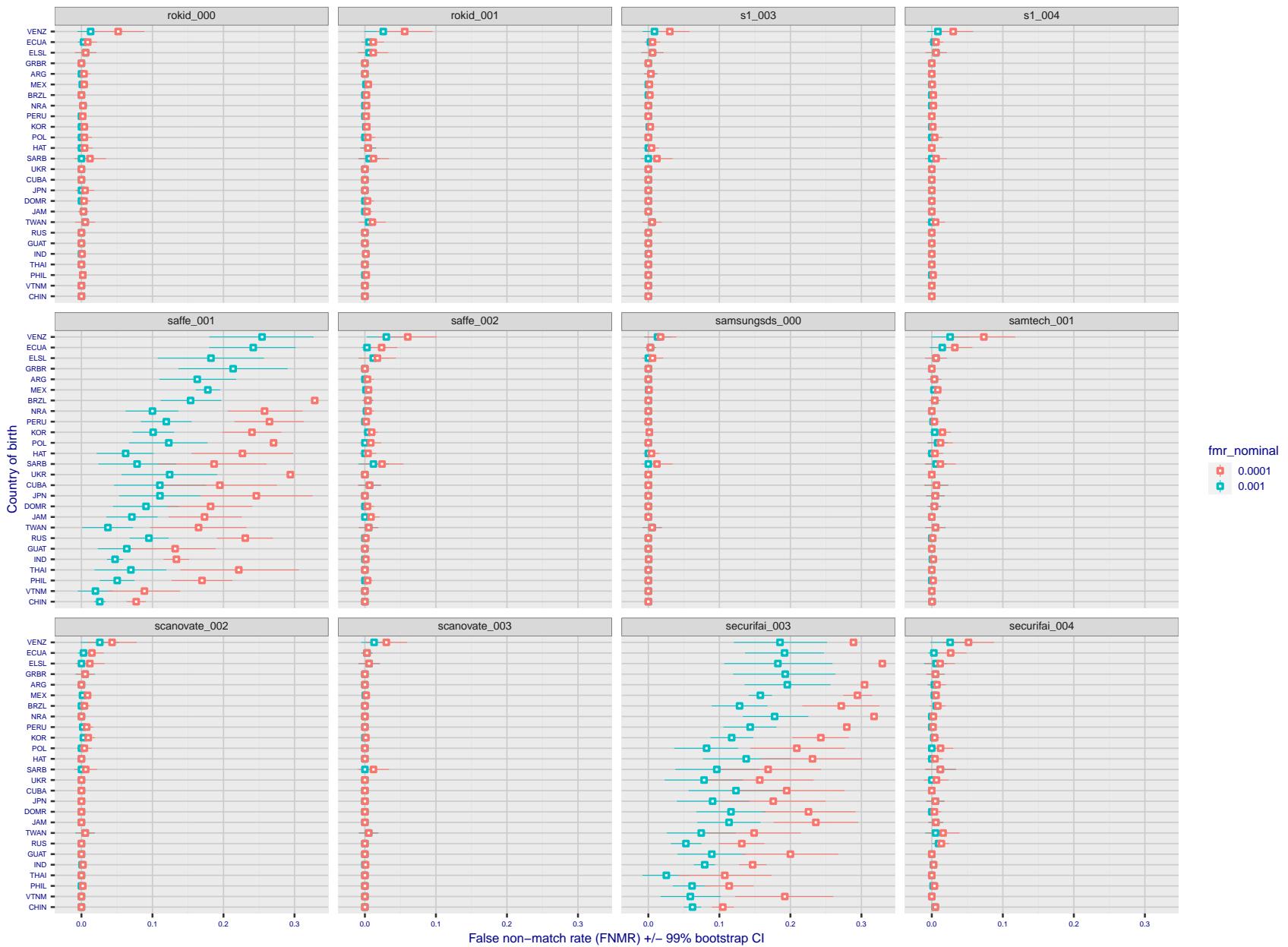


Figure 253: For the visa images, the dots show FNMR by country of birth for two globally set operating thresholds corresponding to $FMR = \{0.001, 0.0001\}$ computed over all on the order of 10^{10} impostor scores. The FMR in each bin will vary also - see subsequent impostor heatmaps in sec. 3.6.1. The figures shows an order of magnitude variation in FNMR across country of birth; these effects are likely due quality variations, then demographics like age and race. The error rates in some cases are zero, and in others the DET is flat so the error rates at the two thresholds are identical. The lines span 1% and 99% of bootstrap replicated FNMR estimates.

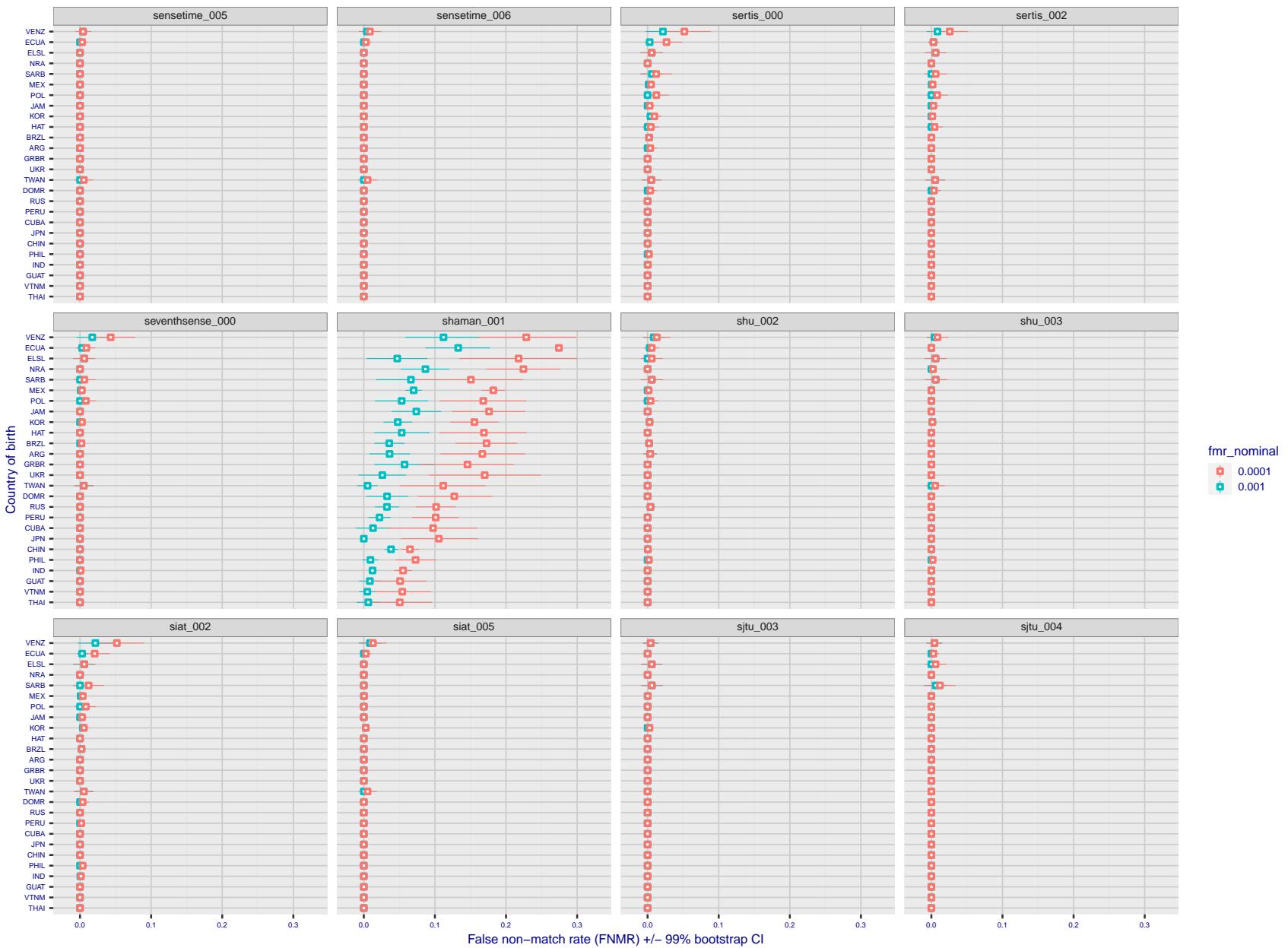


Figure 254: For the visa images, the dots show FNMR by country of birth for two globally set operating thresholds corresponding to $\text{FMR} = \{0.001, 0.0001\}$ computed over all on the order of 10^{10} impostor scores. The FMR in each bin will vary also - see subsequent impostor heatmaps in sec. 3.6.1. The figures shows an order of magnitude variation in FNMR across country of birth; these effects are likely due quality variations, then demographics like age and race. The error rates in some cases are zero, and in others the DET is flat so the error rates at the two thresholds are identical. The lines span 1% and 99% of bootstrap replicated FNMR estimates.

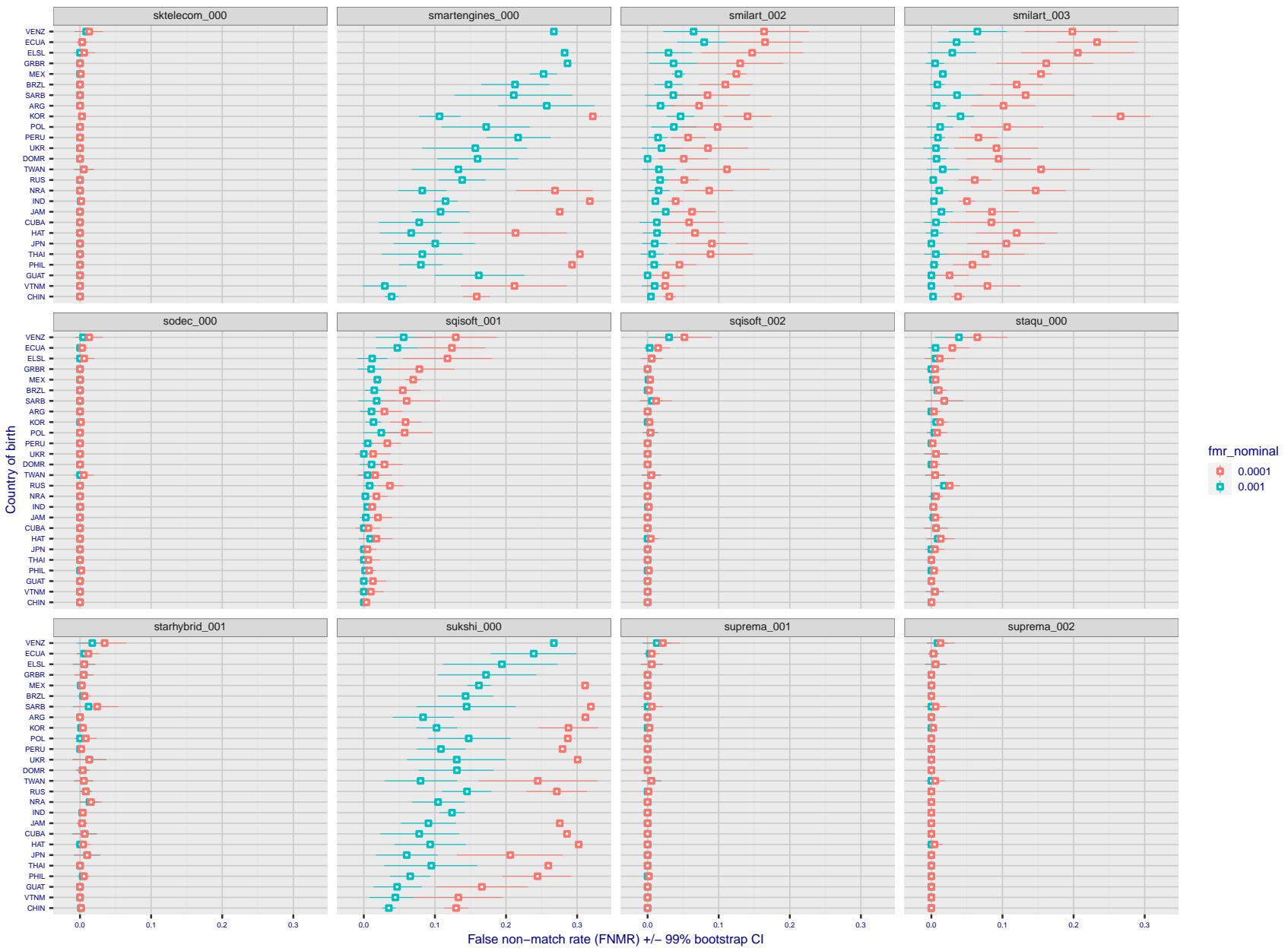


Figure 255: For the visa images, the dots show FNMR by country of birth for two globally set operating thresholds corresponding to $FMR = \{0.001, 0.0001\}$ computed over all on the order of 10^{10} impostor scores. The FMR in each bin will vary also - see subsequent impostor heatmaps in sec. 3.6.1. The figures shows an order of magnitude variation in FNMR across country of birth; these effects are likely due quality variations, then demographics like age and race. The error rates in some cases are zero, and in others the DET is flat so the error rates at the two thresholds are identical. The lines span 1% and 99% of bootstrap replicated FNMR estimates.

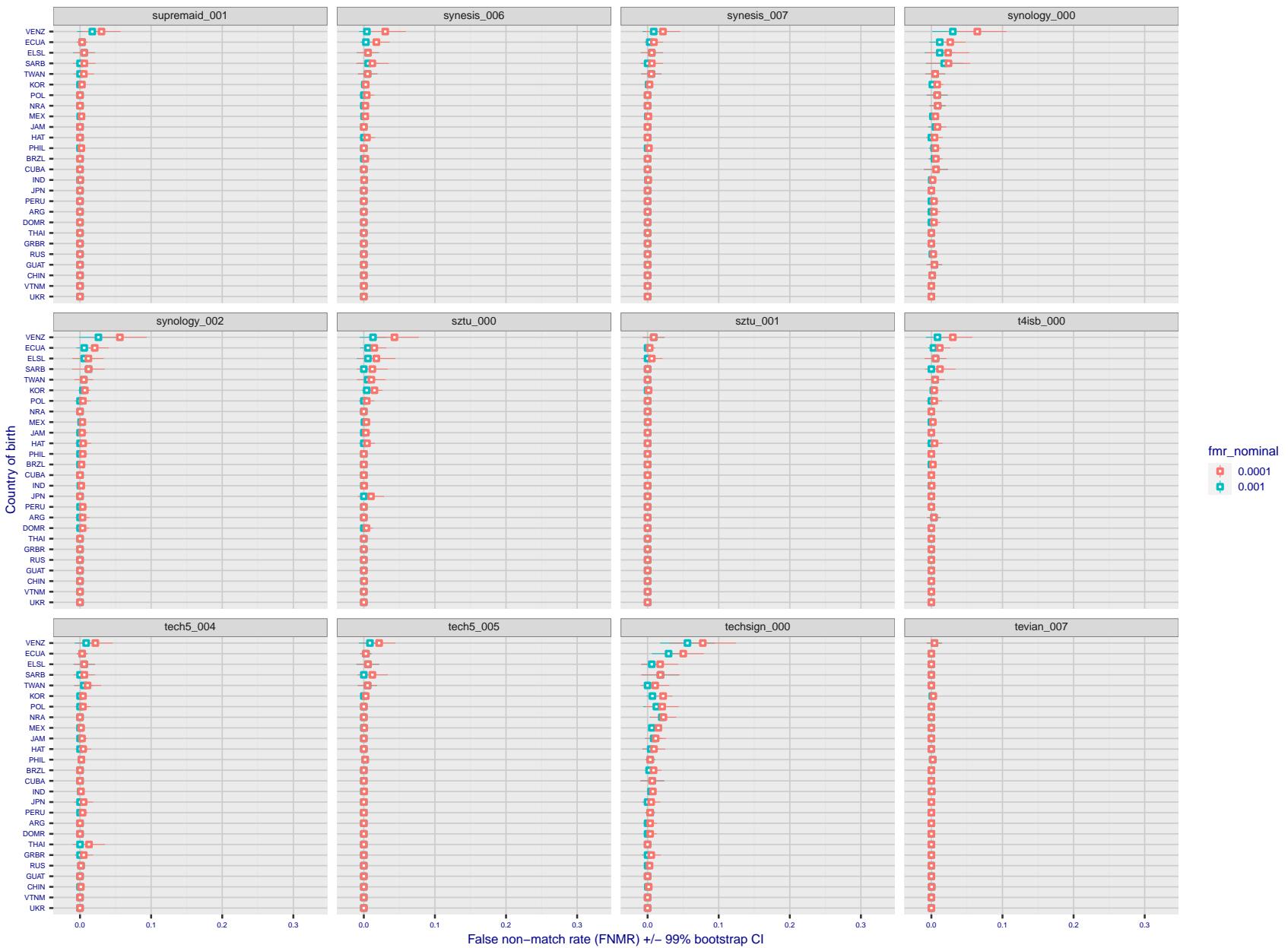


Figure 256: For the visa images, the dots show FNMR by country of birth for two globally set operating thresholds corresponding to $FMR = \{0.001, 0.0001\}$ computed over all on the order of 10^{10} impostor scores. The FMR in each bin will vary also - see subsequent impostor heatmaps in sec. 3.6.1. The figures shows an order of magnitude variation in FNMR across country of birth; these effects are likely due quality variations, then demographics like age and race. The error rates in some cases are zero, and in others the DET is flat so the error rates at the two thresholds are identical. The lines span 1% and 99% of bootstrap replicated FNMR estimates.

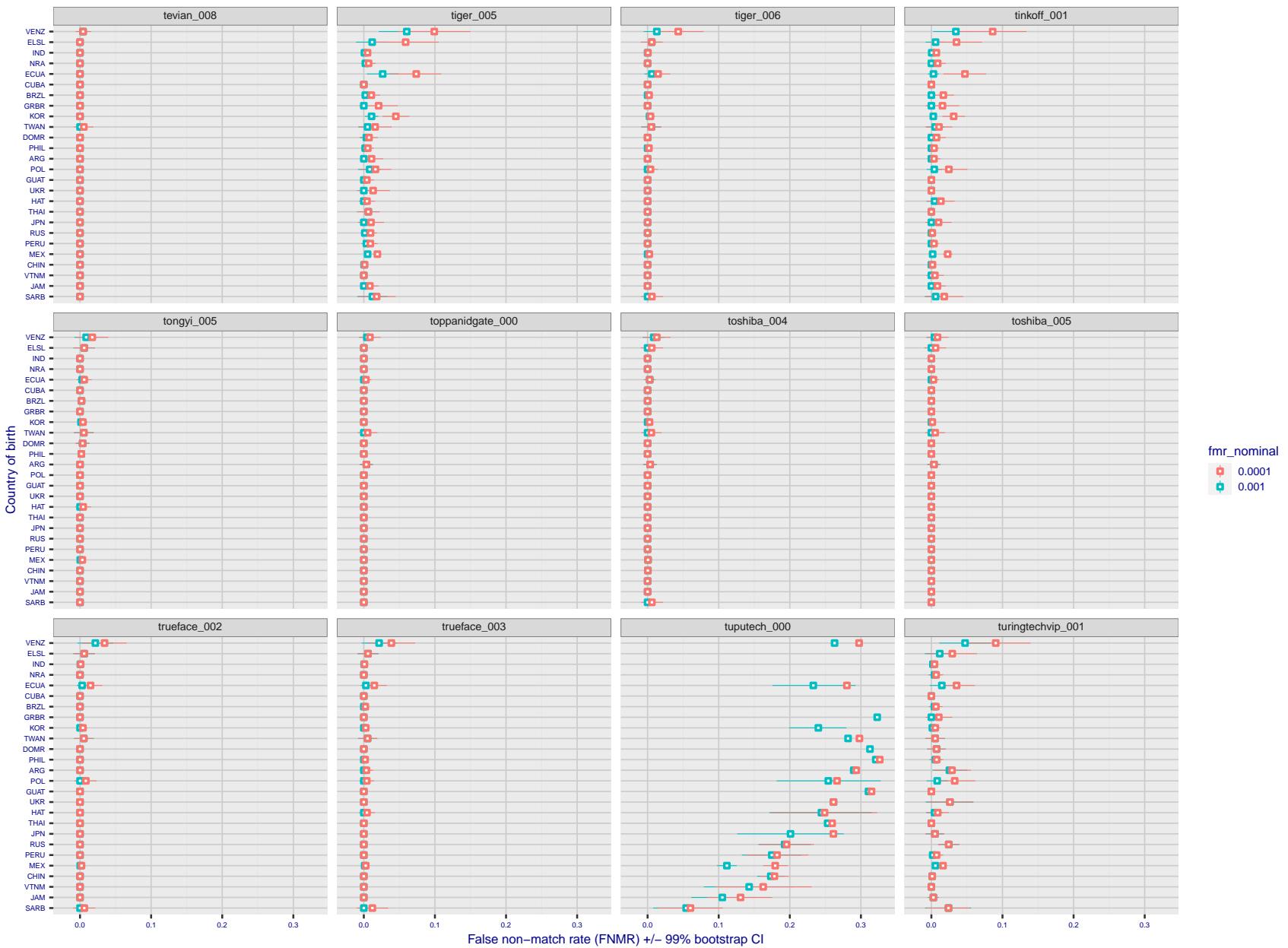


Figure 257: For the visa images, the dots show FNMR by country of birth for two globally set operating thresholds corresponding to $FMR = \{0.001, 0.0001\}$ computed over all on the order of 10^{10} impostor scores. The FMR in each bin will vary also - see subsequent impostor heatmaps in sec. 3.6.1. The figures shows an order of magnitude variation in FNMR across country of birth; these effects are likely due quality variations, then demographics like age and race. The error rates in some cases are zero, and in others the DET is flat so the error rates at the two thresholds are identical. The lines span 1% and 99% of bootstrap replicated FNMR estimates.

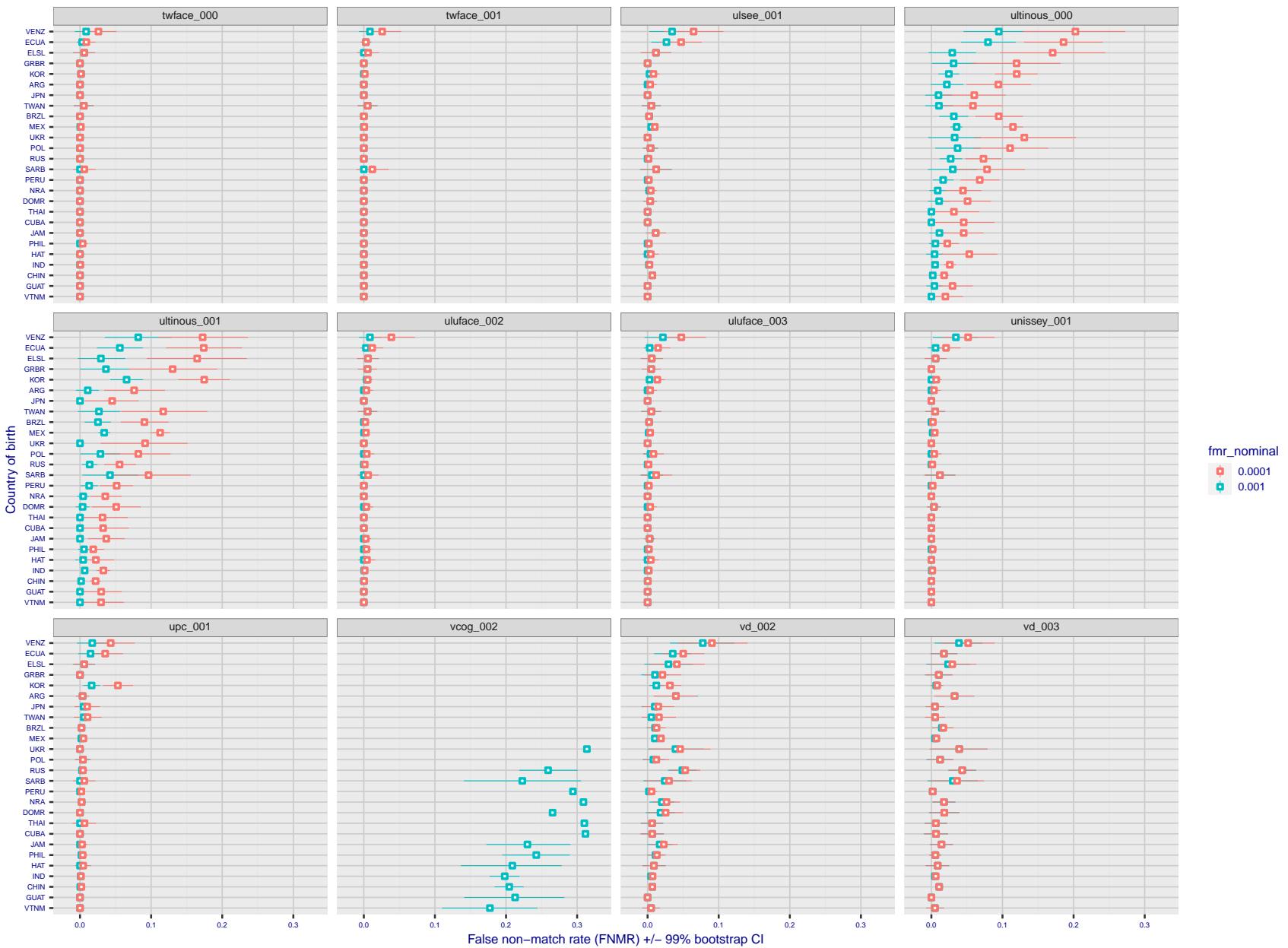


Figure 258: For the visa images, the dots show FNMR by country of birth for two globally set operating thresholds corresponding to $FMR = \{0.001, 0.0001\}$ computed over all on the order of 10^{10} impostor scores. The FMR in each bin will vary also - see subsequent impostor heatmaps in sec. 3.6.1. The figures shows an order of magnitude variation in FNMR across country of birth; these effects are likely due quality variations, then demographics like age and race. The error rates in some cases are zero, and in others the DET is flat so the error rates at the two thresholds are identical. The lines span 1% and 99% of bootstrap replicated FNMR estimates.

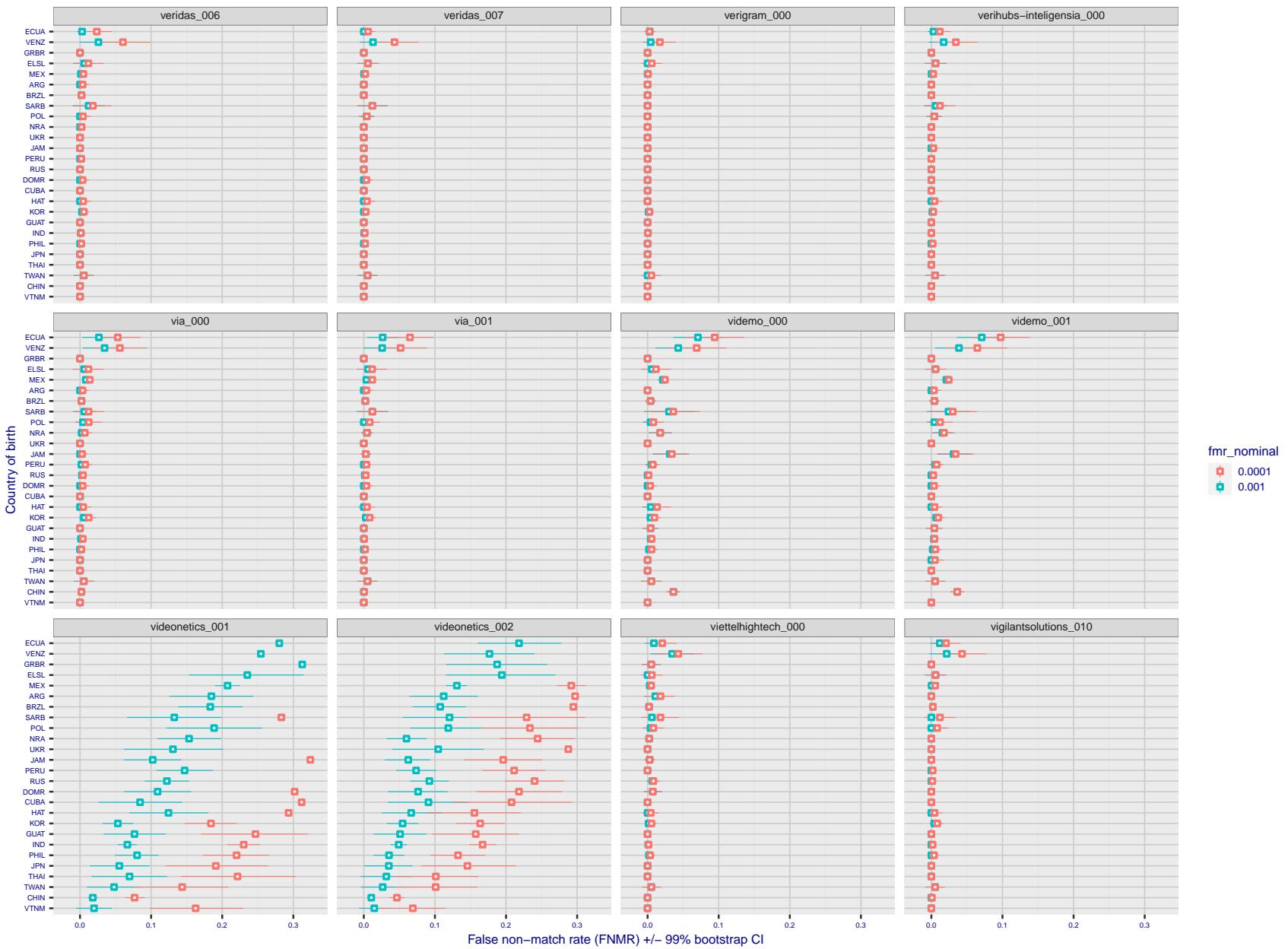


Figure 259: For the visa images, the dots show FNMR by country of birth for two globally set operating thresholds corresponding to $FMR = \{0.001, 0.0001\}$ computed over all on the order of 10^{10} impostor scores. The FMR in each bin will vary also - see subsequent impostor heatmaps in sec. 3.6.1. The figures shows an order of magnitude variation in FNMR across country of birth; these effects are likely due quality variations, then demographics like age and race. The error rates in some cases are zero, and in others the DET is flat so the error rates at the two thresholds are identical. The lines span 1% and 99% of bootstrap replicated FNMR estimates.

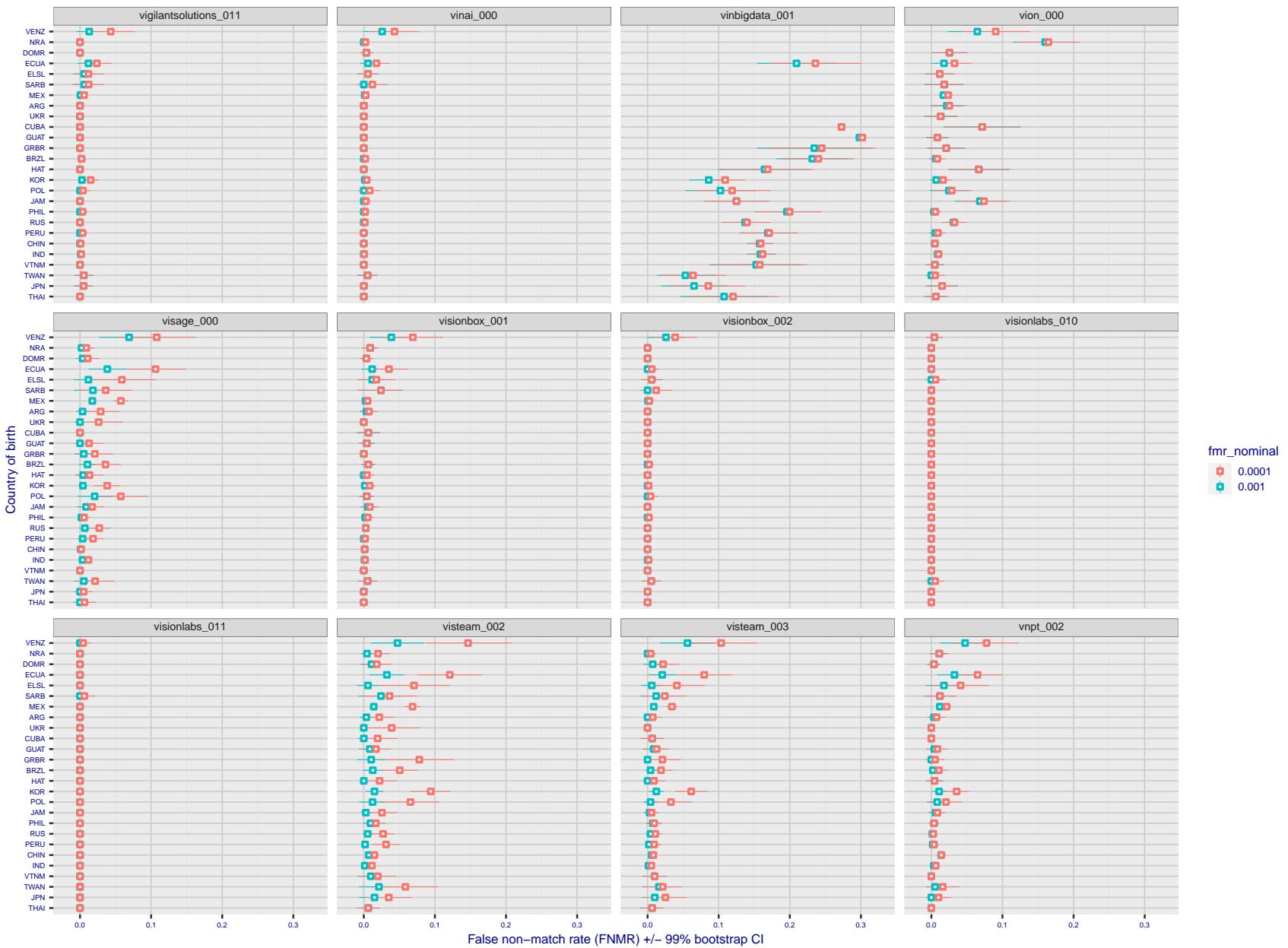


Figure 260: For the visa images, the dots show FNMR by country of birth for two globally set operating thresholds corresponding to $FMR = \{0.001, 0.0001\}$ computed over all on the order of 10^{10} impostor scores. The FMR in each bin will vary also - see subsequent impostor heatmaps in sec. 3.6.1. The figures shows an order of magnitude variation in FNMR across country of birth; these effects are likely due quality variations, then demographics like age and race. The error rates in some cases are zero, and in others the DET is flat so the error rates at the two thresholds are identical. The lines span 1% and 99% of bootstrap replicated FNMR estimates.

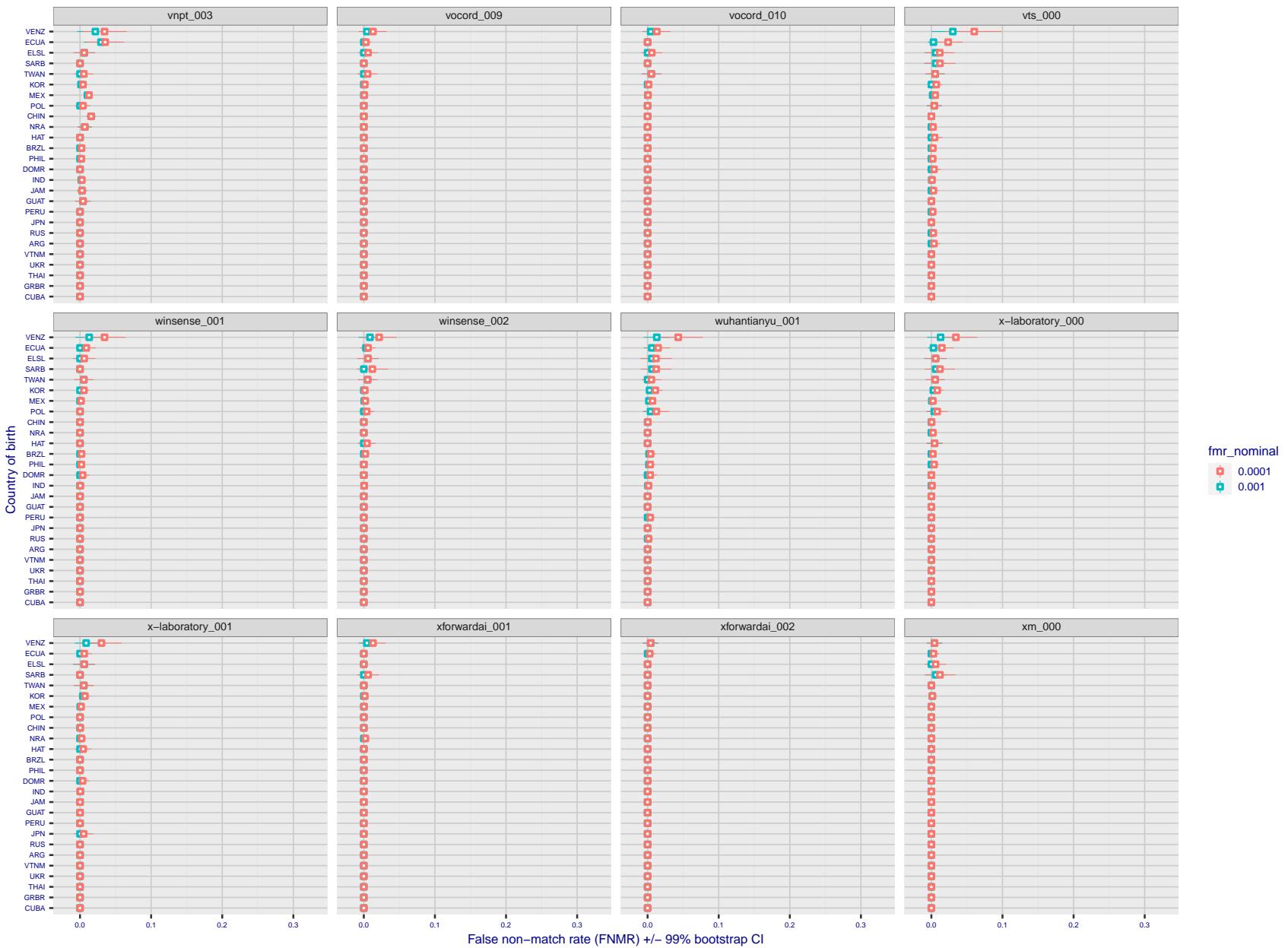


Figure 261: For the visa images, the dots show FNMR by country of birth for two globally set operating thresholds corresponding to $FMR = \{0.001, 0.0001\}$ computed over all on the order of 10^{10} impostor scores. The FMR in each bin will vary also - see subsequent impostor heatmaps in sec. 3.6.1. The figures shows an order of magnitude variation in FNMR across country of birth; these effects are likely due quality variations, then demographics like age and race. The error rates in some cases are zero, and in others the DET is flat so the error rates at the two thresholds are identical. The lines span 1% and 99% of bootstrap replicated FNMR estimates.



Figure 262: For the visa images, the dots show FNMR by country of birth for two globally set operating thresholds corresponding to $FMR = \{0.001, 0.0001\}$ computed over all on the order of 10^{10} impostor scores. The FMR in each bin will vary also - see subsequent impostor heatmaps in sec. 3.6.1. The figures shows an order of magnitude variation in FNMR across country of birth; these effects are likely due quality variations, then demographics like age and race. The error rates in some cases are zero, and in others the DET is flat so the error rates at the two thresholds are identical. The lines span 1% and 99% of bootstrap replicated FNMR estimates.

Caveats: The results may not relate to subject-specific properties. Instead they could reflect image-specific quality differences, which could occur due to collection protocol or software processing variations.

3.5.2 Effect of ageing

Background: Faces change appearance throughout life. This change gradually reduces similarity of a new image to an earlier image. Face recognition algorithms give reduced similarity scores and more frequent false rejections.

Goal: To quantify false non-match rates (FNMR) as a function of elapsed time in an adult population.

Methods: Using the mugshot images, a threshold is set to give FMR = 0.00001 over the entire impostor set. Then FNMR is measured over 1000 bootstrap replications of the genuine scores.

Results: For the visa images, Figure 286 shows how false non-match rates for genuine users, as a function of age group.

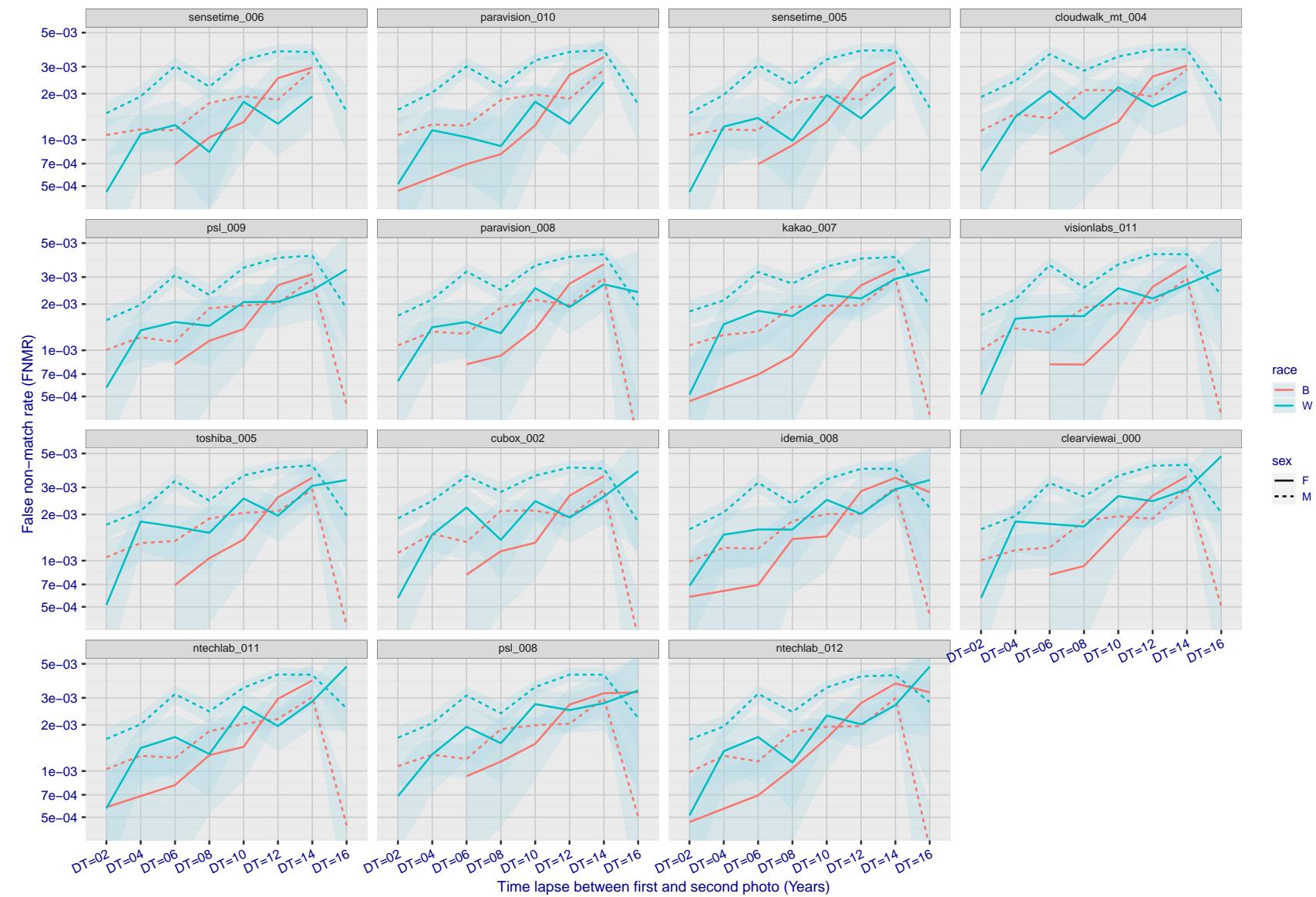


Figure 263: For the mugshot images, FNMR as a function of elapsed time between initial enrollment and second verification images. The panels appear most accurate first, and vertical scale changes on each page. The four traces correspond to images annotated with codes for black female, black male, white female, white male. The threshold is fixed for each algorithm to give FMR = 0.00001 over all (10^8) impostor comparisons. For short time-lapses, the most accurate algorithms give very few errors (FNMR < 0.001) so that the uncertainty estimates are high.

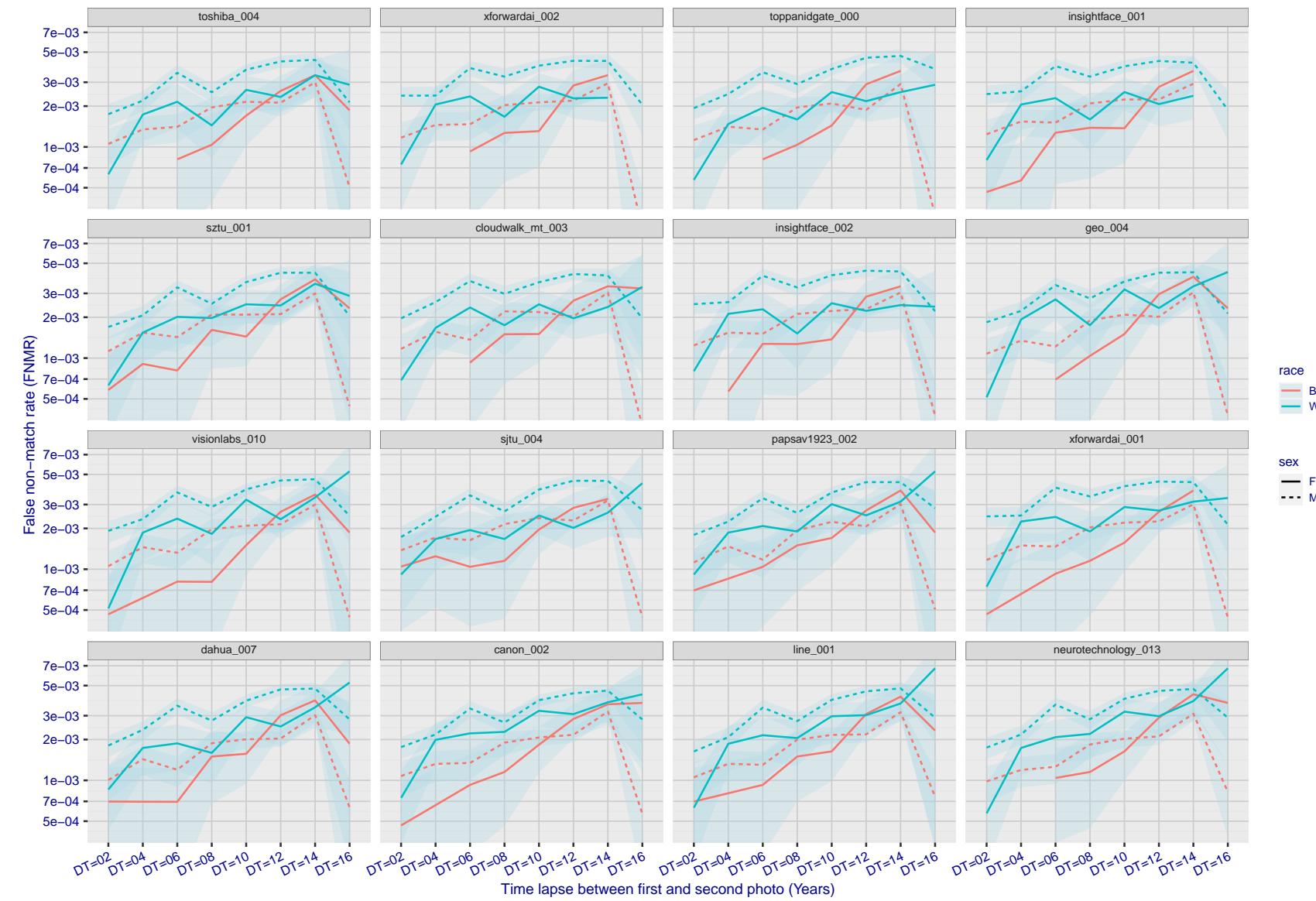


Figure 264: For the mugshot images, FNMR as a function of elapsed time between initial enrollment and second verification images. The panels appear most accurate first, and vertical scale changes on each page. The four traces correspond to images annotated with codes for black female, black male, white female, white male. The threshold is fixed for each algorithm to give FMR = 0.00001 over all (10^8) impostor comparisons. For short time-lapses, the most accurate algorithms give very few errors (FNMR < 0.001) so that the uncertainty estimates are high.

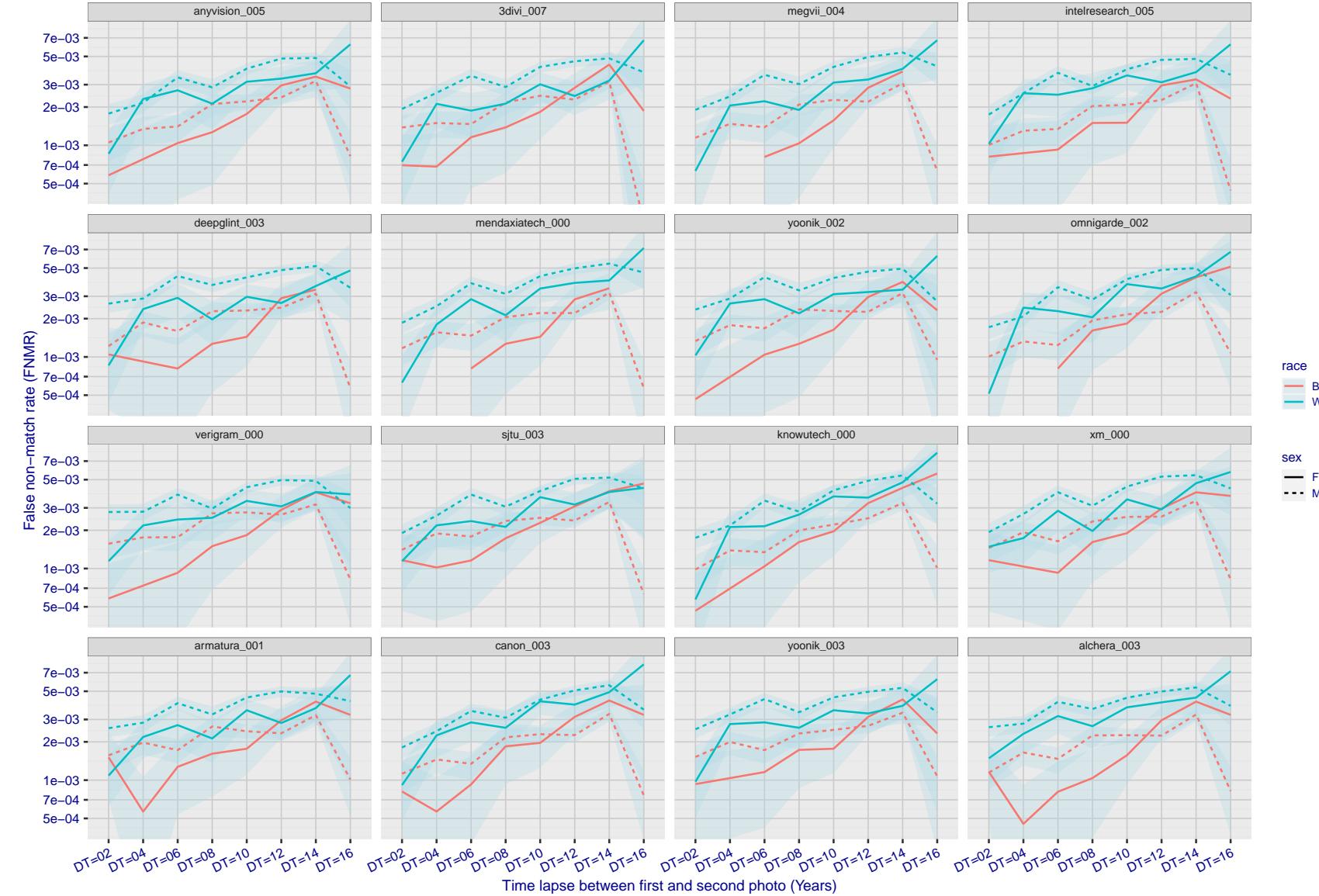
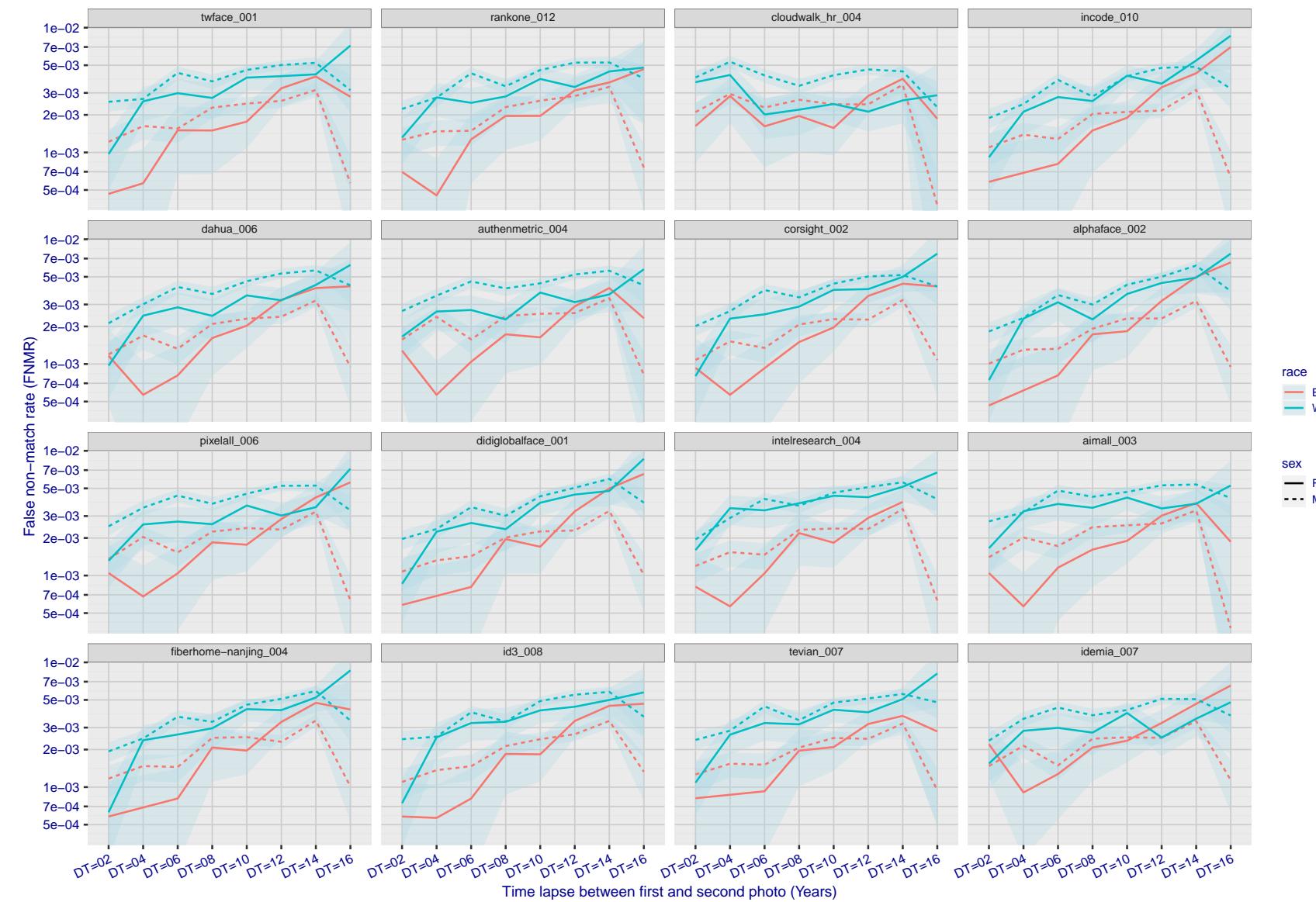


Figure 265: For the mugshot images, FNMR as a function of elapsed time between initial enrollment and second verification images. The panels appear most accurate first, and vertical scale changes on each page. The four traces correspond to images annotated with codes for black female, black male, white female, white male. The threshold is fixed for each algorithm to give $FMR = 0.00001$ over all (10^8) impostor comparisons. For short time-lapses, the most accurate algorithms give very few errors ($FNMR < 0.001$) so that the uncertainty estimates are high.



FNMR(T)
FMR(T)
"False match rate"
"False non-match rate"

Figure 266: For the mugshot images, FNMR as a function of elapsed time between initial enrollment and second verification images. The panels appear most accurate first, and vertical scale changes on each page. The four traces correspond to images annotated with codes for black female, black male, white female, white male. The threshold is fixed for each algorithm to give FMR = 0.00001 over all (10^8) impostor comparisons. For short time-lapses, the most accurate algorithms give very few errors (FNMR < 0.001) so that the uncertainty estimates are high.

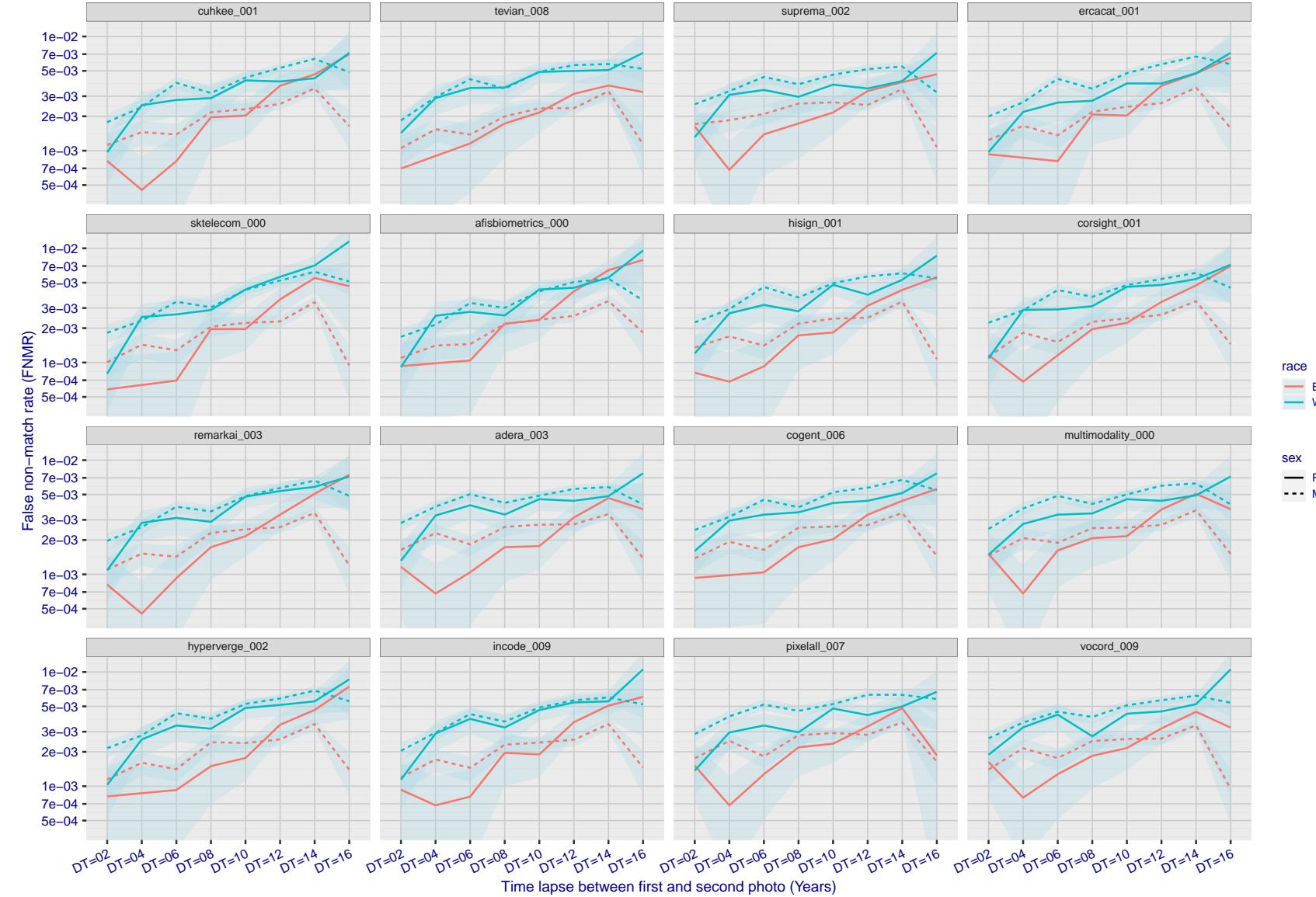


Figure 267: For the mugshot images, FNMR as a function of elapsed time between initial enrollment and second verification images. The panels appear most accurate first, and vertical scale changes on each page. The four traces correspond to images annotated with codes for black female, black male, white female, white male. The threshold is fixed for each algorithm to give FMR = 0.00001 over all (10^8) impostor comparisons. For short time-lapses, the most accurate algorithms give very few errors (FNMR < 0.001) so that the uncertainty estimates are high.

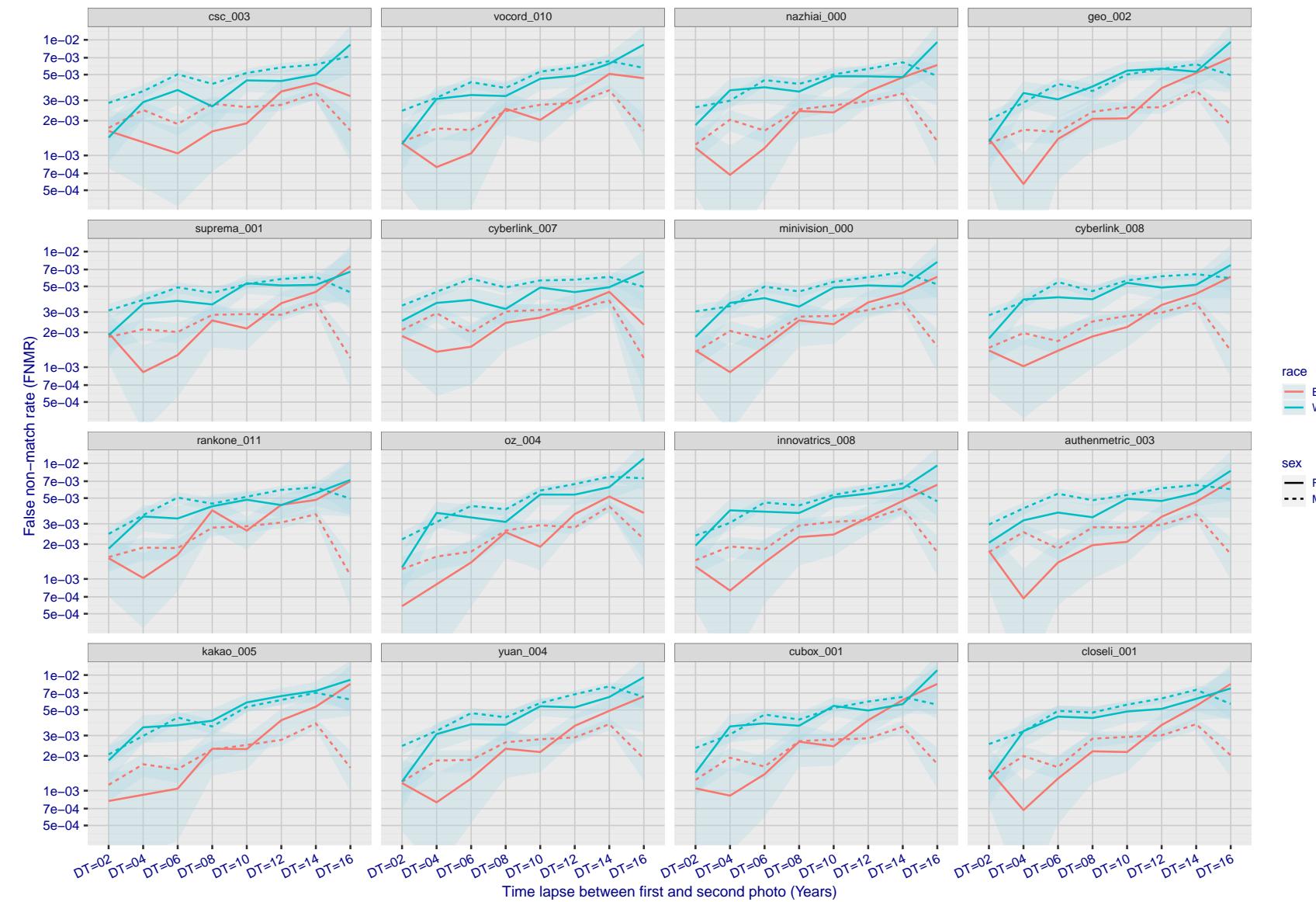


Figure 268: For the mugshot images, FNMR as a function of elapsed time between initial enrollment and second verification images. The panels appear most accurate first, and vertical scale changes on each page. The four traces correspond to images annotated with codes for black female, black male, white female, white male. The threshold is fixed for each algorithm to give $FMR = 0.00001$ over all (10^8) impostor comparisons. For short time-lapses, the most accurate algorithms give very few errors ($FNMR < 0.001$) so that the uncertainty estimates are high.

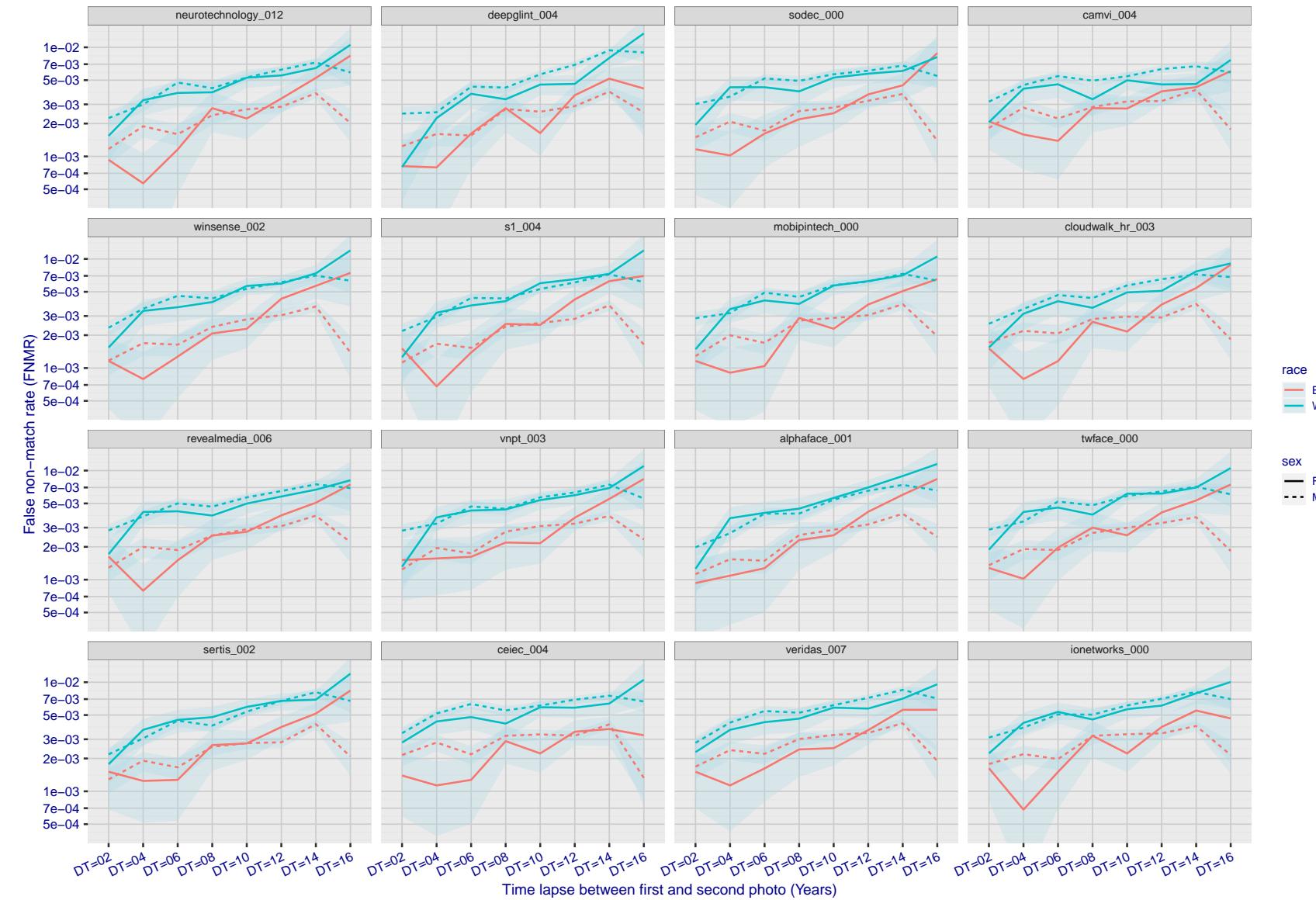


Figure 269: For the mugshot images, FNMR as a function of elapsed time between initial enrollment and second verification images. The panels appear most accurate first, and vertical scale changes on each page. The four traces correspond to images annotated with codes for black female, black male, white female, white male. The threshold is fixed for each algorithm to give $FMR = 0.00001$ over all (10^8) impostor comparisons. For short time-lapses, the most accurate algorithms give very few errors ($FNMR < 0.001$) so that the uncertainty estimates are high.

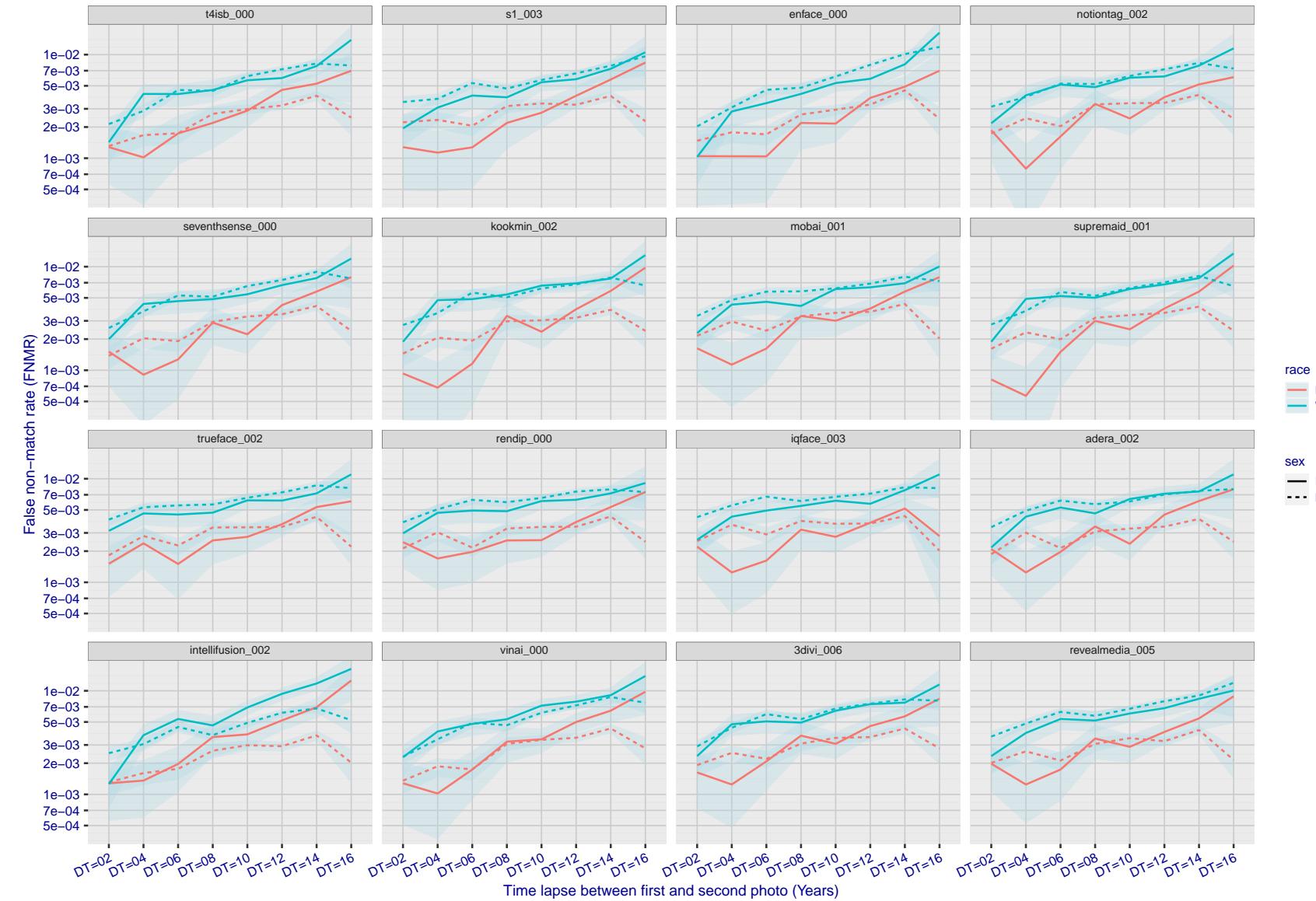


Figure 270: For the mugshot images, FNMR as a function of elapsed time between initial enrollment and second verification images. The panels appear most accurate first, and vertical scale changes on each page. The four traces correspond to images annotated with codes for black female, black male, white female, white male. The threshold is fixed for each algorithm to give $FMR = 0.00001$ over all (10^8) impostor comparisons. For short time-lapses, the most accurate algorithms give very few errors ($FNMR < 0.001$) so that the uncertainty estimates are high.

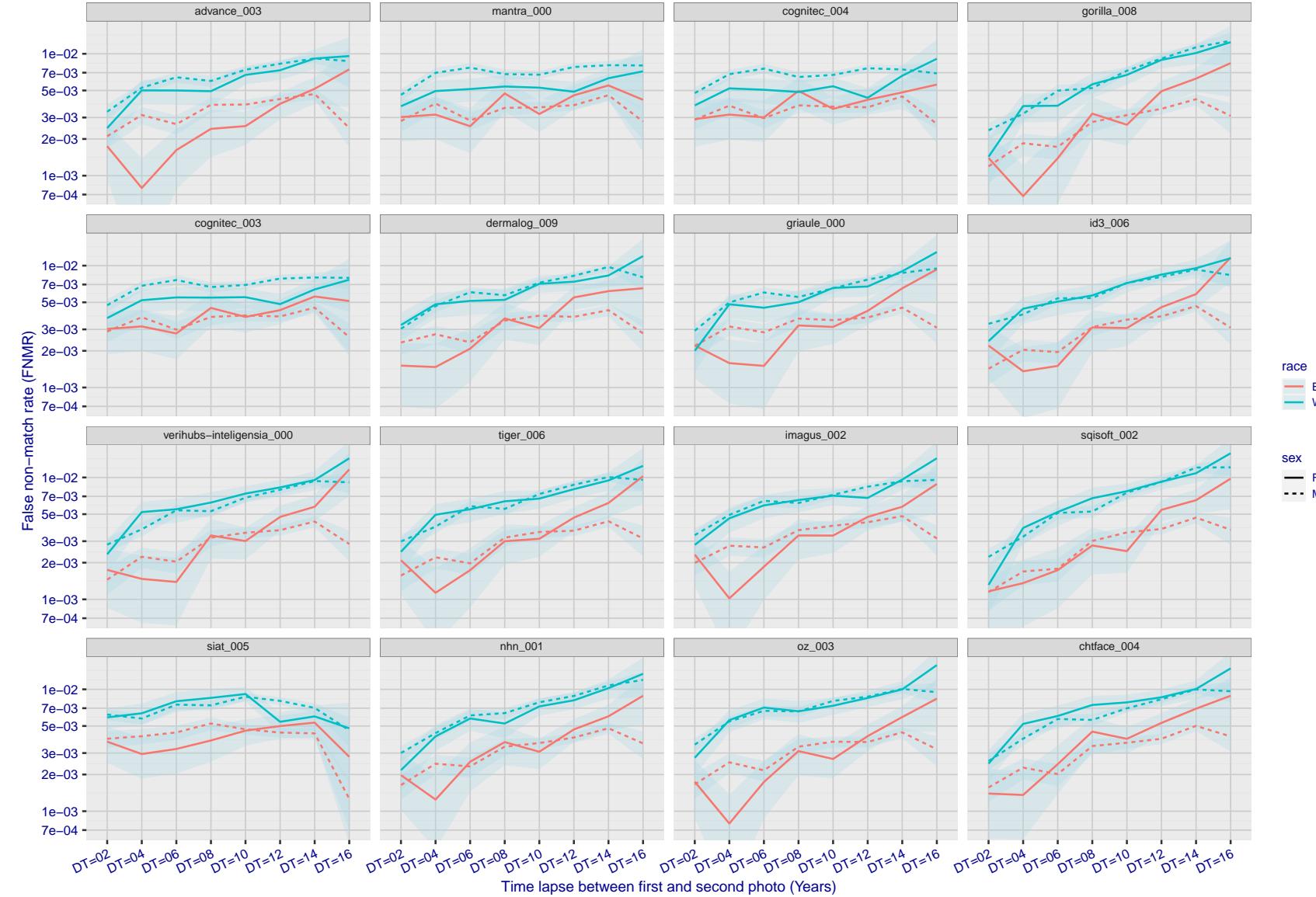


Figure 271: For the mugshot images, FNMR as a function of elapsed time between initial enrollment and second verification images. The panels appear most accurate first, and vertical scale changes on each page. The four traces correspond to images annotated with codes for black female, black male, white female, white male. The threshold is fixed for each algorithm to give $FMR = 0.00001$ over all (10^8) impostor comparisons. For short time-lapses, the most accurate algorithms give very few errors ($FNMR < 0.001$) so that the uncertainty estimates are high.

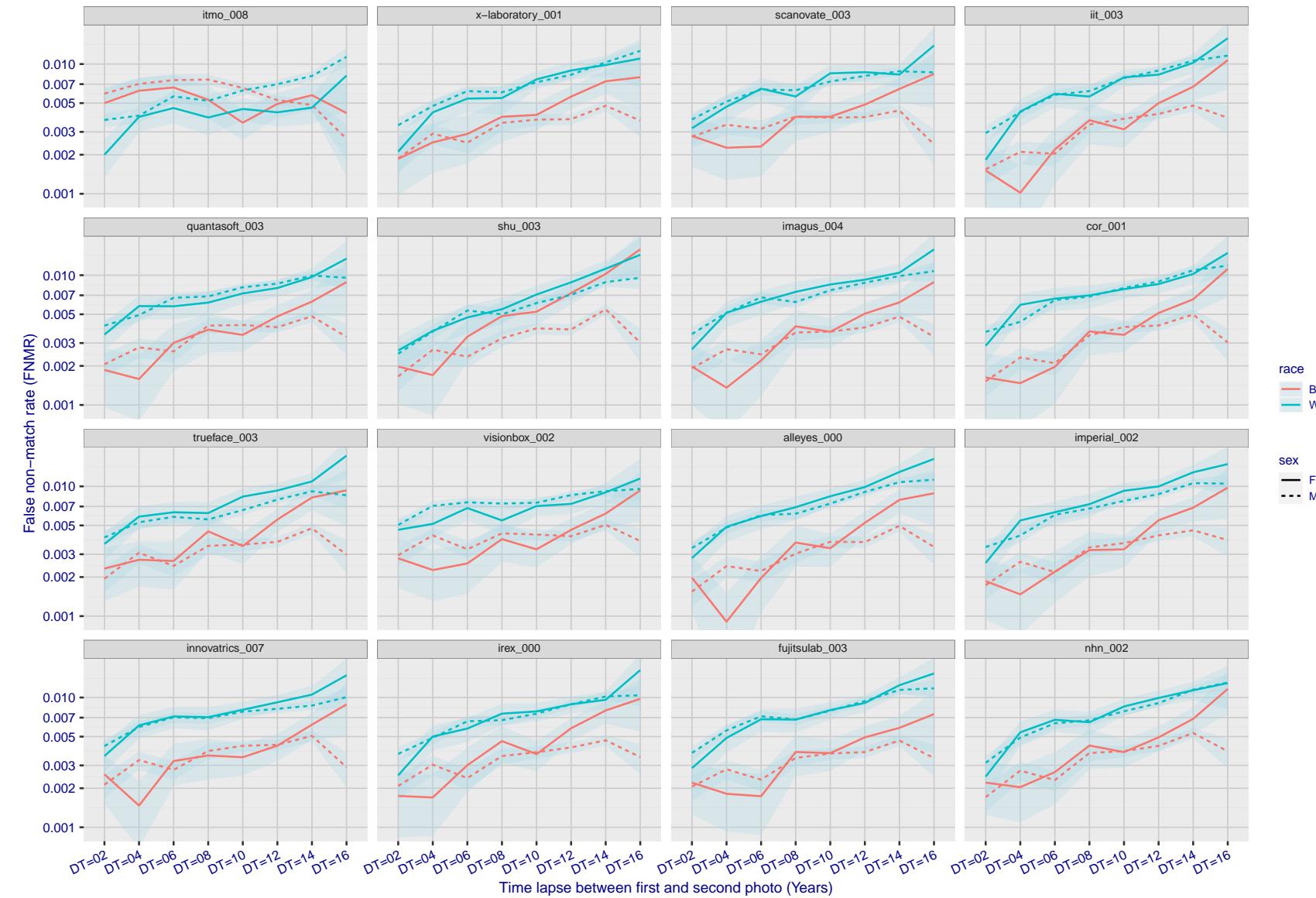


Figure 272: For the mugshot images, FNMR as a function of elapsed time between initial enrollment and second verification images. The panels appear most accurate first, and vertical scale changes on each page. The four traces correspond to images annotated with codes for black female, black male, white female, white male. The threshold is fixed for each algorithm to give FMR = 0.00001 over all (10^8) impostor comparisons. For short time-lapses, the most accurate algorithms give very few errors (FNMR < 0.001) so that the uncertainty estimates are high.

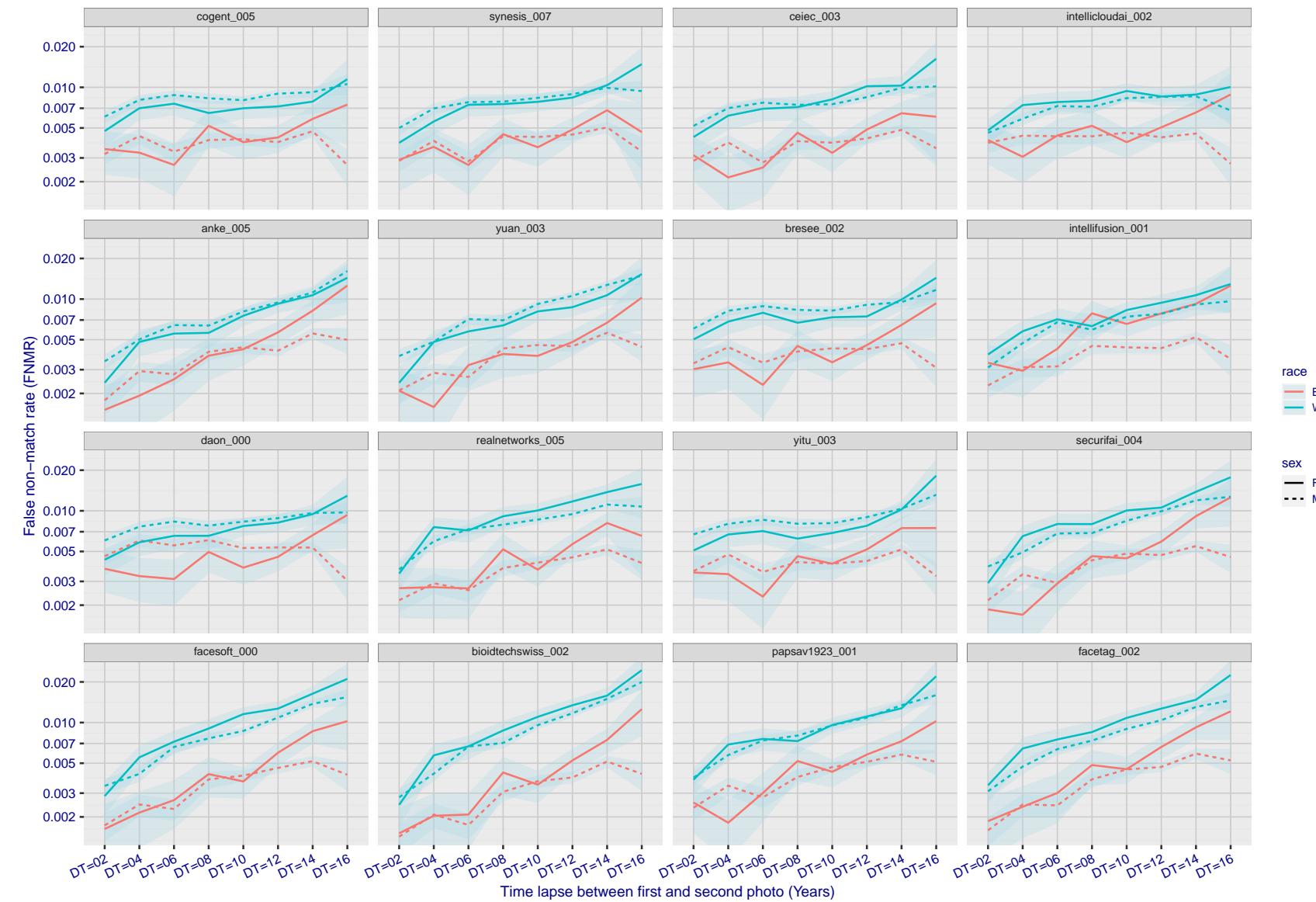


Figure 273: For the mugshot images, FNMR as a function of elapsed time between initial enrollment and second verification images. The panels appear most accurate first, and vertical scale changes on each page. The four traces correspond to images annotated with codes for black female, black male, white female, white male. The threshold is fixed for each algorithm to give FMR = 0.00001 over all (10^8) impostor comparisons. For short time-lapses, the most accurate algorithms give very few errors (FNMR < 0.001) so that the uncertainty estimates are high.

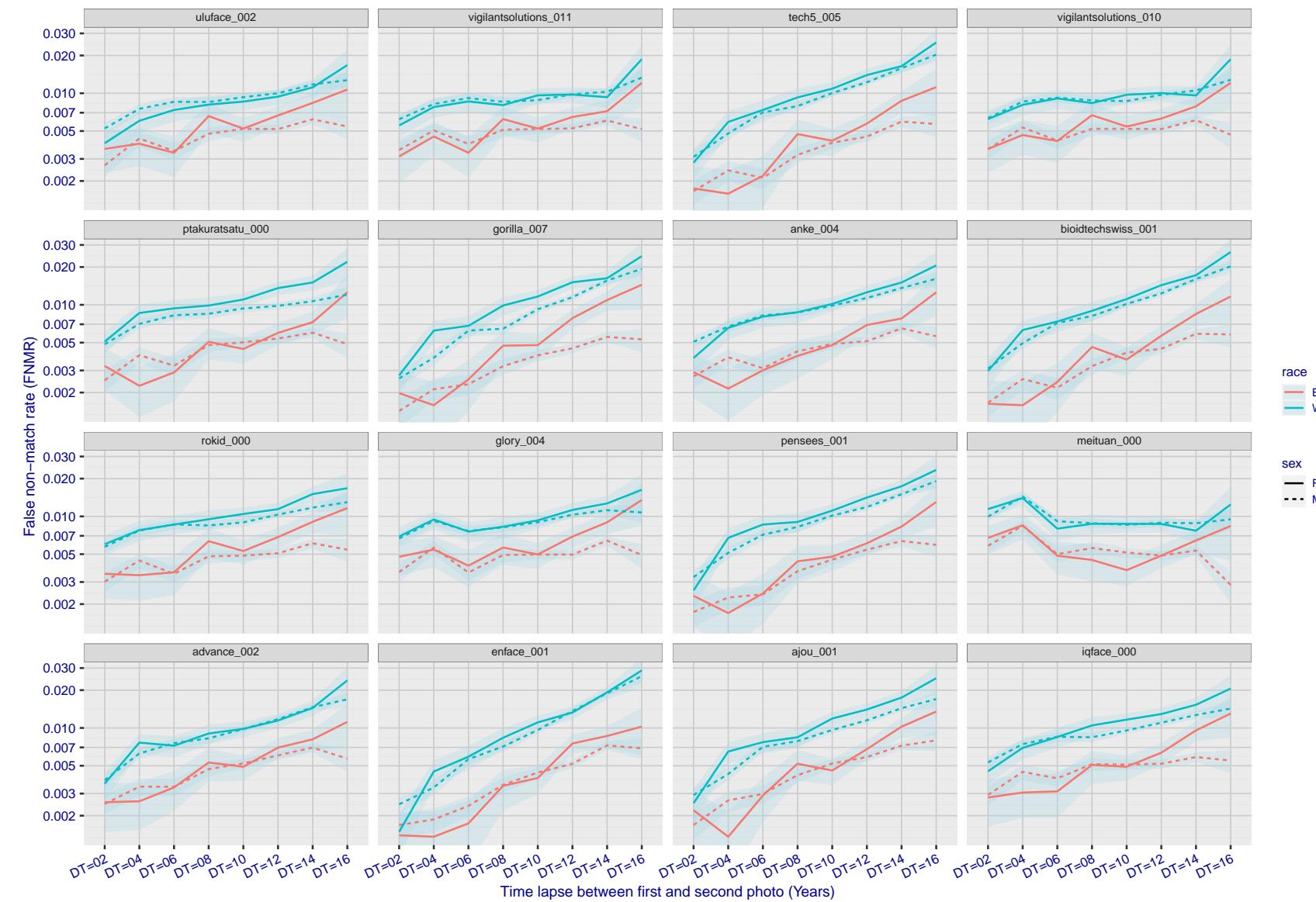


Figure 274: For the mugshot images, FNMR as a function of elapsed time between initial enrollment and second verification images. The panels appear most accurate first, and vertical scale changes on each page. The four traces correspond to images annotated with codes for black female, black male, white female, white male. The threshold is fixed for each algorithm to give FMR = 0.00001 over all (10^8) impostor comparisons. For short time-lapses, the most accurate algorithms give very few errors (FNMR < 0.001) so that the uncertainty estimates are high.

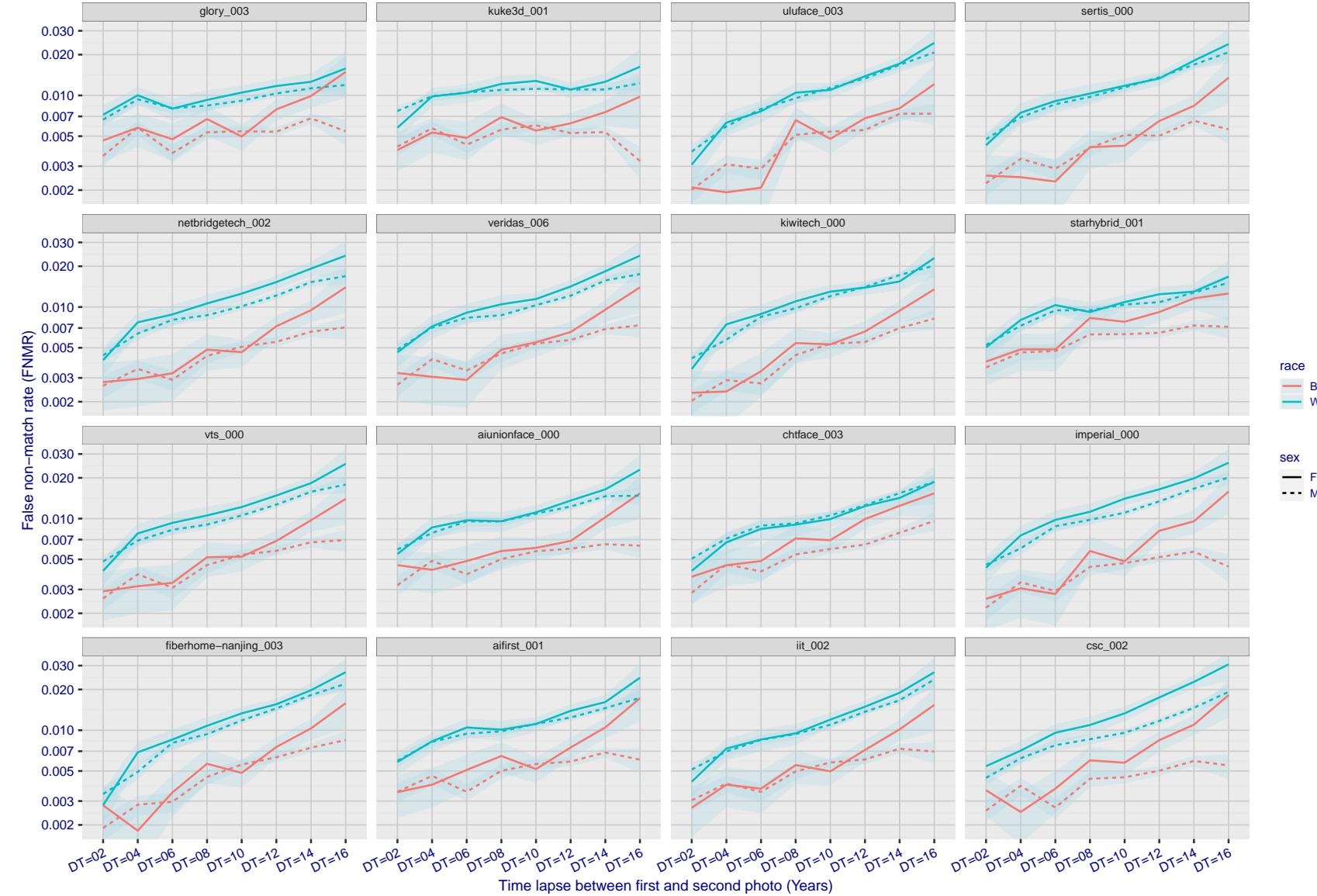


Figure 275: For the mugshot images, FNMR as a function of elapsed time between initial enrollment and second verification images. The panels appear most accurate first, and vertical scale changes on each page. The four traces correspond to images annotated with codes for black female, black male, white female, white male. The threshold is fixed for each algorithm to give FMR = 0.00001 over all (10^8) impostor comparisons. For short time-lapses, the most accurate algorithms give very few errors (FNMR < 0.001) so that the uncertainty estimates are high.

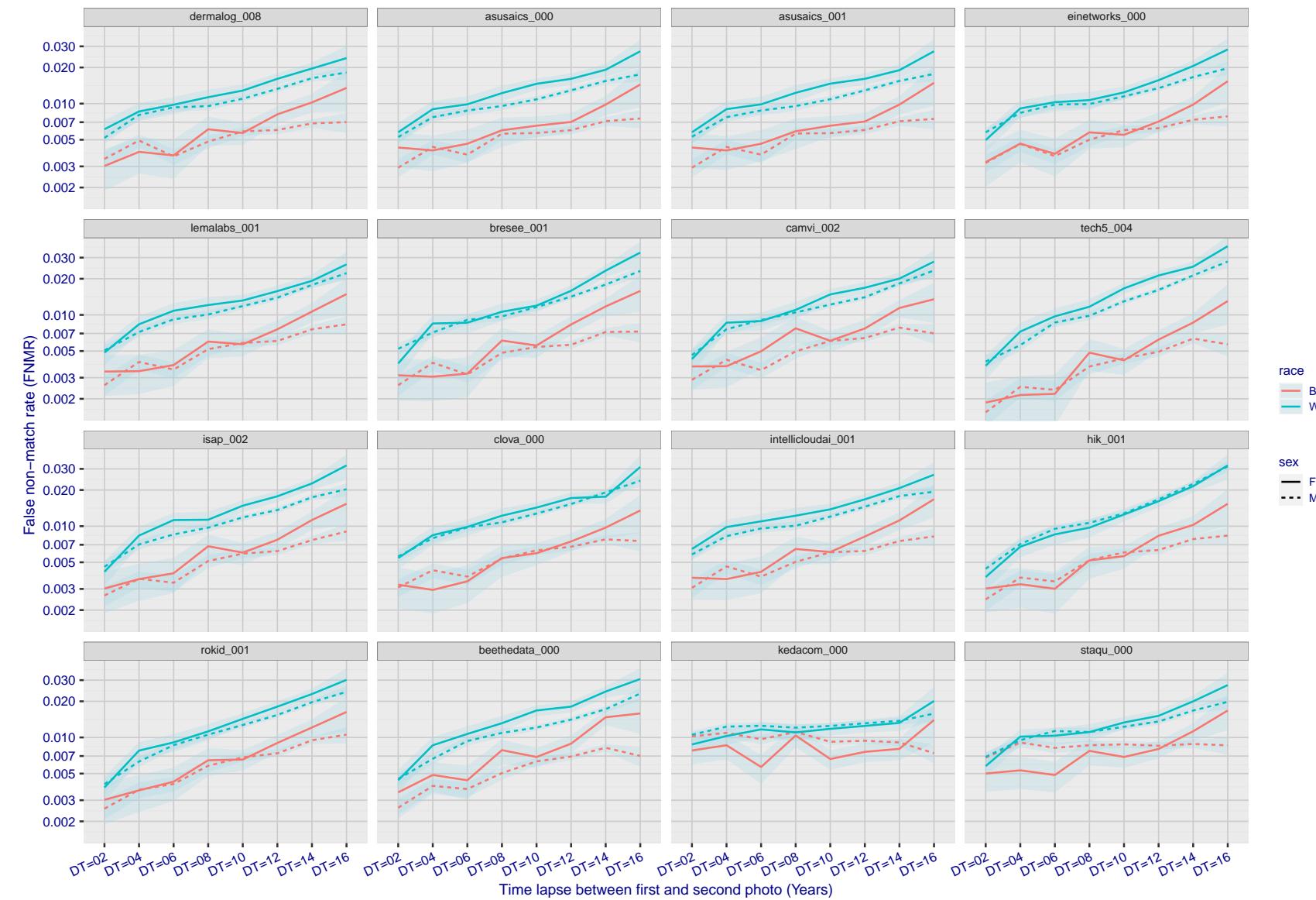


Figure 276: For the mugshot images, FNMR as a function of elapsed time between initial enrollment and second verification images. The panels appear most accurate first, and vertical scale changes on each page. The four traces correspond to images annotated with codes for black female, black male, white female, white male. The threshold is fixed for each algorithm to give FMR = 0.00001 over all (10^8) impostor comparisons. For short time-lapses, the most accurate algorithms give very few errors (FNMR < 0.001) so that the uncertainty estimates are high.

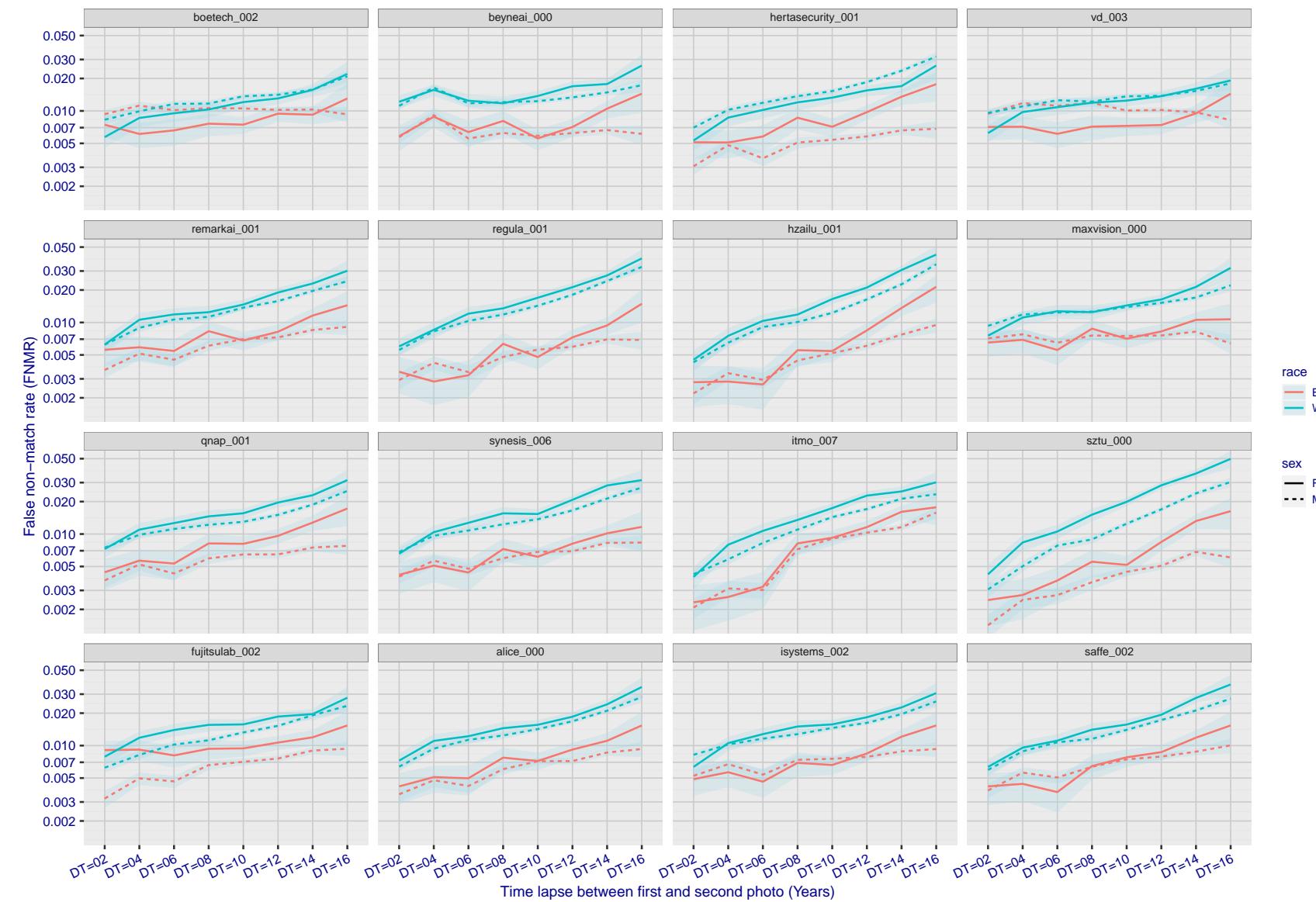


Figure 277: For the mugshot images, FNMR as a function of elapsed time between initial enrollment and second verification images. The panels appear most accurate first, and vertical scale changes on each page. The four traces correspond to images annotated with codes for black female, black male, white female, white male. The threshold is fixed for each algorithm to give FMR = 0.00001 over all (10^8) impostor comparisons. For short time-lapses, the most accurate algorithms give very few errors (FNMR < 0.001) so that the uncertainty estimates are high.

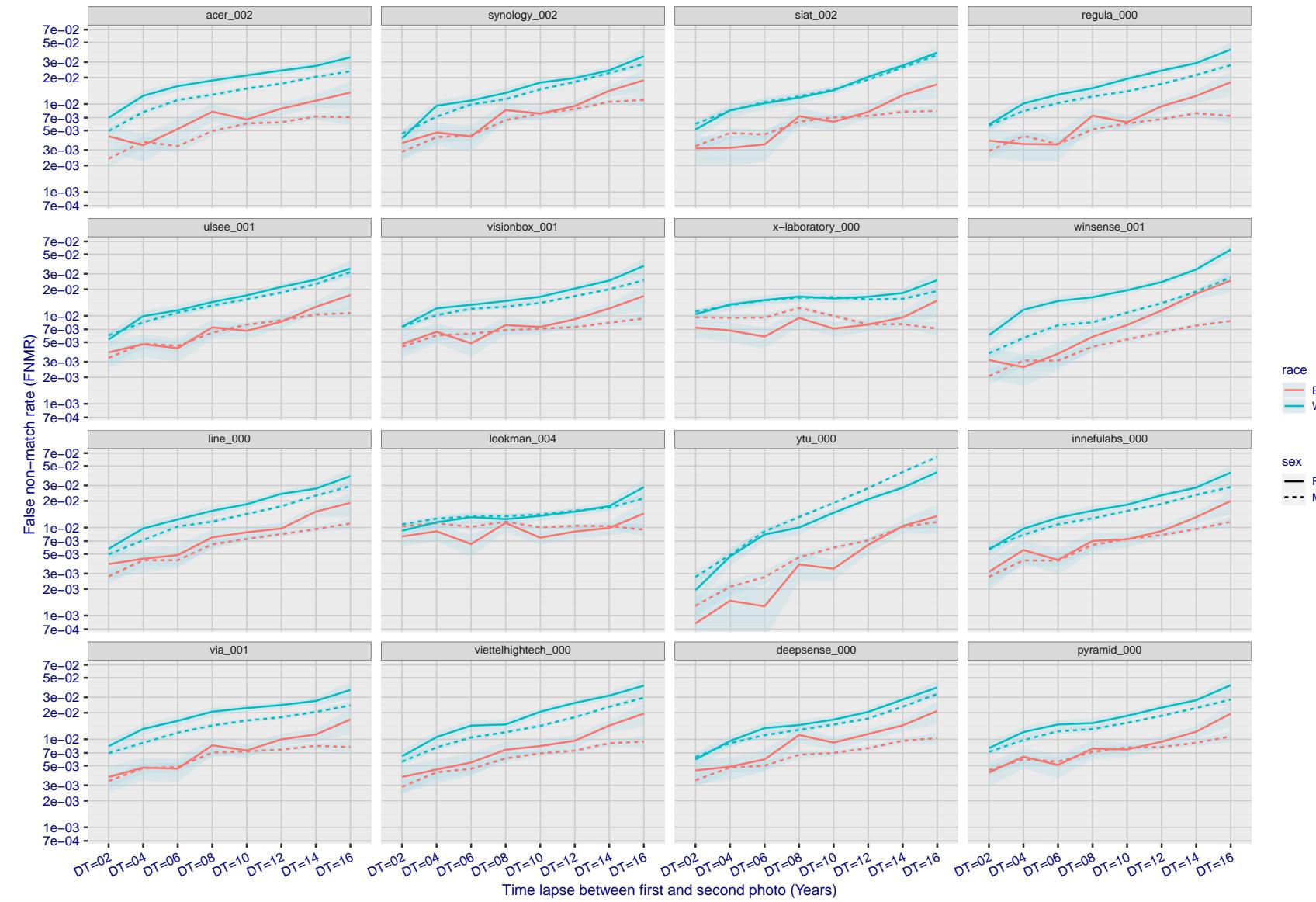


Figure 278: For the mugshot images, FNMR as a function of elapsed time between initial enrollment and second verification images. The panels appear most accurate first, and vertical scale changes on each page. The four traces correspond to images annotated with codes for black female, black male, white female, white male. The threshold is fixed for each algorithm to give $FMR = 0.00001$ over all (10^8) impostor comparisons. For short time-lapses, the most accurate algorithms give very few errors ($FNMR < 0.001$) so that the uncertainty estimates are high.

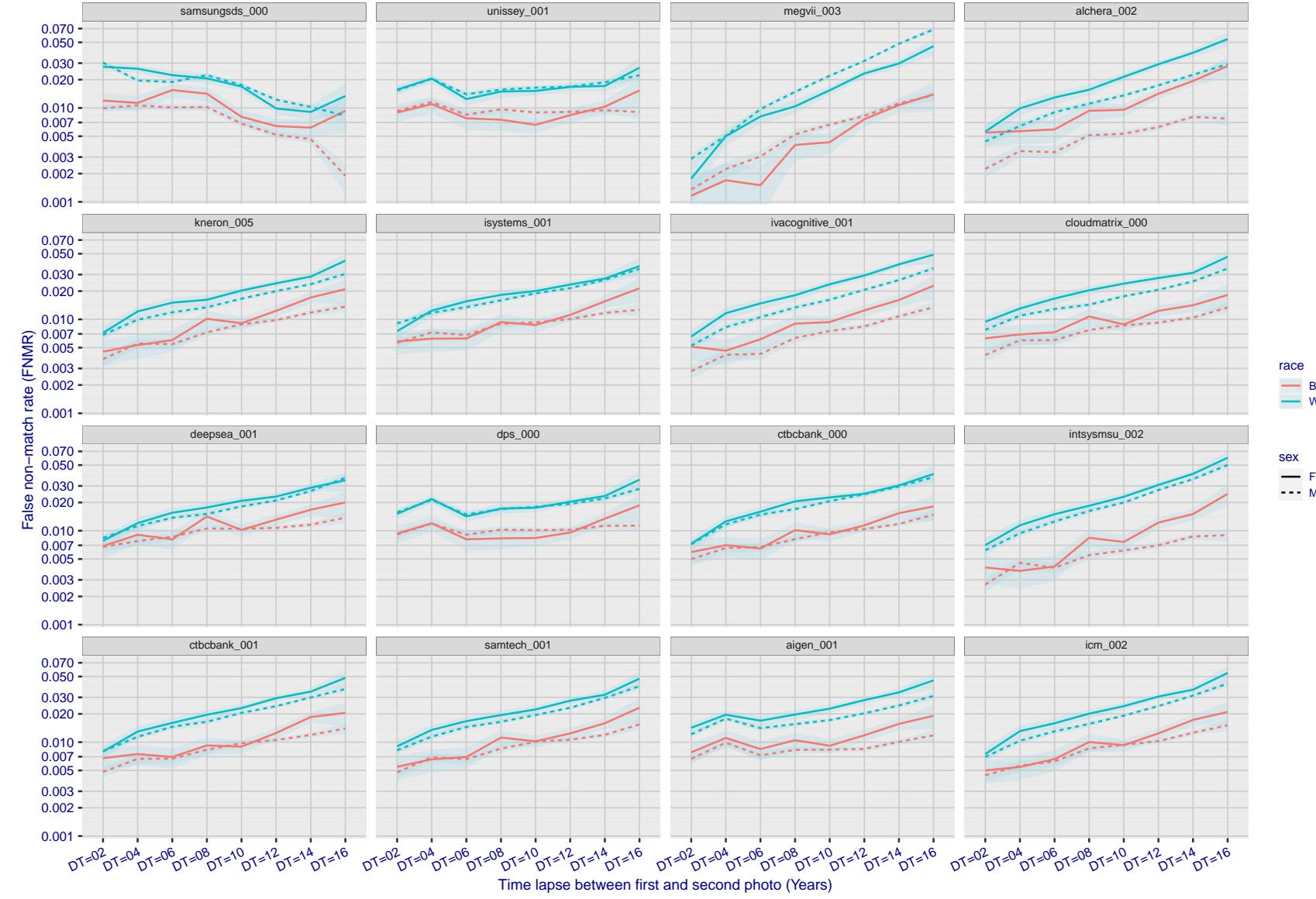


Figure 279: For the mugshot images, FNMR as a function of elapsed time between initial enrollment and second verification images. The panels appear most accurate first, and vertical scale changes on each page. The four traces correspond to images annotated with codes for black female, black male, white female, white male. The threshold is fixed for each algorithm to give FMR = 0.00001 over all (10^8) impostor comparisons. For short time-lapses, the most accurate algorithms give very few errors (FNMR < 0.001) so that the uncertainty estimates are high.

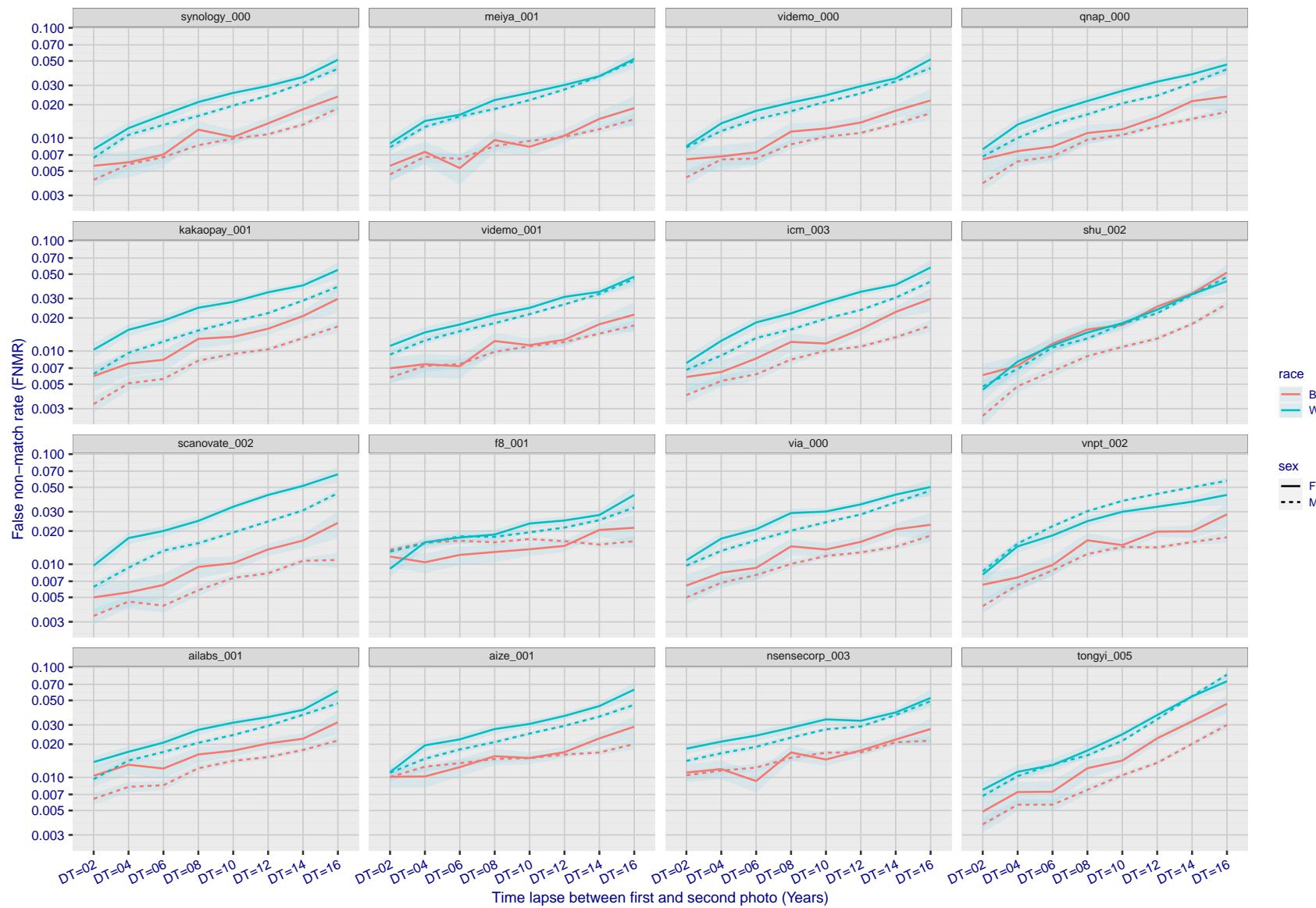


Figure 280: For the mugshot images, FNMR as a function of elapsed time between initial enrollment and second verification images. The panels appear most accurate first, and vertical scale changes on each page. The four traces correspond to images annotated with codes for black female, black male, white female, white male. The threshold is fixed for each algorithm to give FMR = 0.00001 over all (10^8) impostor comparisons. For short time-lapses, the most accurate algorithms give very few errors (FNMR < 0.001) so that the uncertainty estimates are high.

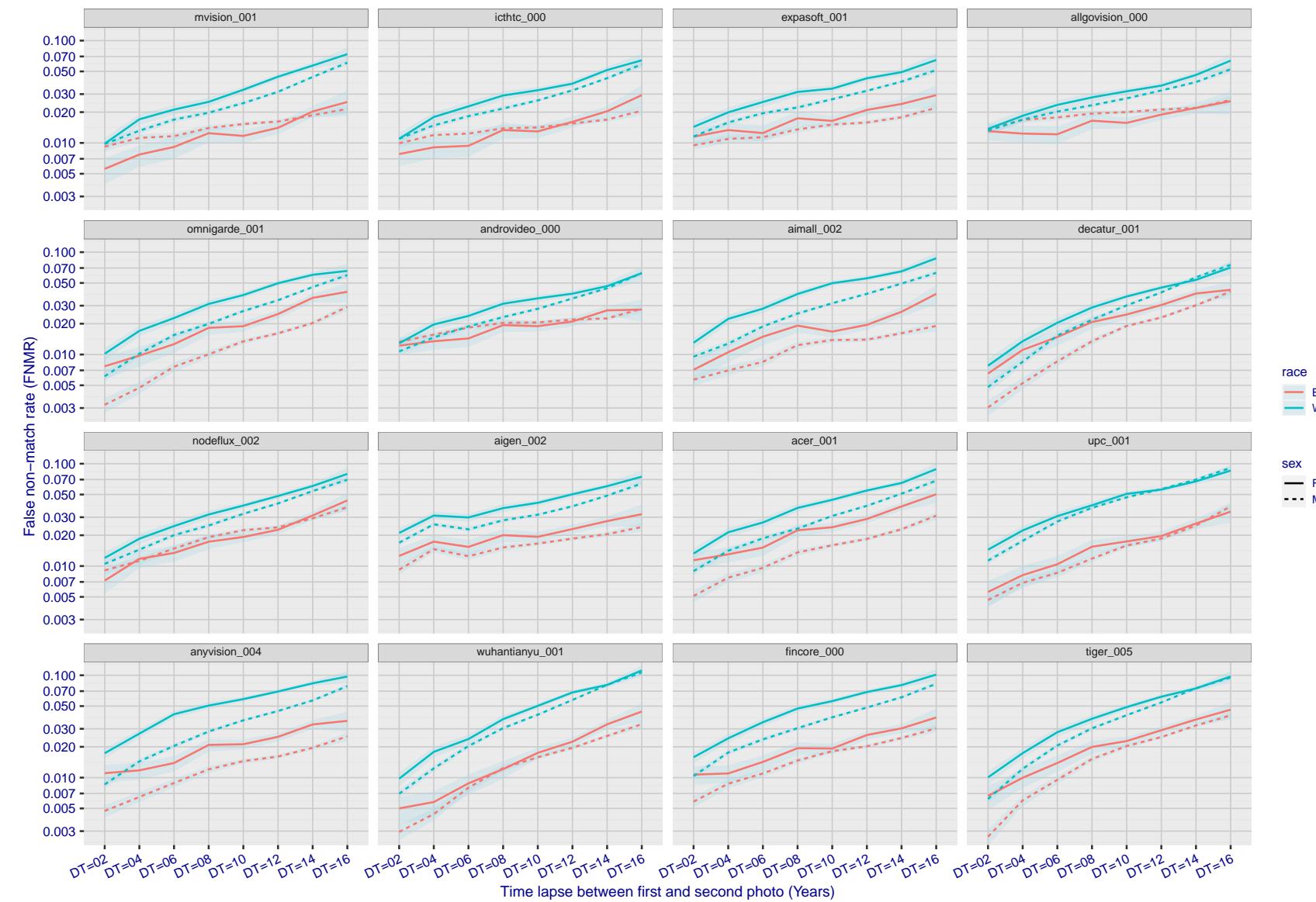


Figure 281: For the mugshot images, FNMR as a function of elapsed time between initial enrollment and second verification images. The panels appear most accurate first, and vertical scale changes on each page. The four traces correspond to images annotated with codes for black female, black male, white female, white male. The threshold is fixed for each algorithm to give $FMR = 0.00001$ over all (10^8) impostor comparisons. For short time-lapses, the most accurate algorithms give very few errors ($FNMR < 0.001$) so that the uncertainty estimates are high.

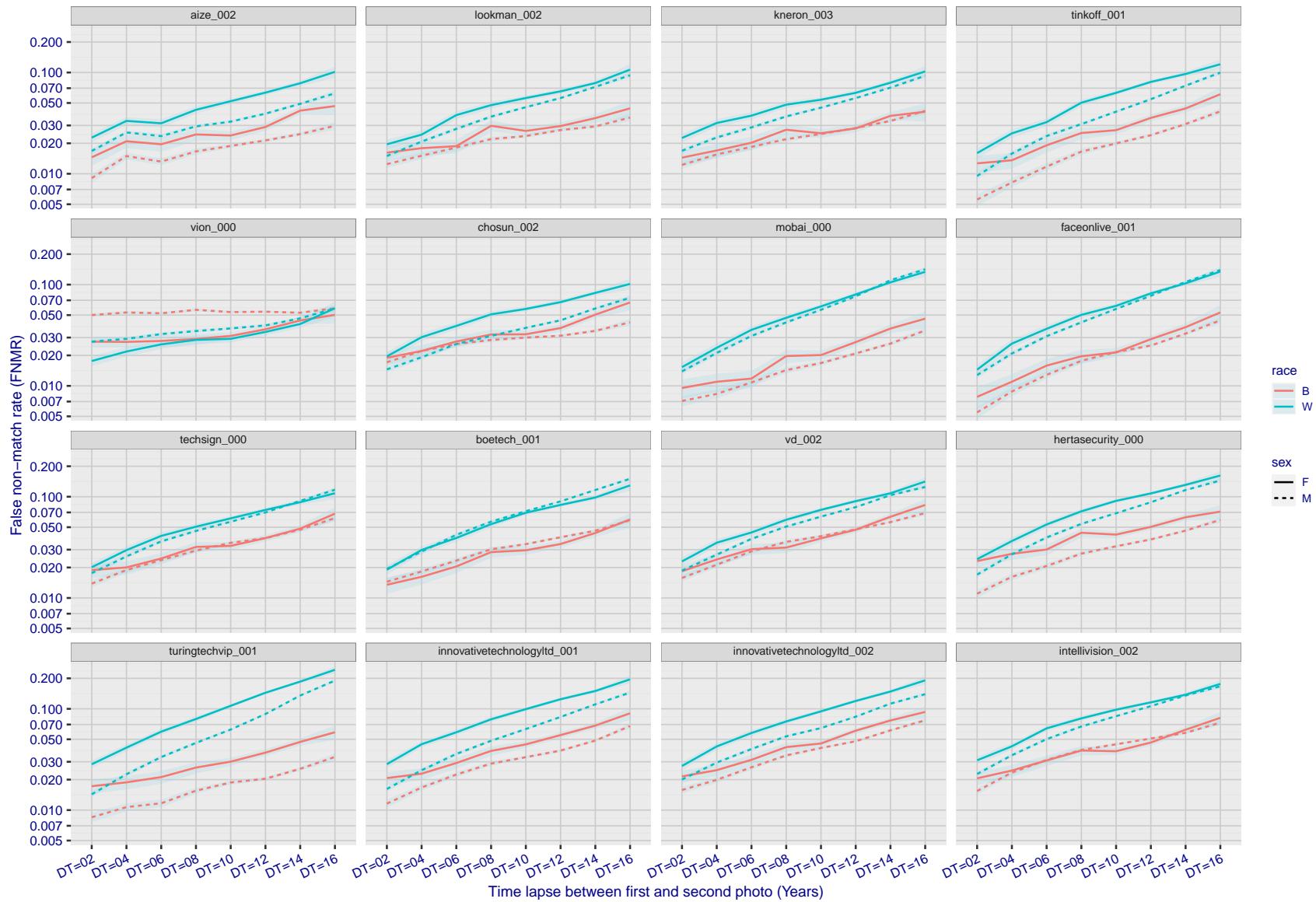


Figure 282: For the mugshot images, FNMR as a function of elapsed time between initial enrollment and second verification images. The panels appear most accurate first, and vertical scale changes on each page. The four traces correspond to images annotated with codes for black female, black male, white female, white male. The threshold is fixed for each algorithm to give $FMR = 0.00001$ over all (10^8) impostor comparisons. For short time-lapses, the most accurate algorithms give very few errors ($FNMR < 0.001$) so that the uncertainty estimates are high.

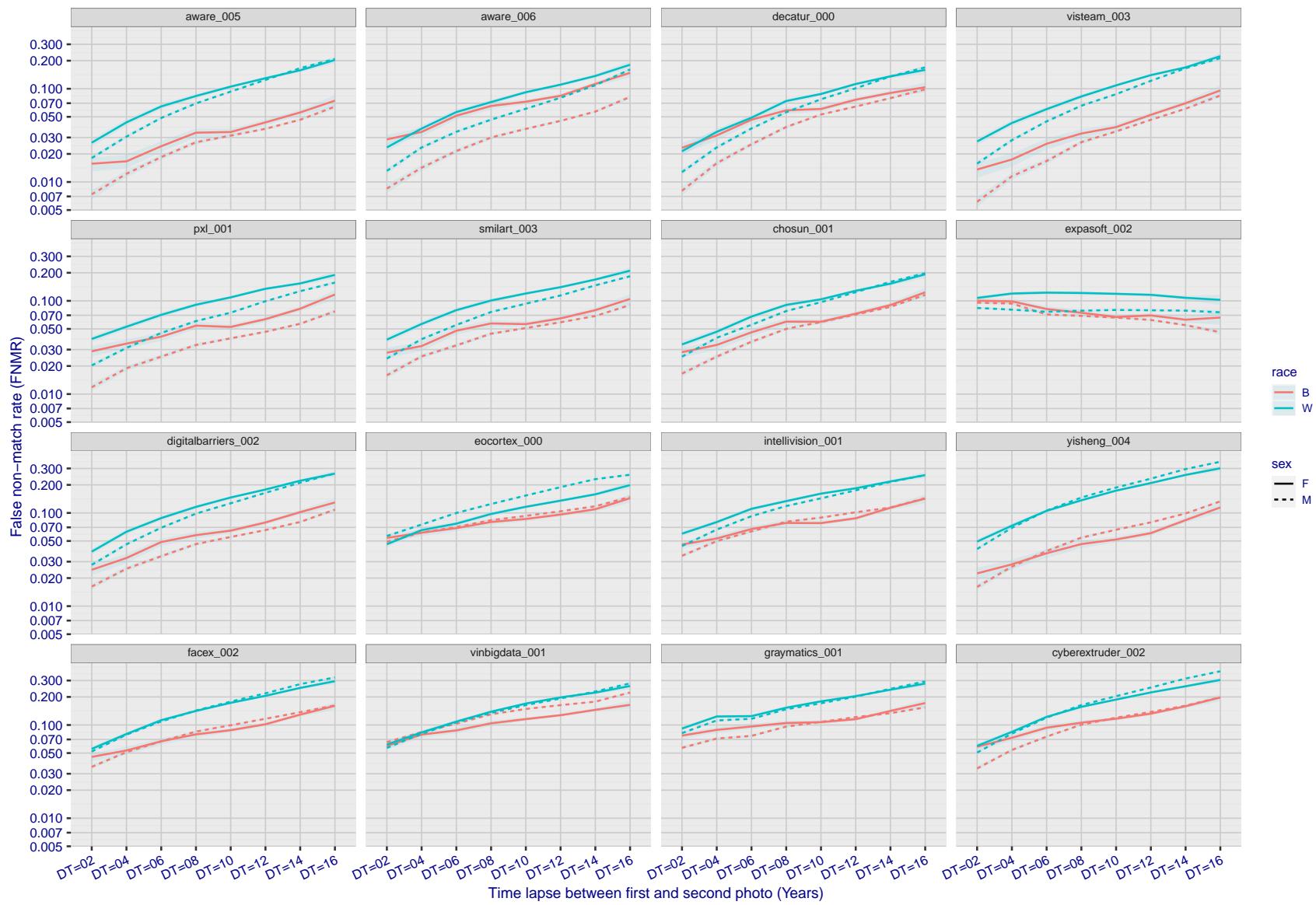


Figure 283: For the mugshot images, FNMR as a function of elapsed time between initial enrollment and second verification images. The panels appear most accurate first, and vertical scale changes on each page. The four traces correspond to images annotated with codes for black female, black male, white female, white male. The threshold is fixed for each algorithm to give FMR = 0.00001 over all (10^8) impostor comparisons. For short time-lapses, the most accurate algorithms give very few errors (FNMR < 0.001) so that the uncertainty estimates are high.

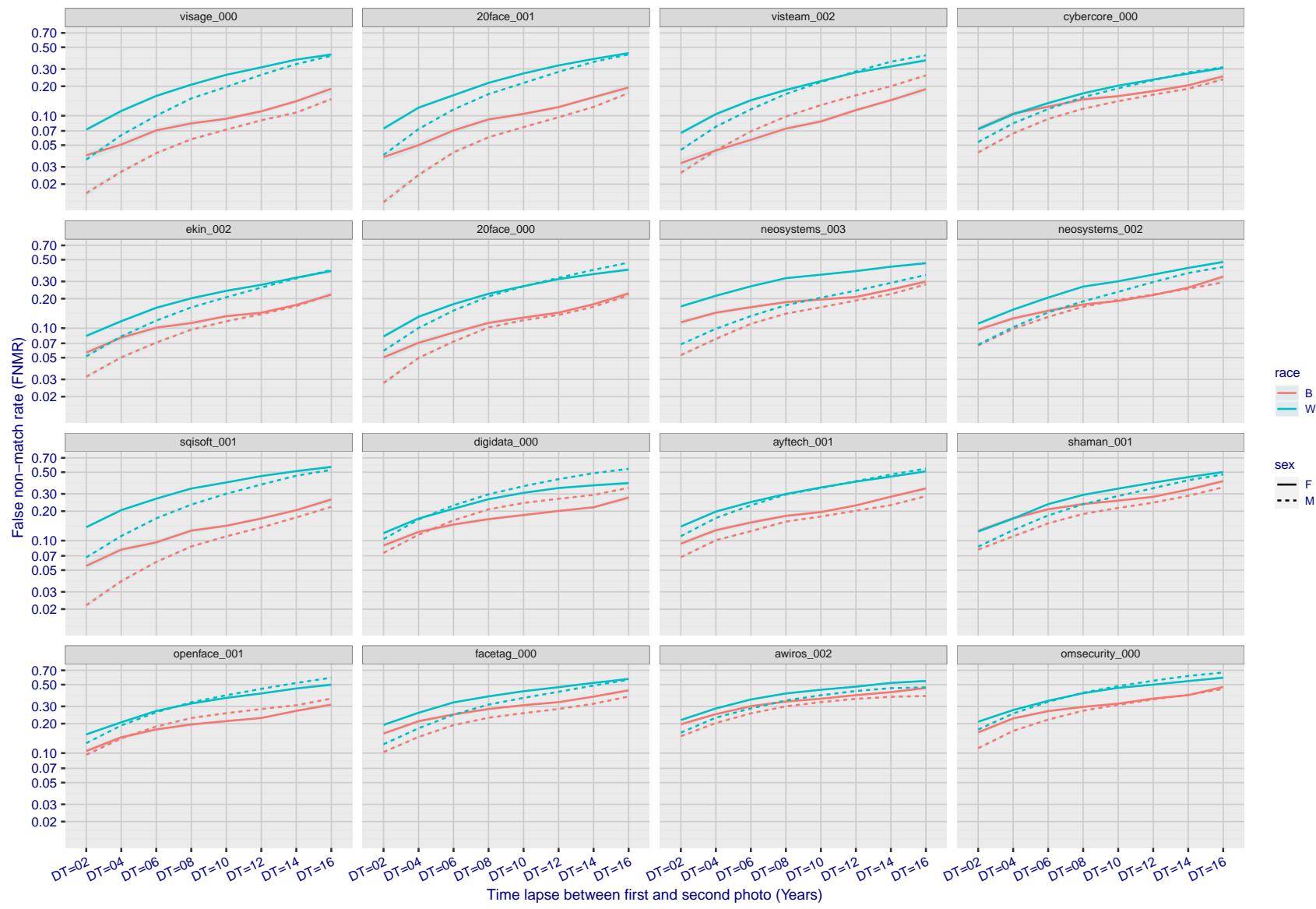


Figure 284: For the mugshot images, FNMR as a function of elapsed time between initial enrollment and second verification images. The panels appear most accurate first, and vertical scale changes on each page. The four traces correspond to images annotated with codes for black female, black male, white female, white male. The threshold is fixed for each algorithm to give $FMR = 0.00001$ over all (10^8) impostor comparisons. For short time-lapses, the most accurate algorithms give very few errors ($FNMR < 0.001$) so that the uncertainty estimates are high.

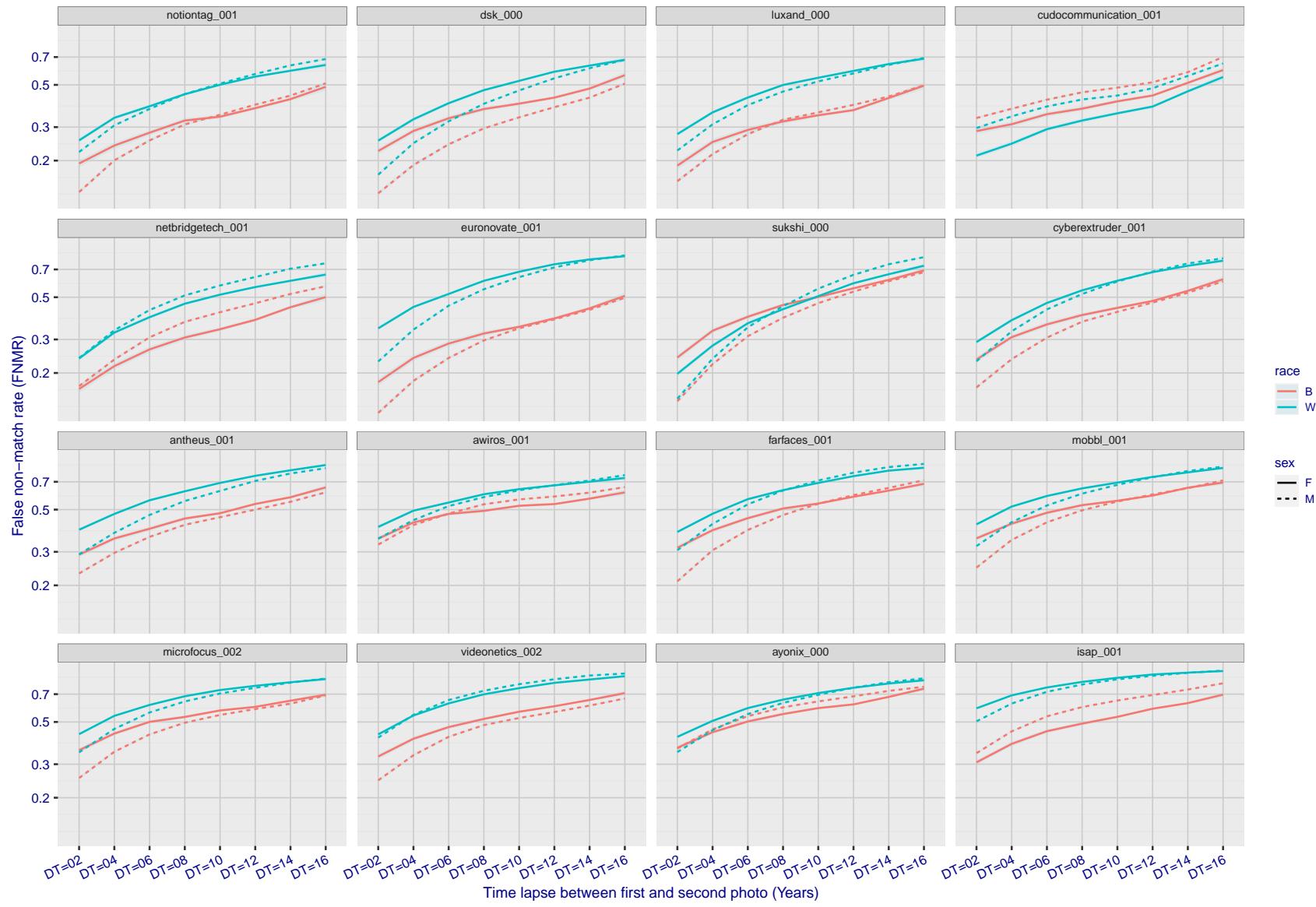


Figure 285: For the mugshot images, FNMR as a function of elapsed time between initial enrollment and second verification images. The panels appear most accurate first, and vertical scale changes on each page. The four traces correspond to images annotated with codes for black female, black male, white female, white male. The threshold is fixed for each algorithm to give FMR = 0.00001 over all (10^8) impostor comparisons. For short time-lapses, the most accurate algorithms give very few errors (FNMR < 0.001) so that the uncertainty estimates are high.

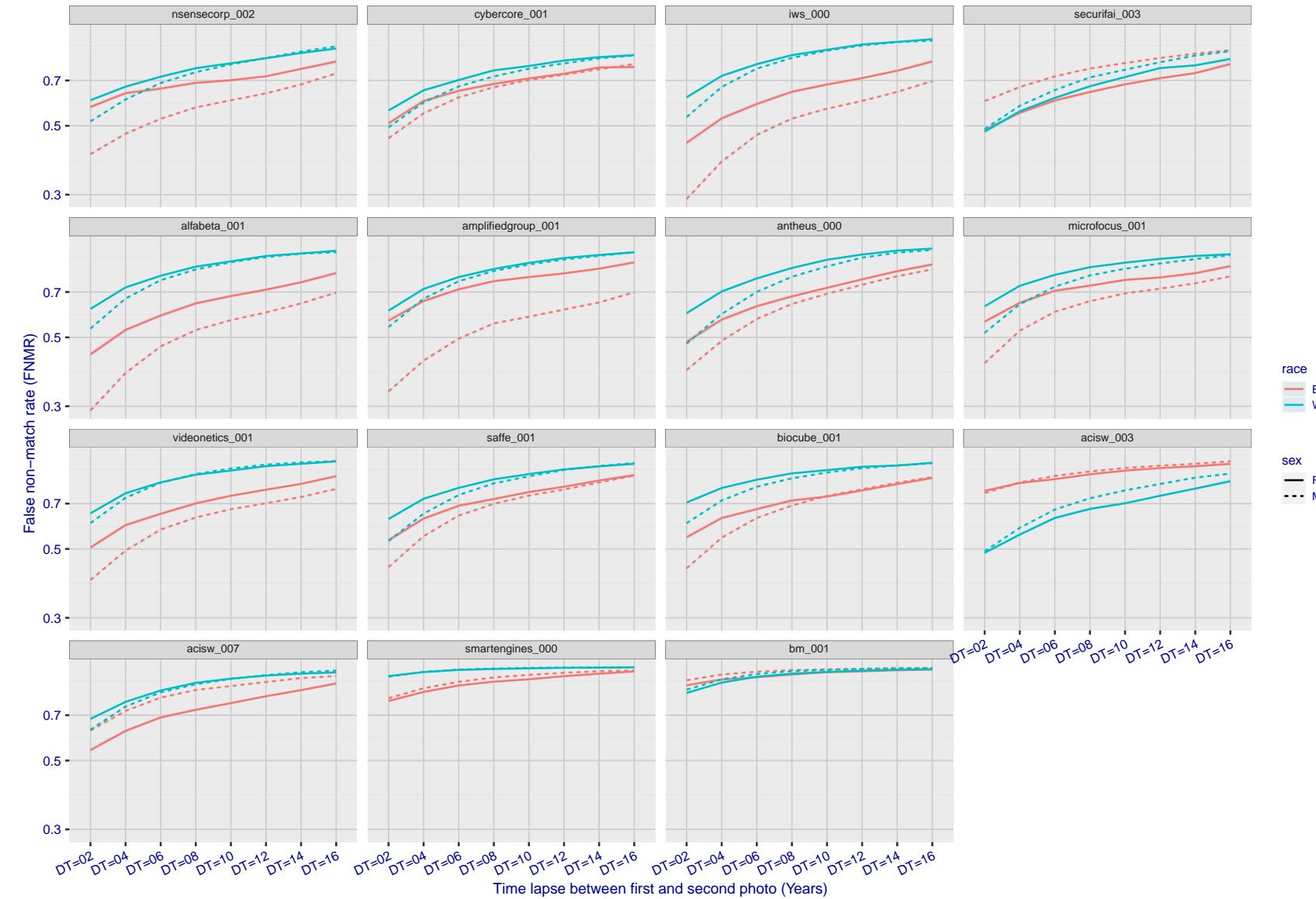


Figure 286: For the mugshot images, FNMR as a function of elapsed time between initial enrollment and second verification images. The panels appear most accurate first, and vertical scale changes on each page. The four traces correspond to images annotated with codes for black female, black male, white female, white male. The threshold is fixed for each algorithm to give FMR = 0.00001 over all (10^8) impostor comparisons. For short time-lapses, the most accurate algorithms give very few errors (FNMR < 0.001) so that the uncertainty estimates are high.

3.5.3 Effect of age on genuine subjects

Background: Faces change appearance throughout life. Face recognition algorithms have previously been reported to give better accuracy on older individuals (See NIST IR 8009).

Goal: To quantify false non-match rates (FNMR) as a function of age, without an ageing component.

Methods: Using the visa images, which span fewer than five years, thresholds are determined that give FMR = 0.001 and 0.0001 over the entire impostor set. Then FNMR is measured over 1000 bootstrap replications of the genuine scores.

Results: For the visa images, Figure 319 shows how false non-match rates for genuine users, as a function of age group. The notable aspects are:

- ▷ Younger subjects give considerably higher FNMR. This is likely due to rapid growth and change in facial appearance.
- ▷ FNMR trends down throughout life. The last bin, AGE > 72, contains fewer than 140 mated pairs, and may be affected by small sample size.

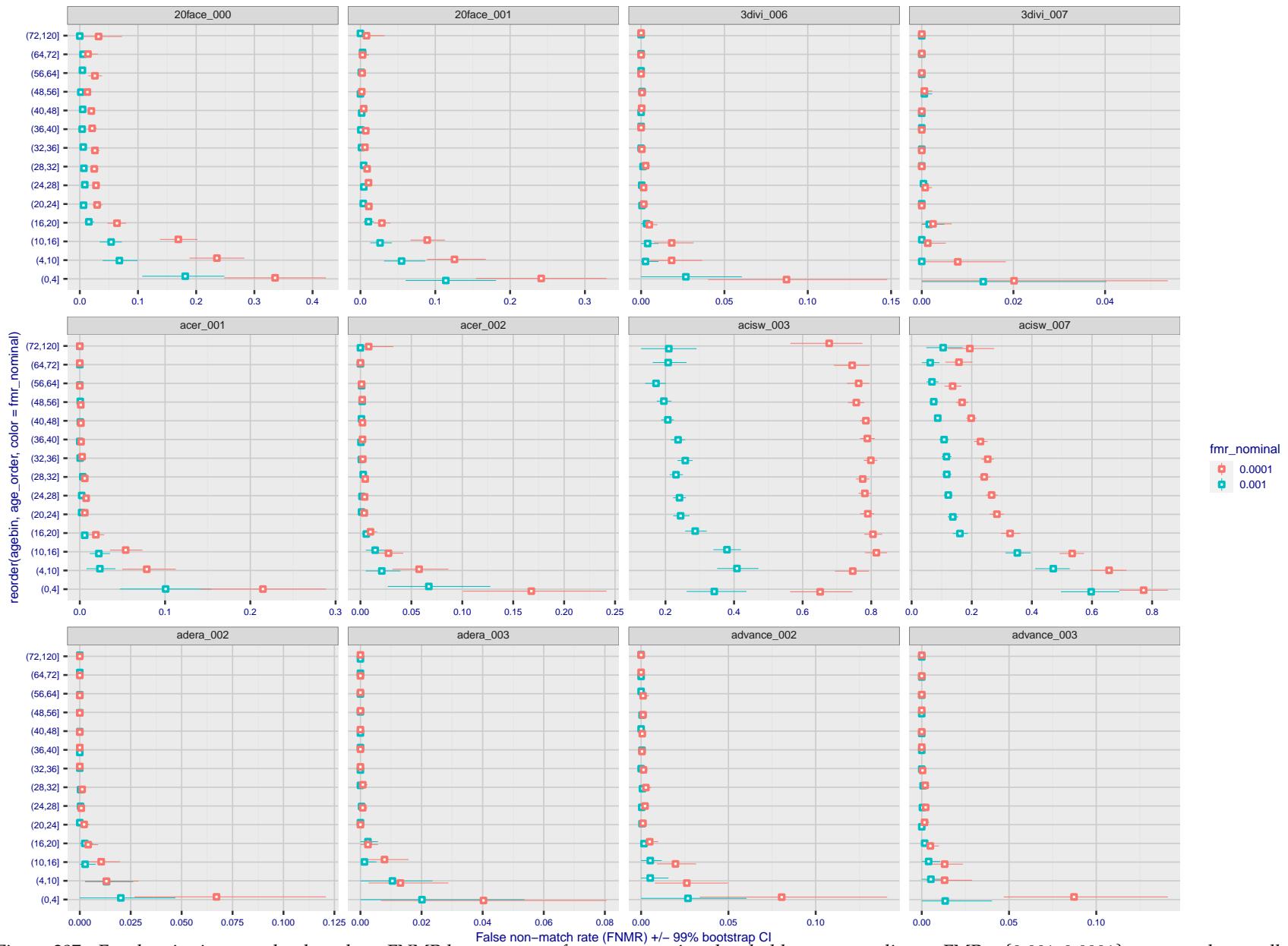


Figure 287: For the visa images, the dots show FNMR by age group for two operating thresholds corresponding to $FMR = \{0.001, 0.0001\}$ computed over all on the order of 10^{10} impostor scores. The FMR in each bin will vary also - see subsequent impostor heatmaps in sec. 3.6.2. Given a pair of face images taken at different times, we assign the comparison to the bin that is the arithmetic average of the subject's ages. This plot shows only the effect of age, not ageing. The number of comparisons in each bin is generally in the thousands, however the first and last bins are computed over 149 and 124 respectively. The error rates in some (adult) cases are zero, and in others the DET is flat so the error rates at the two thresholds are identical. The lines span 1% and 99% of bootstrap replicated FNMR estimates.

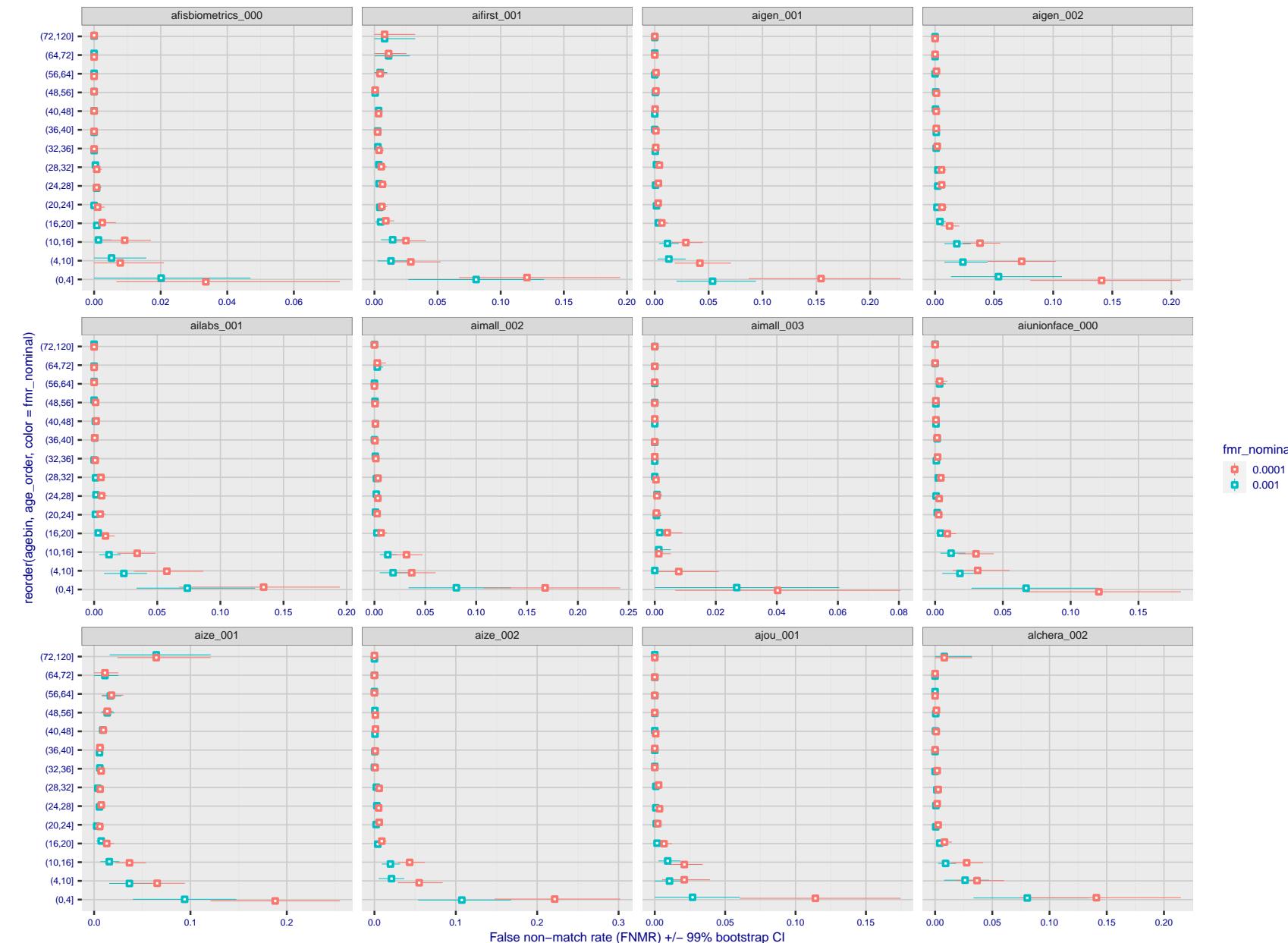


Figure 288: For the visa images, the dots show FNMR by age group for two operating thresholds corresponding to $FMR = \{0.001, 0.0001\}$ computed over all on the order of 10^{10} impostor scores. The FMR in each bin will vary also - see subsequent impostor heatmaps in sec. 3.6.2. Given a pair of face images taken at different times, we assign the comparison to the bin that is the arithmetic average of the subject's ages. This plot shows only the effect of age, not ageing. The number of comparisons in each bin is generally in the thousands, however the first and last bins are computed over 149 and 124 respectively. The error rates in some (adult) cases are zero, and in others the DET is flat so the error rates at the two thresholds are identical. The lines span 1% and 99% of bootstrap replicated FNMR estimates.

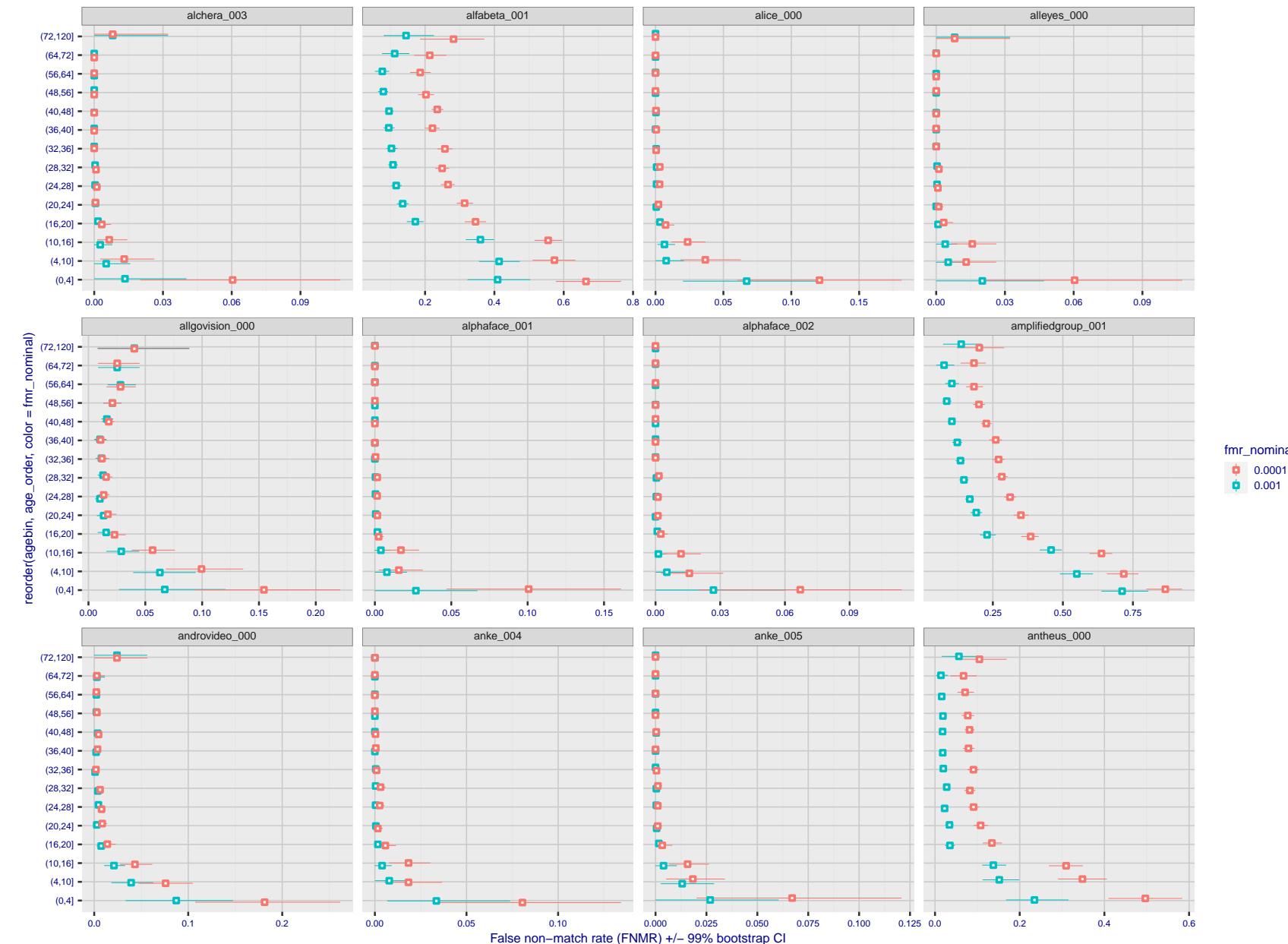


Figure 289: For the visa images, the dots show FNMR by age group for two operating thresholds corresponding to $FMR = \{0.001, 0.0001\}$ computed over all on the order of 10^{10} impostor scores. The FMR in each bin will vary also - see subsequent impostor heatmaps in sec. 3.6.2. Given a pair of face images taken at different times, we assign the comparison to the bin that is the arithmetic average of the subject's ages. This plot shows only the effect of age, not ageing. The number of comparisons in each bin is generally in the thousands, however the first and last bins are computed over 149 and 124 respectively. The error rates in some (adult) cases are zero, and in others the DET is flat so the error rates at the two thresholds are identical. The lines span 1% and 99% of bootstrap replicated FNMR estimates.

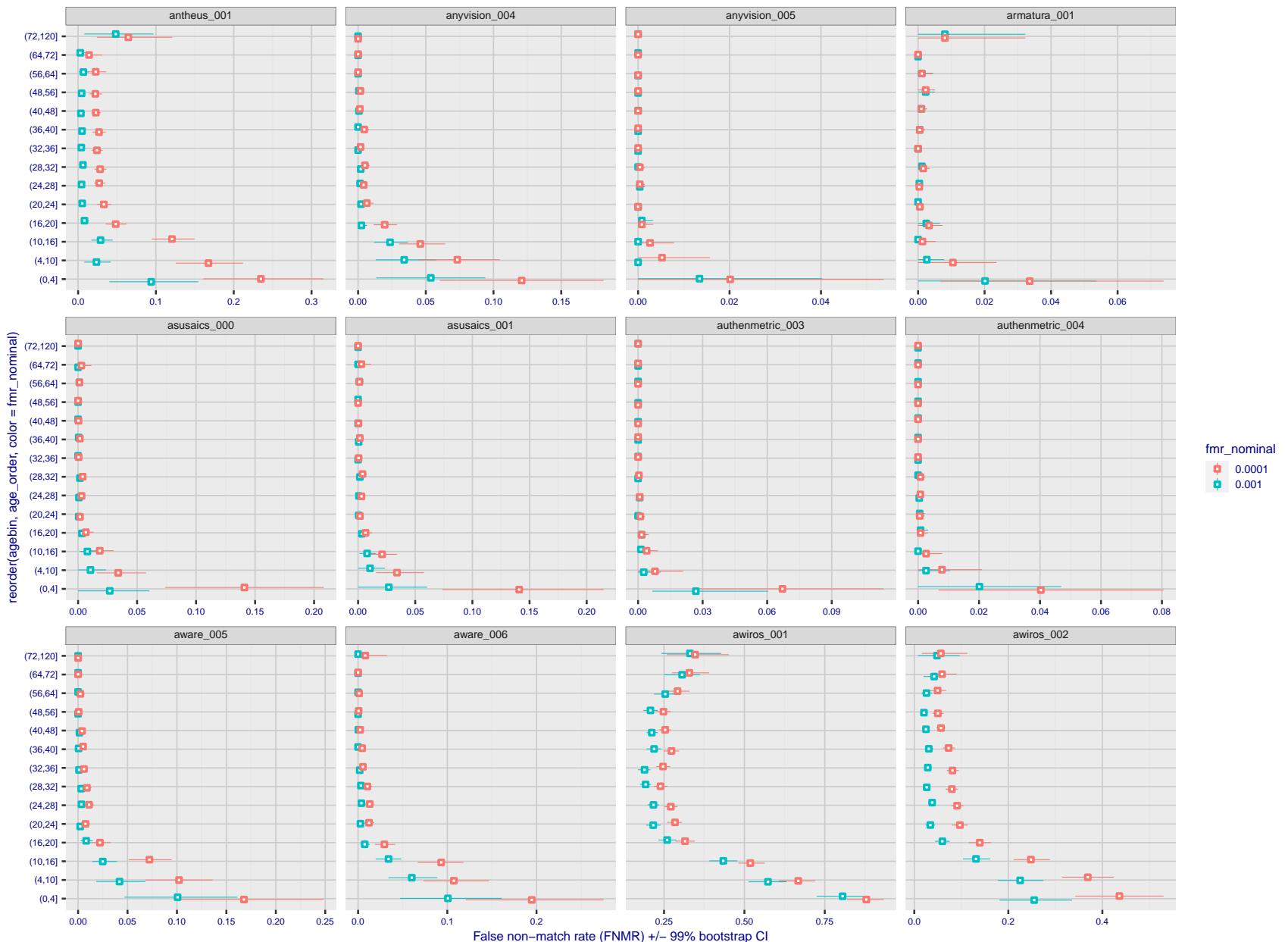


Figure 290: For the visa images, the dots show FNMR by age group for two operating thresholds corresponding to $FMR = \{0.001, 0.0001\}$ computed over all on the order of 10^{10} impostor scores. The FMR in each bin will vary also - see subsequent impostor heatmaps in sec. 3.6.2. Given a pair of face images taken at different times, we assign the comparison to the bin that is the arithmetic average of the subject's ages. This plot shows only the effect of age, not ageing. The number of comparisons in each bin is generally in the thousands, however the first and last bins are computed over 149 and 124 respectively. The error rates in some (adult) cases are zero, and in others the DET is flat so the error rates at the two thresholds are identical. The lines span 1% and 99% of bootstrap replicated FNMR estimates.



Figure 291: For the visa images, the dots show FNMR by age group for two operating thresholds corresponding to $FMR = \{0.001, 0.0001\}$ computed over all on the order of 10^{10} impostor scores. The FMR in each bin will vary also - see subsequent impostor heatmaps in sec. 3.6.2. Given a pair of face images taken at different times, we assign the comparison to the bin that is the arithmetic average of the subject's ages. This plot shows only the effect of age, not ageing. The number of comparisons in each bin is generally in the thousands, however the first and last bins are computed over 149 and 124 respectively. The error rates in some (adult) cases are zero, and in others the DET is flat so the error rates at the two thresholds are identical. The lines span 1% and 99% of bootstrap replicated FNMR estimates.



Figure 292: For the visa images, the dots show FNMR by age group for two operating thresholds corresponding to $FMR = \{0.001, 0.0001\}$ computed over all on the order of 10^{10} impostor scores. The FMR in each bin will vary also - see subsequent impostor heatmaps in sec. 3.6.2. Given a pair of face images taken at different times, we assign the comparison to the bin that is the arithmetic average of the subject's ages. This plot shows only the effect of age, not ageing. The number of comparisons in each bin is generally in the thousands, however the first and last bins are computed over 149 and 124 respectively. The error rates in some (adult) cases are zero, and in others the DET is flat so the error rates at the two thresholds are identical. The lines span 1% and 99% of bootstrap replicated FNMR estimates.

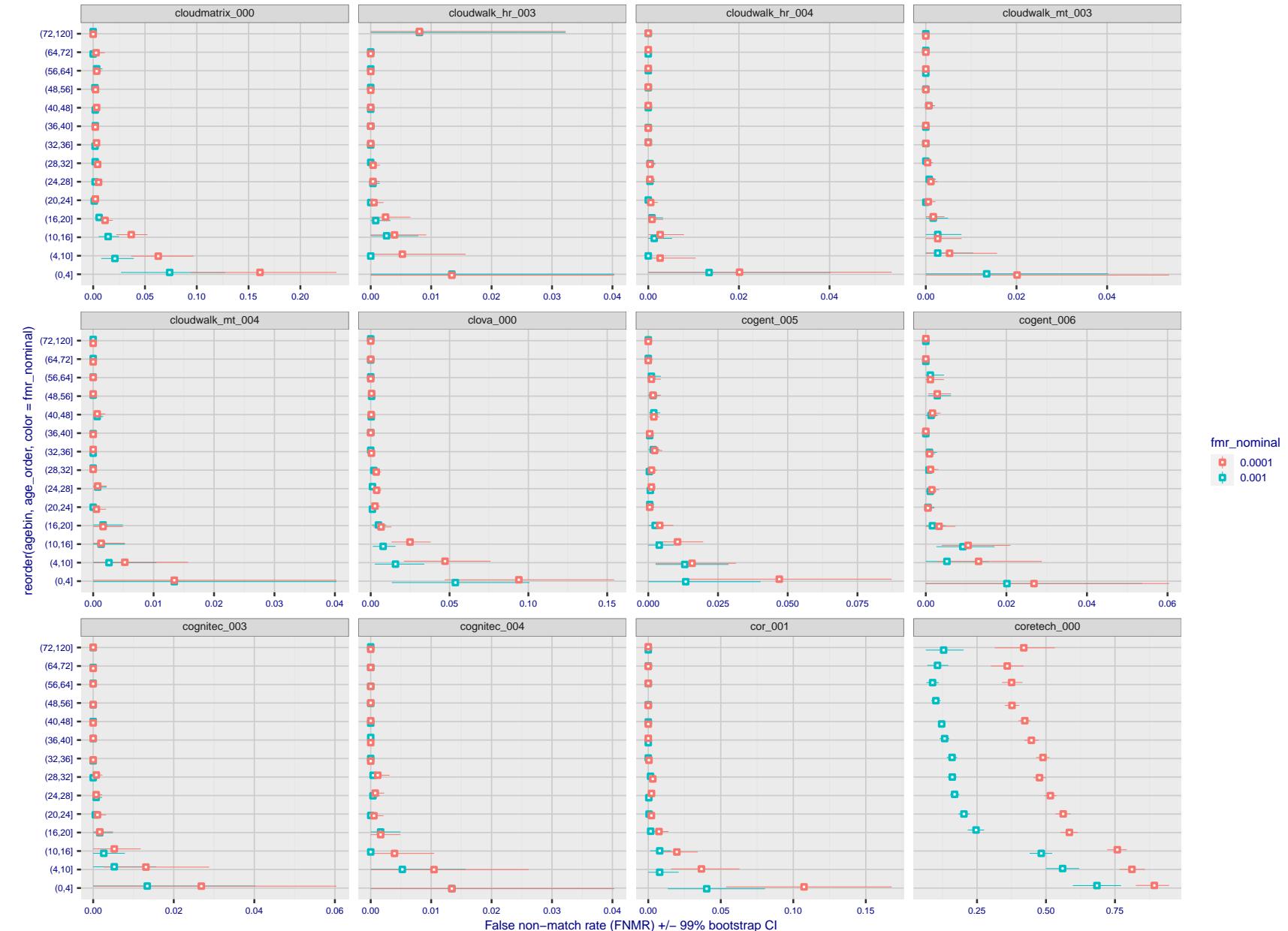


Figure 293: For the visa images, the dots show FNMR by age group for two operating thresholds corresponding to $FMR = \{0.001, 0.0001\}$ computed over all on the order of 10^{10} impostor scores. The FMR in each bin will vary also - see subsequent impostor heatmaps in sec. 3.6.2. Given a pair of face images taken at different times, we assign the comparison to the bin that is the arithmetic average of the subject's ages. This plot shows only the effect of age, not ageing. The number of comparisons in each bin is generally in the thousands, however the first and last bins are computed over 149 and 124 respectively. The error rates in some (adult) cases are zero, and in others the DET is flat so the error rates at the two thresholds are identical. The lines span 1% and 99% of bootstrap replicated FNMR estimates.

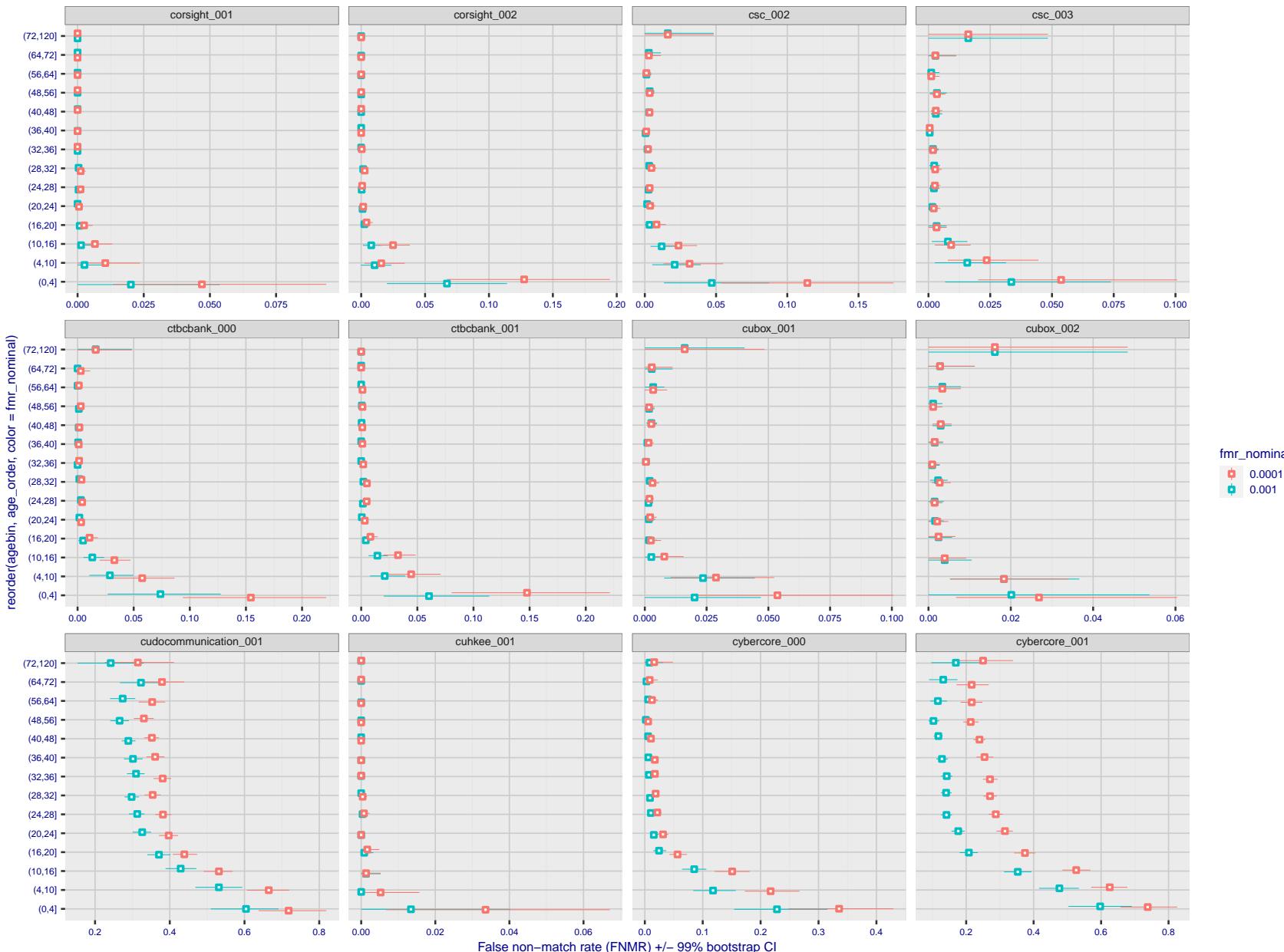


Figure 294: For the visa images, the dots show FNMR by age group for two operating thresholds corresponding to $FMR = \{0.001, 0.0001\}$ computed over all on the order of 10^{10} impostor scores. The FMR in each bin will vary also - see subsequent impostor heatmaps in sec. 3.6.2. Given a pair of face images taken at different times, we assign the comparison to the bin that is the arithmetic average of the subject's ages. This plot shows only the effect of age, not ageing. The number of comparisons in each bin is generally in the thousands, however the first and last bins are computed over 149 and 124 respectively. The error rates in some (adult) cases are zero, and in others the DET is flat so the error rates at the two thresholds are identical. The lines span 1% and 99% of bootstrap replicated FNMR estimates.



Figure 295: For the visa images, the dots show FNMR by age group for two operating thresholds corresponding to $FMR = \{0.001, 0.0001\}$ computed over all on the order of 10^{10} impostor scores. The FMR in each bin will vary also - see subsequent impostor heatmaps in sec. 3.6.2. Given a pair of face images taken at different times, we assign the comparison to the bin that is the arithmetic average of the subject's ages. This plot shows only the effect of age, not ageing. The number of comparisons in each bin is generally in the thousands, however the first and last bins are computed over 149 and 124 respectively. The error rates in some (adult) cases are zero, and in others the DET is flat so the error rates at the two thresholds are identical. The lines span 1% and 99% of bootstrap replicated FNMR estimates.



Figure 296: For the visa images, the dots show FNMR by age group for two operating thresholds corresponding to $FMR = \{0.001, 0.0001\}$ computed over all on the order of 10^{10} impostor scores. The FMR in each bin will vary also - see subsequent impostor heatmaps in sec. 3.6.2. Given a pair of face images taken at different times, we assign the comparison to the bin that is the arithmetic average of the subject's ages. This plot shows only the effect of age, not ageing. The number of comparisons in each bin is generally in the thousands, however the first and last bins are computed over 149 and 124 respectively. The error rates in some (adult) cases are zero, and in others the DET is flat so the error rates at the two thresholds are identical. The lines span 1% and 99% of bootstrap replicated FNMR estimates.

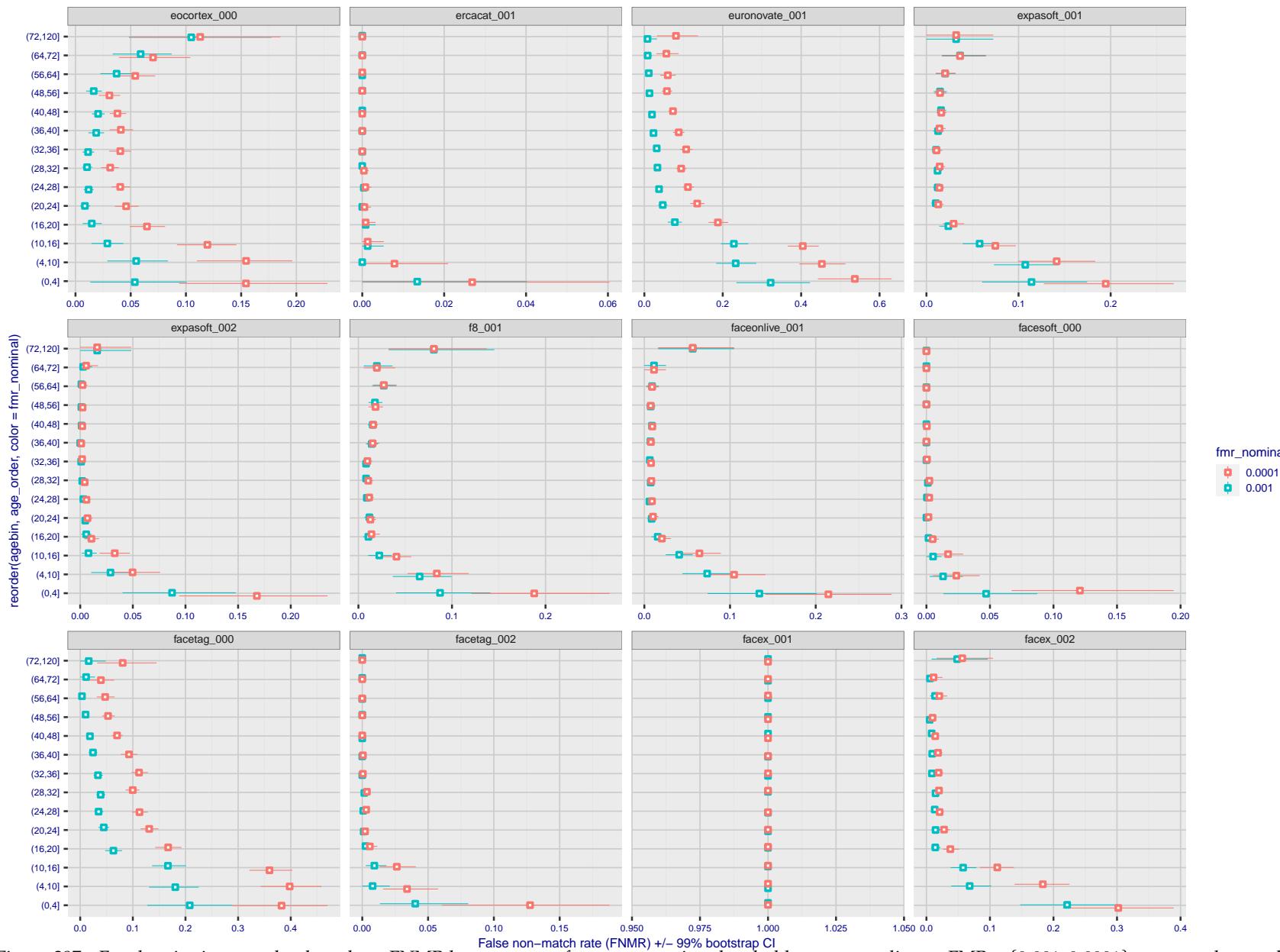
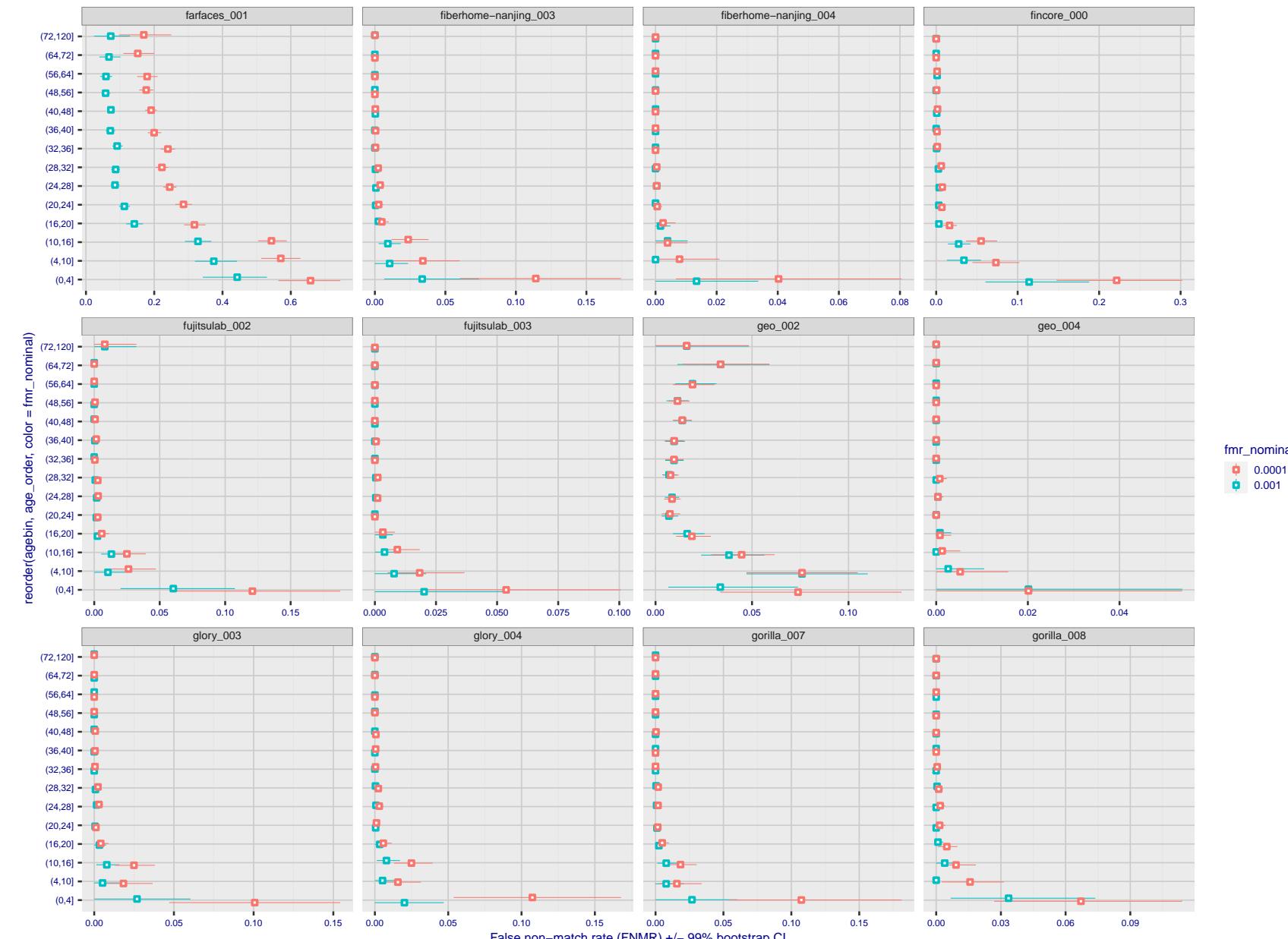


Figure 297: For the visa images, the dots show FNMR by age group for two operating thresholds corresponding to $FMR = \{0.001, 0.0001\}$ computed over all on the order of 10^{10} impostor scores. The FMR in each bin will vary also - see subsequent impostor heatmaps in sec. 3.6.2. Given a pair of face images taken at different times, we assign the comparison to the bin that is the arithmetic average of the subject's ages. This plot shows only the effect of age, not ageing. The number of comparisons in each bin is generally in the thousands, however the first and last bins are computed over 149 and 124 respectively. The error rates in some (adult) cases are zero, and in others the DET is flat so the error rates at the two thresholds are identical. The lines span 1% and 99% of bootstrap replicated FNMR estimates.



FNMR(T)
FMR(T)
"False non-match rate"
"False match rate"

Figure 298: For the visa images, the dots show FNMR by age group for two operating thresholds corresponding to $FMR = \{0.001, 0.0001\}$ computed over all on the order of 10^{10} impostor scores. The FMR in each bin will vary also - see subsequent impostor heatmaps in sec. 3.6.2. Given a pair of face images taken at different times, we assign the comparison to the bin that is the arithmetic average of the subject's ages. This plot shows only the effect of age, not ageing. The number of comparisons in each bin is generally in the thousands, however the first and last bins are computed over 149 and 124 respectively. The error rates in some (adult) cases are zero, and in others the DET is flat so the error rates at the two thresholds are identical. The lines span 1% and 99% of bootstrap replicated FNMR estimates.

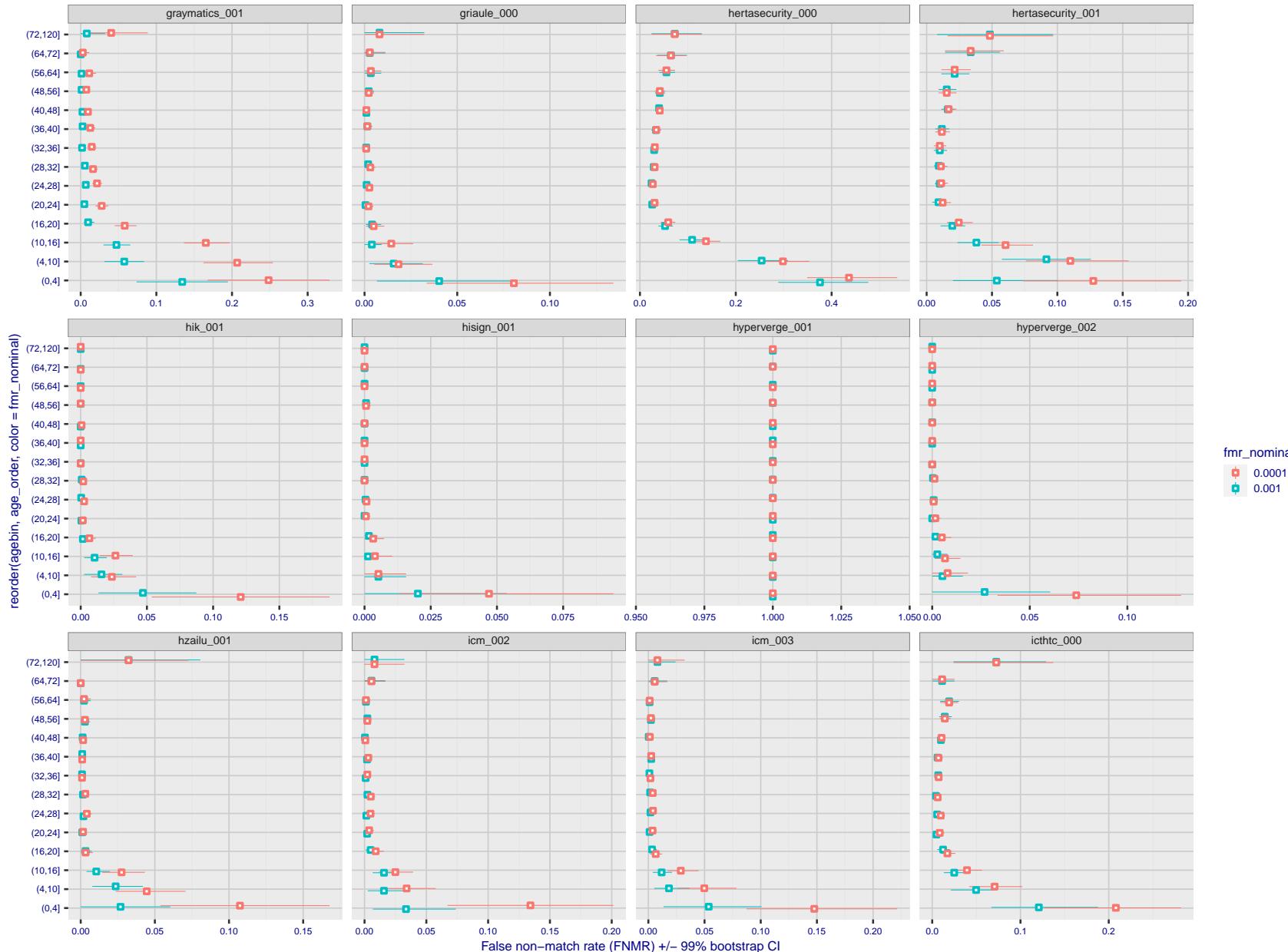


Figure 299: For the visa images, the dots show FNMR by age group for two operating thresholds corresponding to $FMR = \{0.001, 0.0001\}$ computed over all on the order of 10^{10} impostor scores. The FMR in each bin will vary also - see subsequent impostor heatmaps in sec. 3.6.2. Given a pair of face images taken at different times, we assign the comparison to the bin that is the arithmetic average of the subject's ages. This plot shows only the effect of age, not ageing. The number of comparisons in each bin is generally in the thousands, however the first and last bins are computed over 149 and 124 respectively. The error rates in some (adult) cases are zero, and in others the DET is flat so the error rates at the two thresholds are identical. The lines span 1% and 99% of bootstrap replicated FNMR estimates.

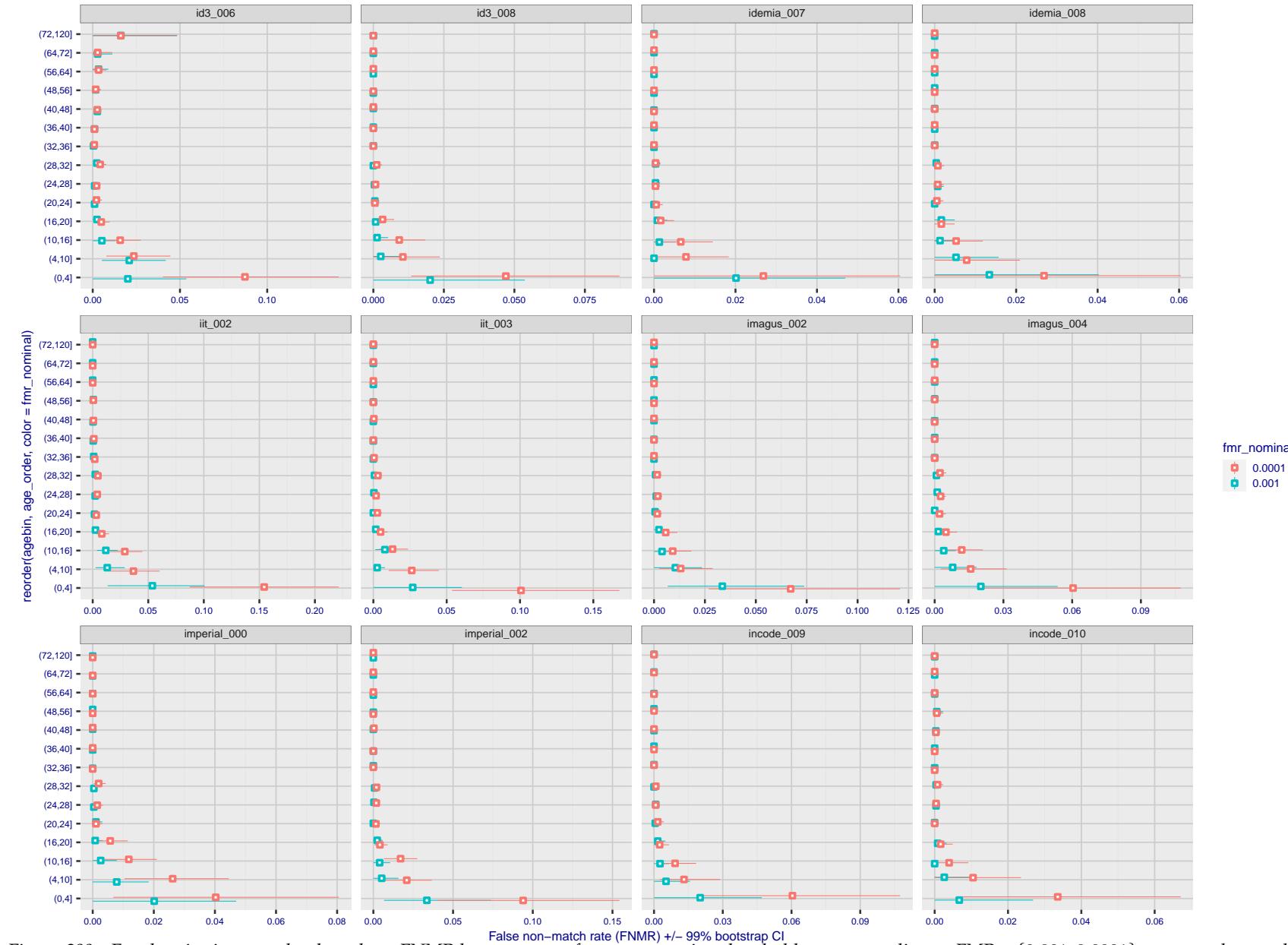


Figure 300: For the visa images, the dots show FNMR by age group for two operating thresholds corresponding to $FMR = \{0.001, 0.0001\}$ computed over all on the order of 10^{10} impostor scores. The FMR in each bin will vary also - see subsequent impostor heatmaps in sec. 3.6.2. Given a pair of face images taken at different times, we assign the comparison to the bin that is the arithmetic average of the subject's ages. This plot shows only the effect of age, not ageing. The number of comparisons in each bin is generally in the thousands, however the first and last bins are computed over 149 and 124 respectively. The error rates in some (adult) cases are zero, and in others the DET is flat so the error rates at the two thresholds are identical. The lines span 1% and 99% of bootstrap replicated FNMR estimates.

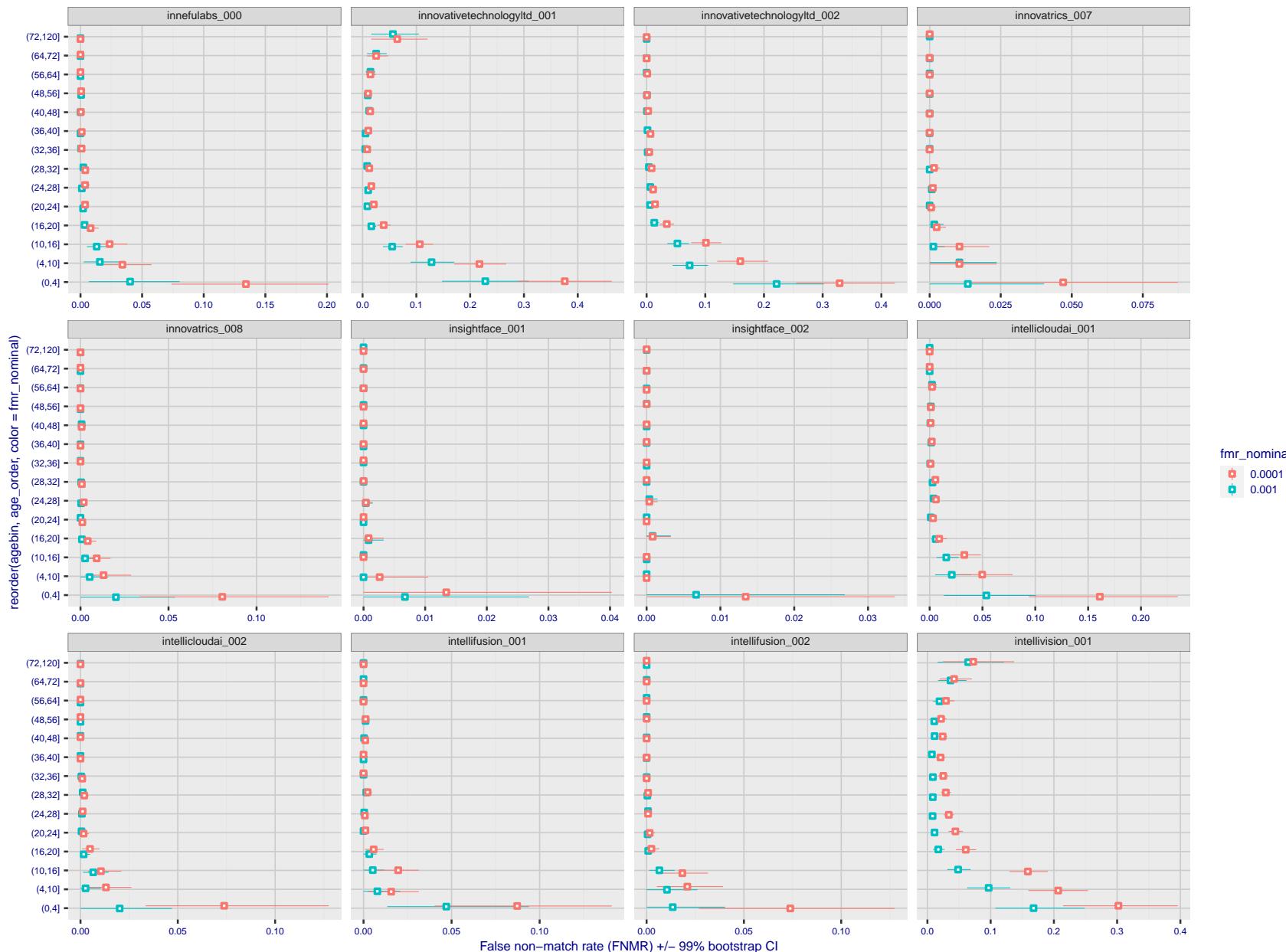


Figure 301: For the visa images, the dots show FNMR by age group for two operating thresholds corresponding to $FMR = \{0.001, 0.0001\}$ computed over all on the order of 10^{10} impostor scores. The FMR in each bin will vary also - see subsequent impostor heatmaps in sec. 3.6.2. Given a pair of face images taken at different times, we assign the comparison to the bin that is the arithmetic average of the subject's ages. This plot shows only the effect of age, not ageing. The number of comparisons in each bin is generally in the thousands, however the first and last bins are computed over 149 and 124 respectively. The error rates in some (adult) cases are zero, and in others the DET is flat so the error rates at the two thresholds are identical. The lines span 1% and 99% of bootstrap replicated FNMR estimates.

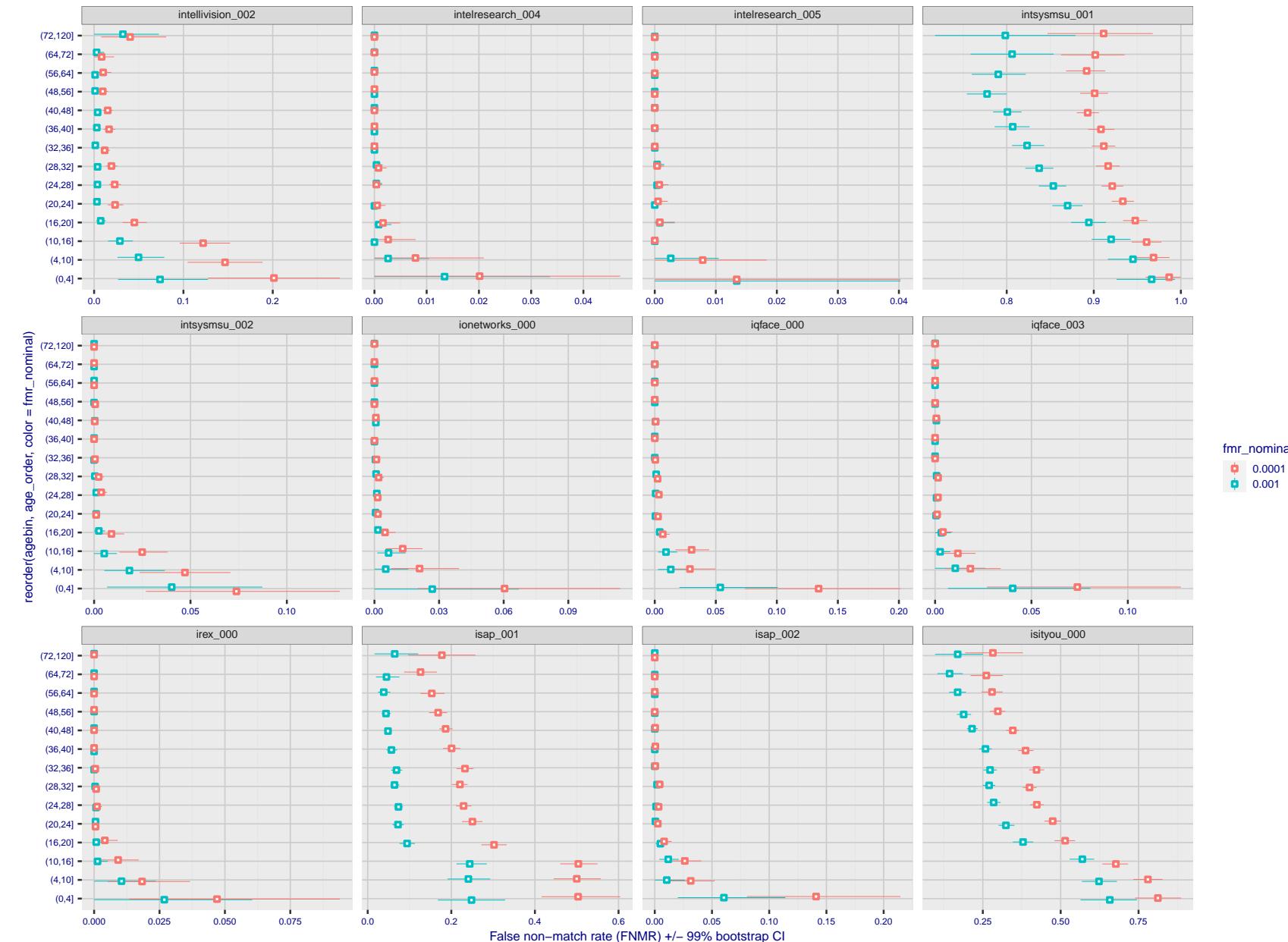


Figure 302: For the visa images, the dots show FNMR by age group for two operating thresholds corresponding to $FMR = \{0.001, 0.0001\}$ computed over all on the order of 10^{10} impostor scores. The FMR in each bin will vary also - see subsequent impostor heatmaps in sec. 3.6.2. Given a pair of face images taken at different times, we assign the comparison to the bin that is the arithmetic average of the subject's ages. This plot shows only the effect of age, not ageing. The number of comparisons in each bin is generally in the thousands, however the first and last bins are computed over 149 and 124 respectively. The error rates in some (adult) cases are zero, and in others the DET is flat so the error rates at the two thresholds are identical. The lines span 1% and 99% of bootstrap replicated FNMR estimates.



Figure 303: For the visa images, the dots show FNMR by age group for two operating thresholds corresponding to $FMR = \{0.001, 0.0001\}$ computed over all on the order of 10^{10} impostor scores. The FMR in each bin will vary also - see subsequent impostor heatmaps in sec. 3.6.2. Given a pair of face images taken at different times, we assign the comparison to the bin that is the arithmetic average of the subject's ages. This plot shows only the effect of age, not ageing. The number of comparisons in each bin is generally in the thousands, however the first and last bins are computed over 149 and 124 respectively. The error rates in some (adult) cases are zero, and in others the DET is flat so the error rates at the two thresholds are identical. The lines span 1% and 99% of bootstrap replicated FNMR estimates.



Figure 304: For the visa images, the dots show FNMR by age group for two operating thresholds corresponding to FMR = {0.001, 0.0001} computed over all on the order of 10^{10} impostor scores. The FMR in each bin will vary also - see subsequent impostor heatmaps in sec. 3.6.2. Given a pair of face images taken at different times, we assign the comparison to the bin that is the arithmetic average of the subject's ages. This plot shows only the effect of age, not ageing. The number of comparisons in each bin is generally in the thousands, however the first and last bins are computed over 149 and 124 respectively. The error rates in some (adult) cases are zero, and in others the DET is flat so the error rates at the two thresholds are identical. The lines span 1% and 99% of bootstrap replicated FNMR estimates.

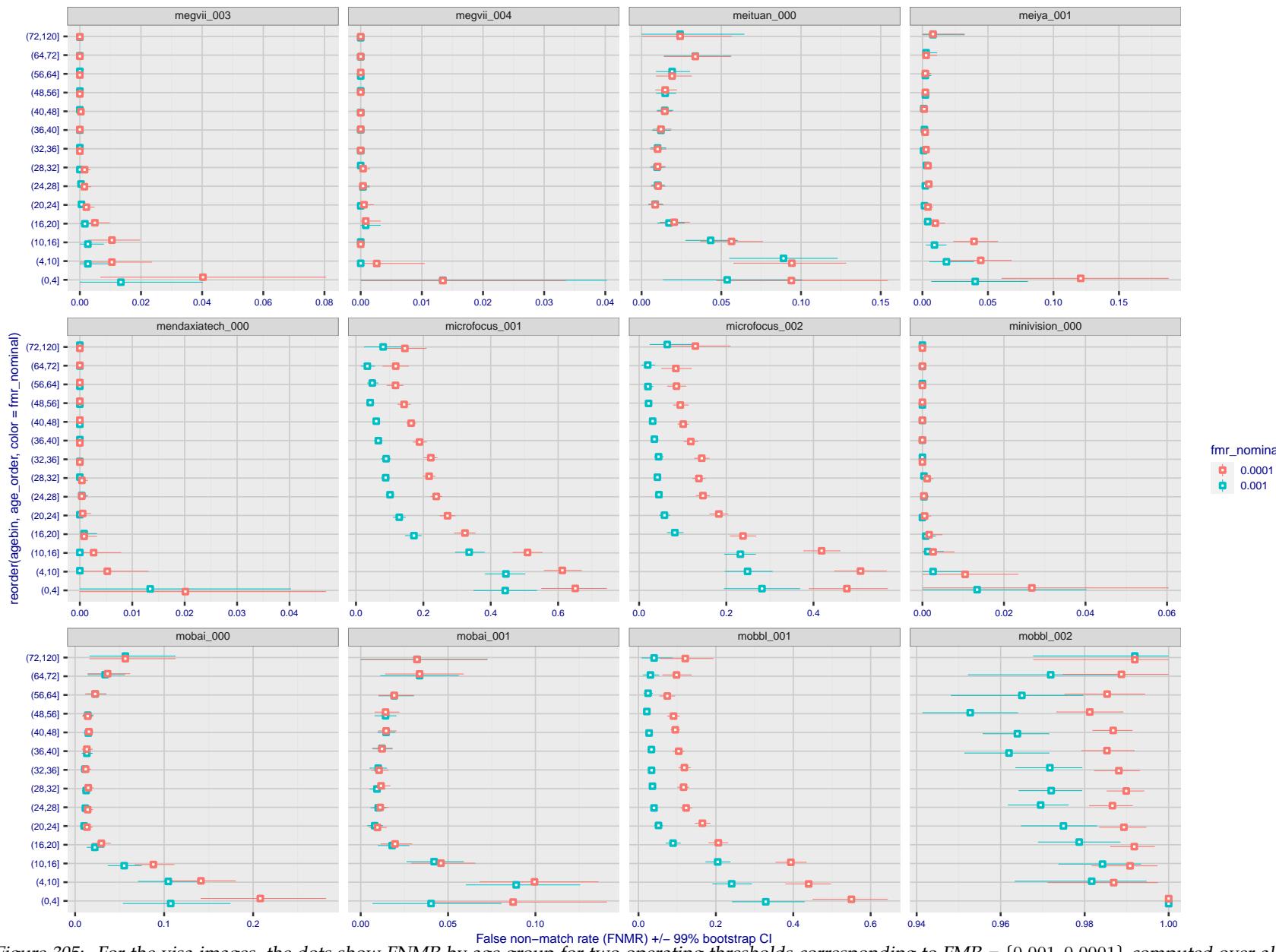


Figure 305: For the visa images, the dots show FNMR by age group for two operating thresholds corresponding to $FMR = \{0.001, 0.0001\}$ computed over all on the order of 10^{10} impostor scores. The FMR in each bin will vary also - see subsequent impostor heatmaps in sec. 3.6.2. Given a pair of face images taken at different times, we assign the comparison to the bin that is the arithmetic average of the subject's ages. This plot shows only the effect of age, not ageing. The number of comparisons in each bin is generally in the thousands, however the first and last bins are computed over 149 and 124 respectively. The error rates in some (adult) cases are zero, and in others the DET is flat so the error rates at the two thresholds are identical. The lines span 1% and 99% of bootstrap replicated FNMR estimates.



Figure 306: For the visa images, the dots show FNMR by age group for two operating thresholds corresponding to $FMR = \{0.001, 0.0001\}$ computed over all on the order of 10^{10} impostor scores. The FMR in each bin will vary also - see subsequent impostor heatmaps in sec. 3.6.2. Given a pair of face images taken at different times, we assign the comparison to the bin that is the arithmetic average of the subject's ages. This plot shows only the effect of age, not ageing. The number of comparisons in each bin is generally in the thousands, however the first and last bins are computed over 149 and 124 respectively. The error rates in some (adult) cases are zero, and in others the DET is flat so the error rates at the two thresholds are identical. The lines span 1% and 99% of bootstrap replicated FNMR estimates.

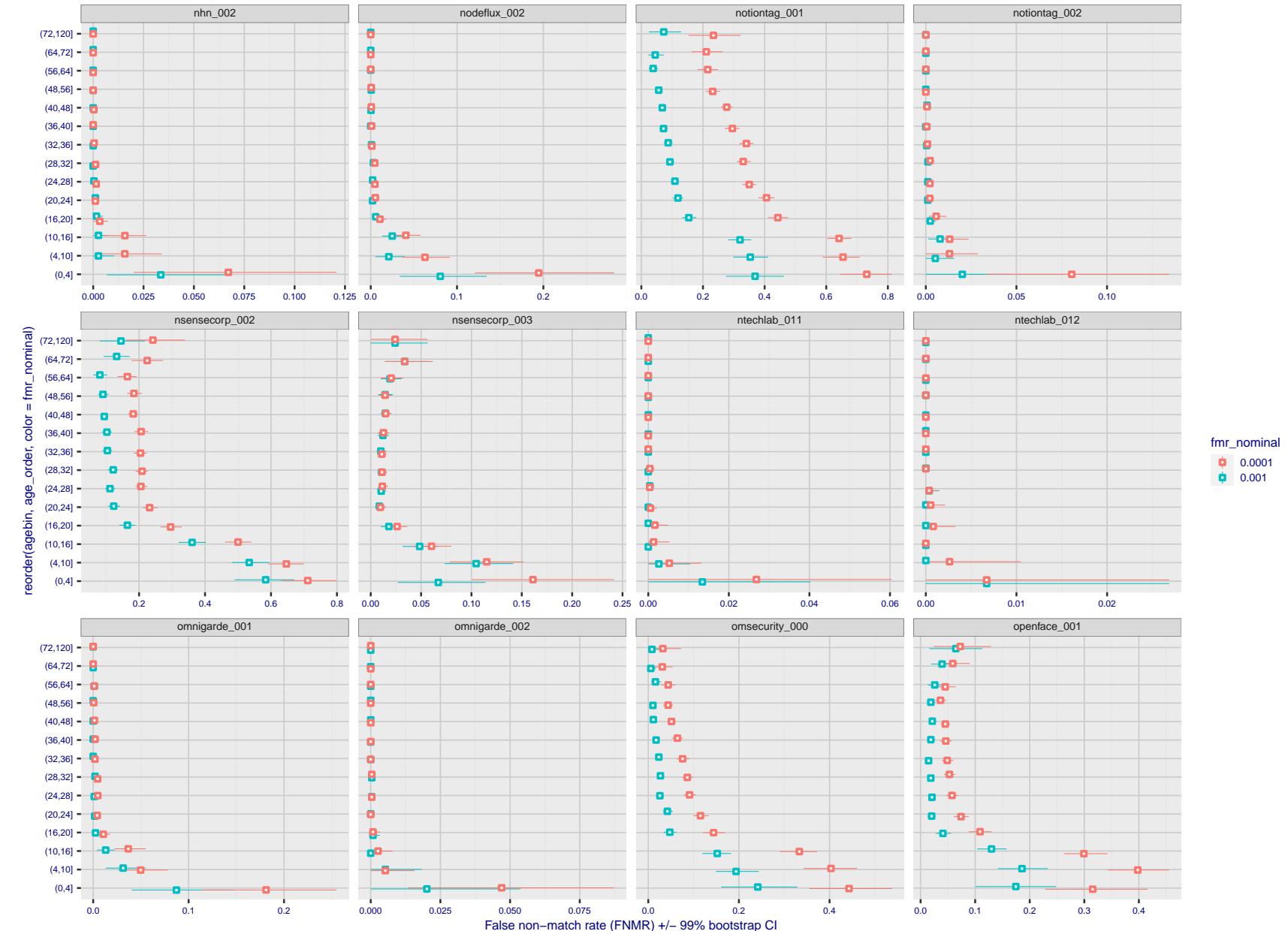


Figure 307: For the visa images, the dots show FNMR by age group for two operating thresholds corresponding to $FMR = \{0.001, 0.0001\}$ computed over all on the order of 10^{10} impostor scores. The FMR in each bin will vary also - see subsequent impostor heatmaps in sec. 3.6.2. Given a pair of face images taken at different times, we assign the comparison to the bin that is the arithmetic average of the subject's ages. This plot shows only the effect of age, not ageing. The number of comparisons in each bin is generally in the thousands, however the first and last bins are computed over 149 and 124 respectively. The error rates in some (adult) cases are zero, and in others the DET is flat so the error rates at the two thresholds are identical. The lines span 1% and 99% of bootstrap replicated FNMR estimates.



Figure 308: For the visa images, the dots show FNMR by age group for two operating thresholds corresponding to $FMR = \{0.001, 0.0001\}$ computed over all on the order of 10^{10} impostor scores. The FMR in each bin will vary also - see subsequent impostor heatmaps in sec. 3.6.2. Given a pair of face images taken at different times, we assign the comparison to the bin that is the arithmetic average of the subject's ages. This plot shows only the effect of age, not ageing. The number of comparisons in each bin is generally in the thousands, however the first and last bins are computed over 149 and 124 respectively. The error rates in some (adult) cases are zero, and in others the DET is flat so the error rates at the two thresholds are identical. The lines span 1% and 99% of bootstrap replicated FNMR estimates.

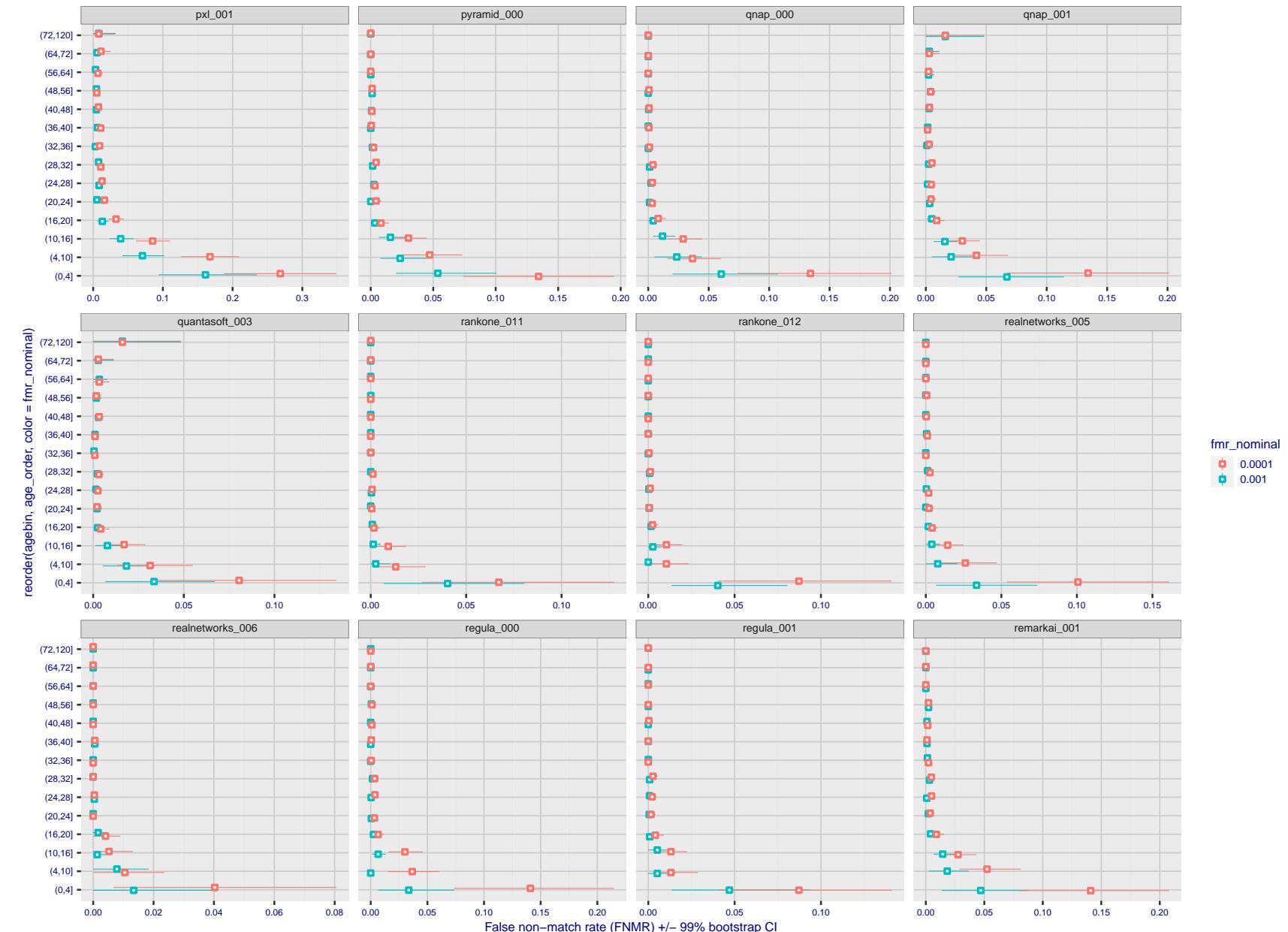


Figure 309: For the visa images, the dots show FNMR by age group for two operating thresholds corresponding to $FMR = \{0.001, 0.0001\}$ computed over all on the order of 10^{10} impostor scores. The FMR in each bin will vary also - see subsequent impostor heatmaps in sec. 3.6.2. Given a pair of face images taken at different times, we assign the comparison to the bin that is the arithmetic average of the subject's ages. This plot shows only the effect of age, not ageing. The number of comparisons in each bin is generally in the thousands, however the first and last bins are computed over 149 and 124 respectively. The error rates in some (adult) cases are zero, and in others the DET is flat so the error rates at the two thresholds are identical. The lines span 1% and 99% of bootstrap replicated FNMR estimates.

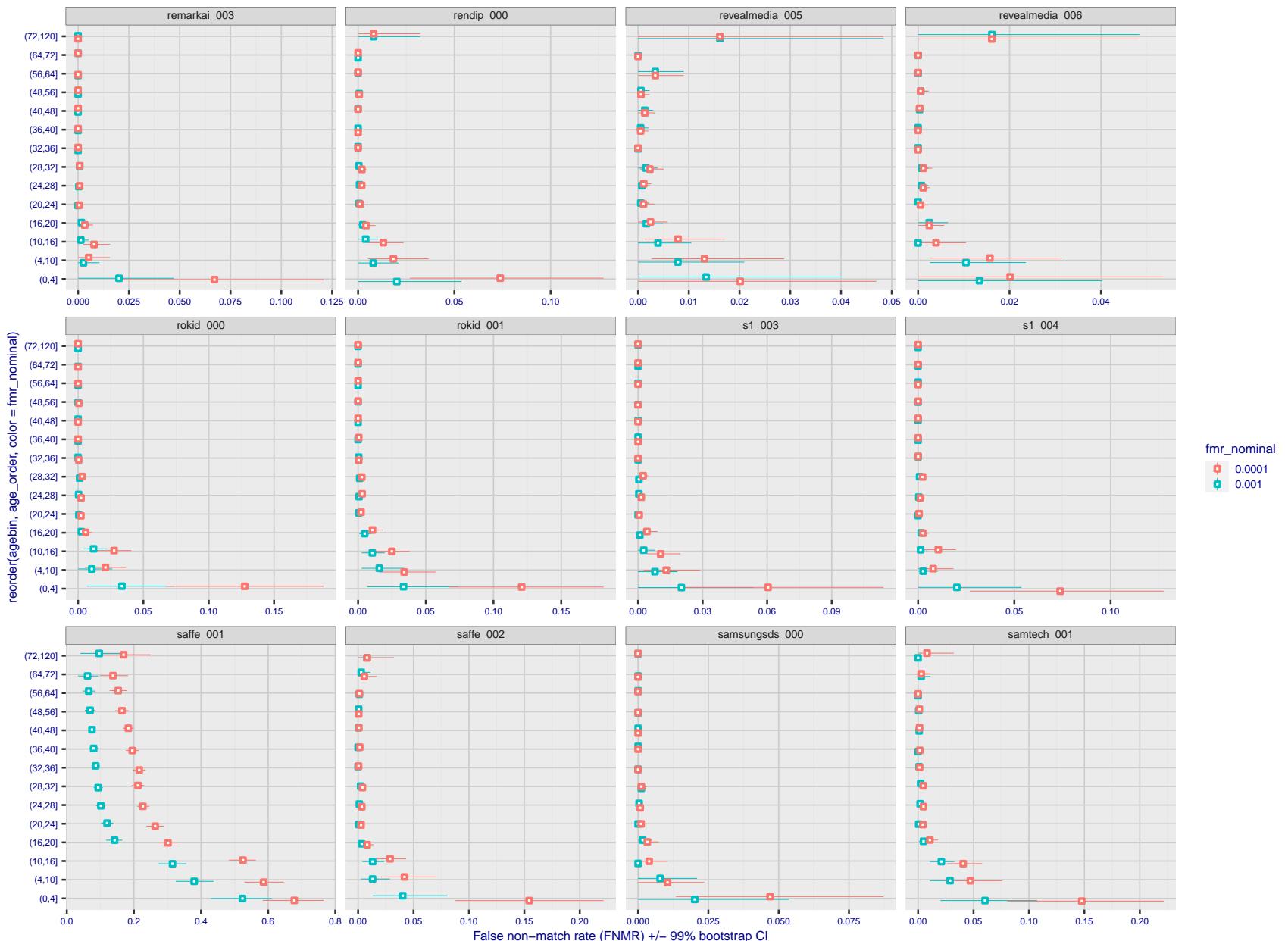


Figure 310: For the visa images, the dots show FNMR by age group for two operating thresholds corresponding to $FMR = \{0.001, 0.0001\}$ computed over all on the order of 10^{10} impostor scores. The FMR in each bin will vary also - see subsequent impostor heatmaps in sec. 3.6.2. Given a pair of face images taken at different times, we assign the comparison to the bin that is the arithmetic average of the subject's ages. This plot shows only the effect of age, not ageing. The number of comparisons in each bin is generally in the thousands, however the first and last bins are computed over 149 and 124 respectively. The error rates in some (adult) cases are zero, and in others the DET is flat so the error rates at the two thresholds are identical. The lines span 1% and 99% of bootstrap replicated FNMR estimates.

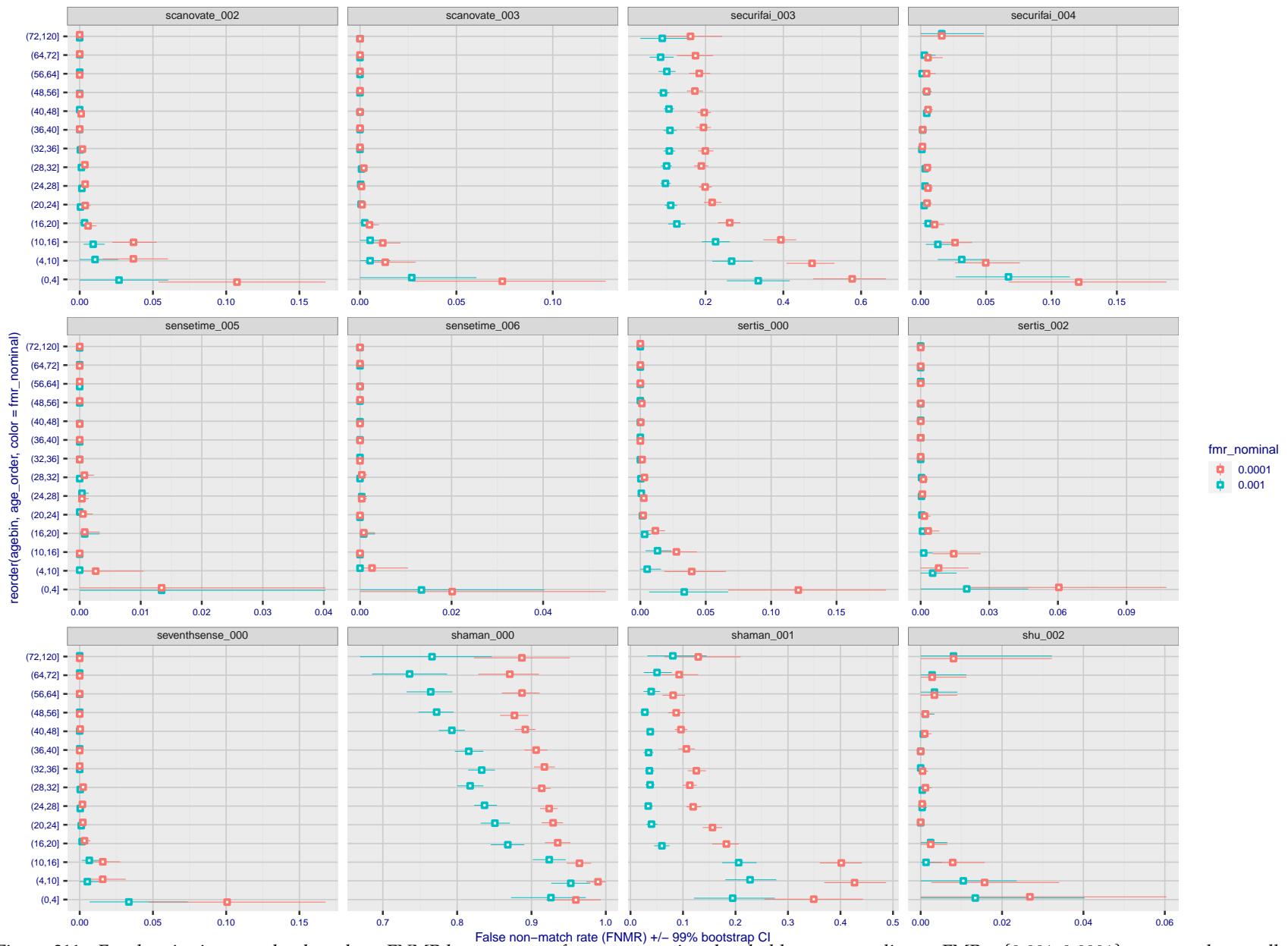


Figure 311: For the visa images, the dots show FNMR by age group for two operating thresholds corresponding to $FMR = \{0.001, 0.0001\}$ computed over all on the order of 10^{10} impostor scores. The FMR in each bin will vary also - see subsequent impostor heatmaps in sec. 3.6.2. Given a pair of face images taken at different times, we assign the comparison to the bin that is the arithmetic average of the subject's ages. This plot shows only the effect of age, not ageing. The number of comparisons in each bin is generally in the thousands, however the first and last bins are computed over 149 and 124 respectively. The error rates in some (adult) cases are zero, and in others the DET is flat so the error rates at the two thresholds are identical. The lines span 1% and 99% of bootstrap replicated FNMR estimates.

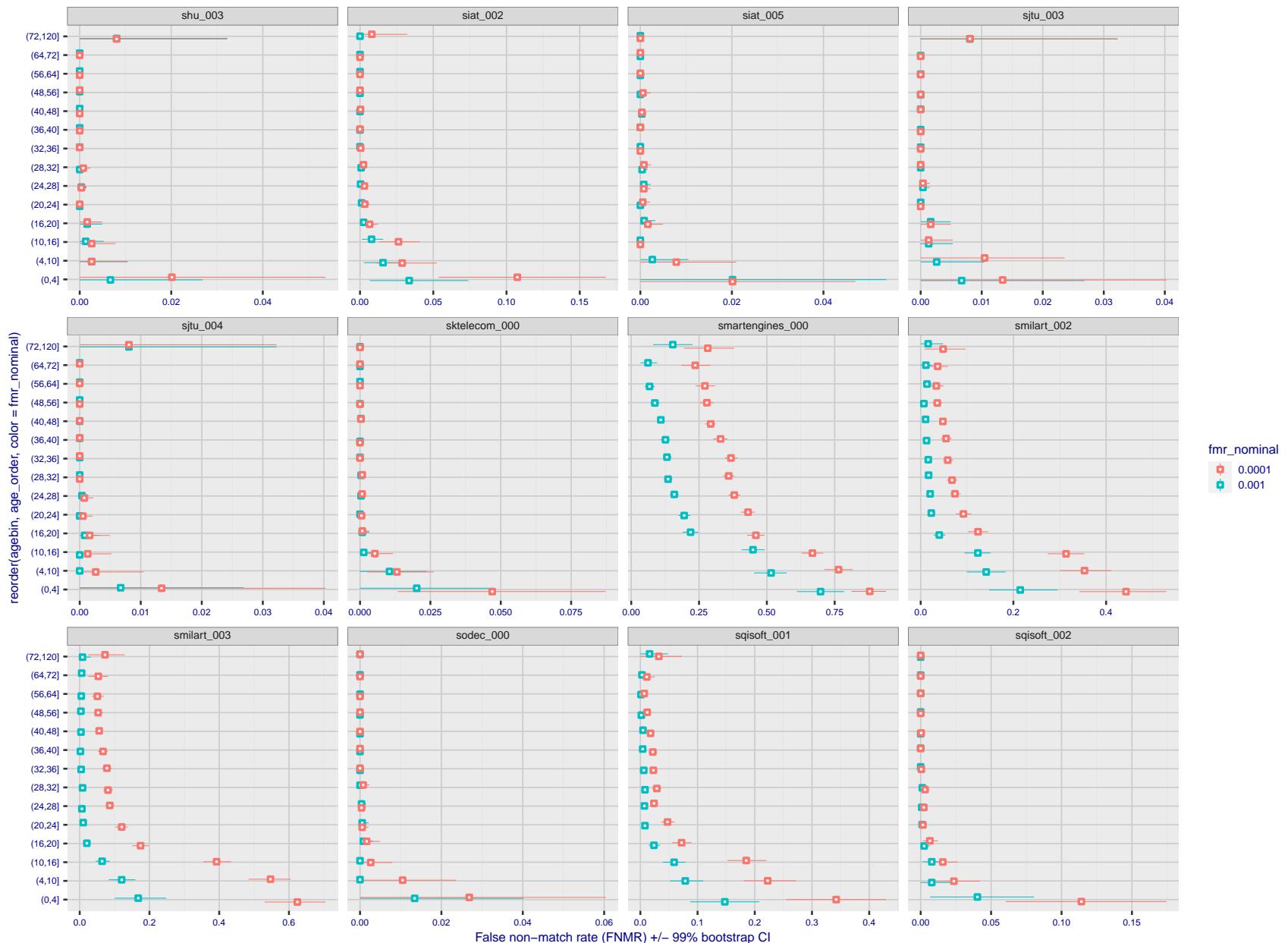


Figure 312: For the visa images, the dots show FNMR by age group for two operating thresholds corresponding to $FMR = \{0.001, 0.0001\}$ computed over all on the order of 10^{10} impostor scores. The FMR in each bin will vary also - see subsequent impostor heatmaps in sec. 3.6.2. Given a pair of face images taken at different times, we assign the comparison to the bin that is the arithmetic average of the subject's ages. This plot shows only the effect of age, not ageing. The number of comparisons in each bin is generally in the thousands, however the first and last bins are computed over 149 and 124 respectively. The error rates in some (adult) cases are zero, and in others the DET is flat so the error rates at the two thresholds are identical. The lines span 1% and 99% of bootstrap replicated FNMR estimates.

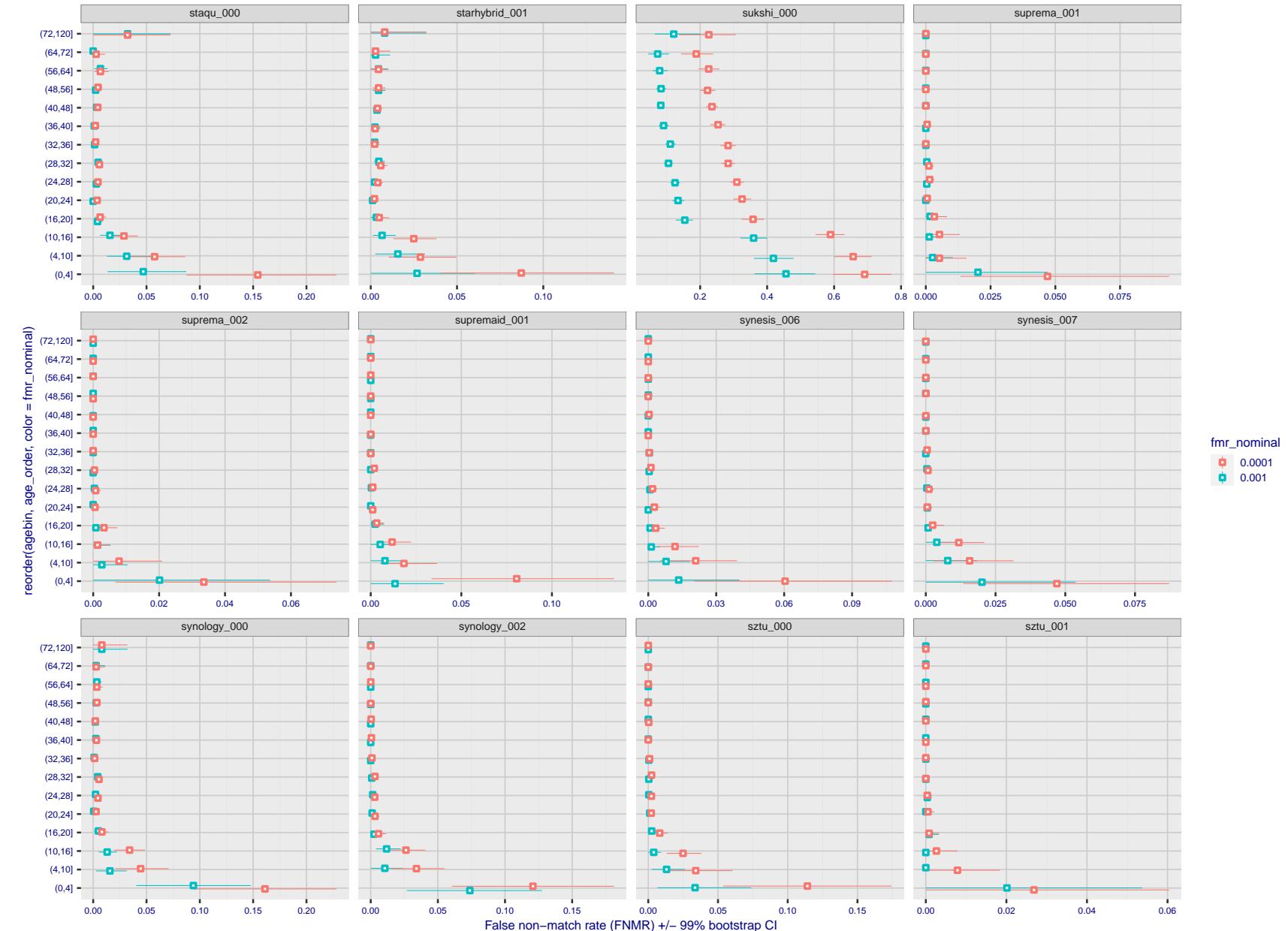


Figure 313: For the visa images, the dots show FNMR by age group for two operating thresholds corresponding to $FMR = \{0.001, 0.0001\}$ computed over all on the order of 10^{10} impostor scores. The FMR in each bin will vary also - see subsequent impostor heatmaps in sec. 3.6.2. Given a pair of face images taken at different times, we assign the comparison to the bin that is the arithmetic average of the subject's ages. This plot shows only the effect of age, not ageing. The number of comparisons in each bin is generally in the thousands, however the first and last bins are computed over 149 and 124 respectively. The error rates in some (adult) cases are zero, and in others the DET is flat so the error rates at the two thresholds are identical. The lines span 1% and 99% of bootstrap replicated FNMR estimates.



Figure 314: For the visa images, the dots show FNMR by age group for two operating thresholds corresponding to $FMR = \{0.001, 0.0001\}$ computed over all on the order of 10^{10} impostor scores. The FMR in each bin will vary also - see subsequent impostor heatmaps in sec. 3.6.2. Given a pair of face images taken at different times, we assign the comparison to the bin that is the arithmetic average of the subject's ages. This plot shows only the effect of age, not ageing. The number of comparisons in each bin is generally in the thousands, however the first and last bins are computed over 149 and 124 respectively. The error rates in some (adult) cases are zero, and in others the DET is flat so the error rates at the two thresholds are identical. The lines span 1% and 99% of bootstrap replicated FNMR estimates.



Figure 315: For the visa images, the dots show FNMR by age group for two operating thresholds corresponding to $FMR = \{0.001, 0.0001\}$ computed over all on the order of 10^{10} impostor scores. The FMR in each bin will vary also - see subsequent impostor heatmaps in sec. 3.6.2. Given a pair of face images taken at different times, we assign the comparison to the bin that is the arithmetic average of the subject's ages. This plot shows only the effect of age, not ageing. The number of comparisons in each bin is generally in the thousands, however the first and last bins are computed over 149 and 124 respectively. The error rates in some (adult) cases are zero, and in others the DET is flat so the error rates at the two thresholds are identical. The lines span 1% and 99% of bootstrap replicated FNMR estimates.

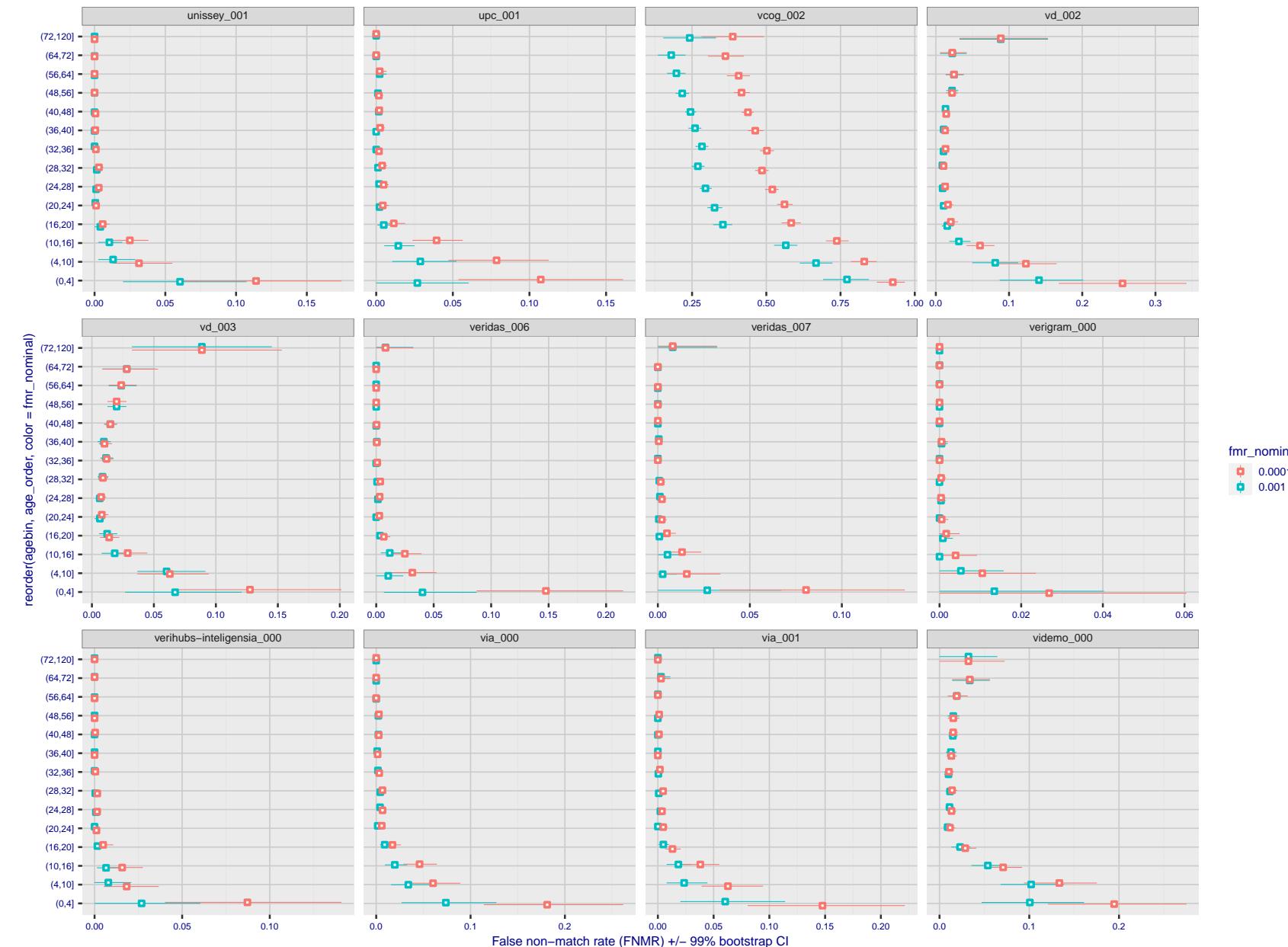


Figure 316: For the visa images, the dots show FNMR by age group for two operating thresholds corresponding to $FMR = \{0.001, 0.0001\}$ computed over all on the order of 10^{10} impostor scores. The FMR in each bin will vary also - see subsequent impostor heatmaps in sec. 3.6.2. Given a pair of face images taken at different times, we assign the comparison to the bin that is the arithmetic average of the subject's ages. This plot shows only the effect of age, not ageing. The number of comparisons in each bin is generally in the thousands, however the first and last bins are computed over 149 and 124 respectively. The error rates in some (adult) cases are zero, and in others the DET is flat so the error rates at the two thresholds are identical. The lines span 1% and 99% of bootstrap replicated FNMR estimates.

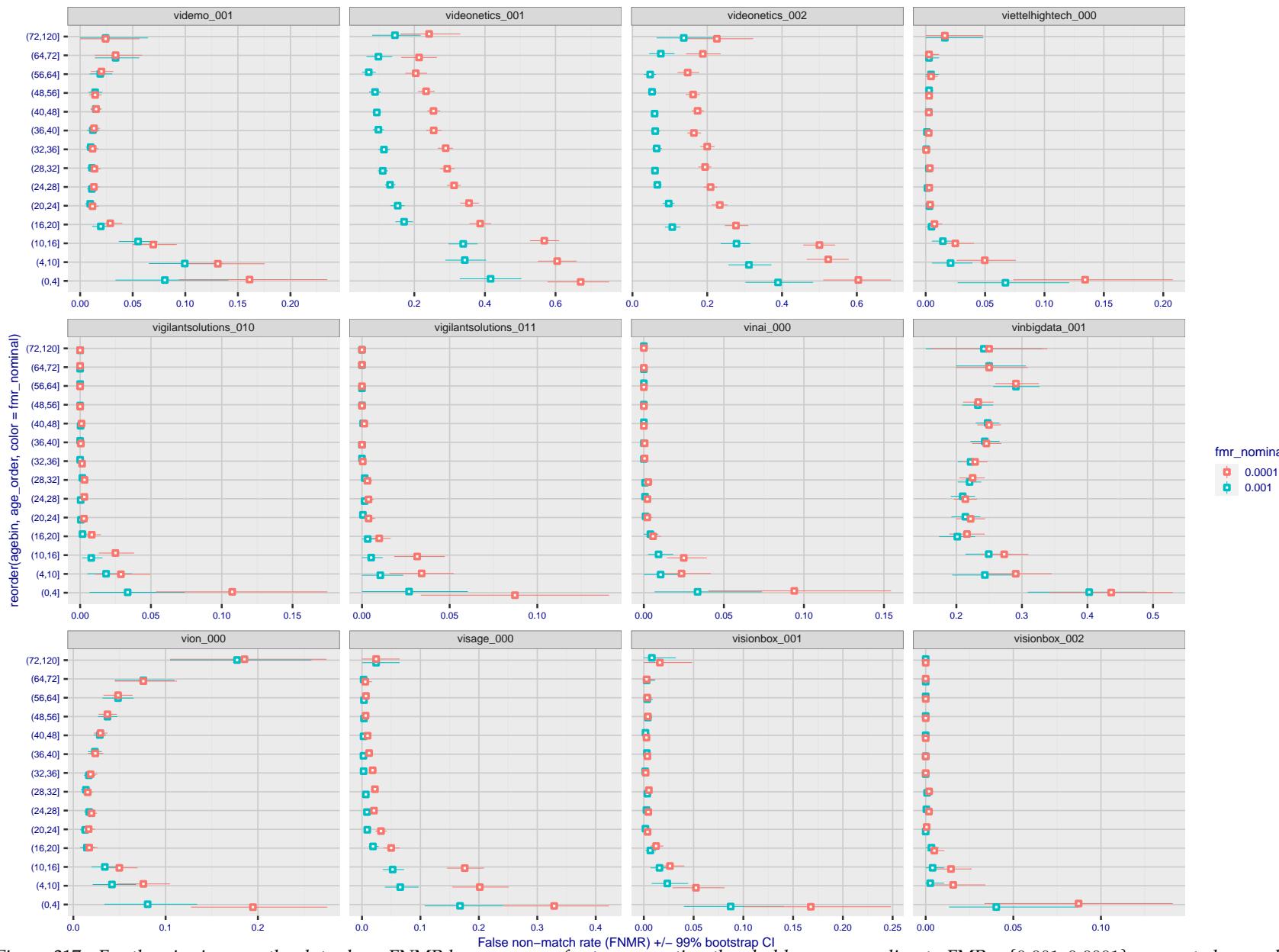


Figure 317: For the visa images, the dots show FNMR by age group for two operating thresholds corresponding to $FMR = \{0.001, 0.0001\}$ computed over all on the order of 10^{10} impostor scores. The FMR in each bin will vary also - see subsequent impostor heatmaps in sec. 3.6.2. Given a pair of face images taken at different times, we assign the comparison to the bin that is the arithmetic average of the subject's ages. This plot shows only the effect of age, not ageing. The number of comparisons in each bin is generally in the thousands, however the first and last bins are computed over 149 and 124 respectively. The error rates in some (adult) cases are zero, and in others the DET is flat so the error rates at the two thresholds are identical. The lines span 1% and 99% of bootstrap replicated FNMR estimates.



Figure 318: For the visa images, the dots show FNMR by age group for two operating thresholds corresponding to $FMR = \{0.001, 0.0001\}$ computed over all on the order of 10^{10} impostor scores. The FMR in each bin will vary also - see subsequent impostor heatmaps in sec. 3.6.2. Given a pair of face images taken at different times, we assign the comparison to the bin that is the arithmetic average of the subject's ages. This plot shows only the effect of age, not ageing. The number of comparisons in each bin is generally in the thousands, however the first and last bins are computed over 149 and 124 respectively. The error rates in some (adult) cases are zero, and in others the DET is flat so the error rates at the two thresholds are identical. The lines span 1% and 99% of bootstrap replicated FNMR estimates.



Figure 319: For the visa images, the dots show FNMR by age group for two operating thresholds corresponding to $FMR = \{0.001, 0.0001\}$ computed over all on the order of 10^{10} impostor scores. The FMR in each bin will vary also - see subsequent impostor heatmaps in sec. 3.6.2. Given a pair of face images taken at different times, we assign the comparison to the bin that is the arithmetic average of the subject's ages. This plot shows only the effect of age, not ageing. The number of comparisons in each bin is generally in the thousands, however the first and last bins are computed over 149 and 124 respectively. The error rates in some (adult) cases are zero, and in others the DET is flat so the error rates at the two thresholds are identical. The lines span 1% and 99% of bootstrap replicated FNMR estimates.

Caveats: None.

3.6 Impostor distribution stability

3.6.1 Effect of birth place on the impostor distribution

Background: Facial appearance varies geographically, both in terms of skin tone, cranio-facial structure and size. This section addresses whether false match rates vary intra- and inter-regionally.

Goals:

- ▷ To show the effect of birth region of the impostor and enrollee on false match rates.
- ▷ To determine whether some algorithms give better impostor distribution stability.

Methods:

- ▷ For the visa images, NIST defined 10 regions: Sub-Saharan Africa, South Asia, Polynesia, North Africa, Middle East, Europe, East Asia, Central and South America, Central Asia, and the Caribbean.
- ▷ For the visa images, NIST mapped each country of birth to a region. There is some arbitrariness to this. For example, Egypt could reasonably be assigned to the Middle East instead of North Africa. An alternative methodology could, for example, assign the Philippines to *both* Polynesia and East Asia.
- ▷ FMR is computed for cases where all face images of impostors born in region r_2 are compared with enrolled face images of persons born in region r_1 .

$$\text{FMR}(r_1, r_2, T) = \frac{\sum_{i=1}^{N_{r_1, r_2}} H(s_i - T)}{N_{r_1, r_2}} \quad (5)$$

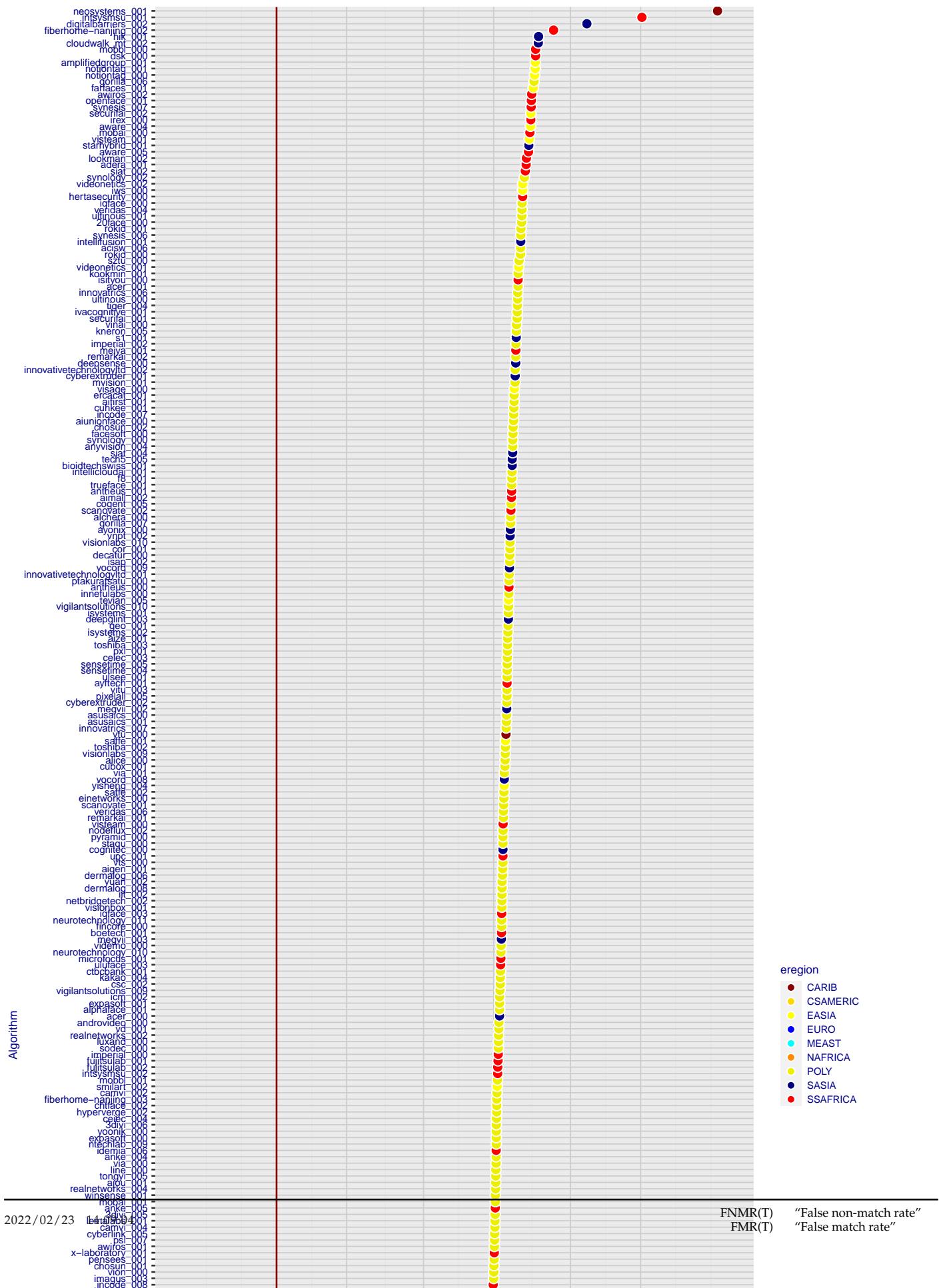
where the same threshold, T , is used in all cells, and H is the unit step function. The threshold is set to give $\text{FMR}(T) = 0.001$ over the entire set of visa image impostor comparisons.

- ▷ This analysis is then repeated by country-pair, but only for those country pairs where both have at least 1000 images available. The countries¹ appear in the axes of graphs that follow.
- ▷ The mean number of impostor scores in any cross-region bin is 33 million. The smallest number of impostor scores in any bin is 135000, for Central Asia - North Africa. While these counts are large enough to support reasonable significance, the number of individual faces is much smaller, on the order of $N^{0.5}$.
- ▷ The numbers of impostor scores in any cross-country bin is shown in Figure ??.

Results: Subsequent figures show heatmaps that use color to represent the base-10 logarithm of the false match rate. Red colors indicate high (bad) false match rates. Dark colors indicate benign false match rates. There are two series of graphs corresponding to aggregated geographical regions, and to countries. The notable observations are:

- ▷ The on-diagonal elements correspond to within-region impostors. FMR is generally above the nominal value of $\text{FMR} = 0.001$. Particularly there is usually higher FMR in, Sub-Saharan Africa, South Asia, and the Caribbean. Europe and Central Asia, on the other hand, usually give FMR closer to the nominal value.
- ▷ The off-diagonal elements correspond to across-region impostors. The highest FMR is produced between the Caribbean and Sub-Saharan Africa.
- ▷ Algorithms vary.

¹These are Argentina, Australia, Brazil, Chile, China, Costa Rica, Cuba, Czech Republic, Dominican Republic, Ecuador, Egypt, El Salvador, Germany, Ghana, Great Britain, Greece, Guatemala, Haiti, Hong Kong, Honduras, Indonesia, India, Israel, Jamaica, Japan, Kenya, Korea, Lebanon, Mexico, Malaysia, Nepal, Nigeria, Peru, Philippines, Pakistan, Poland, Romania, Russia, South Africa, Saudi Arabia, Thailand, Trinidad, Turkey, Taiwan, Ukraine, Venezuela, and Vietnam.



- ▷ We computed the same quantities for a global FMR = 0.0001. The effects are similar.

Caveats:

- ▷ The effects of variable impostor rates on one-to-many identification systems may well differ from what's implied by these one-to-one verification results. Two reasons for this are a) the enrollment galleries are usually imbalanced across countries of birth, age and sex; b) one-to-many identification algorithms often implement techniques aimed at stabilizing the impostor distribution. Further research is necessary.
- ▷ In principle, the effects seen in this subsection could be due to differences in the image capture process. We consider this unlikely since the effects are maintained across geography - e.g. Caribbean vs. Africa, or Japan vs. China.

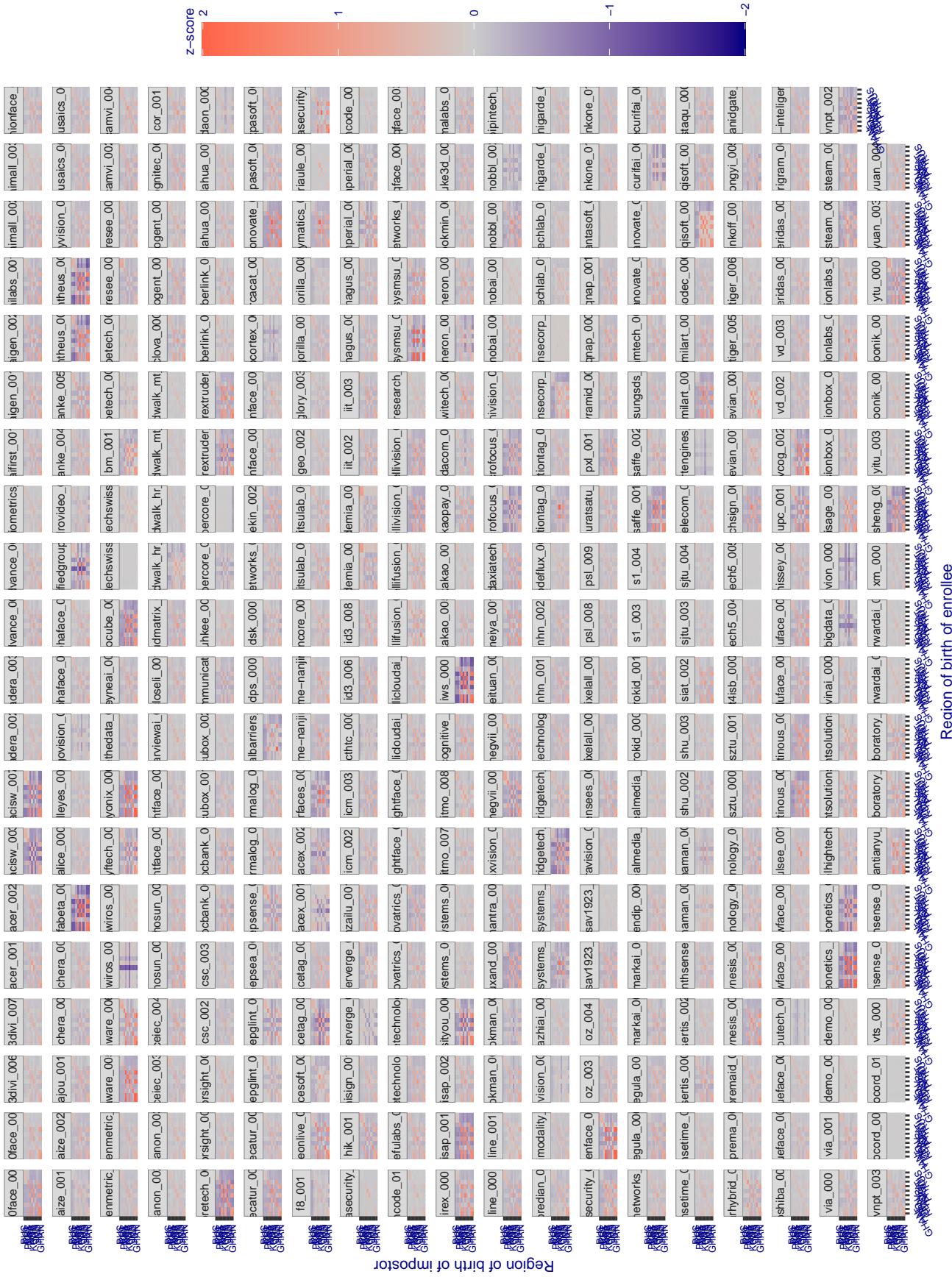


Figure 321: For visa images, the heatmap shows how the mean of the impostor distribution for the country pair (a,b) is shifted relative to the mean of the global impostor distribution, expressed as a number of standard deviations of the global impostor distribution. This statistic is designed to show shifts in the entire impostor distribution, not just tail effects that manifest as the anomalously high (or low) false match rates that appear in the subsequent figures. The countries are chosen to show that skin tone alone does not explain impostor distribution shifts. The reduced shift in Asian populations with the Yitu and Tong YiTrans algorithms, is accompanied by positive shifts in the European populations. This reversal relative to most other algorithms, may derive from use of nationally weighted training sets. The figure is computed from same-sex and same-age impostor pairs.

3.6.2 Effect of age on impostors

Background: This section shows the effect of age on the impostor distribution. The ideal behaviour is that the age of the enrollee and the impostor would not affect impostor scores. This would support FMR stability over sub-populations.

Goals:

- ▷ To show the effect of relative ages of the impostor and enrollee on false match rates.
- ▷ To determine whether some algorithms have better impostor distribution stability.

Methods:

- ▷ Define 14 age group bins, spanning 0 to over 100 years old.
- ▷ Compute FMR over all impostor comparisons for which the subjects in the enrollee and impostor images have ages in two bins.
- ▷ Compute FMR over all impostor comparisons for which the subjects are additionally of the same sex, and born in the same geographic region.

Results:

The notable aspects are:

- ▷ Diagonal dominance: Impostors are more likely to be matched against their same age group.
- ▷ Same sex and same region impostors are more successful. On the diagonal, an impostor is more likely to succeed by posing as someone of the same sex. If $\Delta \log_{10} \text{FMR} = 0.2$, then same-sex same-region FMR exceeds the all-pairs FMR by factor of $10^{0.2} = 1.6$.
- ▷ Young children impostors give elevated FMR against young children. Older adult impostor give elevated FMR against older adults. These effects are quite large, for example if $\Delta \log_{10} \text{FMR} = 1.0$ larger than a 32 year old, then these groups have higher FMR by a factor of $10^1 = 10$. This would imply an FMR above 0.01 for a nominal (global) FMR = 0.001.
- ▷ Algorithms vary.
- ▷ We computed the same quantities for a global FMR = 0.0001. The effects are similar.

Note the calculations in this section include impostors paired across all countries of birth.

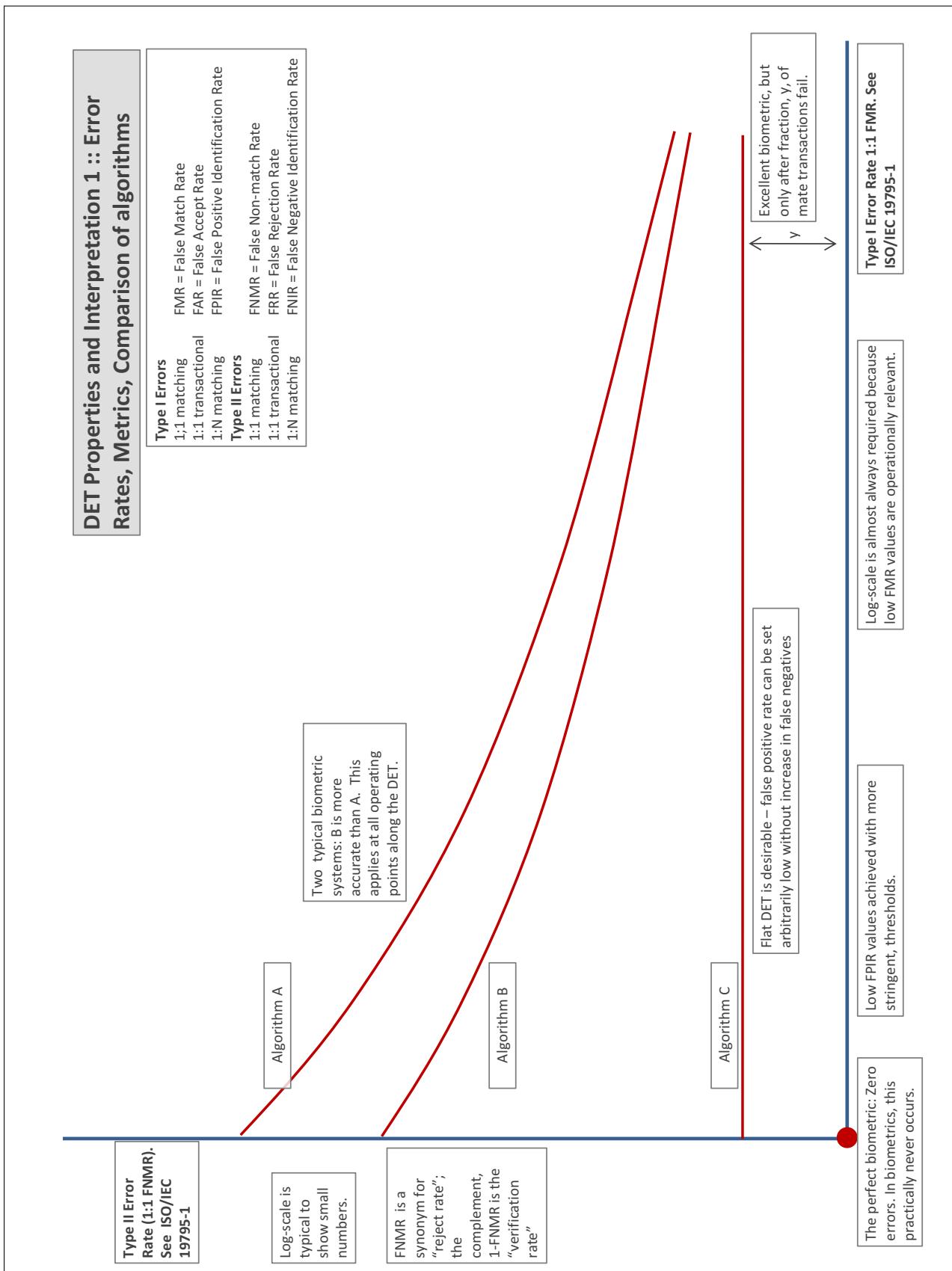
Accuracy Terms + Definitions

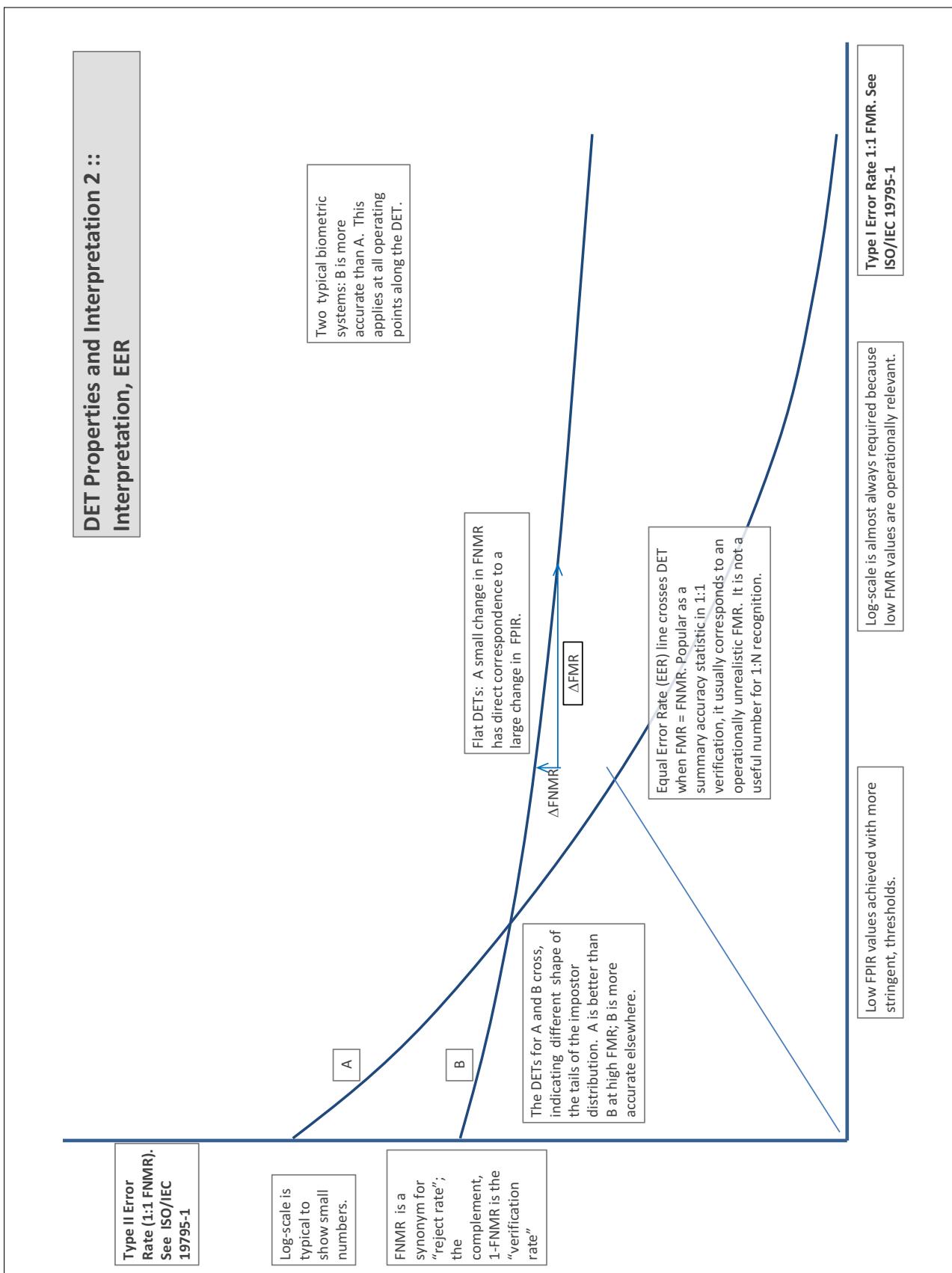
In biometrics, Type II errors occur when two samples of one person do not match – this is called a **false negative**. Correspondingly, Type I errors occur when samples from two persons do match – this is called a **false positive**. Matches are declared by a biometric system when the native comparison score from the recognition algorithm meets some **threshold**. Comparison scores can be either **similarity scores**, in which case higher values indicate that the samples are more likely to come from the same person, or **dissimilarity scores**, in which case higher values indicate different people. Similarity scores are traditionally computed by **fingerprint** and **face** recognition algorithms, while dissimilarities are used in **iris recognition**. In some cases, the dissimilarity score is a distance; this applies only when **metric** properties are obeyed. In any case, scores can be either **mate** scores, coming from a comparison of one person's samples, or **nonmate** scores, coming from comparison of different persons' samples. The words **genuine** or **authentic** are synonyms for mate, and the word **impostor** is used as a synonym for nonmatch. The words mate and nonmatch are traditionally used in identification applications (such as law enforcement search, or background checks) while genuine and impostor are used in verification applications (such as access control).

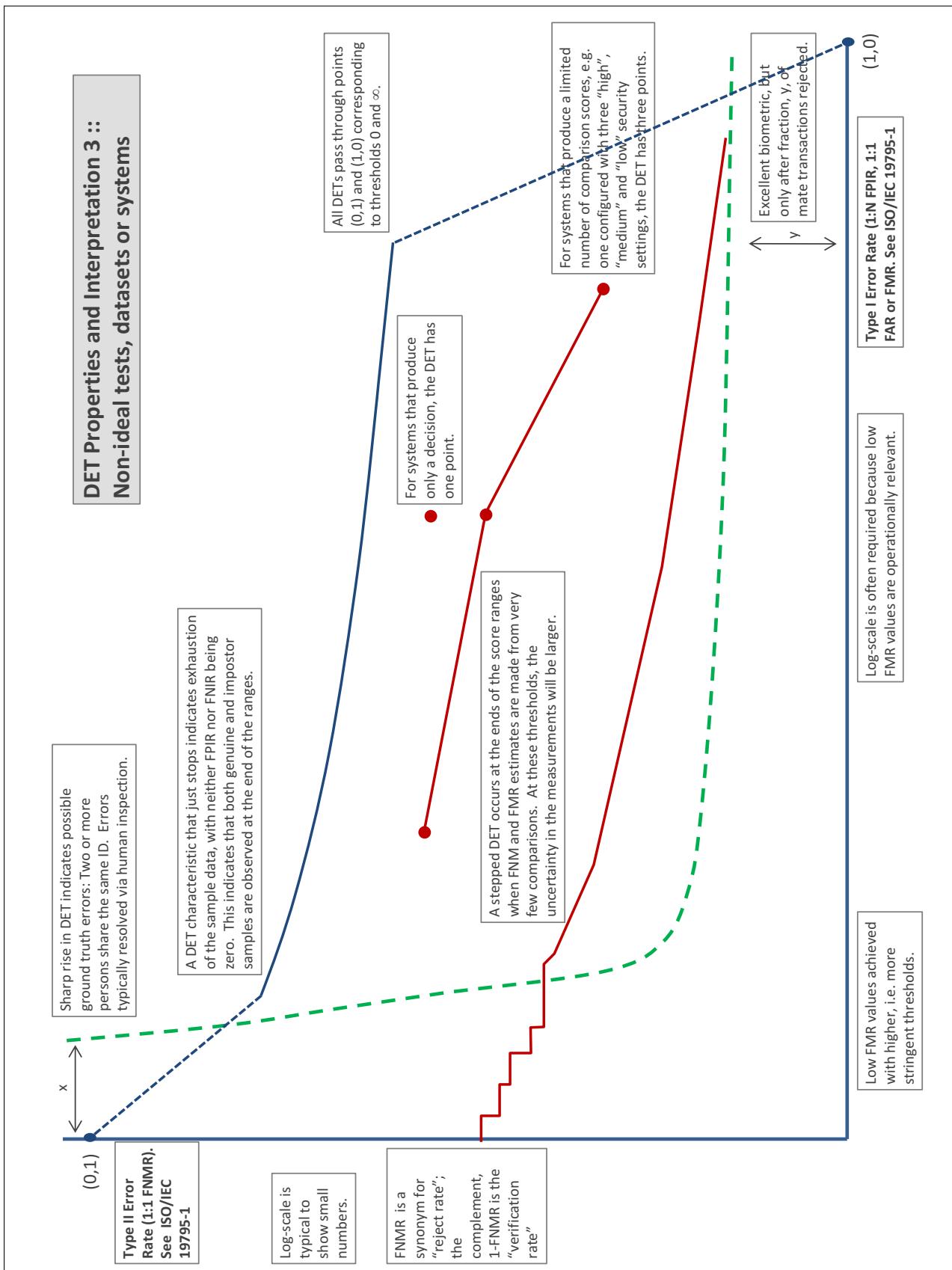
A **error tradeoff** characteristic represents the tradeoff between Type II and Type I classification errors. For verification this plots false non-match rate (FNMR) vs. false match rate (FMR) parametrically with T.

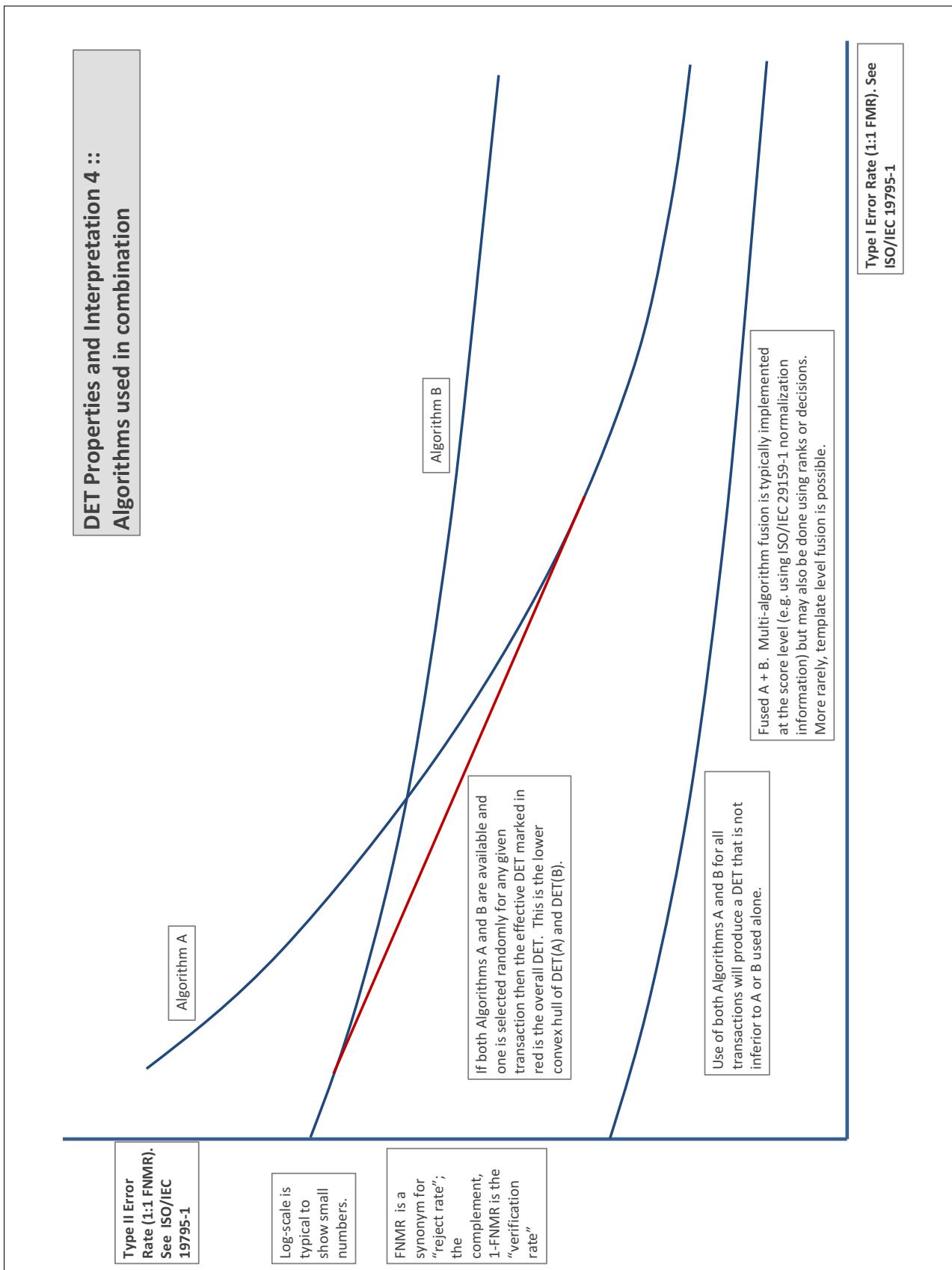
The error tradeoff plots are often called **detection error tradeoff (DET)** characteristics or **receiver operating characteristic (ROC)**. These serve the same function but differ, for example, in plotting the complement of an error rate (e.g., $TMR = 1 - FNMR$) and in transforming the axes most commonly using logarithms, to show multiple decades of FMR. More rarely, the function might be the inverse Gaussian function.

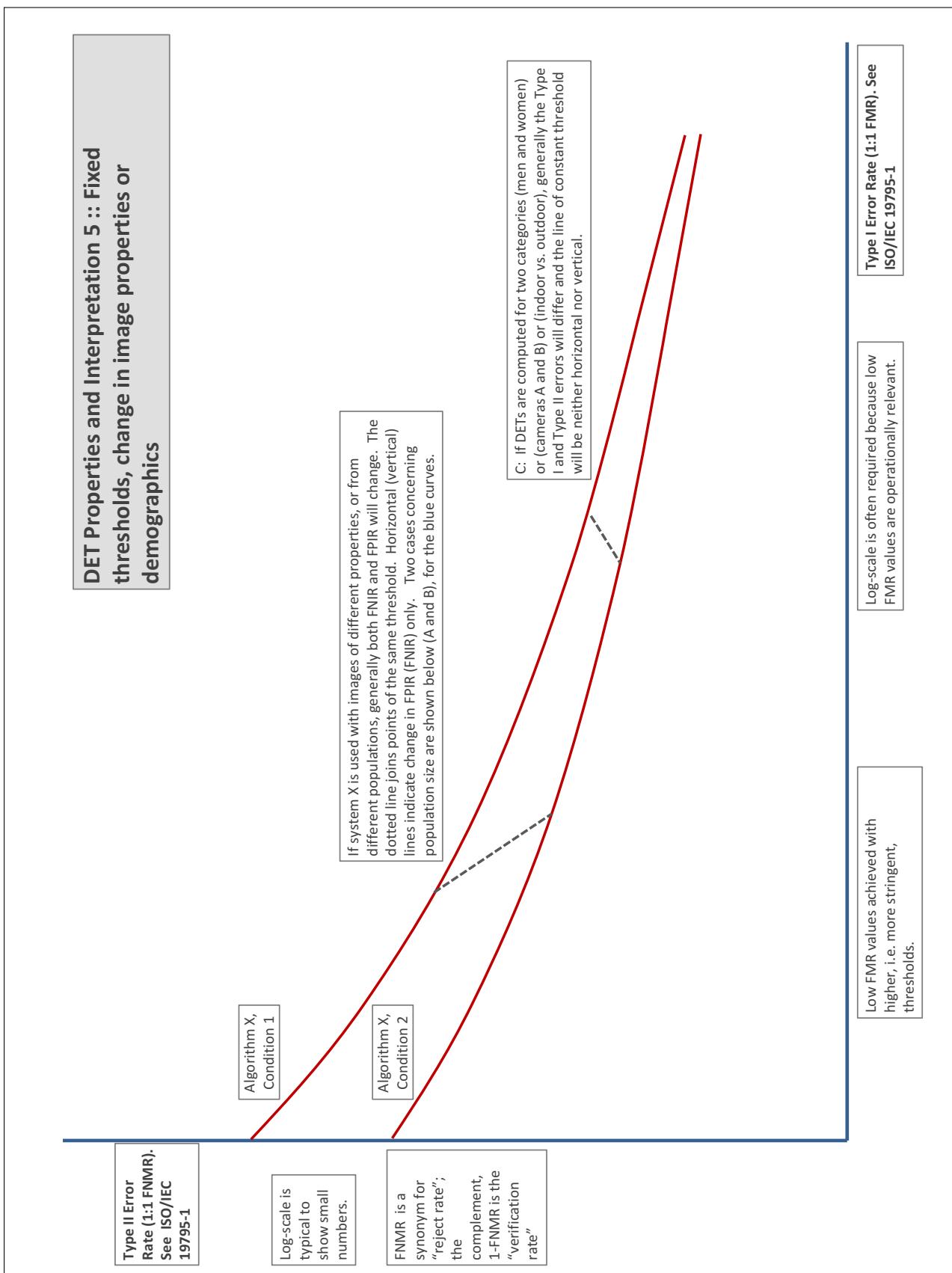
More detail and generality is provided in formal biometrics testing standards, see the various parts of [ISO/IEC 19795 Biometrics Testing and Reporting](#). More terms, including and beyond those to do with accuracy, see [ISO/IEC 2382-37 Information technology -- Vocabulary -- Part 37: Harmonized biometric vocabulary](#)











References

- [1] P. Jonathon Phillips, Amy N. Yates, Ying Hu, Carina A. Hahn, Eilidh Noyes, Kelsey Jackson, Jacqueline G. Cavazos, Géraldine Jeckeln, Rajeev Ranjan, Swami Sankaranarayanan, Jun-Cheng Chen, Carlos D. Castillo, Rama Chellappa, David White, and Alice J. O'Toole. Face recognition accuracy of forensic examiners, superrecognizers, and face recognition algorithms. *Proceedings of the National Academy of Sciences*, 115(24):6171–6176, 2018.